Molecular Tools for G-Protein Coupled Receptors: Synthesis, Pharmacological Characterization and [^{3}H]-Labeling of Subtype-selective Ligands for Histamine H_4 and NPY Y_2 Receptors

Dissertation

zur Erlangung des Doktorgrades der Naturwissenschaften (Dr. rer. nat.)

an der Fakultät für Chemie und Pharmazie

der Universität Regensburg

vorgelegt von

Paul Baumeister

aus Zinzenzell

2014

Die vorliegende Arbeit entstand in der Zeit von April 2010 bis April 2014 unter der Anleitung von Herrn Prof. Dr. Armin Buschauer am Institut für Pharmazie der Naturwissenschaftlichen Fakultät IV – Chemie und Pharmazie – der Universität Regensburg.

Das Promotionsgesuch wurde eingereicht im Juni 2014.

Tag der mündlichen Prüfung: 18.07.2014

Prüfungsausschuss: Prof. Dr. J. Heilmann (Vorsitzender)

Prof. Dr. A. Buschauer (Erstgutachter)

Prof. Dr. S. Elz (Zweitgutachter)

Prof. Dr. J. Wegener (Drittprüfer)

„If you don’t turn your life into a story,

you just become a part of someone else’s story.“

Terry Pratchett

Danksagung

An dieser Stelle möchte mich ganz herzlich bei allen bedanken, die zum Gelingen dieser Arbeit beigetragen haben und mich während der Promotionszeit begleitet haben. Besonders möchte ich danken:

Meinem Doktorvater Herrn Prof. Dr. Armin Buschauer für das Vertrauen und die Möglichkeit dieses interessante und herausfordernde Projekt zu verwirklichen, seine wissenschaftlichen Anregungen, für die mir gewährte forscherische Freiheit, seine konstruktive Kritik bei der Durchsicht der Arbeit, sein stets offenes Ohr, sowie die Mentorenschaft in der Emil-Fischer-Graduiertenschule;

Herrn Prof. Dr. Günther Bernhardt für seine stete Hilfsbereitschaft und sein Interesse am Fortschritt der Arbeit, sein Fachwissen, die Durchsicht der Arbeit, die Co-Mentorenschaft in der Emil-Fischer-Graduiertenschule, sowie für hervorragenden Sommerfeste;

Herrn Prof. Dr. Sigurd Elz für die Erstellung des Zweitgutachtens und die Teilnahme an der mündlichen Prüfung;

Herrn Prof. Dr. Joachim Wegener für die Bereitschaft als Drittprüfer an der mündlichen Prüfung teilzunehmen und die Co-Mentorenschaft in der Emil-Fischer-Graduiertenschule;

Herrn Prof. Dr. Jörg Heilmann für die Teilnahme als Vorsitzender in der mündlichen Prüfung;

Herrn Dr. Max Keller für seine fachliche und soziale Kompetenz, die hervorragende Zusammenarbeit, aufmunternde Worte, seine Motivation, die Bereitstellung von Synthesebausteinen und die gemütlichen Abende bei selbstgemachtem Wein;

Herrn Dr. Patrick Igel und Herrn Dr. Roland Geyer für die ausführliche Einführung in die Histamin-Welt, die fachlichen Tipps und die Bereitstellung von Synthesebausteinen;

Herrn Dr. Nikola Pluym für die ausführliche Einführung in die NPY-Welt, die fachlichen Diskussionen, seine soziale Kompetenz, die Bereitstellung von Synthesebausteinen und die Einführung in die Welt der Radioligandsynthese;

Herrn Dr. Thilo Spruss, Herrn Franz Wiesenmayer und Frau Petra Pistor für die Betreuung und Unterstützung bei der Durchführung der Tierversuche, sowie für das Anfertigen der Kryoschnitte von Gewebeproben und deren histologischen Färbung;

Herrn Dr. Uwe Nordemann für die Durchführung der HEK293 Zellexperimente mit [^{3}H]JNJ7777120 und die Einweisung in die Welt der Radioligandsynthese;

Frau Nicole Kagermeier für die fachlichen Diskussionen und die Durchführung der HEK293 Zellexperimente mit [^{3}H]UR-DE257;

Frau Maria Beer-Krön, Frau Dita Fritsch, Frau Susanne Bollwein, Frau Elvira Schreiber und Frau Brigitte Wenzl für die tatkräftige Unterstützung bei der Durchführung vieler Assays, HPLC-Läufe und der Zellkultivierung;

Herrn Peter Richthammer für die zahlreichen netten Gespräche, seine stete Hilfsbereitschaft und Kompetenz bei allen technischen Herausforderungen und für die gute Zusammenarbeit bei der Durchführung der verschiedenen Praktika;

Frau Uta Hasselmann, Frau Karin Reindl und Frau Silvia Heinrich für die stets freundliche Unterstützung bei allen organisatorischen Angelegenheiten;

Frau Edith Bartole, Frau Shiwen Xue, Herrn Josef Auburger, Herrn Michael Schupfner und Herrn Markus Friedrich für die Durchführung von Versuche im Rahmen Ihrer Praktika;

Allen Laborkollegen, allen Mitgliedern der Histamin-Gruppe und der NPY-Gruppe für die angenehme, inspirierenden und gelegentlich auch amüsanten Atmosphäre und die sehr gute Zusammenarbeit;

Frau Edith Bartole und Frau Sabrina Biselli für die gute Zusammenarbeit im Rahmen der Betreuung Ihrer Masterarbeiten;

Allen Mitarbeitern der analytischen Abteilung der Universität Regensburg für die Aufnahme und Hilfestellung bei der Interpretation der NMR- und Massenspektren. Ein besonderer Dank geht hierbei an Herrn Fritz Kastner und Herrn Josef Kiermaier für die hilfreichen Diskussionen und die Ermittlung zahlreicher analytischer Daten;

Allen Mitgliedern der Arminia Buschauer für die tolle Zeit am Lehrstuhl, die stets gute Kollegialität, Arbeitsatmosphäre und Zusammenarbeit;

Frau Dr. Stefanie Bauer, Herrn Dr. Roland Geyer, Herrn Stefan Huber, Frau Nicole Kagermeier, Herrn Dr. Nikola Pluym, Frau Edith Bartole, Herrn Steffen Pockes und Frau Maria Beer-Kroen für die vielen netten Gespräche und schöne Zeit;

Den Mitarbeitern der FAU Erlangen, Herrn Prof. Dr. Peter Gmeiner, Herrn Prof. Dr. Markus Heinrich, Frau Dr. Nuska Tschammer, Herrn Dr. Viachaslau Bernat, Herrn Dr. Harald Hübner und Michael Fürst für die gute Zusammenarbeit;

Herrn Prof. Dr. Oliver Reiser und Dr. Julian Bodensteiner für die gute Zusammenarbeit;

Der Deutschen Forschungsgemeinschaft für die finanzielle Förderung im Rahmen des Graduiertenkollegs GRK 760;

Special thanks to my coworkers and friends Jianfei Wan and Xueke She for the great opportunity to visit their homeland China, all the hospitality, patience and unforgettable impressions. **谢谢**! 干杯!

Meinen Freunden und dem Trimmverein Regensburg, auf die man sich immer verlassen konnte, wenn es darauf ankam. ‚*Reich sind nur die, die wahre Freunde haben' (Thomas Fuller)*;

Den Herren Dr. Daniel Bücherl, Petr Jirásek und Michel Leonhardt für die allmorgendliche Frühstücksrunde, sowie die moralische und fachliche Unterstützung;

Zuletzt all denjenigen, die das Leben lebenswert machen und mehr als nur Dank verdienen: meinen Eltern, meinen Geschwistern und meiner Freundin Marina. Ihnen ist die vorliegende Arbeit gewidmet.

Publications (published results prior to the submission of this thesis):

(1) Baumeister, P., Erdmann, D., Biselli, S., Kagermeier, N., Bernhardt, G., Buschauer, A.: [^{3}H]UR-DE257: A Selective and Highly Potent Tritium-Labeled Squaramide-type Histamine H_2 Receptor Antagonist. *ChemMedChem* **2014**, in preparation.

(2) Geyer, R., Kaske, M., Baumeister, P., Buschauer, A.: Synthesis and Functional Characterization of Imbutamine Analogs as Histamine H_3 and H_4 Receptor Ligands. *Arch. Pharm. Chem. Life Sci.* **2014**, 347, 77–88.

(3) Pluym, N., Baumeister, P., Keller, M., Bernhardt, G., Buschauer, A.: [^{3}H]UR-PLN196: A Selective Nonpeptide Radioligand and Insurmountable Antagonist for the Neuropeptide Y Y_2 Receptor. *ChemMedChem Comm.* **2013**, 8, 587-593.

(4) Bodensteiner, J., Baumeister, P., Geyer, R., Buschauer, A., Reiser, O.: Synthesis and Pharmacological Characterization of New Tetrahydrofuran Based Compounds as Conformationally Constrained Histamine Receptor Ligands. *Org. Biomol. Chem.* **2013**, 11, 4040-4055.

(5) Bernat, V., Heinrich, M., Baumeister, P., Buschauer, A., Tschammer, N.: Synthesis and Application of the First Radioligand Targeting the Allosteric Binding Pocket of Chemokine Receptor CXCR3. *ChemMedChem* **2012**, 7 (8), 1481-1489.

Short Lecture:

Baumeister, P.: The First Selective Tritium-labeled Nonpeptide Radioligands for the NPY Y_2 Receptor. *Christmas Colloquium 2012 of the Department of Organic Chemistry*, University of Regensburg, 19.12.2012.

Poster Presentations:

03/2013 Annual Meeting of the GDCh, Fachgruppe Medizinische Chemie, Frontiers in Medicinal Chemistry, München.

Baumeister, P., Pluym, N., Keller, M., Bernhardt, G., Buschauer, A.:
Subtype-selective Nonpeptide NPY Y_2 Receptor Radioligands.

09/2012 XXIInd International Symposium on Medicinal Chemistry (ISMC), Berlin.

Baumeister, P., Erdmann, D., Bernhardt, G., Buschauer, A.: [^{3}H]UR-DE257:
A New Tritium-labeled Histamine H_2 Receptor Antagonist.

Bernat, V., Heinrich, M., Baumeister, P., Buschauer, A., Tschammer, N.:
Synthesis and Application of the First Small-Molecule Radioligand Targeting the Human Chemokine Receptor CXCR3. Best Poster Award

09/2012 6th Summer School in Medicinal Chemistry, Regensburg.

Geyer, R., Nordemann, U., Baumeister, P., Bernhardt, G., Buschauer, A.:
trans-(+)-(1*S*,3*S*)-UR-RG98: Synthesis, Absolute Configuration and Pharmacological Characterization of a Highly Potent and Selective Histamine H_4 Receptor Agonist.

03/2011 Annual Meeting of the GDCh, Fachgruppe Medizinische Chemie, Frontiers in Medicinal Chemistry, Saarbrücken.

Baumeister, P., Buschauer, A.:
2-Arylbenzimidazoles as Potent Human Histamine H_4 Receptor Agonists.

Professional Training:

04/2013 Fortbildung für Projektleiter und Beauftragter für Biologische Sicherheit (§15 und 17 Gentechniksicherheitsverordnung).
Regensburg, Germany.

06/2010 Umgang mit offenen radioaktiven Stoffen.
Regensburg, Germany.

03/2010 – 03/2012 Member of the Research Training Group (Graduiertenkolleg 760) "Medicinal Chemistry: Molecular Recognition – Ligand Receptor Interactions" of the German Research Foundation.
Regensburg, Germany.

06/2012 – 04/2014 Member of the Emil Fischer Graduate School of Pharmaceutical Sciences and Molecular Medicine.
Regensburg, Erlangen, Germany.

Contents

Chapter 1

Introduction

1.1 G-Protein-coupled receptors

1.1.1 GPCRs as drug targets and their classification

G-Protein-coupled receptors (GPCRs) constitute the largest group of integral membrane proteins that transmit a wide variety of signals across the cell membrane.[1] GPCRs respond to a broad range of extracellular stimuli such as biogenic amines, purines, lipids, amino acids, peptides and proteins, odorants, pheromones, ions and even photons.[2] More than 800 GPCRs are encoded in the human genome (approximately 2-3% of the human genome) including about 400 functional non-olfactory receptors.[3] For roughly 120 of the latter, referred to as orphan receptors, endogenous ligands are not known to date.[4] More than 50 GPCRs are targeted by approved drugs,[5] which represent 30 - 40 % of all marketed drugs,[6] emphasizing the current value in the treatment of human diseases, as well as the prospects for the development of GPCR ligands as future drugs. Based on structural differences, mammalian GPCRs were classified in five groups: rhodopsin, secretin, adhesion, glutamate and frizzled/taste2.[7] The common structural features of the GPCR superfamily are seven membrane-spanning helices, connected by three alternating intracellular and extracellular loops and flanked by an extracellular N-terminus and an intracellular C-terminus, respectively. The rhodopsin-like family, also referred to as class A of GPCRs, is by far the largest and best studied subgroup containing receptors for odorants, small molecules such as biogenic amines, peptides and glycoprotein hormones (~700 GPCRs). The binding sites of small endogenous ligands are located within the seven transmembrane (TM) domains, whereas binding of more space filling ligands, for example peptides and glycoproteins, occurs at the amino terminus (N-terminus), extracellular loops and amino acids located at the top of the TM helices.[8]

1.1.2 G-Protein activation, ligand classification and signal transduction

Several models have been proposed for the molecular mechanism involved in the activation of GPCRs upon interaction with appropriate ligands. Among them, the cubic ternary model[9-11] is considered most suitable for explaining the pharmacodynamic activities of the majority of interacting ligands (cf. Figure 1.1). This model distinguishes between an active (R*) and an inactive (R) receptor state. These two states are in equilibrium and are allowed to isomerize independently from agonist binding. This kind of a spontaneous activation of the receptor in the absence of agonists is referred to as constitutive activity.[12] Both receptor states are able to bind G-proteins, but only the active receptor – G-protein complex (R*G) induces GDP/GTP exchange, resulting in signal transduction.

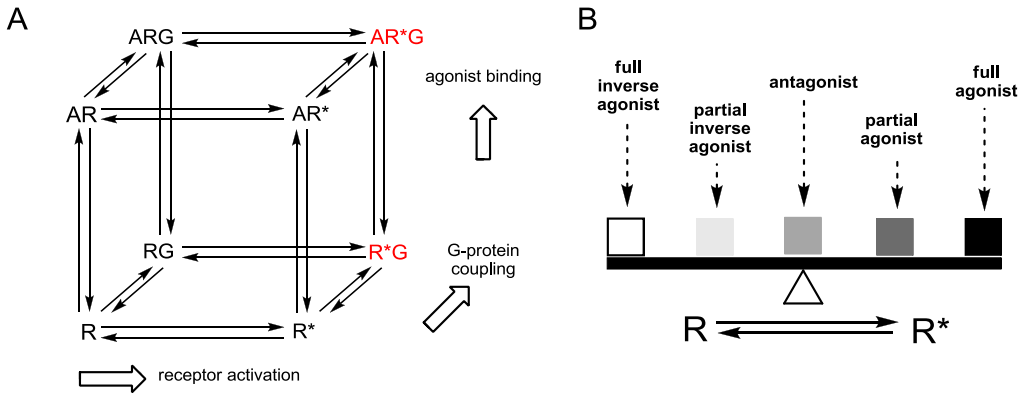

Figure 1.1 A. Two-state cubic ternary complex model of GPCR activation (R: inactive state of the receptor, R*: active state of the receptor, G: G-Protein, A: agonist). Signaling complexes mediating GDP/GTP exchange are highlighted in red. B. Ligand classification according to their capability of shifting the equilibrium to either side of both states. According to Seifert *et al.*[12]

Ligands are classified according to their capability of shifting the equilibrium to either side of both states. Full agonists preferentially bind to the R* state, stabilizing the active conformation and thereby enhancing the functional response. On the opposite, inverse agonists particularly interact with and stabilize the inactive conformation R of the receptor and reduce the percentage of spontaneously active receptors. Neutral antagonists bind to both conformations with the same affinity without altering the equilibrium, but impairing the binding of other ligands. Partial agonists and partial inverse agonists are less effective in stabilizing the active or the inactive receptor conformation, respectively.[13] However, the two-state model of GPCR activation cannot sufficiently explain all observed experimental findings. The function of GPCRs is considered much more complex in terms of ligand binding (orthosteric, allosteric), different conformational states, accessory protein interaction, phosphorylation, G-Protein coupling, oligomerization and internalization.[14-17] Furthermore, there is growing evidence of several inactive and active receptor conformations,[18] suggesting that structurally different ligands stabilize distinct receptor conformations, resulting in different biological responses.[19] In summary, the two-state model provides a molecular basis for classical concepts of pharmacology and helps to explain the properties of drugs acting as agonist, antagonist and inverse agonist, but the real situation is not completely reflected. After activation, the majority of GPCRs is able to transduce signals into cells through G-Protein coupling.[20] Agonist binding to extracellular or transmembrane domains of a GPCR (or agonist-free constitutive activity) promotes conformational changes that initiate coupling of intracellular receptor domains to a heterotrimeric G-Protein. This agonist-receptor-G-Protein complex, termed as ternary complex, triggers a G-Protein conformational change and results in the release of GDP from the Gα-subunit. Subsequently, the activated heterotrimeric G-Protein dissociates into Gα-GTP and Gβγ subunits, both of which then interact with effector proteins like enzymes or ion channels resulting in cellular biological responses.[21] The intrinsic GTPase activity of the GTP-bound Gα subunit terminates the signal by the

hydrolysis of GTP to GDP, i. e. the cycle is completed by reversion of the G-Protein to the inactive heterotrimeric state (see Figure 1.2). Subsequently, the GDP-bound Gα-subunit re-associates with Gβγ enabling the next G-Protein cycle.[22] According to the structure and signaling pathway of the Gα-subunits, G-Proteins are divided into four main families, termed G_s, $G_{i/o}$, $G_{q/11}$ and $G_{12/13}$.[23] The $G\alpha_s$ family activates adenylyl cyclases (AC 1–9), resulting in increased cellular levels of the second messenger cAMP (3´-5´-cyclic adenosine monophosphate). By contrast, the $G\alpha_i$ family shows inverse effects, inhibiting the AC activity (AC 5 and AC 6). cAMP regulates various cellular effects such as activation of the protein kinase A (PKA) or the mitogen-activated protein kinase (MAPK) pathway, both modulating gene expression.[24] Members of the $G\alpha_{q/11}$ family activate the phospholipases Cβ1-3 (PLCβ), which catalyze the hydrolysis of phosphatidylinositol 4,5-bisphosphate (PIP_2) to 1,2-diacylglycerol (DAG) and inositol-1,4,5- trisphosphate (IP_3). The latter second messenger controls calcium efflux from the endoplasmic reticulum. DAG and the released calcium control the activity of several protein kinase C (PKC) isoforms, which in turn activate a number of other proteins by phosphorylation.[25,26] Finally, the $G\alpha_{12}$ proteins interact with Ras homology GEFs (guanine-nucleotide exchange factor) (RhoGEFs) that regulate cytoskeletal assembly.[27] Not only the Gα-subunit, but also the Gβγ-heterodimers are involved in signal transduction and regulate certain effectors such as PLCβ and ion channels.[28]

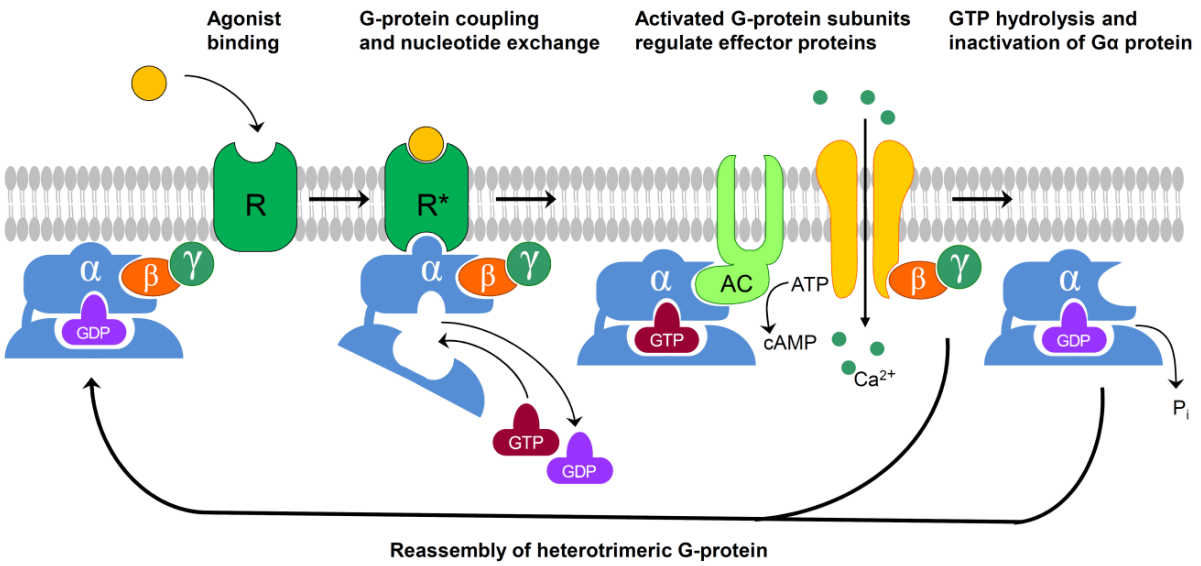

Figure 1.2 Activation of a heterotrimeric G-Protein by interaction with an agonist-occupied GPCR. The activated receptor is represented by R*, whereas the inactive form is termed R. The dissociated subunits regulate their respective effector proteins such as adenylyl cyclase (AC) and calcium channels. Further details are described in the text (modified from[29]).

1.1.3 G-Protein independent signaling, β-arrestin and functional selectivity

Although the vast majority of GPCRs is able to transduce signals into cells *via* G-Protein coupling, recent work has indicated that GPCRs participate in numerous other protein-protein interactions, which generate intracellular signals independent of G-Protein activation.[24] For instance, GPCR dimerization, the interaction with receptor activity-modifying proteins (RAMPs) and the binding of various scaffolding proteins to GPCRs modulate GPCR signaling.[20] Most compelling, the discovery that β-arrestins (arrestin 2 and 3) function as alternative transducers of GPCR signals, has challenged the basic concept of GPCR signaling.[20,30,31] Originally regarded as mediators of GPCR desensitization (through internalization into clathrin-coated pits),[32,33] β-arrestins are ubiquitously expressed cellular regulatory proteins that are meanwhile recognized as true adapter proteins that transduce signals to multiple effector pathways such as MAPKs (mitogen-activated protein kinase), SRC (v-src avian sarcoma (Schmidt-Ruppin A-2) viral oncogene homolog), nuclear factor κB (Nf-κB) and phosphatidylinositol 3-kinase (PIK3).[34] An updated model of signal transduction should comprise signaling by G-proteins and/or β-arrestins, as well as desensitization and internalization by β-arrestins.[34] The selective stimulation of some, but not all, possible signaling pathways has been postulated as 'functional selectivity',[35] also known as 'biased agonism'[36] or differential receptor-linked effector actions.[37,38] Apparently, depending on the ligand, the conformational changes of GPCRs are biased, giving rise to different behavior and interactions.[16] Such biased ligands are not only useful tools to investigate GPCR signaling, but might also harbor a potential as fine-tuned therapeutics.[39] Besides, allosteric ligands, which could modulate the signaling cascades and biochemical responses triggered by endogenous ligands, can also impose biased agonism, showing promise in clinical pharmacology.[40]

1.2 Histamine and the histamine receptor family

1.2.1 Histamine as endogenous ligand

The biogenic amine histamine (2-(1*H*-imidazol-4-yl)ethanamine) is a local mediator, immunomodulator and neurotransmitter targeting the histaminergic system. First biological effects of histamine like vasodilatation and smooth muscle contraction have been reported more than one hundred years ago.[41] Histamine contains two basic functionalities, a primary aliphatic amine and imidazole. At physiological pH, the amine group is protonated, and two different tautomers of this monocation are the predominating forms (Figure 1.3).[42]

In the body, histamine is synthesized from the amino acid L-histidine through decarboxylation.[43,44] Nowadays, histamine is considered , an ubiquitous and multifunctional biogenic amine which is involved in various physiological and pathophysiological processes. High tissue concentrations of histamine are found in particular in the lungs, the skin, connective tissues and the gastrointestinal tract.[44] It is stored in mast cells,[45] basophils,[46] platelets,[46] enterochromaffin-like cells (ECL) of the stomach,[47] endothelial cells,[48] and it is also found in neurons.[49] In the brain, histaminergic neurons are involved in the sleep-wake cycle, energy and endocrine homeostasis, synaptic plasticity and learning.[50] In mast cells and basophils, histamine is stored in secretory granules and released during allergic conditions, resulting in smooth muscle contraction, vasodilatation and an increase in vascular permeability.[51] After release, in response to immunological and non-immunological stimuli, histamine is degraded by two catabolic pathways. The first pathway involves methylation of histamine by histamine *N*-methyltransferase and the second pathway involves oxidative deamination by diamine oxidase.[52] The biological effects are mediated by the interaction with currently four histamine receptor (HR) subtypes, termed H_1R, H_2R, H_3R and H_4R, all belonging to the rhodopsin-like family A of GPCRs.[44,53-55]

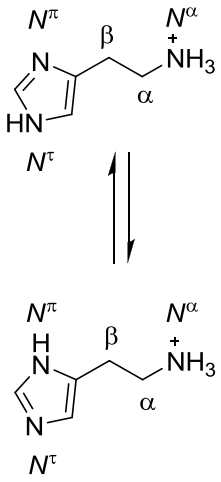

Figure 1.3 Tautomeric forms of the histamine monocation.

1.2.2 Histamine receptors and their ligands

In this chapter, various molecular pharmacological aspects of the four histamine receptor subtypes, including the availability of selective agonists and antagonists, will be discussed. In 1966 the term histamine H_1 receptor (H_1R) was introduced by *Ash* and *Schild*, who suggested the existence of a second HR subtype (non-H_1 receptor, H_2R) as not all effects provoked by histamine could be antagonized by classical antihistamines.[56] Activation of the H_1R has long been known to be associated with allergic conditions.[44,57] As a consequence, antagonists of this receptor subtype (popularly referred to as antihistamines) have been used as anti-allergic drugs since the 1940s.[44] The H_2R plays a pivotal role in gastric acid secretion,[58] and H_2R antagonists have been used as antiulcer drugs ('H_2R blockers').[57] The histamine H_3R is located predominantly in the central nervous system (CNS) and acts both as a presynaptic autoreceptor,[59] modulating histamine release from histaminergic neurons, and as an inhibitory heteroreceptor.[60,61] H_3R antagonists are being investigated as potential drugs for therapeutic applications against a variety of CNS disorders such as Alzheimer's disease, attention-deficit/hyperactivity disorder (ADHD), epilepsy, migraine, narcolepsy, obesity, schizophrenia and depression.[62] In the years 2000 and 2001, the H_4R was identified and cloned independently by

several research groups.[63-69] It is considered as a new therapeutic target for the modulation of various inflammatory and immunological processes and disorders.[70-73]

1.2.2.1 The histamine H_1 receptor

The histamine H_1 receptor (H_1R) was first cloned in 1993.[74] The corresponding receptor protein consists of 487 amino acids.[74] It is mainly expressed on smooth muscle cells, endothelial cells and in the CNS and is involved in the pathophysiology of allergy and inflammatory reactions.[75] *Via* the H_1R, histamine induces, for instance, vasodilatation, bronchoconstriction, increased vascular permeability, pain and itching upon insect stings.[76] Upon agonist stimulation, the H_1R predominantly couples to the pertussis-toxin insensitive $G\alpha_{q/11}$ proteins. Its stimulation triggers the inositol phospholipid signaling system, resulting in the formation of IP_3 and DAG (cf Chapter 1.1.2), which results in Ca^{2+}-mobilization from intracellular stores and activation of protein kinase C.[75,77] H_1R antagonists (antihistamines) have been used for decades for the treatment of allergic disorders (e.g. allergic rhinitis, chronic urticarial and atopic dermatitis), nausea and vomiting, and for sedation.[78,79] First generation antihistamines, such as mepyramine or diphenhydramine, are highly lipophilic compounds which cross the blood brain barrier, block central H_1 receptors and cause sedation.[44] More polar H_1R antagonists such as cetirizine and fexofenadine were developed to reduce this undesired effect in the treatment of allergic diseases ('non-sedative' second generation of H_1R blockers).[57,80] Mepyramine is still the most commonly used reference H_1R antagonist and radioligand ([^{3}H]mepyramine) for pharmacological studies.[81] Besides, H_1R agonists such as 2-methylhistamine and supra(histaprodifen), have been used as pharmacological tools to study H_1R functions in cellular systems.[82] So far, betahistine is the only marketed H_1R agonist; the drug is therapeutically used in the treatment of Menière`s disease (cf. Figure 1.4).[83,84]

1.2.2.2 The histamine H_2 receptor

The histamine H_2R was pharmacologically characterized by Black *et al.* in 1972,[58] using the first H_2R antagonist burimamide, which was able to block the histamine-mediated gastric acid secretion and the positive chronotropic effect on the heart. In 1991, Gantz and coworkers were able to clone the canine and human H_2Rs.[85,86] The human H_2R consists of 359 amino acids and is expressed in a variety of tissues including brain, uterus, airways, gastric parietal cells and the heart.[57,87] The H_2R primarily couples to the $G\alpha_s$ family of G-Proteins, leading to an increase in intracellular cAMP levels and the activation of PKA (cf. Section 1.1.2).[85,88,89] Depending on the used cell system, the H_2R may additionally trigger calcium signaling by coupling to the $G\alpha_{q/11}$ G-Protein.[90-92]

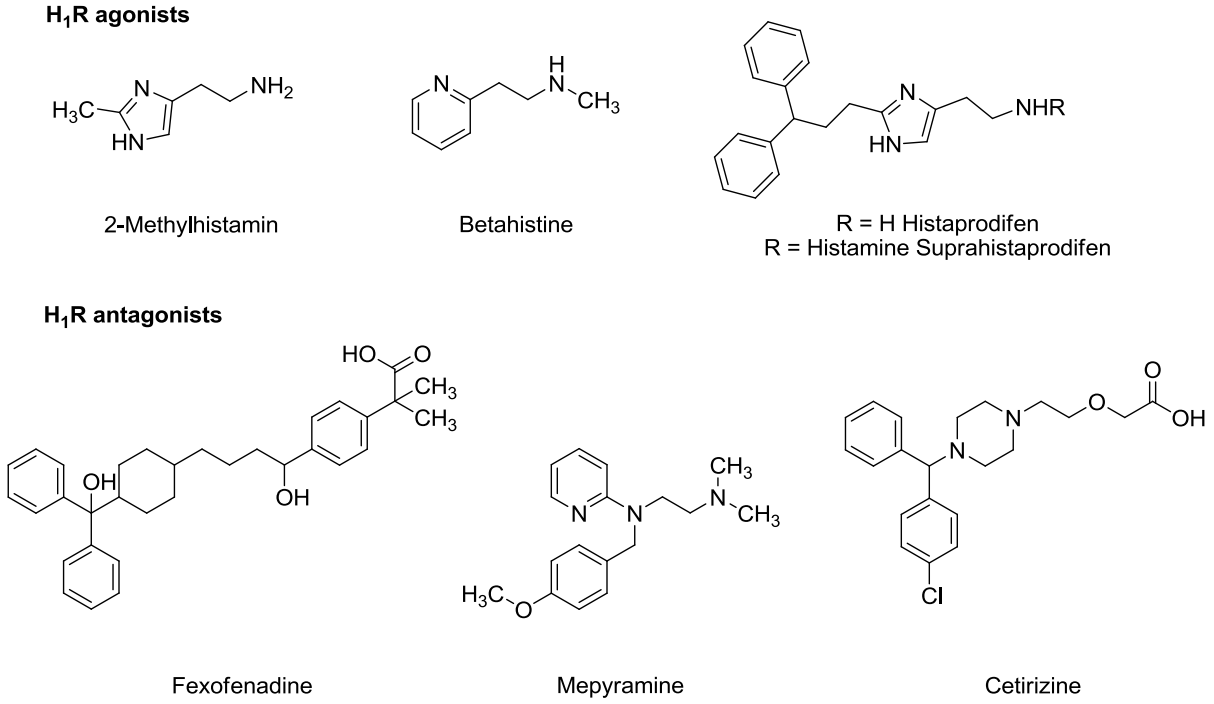

Figure 1.4 Structures of selected H_1R agonists and antagonists.

An essential physiological function of the H_2R is the control of gastric acid secretion from parietal cells.[58] Activation of cardiac H_2Rs mediates positive chronotropic and inotropic effects,[93] and histamine-mediated smooth muscle relaxation has been documented in airways, uterus and blood vessels.[94] The first marketed H_2R antagonist cimetidine revolutionized the treatment of peptic ulcer and gastro-oesophageal reflux disease.[44] Following cimetidine, several other H_2R antagonists ranitidine, famotidine, nizatidine and roxatidine have been successfully used in the treatment of gastric and duodenal symptoms (ulcers),[95] but are nowadays mostly replaced by more effective proton pump inhibitors, such as omeprazole, and by eradication of *Helicobacter pylori*.[44,96-98] Apart from marketed drugs, numerous structurally related compounds,[87] e.g. iodoaminopotentidine,[99] BMY25368,[100] and tiotidine,[101] are known as H_2R antagonists (structures are given in Figure 1.6). For radioligand binding studies [^{3}H]tiotidine[102] and [^{125}I]iodaminopotentidine[103-105] were used. More information about available radioligands and the characterization of a new H_2R radioligand is given in Chapter 5. Recently, a series of H_2R antagonists was developed in our working group, replacing the cyanoguanidine group of potentidine-related piperidinomethylphenoxyalkylamines by squaramides. Additional coupling with ω-aminoalkyl spacers allows for labeling reactions or bivalent ligand construction.[106] Whereas H_2R antagonists became standard drugs for the treatment of gastric and duodenal ulcers,[107,108] H_2R agonists have been mainly used as pharmacological tools to study the physiological and pathophysiological role of this histamine receptor. A first step towards a selective H_2R agonist was the discovery of dimaprit and amthamine, which were found to be almost as active as histamine at the H_2R, but hardly display any H_1R agonism.[109,110] Highly potent and selective

guanidine-type H_2R agonists like impromidine[111,112] and arpromidine[113] had been developed,[114] which, however, showed poor oral bioavailability.[87] Drug-like properties were improved according to a bioisosteric approach, by an exchange of the guanidine by an acylguanidine moiety, resulting in N^G-acylated imidazolylpropylguanidines (e.g. UR-AK24, Figure 4.1, Chapter 4).[115] Further improvement, concerning selectivity was achieved by the introduction of a 2-amino-4-methylthiazol-5-yl moiety as a bioisostere of the imidazole ring.[116] Thus, N^G-acylated aminothiazolylpropylguanidines (e.g. UR-BIT24) combine the high selectivity for the H_2R with improved pharmacokinetic properties, resulting in valuable pharmacological tools to evaluate the physiological role of H_2Rs. Recently, the application of the bivalent ligand approach to acylguanidines yielded agonists, which are highly selective and up to 4000 times more potent than histamine at the guinea pig right atrium.[117] Furthermore, another indication for the clinical use of histamine as H_2R agonist evolved, based on the finding that histamine ameliorates the course of acute myeloid leukemia.[118-120]

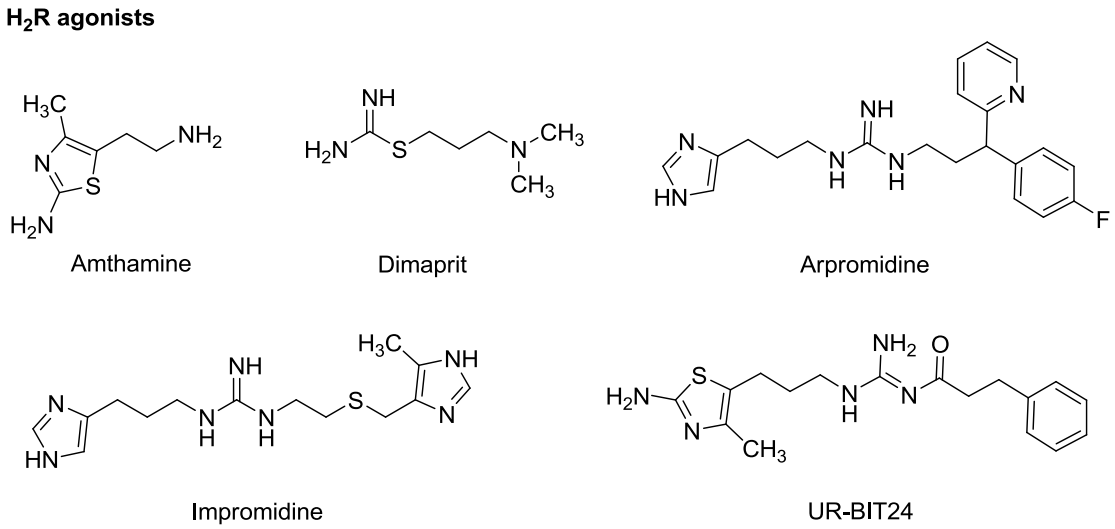

Figure 1.5 Structures of selected H_2R agonists.

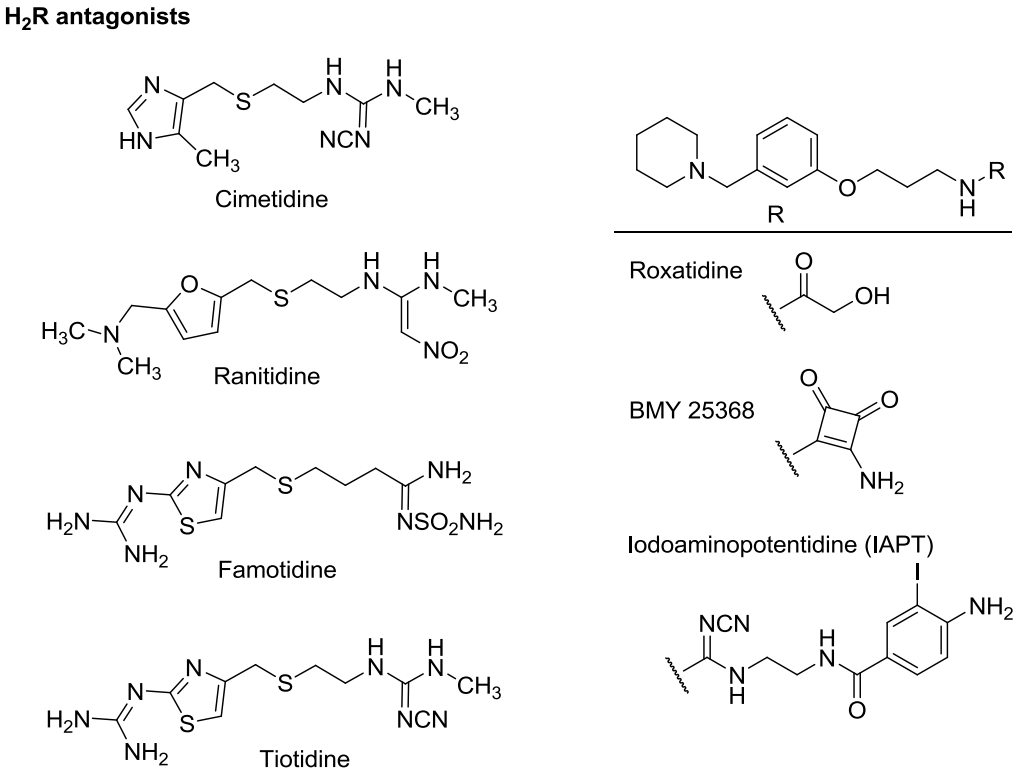

Figure 1.6 Structures of selected H_2R antagonists.

1.2.2.3 The histamine H_3 receptor

The histamine H_3R was discovered by Arrang *et al.* in 1983[59] and cloned in 1999.[121] The hH_3R consists of 445 amino acids[122] and is mainly expressed in the CNS, where it acts as a presynaptic auto- and heteroreceptor, controlling the release of histamine and various other neurotransmitters, including dopamine,[123] serotonin,[124] noradrenalin[46] and acetylcholine.[125] The H_3R is suggested to be involved in various CNS functions, for instance, the regulation of locomotor activity, wakefulness and food intake, thermoregulation and memory.[126] In the periphery, H_3R activation was shown to occur in the cardiovascular system, the gastrointestinal tract and the airways.[127-130] The activation of H_3Rs leads to a decrease in intracellular cAMP levels *via* coupling to $G_{i/o}$ proteins and inhibition of the adenylyl cyclase. Besides, activation of phospholipase A_2 (PLA_2), MAPKs and phosphatidyl inositol 3-kinase, inhibition of the Na^+/H^+ exchanger and modulation of intracellular calcium was demonstrated.[131,132] Antagonists for the H_3R are promising agents[131,133,134] in several therapeutic areas including dementia, Alzheimer`s disease, narcolepsy, deficit hyperactivity disorder, schizophrenia as well as for the treatment of myocardial ischemic arrhythmias, migraine and inflammatory and gastric acid-related diseases.[62,122,135-140]

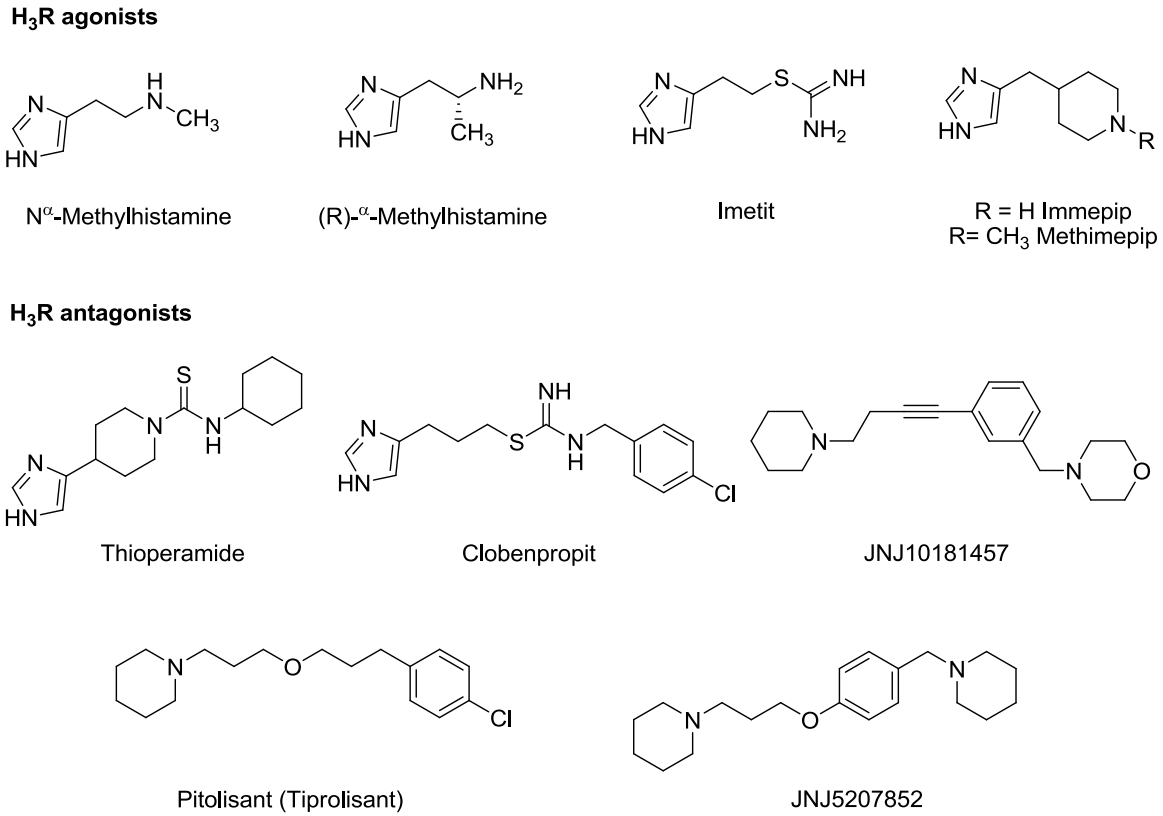

Figure 1.7 Structures of selected H_3R agonists and antagonists.

The first potent H_3R antagonists, thioperamide[141] and clobenpropit[142] were derived from the structure of histamine and have an imidazole ring in common. To improve the drug-like properties and to prevent potential drug-drug interactions, several pharmaceutical companies developed non-imidazole H_3R antagonists, for instance JNJ10181457 and JNJ5207852.[133,143] Recently, the H_3R antagonist pitolisant (tiprolisant) has been introduced as an orphan drug for the treatment of narcolepsy.[144,145] Typical H_3R agonists are N^{α}-methylhistamine and (*R*)-α-methylhistamine[141] as well as imetit[146] and the H_3R selective ligands immepip and methimepip,[137] which are structurally less related to histamine (structures are shown in Figure 1.7). Almost exclusively, the application of the H_3R agonists [^{3}H]histamine, [^{3}H]N^{α}-methylhistamine and [^{3}H](*R*)-α-methylhistamine, as well as of the inverse agonist [^{125}I]iodophenpropit or of the antagonist [^{3}H]thioperamide have been described in radioligand binding experiments.[107,147,148]

1.2.2.4 The histamine H_4 receptor

In 1975, Clark and co-workers reported on histamine induced chemotaxis of human eosinophils that was not inhibited by H_1 or H_2 receptor antagonists.[149] Two decades later, Raible and colleagues suggested a novel HR subtype on human eosinophils. The authors observed that the histamine triggered calcium mobilization in human eosinophils could be blocked by the H_3R antagonist

thioperamide. However, the potent H_3R agonist (*R*)-α-methylhistamine was less potent than histamine in inducing calcium mobilization; this was not compatible with a H_3R mediated effect.[150,151] Finally, the human H_4R was identified and cloned – at that time as an orphan receptor – in 2000 and 2001, independently by several research groups.[63-69] Cloning of the H_3R gene provided the basis for a fourth histamine receptor subtype due to their high sequence homology (about 40% overall sequence identity and about 58% sequence identity within the transmembrane domains).[121] The human receptor subtype consists of 390 amino acids and, as in case of the H_3R, couples to $G_{i/o}$-proteins, resulting in adenylyl cyclase inhibition,[64,152] activation of MAPKs[67] and calcium mobilization.[153] Besides the coupling to G-Proteins, the activation of β-arrestin by several H_4R ligands was recently reported.[154-156] The H_4R was suggested to be expressed in bone marrow and immunocytes such as mast cells, basophils, eosinophils, monocytes, T-lymphocytes and dendritic cells.[157,158] Furthermore, detection of the H_4R was purported on nerves from the nasal mucosa, in the enteric and, together with the other histamine receptor subtypes, in the central nervous system.[152] Based on studies with H_4R knockout mice, it has been suggested that the H_4R plays a proinflammatory role in bronchial asthma, atopic dermatitis, allergic rhinitis, and pruritus.[44,53,152,159] If so, H_4R antagonists could be useful drugs for the treatment of these conditions.[51,53,152,160] The H_4R was also suggested as a new therapeutic target for the treatment of colitis, pain, cancer, rheumatoid arthritis and multiple sclerosis.[70-72,161,162] The supposed role of the H_4R in immunological responses overlaps with the function of the H_1R, suggesting that combined H_1- and H_4-receptor ligands might be beneficial for the treatment of inflammatory diseases.[51,163-166] In search for novel H_4R antagonists or inverse agonists, the imidazole-containing H_3R inverse agonist thioperamide has been identified as H_4R inverse agonist with similar potency and has been frequently used as a reference compound (structure is given in Figure 1.7).[167] A high-throughput screening campaign led to the identification of the indole carboxamide JNJ7777120 as a selective H_4R antagonist.[168] JNJ7777120 has been widely used as the prototypical H_4R antagonist in animal models to assess the (patho)physiological role of the H_4R.[51]. However, *in vivo* results of JNJ7777120 must be interpreted with caution in view of partial agonistic activity at murine H_4R orthologs *in vitro,*[169] β-arrestin recruitment to the hH_4R[154-156] and off-target effects at higher concentrations.[170] For a more detailed view at JNJ7777120 cf. Chapter 6. Meanwhile, other highly selective and potent H_4R antagonists, e.g. with quinazoline[171] and pyrimidine[160,172] scaffold, have been developed (cf. Figure 1.8; an overview is given by Schreeb *et al.*[173]). Some H_4R ligands had entered clinical studies, e.g. UR-63325, the first H_4R antagonist from which clinical data were reported,[174,175] ZPL-38937887 (formerly PF-03893787)[172] and JNJ39758979.[160] To further investigate the pathophysiological role of the H_4R, selective agonists are of particular interest as pharmacological tools.

H_4R agonists

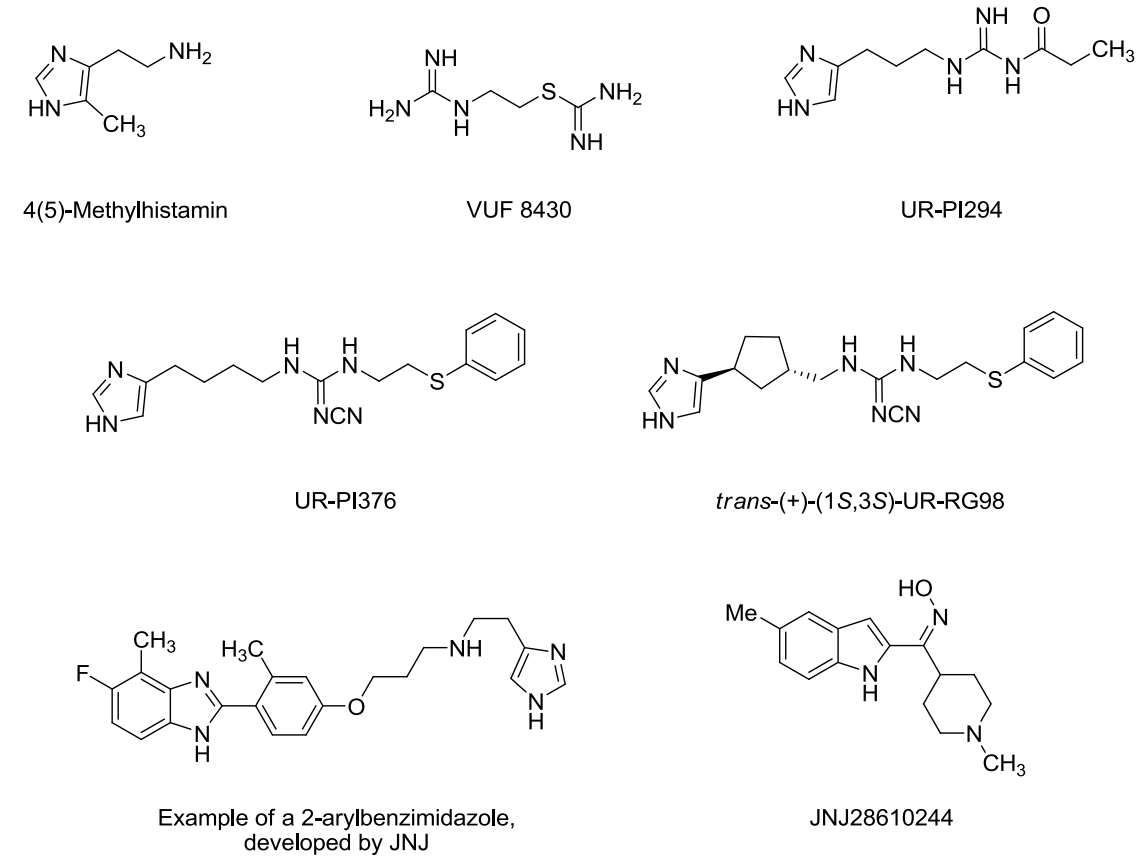

H_4R antagonists

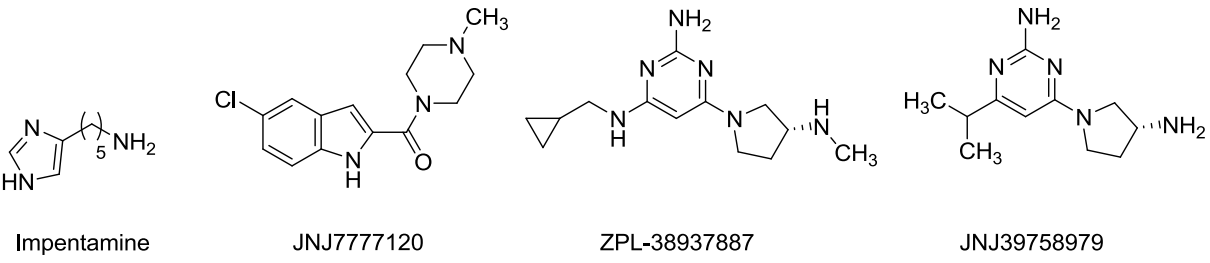

Figure 1.8 Structures of selected H_4R agonists and antagonists.

Due to the high sequence homology of the H_4R with the H_3R, especially in the transmembrane domains, it is not surprising that the H_4R is activated by numerous compounds which were originally designed as H_3R agonists, and, consequently, contain an imidazole ring, for instance (*R*)-α-methylhistamine, N^{α}-methylhistamine and imetit (Figure 1.7).[167,176] Histamine and its homologs homohistamine (spacer length of three methylene groups) and imbutamine (four methylene groups) are agonists with similar hH_3R and hH_4R affinity, whereas the higher homolog impentamine (five methylene groups) is an almost full hH_3R agonist but shows no agonistic activity at the hH_4R.[167,177,178] The hH_3R inverse agonist clobenpropit[142] turned out to be a potent partial agonist at the hH_4R and one of the few compounds that activate the hH_4R, but not the hH_3R, rendering clobenpropit an

interesting pharmacological tool (structure is shown in Figure 1.7).[167] The first ligands with improved selective H_4R activation were the cyanoguanidine OUP-16, a chiral tetrahydrofurane related to imifuramine,[179] and 5-methylhistamine (also referred to as 4-methylhistamine),[167] which was initially reported as a selective H_2R agonist.[58] The dimaprit analog VUF 8430[180] turned out to be an H_4R agonist with about 100- and 30-fold selectivity over the other H_2R and the H_3R, respectively (cf. Chapter 4).[180] Similarly, N^G-acylated imidazolylpropylguanidine-type H_2R agonists such as UR-AK24 were shown to be more potent at the hH_3R and hH_4R. Truncation of the N^G-acyl groups resulted in potent, nearly full, H_4R agonists such as UR-PI294, which possesses improved selectivity over the hH_1R and hH_2R, but shows residual activity at the hH_3R (cf. Chapter 4).[181] Aiming at improved selectivity for the H_4R, the acylguanidine moiety was replaced by a non-basic cyanoguanidine group. Further structural optimization led to highly potent and selective cyanoguanidine-type H_4R agonists such as UR-PI376 and *trans*-(+)-(1*S*,3*S*)-UR-RG98.[182,183] Another recently reported structural class of ligands comprising selective H_4R agonists are 2-arylbenzimidazoles (Lee-Dutra *et al.*, 2006), previously developed as H_4R antagonists by Johnson & Johnson.[184] One of these compounds, which is characterized by a histamine substructure, has sub-nanomolar hH_4R affinity and is among the most potent hH_4R agonists described so far.[185] For a more detailed view at this class of compounds cf. Chapter 3. Very recently, *Z*-configured oxime analogs of the selective H_4R antagonists JNJ7777120[186] and JNJ10191584 (VUF 6002)[187] were reported as a new class of H_4R agonists.[188] All of them are selective for the hH_4R and show only low (if any) affinities for the other histamine receptor subtypes. The oxime-type compounds are of particular value as pharmacological tools for the study of the H_4R in rodents. In contrast to these oxime-type ligands, numerous other H_4R agonists (and antagonists) show pronounced species-dependent discrepancies regarding potencies, receptor selectivities and even opposite qualities of action.[54,90,169,176,189] Thus, the predictive value of translational animals may be severely compromised due to ortholog dependent discrepancies. Except for the monkey H_4R, which shows an overall amino acid homology with the human H_4R of 93%,[189] homologies range from 65 to 71%. Accordingly, the sequence differences between human, rat, and mouse H_4R have been reported to cause significant differences in affinity for the endogenous agonist histamine.[190] Hence, future prospects of H_4R agonists (and antagonists) as molecular tools to study the H_4R *in vivo* will strongly depend on balanced activities on the receptor orthologs of humans and laboratory animals. A general overview of published radioligands for the H_4R is given in Chapter 6.

1.3 NPY and the NPY receptor family

1.3.1 Neuropeptide Y

The 36 amino acid peptides pancreatic polypeptide (PP), neuropeptide Y (NPY, cf. Figure 1.9) and peptide YY (PYY) are structurally related peptides, which bind to G-Protein coupled receptors of the NPY receptor family. NPY, one of the most abundant neuropeptides in the central and peripheral nervous system,[192] was first isolated by Tatemoto and coworkers from porcine brain in 1982,[193] and was proven to be highly conserved in various species. For all these peptides, C-terminal amidation is essential for biological activity.[194] NPY receptors are widely distributed in the central and peripheral nervous system. They are involved in the regulation of numerous physiological processes such as blood pressure, food intake, pain sensitivity, anxiety/anxiolysis, depression, obesity and hormone release.[195,196]

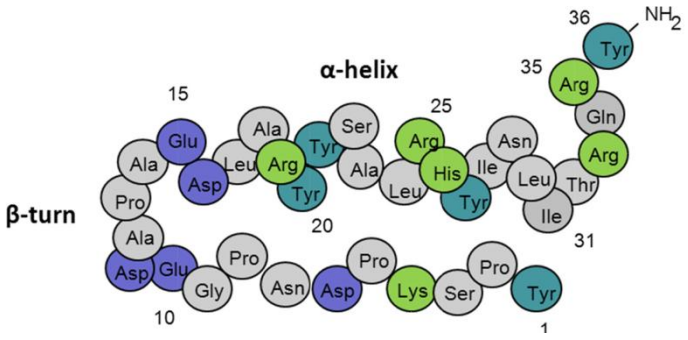

Figure 1.9 Tertiary structure of porcine NPY according to Allen *et al.*[191] basic residues (green); acid residues (blue); tyrosine residues (cyan).

1.3.2 NPY receptors and their ligands

The diverse biological effects of NPY are mediated by the activation of different receptor subtypes which are all members of the GPCR superfamily. To date, five mammalian NPY receptor subtypes, termed Y_1, Y_2, Y_4, Y_5 and y_6 receptor, have been cloned.[197-204] The y_6 receptor was found to be functional in mice, but non-functional in most mammalian species.[205] All NPY receptor subtypes were shown to activate pertussis toxin sensitive $G_{i/o}$ proteins, mediating the inhibition of forskolin-stimulated cAMP accumulation.[206,207]

1.3.2.1 The NPY Y_2 receptor and its ligands

In 1986, the Y_2 receptor was identified by pharmacological studies with *N*-terminally truncated analogs of NPY and PYY using vascular preparations (e.g. NPY(3-36) and NPY(13-36)).[194] The cloned hY_2R consists of 381 amino acids and has only ~30% identity to the Y_1R and the Y_4R, respectively. This receptor subtype turned out to be highly conserved across species with a sequence homology of 90-96%.[204,208-210] The argininamide BIIE 0246,[211] the first reported potent and selective Y_2R antagonist, proved to be a valuable tool for the study of Y_2R. Meanwhile, there is growing interest in the Y_2R as a therapeutic target, not least stimulated by recently published brainpenetrant, orally available Y_2R

antagonists such as JNJ31020028,[212] JNJ5207787[213] and SF-11[214], as well as structural analogs of the latter, such as CYM 9552 or CYM 9484,[215] and imidazolidine-2,4-diones, such as NVP-833[216] (for a recent review cf. Mittapalli *et al.,*[217] structures are presented in Figure 1.10). Aiming at potent and subtype-selective tracers for the Y_2R, a series of derivatives of argininamide-type Y_2R antagonist BIIE 0246 was synthesized in our working group.[218,223]

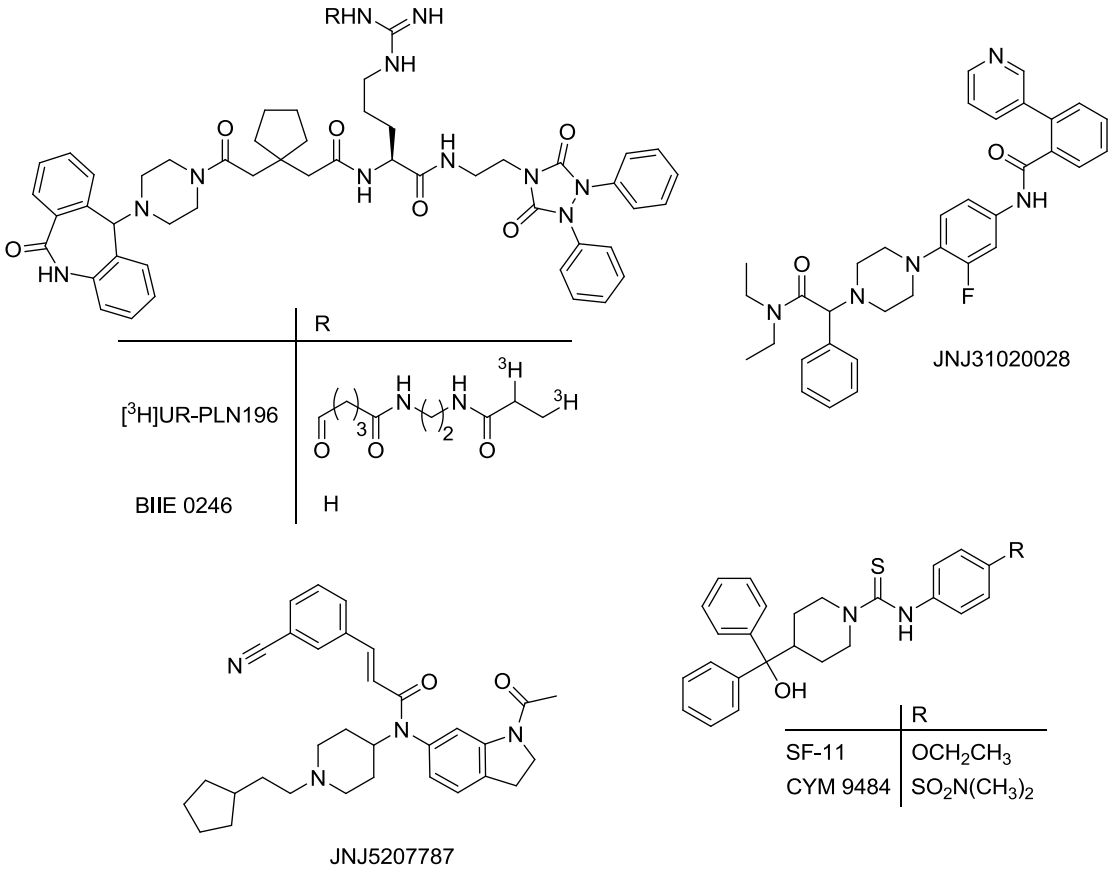

Figure 1.10 Structures of selected Y_2R antagonists.

Most of the resulting N^G-substituted (*S*)-argininamides related to BIIE0246 showed Y_2R antagonistic activities and binding affinities similar to those of the parent compound, corroborating the hypothesis that the guanidine–acylguanidine exchange is a promising and broadly applicable bioisosteric approach.[218] Radioligands used for the study of Y_2R are, for instance, [^{3}H]NPY,[219,220] [^{125}I]PYY,[221] and [^{125}I]PYY(3–36),[222,223] which are devoid of subtype selectivity. Attachment of a [2,3-$^3H_2$]propionyl group through an appropriate linker to the guanidine group of above mentioned (*S*)-argininamide-type NPY Y_2R antagonist resulted in the first selective nonpeptide radioligand for the Y_2R ([^{3}H]UR-PLN196).[224]

1.3.2.2 Ligands for the NPY Y_1, Y_4 and Y_5 receptors

In the last two decades, a multitude of highly potent and selective non-peptidic Y_1R antagonists with affinities in the nanomolar and subnanomolar range have been developed, including BIBP 3226[225] and J-104870 (Figure 1.11).[226] For a review see Brennauer *et al.*[227] The investigation of a series of N^G-substituted BIBP 3226 derivatives revealed that especially electron-withdrawing substituents such as acyl, alkoxycarbonyl and carbamoyl are tolerated. Therefore, a bioisosterism of guanidines and acylguanidines was suggested for this class of compounds.[228-230] High-affinity radioligands for the characterization of the Y_1R are, apart from [^{125}I]NPY and [^{3}H]BIBP 3226, two N^G-acylated argininamides from our laboratory, [^{3}H]UR-MK114[231] and [^{3}H]UR-MK136.[232] Both compounds are highly potent and selective radiotracers for the Y_1R.

The peptide VD-11, an analog of the C-terminus of NPY, was reported to act as a competitive antagonist at the Y_4R.[233] However, high-affinity non-peptide Y_4R ligands are not known so far. Acylguanidines such as UR-AK49 (Figure 1.11), which were designed as histamine H_2 receptor ligands, proved to be weak Y_4R antagonists.[234,235] These compounds may serve as lead structures towards potent small molecule antagonists for the Y_4R. Recently, UR-MK188, a dimeric argininamide-type neuropeptide Y receptor antagonist was reported to be the most potent Y_4R antagonist known so far.[236] Up to date, nonpeptidic selective radioligands for the Y_4R are not described in literature.

In case of the Y_5R, the situation is comparable to the Y_1R. The search for new drugs for the treatment of obesity led to numerous highly potent and selective non-peptidic antagonists with broad structural diversity. Some of these compounds have entered clinical trials. Along these lines, MK-0557 (Merck & Co., Inc.) was tested in phase II trials, but was withdrawn due to lack of significant effect on body weight.[237] A selection of Y_5R antagonists with K_i values in the low nanomolar range is given in Figure 1.11 (for a review see Brennauer *et al.*[227]). Recently, a Y_5R selective radioligand was reported as an insurmountable pseudo-irreversible non-peptide antagonist.[238]

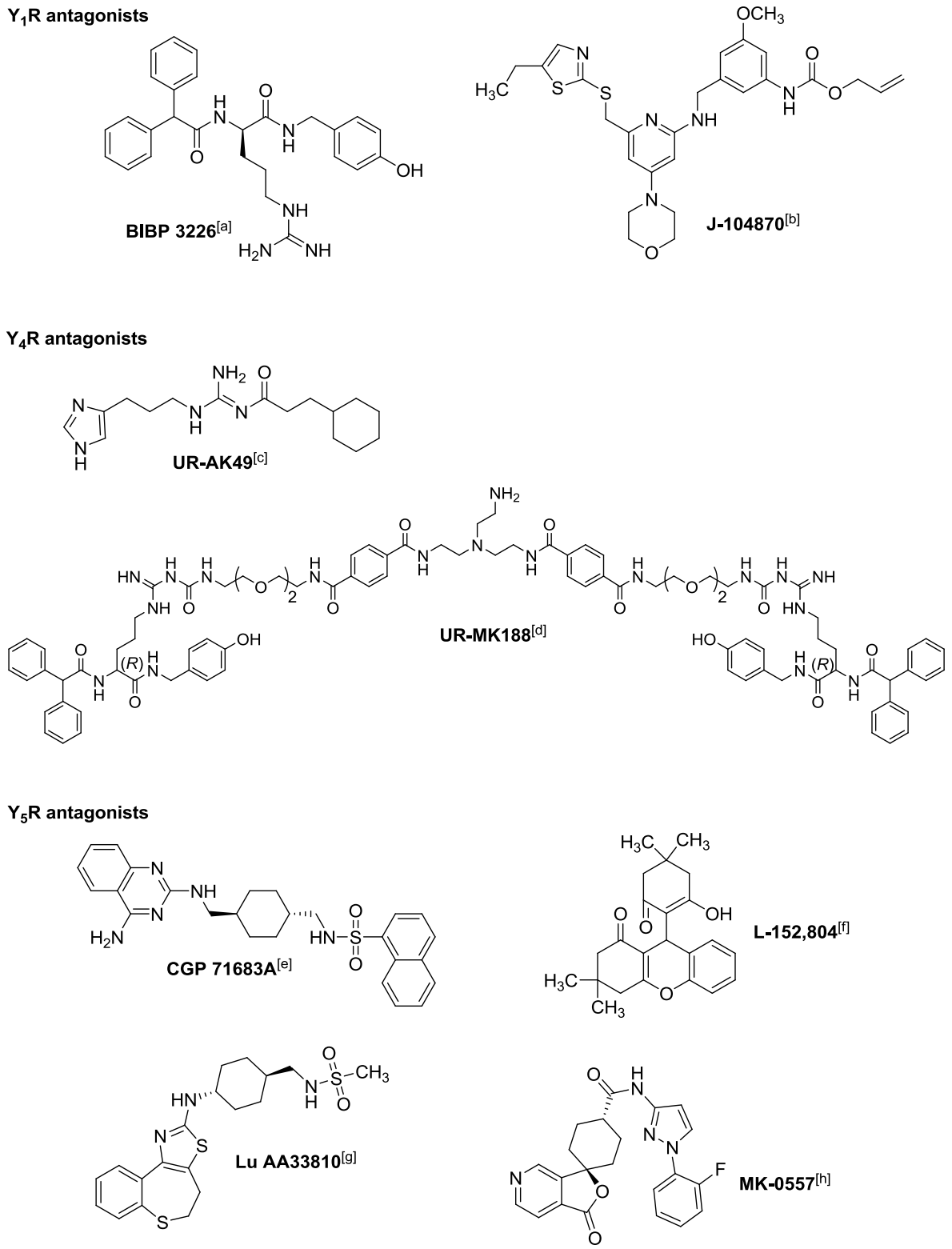

Figure 1.11 Examples of nonpeptidic selective Y_1R, Y_4R and Y_5R antagonists. [a] Rudolf *et al.*;[225] [b] Kanatani *et al.*;[239] [c] Ziemek *et al.*;[235] [d] Keller *et al.*;[236] [e] Criscione *et al.*;[240] [f] Kanatani *et al.*;[241] [g] Walker *et al.*;[242] [h] Erondu *et al.*[243]

1.4 Receptor–ligand binding assays

Receptor screening methodologies make use of either the determination of a functional response (e.g. cell proliferation or changes in the concentration of second messengers such as Ca^{2+} or the interaction of a ligand with its receptor.[244] Binding of a ligand to its receptor is the initial and indispensable step in the cascade of reactions that finally cause a pharmacological effect.[245]

Various assay technologies measuring receptor–ligand interactions are available and can be used in multiple ways. Firstly, they can be applied as a tool for basic research on the receptor itself by determining receptor distribution and identifying receptor subtypes. Secondly, screening of new chemical entities and the discovery of endogenous ligands is facilitated by receptor–ligand binding assays, despite the fact that receptor–ligand binding assays do not predict pharmacological activity (agonism or antagonism) of compounds.[246] Finally, binding assays can be used to quantify an analyte that is present in a biological matrix with high sensitivity and reproducibility by comparing the displaced amount of labeled ligand with standard curves constructed with known concentrations of the analyte.[244]

Assays requiring a labeled ligand or receptor are divided in radioactive and non-radioactive assay technologies. While radioreceptor assays are fast, sensitive, easy to use and reproducible, their major disadvantages are that they are potentially hazardous to human health, produce radioactive waste, require special laboratory conditions and licenses, and there is a need for separation of bound from free ligand.[247] This has led to the development of non-radioactive assays based on technologies using either colorimetry, fluorescence or (chemo-/bio-) luminescence.[244] Such optical methods comprise fluorescence polarization (FP),[248] fluorescence/bioluminescence resonance energy transfer (FRET/BRET),[249] flow cytometry[250] or total internal reflection fluorescence (TIRF).[251] Furthermore, surface plasmon resonance (SPR),[252] affinity selection mass spectrometry (AS-MS)[253] and nuclear magnetic resonance spectroscopy (NMR)[254] allow for label-free assays. In summary, a shift from radioactive to fluorescence-based or label-free detection of receptor–ligand interactions has been observed over the past years.

However, most of the new approaches are not well established and validated. Therefore radioligand binding is still an indispensable procedure in drug research, especially in the screening of compound libraries. The major advantage of radioligand binding is the robustness of the readout.[244] In the following, radiochemistry-based techniques commonly applied for the investigation of ligand-receptor interactions with focus on radioligand binding experiment will be presented.[255]

1.4.1 Radioligand Binding Methods

A number of different receptor sources can be employed, such as whole animals, slices of tissue, whole cells, membrane fractions, cytosolic extracts, and purified solubilized receptor proteins.[247] There are three basic types of radioligand binding experiments: Firstly, saturation experiments by which the affinity of the radioligand for the receptor of interest and the number of specific binding sites can be determined;[256] secondly, kinetic experiments whereby the rate constants of association and dissociation of a radioligand are accessible.[257] Thirdly, radioligand binding assays are widely used to identify unlabeled compounds which specifically bind to certain receptors. An unlabeled compound that is able to bind to the receptor of interest will compete with the radiolabeled ligand. Thus, competition curves using increasing concentrations of the unlabeled ligand can be constructed and the affinity of the unlabeled ligand for the receptor can be calculated.[258]

1.4.1.1 Selection of radioligands

In choosing the appropriate radioligand for a radioreceptor assay, several criteria have to be met. Firstly, the radioligand should be selective and possess a high affinity for the respective receptor (the radioligand should bind selectively to the receptor type or subtypes of interest under assay conditions. Secondly, the radioligand should be radiochemically pure and have a high specific activity. Furthermore, the radioligand should be chemically stable and resistant to enzymatic degradation. Finally, in case of optically active ligands, the eutomer of the radioligand is preferred, to avoid interference and to prevent complicate analysis as a consequence of the presence of the less active enantiomer.[244,259] Further important issues to consider, include the choice of the radioisotope (preferably ^{3}H or ^{125}I, occasionally $^{32/33}P$ and ^{35}S), the extent of nonspecific binding, and whether the radioligand is an agonist or an antagonist. Tritium as a radioisotope, compared to 125-iodine, has a longer half-life (12.3 years vs. 60 days), which is of advantage with respect to performing both synthesis and pharmacological studies, and the compound is more convenient to handle with respect to safety precautions.[260] Because of their short half-lives, iodinated radioligands are usually purchased or prepared every 4-6 weeks, whereas tritiated ligands can often be used for several months or even years. An advantage of iodinated radioligands is their higher specific activity (up to 2200 vs. 30-100 Ci/mmol), which makes them particularly useful when the density of receptors is low or the amount of tissue is small. It is more convenient and less expensive to use iodinated ligands, since scintillation fluid is not needed, thus eliminating purchasing and disposal costs.[261] Agonist radioligands may label only a portion of the total receptor population (the high affinity state in case of GPCRs), whereas antagonist ligands label all receptors. On the other hand, a radiolabeled agonist may more accurately reflect receptor alterations of biological significance. Nonspecific binding is binding to sites other than the receptors of interest. This can include other receptors, non-receptor

binding sites in the tissue (e.g., the lipid bilayer), and also binding to filter material. Usually, the radioligand with the lowest nonspecific binding is best. An assay is considered barely adequate if 50% of the total binding is specific, 70% is good, and 90% is excellent.[257] Membrane preparations are most widely used and probably provide the most reproducible and reliable data. Nevertheless, radioligand binding techniques can be applied to other preparations, such as purified receptors, solubilized receptors, whole cells, and tissue slices. The choice of preparation depends on the question to be addressed.[247] Further aspects of interest are an appropriate choice of the assay conditions and an efficient technique for the separation of free and bound radioligands (cf.[247,261,262]). In conclusion, the basic principle of radioligand binding is quite simple, but careful application of these assays requires careful consideration of the above mentioned details. When properly conducted and appropriately interpreted, these assays can be an extremely powerful tool for the study of receptors.[261]

1.4.2 Radioligands for the histamine H_2, H_4 and NPY Y_2 receptor

Information about available radioligands for the histamine H_2, H_4 and NPY Y_2 receptor and the characterization of new radioligands is given in Chapter 5-7.

1.5 References

1. Fredriksson, R.; Lagerstrom, M. C.; Lundin, L.-G.; Schioth, H. B. The G-Protein-Coupled Receptors in the Human Genome Form Five Main Families. Phylogenetic Analysis, Paralogon Groups, and Fingerprints. *Mol. Pharmacol.* **2003**, 63, 1256-1272.
2. Liapakis, G.; Cordomi, A.; Pardo, L. The G-protein coupled receptor family: actors with many faces. *Curr. Pharm. Des.* **2012**, 18, 175-185.
3. Sharman, J. L.; Benson, H. E.; Pawson, A. J.; Lukito, V.; Mpamhanga, C. P.; Bombail, V.; Davenport, A. P.; Peters, J. A.; Spedding, M.; Harmar, A. J. IUPHAR-DB: updated database content and new features. *Nucleic Acids Res.* **2013**, 41, D1083-1088.
4. Alexander, S. P. H.; Benson, H. E.; Faccenda, E.; Pawson, A. J.; Sharman, J. L.; Spedding, M.; Peters, J. A.; Harmar, A. J.; Collaborators, C. The Concise Guide to PHARMACOLOGY 2013/14: G-Protein-Coupled Receptors. *Br. J. Pharmacol.* **2013**, 170, 1459-1581.
5. Overington, J. P.; Al-Lazikani, B.; Hopkins, A. L. How many drug targets are there? *Nat. Rev. Drug Discov.* **2006**, 5, 993-996.
6. Stevens, R. C.; Cherezov, V.; Katritch, V.; Abagyan, R.; Kuhn, P.; Rosen, H.; Wuthrich, K. The GPCR Network: a large-scale collaboration to determine human GPCR structure and function. *Nat. Rev. Drug Discov.* **2013**, 12, 25-34.
7. Lagerstrom, M. C.; Schioth, H. B. Structural diversity of G-Protein-coupled receptors and significance for drug discovery. *Nat. Rev. Drug Discov.* **2008**, 7, 339-357.
8. Kristiansen, K. Molecular mechanisms of ligand binding, signaling, and regulation within the superfamily of G-protein-coupled receptors: molecular modeling and mutagenesis approaches to receptor structure and function. *Pharmacol. Ther.* **2004**, 103, 21-80.
9. Weiss, J. M.; Morgan, P. H.; Lutz, M. W.; Kenakin, T. P. The Cubic Ternary Complex Receptor-Occupancy Model I. Model Description. *J. Theor. Biol.* **1996**, 178, 151-167.
10. Weiss, J. M.; Morgan, P. H.; Lutz, M. W.; Kenakin, T. P. The Cubic Ternary Complex Receptor-Occupancy Model II. Understanding Apparent Affinity. *J. Theor. Biol.* **1996**, 178, 169-182.
11. Weiss, J. M.; Morgan, P. H.; Lutz, M. W.; Kenakin, T. P. The cubic ternary complex receptor-occupancy model. III. resurrecting efficacy. *J. Theor. Biol.* **1996**, 181, 381-397.
12. Seifert, R.; Wenzel-Seifert, K. Constitutive activity of G-protein-coupled receptors: cause of disease and common property of wild-type receptors. *Naunyn. Schmiedebergs Arch. Pharmacol.* **2002**, 366, 381-416.
13. Kenakin, T. Drug efficacy at G-protein coupled receptors. *Annu. Rev. Pharmacol. Toxicol.* **2002**, 42, 349-379.
14. Vauquelin, G.; Van Liefde, I.; Birzbier, B. B.; Vanderheyden, P. M. L. New insights in insurmountable antagonism. *Fundam. Clin. Pharmacol.* **2002**, 16, 263-272.
15. Bridges, T. M.; Lindsley, C. W. G-protein-coupled receptors: from classical modes of modulation to allosteric mechanisms. *ACS Chem. Biol.* **2008**, 3, 530-541.
16. Kenakin, T. New concepts in drug discovery: collateral efficacy and permissive antagonism. *Nat. Rev. Drug Discov.* **2005**, 4, 919-927.
17. May, L. T.; Leach, K.; Sexton, P. M.; Christopoulos, A. Allosteric Modulation of G-Protein-Coupled Receptors. *Annu. Rev. Pharmacol. Toxicol.* **2007**, 47, 1-51.
18. Perez, D. M.; Karnik, S. S. Multiple Signaling States of G-Protein-Coupled Receptors. *Pharmacol. Rev.* **2005**, 57, 147-161.
19. Kenakin, T. Ligand-selective receptor conformations revisited: the promise and the problem. *Trends Pharmacol. Sci.* **2003**, 24, 346-354.
20. Luttrell, L. M. Reviews in molecular biology and biotechnology: transmembrane signaling by G-Protein-coupled receptors. *Mol. Biotechnol.* **2008**, 39, 239-264.
21. Johnston, C. A.; Siderovski, D. P. Receptor-mediated activation of heterotrimeric G-proteins: current structural insights. *Mol. Pharmacol.* **2007**, 72, 219-230.

22. Seifert, R. G-Protein-Coupled Receptors as Drug Targets: Analysis of Activation and constitutive Activity. *G-Protein-Coupled Receptors as Drug Targets,* **2005**, Seifert, R., Wieland, T., Eds. Wiley-VCH, 122.140.
23. Cabrera-Vera, T. M.; Vanhauwe, J.; Thomas, T. O.; Medkova, M.; Preininger, A.; Mazzoni, M. R.; Hamm, H. E. Insights into G-Protein structure, function, and regulation. *Endocr. Rev.* **2003**, 24, 765-781.
24. Marinissen, M. J.; Gutkind, J. S. G-protein-coupled receptors and signaling networks: emerging paradigms. *Trends Pharmacol. Sci.* **2001**, 22, 368-376.
25. Mikoshiba, K. IP_3 receptor/Ca^{2+} channel: from discovery to new signaling concepts. *J. Neurochem.* **2007**, 102, 1426-1446.
26. Thomsen, W.; Frazer, J.; Unett, D. Functional assays for screening GPCR targets. *Curr. Opin. Biotechnol.* **2005**, 16, 655-665.
27. Kristiansen, K. Molecular mechanisms of ligand binding, signaling, and regulation within the superfamily of G-protein-coupled receptors: molecular modeling and mutagenesis approaches to receptor structure and function. *Pharmacol. Ther.* **2004**, 103, 21-80.
28. Cabrera-Vera, T. M.; Vanhauwe, J.; Thomas, T. O.; Medkova, M.; Preininger, A.; Mazzoni, M. R.; Hamm, H. E. Insights into G-Protein structure, function, and regulation. *Endocr. Rev.* **2003**, 24, 765-781.
29. Rasmussen, S. G.; DeVree, B. T.; Zou, Y.; Kruse, A. C.; Chung, K. Y.; Kobilka, T. S.; Thian, F. S.; Chae, P. S.; Pardon, E.; Calinski, D.; Mathiesen, J. M.; Shah, S. T.; Lyons, J. A.; Caffrey, M.; Gellman, S. H.; Steyaert, J.; Skiniotis, G.; Weis, W. I.; Sunahara, R. K.; Kobilka, B. K. Crystal structure of the beta2 adrenergic receptor-Gs protein complex. *Nature* **2011**, 477, 549-555.
30. Miller, W. E.; Lefkowitz, R. J. Expanding roles for beta-arrestins as scaffolds and adapters in GPCR signaling and trafficking. *Curr. Opin. Cell Biol.* **2001**, 13, 139-145.
31. Perry, S. J.; Lefkowitz, R. J. Arresting developments in heptahelical receptor signaling and regulation. *Trends Cell Biol.* **2002**, 12, 130-138.
32. Lefkovitz, Z.; Shapiro, R.; Koch, S.; Cappell, M. S. The emerging role of virtual colonoscopy. *Med. Clin. North Am.* **2005**, 89, 111-138, viii.
33. Lefkowitz, R. J.; Shenoy, S. K. Transduction of receptor signals by beta-arrestins. *Science* **2005**, 308, 512-517.
34. Rajagopal, S.; Rajagopal, K.; Lefkowitz, R. J. Teaching old receptors new tricks: biasing seven-transmembrane receptors. *Nat. Rev. Drug Discov.* **2010**, 9, 373-386.
35. Urban, J. D.; Clarke, W. P.; von Zastrow, M.; Nichols, D. E.; Kobilka, B.; Weinstein, H.; Javitch, J. A.; Roth, B. L.; Christopoulos, A.; Sexton, P. M.; Miller, K. J.; Spedding, M.; Mailman, R. B. Functional selectivity and classical concepts of quantitative pharmacology. *J. Pharmacol. Exp. Ther.* **2007**, 320, 1-13.
36. Jarpe, M. B.; Knall, C.; Mitchell, F. M.; Buhl, A. M.; Duzic, E.; Johnson, G. L. [D-Arg1,D-Phe5,D-Trp7,9,Leu11]Substance P acts as a biased agonist toward neuropeptide and chemokine receptors. *J. Biol. Chem.* **1998**, 273, 3097-3104.
37. Roth, B. L. Modulation of phosphatidylinositol-4,5-bisphosphate hydrolysis in rat aorta by guanine nucleotides, calcium and magnesium. *Life Sci.* **1987**, 41, 629-634.
38. Roth, B. L.; Chuang, D. M. Multiple mechanisms of serotonergic signal transduction. *Life Sci.* **1987**, 41, 1051-1064.
39. Mailman, R. B. GPCR functional selectivity has therapeutic impact. *Trends Pharmacol. Sci.* **2007**, 28, 390-396.
40. Christopoulos, A.; Kenakin, T. G-Protein-coupled receptor allosterism and complexing. *Pharmacol. Rev.* **2002**, 54, 323-374.
41. Dale, H. H.; Laidlaw, P. P. The physiological action of beta-iminazolylethylamine. *J. Physiol.* **1910**, 41, 318-344.
42. Ganellin, C. R. The tautomer ratio of histamine. *J. Pharm. Pharmacol.* **1973**, 25, 787-792.
43. Schwartz, J.-C.; Haas, H. L. *The histamine r*EC*eptor*. Wiley Liss. Inc.: New York, **1992**.
44. Parsons, M. E.; Ganellin, C. R. Histamine and its receptors. *Br. J. Pharmacol.* **2006**, 147, S127-S135.
45. Riley, J. F.; West, G. B. Histamine in tissue mast cells. *J. Physiol.* **1952**, 117, 72P-73P.
46. Saxena, S. P.; Brandes, L. J.; Becker, A. B.; Simons, K. J.; LaBella, F. S.; Gerrard, J. M. Histamine is an intracellular messenger mediating platelet aggregation. *Science* **1989**, 243, 1596-1599.

47. Hakanson, R.; Larsson, L. I.; Sundler, F. Endocrine-like cells in rat stomach: effects of 6-hydroxydopa on amine stores and amino acid decarboxylase activities. A chemical, fluorescence histochemical and electron microscopic study. *J. Pharmacol. Exp. Ther.* **1974**, 191, 92-101.
48. Karnushina, I. L.; Palacios, J. M.; Barbin, G.; Dux, E.; Joo, F.; Schwartz, J. C. Studies on a capillary-rich fraction isolated from brain: histaminic components and characterization of the histamine receptors linked to adenylate cyclase. *J. Neurochem.* **1980**, 34, 1201-1208.
49. Schwartz, J. C.; Pollard, H.; Quach, T. T. Histamine as a neurotransmitter in mammalian brain: neurochemical evidence. *J. Neurochem.* **1980**, 35, 26-33.
50. Haas, H. L.; Sergeeva, O. A.; Selbach, O. Histamine in the nervous system. *Physiol. Rev.* **2008**, 88, 1183-1241.
51. Thurmond, R. L.; Gelfand, E. W.; Dunford, P. J. The role of histamine H_1 and H_4 receptors in allergic inflammation: the search for new antihistamines. *Nat. Rev. Drug Discov.* **2008**, 7, 41-53.
52. Ogasawara, M.; Yamauchi, K.; Satoh, Y.; Yamaji, R.; Inui, K.; Jonker, J. W.; Schinkel, A. H.; Maeyama, K. Recent advances in molecular pharmacology of the histamine systems: organic cation transporters as a histamine transporter and histamine metabolism. *J. Pharm. Sci.* **2006**, 101, 24-30.
53. Seifert, R.; Strasser, A.; Schneider, E. H.; Neumann, D.; Dove, S.; Buschauer, A. Molecular and cellular analysis of human histamine receptor subtypes. *Trends Pharmacol. Sci.* **2013**, 34, 33-58.
54. Strasser, A.; Wittmann, H.-J.; Buschauer, A.; Schneider, E. H.; Seifert, R. Species-dependent activities of G-protein-coupled receptor ligands: lessons from histamine receptor orthologs. *Trends Pharmacol. Sci.* **2013**, 34, 13-32.
55. Walter, M.; Stark, H. Histamine receptor subtypes: a century of rational drug design. *Front. Biosci.* **2012**, 4, 461-488.
56. Ash, A. S. F.; Schild, H. O. Receptors Mediating Some Actions of Histamine. *Br. J. Pharmacol. Chemother.* **1966**, 27, 427-&.
57. Hill, S. J.; Ganellin, C. R.; Timmerman, H.; Schwartz, J.-C.; Shankley, N. P.; Young, J. M.; Schunack, W.; Levi, R.; Haas, H. L. International Union of Pharmacology. XIII. Classification of Histamine Receptors. *Pharmacol. Rev.* **1997**, 49, 253-278.
58. Black, J. W.; Duncan, W. A.; Durant, C. J.; Ganellin, C. R.; Parsons, E. M. Definition and antagonism of histamine H_2-receptors. *Nature* **1972**, 236, 385-390.
59. Arrang, J. M.; Garbarg, M.; Schwartz, J. C. Auto-inhibition of brain histamine release mediated by a novel class H_3 of histamine receptor. *Nature* **1983**, 302, 832-837.
60. Arrang, J. M.; Garbarg, M.; Schwartz, J. C. Autoinhibition of histamine synthesis mediated by presynaptic H_3-receptors. *Neuroscience* **1987**, 23, 149-157.
61. Arrang, J. M.; Garbarg, M.; Schwartz, J. C. Autoregulation of histamine release in brain by presynaptic H_3-receptors. *Neuroscience* **1985**, 15, 553-562.
62. Sander, K.; Kottke, T.; Stark, H. Histamine H_3 receptor antagonists go to clinics. *Biol. Pharm. Bull.* **2008**, 31, 2163-2181.
63. Nguyen, T.; Shapiro, D. A.; George, S. R.; Setola, V.; Lee, D. K.; Cheng, R.; Rauser, L.; Lee, S. P.; Lynch, K. R.; Roth, B. L.; O'Dowd, B. F. Discovery of a Novel Member of the Histamine Receptor Family. *Mol. Pharmacol.* **2001**, 59, 427-433.
64. Oda, T.; Morikawa, N.; Saito, Y.; Masuho, Y.; Matsumoto, S. Molecular Cloning and Characterization of a Novel Type of Histamine Receptor Preferentially Expressed in Leukocytes. *J. Biol. Chem.* **2000**, 275, 36781-36786.
65. Coge, F.; Guenin, S.-P.; Rique, H.; Boutin, J. A.; Galizzi, J.-P. Structure and expression of the human histamine H_4-receptor gene. *Biochem. Biophys. Res. Commun.* **2001**, 284, 301-309.
66. Liu, C.; Ma, X.-J.; Jiang, X.; Wilson, S. J.; Hofstra, C. L.; Blevitt, J.; Pyati, J.; Li, X.; Chai, W.; Carruthers, N.; Lovenberg, T. W. Cloning and Pharmacological Characterization of a Fourth Histamine Receptor H_4 Expressed in Bone Marrow. *Mol. Pharmacol.* **2001**, 59, 420-426.
67. Morse, K. L.; Behan, J.; Laz, T. M.; West, R. E., Jr.; Greenfeder, S. A.; Anthes, J. C.; Umland, S.; Wan, Y.; Hipkin, R. W.; Gonsiorek, W.; Shin, N.; Gustafson, E. L.; Qiao, X.; Wang, S.; Hedrick, J. A.; Greene, J.;

Bayne, M.; Monsma, F. J., Jr. Cloning and Characterization of a Novel Human Histamine Receptor. *J. Pharmacol. Exp. Ther.* **2001**, 296, 1058-1066.

68. Nakamura, T.; Itadani, H.; Hidaka, Y.; Ohta, M.; Tanaka, K. Molecular Cloning and Characterization of a New Human Histamine Receptor, hH_4R. *Biochem. Biophys. Res. Commun.* **2000**, 279, 615-620.
69. Zhu, Y.; Michalovich, D.; Wu, H.-L.; Tan, K. B.; Dytko, G. M.; Mannan, I. J.; Boyce, R.; Alston, J.; Tierney, L. A.; Li, X.; Herrity, N. C.; Vawter, L.; Sarau, H. M.; Ames, R. S.; Davenport, C. M.; Hieble, J. P.; Wilson, S.; Bergsma, D. J.; Fitzgerald, L. R. Cloning, Expression, and Pharmacological Characterization of a Novel Human Histamine Receptor. *Mol. Pharmacol.* **2001**, 59, 434-441.
70. Walter, M.; Kottke, T.; Stark, H. The histamine H_4 receptor: Targeting inflammatory disorders. *Eur. J. Pharmacol.* **2011**, 668, 1-5.
71. Marson, C. M. Targeting the histamine H_4 receptor. *Chem. Rev.* **2011**, 111, 7121-7156.
72. In *Histamine H_4 Receptor: A Novel Drug Target in Immunoregulation and Inflammation*, Stark, H., Ed. Versita: London, **2013**.
73. Bodensteiner, J.; Baumeister, P.; Geyer, R.; Buschauer, A.; Reiser, O. Synthesis and pharmacological characterization of new tetrahydrofuran based compounds as conformationally constrained histamine receptor ligands. *Org. Biomol. Chem.* **2013**, 11, 4040-4055.
74. De Backer, M. D.; Gommeren, W.; Moereels, H.; Nobels, G.; Van Gompel, P.; Leysen, J. E.; Luyten, W. H. Genomic cloning, heterologous expression and pharmacological characterization of a human histamine H1 receptor. *Biochem. Biophys. Res. Commun.* **1993**, 197, 1601-1608.
75. Hill, S. J. Distribution, properties, and functional characteristics of three classes of histamine receptor. *Pharmacol. Rev.* **1990**, 42, 45-83.
76. Bongers, G.; de Esch, I.; Leurs, R. Molecular Pharmacology of the Four Histamine Receptors. *Adv. Exp. Med. Biol.* **2010**, 709, 11-19.
77. Leurs, R.; Smit, M. J.; Timmerman, H. Molecular pharmacological aspects of histamine receptors. *Pharmacol. Ther.* **1995**, 66, 413-463.
78. Simons, F. E. Advances in H_1-antihistamines. *N. Engl. J. Med.* **2004**, 351, 2203-2217.
79. Simons, F. E.; Simons, K. J. Histamine and H_1-antihistamines: celebrating a century of progress. *J. Allergy Clin. Immunol.* **2011**, 128, 1139-1150 e1134.
80. Yanai, K.; Rogala, B.; Chugh, K.; Paraskakis, E.; Pampura, A. N.; Boev, R. Safety considerations in the management of allergic diseases: focus on antihistamines. *Curr. Med. Res. Opin.* **2012**, 28, 623-642.
81. Hill, S. J.; Young, J. M.; Marrian, D. H. Specific binding of ^{3}H-mepyramine to histamine H_1 receptors in intestinal smooth muscle. *Nature* **1977**, 270, 361-363.
82. Stark, H. Histamine Receptors. *BIOTREND Reviews* **2007**, 1-10.
83. Barak, N. Betahistine: what's new on the agenda? *Expert Opin. Investig. Drugs* **2008**, 17, 795-804.
84. Seifert, R.; Wenzel-Seifert, K.; Bürckstümmer, T.; Pertz, H. H.; Schunack, W.; Dove, S.; Buschauer, A.; Elz, S. Multiple Differences in Agonist and Antagonist Pharmacology between Human and Guinea Pig Histamine H_1-Receptor. *J. Pharmacol. Exp. Ther.* **2003**, 305, 1104-1115.
85. Gantz, I.; Munzert, G.; Tashiro, T.; Schaffer, M.; Wang, L.; DelValle, J.; Yamada, T. Molecular cloning of the human histamine H_2 receptor. *Biochem. Biophys. Res. Commun.* **1991**, 178, 1386-1392.
86. Gantz, I.; Schaffer, M.; DelValle, J.; Logsdon, C.; Campbell, V.; Uhler, M.; Yamada, T. Molecular cloning of a gene encoding the histamine H_2 receptor. *Proc. Natl. Acad. Sci. U. S. A.* **1991**, 88, 429-433.
87. Dove, S.; Elz, S.; Seifert, R.; Buschauer, A. Structure-activity relationships of histamine H_2 receptor ligands. *Mini. Rev. Med. Chem.* **2004**, 4, 941-954.
88. Johnson, C. L.; Weinstein, H.; Green, J. P. Studies on histamine H_2 receptors coupled to cardiac adenylate cyclase. Blockade by H_2 and H_1 receptor antagonists. *Mol. Pharmacol.* **1979**, 16, 417-428.
89. Klein, I.; Levey, G. S. Activation of myocardial adenyl cyclase by histamine in guinea pig, cat, and human heart. *J. Clin. Invest.* **1971**, 50, 1012-1015.
90. Esbenshade, T. A.; Kang, C. H.; Krueger, K. M.; Miller, T. R.; Witte, D. G.; Roch, J. M.; Masters, J. N.; Hancock, A. A. Differential activation of dual signaling responses by human H_1 and H_2 histamine receptors. *J. Recept. Signal Transduct. Res.* **2003**, 23, 17-31.

91. Mitsuhashi, M.; Mitsuhashi, T.; Payan, D. G. Multiple signaling pathways of histamine H_2 receptors. Identification of an H_2 receptor-dependent Ca^{2+} mobilization pathway in human HL-60 promyelocytic leukemia cells. *J. Biol. Chem.* **1989**, 264, 18356-18362.
92. Wang, L.; Gantz, I.; DelValle, J. Histamine H_2 receptor activates adenylate cyclase and PLC via separate GTP-dependent pathways. *Am. J. Physiol.* **1996**, 271, G613-620.
93. Levi, R. C.; Alloatti, G. Histamine modulates calcium current in guinea pig ventricular myocytes. *J. Pharmacol. Exp. Ther.* **1988**, 246, 377-383.
94. Jolly, S.; Desmecht, D. Functional identification of epithelial and smooth muscle histamine-dependent relaxing mechanisms in the bovine trachea, but not in bronchi. *Comparative Biochemistry and Physiology Part C: Toxicology & Pharmacology* **2003**, 134, 91-100.
95. Ichikawa, T.; Hotta, K.; Ishihara, K. Second-generation histamine H_2-receptor antagonists with gastric mucosal defensive properties. *Mini. Rev. Med. Chem.* **2009**, 9, 581-589.
96. Freston, J. W. Management of Peptic Ulcers: Emerging Issues. *World J. Surg.* **2000**, 24, 250-255.
97. Penston, J. G. Clinical aspects of Helicobacter pylori eradication therapy in peptic ulcer disease. *Aliment. Pharmacol. Ther.* **1996**, 10, 469-486.
98. Alhazzani, W.; Alenezi, F.; Jaeschke, R. Z.; Moayyedi, P.; Cook, D. J. Proton pump inhibitors versus histamine 2 receptor antagonists for stress ulcer prophylaxis in critically ill patients: a systematic review and meta-analysis. *Crit. Care Med.* **2013**, 41, 693-705.
99. Hirschfeld, J.; Buschauer, A.; Elz, S.; Schunack, W.; Ruat, M.; Traiffort, E.; Schwartz, J. C. Iodoaminopotentidine and related compounds: a new class of ligands with high affinity and selectivity for the histamine H_2 receptor. *J. Med. Chem.* **1992**, 35, 2231-2238.
100. Cavanagh, R. L.; Buyniski, J. P. Effect of BMY-25368, a potent and long-acting histamine H_2-receptor antagonist, on gastric secretion and aspirin-induced gastric lesions in the dog. *Aliment. Pharmacol. Ther.* **1989**, 3, 299-313.
101. Yellin, T. O.; Buck, S. H.; Gilman, D. J.; Jones, D. F.; Wardleworth, J. M. ICI 125,211: A new gastric antisecretory agent acting on histamine H_2-receptors. *Life Sci.* **1979**, 25, 2001-2009.
102. Gajtkowski, G. A.; Norris, D. B.; Rising, T. J.; Wood, T. P. Specific binding of ^{3}H-tiotidine to histamine H_2 receptors in guinea pig cerebral cortex. *Nature* **1983**, 304, 65-67.
103. Traiffort, E.; Pollard, H.; Moreau, J.; Ruat, M.; Schwartz, J. C.; Martinez-Mir, M. I.; Palacios, J. M. Pharmacological Characterization and Autoradiographic Localization of Histamine H_2 Receptors in Human Brain Identified with [^{125}I]Iodoaminopotentidine. *J. Neurochem.* **1992**, 59, 290-299.
104. Ruat, M.; Traiffort, E.; Bouthenet, M. L.; Souil, E.; Pollard, H.; Moreau, J.; Schwartz, J. C.; Martinez-Mir, I.; Palacios, J. M.; Hirschfeld, J.; et al. Reversible and irreversible labelling of H_1- and H_2 -receptors using novel [^{125}I] probes. *Agents & Actions Suppl.* **1991**, 33, 123-144.
105. Ruat, M.; Traiffort, E.; Bouthenet, M. L.; Schwartz, J. C.; Hirschfeld, J.; Buschauer, A.; Schunack, W. Reversible and irreversible labeling and autoradiographic localization of the cerebral histamine H_2 receptor using [^{125}I]iodinated probes. *Proceedings of the National Academy of Sciences* **1990**, 87, 1658-1662.
106. Erdmann, D. Histamine H_2- and H_3- Receptor Antagonists: Synthesis and Characterization of Radiolabelled and Flourescent Pharmacological Tools. *Doctoral Thesis, University of Regensburg,* **2010**.
107. van der Goot, H.; Timmerman, H. Selective ligands as tools to study histamine receptors. *Eur. J. Med. Chem.* **2000**, 35, 5-20.
108. Yanagisawa, I.; Hirata, Y.; Ishii, Y. Studies on histamine H_2 receptor antagonists. 2. Synthesis and pharmacological activities of *N*-sulfamoyl and *N*-sulfonyl amidine derivatives. *J. Med. Chem.* **1987**, 30, 1787-1793.
109. Eriks, J. C.; Van der Goot, H.; Sterk, G. J.; Timmerman, H. Histamine H_2-receptor agonists. Synthesis, in vitro pharmacology, and qualitative structure-activity relationships of substituted 4- and 5-(2-aminoethyl)thiazoles. *J. Med. Chem.* **1992**, 35, 3239-3246.
110. Parsons, M. E.; Owen, D. A. A.; Ganellin, C. R.; durant, G. J. Dimaprit-[*S*-[3-(*N,N*-dimethylamino)propyl]isothiourea] - A highly specific histamine H_2-receptor agonist. Part 1. Pharmacology. *Agents Actions* **1977**, 7, 31-37.

111. Durant, G. J.; Duncan, W. A. M.; Ganellin, C. R.; Parsons, M. E.; Blakemore, R. C.; Rasmussen, A. C. Impromidine (SKF 92676) is a very potent and specific agonist for histamine H_2 receptors. *Nature* **1978**, 276, 403-405.

112. Durant, G. J.; Ganellin, C. R.; Hills, D. W.; Miles, P. D.; Parsons, M. E.; Pepper, E. S.; White, G. R. The histamine H_2 receptor agonist impromidine: synthesis and structure-activity considerations. *J. Med. Chem.* **1985**, 28, 1414-1422.

113. Buschauer, A.; Baumann, G. Structure-activity relationships of histamine H_2-agonists, a new class of positive inotropic drugs. *Agents Actions. Suppl.* **1991**, 33, 231-256.

114. Timmerman, H. Routes to Histamine H_2-Agonists. *Quant. Struct.-Act. Relat.* **1992**, 11, 219-223.

115. Ghorai, P.; Kraus, A.; Keller, M.; Götte, C.; Igel, P.; Schneider, E.; Schnell, D.; Bernhardt, G. n.; Dove, S.; Zabel, M.; Elz, S.; Seifert, R.; Buschauer, A. Acylguanidines as Bioisosteres of Guanidines: N^G-Acylated Imidazolylpropylguanidines, a New Class of Histamine H_2 Receptor Agonists. *J. Med. Chem.* **2008**, 51, 7193-7204.

116. Kraus, A.; Ghorai, P.; Birnkammer, T.; Schnell, D.; Elz, S.; Seifert, R.; Dove, S.; Bernhardt, G.; Buschauer, A. N^G-Acylated Aminothiazolylpropylguanidines as Potent and Selective Histamine H_2 Receptor Agonists. *ChemMedChem* **2009**, 4, 232-240.

117. Birnkammer, T.; Spickenreither, A.; Brunskole, I.; Lopuch, M.; Kagermeier, N.; Bernhardt, G.; Dove, S.; Seifert, R.; Elz, S.; Buschauer, A. The Bivalent Ligand Approach Leads to Highly Potent and Selective Acylguanidine-Type Histamine H_2 Receptor Agonists. *J. Med. Chem.* **2012**, 55, 1147-1160.

118. Aurelius, J.; Martner, A.; Brune, M.; Palmqvist, L.; Hansson, M.; Hellstrand, K.; Thoren, F. B. Remission maintenance in acute myeloid leukemia: impact of functional histamine H_2 receptors expressed by leukemic cells. *Haematologica* **2012**, 97, 1904-1908.

119. Berry, S. M.; Broglio, K. R.; Berry, D. A. Addressing the incremental benefit of histamine dihydrochloride when added to interleukin-2 in treating acute myeloid leukemia: a Bayesian meta-analysis. *Cancer Invest.* **2011**, 29, 293-299.

120. Buyse, M.; Squifflet, P.; Lucchesi, K. J.; Brune, M. L.; Castaigne, S.; Rowe, J. M. Assessment of the consistency and robustness of results from a multicenter trial of remission maintenance therapy for acute myeloid leukemia. *Trials* **2011**, 12, 86.

121. Lovenberg, T. W.; Roland, B. L.; Wilson, S. J.; Jiang, X.; Pyati, J.; Huvar, A.; Jackson, M. R.; Erlander, M. G. Cloning and Functional Expression of the Human Histamine H_3 Receptor. *Mol. Pharmacol.* **1999**, 55, 1101-1107.

122. Berlin, M.; Boyce, C. W.; de Lera Ruiz, M. Histamine H_3 Receptor as a Drug Discovery Target. *J. Med. Chem.* **2011**, 54, 26-53.

123. Schlicker, E.; Fink, K.; Detzner, M.; Göthert, M. Histamine inhibits dopamine release in the mouse striatum via presynaptic H_3 receptors. *J. Neural Transm.* **1993**, 93, 1-10.

124. Schlicker, E.; Betz, R.; Göthert, M. Histamine H_3 receptor-mediated inhibition of serotonin release in the rat brain cortex. *Naunyn-Schmiedeberg's Arch. Pharmacol.* **1988**, 337, 588-590.

125. Clapham, J.; Kilpatrick, G. J. Histamine H_3 receptors modulate the release of [^{3}H]-acetylcholine from slices of rat entorhinal cortex: evidence for the possible existence of H_3 receptor subtypes. *Br. J. Pharmacol.* **1992**, 107, 919-923.

126. Bakker, R. A.; Dees, G.; Carrillo, J. J.; Booth, R. G.; Lopez-Gimenez, J. F.; Milligan, G.; Strange, P. G.; Leurs, R. Domain Swapping in the Human Histamine H_1 Receptor. *J. Pharmacol. Exp. Ther.* **2004**, 311, 131-138.

127. Bertaccini, G.; Coruzzi, G. An update on histamine H_3 receptors and gastrointestinal functions. *Dig. Dis. Sci.* **1995**, 40, 2052-2063.

128. Delaunois, A.; Gustin, P.; Garbarg, M.; Ansay, M. Modulation of acetylcholine, capsaicin and substance P effects by histamine H_3 receptors in isolated perfused rabbit lungs. *Eur. J. Pharmacol.* **1995**, 277, 243-250.

129. Malinowska, B.; Godlewski, G.; Schlicker, E. Histamine H_3 receptors - general characterization and their function in the cardiovascular system. *J. Physiol. Pharmacol.* **1998**, 49, 191-211.

130. Schwartz, J. C.; Arrang, J. M.; Garbarg, M.; Pollard, H. Plenary lecture. A third histamine receptor subtype: characterisation, localisation and functions of the H_3-receptor. *Agents Actions* **1990**, 30, 13-23.
131. Leurs, R.; Bakker, R. A.; Timmerman, H.; de Esch, I. J. P. The histamine H_3 receptor: from gene cloning to H_3 receptor drugs. *Nat. Rev. Drug Discov.* **2005**, 4, 107-120.
132. Bongers, G.; Bakker, R. A.; Leurs, R. Molecular aspects of the histamine H_3 receptor. *Biochem. Pharmacol.* **2007**, 73, 1195-1204.
133. Bonaventure, P.; Letavic, M.; Dugovic, C.; Wilson, S.; Aluisio, L.; Pudiak, C.; Lord, B.; Mazur, C.; Kamme, F.; Nishino, S.; Carruthers, N.; Lovenberg, T. Histamine H_3 receptor antagonists: from target identification to drug leads. *Biochem. Pharmacol.* **2007**, 73, 1084-1096.
134. Hancock, A. A. H_3 receptor antagonists/inverse agonists as anti-obesity agents. *Curr. Opin. Investig. Drugs* **2003**, 4, 1190-1197.
135. Leurs, R.; Vischer, H. F.; Wijtmans, M.; de Esch, I. J. En route to new blockbuster anti-histamines: surveying the offspring of the expanding histamine receptor family. *Trends Pharmacol. Sci.* **2011**, 32, 250-257.
136. de Esch, I. J. P.; Belzar, K. J. Histamine H_3 Receptor Agonists. *Mini. Rev. Med. Chem.* **2004**, 4, 955-963.
137. Kitbunnadaj, R.; Zuiderveld, O. P.; DeEsch, I. J. P.; Vollinga, R. C.; Bakker, R.; Lutz, M.; Spek, A. L.; Cavoy, E.; Deltent, M. F.; Menge, W. M. P. B.; Timmerman, H.; Leurs, R. Synthesis and Structure-Activity Relationships of Conformationally Constrained Histamine H_3 Receptor Agonists. *J. Med. Chem.* **2003**, 46, 5445-5457.
138. Celanire, S.; Wijtmans, M.; Talaga, P.; Leurs, R.; de Esch, I. J. P. Keynote review: Histamine H_3 receptor antagonists reach out for the clinic. *Drug Discov. Today* **2005**, 10, 1613-1627.
139. Cramp, S.; Dyke, H. J.; Higgs, C.; Clark, D. E.; Gill, M.; Savy, P.; Jennings, N.; Price, S.; Lockey, P. M.; Norman, D.; Porres, S.; Wilson, F.; Jones, A.; Ramsden, N.; Mangano, R.; Leggate, D.; Andersson, M.; Hale, R. Identification and hit-to-lead exploration of a novel series of histamine H_4 receptor inverse agonists. *Bioorg. Med. Chem. Lett.* **2010**, 20, 2516-2519.
140. Millan-Guerrero, R. O.; Pineda-Lucatero, A. G.; Hernandez-Benjamin, T.; Tene, C. E.; Pacheco, M. F. N^a-methylhistamine safety and efficacy in migraine prophylaxis: phase I and phase II studies. *Headache* **2003**, 43, 389-394.
141. Arrang, J. M.; Garbarg, M.; Lancelo, J. C.; Lecomte, J. M.; Pollard, H.; Robba, M.; Schunack, W.; Schwartz, J. C. Highly potent and selective ligands for histamine H_3-receptors. *Nature* **1987**, 327, 117-123.
142. van der Goot, H.; Schepers, M. J. P.; Sterk, G. J.; Timmerman, H. Isothiourea analogs of histamine as potent agonists or antagonists of the histamine H_3-receptor. *Eur. J. Med. Chem.* **1992**, 27, 511-517.
143. Cowart, M.; Altenbach, R.; Black, L.; Faghih, R.; Zhao, C.; Hancock, A. A. Medicinal Chemistry and Biological Properties of Non-Imidazole Histamine H_3 Antagonists. *Mini. Rev. Med. Chem* **2004**, 4, 979-992.
144. Inocente, C.; Arnulf, I.; Bastuji, H.; Thibault-Stoll, A.; Raoux, A.; Reimao, R.; Lin, J. S.; Franco, P. Pitolisant, an inverse agonist of the histamine H_3 receptor: an alternative stimulant for narcolepsy-cataplexy in teenagers with refractory sleepiness. *Clin. Neuropharmacol.* **2012**, 35, 55-60.
145. Schwartz, J. C. The histamine H_3 receptor: from discovery to clinical trials with pitolisant. *Br. J. Pharmacol.* **2011**, 163, 713-721.
146. van der Goot, H.; Eriks, J. C.; Leurs, R.; Timmerman, H. Amselamine, a new selective histamine H_2-receptor agonist. *Bioorg. Med. Chem. Lett.* **1994**, 4, 1913-1916.
147. Alves-Rodrigues, A.; Leurs, R.; Wu, T. S.; Prell, G. D.; Foged, C.; Timmerman, H. [^{3}H]-thioperamide as a radioligand for the histamine H_3 receptor in rat cerebral cortex. *Br. J. Pharmacol.* **1996**, 118, 2045-2052.
148. Jansen, F. P.; Rademaker, B.; Bast, A.; Timmerman, H. The first radiolabeled histamine H_3 receptor antagonist, [^{125}I]iodophenpropit: saturable and reversible binding to rat cortex membranes. *Eur. J. Pharmacol.* **1992**, 217, 203-205.

149. Clark, R. A.; Gallin, J. I.; Kaplan, A. P. The selective eosinophil chemotactic activity of histamine. *J. Exp. Med.* **1975**, 142, 1462-1476.
150. Raible, D. G.; Lenahan, T.; Fayvilevich, Y.; Kosinski, R.; Schulman, E. S. Pharmacologic characterization of a novel histamine receptor on human eosinophils. *Am. J. Respir. Crit. Care Med.* **1994**, 149, 1506-1511.
151. Raible, D. G.; Schulman, E. S.; DiMuzio, J.; Cardillo, R.; Post, T. J. Mast cell mediators prostaglandin-D_2 and histamine activate human eosinophils. *J. Immunol.* **1992**, 148, 3536-3542.
152. Leurs, R.; Chazot, P. L.; Shenton, F. C.; Lim, H. D.; de Esch, I. J. Molecular and biochemical pharmacology of the histamine H_4 receptor. *Br. J. Pharmacol.* **2009**, 157, 14-23.
153. Hofstra, C. L.; Desai, P. J.; Thurmond, R. L.; Fung-Leung, W. P. Histamine H_4 receptor mediates chemotaxis and calcium mobilization of mast cells. *J. Pharmacol. Exp. Ther.* **2003**, 305, 1212-1221.
154. Nijmeijer, S.; Vischer, H. F.; Rosethorne, E. M.; Charlton, S. J.; Leurs, R. Analysis of multiple histamine H_4 receptor compound classes uncovers Galphai protein- and beta-arrestin2-biased ligands. *Mol. Pharmacol.* **2012**, 82, 1174-1182.
155. Rosethorne, E. M.; Charlton, S. J. Agonist-biased signaling at the histamine H_4 receptor: JNJ7777120 recruits beta-arrestin without activating G-Proteins. *Mol. Pharmacol.* **2011**, 79, 749-757.
156. Seifert, R.; Schneider, E. H.; Dove, S.; Brunskole, I.; Neumann, D.; Strasser, A.; Buschauer, A. Paradoxical stimulatory effects of the "standard" histamine H_4-receptor antagonist JNJ7777120: the H_4 receptor joins the club of 7 transmembrane domain receptors exhibiting functional selectivity. *Mol. Pharmacol.* **2011**, 79, 631-638.
157. Zhang, M.; Thurmond, R. L.; Dunford, P. J. The histamine H_4 receptor: A novel modulator of inflammatory and immune disorders. *Pharmacol. Ther.* **2007**, 113, 594-606.
158. Damaj, B. B.; Becerra, C. B.; Esber, H. J.; Wen, Y.; Maghazachi, A. A. Functional expression of H_4 histamine receptor in human natural killer cells, monocytes, and dendritic cells. *J. Immunol.* **2007**, 179, 7907-7915.
159. Kollmeier, A.; Francke, K.; Chen, B.; Dunford, P. J.; Greenspan, A. J.; Xia, Y.; Xu, X. L.; Zhou, B.; Thurmond, R. The H_4 receptor antagonist, JNJ 39758979, is effective in reducing histamine-induced pruritus in a randomized clinical study in healthy subjects. *J. Pharmacol. Exp. Ther.* **2014**.
160. Thurmond, R. L.; Chen, B.; Dunford, P. J.; Greenspan, A. J.; Karlsson, L.; La, D.; Ward, P.; Xu, X. L. Clinical and Preclinical Characterization of the Histamine H_4 Receptor Antagonist JNJ-39758979. *J. Pharmacol. Exp. Ther.* **2014**, 349, 176-184.
161. Tiligada, E. Perspectives in H_4R Research and Therapeutic Exploitation. In *Histamine H_4 Receptor: A Novel Drug Target in Immunoregulation and Inflammation*, Stark, H., Ed. Versita: London, **2013**; pp 333-352.
162. Ballerini, C.; Aldinucci, A.; Luccarini, I.; Galante, A.; Manuelli, C.; Blandina, P.; Katebe, M.; Chazot, P. L.; Masini, E.; Passani, M. B. Antagonism of histamine H_4 receptors exacerbates clinical and pathological signs of experimental autoimmune encephalomyelitis. *Br. J. Pharmacol.* **2013**, 170, 67-77.
163. Deml, K.-F.; Beermann, S.; Neumann, D.; Strasser, A.; Seifert, R. Interactions of Histamine H_1-Receptor Agonists and Antagonists with the Human Histamine H_4-Receptor. *Mol. Pharmacol.* **2009**, 76, 1019-1030.
164. Wagner, E.; Wittmann, H. J.; Elz, S.; Strasser, A. Pharmacological profile of astemizole-derived compounds at the histamine H_1 and H_4 receptor-H_1/H_4 receptor selectivity. *Naunyn-Schmiedeberg's Arch. Pharmacol.* **2014**, 387, 235-250.
165. Deiteren, A.; De Man, J. G.; Ruyssers, N. E.; Moreels, T. G.; Pelckmans, P. A.; De Winter, B. Y. Histamine H_4 and H_1 receptors contribute to postinflammatory visceral hypersensitivity. *Gut* **2014**.
166. Matsushita, A.; Seike, M.; Okawa, H.; Kadawaki, Y.; Ohtsu, H. Advantages of histamine H_4 receptor antagonist usage with H_1 receptor antagonist for the treatment of murine allergic contact dermatitis. *Exp. Dermatol.* **2012**, 21, 714-715.
167. Lim, H. D.; van Rijn, R. M.; Ling, P.; Bakker, R. A.; Thurmond, R. L.; Leurs, R. Evaluation of histamine H_1-, H_2-, and H_3-receptor ligands at the human histamine H_4 receptor: identification of 4-methylhistamine as the first potent and selective H_4 receptor agonist. *J. Pharmacol. Exp. Ther.* **2005**, 314, 1310-1321.

168. Jablonowski, J. A.; Grice, C. A.; Chai, W.; Dvorak, C. A.; Venable, J. D.; Kwok, A. K.; Ly, K. S.; Wei, J.; Baker, S. M.; Desai, P. J.; Jiang, W.; Wilson, S. J.; Thurmond, R. L.; Karlsson, L.; Edwards, J. P.; Lovenberg, T. W.; Carruthers, N. I. The First Potent and Selective Non-Imidazole Human Histamine H_4 Receptor Antagonists. *J. Med. Chem.* **2003**, 46, 3957-3960.

169. Schnell, D.; Brunskole, I.; Ladova, K.; Schneider, E.; Igel, P.; Dove, S.; Buschauer, A.; Seifert, R. Expression and functional properties of canine, rat, and murine histamine H_4 receptors in Sf9 insect cells. *Naunyn-Schmiedeberg's Arch. Pharmacol.* **2011**, 383, 457-470.

170. Nordemann, U.; Wifling, D.; Schnell, D.; Bernhardt, G.; Stark, H.; Seifert, R.; Buschauer, A. Luciferase Reporter Gene Assay on Human, Murine and Rat Histamine H_4 Receptor Orthologs: Correlations and Discrepancies between Distal and Proximal Readouts. *PLoS ONE* **2013**, 8, e73961.

171. Smits, R. A.; de Esch, I. J. P.; Zuiderveld, O. P.; Broeker, J.; Sansuk, K.; Guaita, E.; Coruzzi, G.; Adami, M.; Haaksma, E.; Leurs, R. Discovery of Quinazolines as Histamine H_4 Receptor Inverse Agonists Using a Scaffold Hopping Approach. *J. Med. Chem.* **2008**, 51, 7855-7865.

172. Mowbray, C. E.; Bell, A. S.; Clarke, N. P.; Collins, M.; Jones, R. M.; Lane, C. A.; Liu, W. L.; Newman, S. D.; Paradowski, M.; Schenck, E. J.; Selby, M. D.; Swain, N. A.; Williams, D. H. Challenges of drug discovery in novel target space. The discovery and evaluation of PF-3893787: a novel histamine H_4 receptor antagonist. *Bioorg. Med. Chem. Lett.* **2011**, 21, 6596-6602.

173. Schreeb, A.; Łażewska, D.; Dove, S.; Buschauer, A.; Kieć-Kononowicz, K.; Stark, H. Histamine H_4 Receptor Ligands. In *Histamine H_4 Receptor: A Novel Drug Target in Immunoregulation and Inflammation*, Stark, H., Ed. Versita: London, **2013**; pp 21-62.

174. Salcedo, C.; Pontes, C.; Merlos, M. Is the H_4 receptor a new drug target for allergies and asthma? *Front. Biosci.* **2013**, 5, 178-187.

175. Lazewska, D.; Kiec-Kononowicz, K. Azines as histamine H_4 receptor antagonists. *Front. Biosci.* **2012**, 4, 967-987.

176. Igel, P.; Dove, S.; Buschauer, A. Histamine H_4 receptor agonists. *Bioorg. Med. Chem. Lett.* **2010**, 20, 7191-7199.

177. Gbahou, F.; Vincent, L.; Humbert-Claude, M.; Tardivel-Lacombe, J.; Chabret, C.; Arrang, J. M. Compared pharmacology of human histamine H_3 and H_4 receptors: structure-activity relationships of histamine derivatives. *Br. J. Pharmacol.* **2006**, 147, 744-754.

178. Geyer, R.; Kaske, M.; Baumeister, P.; Buschauer, A. Synthesis and Functional Characterization of Imbutamine Analogs as Histamine H_3 and H_4 Receptor Ligands. *Arch. Pharm. (Weinheim).* **2014**, 347, 77-88.

179. Hashimoto, T.; Harusawa, S.; Araki, L.; Zuiderveld, O. P.; Smit, M. J.; Imazu, T.; Takashima, S.; Yamamoto, Y.; Sakamoto, Y.; Kurihara, T.; Leurs, R.; Bakker, R. A.; Yamatodani, A. A Selective Human H_4-Receptor Agonist: (-)-2-Cyano-1-methyl-3-(2*R*,5*R*)-5-[1*H*-imidazol-4(5)-yl]tetrahydrofuran-2-ylmethylguanidine. *J. Med. Chem.* **2003**, 46, 3162-3165.

180. Lim, H. D.; Smits, R. A.; Bakker, R. A.; vanDam, C. M. E.; deEsch, I. J. P.; Leurs, R. Discovery of *S*-(2-Guanidylethyl)-isothiourea (VUF 8430) as a Potent Nonimidazole Histamine H_4 Receptor Agonist. *J. Med. Chem.* **2006**, 49, 6650-6651.

181. Igel, P.; Schneider, E.; Schnell, D.; Elz, S.; Seifert, R.; Buschauer, A. N^G-Acylated Imidazolylpropylguanidines as Potent Histamine H_4 Receptor Agonists: Selectivity by Variation of the N^G-Substituent. *J. Med. Chem.* **2009**, 52, 2623-2627.

182. Geyer, R. Hetarylalkyl(aryl)cyanoguanidines as histamine H_4 receptor ligands: Synthesis, chiral separation, pharmacological characterization, structureactivity and -selectivity relationships. Doctoral thesis, University of Regensburg, Regensburg, **2011**.

183. Igel, P.; Geyer, R.; Strasser, A.; Dove, S.; Seifert, R.; Buschauer, A. Synthesis and Structure−Activity Relationships of Cyanoguanidine-Type and Structurally Related Histamine H_4 Receptor Agonists. *J. Med. Chem.* **2009**, 52, 6297-6313.

184. Lee-Dutra, A.; Arienti, K. L.; Buzard, D. J.; Hack, M. D.; Khatuya, H.; Desai, P. J.; Nguyen, S.; Thurmond, R. L.; Karlsson, L.; Edwards, J. P.; Breitenbucher, J. G. Identification of 2-arylbenzimidazoles as potent human histamine H_4 receptor ligands. *Bioorg. Med. Chem. Lett.* **2006**, 16, 6043-6048.

185. Savall, B. M.; Edwards, J. P.; Venable, J. D.; Buzard, D. J.; Thurmond, R.; Hack, M.; McGovern, P. Agonist/antagonist modulation in a series of 2-aryl benzimidazole H_4 receptor ligands. *Bioorg. Med. Chem. Lett.* **2010**, 20, 3367-3371.

186. Thurmond, R. L.; Desai, P. J.; Dunford, P. J.; Fung-Leung, W. P.; Hofstra, C. L.; Jiang, W.; Nguyen, S.; Riley, J. P.; Sun, S.; Williams, K. N.; Edwards, J. P.; Karlsson, L. A potent and selective histamine H_4 receptor antagonist with anti-inflammatory properties. *J. Pharmacol. Exp. Ther.* **2004**, 309, 404-413.

187. Varga, C.; Horvath, K.; Berko, A.; Thurmond, R. L.; Dunford, P. J.; Whittle, B. J. Inhibitory effects of histamine H_4 receptor antagonists on experimental colitis in the rat. *Eur. J. Pharmacol.* **2005**, 522, 130-138.

188. Yu, F.; Wolin, R. L.; Wei, J.; Desai, P. J.; McGovern, P. M.; Dunford, P. J.; Karlsson, L.; Thurmond, R. L. Pharmacological characterization of oxime agonists of the histamine H_4 receptor. *J. Receptor Channel Res.* **2010**, 3, 37-49.

189. Lim, H. D.; de Graaf, C.; Jiang, W.; Sadek, P.; McGovern, P. M.; Istyastono, E. P.; Bakker, R. A.; de Esch, I. J.; Thurmond, R. L.; Leurs, R. Molecular determinants of ligand binding to H_4R species variants. *Mol. Pharmacol.* **2010**, 77, 734-743.

190. Liu, C.; Wilson, S. J.; Kuei, C.; Lovenberg, T. W. Comparison of human, mouse, rat, and guinea pig histamine H_4 receptors reveals substantial pharmacological species variation. *J. Pharmacol. Exp. Ther.* **2001**, 299, 121-130.

191. Allen, J.; Novotny, J.; Martin, J.; Heinrich, G. Molecular structure of mammalian neuropeptide Y: analysis by molecular cloning and computer-aided comparison with crystal structure of avian homologue. *Proc. Natl. Acad. Sci. U. S. A.* **1987**, 84, 2532-2536.

192. Gray, T. S.; Morley, J. E. Neuropeptide Y: anatomical distribution and possible function in mammalian nervous system. *Life Sci.* **1986**, 38, 389-401.

193. Tatemoto, K.; Carlquist, M.; Mutt, V. Neuropeptide Y - a novel brain peptide with structural similarities to peptide YY and pancreatic polypeptide. *Nature* **1982**, 296, 659-660.

194. Wahlestedt, C.; Yanaihara, N.; Hakanson, R. Evidence for different pre-and post-junctional receptors for neuropeptide Y and related peptides. *Regul. Pept.* **1986**, 13, 307-318.

195. Brothers, S. P.; Wahlestedt, C. Therapeutic potential of neuropeptide Y (NPY) receptor ligands. *EMBO Molecular Medicine* **2010**, 2, 429-439.

196. Yulyaningsih, E.; Zhang, L.; Herzog, H.; Sainsbury, A. NPY receptors as potential targets for anti-obesity drug development. *Br. J. Pharmacol.* **2011**, 163, 1170-1202.

197. Gerald, C.; Walker, M. W.; Criscione, L.; Gustafson, E. L.; Batzl-Hartmann, C.; Smith, K. E.; Vaysse, P.; Durkin, M. M.; Laz, T. M.; Linemeyer, D. L.; Schaffhauser, A. O.; Whitebread, S.; Hofbauer, K. G.; Taber, R. I.; Branchek, T. A.; Weinshank, R. L. A receptor subtype involved in neuropeptide-Y-induced food intake. *Nature* **1996**, 382, 168-171.

198. Gerald, C.; Walker, M. W.; Vaysse, P. J.; He, C.; Branchek, T. A.; Weinshank, R. L. Expression cloning and pharmacological characterization of a human hippocampal neuropeptide Y/peptide YY Y_2 receptor subtype. *J. Biol. Chem.* **1995**, 270, 26758-26761.

199. Gregor, P.; Millham, M. L.; Feng, Y.; DeCarr, L. B.; McCaleb, M. L.; Cornfield, L. J. Cloning and characterization of a novel receptor to pancreatic polypeptide, a member of the neuropeptide Y receptor family. *FEBS Lett.* **1996**, 381, 58-62.

200. Herzog, H.; Hort, Y. J.; Ball, H. J.; Hayes, G.; Shine, J.; Selbie, L. A. Cloned human neuropeptide Y receptor couples to two different second messenger systems. *Proc. Natl. Acad. Sci. U. S. A.* **1992**, 89, 5794-5798.

201. Hu, Y.; Bloomquist, B. T.; Cornfield, L. J.; DeCarr, L. B.; Flores-Riveros, J. R.; Friedman, L.; Jiang, P.; Lewis-Higgins, L.; Sadlowski, Y.; Schaefer, J.; Velazquez, N.; McCaleb, M. L. Identification of a novel hypothalamic neuropeptide Y receptor associated with feeding behavior. *J. Biol. Chem.* **1996**, 271, 26315-26319.

202. Larhammar, D.; Blomqvist, A. G.; Yee, F.; Jazin, E.; Yoo, H.; Wahlested, C. Cloning and functional expression of a human neuropeptide Y/peptide YY receptor of the Y_1 type. *J. Biol. Chem.* **1992**, 267, 10935-10938.

203. Lundell, I.; Blomqvist, A. G.; Berglund, M. M.; Schober, D. A.; Johnson, D.; Statnick, M. A.; Gadski, R. A.; Gehlert, D. R.; Larhammar, D. Cloning of a human receptor of the NPY receptor family with high affinity for pancreatic polypeptide and peptide YY. *J. Biol. Chem.* **1995**, 270, 29123-29128.
204. Rose, P. M.; Fernandes, P.; Lynch, J. S.; Frazier, S. T.; Fisher, S. M.; Kodukula, K.; Kienzle, B.; Seethala, R. Cloning and functional expression of a cDNA encoding a human type 2 neuropeptide Y receptor. *J. Biol. Chem.* **1995**, 270, 29038.
205. Larhammar, D.; Wraith, A.; Berglund, M. M.; Holmberg, S. K.; Lundell, I. Origins of the many NPY-family receptors in mammals. *Peptides* **2001**, 22, 295-307.
206. Michel, M. C.; Beck-Sickinger, A.; Cox, H.; Doods, H. N.; Herzog, H.; Larhammar, D.; Quirion, R.; Schwartz, T.; Westfall, T. XVI. International Union of Pharmacology recommendations for the nomenclature of neuropeptide Y, peptide YY, and pancreatic polypeptide receptors. *Pharmacol. Rev.* **1998**, 50, 143-150.
207. Westlind-Danielsson, A.; Unden, A.; Abens, J.; Andell, S.; Bartfai, T. Neuropeptide Y receptors and the inhibition of adenylate cyclase in the human frontal and temporal cortex. *Neurosci. Lett.* **1987**, 74, 237-242.
208. Gehlert, D. R.; Beavers, L. S.; Johnson, D.; Gackenheimer, S. L.; Schober, D. A.; Gadski, R. A. Expression cloning of a human brain neuropeptide Y Y_2 receptor. *Mol. Pharmacol.* **1996**, 49, 224-228.
209. Parker, M. S.; Sah, R.; Balasubramaniam, A.; Sallee, F. R.; Sweatman, T.; Park, E. A.; Parker, S. L. Dimers of the neuropeptide Y (NPY) Y_2 receptor show asymmetry in agonist affinity and association with G-Proteins. *J. Recept. Signal Transduct. Res.* **2008**, 28, 437-451.
210. Parker, S. L.; Kane, J. K.; Parker, M. S.; Berglund, M. M.; Lundell, I. A.; Li, M. D. Cloned neuropeptide Y (NPY) Y_1 and pancreatic polypeptide Y_4 receptors expressed in Chinese hamster ovary cells show considerable agonist-driven internalization, in contrast to the NPY Y_2 receptor. *Eur. J. Biochem.* **2001**, 268, 877-886.
211. Doods, H.; Gaida, W.; Wieland, H. A.; Dollinger, H.; Schnorrenberg, G.; Esser, F.; Engel, W.; Eberlein, W.; Rudolf, K. BIIE 0246: a selective and high affinity neuropeptide Y Y_2 receptor antagonist. *Eur. J. Pharmacol.* **1999**, 384, R3-5.
212. Shoblock, J. R.; Welty, N.; Nepomuceno, D.; Lord, B.; Aluisio, L.; Fraser, I.; Motley, S. T.; Sutton, S. W.; Morton, K.; Galici, R.; Atack, J. R.; Dvorak, L.; Swanson, D. M.; Carruthers, N. I.; Dvorak, C.; Lovenberg, T. W.; Bonaventure, P. In vitro and in vivo characterization of JNJ-31020028 (*N*-(4-{4-[2-(diethylamino)-2-oxo-1-phenylethyl]piperazin-1-yl}-3-fluorophenyl)-2-pyridin-3-ylbenzamide), a selective brain penetrant small molecule antagonist of the neuropeptide Y Y_2 receptor. *Psychopharmacology (Berl).* **2010**, 208, 265-277.
213. Bonaventure, P.; Nepomuceno, D.; Mazur, C.; Lord, B.; Rudolph, D. A.; Jablonowski, J. A.; Carruthers, N. I.; Lovenberg, T. W. Characterization of *N*-(1-Acetyl-2,3-dihydro-1H-indol-6-yl)-3-(3-cyano-phenyl)-*N*-[1-(2-cyclopen tyl-ethyl)-piperidin-4yl]acrylamide (JNJ-5207787), a small molecule antagonist of the neuropeptide Y Y_2 receptor. *J. Pharmacol. Exp. Ther.* **2004**, 308, 1130-1137.
214. Brothers, S. P.; Saldanha, S. A.; Spicer, T. P.; Cameron, M.; Mercer, B. A.; Chase, P.; McDonald, P.; Wahlestedt, C.; Hodder, P. S. Selective and brain penetrant neuropeptide Y Y_2 receptor antagonists discovered by whole-cell high-throughput screening. *Mol. Pharmacol.* **2010**, 77, 46-57.
215. Mittapalli, G. K.; Vellucci, D.; Yang, J.; Toussaint, M.; Brothers, S. P.; Wahlestedt, C.; Roberts, E. Synthesis and SAR of selective small molecule neuropeptide Y Y_2 receptor antagonists. *Bioorg. Med. Chem. Lett.* **2012**, 22, 3916-3920.
216. Nozulak, J.; Oser, D.; Daehler, J.; Orain, D.; Cotesta, S.; Uzunov, D. Discovery of imidazolidine-2,4-diones as selective NPY Y_2 receptor antagonists. XXIInd International Symposium on Medicinal Chemistry, September 2-6, 2012, Berlin, Germany, **2012**; *Wiley-VCH* **2012**, *ChemMedChem*, Book of Abstracts, 306-307.
217. Mittapalli, G. K.; Roberts, E. Ligands of the neuropeptide Y Y_2 receptor. *Bioorg. Med. Chem. Lett.* **2014**, 24, 430-441.

218. Pluym, N.; Brennauer, A.; Keller, M.; Ziemek, R.; Pop, N.; Bernhardt, G.; Buschauer, A. Application of the Guanidine-Acylguanidine Bioisosteric Approach to Argininamide-Type NPY Y_2 Receptor Antagonists. *ChemMedChem* **2011**.

219. Chang, R. S.; Lotti, V. J.; Chen, T. B. Specific [^{3}H]propionyl-neuropeptide Y (NPY) binding in rabbit aortic membranes: comparisons with binding in rat brain and biological responses in rat vas deferens. *Biochem. Biophys. Res. Commun.* **1988**, 151, 1213-1219.

220. Widdowson, P. S.; Halaris, A. E. A comparison of the binding of [^{3}H]proprionyl-neuropeptide Y to rat and human frontal cortical membranes. *J. Neurochem.* **1990**, 55, 956-962.

221. Martel, J. C.; Fournier, A.; St Pierre, S.; Quirion, R. Quantitative autoradiographic distribution of [^{125}I]Bolton-Hunter neuropeptide Y receptor binding sites in rat brain. Comparison with [^{125}I]peptide YY receptor sites. *Neuroscience* **1990**, 36, 255-283.

222. Dumont, Y.; Fournier, A.; St-Pierre, S.; Quirion, R. Characterization of neuropeptide Y binding sites in rat brain membrane preparations using [^{125}I][Leu31, Pro34] peptide YY and [^{125}I]Peptide YY3-36 as selective Y_1 and Y_2 radioligands. *J. Pharmacol. Exp. Ther.* **1995**, 272, 673-680.

223. Dumont, Y.; Fournier, A.; St-Pierre, S.; Quiron, R. Autoradiographic distribution of [^{125}I][Leu31,Pro34]PYY and [^{125}I]PYY3-36 binding sites in the rat brain evaluated with two newly developed Y_1 and Y_2 receptor radioligands. *Synapse (N. Y.)* **1996**, 22, 139-158.

224. Pluym, N.; Baumeister, P.; Keller, M.; Bernhardt, G.; Buschauer, A. [^{3}H]UR-PLN196: a selective nonpeptide radioligand and insurmountable antagonist for the neuropeptide Y Y_2 receptor. *ChemMedChem* **2013**, 8, 587-593.

225. Rudolf, K.; Eberlein, W.; Engel, W.; Wieland, H. A.; Willim, K. D.; Entzeroth, M.; Wienen, W.; Beck-Sickinger, A. G.; Doods, H. N. The first highly potent and selective non-peptide neuropeptide Y Y_1 receptor antagonist: BIBP 3226. *Eur. J. Pharmacol.* **1994**, 271, R11-13.

226. Kanatani, A.; Kanno, T.; Ishihara, A.; Hata, M.; Sakuraba, A.; Tanaka, T.; Tsuchiya, Y.; Mase, T.; Fukuroda, T.; Fukami, T.; Ihara, M. The novel neuropeptide Y Y_1 receptor antagonist J-104870: a potent feeding suppressant with oral bioavailability. *Biochem. Biophys. Res. Commun.* **1999**, 266, 88-91.

227. Brennauer, A.; Dove, S.; Buschauer, A. Structure-activity relationships of nonpeptide neuropeptide Y receptor antagonists. *Handbook of Experimental Pharmacology* **2004**, 162, 505-546.

228. Brennauer, A. Acylguanidines as bioisosteric groups in argininamide-type neuropeptide Y Y_1 and Y_2 receptor antagonists: synthesis, stability and pharmacological activity. Doctoral thesis, Universität Regensburg, Regensburg, **2006**.

229. Hutzler, C. Synthese und pharmakologische Aktivität neuer Neuropeptid Y Rezeptorliganden: Von *N,N*-disubstituierten Alkanamiden zu hochpotenten Y_1-Antagonisten der Argininamid-Reihe Doctoral thesis, Universität Regensburg, Regensburg, **2001**.

230. Keller, M. Guanidine-acylguanidine bioisosteric approach to adress peptidergic receptors: pharmacological and diagnostic tools for the NPY Y_1 receptor and versatile building blocks based on arginine substitutes. Doctoral thesis, University of Regensurg, Regensburg, **2008**.

231. Keller, M.; Pop, N.; Hutzler, C.; Beck-Sickinger, A. G.; Bernhardt, G.; Buschauer, A. Guanidine-acylguanidine bioisosteric approach in the design of radioligands: synthesis of a tritium-labeled N^G-propionylargininamide ([^{3}H]-UR-MK114) as a highly potent and selective neuropeptide Y Y_1 receptor antagonist. *J. Med. Chem.* **2008**, 51, 8168-8172.

232. Keller, M.; Bernhardt, G.; Buschauer, A. [^{3}H]UR-MK136: A Highly Potent and Selective Radioligand for Neuropeptide Y Y_1 Receptors. *ChemMedChem* **2011**, 6, 1566-1571.

233. Parker, M. S.; Sah, R.; Sheriff, S.; Balasubramaniam, A.; Parker, S. L. Internalization of cloned pancreatic polypeptide receptors is accelerated by all types of Y_4 agonists. *Regul. Pept.* **2005**, 132, 91-101.

234. Pop, N.; Igel, P.; Brennauer, A.; Cabrele, C.; Bernhardt, G. N.; Seifert, R.; Buschauer, A. Functional reconstitution of human neuropeptide Y (NPY) Y_2 and Y_4 receptors in Sf9 insect cells. *J. Recept. Signal Transduct. Res.* **2011**, 31, 271-285.

235. Ziemek, R.; Schneider, E.; Kraus, A.; Cabrele, C.; Beck-Sickinger, A. G.; Bernhardt, G.; Buschauer, A. Determination of affinity and activity of ligands at the human neuropeptide Y Y_4 receptor by flow cytometry and aequorin luminescence. *J. Recept. Signal Transduct. Res.* **2007**, 27, 217-233.

236. Keller, M.; Kaske, M.; Holzammer, T.; Bernhardt, G.; Buschauer, A. Dimeric argininamide-type neuropeptide Y receptor antagonists: chiral discrimination between Y_1 and Y_4 receptors. *Bioorg. Med. Chem.* **2013**, 21, 6303-6322.
237. Sato, N.; Ogino, Y.; Mashiko, S.; Ando, M. Modulation of neuropeptide Y receptors for the treatment of obesity. *Expert Opin. Ther. Pat.* **2009**, 19, 1401-1415.
238. Mullins, D.; Adham, N.; Hesk, D.; Wu, Y.; Kelly, J.; Huang, Y.; Guzzi, M.; Zhang, X.; McCombie, S.; Stamford, A.; Parker, E. Identification and characterization of pseudoirreversible nonpeptide antagonists of the neuropeptide Y Y_5 receptor and development of a novel Y_5-selective radioligand. *Eur. J. Pharmacol.* **2008**, 601, 1-7.
239. Kanatani, A.; Kanno, T.; Ishihara, A.; Hata, M.; Sakuraba, A.; Tanaka, T.; Tsuchiya, Y.; Mase, T.; Fukuroda, T.; Fukami, T.; Ihara, M. The novel neuropeptide Y Y_1 receptor antagonist J-104870: a potent feeding suppressant with oral bioavailability. *Biochem. Biophys. Res. Commun.* **1999**, 266, 88-91.
240. Criscione, L.; Rigollier, P.; Batzl-Hartmann, C.; Rueger, H.; Stricker-Krongrad, A.; Wyss, P.; Brunner, L.; Whitebread, S.; Yamaguchi, Y.; Gerald, C.; Heurich, R. O.; Walker, M. W.; Chiesi, M.; Schilling, W.; Hofbauer, K. G.; Levens, N. Food intake in free-feeding and energy-deprived lean rats is mediated by the neuropeptide Y_5 receptor. *J. Clin. Invest.* **1998**, 102, 2136-2145.
241. Kanatani, A.; Ishihara, A.; Iwaasa, H.; Nakamura, K.; Okamoto, O.; Hidaka, M.; Ito, J.; Fukuroda, T.; MacNeil, D. J.; Van der Ploeg, L. H.; Ishii, Y.; Okabe, T.; Fukami, T.; Ihara, M. L-152,804: orally active and selective neuropeptide Y Y_5 receptor antagonist. *Biochem. Biophys. Res. Commun.* **2000**, 272, 169-173.
242. Walker, M. W.; Wolinsky, T. D.; Jubian, V.; Chandrasena, G.; Zhong, H.; Huang, X.; Miller, S.; Hegde, L. G.; Marsteller, D. A.; Marzabadi, M. R.; Papp, M.; Overstreet, D. H.; Gerald, C. P.; Craig, D. A. The novel neuropeptide Y Y_5 receptor antagonist Lu AA33810 [*N*-[[*trans*-4-[(4,5-dihydro[1]benzothiepino[5,4-*d*]thiazol-2-yl)amino]cycloh exyl]methyl]-methanesulfonamide] exerts anxiolytic- and antidepressant-like effects in rat models of stress sensitivity. *J. Pharmacol. Exp. Ther.* **2009**, 328, 900-911.
243. Erondu, N.; Gantz, I.; Musser, B.; Suryawanshi, S.; Mallick, M.; Addy, C.; Cote, J.; Bray, G.; Fujioka, K.; Bays, H.; Hollander, P.; Sanabria-Bohorquez, S. M.; Eng, W.; Langstrom, B.; Hargreaves, R. J.; Burns, H. D.; Kanatani, A.; Fukami, T.; MacNeil, D. J.; Gottesdiener, K. M.; Amatruda, J. M.; Kaufman, K. D.; Heymsfield, S. B. Neuropeptide Y_5 receptor antagonism does not induce clinically meaningful weight loss in overweight and obese adults. *Cell Metabolism* **2006**, 4, 275-282.
244. de Jong, L. A.; Uges, D. R.; Franke, J. P.; Bischoff, R. Receptor-ligand binding assays: technologies and applications. *Journal of chromatography. B, Analytical technologies in the biomedical and life sciences* **2005**, 829, 1-25.
245. Major, J. S. Minireview: Challenges of High Throughput Screening Against Cell Surface Receptors. *J. R*EC*ept. Signal Transduct. Res.* **1995**, 15, 595-607.
246. Crevat-Pisano, P.; Hariton, C.; Rolland, P. H.; Cano, J. P. Fundamental aspects of radioreceptor assays. *J. Pharm. Biomed. Anal.* **1986**, 4, 697-716.
247. Keen, M. The problems and pitfalls of radioligand binding. *Methods Mol. Biol.* **1995**, 41, 1-16.
248. Jameson, D. M.; Ross, J. A. Fluorescence polarization/anisotropy in diagnostics and imaging. *Chem. Rev.* **2010**, 110, 2685-2708.
249. Lohse, M. J.; Nuber, S.; Hoffmann, C. Fluorescence/bioluminescence resonance energy transfer techniques to study G-protein-coupled receptor activation and signaling. *Pharmacol. Rev.* **2012**, 64, 299-336.
250. Black, C. B.; Duensing, T. D.; Trinkle, L. S.; Dunlay, R. T. Cell-based screening using high-throughput flow cytometry. *ASSAY and Drug Development Technologies* **2011**, 9, 13-20.
251. Tian, Y.; Martinez, M. M.; Pappas, D. Fluorescence correlation spectroscopy: a review of biochemical and microfluidic applications. *Appl. Spectrosc.* **2011**, 65, 115A-124A.
252. Maynard, J. A.; Lindquist, N. C.; Sutherland, J. N.; Lesuffleur, A.; Warrington, A. E.; Rodriguez, M.; Oh, S.-H. Surface plasmon resonance for high-throughput ligand screening of membrane-bound proteins. *Biotechnol. J.* **2009**, 4, 1542-1558.

253. Jonker, N.; Kool, J.; Irth, H.; Niessen, W. M. Recent developments in protein-ligand affinity mass spectrometry. *Anal. Bioanal. Chem.* **2011**, 399, 2669-2681.
254. Lepre, C. A.; Moore, J. M.; Peng, J. W. Theory and applications of NMR-based screening in pharmaceutical research. *Chem. Rev.* **2004**, 104, 3641-3676.
255. Davenport, A. P.; Kuc, R. E. Radioligand-binding and molecular-imaging techniques for the quantitative analysis of established and emerging orphan receptor systems. *Methods Mol. Biol.* **2005**, 306, 93-120.
256. Bylund, D. B.; Murrin, L. C. Radioligand saturation binding experiments over large concentration ranges. *Life Sci.* **2000**, 67, 2897-2911.
257. Bylund, D. B.; Toews, M. L. Radioligand binding methods for membrane preparations and intact cells. In *Receptor Signal Transduction Protocols*, 2011/05/25 ed.; Willars, G. B.; Challiss, R. A. J., Eds., Springer: Leicester, **2011**; Vol. 746, pp 135-164.
258. Bereford, I. J. M.; Allen, M. J. *Radioisotopes in Biology*. Second Edition ed.; Oxford University Press: New York, **2002**.
259. Smisterova, J.; Ensing, K.; De Zeeuw, R. A. Methodological aspects of quantitative receptor assays. *J. Pharm. Biomed. Anal.* **1994**, 12, 723-745.
260. McFarthing, K. G. *Receptor-Ligand Interactions* Oxford University Press: New York, **1992**.
261. Bylund, D. B.; Toews, M. L. Radioligand binding methods: practical guide and tips. *Am. J. Physiol.* **1993**, 265, L421-429.
262. Lazareno, S. Quantification of receptor interactions using binding methods. *J. Recept. Signal Transduct. Res.* **2001**, 21, 139-165.

Chapter 2

Scope and Objectives

The discovery of the histamine H_4 receptor almost 15 years ago, has stimulated the evaluation of this GPCR as a new therapeutic target for the modulation of various inflammatory and immunological disorders.[1] Nevertheless, its biological role is far from being understood. The analysis of the (patho)physiological mechanisms of the H_4R and the validation as a drug target using antagonists and agonists in translational animal models are seriously hampered by substantial species-dependent differences regarding potencies, receptor selectivity and even by opposite activities of available ligands.[2,3] Hence, potent and selective ligands including agonists are required as pharmacological tools to further explore the (patho)physiological function of the H_4R. Therefore, this work aimed at the design and synthesis of potent and selective H_4R agonists. Recently, Savall *et al.* identified 2-arylbenzimidazoles as highly potent and selective H_4R ligands.[4] Highest agonistic activity and selectivity over the other HR subtypes was reported to reside in a compound with a specific substitution pattern, including methyl and fluorine residues, at the benzimidazole and a histamine moiety. Starting from this compound as a lead, in one subproject of this work a library of structurally related analogs was designed and synthesized to elucidate the structure-activity and structure-selectivity relationships of this class of compounds.

The early pharmacological and physiological characterization of the H_4R was based on investigations using compounds identified as H_4R agonists or antagonists among known ligands of the other histamine receptor subtypes.[5] As the hH_4R shares the highest sequence homology with the hH_3R, it is not astonishing that numerous hH_3R ligands, especially ligands incorporating an imidazole moiety as the endogenous ligand histamine, bind to the hH_4R as well. N^G-alkylated and acylated imidazolylpropylguanidines were originally developed as H_2R agonists.[6-8] However, several of them were found to be potent at the H_3R and H_4R, too.[9] VUF 8430, (*S*-(2-guanidinylethyl)isothiourea), also initially designed as an H_2R agonist, proved to be a potent hH_4R agonist with ~30-fold selectivity over the hH_3R (full agonism) and negligible affinity for hH_1R and hH_2R.[10,11] Aiming at H_4R agonists with increased selectivity for the H_4R over the other HR subtypes, the second part of this work was focused on the combination of an imidazole-free molecule like VUF 8430 with the acylguanidine moiety of the N^G-acylated imidazolylpropylguanidines.

The theory of radioligands binding is simple, the experiments can be conveniently performed and applied to a wide range of preparations, including purified and solubilized receptors, membrane preparations, whole cells, tissue slices, and even whole animals.[12] However, radioligands are not commercially available for every target. Furthermore, the applicability of available radioligands is often compromised by moderate affinity, lack of selectivity towards related receptor subtypes, high nonspecific binding and radiochemical instability.[13] Therefore, another aim of this work was the

synthesis and pharmacological characterization of tritium-labeled radioligands for G-Protein coupled receptors (GPCRs).

There has been a shortage of high affinity radioligands for the investigation of the histamine H_2 receptor. For example, [^{3}H]tiotidine,[14] which shows a high degree of unspecific binding, and [^{125}I]iodoaminopotentidine,[15] which has a short half-life and is more difficult to handle with respect to safety precautions, are no longer commercially available. Within a series of H_2R antagonists with piperidinomethylphenoxyalkyl moieties connected to a squaric amide residue, UR-DE257 showed the highest affinity and selectivity for the H_2R.[16] As a subproject of this thesis, the radiosynthesis and the pharmacological characterization of [^{3}H]UR-DE257 are described.

JNJ7777120 ((5-chloro-1*H*-indol-2-yl)(4-methylpiperazine-1-yl)methanone) has been described as the first potent and selective H_4R antagonist in 2003.[17] Its radiolabeled analog was published, but is not commercially available.[18] Hence, a further aim was to synthesize [^{3}H]JNJ7777120 in house and to evaluate the suitability of this radioligand to study various H_4R orthologs.

To better understand the biological role of the different NPY receptor subtypes, especially of the NPY Y_2R, pharmacological tools such as radio- and fluorescent ligands are required.[19] Aiming at potent and subtype selective tracers for the Y_2R, a series of derivatives of BIIE 0246 was synthesized in our laboratory.[20] Application of the guanidine-acylguanidine bioisosteric approach resulted in the first tritiated Y_2R selective non-peptide radioligand, [^{3}H]UR-PLN196.[21] More detailed binding and functional studies revealed insurmountable antagonism versus pNPY and pseudo-irreversible binding at the Y_2R. In the final part, the synthesis and characterization of [^{3}H]UR-PLN208, a structurally related radiotracer is reported and binding as well as functional data are compared with [^{3}H]UR-PLN196 and their unlabeled analogs.

In summary, the first aim of this doctoral thesis was to design, synthesize and pharmacologically characterize new H_4R agonists to gain more information about structure-activity and structure-selectivity relationships and to develop H_4R subtype and selective compounds, which could serve as molecular determinants. The second part of this work focused on the synthesis of tritium-labeled radioligands for different GPCRs and their applicability as pharmacological tools.

2.1 References

1. Igel, P.; Dove, S.; Buschauer, A. Histamine H_4 receptor agonists. *Bioorg. Med. Chem. Lett.* **2010**, 20, 7191-7199.
2. Strasser, A.; Wittmann, H.-J.; Buschauer, A.; Schneider, E. H.; Seifert, R. Species-dependent activities of G-protein-coupled receptor ligands: lessons from histamine receptor orthologs. *Trends Pharmacol. Sci.* **2013**, 34, 13-32.
3. Schnell, D.; Brunskole, I.; Ladova, K.; Schneider, E.; Igel, P.; Dove, S.; Buschauer, A.; Seifert, R. Expression and functional properties of canine, rat, and murine histamine H_4 receptors in Sf9 insect cells. *Naunyn-Schmiedeberg's Arch. Pharmacol.* **2011**, 383, 457-470.
4. Savall, B. M.; Edwards, J. P.; Venable, J. D.; Buzard, D. J.; Thurmond, R.; Hack, M.; McGovern, P. Agonist/antagonist modulation in a series of 2-aryl benzimidazole H_4 receptor ligands. *Bioorg. Med. Chem. Lett.* **2010**, 20, 3367-3371.
5. Lim, H. D.; van Rijn, R. M.; Ling, P.; Bakker, R. A.; Thurmond, R. L.; Leurs, R. Evaluation of histamine H_1-, H_2-, and H_3-receptor ligands at the human histamine H_4 receptor: identification of 4-methylhistamine as the first potent and selective H_4 receptor agonist. *J. Pharmacol. Exp. Ther.* **2005**, 314, 1310-1321.
6. Ghorai, P.; Kraus, A.; Birnkammer, T.; Geyer, R.; Bernhardt, G.; Dove, S.; Seifert, R.; Elz, S.; Buschauer, A. Chiral N^G-acylated hetarylpropylguanidine-type histamine H_2 receptor agonists do not show significant stereoselectivity. *Bioorg. Med. Chem. Lett.* **2010**, 20, 3173-3176.
7. Ghorai, P.; Kraus, A.; Keller, M.; Götte, C.; Igel, P.; Schneider, E.; Schnell, D.; Bernhardt, G.; Dove, S.; Zabel, M.; Elz, S.; Seifert, R.; Buschauer, A. Acylguanidines as Bioisosteres of Guanidines: N^G-Acylated Imidazolylpropylguanidines, a New Class of Histamine H_2 Receptor Agonists. *J. Med. Chem.* **2008**, 51, 7193-7204.
8. Dove, S.; Elz, S.; Seifert, R.; Buschauer, A. Structure-activity relationships of histamine H_2 receptor ligands. *Mini. Rev. Med. Chem.* **2004**, 4, 941-954.
9. Igel, P.; Schneider, E.; Schnell, D.; Elz, S.; Seifert, R.; Buschauer, A. N^G-Acylated Imidazolylpropylguanidines as Potent Histamine H_4 Receptor Agonists: Selectivity by Variation of the N^G-Substituent. *J. Med. Chem.* **2009**, 52, 2623-2627.
10. Black, J. W.; Duncan, W. A.; Durant, C. J.; Ganellin, C. R.; Parsons, E. M. Definition and antagonism of histamine H_2-receptors. *Nature* **1972**, 236, 385-390.
11. Lim, H. D.; Smits, R. A.; Bakker, R. A.; vanDam, C. M. E.; deEsch, I. J. P.; Leurs, R. Discovery of *S*-(2-Guanidylethyl)-isothiourea (VUF 8430) as a Potent Nonimidazole Histamine H_4 Receptor Agonist. *J. Med. Chem.* **2006**, 49, 6650-6651.
12. Keen, M. The problems and pitfalls of radioligand binding. *Methods Mol. Biol.* **1995**, 41, 1-16.
13. Bylund, D. B.; Toews, M. L. Radioligand binding methods for membrane preparations and intact cells. In *Receptor Signal Transduction Protocols*, 2011/05/25 ed.; Willars, G. B.; Challiss, R. A. J., Eds., Springer: Leicester, **2011**; Vol. 746, pp 135-164.
14. Gajtkowski, G. A.; Norris, D. B.; Rising, T. J.; Wood, T. P. Specific binding of ^{3}H-tiotidine to histamine H_2 receptors in guinea pig cerebral cortex. *Nature* **1983**, 304, 65-67.
15. Ruat, M.; Traiffort, E.; Bouthenet, M. L.; Schwartz, J. C.; Hirschfeld, J.; Buschauer, A.; Schunack, W. Reversible and irreversible labeling and autoradiographic localization of the cerebral histamine H_2 receptor using [^{125}I]iodinated probes. *Proc. Natl. Acad. Sci. U.S.A.* **1990**, 87, 1658-1662.
16. Erdmann, D. Histamine H_2- and H_3- Receptor Antagonists: Synthesis and Characterization of Radiolabelled and Flourescent Pharmacological Tools. University of Regensburg, Regensburg, Doctoral Thesis, **2010**.
17. Jablonowski, J. A.; Grice, C. A.; Chai, W.; Dvorak, C. A.; Venable, J. D.; Kwok, A. K.; Ly, K. S.; Wei, J.; Baker, S. M.; Desai, P. J.; Jiang, W.; Wilson, S. J.; Thurmond, R. L.; Karlsson, L.; Edwards, J. P.; Lovenberg, T. W.; Carruthers, N. I. The First Potent and Selective Non-Imidazole Human Histamine H_4 Receptor Antagonists. *J. Med. Chem.* **2003**, 46, 3957-3960.

18. Thurmond, R. L.; Desai, P. J.; Dunford, P. J.; Fung-Leung, W. P.; Hofstra, C. L.; Jiang, W.; Nguyen, S.; Riley, J. P.; Sun, S.; Williams, K. N.; Edwards, J. P.; Karlsson, L. A potent and selective histamine H_4 receptor antagonist with anti-inflammatory properties. *J. Pharmacol. Exp. Ther.* **2004**, 309, 404-413.
19. Mittapalli, G. K.; Roberts, E. Ligands of the neuropeptide Y Y_2 receptor. *Bioorg. Med. Chem. Lett.* **2014**, 24, 430-441.
20. Pluym, N. Application of the Guanidine–Acylguanidine Bioisosteric Approach to NPY Y_2 Receptor Antagonists: Bivalent, Radiolabeled and Fluorescent Pharmacological Tools. University of Regensburg, Regensburg, Doctoral thesis, **2011**.
21. Pluym, N.; Baumeister, P.; Keller, M.; Bernhardt, G.; Buschauer, A. [^{3}H]UR-PLN196: a selective nonpeptide radioligand and insurmountable antagonist for the neuropeptide Y Y_2 receptor. *ChemMedChem* **2013**, 8, 587-593.

Chapter 3

Synthesis and Pharmacological Characterization of 2-Arylbenzimidazoles as Potent and Selective Histamine H_4 Receptor Ligands

3.1 Introduction

Although the number of ligands addressing the H_4R is continuously increasing, their potential value in the treatment of immunological and inflammatory diseases such as asthma and rheumatoid arthritis has still to be proven. Potent and selective ligands including agonists are required as pharmacological tools to further explore the (patho)physiological function of the H_4R. However, the investigation of numerous H_4R agonists in animal models is hampered by species-dependent discrepancies regarding potencies and histamine receptor subtype selectivities.[1,2] Recently, Savall *et al.* identified 2-arylbenzimidazoles as highly potent and selective hH_4R ligands.[3] Highest potency and selectivity over the other H_xR subtypes were reported to reside in a compound with a specific substitution pattern including methyl and fluorine residues at the benzimidazole and a histamine moiety (**3.16** cf. Figure 3.1 and Scheme 3.2). As part of a project on histamine H_4R ligands, the aim of the present work was to synthesize a small library of compounds related to **3.16** and to elucidate the structure-activity- and structure-selectivity relationships on human histamine receptors ($hH_{1,2,3,4}R$) and the murine H_4R, recombinantly expressed in Sf9 insect cells, using GTPγS binding- and steady-state GTPase-assays, as well as radioligand binding experiments.

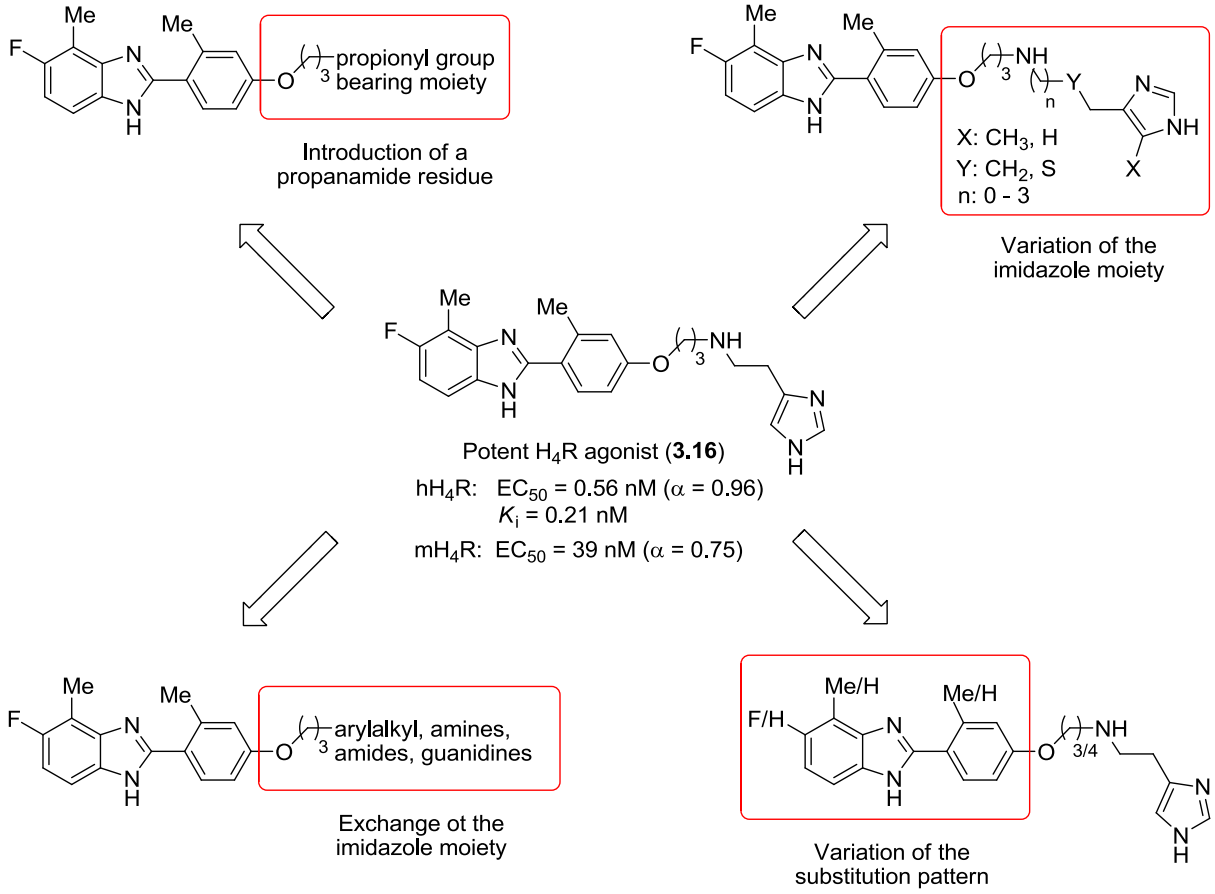

Figure 3.1 Structural variation in a series of 2-arylbenzimidazoles derived from **3.16**.[3]

Emphasis will be put on the substitution pattern at the benzimidazole moiety of **3.16**. Moreover, the number of basic centers will be varied to elucidate their influence on hH_4R binding and selectivity. The imidazole-bearing moiety will be modified with respect to a series of histamine analogs previously published[1,4] and replaced by non-imidazole moieties, aiming at improved H_4R selectivity compared to the other H_xR subtypes. In our laboratory the introduction of a tritium-labeled propionyl group is well-established as a strategy for the development of new radioligands.[5-8] Therefore, a series of 2-arylbenzimidazoles bearing a propionic amide or a N^G-propionylated acylguanidine group was synthesized in 'cold form' and investigated for binding to the H_xR subtypes.

3.2 Chemistry

As shown in Scheme 3.1 and Scheme 3.2, the 2-arylbenzimidazoles **3.16**-**3.20** were synthesized following the procedure of Savall *et al.*[9] starting with an oxidation of the respective benzene-1,2-diamine and 4-hydroxybenzaldehyde derivative with $Na_2S_2O_5$ to form the benzimidazoles **3.7**-**3.10**. *O*-Alkylation with the respective bromo-chloro-alkane and coupling with trityl-protected histamine **3.2**, followed by acidic deprotection, led to the 2-arylbenzimidazoles **3.16**-**3.20**. The protection of the histamine was carried out with triphenylmethyl chloride (Trl-Cl) according to Ghorai *et al.*[10] (cf. Scheme 3.2). The synthesis of **3.22** and **3.23** followed the same principle. Alkylation with Boc-protected 3-bromopropanamine **3.21** and acidic deprotection yielded **3.22** and **3.23**, which were both pharmacologically investigated and used as building blocks for further synthesis.

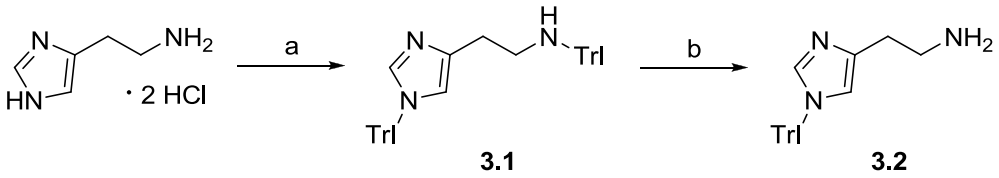

Scheme 3.1 Synthesis of **3.2**. Reagents and conditions: (a) Trl-Cl, NEt_3, $CHCl_3$, 0 °C-rt, 27 h, 46%; (b) 5% TFA in CH_2Cl_2, 0 °C - rt, 4 h, 61%.

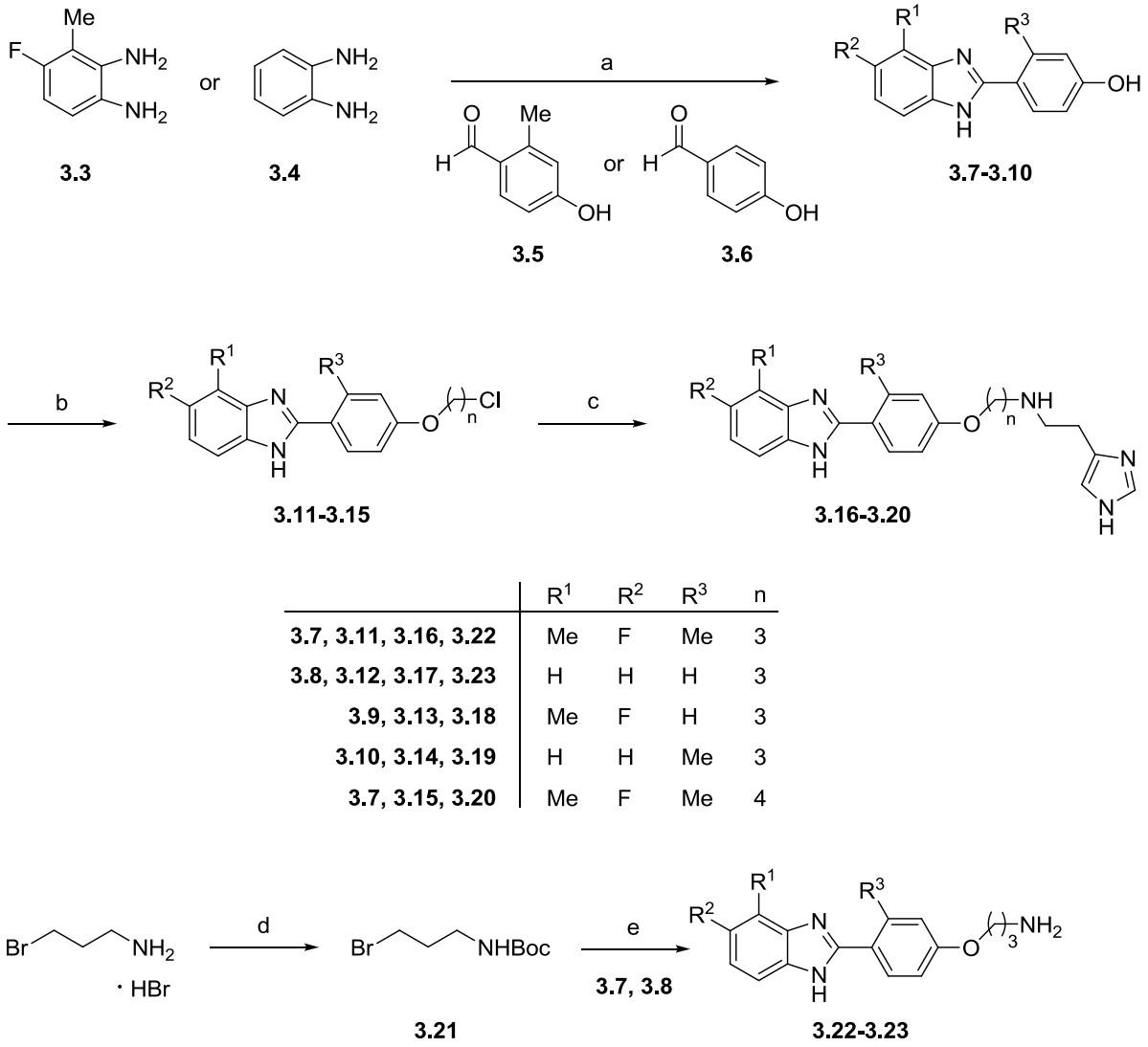

	R^1	R^2	R^3	n
3.7, 3.11, 3.16, 3.22	Me	F	Me	3
3.8, 3.12, 3.17, 3.23	H	H	H	3
3.9, 3.13, 3.18	Me	F	H	3
3.10, 3.14, 3.19	H	H	Me	3
3.7, 3.15, 3.20	Me	F	Me	4

Scheme 3.2 Synthesis of the benzimidazole derivatives **3.16**-**3.20**, **3.22** and **3.23**. Reagents and conditions: (a) **3.5** or **3.6**, $Na_2S_2O_5$, DMF, 90 °C, 2 h, 61-95%; (b) Cs_2CO_3, MeCN, 1-bromo-3-chloropropane or 1-bromo-4-chlorobutane, 70 °C, 17 h, 16-62%; (c) K_2CO_3, NaI, 2-(1-trityl-1*H*-imidazol-4-yl)ethanamine (**3.2**), *n*-butanol, 90 °C, 15-94 h, 14-24%; (d) 3-bromopropylamine hydrobromide, Boc_2O, DIPEA, CH_2Cl_2, rt, 18 h, 74%; (e) 1) **3.7** or **3.8**, Cs_2CO_3, MeCN, 70 °C, 17 h; 2). TFA, CH_2Cl_2, rt, 5-8 h, 27-30%.

The guanidine **3.26** was prepared, according to Feichtinger *et al.*[11], from guanidine hydrochloride by di-Boc protection (**3.24**), followed by the reaction of **3.24** with trifluoromethane sulfonic anhydride to give **3.25**. Subsequently, **3.23** was treated with the guanidinylating reagent **3.25** under mild basic conditions releasing triflic amide, which could be easily removed by aqueous work-up. Finally, cleavage of the Boc-protecting groups gave **3.26** (cf. Scheme 3.3).

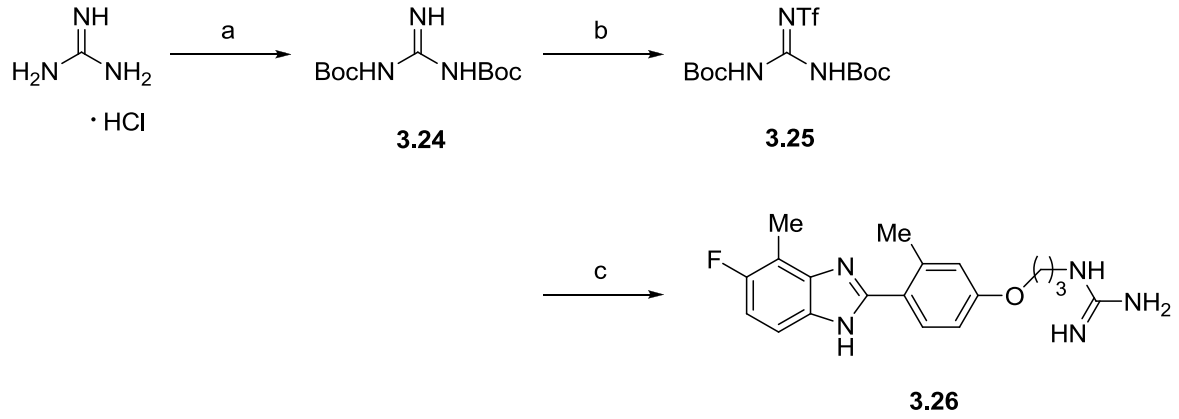

Scheme 3.3 Synthesis of the guanidine derivative **3.26**. Reagents and conditions: (a) Guanidine hydrochloride, Boc_2O, NaOH, water/dioxane, 0 °C-rt, 26 h, 35%; (b) triflic anhydride, NEt_3, CH_2Cl_2, -78 °C-rt, 4h, 81%; (c) **3.22**, NEt_3, CH_2Cl_2, rt, 3 h, 33%.

The N^G-acylated guanidine **3.30** was prepared according to the synthetic pathway outlined in Scheme 3.4 from amine **3.22** and *N*-Boc-protected *N*'-(propionyl)-*S*-methylisothiourea (**3.29**), which was obtained *via* a three-step synthesis. *N*-Boc protected *S*-methylisothiourea (**3.28**) was synthesized as described previously.[12-14] Subsequently, **3.28** was treated with propionic acid under standard conditions for amide coupling, using TBTU and NEt_3.[15] Treatment of the amine **3.22** with the guanidinylating reagent **3.29** in the presence of $HgCl_2$ - the metal ion reacts as a desulfurizing agent *via* complex formation[16,17] - followed by Boc-deprotection with trifluoroacetic acid yielded the acylguanidine **3.30.**

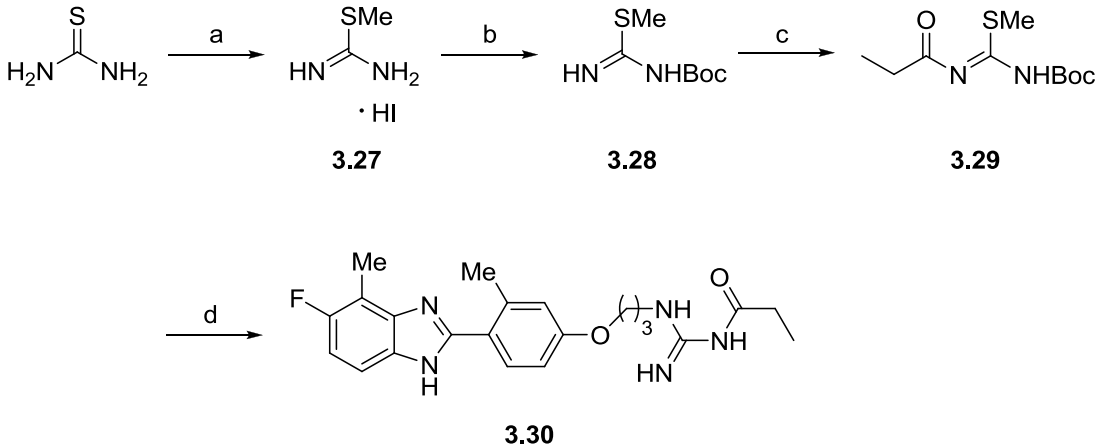

Scheme 3.4 Synthesis of the acylated guanidine **3.30**. Reagents and conditions: (a) Thiourea, MeI, MeOH, rt, 1 h, 98%; (b) Boc_2O, NEt_3, rt, 20 h, 74%; (c) propionic acid, TBTU, DIPEA, rt, O/N, 89%; (d) 1) **3.22** (as free base), $HgCl_2$, NEt_3, CH_2Cl_2, rt, 20 h; 2) TFA, CH_2Cl_2, rt, 5 h, 71%.

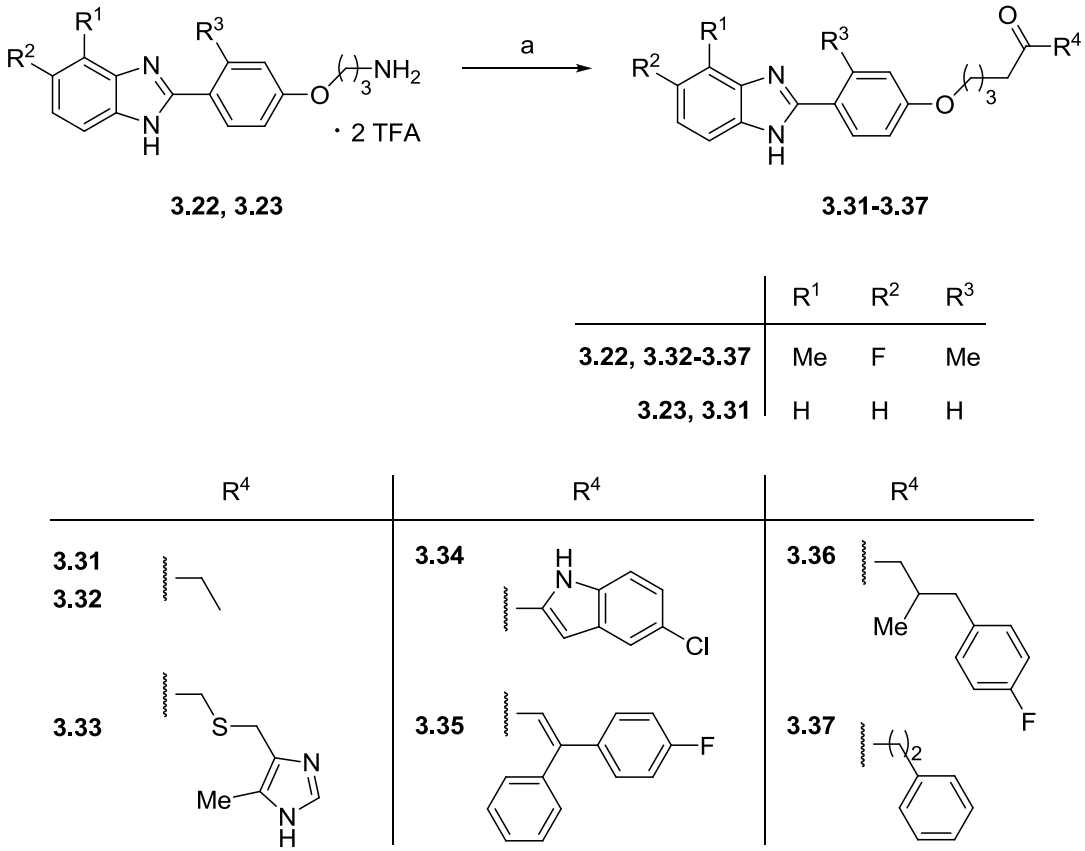

Scheme 3.5 Synthesis of the amides **3.31**-**3.37**. Reagents and conditions: (a) For **3.31**, **3.32**: **3.22** or **3.23**, propionic acid, EDC × HCl, HOBt × H_2O, DIPEA, THF, rt, 22 h, 41-48%; for **3.33**-**3.36**: **3.22**, respective acid, TBTU, DIPEA, DMF, rt, 20 h, 13-55%; for **3.37**: **3.22**, 3-phenylpropanoyl chloride, DIPEA, CH_2Cl_2, 0 °C-rt, 9 h, 59%.

The amides **3.31**-**3.37** were prepared as highlighted in Scheme 3.5. The guanidine building blocks **3.22** and **3.23** were coupled to propionic acid using EDC and HOBt as coupling reagents to give the amides **3.31** and **3.32**. The compounds **3.33**-**3.36** were synthesized by acylation with UR-PG139[10] (for **3.33**), 5-chloroindole-2-carboxylic acid (for **3.34**), UR-PG17[18] (for **3.35**) and UR-AK318[12] (for **3.36**) using TBTU as coupling reagent. 5-Chloroindole-2-carboxylic acid (TCI, Tokyo, Japan) is commercially available, UR-AK318,[19] UR-PG17 and UR-PG139[18] were available in our laboratory. The amine **3.22** was allowed to react with the commercially available 3-phenylpropanoyl chloride under basic conditions to afford compound **3.37**.

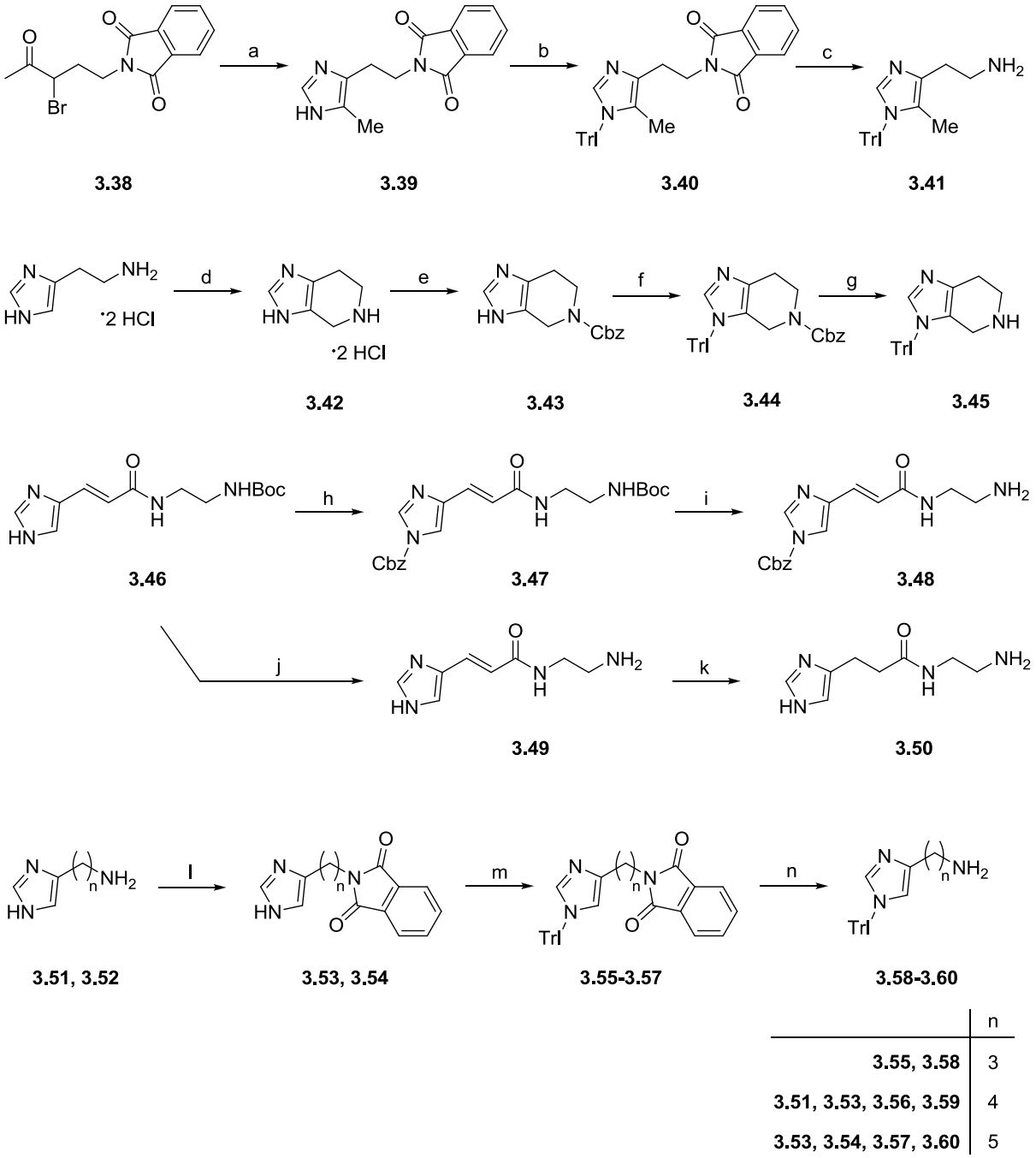

	n
3.55, 3.58	3
3.51, 3.53, 3.56, 3.59	4
3.53, 3.54, 3.57, 3.60	5

Scheme 3.6 Synthesis of the imidazole derivatives **3.41, 3.45, 3.48**-**3.50** and **3.58**-**3.60** . Reagents and conditions: (a) Formamide, 170 °C, 4 h, 48%; (b) Trl-Cl, NEt_3, MeCN, rt, 27 h, 95%; (c) hydrazine x H_2O, EtOH, rt, 24 h, 96%; (d) histamine x 2 HCl, dimethoxymethane, 0.01 M HCl, reflux, 19 h, 72%; (e) benzyl succinimidyl carbonate, NEt_3, CH_2Cl_2, 0 °C-rt, 1 h, 58%; (f) Trl-Cl, NEt_3, MeCN, rt, 24 h, 66%; (g) Pd/C, H_2, MeOH, rt, 4 h, 90%; (h) benzyl chloroformate, NEt_3, DMF, rt, 24 h, 81%; (i) TFA, CH_2Cl_2, rt, 4 h , 96%; (j) TFA, CH_2Cl_2, rt, 4 h , 98%; (k) Pd/C, H_2, MeOH, rt, 20 h, 88%; (l) phthalic anhydride, NEt_3, toluene, reflux, 24 h, 48-53%; (m) Trl-Cl, NEt_3, MeCN, rt, 24 h, 40-91%; (n) hydrazine x H_2O, EtOH or *n*-BuOH, rt, 24 h, 96-100%.

The amines required for the preparation of imidazole-containing ligands **3.62**-**3.64**, **3.67**, **3.70** and **3.71** had to be protected as depicted in Scheme 3.6. The trityl-protected 5-methylhistamine derivative **3.41** was prepared starting from 2-(3-bromo-4-oxopentyl)isoindoline-1,3-dione (**3.38**),[20]

which was allowed to react with formamide according to a *Bredereck* synthesis[21] to give the imidazole **3.39**. After trityl protection of the imidazole (**3.40**) and hydrazinolysis of the phthalimide group, **3.41** was obtained in good yield. The intermediate **3.42** (spinaceamine) was achieved by a modified *Pictet-Spengler* reaction[22,23] with histamine and dimethoxymethane in 0.01 M HCl. Cbz-protection of the amine with benzyl succinimidyl carbonate, followed by trityl-protection of the imidazole and cleavage of the Cbz group by hydrogenolysis gave **3.45**. The imidazole derivatives **3.49** and **3.50**, which were also tested for hH_4R affinity, were obtained from UR-MK251 (**3.46**), which was synthesized by Dr. Max Keller, after acidic Boc-deprotection (**3.49**) and hydrogenation over Pd/C catalyst (**3.50**). For the coupling with the benzimidazole **3.22**, the imidazole in UR-MK251 (**3.46**) was protected with Cbz. Subsequently, the Boc group was removed under acidic conditions to produce the primary amine **3.48**. To incorporate homohistamine (n = 3) in **3.22**, compound **3.55**[24] was converted to **3.58** by hydrazinolysis of the phthalimide group. Imbutamine (**3.51**,[20] n = 4) and impentamine (**3.52**,[24] n = 5), were available in our laboratory. Compounds **3.53** and **3.54** were obtained from the reaction of the corresponding amine (**3.51** or **3.52**) with phthalic anhydride. Trityl protection of the imidazole, followed by hydrazinolysis of the phthalimide group afforded the trityl protected primary amines **3.59** and **3.60**.

Preparation of the compounds **3.62**-**3.73** (cf. Scheme 3.7) started from **3.11** (cf. Scheme 3.2), which was converted to the corresponding iodinated analog (**3.61**) under *Finkelstein*[25] conditions. Conversion of the respective primary amines (**3.41** for **3.62**; **3.58** for **3.63**, **3.59** for **3.64**, 5-methylimbutamine[20] for **3.65**, thia-5-methylimbutamine[26] for **3.66**, **3.60** for **3.67**, mono-Boc protected ethandiamine UR-MK74,[27] for **3.68**, **6.1** for **3.69**, **3.48** for **3.70**, **3.45** for **3.71**, **6.3** for **3.72**) to the secondary amines **3.62-3.73** was performed by heating in a microwave oven with **3.61** in acetonitrile (Scheme 3.7). Subsequently, acidic deprotection was performed if required. Preparation of **3.75** started from the *N*-Boc-protected derivative of **3.68** (**3.73**), followed by Cbz-protection of the secondary amine. Subsequently, acidic Boc-deprotection, propionylation with succinimidyl propionate under basic conditions and cleavage of the Cbz group by hydrogenolysis yielded **3.75**. Hydrogenolysis was performed in methanol in the presence of TFA to prevent methylation of the secondary amine.[28] The propionylated compound **3.76** was obtained by conversion of **3.69** with the help of succinimidyl propionate.

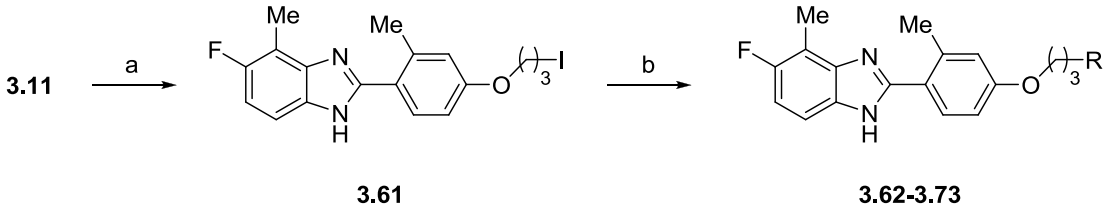

3.61 **3.62-3.73**

	X	Y	n
3.62	CH_3	CH_2	0
3.63	H	CH_2	1
3.64	H	CH_2	2
3.65	CH_3	CH_2	2
3.66	CH_3	S	2
3.67	H	CH_2	3

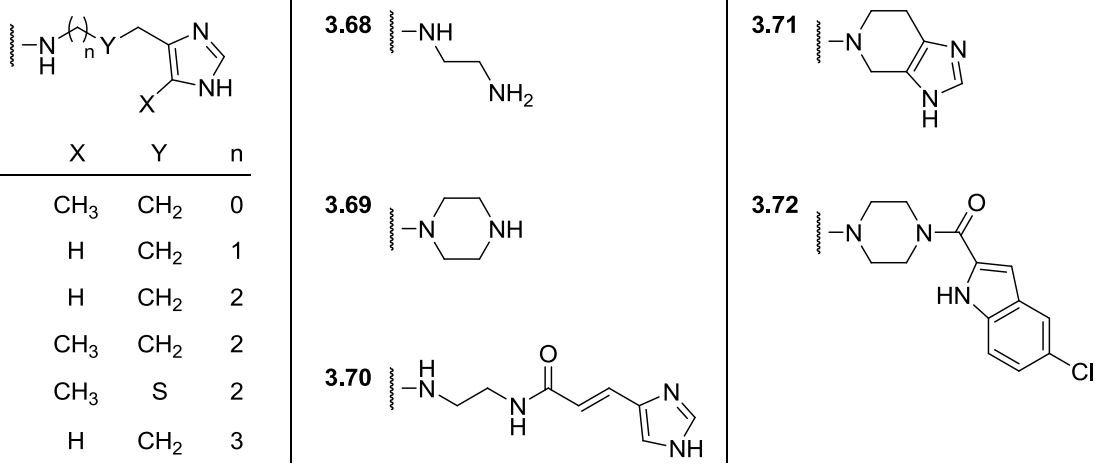

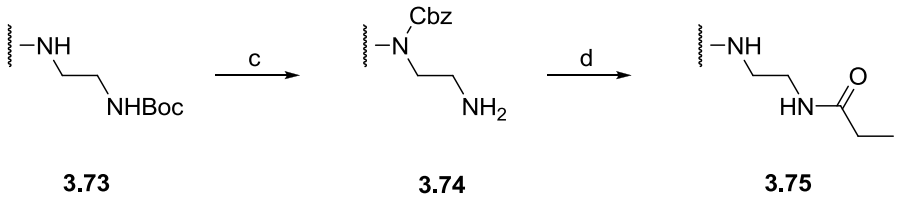

3.73 **3.74** **3.75**

3.76

Scheme 3.7 Synthesis of the compounds **3.61**-**3.76**. Reagents and conditions: (a) NaI, acetone, reflux, 72 h, 90%; (b) 1) respective amine, K_2CO_3, MeCN, microwave 130 °C, 20 min, for **3.62**-**3.64** and **3.67**-**3.73**: 2) TFA, CH_2Cl_2, rt, 5-8 h, 28-65%; (c) 1) benzyl chloroformate, NEt_3, CH_2Cl_2, 0 °C-rt, 24 h; 2) TFA, CH_2Cl_2, rt, 4 h, 55%; (d) 1) succinimidyl propionate, NEt_3, MeCN/DMF, 24 h, rt; 2) Pd/C, H_2, TFA, MeOH, rt, 16 h, 65%; (e) succinimidyl propionate, NEt_3, MeCN, 24 h, rt, 76%.

3.3 Pharmacological Results and Discussion

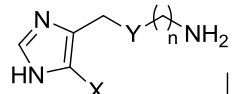

	X	Y	n
Histamine	H	CH_2	0
Homohistamine	H	CH_2	1
Imbutamine	H	CH_2	2
Impentamine	H	CH_2	3
5-Methylhistamine	CH_3	CH_2	0
5-Methylimbutamine	CH_3	CH_2	2
Thia-5-Methyl-imbutamine	CH_3	S	2

Figure 3.2 Structure of histamine and its analogs.

The synthesized 2-arylbenzimidazoles **3.16**-**3.20**, **3.22**, **3.23**, **3.26**, **3.30**-**3.37**, **3.62**-**3.72**, **3.75** and **3.76**, as well as the building blocks **3.42** (spinaceamine), **3.49** and **3.50** were investigated at the hH_1R, hH_2R, hH_3R and hH_4R in radioligand binding assays using membrane preparations of Sf9 insect cells expressing the hH_1R + RGS4, hH_2R–$Gs_{\alpha s}$ fusion protein, hH_3R + $G\alpha_{i2}$ + $G\beta_1\gamma_2$ or hH_4R + $G\alpha_{i2}$ + $G\beta_1\gamma_2$, respectively.[29] Moreover, the reference H_4R ligands histamine, homohistamine, imbutamine, impentamine, 5-methylhistamine, 5-methylimbutamine and thia-5-methylimbutamine[30] were included (Figure 3.2). The most promising compounds **3.16**-**3.19**, **3.22**, **3.23**, **3.30**-**3.32**, **3.62**-**3.65**, **3.67**, **3.70** and **3.71** were tested for agonism and antagonism at the hH_1R in [^{33}P]GTPase binding assays using membrane preparations of Sf9 insect cells expressing the hH_1R + RGS4,[31-34] at the hH_2R, hH_3R and hH_4R in [^{35}S]GTPγS binding assays using membrane preparations of Sf9 insect cells expressing the hH_2R–$Gs_{\alpha s}$ fusion protein,[35,36] expressing the hH_3R + $G\alpha_{i2}$ + $G\beta_1\gamma_2$[37,38] or expressing the hH_4R plus $G\alpha_{i2}$ plus $G\beta_1\gamma_2$ (cf. Figure 3.3).[33] To verify whether the response was H_4R mediated, the K_b values of standard neutral antagonists were determined from the concentration-dependent inhibition of 2-arylbenzimidazole **3.16**induced increase in [^{35}S]GTPγS binding. Moreover, with respect to the potential use of the synthesized H_4R ligands in translational animal models, selected compounds were analysed in radioligand binding studies using HEK293 cells stably expressing the murine H_4R and in [^{35}S]GTPγS binding assays using membrane preparations of Sf9 insect cells expressing the mH_4R + $G\alpha_{i2}$ + $G\beta_1\gamma_2$. In the following, agonistic potencies are expressed as EC_{50} values. Intrinsic activities (α) refer to the maximal response induced by the standard agonist histamine, unless otherwise stated. Compounds identified to be inactive as agonists (α< 0.1 or negative values, respectively), were also investigated in the antagonist mode. The corresponding K_b values of neutral antagonists and inverse agonists were determined from the concentration-dependent inhibition of the histamine-induced increase in [^{35}S]GTPγS binding or [^{33}P]GTPase cleavage. Binding data represent K_i values determined by displacement of [^{3}H]pyrilamine (hH_1R), [^{3}H]UR-DE257 (hH_2R), [^{3}H]N^{α}-methylhistamine (hH_3R), [^{3}H]histamine (hH_4R) or [^{3}H]UR-PI294[5] (mH_4R).

3.3.1 Histamine receptor subtype affinities of the synthesized compounds

3.3.1.1 Variation of the substitution pattern

The investigation of compound **3.16** in radioligand binding assays revealed discrepancies compared to published data (Figure 3.4, Table 3.1).[3] The affinity was 50-fold lower at the hH_4R (K_i = 11.2 ± 1.8 nM) than reported by Savall *et al.* (0.21 nM).[3] The pharmacological evaluation of the 2-arylbenzimidazoles **3.17**-**3.19** with a modified substitution pattern at the hH_4R revealed nearly identical K_i values (8.5 to 14.4 nM). As shown for compound **3.20**, the elongation of the linker had no effect on hH_4R affinity. The hH_3R affinities of **3.16**-**3.20** were comparable (486-1270 nM), however the hH_2R affinities for **3.17** and **3.18** were 10-fold lower than those of **3.16** and **3.19**, indicating that the omission of the *O*-methyl group at the phenyl ring increases the hH_4R selectivity compared to the hH_2R. Nevertheless, this group is important for functional activity at hH_4R and affinity at the mH_4R (see below). The hH_1R affinities were low and comparable to the reported data (K_i = 5380-16500 nM).[3]

3.3.1.2 Structural variations of arylbenzimidazole-type hH_4R ligands

As an imidazole moiety is known to reduce hH_4R selectivity compared to the other histamine receptor subtypes, the compounds **3.26**, **3.34**-**3.37**, **3.68**, **3.69** and **3.72** were investigated for their affinity at the hH_4R and selectivity towards the other H_xR subtypes. Unfortunately, most of the tested compounds had only very weak affinity at the hH_4R. The guanidine **3.26** revealed a lower affinity at the hH_4R compared to **3.16**, no affinity at the hH_3R, but retained affinity at the hH_2R. The carboxamide **3.34-3.37** showed almost no binding to the hH_xR subtypes. It may be speculated that bulky aromatic residues are not tolerated in this position. It is more likely that, apart from the benzimidazole moiety, an additional basic center should be present to enable H_3R and H_4R binding. However, a guanidine group alone appears to be inappropriate. The introduction of a diamine led to a decrease in hH_4R binding in case of **3.68** (20-fold) and **3.69** (4-fold), whereas the selectivities over the other H_xR subtypes remained unchanged for both compounds. The incorporation of a moiety that corresponds to the structure of the H_4R antagonist JNJ7777120 (**3.72**, cf. Chapter 6) resulted in a drastic loss in affinity at the hH_4R as well as for the hH_2R and hH_3R. Summed up, only compounds bearing two basic amino functions showed sufficient affinity at the hH_4R. The most promising bioisosteres of the imidazole ring are nitrogen-containing aliphatic residues or heterocycles bearing two basic moieties.

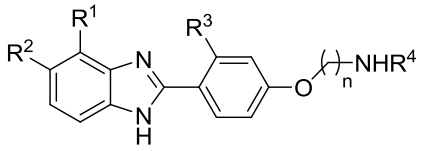

	R^1	R^2	R^3	R^4	n
3.16	Me	F	Me	Histamine	3
3.17	H	H	H	Histamine	3
3.18	Me	F	H	Histamine	3
3.19	H	H	Me	Histamine	3
3.20	Me	F	Me	Histamine	4
3.22	Me	F	Me	H	3
3.23	H	H	H	H	3
3.31	H	H	H	$C(O)CH_2CH_3$	3
3.32	Me	F	Me	$C(O)CH_2CH_3$	3

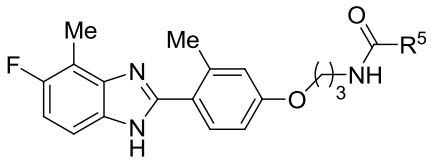

R^5	R^5
3.33 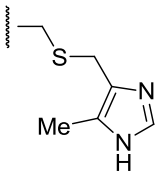	**3.36** 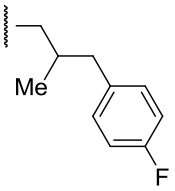
3.34 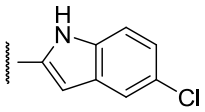	**3.37** 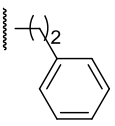
3.35 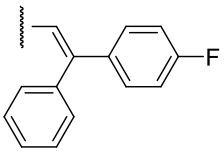	

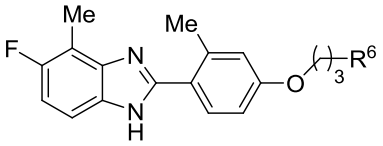

R^6	R^6	R^6
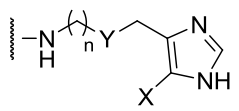	**3.26** 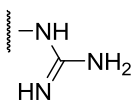	**3.71** 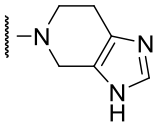
	3.30 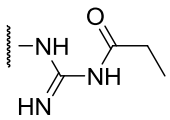	**3.72** 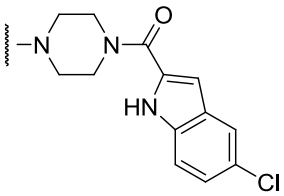
	3.68 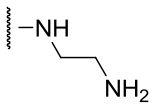	**3.75** 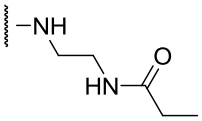
	3.69 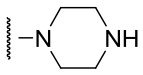	**3.76** 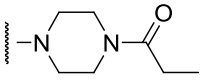
	3.70 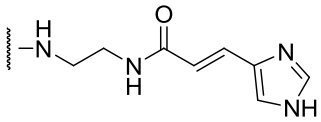	

	X	Y	n
3.62	CH_3	CH_2	0
3.63	H	CH_2	1
3.64	H	CH_2	2
3.65	CH_3	CH_2	2
3.66	CH_3	S	2
3.67	H	CH_2	3

Figure 3.3 Structures of the investigated 2-arylbenzimidazoles.

The data for higher homologs of histamine and their ring-substituted or conformationally constrained analogs coupled with a 2-arylbenzimidazole building-block (**3.62**-**3.67**, **3.71**), compared

to the histamine analog **3.16** and previously published data,[4] are summarized in Table 3.1. In general, these compounds, except for **3.66** (K_i = 13.1 nM), revealed similar hH_4R affinities (K_i = 0.58-8.7 nM) and were higher as for **3.16**. Highest affinity for the hH_4R within this series resided in compound **3.64**; the K_i value was in the sub-nanomolar range (0.58 nM) and 20-fold lower than that determined for **3.16** in our laboratory. Lowest hH_3R affinity was found for **3.71** (for hH_4R: K_i = 5.1 nM, ref: 3.3 nM;[3] for hH_3R: K_i = 18400 nM, cf. Figure 3.4) corresponding to an over 3600-fold selectivity for the hH_4R and also an over 270-fold selectivity over the hH_2R. Contrary to this, spinaceamine (**3.42**) alone afforded almost no hH_4R affinity. By analogy with histamine and imbutamine, methyl substitution at the 5-imidazolyl ring resulted in a preference for the hH_4R (for **3.62**: 480-fold, for **3.65**: 145-fold over the hH_3R). The selectivities for the demethylated homologs were lower (60-fold for **3.16** and 85-fold for **3.64**, respectively). In addition, the derivative **3.67**, providing a five membered linker, showed a slight preference for the hH_3R (K_i = 4.8 nM) than for the hH_4R (K_i = 8.7 nM) and remarkably high affinity for the hH_2R (K_i = 41.2 nM). Highest binding affinity at the hH_2R was determined for imidazole **3.70**. With a K_i value of 14.5 nM at the hH_2R this compound revealed almost 50-fold selectivity for the hH_2R over the hH_3R and almost 150-fold selectivity over the hH_4R, respectively. In contrast, the structurally related building block **3.49**, as well as its reduced derivative **3.50**, showed no affinity at the hH_2R. This makes **3.70** an excellent starting point to explore the structural requirements for hH_2R selectivity in this class of compounds. Hence, imidazole derivatives with further elongated spacers would most probably not result in improved hH_4R affinity. Instead, future prospects herein should focus on the synthesis of conformationally constrained spacers to further explore the structure-activity relationships of hH_4R preferring 2-arylbenzimidazoles. The K_i values of **3.62**-**3.67** and **3.71** at the hH_2R were comparable and in the range of 200 to 1400 nM.

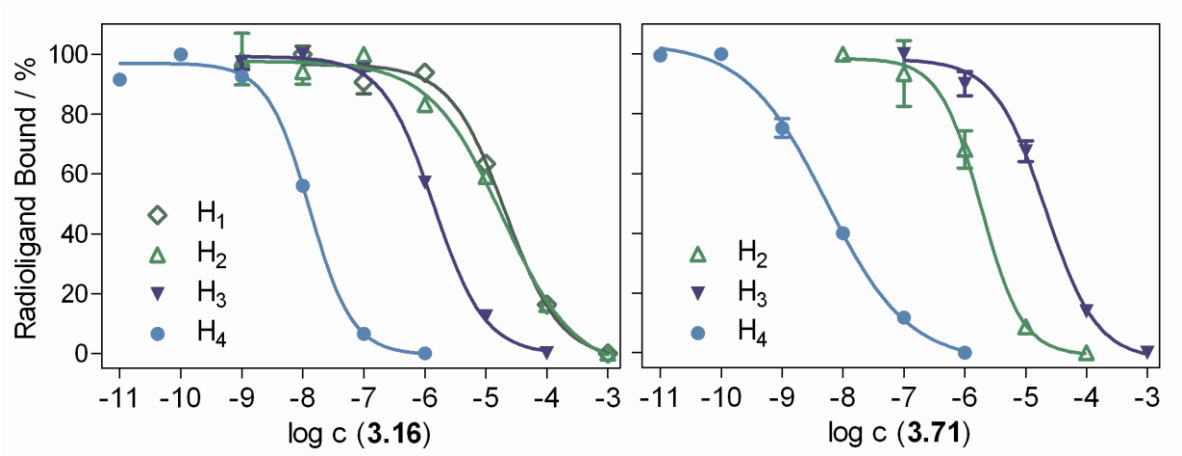

Figure 3.4 Competition binding curves of **3.16** and **3.71** at hH_xR subtypes.

Regardless of being known as a building block for the preparation of cimetidine, compound **3.66**, the thia-analog of 5-methylimbutamine, did not prefer the H_2R, but revealed an over 240-fold selectivity for the hH_4R compared to the hH_2R and an over 360-fold selectivity over the hH_3R, although the hH_4R affinity (K_i = 13.1 nM) was lower than for other homologs in this series. In contrast, compound **3.30**, in which the secondary amine of **3.66** is exchanged by an amide, showed an over 350-fold higher hH_4R affinity, indicating that this basic functionality is crucial for hH_4R binding.

3.3.1.3 Introduction of a propionyl group

The introduction of a tritium-labeled propionyl group has been established as a strategy for the synthesis of new radioligands for GPCRs.[5-8] Therefore, a series of 2-arylbenzimidazoles with a propionic amide or a N^G-propionyl guanidine moiety was synthesized and investigated for affinity towards the H_xR subtypes. These investigationsligands revealed quite promising results, stimulating the search for hH_4R radioligands. The results for the propionyl group bearing molecules **3.30**-**3.32**, **3.75** and **3.76** are presented in Table 3.1. Propionylation of the amino group in **3.22** and **3.23** abolished the hH_4R binding, obviously due to the missing basic center in this changed part of the molecule as mentioned above. The propionylation of the primary amine in **3.68** led to a 17-fold loss of affinity at the hH_4R (**3.75**, K_i = 3850 nM). Highest affinity for the hH_4R within this set of propionylated compounds was determined for **3.76** with a K_i of 132 nM. The exchange of the ethylene linker in **3.75** with a piperazine afforded an almost 30-fold increase in affinity. Unlike most of the other investigated compounds, **3.76** showed almost no binding to the hH_2R and hH_3R. Even though the affinity of **3.76** is too low for being considered a potential radioligand, the lack of affinity at the other hH_xR subtypes is a promising starting point for the development of new 2-arylbenzimidazole-type ligands, including compounds bearing different nitrogen-containing heterocycles as well as an appropriate group for radiolabeling in the center of the molecule. Surprisingly, ligand **3.30** bound to the hH_2R with a K_i value in a low three-digit nanomolar range (K_i = 101 nM), with an over 360-fold selectivity over the hH_3R receptor and a 30-fold selectivity over the hH_4R. This compound could be a starting point in the search for novel hH_2R ligands (cf. **3.70**), especially regarding radioligands, because the available radioligands (cf. Chapter 5) are far from being ideal.

Table 3.1 K_i values of the synthesized 2-arylbenzimidazoles and histamine analogs at the hH_xR subtypes determined in radioligand binding studies.[a]

Compound	hH_1R		hH_2R		hH_3R		hH_4R		Selectivity
	K_i / nM	n	K_i / nM	n	K_i / nM	n	K_i / nM	n	H_2:H_3:H_4
Histamine	200[b]		534 ± 52	3	20.1 ± 3.1	4	13.1 ± 1.1	4	41 : 1.5 : 1
Homohistamine	n.d.		n.d.		94.4 ± 0.4	2	31.8 ± 11.3	3	- : 3 : 1
Imbutamine	n.d.		n.d.		4.3 ± 0.8	2	12.7 ± 0.8	2	- : 1 : 3
Impentamine	n.d.		n.d.		36.9 ± 7.0	2	627 ± 63	3	- : 1 : 17
5-Methylhistamine	n.d.		n.d.		9940 ± 1400	2	28.5 ± 4.4	3	- : 349 : 1
5-Methylimbutamine	n.d.		n.d.		639 ± 227	2	68.8 ± 14.5	3	- : 9.3 : 1
Thia-5-Methylimbutamine	n.d.		n.d.		1670	1	1460	1	- : 1.2 : 1
3.16	10800 ± 840	2	548 ± 208	3	673 ± 190	2	11.2 ± 1.8	3	49 : 60 : 1
3.17	10400 ± 400	2	6490 ± 270	2	1020 ± 30	2	8.5 ± 0.4	2	764 : 120 : 1
3.18	5380 ± 360	2	3660 ± 704	2	486 ± 15	2	14.4 ± 0.5	2	254 : 34 : 1
3.19	16500 ± 1500	2	516 ± 168	2	1270 ± 130	2	10.5 ± 0.5	2	49 : 121 : 1
3.20	n.d.		734 ± 170	2	810 ± 110	3	7.0 ± 2.0	3	105 : 116 : 1
3.26	n.d.		2000 ± 565	2	> 50000	2	3100 ± 120	2	1 : - : 1.6
3.30	n.d.		101 ± 16	3	36800 ± 13200	3	3350 ± 1040	2	1 : 364 : 33
3.31	n.d.		n.a.[c]	2	n.a.[c]	2	> 30000	2	-
3.32	n.d.		n.a.[c]	2	n.a.[c]	2	> 50000	2	-
3.33	n.d.		> 10000	2	> 50000	2	4610 ± 1360	3	-
3.34	n.d.		n.a.[c]	2	5550 ± 2260	2	n.a.[c]	2	-
3.35	n.d.		> 30000	2	> 30000	2	> 50000	2	-
3.36	n.d.		n.a.[c]	2	n.a.	2	> 50000	2	-
3.37	n.d.		n.d.	-	n.a.[c]	2	n.a.[c]	2	-

Table 3.1 (continued)

Compound	hH_1R		hH_2R		hH_3R		hH_4R		Selectivity
	K_i / nM	n	K_i / nM	n	K_i / nM	n	K_i / nM	n	H_2:H_3:H_4
3.42	n.d.		> 30000	2	7880 ± 290	2	5050 ± 54	2	- : 1.6 : 1
3.49	n.d.		n.a.[c]	2	n.a.[c]	2	2350 ± 360	2	-
3.50	n.d.		n.a.[c]	2	9450 ± 1280	3	n.a.[c]	2	-
3.62	n.d.		377 ± 111	3	1190 ± 10	2	2.5 ± 0.6	5	151 : 476 : 1
3.63	n.d.		308 ± 57	2	68.4 ± 9.8	3	3.6 ± 1.6	3	86 : 19 : 1
3.64	n.d.		223 ± 84	2	49.0 ± 14.1	3	0.58 ± 0.20	4	385 : 85 : 1
3.65	n.d.		391 ± 194	2	421 ± 19	4	2.9 ± 0.2	3	135 : 145 : 1
3.66	n.d.		3140 ± 580	2	4750 ± 470	2	13.1 ± 1.5	4	240 : 363 : 1
3.67	n.d.		41.2 ± 5.8	2	4.8 ± 0.5	2	8.7 ± 2.3	4	8.6 : 1 : 1.8
3.68	n.d.		> 20000	2	9830 ± 1550	2	231 ± 28	2	- : 43 : 1
3.69	n.d.		> 10000	2	4150 ± 1040	3	40.0 ± 19.8	2	- : 104 : 1
3.70	n.d.		14.5 ± 3.8	3	686 ± 21	2	2150 ± 970	3	1 : 47 : 148
3.71	n.d.		1390 ± 190	2	18400 ± 990	2	5.1 ± 0.9	3	273 : 3610 : 1
3.72	n.d.		> 20000	2	> 40000	2	6940 ± 410	2	-
3.75	n.d.		> 20000	2	>40000	2	3850 ± 840	2	-
3.76	n.d.		> 50000	2	> 80000	2	132 ± 51	3	-

[a] Determination of hH_1R binding by displacement of [^{3}H]pyrilamine (5 nM) from Sf9 cell membranes expressing the hH_1R + RGS4, hH_2R binding by displacement of [^{3}H]UR-DE257 (30 nM) from Sf9 cell membranes expressing the hH_2R–$Gs_{\alpha s}$, hH_3R binding by displacement of [^{3}H]N^{α}-methylhistamine (3 nM) from Sf9 cell membranes expressing the hH_3R + $G\alpha_{i2}$ + $G\beta_1\gamma_2$ or hH_4R binding by displacement of [^{3}H]histamine (15 nM) from Sf9 cell membranes expressing the hH_4R + $G\alpha_{i2}$ + $G\beta_1\gamma_2$ was determined as described in the *Pharmacology section*. [b] Data taken from Igel *et al.* 2010.[5] [c] Means no affinity; measured at a ligand concentration of 100 µM. n.d. means not determined. n gives the number of independent experiments performed in triplicate each.

3.3.1.4 Functional activities at recombinant human histamine receptor subtypes

Selected compounds were investigated for agonism or antagonism at hH_1R in functional GTPase assay and at hH_2R, hH_3R and hH_4R subtypes in functional [^{35}S]GTPγS assays using the above mentioned membrane preparations. In general, the determined EC_{50} or K_b values of the tested compounds were in good accordance to the K_i values determined in radioligand binding assays (cf. Table 3.1 and Table 3.2). The hH_4R agonistic potency for **3.16** in the GTPγS assays was 5-times lower compared to the data determined by Savall *et al.* in a reporter gene assay.[3] The EC_{50} values of **3.16**-**3.19** at the hH_4R are in the one-digit nM range (2 to 4 nM). These four compounds acted as full or almost full agonists (α: 0.8-1.0). The lack of 5-F and/or 6-Me caused a change in H_4R selectivity. In particular, the antagonistic activity at the hH_1R and hH_2R (**3.16**) turned into agonism. The hH_2R affinity increased, whereas the activities at the hH_1R remained negligibly low. EC_{50} values at the hH_2R and hH_3R ranged from 300 to 10000 nM. Therefore, the specific substitution pattern is important for the functional activity, even when the affinity at the hH_4R is not influenced. The primary amines **3.22** and **3.23** did not show notable affinity for hH_2, hH_3 and hH_4 receptors and acted as weak antagonists at all hH_xR subtypes. The propionamides **3.31** and **3.32** had negligible activity at the hH_2R and were inactive at the hH_3R. Compound **3.32** (EC_{50} = 1500 nM, α: 0.35) was a moderate partial agonist at the hH_4R, superior to **3.31** (EC_{50} = 4430 nM, α: 0.66) in potency but not in intrinsic activity. The 2-arylbenzimidazoles **3.62**-**3.65** and **3.67** bearing histamine-like moieties had higher potencies at the hH_4R than the parent compound **3.16** (K_i: ~0.3 to 2 nM). Moreover these compounds acted as full agonists (α: ~1), which also holds for the histamine analogs 5-methylhistamine, homohistamine, imbutamine and 5-methylimbutamine.[4] These results are in agreement with data from previous studies on imidazole-type hH_4R agonists, suggesting that ethylamine and butylamine side chains are eqalent substructures. Selectivities over the hH_2R were high and ranged from 1100 to 15000-fold. Selectivities over the hH_3R were similar to **3.16** and decreased with the length of the alkyl linker. The introduction of the 5-methyl group led to a strong increase in selectivity towards the hH_2R (over 15000-fold). In addition, compound **3.67**, comprising the longest spacer within this series (n = 5), was an almost full hH_3R agonist, but, in accordance with the data for impentamine,[4] showed no agonistic activity at the hH_4R. The spacer length of five methylene groups obviously prevents optimal orientation of the ligand in the binding pocket of the hH_4R. Highest selectivity over the hH_3R was obtained for **3.71** (EC_{50} = 2.64 nM; α: 0.35, over 34000-fold selectivity over the hH_3R) and 1300-fold selectivity over the hH_2R. For **3.30**, the K_i values at the hH_2R (K_i = 101 nM) could not be confirmed in the GTPγS assay (K_b = 2350 nM, α: -0.23). Compound **3.70** revealed a K_b value of 18.6 nM (α: -0.20), which makes **3.70** a promising candidate for structural optimization toward new H_2R antagonists.

Table 3.2 Potencies and efficacies of selected synthesized compounds at the hH_xR subtypes in functional [^{35}S]GTPγS assays[a] and [^{33}P]GTPase assays.[b]

Compound	hH_1R			hH_2R			hH_3R			hH_4R		
	EC_{50} or (K_b) / nM	α	n	EC_{50} or (K_b) / nM	α	n	EC_{50} or (K_b) / nM	α	n	EC_{50} or (K_b) / nM	α	n
Histamine	190 ± 8[c]			1200 ± 300[c]	1.00		23.2 ± 7.2[d,e]	1.00	2	10.2 ± 1.8[f,g]	1.00	4
Homohistamine		n.d.			n.d.		103 ± 63[h]	0.81 ± 0.06	3	19.3 ± 2.2[i]	0.77 ± 0.06	3
Imbutamine		n.d.			n.d.		3.13 ± 1.1[j]	0.82 ± 0.13	3	66.1 ± 24.6[k]	0.69 ± 0.07	4
Impentamine		n.d.			n.d.		(57.6 ± 28.8)[l]	0.13 ± 0.02	2	(n.d.)	-0.01 ± 0.02	3
5-Methylhistamine		n.d.			n.d.		12000 ± 3130	0.70 ± 0.11	3	70.3 ± 44.1[m]	0.98 ± 0.03	3
5-Methylimbutamine		n.d.			n.d.		980	0.36 ± 0.11	2	59.4 ± 20.2	0.80 ± 0.08	5
Thia-5-Methylimbutamine		n.d.			n.d.		751 ± 303	0.49 ± 0.05	3	1590 ± 1300	0.70 ± 0.01	3
3.16	(> 10000)	-0.07 ± 0.12	2	(686 ± 175)	-0.05 ± 0.02	2	(1520 ± 220)	-0.09 ± 0.07	2	2.71 ± 0.55	0.92 ± 0.04	4
3.17	> 10000	0.52 ± 0.19	2	413 ± 85	0.30 ± 0.07	2	(641 ± 34)	-0.04 ± 0.12	2	2.62 ± 0.25	1.00 ± 0.03	2
3.18	(> 10000)	0.06 ± 0.09	2	(865 ± 163)	-0.03 ± 0.09	2	(242 ± 30)	-0.52 ± 0.22	2	3.54 ± 0.00	0.96 ± 0.13	2
3.19	> 10000	0.44 ± 0.17	2	278 ± 4	0.31 ± 0.03	2	(660 ± 1)	0.06 ± 0.01	2	2.36 ± 0.08	0.81 ± 0.02	2
3.22	(> 10000)	n.d.	2	(> 10000)	-0.24 ± 0.08	2	(> 10000)	-1.24 ± 0.23	2	(> 10000)	-0.48 ± 0.07	2
3.23	(> 10000)	n.d.	2	(> 10000)	-0.09 ± 0.00	2	(> 10000)	-0.72 ± 0.11	2	(> 10000)	-0.06 ± 0.09	2
3.30		n.d.		(2350 ± 1100)	-0.47 ± 0.00	2		n.d.			n.d.	
3.31	(> 10000)	n.d.	2	(> 10000)	-0.10 ± 0.02	2		Inactive[n]		4430 ± 1570	0.66 ± 0.02	2
3.32	(> 10000)	n.d.	2	(> 10000)	-0.09 ± 0.09	2		Inactive[n]		1500 ± 182	0.35 ± 0.20	2

Table 3.2 (continued)

Compound	hH_1R			hH_2R			hH_3R			hH_4R		
	EC_{50} or (K_b) / nM	α	n	EC_{50} or (K_b) / nM	α	n	EC_{50} or (K_b) / nM	α	n	EC_{50} or (K_b) / nM	α	n
3.62	n.d.			(4340 ± 910)	-0.09 ± 0.01	3	(107 ± 23)	-0.66 ± 0.13	2	0.283 ± 0.17	1.02 ± 0.07	4
3.63	n.d.			(3040 ± 660)	-0.26 ± 0.06	3	(210 ± 4)	0.10	2	1.98 ± 0.57	1.13 ± 0.04	2
3.64	n.d.			(1340 ± 230)	-0.21 ± 0.02	3	(27.0 ± 9.9)	-0.06 ± 0.16	2	1.15 ± 0.78	1.03 ± 0.06	5
3.65	n.d.			n.d.			n.d.			0.488 ± 0.20	1.02 ± 0.10	5
3.67	n.d.			(719 ± 294)	-0.25 ± 0.05	3	30.0 ± 4.0	0.79 ± 0.04	3	(18.1 ± 2.7)[o]	-0.27 ± 0.12	3
3.70	n.d.			(18.6 ± 6.3)	-0.20 ± 0.01	2	n.d.			n.d.		
3.71	n.d.			(3420 ± 750)	-0.23 ± 0.01	3	(> 90000)	-0.70 ± 0.08	2	2.64 ± 0.96	0.97 ± 0.06	4

[a] [^{35}S]GTPγS functional binding assays with membrane preparations of Sf9 cells expressing the hH_3R + $G\alpha_{i2}$ + $G\beta_1\gamma_2$ or the hH_4R + $G\alpha_{i2}$ + $G\beta_1\gamma_2$ or the hH_2R-$Gs_{\alpha s}$ fusion protein were performed as described in section *Pharmacological methods*. [b] Steady-state GTPase activity in Sf9 cell membranes expressing the hH_1R + RGS4 was determined as described in section *Pharmacological methods*. [a,b] Reaction mixtures contained ligands at a concentration from 1 nM to 1 mM as appropriate to generate saturated concentration-response curves. The intrinsic activity (α) of histamine was set to 1.00 and α values of other compounds were referred to this value. The α values of neutral antagonists and inverse agonists were determined at a concentration of 10 µM. The K_b values of neutral antagonists and inverse agonists were determined in the antagonist mode versus histamine (1 µM for the hH_1R and the hH_2R, 100nM for the hH_3R and the hH_4R, respectively) as the agonist. K_b values were calculated according to the Cheng-Prusoff equation.[39] [c] Data taken from Xie *et al.* 2006.[40] [d] ref[5]: EC_{50} 25 nM. [e] ref[41]: EC_{50} 13 nM. [f] ref[5]: EC_{50} 12 nM. [g] ref[41]: EC_{50} 11 nM. [h] ref[41]: EC_{50} 40 nM. [i] ref[41]: EC_{50} 200 nM. [j] ref[41]: EC_{50} 0.6 nM. [k] ref[5]: EC_{50} 32 nM. [l] ref[41]: EC_{50} 4 nM. [m] ref[5]: EC_{50} 71 nM. Data from the literature: [d,f,m] EC_{50} values determined in the steady-state GTPase assay on membranes of Sf9 cells expressing the human hH_3R or hH_4R.[5] [g–j,l] EC_{50} values determined from the inhibition of 1mM forskolin-induced CRE-β-galactosidase activity in SK-N-MC/ hH_3 or SK-N-MC/hH_4 cells.[41] [n] Measured at a ligand concentration of 100 µM. [o] The K_b values of **3.67** were determined in the antagonist mode versus **3.16** (100 nM); cf. 3.3.2. n.d. means not determined. n gives the number of independent experiments performed in triplicate each.

3.3.2 Inhibition of the hH_4R agonistic effect of **3.16** by standard H_4R antagonists

The pharmacological characterization (competition binding experiments, GTPγS- and GTPase assays) of all compounds was determined using membranes of Sf9 insect cells expressing the respective H_xR subtype. When using membranes instead of intact cells, G-proteins are directly accessible to the evaluated compounds. Thus, the possibility of direct, receptor independent G-protein activation has to be taken into account. In addition, most of the investigated ligands, including the previously published potent H_4R agonist **3.16**, contain the imidazole ring as a polar basic moiety combined with a more lipophilic residue. Therefore, and because of the cationic-amphiphilic properties of the molecule, a direct interaction of **3.16** with G-proteins cannot be ruled out. Such implications have been deetected for many compounds, mainly peptides, but also for cationic-amphiphilic HR ligands.[42-45] Hence, [^{35}S]GTPγS binding was induced with **3.16** (100 nM) and the effect of increasing concentrations of the standard H_4R antagonists JNJ7777120 and iodophenpropit and the inverse agonist thioperamide, was evaluated. As shown in Figure 3.5, [^{35}S]GTPγS binding was successfully inhibited by all three ligands in a concentration-dependent manner. As anticipated, thioperamide was more effective than the other standard H_4R antagonists due to its inverse agonistic activity at the hH_4R.

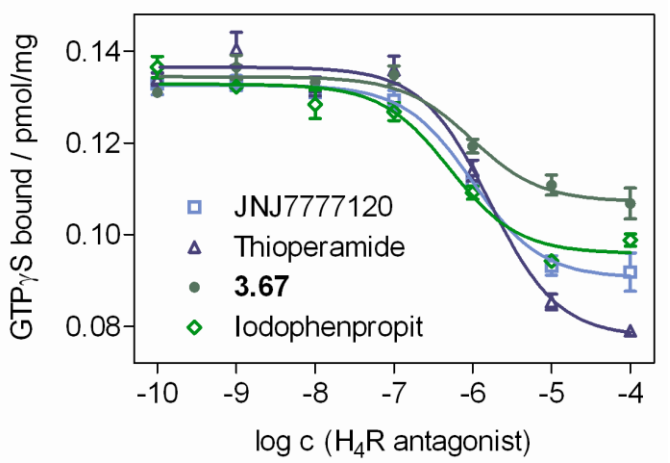

Compound	K_b / nM	$K_{b(ref)}$ / nM[a]
Thioperamide	103 ± 48	148 ± 16[a]
JNJ7777120	34.6 ± 4.7	25.1 ± 2.7[a]
Iodophenpropit	26.8 ± 9.1	20.9 ± 2.3[b]
3.67	18.1 ± 2.7	8.7 ± 2.3[c]

Figure 3.5 Inhibition of the 2-arylbenzimidazole **3.16** stimulated [^{35}S]GTPγS binding at the hH_4R by the H_4R antagonists iodophenpropit and JNJ7777120 and the inverse agonist thioperamide. Functional [^{35}S]GTPγS binding assays with membrane preparations of Sf9 cells expressing the hH_4R + $G\alpha_{i2}$ + $G\beta_1\gamma_2$ was performed as described in section *Pharmacological methods*. Reaction mixtures contained 100 nM of **3.16**. Data were analyzed by nonlinear regression and were best fit to sigmoidal concentration-response curves. Data points shown are the means of two independent experiments performed in triplicate each. [a] K_b values of the reference H_4R antagonists were taken from Wifling *et al.*[46]; [b] Wifling, D. Personal communication, University of Regensburg. **2014**; [c] K_i value, cf. Table 3.1.

The K_b values determined for thioperamide, iodophenpropit and JNJ7777120 for inhibition of the response to **3.16** in the functional assay were in good agreement with K_b values from binding studies reported by Wifling *et al.* (Figure 3.5).[41,46] These results suggest that **3.16** competes with the H_4R antagonists for the same binding site. Furthermore, **3.76** was found to be an antagonist at the hH_4R, with a K_b value of 18.1 nM, which was in good agreement to the K_i value from [^{3}H]histamine binding studies. Summed up, these data confirm that the 2-arylbenzimidazole **3.16** acts as a hH_4R agonist in the [^{35}S]GTPγS binding assay without direct G-protein stimulation.

3.3.2.1 Potencies, efficacies and affinities at the mH_4R

Nowadays GPCR ligands are routinely optimized for activity at the human receptor of interest. The analysis of the (patho)physiological role of the H_4R and its validation as a possible drug target using antagonists and agonists in translational animal models are seriously hampered by tremendous species-dependent differences regarding potencies (up to several orders of magnitude, depending on the assay system) of the pharmacological tools.[46-49] The reason behind is the low homology of the human H_4R and most of the H_4R species variants (hH_4R and mH_4R: 68%, hH_4R and rH_4R: 69%).[1,50] Therefore, with respect to future in vivo studies and better understanding the differences between the murine and human H_4R's, the activities of H_4R ligands on species orthologues, in particular on the murine H_4R, should be taken into consideration. To elucidate the potential use of the synthesized 2-arylbenzimidazoles in murine models, selected compounds (**3.16**-**3.19**) were investigated in radioligand binding studies determined on HEK-293 cells expressing the mH_4R (HEK293-FLAG-mH_4R-His_6)[51] using [^{3}H]UR-PI294[5] as radioligand. In addition, compounds **3.16**, **3.62**-**3.65**, **3.67** and **3.71** were tested in functional [^{35}S]GTPγS assays using membrane preparations of Sf9 insect cells coexpressing the mH_4R + $G\alpha_{i2}$ + $G\beta_1\gamma_2$.[49] The results are summarized in Table 3.3. The investigated compounds **3.16**-**3.20** showed preference for the human H_4R compared to the murine ortholog in radioligand binding affinity. The affinity of **3.16** was 10-fold lower at the mH_4R (K_i = 113 ± 21 nM) than reported.[3] The lack of the typical substitution pattern (F and/or Me) led to a 4-6 fold decrease in mH_4R affinity relative to compound **3.16**. In the functional [^{35}S]GTPγS assays, **3.16** acted as full agonist (α = 1.04) with a EC_{50} value of 139 nM, which was in good accordance to binding data and corresponded to 50-fold lower potency compared to the hH_4R (cf. Table 3.2).The histamine homologs **3.62**-**3.65** also revealed increased functional activities on the mH_4R compared to the data for the hH_4R (14- to 170-fold), but were still almost full agonists (α: 0.68-0.99).

Table 3.3 Affinities, potencies and efficacies of selected synthesized compounds at the mH_4R in radioligand binding studies[a] and functional [^{35}S]GTPγS assays[b]

Compound	mH_4R				
	K_i / nM[a]	n	EC_{50} or (K_b) / nM[b]	α	n
Histamine	129 ± 36	2	3220 ± 424	1.00	3
3.16	113 ± 21	3	139 ± 22	1.04 ± 0.08	3
3.17	595 ± 151	3		n.d.	
3.18	520 ± 3	3		n.d.	
3.19	365 ± 142	3		n.d.	
3.62	n.d.		47.4 ± 14.1	0.99 ± 0.06	3
3.63	n.d.		55.2 ± 15.2	0.74 ± 0.14	3
3.64	n.d.		21.3 ± 3.6	0.68 ± 0.09	3
3.65	n.d.		7.0 ± 0.15	0.80 ± 0.19	3
3.67	n.d.		(1340 ± 0)	0.02 ± 0.06	2
3.71	n.d.		(6230 ± 220)	-0.06 ± 0.07	3

[a] Determination of mH_4R binding by displacement of [^{3}H]UR-PI294[5] (5 nM) from HEK293-FLAG-mH_4R-His_6 cells; [b] [^{35}S]GTPγS functional binding assays with membrane preparations of Sf9 cells expressing the mH_4R + $G\alpha_{i2}$ + $G\beta_1\gamma_2$ were performed as described in section *Pharmacological methods*. Reaction mixtures contained ligands at a concentration from 1 nM to 1 mM as appropriate to generate saturated concentration-response curves. The intrinsic activity (α) of histamine was set to 1.00 and α values of other compounds were referred to this value. The α values of neutral antagonists and inverse agonists were determined at a concentration of 10 μM. The K_b values of neutral antagonists and inverse agonists were determined in the antagonist mode versus histamine (10 μM) as the agonist. K_b values were calculated according to the Cheng-Prusoff equation.[39] n.d. means not determined. n gives the number of independent experiments performed in triplicate each.

Highest potency was found for the 5-methylimbutamine derivative **3.65** with an excellent EC_{50} value of 7 nM (α = 0.80), regardless of a 14-fold decrease in activity compared to the hH_4R. It bears mentioning that the introduction of the 5-methyl residue in **3.62** and **3.65** increased activity of the corresponding parent compounds **3.16** and **3.64** in the same way at both the mH_4R and the hH_4R. By analogy with the hH_4R, the impentamine derivative **3.67** behaved as a neutral antagonist at the mH_4R, too, with a K_b value of 1340 nM and an intrinsic activity of 0.02, accompanied by a 74-fold loss of activity compared to the hH_4R. The reported weak antagonism for **3.71** at the mH_4R in a reporter gene assay was confirmed (K_b = 6230 nM, α = -0.06; pA_{2ref} = 15800 nM[3]). This means that the hH_4R agonism had switched to antagonism at the murine ortholog, making **3.71** an interesting ligand to explore the molecular determinant of differential H_4R ortholog activation, e. g., by molecular modeling studies. In summary, similar to the results of previous studies with agonists such as UR-PI376[52] and *trans*-(+)-(1*S*,3*S*)-UR-RG98,[20] the investigation of this class of 2-arylbenzimidazoles uncovered differences between activities on the human and murine H_4R ortholog. Compound **3.65**, bearing a 5-methylimbutamine residue was the most potent agonist at the murine H_4R and may be

considered a potential pharmacological tool in mouse models. Compounds such as **3.71** may be of special interest in future studies due to biased signaling for human and murine orthologs within one type of functional assay.

3.3.3 Muscarinic receptor subtype affinities of **3.16** on CHO-M_1 and CHO-M_2 cells

Numerous compounds bearing a benzimidazole moiety with different pharmacological activities are known from the literature, e.g., as angiotensin AT_1 receptor antagonists or proton-pump inhibitors.[53,54] In order to further explore the selectivity of the synthesized 2-arylbenzimidazoles, **3.16** was tested exemplarily in radioligand binding assays at human muscarinic M_1 and M_2 receptors stably expressed in CHO cells, which were available in our laboratories. For both muscarinic receptor subtypes the determined K_i values were in the micromolar range, amounting 6350 nM for the hM_1R and 2510 nM for the hM_2R, respectively, corresponding to 570-fold or 220-fold lower affinity compared to the hH_4R. Hence, the inclusion of other targets, GPCRs as well as non-GPCR receptors, is important for additional pharmacological investigation of these benzimidazole-type ligands.

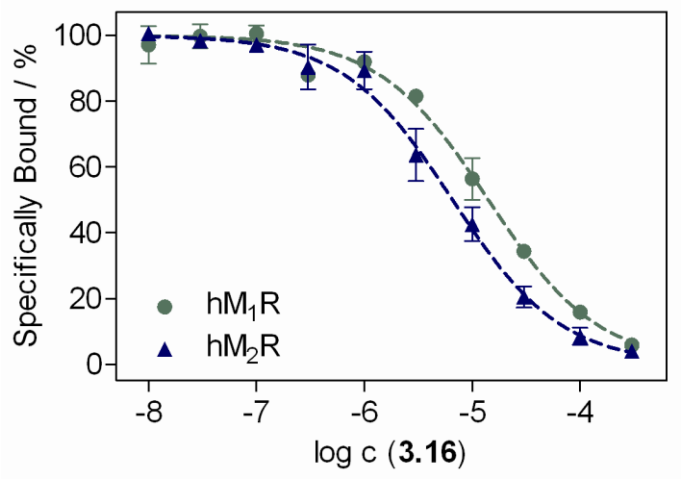

	K_i / nM	n
hM_1R[a]	6350 ± 490	2
hM_2R[a]	2510 ± 152	2

Figure 3.6 Competition binding curves of **3.16** at the $hM_{1/2}R$ subtypes. [a] Determination of hM_1R or hM_2R binding data by displacement of [^{3}H]*N*-methylscopolamine (0.2 nM) from CHO-K9 cells expressing the hM_1R or the hM_2R (cf. *Pharmacology section*). n gives the number of independent experiments performed in triplicate each.

3.4 Summary and Outlook

In search for new selective and potent hH_4R and mH_4R agonists we tested a series of 2-arylbenzimidazoles starting from the structure of the recently published H_4R agonist **3.16**.[3] Radioligand binding studies and GTPγS assays using membranes of Sf9 insect cells expressing the respective human histamine receptor subtype revealed 20-fold lower affinity and potency of **3.16** at the hH_4R compared to the data gained from different assays and reported in the literature. Further investigations showed that the substitution pattern at the 2-arylbenzimidazole is not essential for the

activity at the hH_4R, but is important for functional selectivity over the other hH_xR subtypes as well as for mH_4R affinity. Aiming at improved selectivity for the H_4R, the histamine motif in **3.16** was methyl-substituted or varied regarding the chain. Extension of the carbon chain between imidazole and amino group from two (as in the histamine derivative **3.16**) up to four methylene groups (imbutamine derivative **3.64**) was tolerated, revealing higher affinities and potencies, in part in the sub-nanomolar range. By incorporation of impentamine (**3.67**) agonism switched to antagonism at the hH_4R, and antagonism to agonism at the hH_3R. In addition, compound **3.67** showed higher affinity at the hH_3R than at the hH_4R (cf. Figure 3.6).

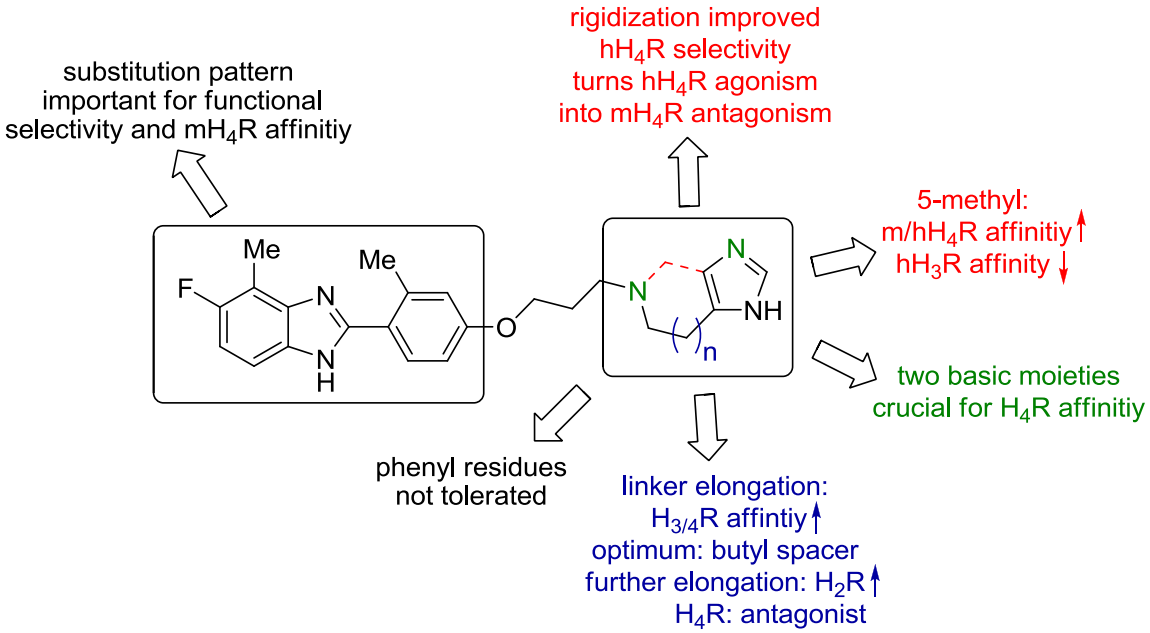

Figure 3.7 Structure-activity relationships of 2-arylbenzimidazole-type H_4R ligands.

Besides the introduction of a 5-methyl substituent at the imidazole ring, rigidization to a spinaceamine derivative (**3.71**) was most effective regarding H_4R selectivity. Structural changes with the aim to replace the imidazole moiety, for example by introduction of guanidines, amides and aromatic residues, resulted in a decrease in affinity at the hH_4R. Thus, only compounds bearing two basic amino functions showed moderate to very high affinity at the hH_4R. With respect to future studies in this field, the most nitrogen-containing aliphatic residues or heterocycles bearing two basic moieties should be considered as promising bioisosteres for replacement of the imidazole ring. The imidazole **3.70**, in which the linker connecting the secondary amine and the imidazole has a length of six atoms, has high affinity at the hH_2R, with almost 50-fold selectivity over the hH_3R and almost 150 fold selectivity over the hH_4R, respectively. These data suggest that the 2-arylbenzimidazole scaffold alone is not the key to hH_4R affinity. As displayed, high affinity and selectivity is possible for the hH_2R, hH_3R and hH_4R as well, depending on appropriate 'decoration' of the scaffold. Affinities

and activities for this class of 2-arylbenzimidazoles at the mH_4R were lower compared to the data for the hH_4R. Such differences were to be expected due to the low homology of hH_4R and mH_4R (68%) and in view of published data for various H_4R ligands. Nevertheless, the 5-methylimbutamine derivative **3.65**, suprisingly, revealed a one-digit nanomolar EC_{50} value with almost full mH_4R agonist activity; this compound might be useful as a pharmacological tool for studies on murine receptors. Moreover, the conformationally constrained analog **3.71** proved to be an agonist at the hH_4R and an antagonist at the mH_4R, respectively. This makes **3.71** an interesting tool for investigations on the differences in the activation mechanisms of H_4R orthologs at the molecular level and an auspicious scaffold for molecular modeling studies as well as ligand-based rational design.

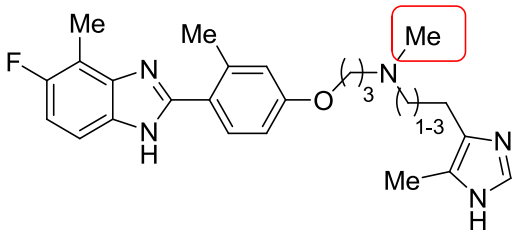

Figure 3.8 Methylated 2-arylbenzimidazoles.

The construction of propionic amides as potential radioligands for the human and murine H_4R based on the arylbenzimidazole scaffold yielded compounds with strongly decreased affinity, obviously due to the loss of basicity by conversion of an amino group to a non-basic carboxylic amide. Therefore, to further pursue the [^{3}H]propionylation strategy, future projects should focus on attaching the propionic residues in a different part of the molecule, e. g. at the functionalized heterocyle, to retain at least two basic moieties in the core structure of the molecule. As an alternative approach enabling tritium labeling, the introduction of a methyl group residue at a basic center could be explored, e.g. the methylation of the secondary amine in **3.62** or **3.65** with the help of methyl iodide or methyl tosylate (Figure 3.8). Both alkylating agents are commercially available for radiolabeling in high specific activity and the labeling strategy with [^{3}H]MeI has been established in our laboratory (cf. Chapter 6 and Appendix). By analogy, according to this concept, the methylation of **3.70** could be explored to generate a new radioligand for the hH_2R.

In conclusion, the search for potent and selective H_4R agonists bearing a 2-arylbenzimidazole scaffold derived from **3.16** resulted in a series of ligands with high affinity and functional activity. The results may contribute to a better understanding of the structure-activity- and structure-selectivity relationships of H_4R ligands on human and murine receptor orthologs. Moreover, selected compounds harbor the potential of being used as pharmacological tools to further investigate the (patho)physiological function of the H_4R. In addition, high affinity at the hH_2R, the hH_3R, the hH_4R and the mH_4R depending on the substitution pattern make the 2-arylbenzimidazole building block an extremely versatile scaffold to play around with subtype, functional and ortholog selectivity in the field of histamine receptors.

3.5 Experimental Section

3.5.1 Chemistry

3.5.1.1 General conditions

Chemicals and solvents were purchased from the following suppliers: Merck KGaA (Darmstadt, Germany), Acros Organics (Geel, Belgium), Sigma Aldrich GmbH (Munich, Germany) and TCI (Tokyo, Japan). All solvents were of analytical grade or distilled prior to use and stored over molecular sieves (4 Å) under protective gas. Deuterated solvents for NMR spectroscopy were from Deutero GmbH (Kastellaun, Germany). DMF was purchased from Sigma-Aldrich Chemie GmbH and stored over 3 Å molecular sieves. Millipore water was used throughout for the preparation of buffers and HPLC eluents. If moisture-free conditions were required, reactions were performed in dried glassware under inert atmosphere (argon or nitrogen). Column chromatography was carried out using Merck silica gel Geduran 60 (0.063-0.200 mm) and Merck silica gel 60 (0.040-0.063 mm) for flash-column chromatography. In certain cases, flash-chromatography was performed on an Intelli Flash-310 Flash-Chromatography Workstation from Varian Deutschland GmbH (Darmstadt, Germany). Reactions were monitored by thin layer chromatography (TLC) on Merck silica gel 60 F254 aluminium sheets and spots were visualized with UV light at 254 nm and/or iodine vapor, ninhydrine spray, vanillin solution, or ammonium molybdate/cerium(IV) sulfate solution. IR spectra were measured on a FTS 3000 MX spectrometer (Excalibur Series) from Bio-Rad (USA) equipped with an attenuated total reflectance (ATR) unit (Specac Golden Gate Diamond Single Reflection ATR System). UV- and VIS spectra were recorded on a Cary 100 UV/VIS photometer (Varian Inc., Mulgrave, Victoria, Australia). Nuclear Magnetic Resonance (^{1}H NMR and ^{13}C NMR) spectra were recorded on an Avance-300 (^{1}H: 300 MHz, ^{13}C: 75 MHz), Avance-400 (^{1}H: 400 MHz, ^{13}C: 101 MHz), or Avance-600 (^{1}H: 600 MHz, ^{13}C: 151 MHz) NMR spectrometer from Bruker BioSpin (Karlsruhe, Germany). Tetramethylsilane was added as internal standard (chemical shift δ = 0 ppm) to all samples. Multiplicities are specified with the following abbreviations: s (singlet), d (doublet), t (triplet), q (quartet), p (quintet), m (multiplet), bs (for broad singulett), as well as combinations thereof. The multiplicity of carbon atoms (^{13}C-NMR) was determined by DEPT 135 and DEPT 90 (distortionless enhancement by polarization transfer): "+" primary and tertiary carbon atom (positive DEPT 135 signal), "-" secondary carbon atom (negative DEPT 135 signal), "quat" quaternary carbon atom. In certain cases 2D-NMR techniques (HSQC, HMQC, HMBC, and COSY) were used to assign ^{1}H and ^{13}C chemical shifts. Low-resolution mass spectrometry (LRMS) was performed on a Finnigan ThermoQuest TSQ 7000 instrument using an electrospray ionization (ESI) source or on a Finnigan SSQ 710A instrument (EI, 70 eV). The compounds were analyzed by LC-MS using the following LC method (Agilent 1100 Series HPLC): Column: Phenomex Luna C18, 2.5 µm, 50 x 2.1 mm HST (Phenomenex, Aschaffenburg, Germany); column

temperature: 40 °C; flow: 0.40 mL/min; solvent A: MeCN, solvent B: 0.1% aq. formic acid; gradient program: 0–1 min: A/B 5:95, 1–8 min: 5:95–98:2, 8–11 min: 98:2, 11–12 min: 98:2–5:95, 12-15 min: 5:95. High-resolution mass spectrometry (HRMS) was performed on an Agilent 6540 UHD Accurate-Mass Q-TOF LC/MS system (Agilent Technologies, Santa Clara, CA) using an ESI source. Melting points (mp) were measured on a Büchi 530 (Büchi GmbH, Essen, Germany) and are uncorrected. Lyophilisation of the products was done with a Christ alpha 2-4 LD, equipped with a Vacuubrand RZ 6 rotary vane vacuum pump. Preparative HPLC was performed with a pump model K-1800 (Knauer, Berlin, Germany), the column was a Eurospher-100 (250 x 32 mm) (Knauer, Berlin, Germany) or a Nucleodur 100-5 C18 ec (250 × 21 mm, 5 µm (Macherey-Nagel, Düren, Germany), which was attached to the UV-detector model K-2000 (Knauer, Berlin, Germany). UV-detection was done at 220 or 254 nm. The temperature was between RT and 30 °C and the flow rate between 18 and 37 mL/min. The mobile phase was 0.1% TFA in millipore water and MeCN. All compounds were filtered through PTFE-filters (25 mm, 0.2 µm, Phenomenex Ltd., Aschaffenburg, Germany) prior to preparative HPLC. Analytical HPLC analysis was performed on a system from Merck, composed of an L-5000 controller, a 655A-12 pump, a 655A-40 auto sampler and an L-4250 UV-VIS detector. Except for **3.30**, **3.37**, **3.42**, **3.62**, **3.63** and **3.68** the column was a Eurospher-100 (250 x 4 mm, 5 µm) (Knauer, Berlin, Germany, t_0 = 3.32 min) at a flow rate of 0.8 mL/min. For **3.30**, **3.37**, **3.42**, **3.62**, **3.63** and **3.68** the column was a Luna C18(2) (150 × 4.6 mm, 3 µm) (Phenomenex, Aschaffenburg, Germany, t_0 = 2.88 min). UV detection was done at 220 nm. Mixtures of 0.05% TFA in MeCN and 0.05% aq. TFA were used as mobile phase. Helium degassing prior to HPLC analysis was necessary. Compound purities were calculated as percentage peak area of the analyzed compound by UV detection at 220 nm. The capacity (retention) factors were calculated according to $k = (t_R\text{-}t_0)/t_0$.

3.5.2 Chemistry

3.5.2.1 Preparation of the imidazole **3.2**

N-Trityl-2-(1-trityl-1H-imidazol-4-yl)ethanamine (3.1)[55,56]

To a solution of histamine dihydrochloride (3.7 g, 20 mmol, 1 eq) and NEt_3 (8.1 g, 80 mmol, 4 eq) in $CHCl_3$ (50 mL) was added dropwise a solution of trityl chloride (22.3 g, 80 mmol, 4 eq) in $CHCl_3$ (50 mL) under external cooling with ice within 1.5 h. The mixture was allowed to warm up at rt and stirred for 27 h. The solvent was evaporated under reduced pressure, and the solid residue was suspended in 100 mL of water. After stirring for 1 h, the product was extracted with $CHCl_3$ (2 x 150 mL), dried over anhydrous Na_2SO_4 and concentrated *in vacuo*. The crude product was purified by flash-chromatography (eluent CH_2Cl_2 (A), MeOH (B); gradient: 0 to 30 min: A/B 100/0 – 90/1 (*v/v*), SF 15-120 g) and afforded a yellow foam-like solid (5.3 g, 46%), mp 210 °C (lit.[55] 202-203 °C). R_f = 0.6

(CH_2Cl_2/MeOH 25:1. ^{1}H-NMR (300 MHz, $CDCl_3$): δ (ppm) 2.40 (t, *J* = 6.2, 2H), 2.73 (t, *J* = 6.2, 2H), 6.51 (s, 1H), 7.08-7.31 (m, 24H), 7.34 (d, *J* = 1.0, 1H), 7.35-7.45 (m, 6H). ^{13}C-NMR (75 MHz, $CDCl_3$): δ (ppm) 29.59, 42.89, 70.87, 75.18, 118.62, 126.19, 127.82, 128.06, 128.11, 128.80, 129.87, 138.47, 140.19, 142.71, 146.48. MS (LC-MS, ESI): *m/z* 596.3 [M+H$^+$]. $C_{43}H_{37}N_3$ (595.77).

2-(1-Trityl-1H-imidazol-4-yl)ethanamine (3.2)[55,56]

To a solution of **3.1** (4.7 g, 7.92 mmol) in CH_2Cl_2 (25 mL) at 0 °C, 1.3 mL of TFA (1.94 g, 17.0 mmol, 2.15 eq) were added dropwise. After stirring for 10 min at the same temperature, the mixture was allowed to warm up to rt and was stirred for additional 4 h. After removing the solvent, the residue was neutralized with saturated $NaHCO_{3(aq)}$ (100 mL) and extracted with $CHCl_3$ (3 x 100 mL), washed with water (400 mL), brine (400 mL) and dried over anhydrous Na_2SO_4. After removing the solvent, the residue was chromatographed with $CHCl_3$/MeOH/NEt_3 (94/5/1) on silica to obtain a yellow foam-like solid (2.0 g, 61%), mp 111 °C (lit.[55] 126-128 °C). R_f = 0.25 ($CHCl_3$/MeOH/NEt_3 94/5/1). ^{1}H-NMR (300 MHz, $CDCl_3$): δ (ppm) 2.84 (t, *J* = 6.5, 2H), 3.20 (t, *J* = 6.8, 2H), 6.58 (s, 1H), 7.16-7.01 (m, 6H). 7.37-7.22 (m, 10H). ^{13}C-NMR (75 MHz, $CDCl_3$): δ (ppm) 27.27, 40.70, 75.39, 118.72, 128.18, 129.80, 138.04, 138.52, 142.31. MS (LC-MS, ESI): *m/z* 354.0 [M+H$^+$]. $C_{24}H_{23}N_3$ (353.46).

3.5.2.2 Preparation of the benzimidazoles **3.7**-**3.10**

General procedure for the synthesis of the benzimidazoles 3.7-3.10[9]

A solution of the pertinent phenylenediamine (**3.3** or **3.4**, 1.00-1.04 eq) and the respective benzaldehyde (**3.5** or **3.6**, 1 eq) in DMF was treated with $Na_2S_2O_5$ (1 eq). After heating for 2 h at 90 °C, the reaction mixture was cooled to rt and then diluted with ice/water. The resulting suspension was stirred for 4 h, then cooled to 0 °C and filtered through a glass fritted funnel, the solid washed with cold water and dried *in vacuo*.

4-(5-Fluoro-4-methyl-1H-benzo[d]imidazole-2-yl)-3-methylphenol (3.7)

The title compound was prepared from **3.3** (8.6 g, 0.061 mol, 1 eq), **3.5** (8.4 g, 0.061 mol, 1 eq) and $Na_2S_2O_5$ (11.7 g, 0.061 mol, 1 eq) in DMF (120 mL) according to the general procedure yielding a brown solid (15.6 g, 99%), mp >261 °C (decomposed). R_f = 0.14 (CH_2Cl_2/MeOH 90/10). ^{1}H-NMR (300 MHz, DMSO-d_6): δ (ppm) 2.45 (s, 3H), 2.52 (d, *J* = 0.9, 3H), 6.83-6.94 (m, 2H), 7.33-7.44 (m, 1H), 7.62 (d, *J* = 8.3, 1H), 7.67 (dd, *J* = 8.9, 4.3, 1H), 10.76 (bs, TFA). ^{13}C-NMR (75 MHz, DMSO-d_6 + 10 µL TFA): δ (ppm) 9.37 (d, *J* = 3.3), 19.84, 110.77 (d, *J* = 23.4), 112.45 (d, *J* = 10.2), 113.63, 113.74 (d, *J* =

26.5), 114.15, 118.09, 128.49, 132.57 (d, *J* = 10.1), 133.01, 139.95, 151.42 (d, *J* = 1.1), 157.86 (d, *J* = 238.7), 158.47 (q, *J* = 32.8, TFA), 161.23. MS (LC-MS, ESI): *m/z* 256.9 [M+H$^+$]. HRMS (ESI-MS): *m/z* [M+H$^+$] calcd. for $C_{15}H_{14}FN_2O^+$: 257.1085, found: 257.1085.

4-(1H-Benzo[d]imidazol-2-yl)phenol (3.8)[57]

The title compound was prepared from **3.4** (5.1 g, 0.047 mol, 1.04 eq), **3.6** (5.5 g, 0.045mol, 1 eq) and $Na_2S_2O_5$ (8.6 g, 0.045 mol, 1 eq) in DMF (90 mL) according to the general procedure yielding a tan solid (6.8 g, 72%), mp >272 °C (decomposed, lit.[57] 279 °C) . R_f = 0.31 (CH_2Cl_2/MeOH 96/4). ^{1}H-NMR (300 MHz, DMSO-d_6): δ (ppm) 7.06 (d, *J* = 8.8, 2H), 7.44 (dd, *J* = 3.2, 6.1, 2H), 7.74 (dd, *J* = 3.1, 6.1, 2H), 8.11 (d, *J* = 8.8, 2H), 10.76 (bs, TFA). ^{13}C-NMR (75 MHz, DMSO-d_6 + 10 µL TFA): δ (ppm) 113.85 (2C), 114.08, 116.63 (2C), 125.21 (2C), 130.05 (2C), 132.56 (2C), 149.79, 158.47 (q, *J* = 32.8, TFA), 162.34. MS (GC-MS, EI): *m/z* 210.1 [M$^{+\bullet}$]. $C_{13}H_{10}N_2O$ (210.23).

4-(5-Fluoro-4-methyl-1H-benzo[d]imidazol-2-yl)phenol (3.9)[9]

The title compound was prepared from **3.3** (200 mg, 1.43 mmol, 1.04 eq), **3.6** (167 mg, 1.37 mmol, 1 eq) and $Na_2S_2O_5$ (260 mg, 1.37 mmol, 1 eq) in DMF (3 mL) according to the general procedure yielding a yellow powder (216 mg, 65%), mp >249 °C (decomposed). R_f = 0.17 (CH_2Cl_2/MeOH 96/4). ^{1}H-NMR (300 MHz, DMSO-d_6 + 10 µL TFA): δ (ppm) 2.52 (d, *J* = 1.1, 1H), 7.08 (d, *J* = 8.8, 2H), 7.30-7.40 (m, 1H), 7.61 (dd, *J* = 4.3, 8.9, 1H), 8.09 (d, *J* = 8.8, 2H), 10.86 (bs, TFA). ^{13}C-NMR (75 MHz, DMSO-d_6 + 10 µL TFA): δ (ppm) 9.48 (d, *J* = 3.2), 110.82 (d, *J* = 23.7), 112.07 (d, *J* = 10.0), 113.28, 113.93 (d, *J* = 26.8), 115.41 (q, *J* = 289.1, TFA), 116.63 (2C), 128.08, 130.63 (2C), 132.24 (d, *J* = 10.1), 150.90, 158.16 (d, *J* = 238.9), 158.66 (q, *J* = 37.9, TFA), 162.65. MS (GC-MS, EI): *m/z* 242.2 [M$^{+\bullet}$]. $C_{14}H_{11}FN_2O$ (242.25).

4-(1H-Benzo[d]imidazol-2-yl)-3-methylphenol (3.10)

The title compound was prepared from **3.4** (1.0 g, 9.25 mmol, 1.04 eq), **3.5** (1.2 g, 8.89 mmol, 1 eq) and $Na_2S_2O_5$ (1.7 g, 8.89 mmol, 1 eq) in DMF (18 mL) according to the general procedure yielding a brown powder (0.63 g, 61%), mp >218 °C (decomposed). R_f = 0.16 (CH_2Cl_2/MeOH 96/4). ^{1}H-NMR (300 MHz, DMSO-d_6): δ (ppm) 2.55 (s, 3H), 6.70-6.78 (m, 2H), 7.16 (dd, *J* = 6.0, 3.2, 2H), 7.49-7.56 (m, 1H), 7.58 (d, *J* = 8.2, 2H), 9.76 (s, 1H), 12.43 (bs, 1H). ^{13}C-NMR (75 MHz, DMSO-d_6 + 10 µL TFA): δ (ppm) 19.95, 113.77, 114.07, 115.87 (q, *J* = 291.7, TFA), 117.80, 118.35, 125.83 (2C), 131.65 (2C), 133.10, 140.07, 150.06, 158.85 (q, *J* = 36.4, TFA), 161.52. MS (GC-MS, EI): *m/z* 224.1 [M$^{+\bullet}$]. $C_{14}H_{12}N_2O$ (224.26).

3.5.2.3 Preparation of the benzimidazolylphenyl chloroalkyl ether **3.11**-**3.15**[9]

General procedure for the O-alkylation of (hydroxyphenyl)benzimidazoles[9]

A suspension of the pertinent (hydroxyphenyl)benzimidazole (1.0 eq), and Cs_2CO_3 (1.0-1.5 eq) in MeCN was treated with the respective alkyl halides (1.0-1.1 eq) and the reaction mixture heated to 70 °C for 17 h. The reaction mixture was cooled to rt, diluted with CH_3Cl and filtered through a glass fritted funnel to remove inorganic solids. The filtrate was concentrated under reduced pressure and purified by flash-chromatography.

2-[4-(3-Chloropropoxy)-2-methylphenyl]-5-fluoro-4-methyl-1H-benzo[d]imidazole (3.11)[9]

The title compound was prepared from **3.7** (1.0 g, 3.90 mmol, 1 eq), 1-bromo-3-chloropropane (0.61 g, 3.90 mmol, 1 eq) and Cs_2CO_3 (1.9 g, 5.85 mmol, 1.5 eq) in MeCN (12 mL) according to the general procedure. The crude product was purified by flash-chromatography (eluent hexanes (A), EtOAc (B); gradient: 0 to 30 min: A/B 100/0 – 50/50 (*v/v*), SF 15-24 g) yielding a yellow foam-like solid (0.53 g, 44%), mp >261 °C (decomposed). R_f = 0.46 (CH_2Cl_2/MeOH 96/4). A sample of 50 mg was purified by preparative HPLC (column: Nucleodur 250 × 21 mm; gradient: 0−30 min: MeCN/0.1% aq. TFA 30/70−60/40, t_R = 12.5 min). MeCN was removed under reduced pressure. After lyophilisation **3.11** (hydrotrifluoroacetate) was obtained as white fluffy solid (33.8 mg, 50%) nm. RP-HPLC (220 nm): 99.4% (gradient: 0−30 min: MeCN/0.1% aq. TFA 30/70−60/40, 31-40 min: 90/10, t_R = 22.5 min, k = 10.1). ^{1}H-NMR (400 MHz, DMSO-d_6 + 10 µL TFA): δ (ppm) 2.21 (p, J = 6.3, 2H), 2.50 (s, 3H), 2.52 (d, J = 1.2, 3H), 3.81 (t, J = 6.4, 2H), 4.22 (t, J = 6.1, 2H), 7.06-7.13 (m, 2H), 7.36-7.42 (m, 1H), 7.69 (dd, J = 4.3, 8.9, 1H), 7.73 (d, J = 8.5, 1H), 13.14 (bs, TFA). ^{13}C-NMR (151 MHz, DMSO-d_6 + 10 µL TFA): δ (ppm) 9.37 (d, J = 3.2), 19.82, 31.61, 41.86, 64.81, 110.84 (d, J = 23.6), 112. 51 (d, J = 7.2), 112.55, 113.94 (d, J = 27.0), 115.74 (q, J = 291.2, TFA), 115.93, 117.22, 128.40, 132.48 (d, J = 10.2), 132.97, 140.16, 150.89 (d, J = 1.5), 158.04 (d, J = 239.1), 158.66 (q, J = 36.5, TFA), 161.50. MS (LC-MS, ESI): *m/z* 333.0 [M+H$^+$]. HRMS (EI-MS): *m/z* $M^{+\bullet}$ calcd. for $C_{18}H_{18}ClFN_2O$: 332.1092, found: 332.1092.

2-[4-(3-Chloropropoxy)phenyl]-1H-benzo[d]imidazole (3.12)[9]

The title compound was prepared from **3.8** (5.7 g, 0.027 mol, 1 eq), 1-bromo-3-chloropropane (4.3 g, 0.027 mol, 1 eq) and Cs_2CO_3 (9.2 g, 0.028 mol, 1.04 eq) in MeCN (87 mL) according to the general procedure. The crude product was purified by flash-chromatography (eluent CH_2Cl_2 (A), MeOH (B); gradient: 0 to 60 min: A/B 100/0 – 96/4 (*v/v*), SF 65-400 g) yielding a white powder (3.6 g, 46%), mp 204 °C. R_f = 0.31 (CH_2Cl_2/MeOH 96/4). ^{1}H-NMR (300 MHz, DMSO-d_6): δ (ppm) 2.20 (p, J = 5.9, 2H),

3.79 (t, *J* = 6.1, 2H), 4.20 (t, *J* = 5.5, 2H), 7.24 (d, *J* = 8.5, 2H), 7.44-7.56 (m, 2H), 7.73-7.84 (m, 2H), 8.18 (d, *J* = 8.5, 2H). ^{13}C-NMR (75 MHz, DMSO-d_6): δ (ppm) 31.57, 41.83, 65.03, 113.87 (2C), 115.29, 115.68 (2C), 125.65 (2C), 129.98 (2C), 131.91 (2C), 149.03, 159.20 (d, *J* = 34.9, TFA), 162.39.MS (LC-MS, ESI): *m/z* 287.1 [M+H$^+$]. $C_{16}H_{15}ClN_2O$ (286.76).

2-[4-(3-Chloropropoxy)phenyl]-5-fluoro-4-methyl-1H-benzo[d]imidazole (3.13)

The title compound was prepared from **3.9** (158 mg, 0.652 mmol, 1 eq), 1-bromo-3-chloropropane (113 mg, 0.717 mmol, 1.1 eq) and Cs_2CO_3 (319 g, 0.978 mmol, 1.5 eq) in MeCN (2 mL) according to the general procedure. The crude product was purified by flash-chromatography (eluent hexanes (A), EtOAc (B); gradient: 0 to 40 min: A/B 100/0 – 50/50 (*v/v*), SF 10-4 g) yielding a yellow foam-like solid (129 mg, 62%), mp 146 °C. R_f = 0.35 (CH_2Cl_2/MeOH 96/4). ^{1}H-NMR (400 MHz, DMSO-d_6 + 10 µL TFA): δ (ppm) 2.23 (p, *J* = 6.2, 2H), 2.55 (d, *J* = 1.3, 3H), 3.82 (t, *J* = 6.4, 2H), 4.26 (t, *J* = 6.1, 2H), 7.33 (d, *J* = 9.0, 2H), 7.35-7.41 (m, 1H), 7.65 (dd, *J* = 4.2, 8.8, 1H), 8.20 (d, *J* = 9.0, 2H), 9.93 (bs, TFA). ^{13}C-NMR (101 MHz, DMSO-d_6 + 10 µL TFA): δ (ppm) 9.46 (d, *J* = 3.4), 31.59, 41.85, 65.14, 110.88 (d, *J* = 23.8), 112.18 (d, *J* = 10.4), 114.08 (d, *J* = 27.0), 115.19, 115.26 (q, *J* = 288.7, TFA), 115.71 (2C), 128.15, 130.44 (2C), 132.33 (d, *J* = 10.2), 150.45 (d, *J* = 1.4), 158.18 (d, *J* = 239.1), 158.55 (q, *J* = 38.2, TFA), 162.60. MS (LC-MS, ESI): *m/z* 318.9 [M+H$^+$]. HRMS (ESI-MS): [M+H$^+$] calcd. for $C_{17}H_{17}ClFN_2O^+$: 319.1008, found: 319.1015.

2-[4-(3-Chloropropoxy]-2-methylphenyl)-1H-benzo[d]imidazole (3.14)

The title compound was prepared from **3.10** (377 mg, 1.68 mmol, 1 eq), 1-bromo-3-chloropropane (291 mg, 1.85 mmol, 1.1 eq) and Cs_2CO_3 (822 mg, 2.52 mmol, 1.5 eq) in MeCN (5 mL) according to the general procedure. The crude product was purified by flash-chromatography (eluent hexanes (A), EtOAc (B); gradient: 0 to 45 min: A/B 100/0 – 50/50 (*v/v*), SF 10-8 g) yielding a white powder (82 mg, 16%), mp 192 °C. R_f = 0.40 (CH_2Cl_2/MeOH 96/4). ^{1}H-NMR (400 MHz, DMSO-d_6 + 10 µL TFA): δ (ppm) 2.22 (p, *J* = 6.2, 2H), 2.53 (s, 3H), 3.82 (t, *J* = 6.4, 2H), 4.23 (t, *J* = 6.0, 2H), 7.08-7.15 (m, 2H), 7.59 (dd, *J* = 3.1,6.1, 2H), 7.74 (d, *J* = 8.4, 1H), 7.85 (dd, *J* = 3.1, 6.1, 2H), 8.88 (bs, TFA). ^{13}C-NMR (101 MHz, DMSO-d_6 + 10 µL TFA): δ (ppm) 19.87, 31.59, 41.88, 64.85, 112.81, 114.08, 115.27 (q, *J* = 288.8, TFA), 115.54, 117.41, 125.98, 131.53, 132.98, 140.16, 149.57, 158.52 (q, *J* = 38.1, TFA), 161.66. MS (LC-MS, ESI): *m/z* 301.0 [M+H$^+$]. HRMS (ESI-MS): [M+H$^+$] calcd. for $C_{17}H_{18}ClN_2O^+$: 301.1109, found: 301.1102.

2-[4-(4-Chlorobutoxy)-2-methylphenyl]-5-fluoro-4-methyl-1H-benzo[d]imidazole (3.15)

The title compound was prepared from **3.7** (500 mg, 1.95 mmol, 1 eq), 1-bromo-4-chlorobutane (335 mg, 1.95 mmol, 1 eq) and Cs_2CO_3 (953 mg, 2.93 mmol, 1.5 eq) in MeCN (6 mL) according to the general procedure. The crude product was purified by flash-chromatography (eluent hexanes (A), EtOAc (B); gradient: 0 to 45 min: A/B 100/0 – 75/25 (*v/v*), SF 15-24 g) yielding a yellow sticky oil (360 mg, 53%). R_f = 0.44 (CH_2Cl_2/MeOH 96/4). ^{1}H-NMR (300 MHz, DMSO-d_6): δ (ppm) 1.93-2.03 (m, 4H), 2.53 (s, 3H), 2.57 (s, 3H), 3.64 (t, *J* = 6.2, 2H), 4.04 (t, *J* = 5.7, 2H), 6.75-6.85 (m, 2H), 6.99 (dd, *J* = 10.2, 8.8, 1H), 7.33 (s, 1H), 7.56 (d, *J* = 8.5, 1H). MS (LC-MS, ESI): *m/z* 346.9 [M+H$^+$]. $C_{19}H_{20}ClFN_2O$ (346.83).

3.5.2.4 Preparation of the imidazole derivatives **3.16**-**3.20**

General procedure for the synthesis of the imidazole derivatives 3.16-3.20[9]

The alkyl halides (1 eq) K_2CO_3 (2 eq), NaI (1 eq) and 2-(1-trityl-1*H*-imidazol-4-yl)ethanamine (**3.2**, 3 eq) in *n*-butanol were heated to 90 °C for 15-94 h. The reaction mixture was cooled to rt, diluted with $CHCl_3$ and filtered through a glass fritted funnel to remove inorganic solids. The filtrate was concentrated under reduced pressure and purified by flash-chromatography. The residue was dissolved in CH_2Cl_2, TFA was added and the reaction mixture was stirred until removal of the protecting group was complete (5-8 h, TLC control). After evaporation of the solvent *in vacuo*, the crude product was purified by preparative RP-HPLC.

N-[2-(1H-Imidazol-4-yl)ethyl]-3-[4-(5-fluoro-4-methyl-1H-benzo[d]imidazol-2-yl)-3-methylphenoxy]-propan-1-amine tris(hydrotrifluoroacetate) (3.16)

The title compound was prepared from **3.11** (97 mg, 0.291 mmol, 1 eq), K_2CO_3 (81 mg, 0.583 mmol, 2 eq), NaI (44 mg, 0.291 mmol, 1 eq) and 2-(1-trityl-1*H*-imidazol-4-yl)ethanamine (**3.2**, 309 mg, 0.874 mmol, 3 eq) in *n*-butanol (1.2 mL) by heating for 23 h according to the general procedure. The crude product was purified by flash-chromatography (eluent CH_2Cl_2 (A), MeOH + 1% NEt_3 (B); gradient: 0 to 60 min: A/B 100/0 – 50/50 (*v/v*), SF 10-8 g). Deprotection in CH_2Cl_2 (5 mL) and TFA (1 mL) followed by preparative RP-HPLC (column: Nucleodur 250 × 21 mm; gradient: 0–30 min: MeCN/0.1% aq. TFA 20/80–50/50, t_R = 7.6 min) afforded **3.16** (tris(hydrotrifluoroacetate)) as white fluffy solid (34.5 mg, 19%). R_f = 0.11 (CH_2Cl_2/MeOH/NH_3 80/19/1). UV/VIS (20 mM HCl): λ_{max} 287, 254, 207, 190 nm. RP-HPLC (220 nm): 99.9% (gradient: 0–30 min: MeCN/0.1% aq. TFA 20/80–50/50, 31-40 min: 90/10, t_R = 11.2 min, *k* = 3.0). ^{1}H-NMR (600 MHz, DMSO-d_6 + 10 µL TFA): δ (ppm) 2.12 (p, *J* = 6.9, 2H), 2.50 (s, 3H), 2.53 (s, 3H), 3.07 (t, *J* = 7.5, 2H), 3.13-3.19 (m, 2H), 3.29-3.35 (m, 2H), 4.19 (t, *J* = 6.0,

2H), 7.06-7.10 (m, 2H), 7.42 (d, *J* = 9.2, 1H), 7.54 (s, 1H), 7.70 (dd, *J* = 4.1, 8.9, 1H), 7.74 (d, *J* = 8.4, 1H), 8.87 (t, *J* = 5.1, 2H), 9.05 (d, *J* = 1.2, 1H), 13.82 (bs, TFA), 14.33 (s, 1H), 14.65 (s, 1H). ^{13}C NMR (151 MHz, DMSO-d_6 + 10 µL TFA): δ (ppm) 9.36 (d, *J* = 3.1), 19.78, 21.19, 25.45, 44.27, 45.07, 65.14, 110.85 (d, *J* = 23.6), 112.51, 112.52 (d, *J* = 9.4), 114.10 (d, *J* = 26.7), 115.33 (q, *J* = 289.4, TFA), 115.84, 116.99, 117.13, 128.23, 128.78, 132.32 (d, *J* = 10.1), 133.01, 134.43, 140.11, 150.79, 157.98 (d, *J* = 239.6), 158.41 (q, *J* = 37.7, TFA), 161.40. MS (LC-MS, ESI): *m/z* 408.0 [M+H$^+$]. HRMS (EI-MS): *m/z* M$^{+\bullet}$ calcd. for $C_{23}H_{26}FN_5O$: 407.2121, found: 407.2121.

3-[4-(1H-Benzo[d]imidazol-2-yl)phenoxy]-N-[2-(1H-imidazol-4-yl)ethyl]propan-1-amine tris(hydrotrifluoroacetate) (3.17)

The title compound was prepared from **3.12** (70 mg, 0.244 mmol, 1 eq), K_2CO_3 (68 mg, 0.488 mmol, 2 eq), NaI (37 mg, 0.244 mmol, 1 eq) and 2-(1-trityl-1*H*-imidazol-4-yl)ethanamine (**3.2**, 259 mg, 0.732 mmol, 3 eq) in *n*-butanol (1.5 mL) by heating for 22 h according to the general procedure. The crude product was purified by flash-chromatography (eluent CH_2Cl_2 (A), MeOH + 1% NEt_3 (B); gradient: 0 to 60 min: A/B 100/0 – 50/50 (*v/v*), SF 10-8 g). Deprotection in CH_2Cl_2 (5 mL) and TFA (1 mL) followed by preparative RP-HPLC (column: Nucleodur 250 × 21 mm; gradient: 0−30 min: MeCN/0.1% aq. TFA 20/80−50/50, t_R = 11.1 min) afforded **3.17** (tris(hydrotrifluoroacetate)) as white fluffy solid (20.3 mg, 14%). R_f = 0.10 (CH_2Cl_2/MeOH/NH_3 80/19/1). UV/VIS (20 mM HCl): λ_{max} 308, 253, 202, 191 nm. RP-HPLC (220 nm): 99.6% (gradient: 0−30 min: MeCN/0.1% aq. TFA 20/80−50/50, 31-40 min: 90/10, t_R = 6.9 min, *k* = 1.5). ^{1}H-NMR (600 MHz, DMSO-d_6 + 10 µL TFA): δ (ppm) 2.10-2.17 (p, *J* = 6.3, 2H), 3.07 (t, *J* = 7.5, 2H), 3.13-3.20 (m, 2H), 3.28-3.35 (m, 2H), 4.24 (t, *J* = 6.0, 2H), 7.31 (d, *J* = 8.9, 2H), 7.54 (s, 1H), 7.56 (dd, *J* = 3.1, 6.1, 2H), 7.83 (dd, *J* = 3.1, 6.1, 2H), 8.21 (d, *J* = 8.9, 2H), 8.86 (s, 2H), 9.05 (d, *J* = 1.1, 1H), 13.82 (bs, TFA). ^{13}C NMR (151 MHz, DMSO-d_6 + 10 µL TFA): δ (ppm) 21.18, 25.37, 44.22, 45.05, 65.38, 113.85 (2C), 115.29, 115.33 (q, *J* = 289.4, TFA), 115.77 (2C), 116.98, 125.90 (2C), 128.77, 130.07 (2C), 131.71 (2C), 134.42, 149.07, 158.51 (q, *J* = 37.7, TFA), 162.34. MS (LC-MS, ESI): *m/z* 362.1 [M+H$^+$]. HRMS (EI-MS): *m/z* M$^{+\bullet}$ calcd. for $C_{21}H_{23}FN_5O$: 361.1903, found: 361.1901.

N-[2-(1H-Imidazol-4-yl)ethyl]-3-[4-(5-fluoro-4-methyl-1H-benzo[d]imidazol-2-yl)phenoxy]propan-1-amine tris(hydrotrifluoroacetate) (3.18)

The title compound was prepared from **3.13** (103 mg, 0.323 mmol, 1 eq), K_2CO_3 (89 mg, 0.646 mmol, 2 eq), NaI (48 mg, 0.323 mmol, 1 eq) and 2-(1-Trityl-1*H*-imidazol-4-yl)ethanamine (**3.2**, 343 mg, 0.969 mmol 3 eq) in *n*-butanol (5 mL) by heating for 94 h according to the general procedure. The crude product was purified by flash-chromatography (eluent CH_2Cl_2 (A), MeOH + 1% NEt_3 (B); gradient: 0 to 60 min: A/B 100/0 – 50/50 (*v/v*), SF 10-8 g). Deprotection in CH_2Cl_2 (5 mL) and TFA (1 mL) followed by

preparative RP-HPLC (column: Nucleodur 250 × 21 mm; gradient: 0–30 min: MeCN/0.1% aq. TFA 20/80–50/50, t_R = 11.9 min) afforded **3.18** (tris(hydrotrifluoroacetate)) as white fluffy solid (32.0 mg, 16%). R_f = 0.15 (CH_2Cl_2/MeOH/NH_3 80/19/1). UV/VIS (20 mM HCl): λ_{max} 306, 256, 201, 190 nm. RP-HPLC (220 nm): 99.6% (gradient: 0–30 min: MeCN/0.1% aq. TFA 20/80–50/50, 31-40 min: 90/10, t_R = 10.9 min, k = 2.9). ^{1}H-NMR (600 MHz, DMSO-d_6 + 10 µL TFA): δ (ppm) 2.06-2.20 (m, 2H), 2.55 (d, J = 0.5, 3H), 3.07 (t, J = 7.5, 2H), 3.13-3.25 (m, 2H), 3.27-3.37 (m, 2H), 4.24 (t, J = 6.0, 2H), 7.30 (d, J = 9.0, 2H), 7.34-7.44 (m, 1H), 7.54 (s, 1H), 7.66 (dd, J = 4.1, 8.8, 1H), 8.23 (d, J = 8.9, 2H), 8.87 (s, 2H), 9.05 (d, J = 1.2, 1H), 13.82 (bs, TFA). ^{13}C NMR (151 MHz, DMSO-d_6 + 10 µL TFA): δ (ppm) 9.41 (d, J = 3.2), 21.18, 25.39, 44.23, 45.05, 65.36, 110.83 (d, J = 23.6), 112.19 (d, J = 10.2), 113.91 (d, J = 27.2), 115.33 (q, J = 289.4, TFA), 115.58, 115.65, 116.98, 128.77, 128.41, 130.30, 132.62 (d, J = 9.0), 134.42, 150.45, 158.04 (d, J = 239.42), 158.51 (q, J = 37.7, TFA), 162.26. MS (LC-MS, ESI): *m/z* 394.1 [M+H$^+$]. HRMS (EI-MS): *m/z* M$^{+\bullet}$ calcd. for $C_{21}H_{23}FN_5O$: 393.1965, found: 393.1969.

3-[4-(1H-Benzo[d]imidazol-2-yl)-3-methylphenoxy]-N-[2-(1H-imidazol-4-yl)ethyl]propan-1-amine tris(hydrotrifluoroacetate) (3.19)

The title compound was prepared from **3.13** (69 mg, 0.229 mmol, 1 eq), K_2CO_3 (63 mg, 0.459 mmol, 2 eq), NaI (34 mg, 0.229 mmol, 1 eq) and 2-(1-Trityl-1*H*-imidazol-4-yl)ethanamine (**3.2**, 243 mg, 0.688 mmol 3 eq) in *n*-butanol (4 mL) by heating for 94 h according to the general procedure. The crude product was purified by flash-chromatography (eluent CH_2Cl_2 (A), MeOH + 1% NEt_3 (B); gradient: 0 to 60 min: A/B 100/0 – 50/50 (*v/v*), SF 10-8 g). Deprotection in CH_2Cl_2 (5 mL) and TFA (1 mL) followed by preparative RP-HPLC (column: Nucleodur 250 × 21 mm; gradient: 0–30 min: MeCN/0.1% aq. TFA 20/80–50/50, t_R = 10.5 min) afforded **3.19** (tris(hydrotrifluoroacetate)) as white fluffy solid (25.3 mg, 18%). R_f = 0.09 (CH_2Cl_2/MeOH/NH_3 80/19/1). UV/VIS (20 mM HCl): λ_{max} 294, 250, 206, 191 nm. RP-HPLC (220 nm): 99.8% (gradient: 0–30 min: MeCN/0.1% aq. TFA 20/80–50/50, 31-40 min: 90/10, t_R = 6.5 min, k = 1.3). ^{1}H-NMR (600 MHz, DMSO-d_6 + 10 µL TFA): δ (ppm) 2.10 (p, J = 6.3, 1H), 2.54 (s, 2H), 3.07 (t, J = 7.5, 1H), 3.16 (p, J = 6.3, 1H), 3.28-3.35 (m, 1H), 4.20 (t, J = 6.0, 1H), 7.06-7.11 (m, 1H), 7.54 (d, J = 0.5, 1H), 7.60 (dd, J = 3.1, 6.1, 1H), 7.76 (d, J = 8.4, 1H), 7.86 (dd, J = 3.1, 6.1, 1H), 8.82-8.90 (m, 1H), 9.05 (d, J = 1.3, 1H), 13.91 (bs, TFA). ^{13}C NMR (151 MHz, DMSO-d_6 + 10 µL TFA): δ (ppm) 19.88, 21.19, 25.43, 44.26, 45.06, 65.13, 112.72, 114.07 (2C), 115.31 (q, J = 289.3, TFA), 115.67, 116.99, 117.30, 125.92 (2C), 128.77, 131.59 (2C), 132.93, 134.43, 140.08, 149.46, 158.50 (q, J = 37.8, TFA), 161.44. MS (LC-MS, ESI): *m/z* 376.0 [M+H$^+$]. HRMS (EI-MS): *m/z* M$^{+\bullet}$ calcd. for $C_{22}H_{25}N_5O$: 375.2059, found: 375.2056.

N-[2-(1H-Imidazol-4-yl)ethyl]-4-(4-(5-fluoro-4-methyl-1H-benzo[d]imidazol-2-yl)-3-methylphenoxy)-butan-1-amine tris(hydrotrifluoroacetate) (3.20)

The title compound was prepared from **3.15** (84 mg, 0.263 mmol, 1 eq), K_2CO_3 (73 mg, 0.526 mmol, 2 eq), NaI (39 mg, 0.263 mmol, 1 eq) and 2-(1-trityl-1*H*-imidazol-4-yl)ethanamine (**3.2**, 279 mg, 0.789 mmol 3 eq) by heating in *n*-butanol (2 mL) for 15 h according to the general procedure. The crude product was purified by flash-chromatography (eluent CH_2Cl_2 (A), MeOH + 1% NEt_3 (B); gradient: 0 to 60 min: A/B 100/0 – 50/50 (*v/v*), SF 10-8 g). Deprotection in CH_2Cl_2 (5 mL) and TFA (2 mL) followed by preparative RP-HPLC (column: Nucleodur 250 × 21 mm; gradient: 0−30 min: MeCN/0.1% aq. TFA 20/80−50/50, t_R = 10.6 min) afforded **3.20** (tris(hydrotrifluoroacetate)) as white fluffy solid (37.1 mg, 24%). R_f = 0.09 (CH_2Cl_2/MeOH/NH_3 80/19/1). UV/VIS (20 mM HCl): λ_{max} 292, 250, 207, 192 nm. RP-HPLC (220 nm): 99.8% (gradient: 0−30 min: MeCN/0.1% aq. TFA 10/90−80/20, 31-40 min: 90/10, t_R = 6.5 min, k = 1.3). ^{1}H-NMR (400 MHz, DMSO-d_6 + 10 µL TFA): δ (ppm) 1.72-1.88 (m, 4H), 2.49 (s, 3H), 2.53 (d, *J* = 1.2, 3H), 3.01-3-09 (m, *J* = 7.3, 4H), 3.22-3.32 (m, 2H), 4.13 (t, *J* = 5.7, 2H), 7.04-7.10 (m, 2H), 7.39-7.47 (m, 1H), 7.53 (s, 1H), 7.67-7.75 (m, 2H), 8.72 (s, 2H), 9.05 (d, *J* = 1.3, 1H), 14.10 (bs, TFA). ^{13}C-NMR (101 MHz, DMSO-d_6 + 10 µL TFA): δ (ppm) 9.43 (d, *J* = 3.3) 19.85, 21.26, 22.51, 25.79, 45.12, 46.74, 67.44, 110.96 (d, *J* = 23.9), 112.60 (d, *J* = 10.4), 112.65, 114.22 (d, *J* = 27.9), 115.52 (d, *J* = 289.1, TFA), 115.63, 117.10, 117.21, 128.25, 128.90, 132.34 (d, *J* = 10.2), 133.11, 134.50, 140.23, 150.94, 158.20 (d, *J* = 239.1), 158.69 (q, *J* = 37.5, TFA), 161.81. MS (LC-MS, ESI): *m/z* 422.2 [M+H$^+$]. HRMS (ESI-MS): *m/z* [M+H$^+$] calcd. for $C_{24}H_{29}FN_5O^+$: 422.2351, found: 422.2354.

3.5.2.5 Preparation of the benzimidazolylphenoxyalkylamines **3.22**-**3.23**

tert-Butyl 3-bromopropylcarbamate (3.21)[58,59]

To a solution of 3-bromopropylamine hydrobromide (6.6 g, 30 mmol, 1 eq) and DIPEA (89.3 g, 72 mmol, 2.4 eq) in CH_2Cl_2 (40 mL) was added dropwise a solution of Boc_2O (7.9 g, 36 mmol, 1.2 eq) in CH_2Cl_2 (20 mL) within 10 min. The mixture was stirred at rt for 18 h. The mixture was washed with 0.1 M HCl, brine and water, dried over Na_2SO_4 and concentrated *in vacuo*. The crude product was purified by flash-chromatography (eluent CH_2Cl_2 (A), MeOH (B); gradient: 0 to 30 min: A/B 100/0 – 60/40 (*v/v*), SF 25-80 g) and afforded a colorless oil (5.2 g, 74%). R_f = 0.78 (CH_2Cl_2/MeOH 25:1). ^{1}H-NMR (300 MHz, $CDCl_3$): δ (ppm) 1.41 (s, 9H), 1.93-2.07 (m, 2H), 3.16-3.27 (m, 2H), 3.41 (t, *J* = 6.5, 2H). ^{13}C-NMR (75 MHz, $CDCl_3$): δ (ppm) 28.46, 30.91, 32.78, 39.06, 79.47, 156.08. MS (GC-MS, CI): *m/z* 238.1 [M+H$^+$]. $C_8H_{16}BrNO_2$ (238.12).

General procedure for the synthesis of the benzimidazolylphenoxyalkylamines 3.22-3.23[9]

A suspension of the pertinent (hydroxyphenyl)benzimidazole (1 eq), and Cs_2CO_3 (1.5 eq) in MeCN was treated with the alkyl halide (1 eq) and heated to 70 °C for 17 h. The reaction mixture was cooled to rt, diluted with $CHCl_3$ and filtered through a glass fritted funnel to remove inorganic solids. The filtrate was concentrated under reduced pressure and purified by flash-chromatography. The combined fractions were dissolved in CH_2Cl_2, TFA was added and the reaction mixture was stirred until the protection group was removed (5-8 h, TLC control). After evaporation of the solvent *in vacuo*, the crude product was purified by preparative RP-HPLC.

3-[4-(5-Fluoro-4-methyl-1H-benzo[d]imidazol-2-yl)-3-methylphenoxy]propan-1-amine bis(hydrotrifluoroacetate) (3.22)

The title compound was prepared from **3.7** (1.30 g, 5.00 mmol, 1 eq), **3.21** (1.21 g, 5.00 mmol, 1 eq) and Cs_2CO_3 (2.48 g, 7.61 mmol, 1.5 eq) in MeCN (16 mL) according to the general procedure. The crude product was purified by flash-chromatography (eluent CH_2Cl_2 (A), MeOH (B); gradient: 0 to 30 min: A/B 100/0 – 96/4 (*v/v*), SF 25-40 g) yielding a yellow foam-like solid. Deprotection in CH_2Cl_2 (60 mL) and TFA (10 mL) gave a brown solid as di-TFA-salt (1.05 g, 27%). A sample of 45 mg was purified by preparative HPLC (column: Nucleodur 250 × 21 mm; gradient: 0−30 min: MeCN/0.1% aq. TFA 20/80−50/50, t_R = 10.6 min). MeCN was removed under reduced pressure. After lyophilisation **3.22** (bis(hydrotrifluoroacetate)) was obtained as white fluffy solid (27.5 mg, 61%). R_f = 0.17 (CH_2Cl_2/MeOH/NH_3 80/19/1). UV/VIS (20 mM HCl): λ_{max} 217, 201 nm. RP-HPLC (220 nm): 99.2% (gradient: 0−30 min: MeCN/0.1% aq. TFA 20/80−50/50, 31-40 min: 90/10, t_R = 12.3 min, k = 3.4). ^{1}H-NMR (300 MHz, MeOH-d_4): δ (ppm) 2.15-2.26 (m, 2H), 2.53 (s, 2H), 2.58 (d, J = 1.7, 2H), 3.19 (t, J = 7.4, 2H), 4.24 (t, J = 5.8, 2H), 7.05-7.15 (m, 2H), 7.34-7.43 (m, 1H), 7.64 (dd, J = 4.2, 8.9, 1H), 7.71 (d, J = 8.5, 1H). ^{13}C-NMR (151 MHz, DMSO-d_6 + 10 µL TFA): δ (ppm) 9.36 (d, J = 3.2), 19.76, 26.87, 36.28, 65.13, 110.86 (d, J = 23.7), 112.45 (d, J = 9.8), 112.55, 114.15 (d, J = 26.9), 115.29 (q, J = 289.1, TFA), 115.64, 117.21, 128.15, 132.24 (d, J = 10.0), 133.03, 140.10, 150.83, 158.11 (d, J = 239.1), 158.53 (q, J = 38.0, TFA), 161.53. MS (LC-MS, ESI): *m/z* 314.0 [M+H$^+$]. HRMS (EI-MS): *m/z* $M^{+\bullet}$ calcd. for $C_{18}H_{20}FN_3O$: 313.1590, found: 313.1585.

3-[4-(1H-Benzo[d]imidazol-2-yl)phenoxy]propan-1-amine bis(hydrotrifluoroacetate) (3.23)

The title compound was prepared from **3.8** (2.00 g, 9.51 mmol, 1 eq), **3.21** (2.27 g, 9.51 mmol, 1 eq) and Cs_2CO_3 (4.64 g, 14.3 mmol, 1.5 eq) in MeCN (30 mL) according to the general procedure. The crude product was purified by flash-chromatography (eluent CH_2Cl_2 (A), MeOH (B); gradient: 0 to

30 min: A/B 100/0 – 96/4 (*v/v*), SF 25-60 g) yielding a white solid. Deprotection in CH_2Cl_2 (60 mL) and TFA (10 mL) gave a brown solid as di-TFA-salt (1.40 g, 30%). A sample of 50 mg was purified by preparative HPLC (column: Nucleodur 250 × 21 mm; gradient: 0−30 min: MeCN/0.1% aq. TFA 15/75−40/60, t_R = 12.2 min). MeCN was removed under reduced pressure. After lyophilisation **3.23** (bis(hydrotrifluoroacetate)) was obtained as white fluffy solid (32.4 mg, 65%). R_f = 0.21 (CH_2Cl_2/MeOH/NH_3 80/19/1). UV/VIS (20 mM HCl): λ_{max} 310, 218, 201 nm. RP-HPLC (220 nm): 100% (gradient: 0−30 min: MeCN/0.1% aq. TFA 30/70−60/40, 31-40 min: 90/10, t_R = 7.6 min, *k* = 1.6). ^{1}H-NMR (300 MHz, DMSO-d_6): δ (ppm) 1.99-2.15 (m, 2H), 2.92-3.09 (m, 2H), 4.23 (t, *J* = 6.1, 2H), 7.29 (d, *J* = 9.0, 2H), 7.52 (dd, *J* = 3.2, 6.1, 2H), 7.82 (dd, *J* = 3.1, 6.1, 2H), 7.94 (s, 3H), 8.22 (d, *J* = 8.9, 2H),14.10 (bs, TFA). ^{13}C-NMR (151 MHz, DMSO-d_6 + 10 µL TFA): δ (ppm) 22.76, 36.35, 65.36, 113.84 (2C), 114.35, 115.33 (q, *J* = 289.4, TFA), 115.81 (2C), 125.91 (2C), 130.08 (2C), 131.68 (2C), 149.11, 158.51 (q, *J* = 37.7, TFA), 162.47.MS (LC-MS, ESI): *m/z* 268.1 [M+H$^+$]. HRMS (EI-MS): *m/z* $M^{+\bullet}$ calcd. for $C_{16}H_{17}N_3O$: 267.1372, found: 267.1376.

3.5.2.6 Preparation of the guanidine **3.26**

N,N'-Bis(tert-butoxycarbonyl)guanidine (3.24)[11,60]

1,4-Dioxane (250 mL) was added to a solution of guanidine hydrochloride (12.0 g, 0.126 mol) and NaOH (20.1 g, 0.502 mol) in water (125mL) and the resulting mixture was cooled to 0 °C. Boc_2O (60.3 g, 0.276 mol) was added in one portion and the reaction mixture was allowed to warm to rt within 2 h. After stirring for 26 h the mixture was concentrated under reduced pressure to one third of its original volume. The resulting suspension was diluted with water (250 mL) and extracted with EtOAc (3 x 250 mL), dried over $MgSO_4$ and concentrated *in vacuo*. The crude product was purified by flash-chromatography (eluent CH_2Cl_2 (A), MeOH (B); gradient: 0 to 10 min: A/B 100/0 – 90/10 (*v/v*), 10 to 30 min: A/B 90/10, SF 65-400 g) and afforded a white solid (11.5 g, 35%), mp 145 °C (lit.[11] 144 °C). R_f = 0.4 (CH_2Cl_2/MeOH 50:1). ^{1}H-NMR (300 MHz, DMSO-d_6): δ (ppm) 1.41 (s, 18H), 8.58 (bs, 2H), 10.53 (bs, 1H). ^{13}C NMR (75 MHz, DMSO-d_6): δ (ppm) 27.83, 79.81, 158.19. MS (LC-MS, ESI): *m/z* 260.0 [M+H$^+$]. $C_{11}H_{21}N_3O_4$ (259.30).

N,N'-Di-Boc-N''-(trifluoromethanesulfonyl)guanidine (3.25)[11]

A solution of *N,N'*-di-Boc-guanidine (**3.24**) (8.57 g, 34.0 mmol) and NEt_3 (3.59 g, 35.0 mmol, 1.05 eq) in CH_2Cl_2 (170 mL) was cooled to -78 °C. Triflic anhydride (10.0 g, 35.0 mmol) was added dropwise within 20 min. After the addition was completed, the mixture was allowed to warm to rt within 4 h. The solution was transferred to a separation funnel, washed with saturated $KHSO_{4(aq.)}$ and water and

dried over anhydrous Na_2SO_4. Concentration *in vacuo* afforded a white solid (10.7 g, 81%). mp 96 °C (lit.[11] 115 °C). R_f = 0.9 (CH_2Cl_2/MeOH 50:1). ^{1}H-NMR (300 MHz, DMSO-d_6): δ (ppm) 1.46 (s, 18H), 11.07 (bs, 2H). ^{13}C NMR (75 MHz, DMSO-d_6): δ (ppm) 27.52, 83.40, 150.09, 152.33. MS (LC-MS, ESI): *m/z* 391.1 [M+H$^+$]. $C_{12}H_{20}F_3N_3O_6S$ (391.36).

1-{3-[4-(5-Fluoro-4-methyl-1H-benzo[d]imidazol-2-yl)-3-methylphenoxy]propyl}guanidine bis(hydrotrifluoroacetate) (3.26)

Compound **3.22** (bis(hydrotrifluoroacetate, 200 mg, 0.369 mmol, 1 eq) was added to a solution of *N,N'*-Di-Boc-*N*''-(trifluoromethanesulfonyl)guanidine (**3.25**, 146 mg, 0.369 mmol, 1 eq) and triethylamine (123 mg, 1.22 mmol, 3.3 eq) in dichloromethane (3mL), and the mixture was stirred at rt for 3 h. After completion of the reaction, the mixture was diluted with dichloromethane (7 mL) and washed with saturated $NaHCO_{3(aq)}$ (10 mL) and brine (10 mL), dried over anhydrous Na_2SO_4 and concentrated *in vacuo*. The crude product was purified by flash-chromatography (eluent CH_2Cl_2 (A), MeOH (B); gradient: 0 to 15 min: A/B 100/0 – 50/1 (*v/v*), 15 to 20 min: A/B A/B 50/1 – 5/1 (*v/v*), SF 10-8 g) and afforded a yellow oil (146 mg, 71%). Deprotection in CH_2Cl_2 (30 mL) and TFA (6 mL) gave a brown solid as di-TFA-salt (153 mg, 100%). A sample of 50 mg was purified by preparative HPLC (column: Nucleodur 250 × 21 mm; gradient: 0−30 min: MeCN/0.1% aq. TFA 20/80−50/50, t_R = 11.4 min). MeCN was removed under reduced pressure. After lyophilisation **3.26** (bis(hydrotrifluoroacetate)) was obtained as white fluffy solid (23.4 mg, 47%). R_f = 0.15 (CH_2Cl_2/MeOH/NH_3 80/19/1). UV/VIS (20 mM HCl): λ_{max} 291, 250, 198, 193 nm. RP-HPLC (220 nm): 98.7% (gradient: 0−30 min: MeCN/0.1% aq. TFA 20/80−50/50, 31-40 min: 90/10, t_R = 16.9 min, *k* = 6.3). ^{1}H-NMR (300 MHz, DMSO-d_6 + 10 µL TFA): δ (ppm) 1.98 (p, *J* = 6.2, 2H), 2.49 (s, 3H), 2.53 (s, 3H), 3.30 (q, *J* = 6.5, 2H), 4.14 (t, *J* = 6.0, 2H), 7.05-7.12 (m, 2H), 7.38-7.48 (m, 1H), 7.66-7.75 (m, 2H), 7.78 (t, *J* = 5.4, 1H), 14.10 (bs, TFA). ^{13}C NMR (75 MHz, DMSO-d_6 + 10 µL TFA): δ (ppm) 9.50 (d, *J* = 3.2), 19.88, 28.20, 45.81, 65.38, 108.12 (d, *J* = 13.2), 110.96 (d, *J* = 23.9), 112.64 (d, *J* = 18.1), 112.65, 114.09, 115.34 (q, *J* = 288.9, TFA), 115.63, 128.16, 132.19, 133.16, 140.23, 150.86, 158.54 (d, *J* = 227.2), 158.63 (q, *J* = 38.1, TFA), 161.72. MS (LC-MS, ESI): *m/z* 355.9 [M+H$^+$]. HRMS (ESI-MS): *m/z* [M+H$^+$] calcd. for $C_{19}H_{23}FN_5O^+$: 356.1881, found: 356.1885.

3.5.2.7 Preparation of N^G-propionyl guanidine **3.30**

S-Methylthiouronium iodide (3.27)[12]

Synthesis of **3.27** is described in Chapter 4 (Compound **4.1**).

N-tert-Butoxycarbonyl-S-methylisothiourea (3.28)[12]

Synthesis of **3.28** is described in Chapter 4 (Compound **4.2**).

N-tert-Butoxycarbonyl-N'-(propionyl)-S-methylisothiourea (3.29)[61]

Synthesis of **3.29** is described in Chapter 4 (Compound **4.4**).

N-(N-{3-[4-(5-Fluoro-4-methyl-1H-benzo[d]imidazol-2-yl)-3-methylphenoxy]propyl}carbamimidoyl)-propionamide bis(hydrotrifluoroacetate) (3.30)

Building block **3.22** (bis(hydrotrifluoroacetate), 152 mg, 0.281 mmol, 1 eq) was dissolved in water (10 mL), the solution was alkalized with 0.5 NaOH (pH 11), extracted three times with CH_2Cl_2 (10 mL), the organic phase dried over anhydrous $MgSO_4$ and concentrated *in vacuo* (70 mg, 0.22 mmol, 1 eq). The released base, the guanidinylating reagent **3.29** (55 mg, 0.22 mmol, 1 eq) and $HgCl_2$ (122 mg, 0.45 mmol, 2 eq) were dissolved in 2 mL CH_2Cl_2. NEt_3 (67.8 mg, 0.67 mmol, 3 eq) was added and the mixture was stirred for 20 h at rt. Subsequently, the precipitate was filtered over Celite. Purification by flash-chromatography (eluent CH_2Cl_2 (A), MeOH (B); gradient: 0 to 30 min: A/B 100/0 – 96/4 (*v/v*), SF 10-4 g)) afforded the intermediate as white solid. Deprotection in CH_2Cl_2 (5 mL) and TFA (1 mL) gave a yellow solid as di-TFA-salt (101 mg, 71%). A sample of 45 mg was purified by preparative HPLC (column: Nucleodur 250 × 21 mm; gradient: 0−30 min: MeCN/0.1% aq. TFA 20/80−50/50, t_R = 14.3 min). MeCN was removed under reduced pressure. After lyophilisation **3.30** (bis(hydrotrifluoroacetate)) was obtained as white fluffy solid (27 mg, 27%). R_f = 0.24 (CH_2Cl_2/MeOH/NH_3 80/19/1). UV/VIS (20 mM HCl): λ_{max} 294, 249, 215, 197 nm. RP-HPLC (220 nm): 97.8% (gradient: 0−30 min: MeCN/0.1% aq. TFA 5/95-80/20, 31-40 min: 90/10, t_R = 15.7 min, k = 8.3). ^{1}H-NMR (300 MHz, DMSO-d_6 + 10 µL TFA): δ (ppm) 1.04 (t, J = 7.4, 3H), 2.05 (p, J = 7.4, 2H), 2.45 (q, J = 7.4, 2H), 2.48 (s, 3H), 2.52 (s, 3H), 3.48 (q, J = 6.2, 2H), 4.17 (t, J = 5.8, 2H), 7.05-7.12 (m, 2H), 7.38-7.48 (m, 1H), 7.66-7.76 (m, 2H), 8.79 (s, 1H), 9.42 (s, 1H), 14.10 (bs, TFA). ^{13}C-NMR (75 MHz, DMSO-d_6 + 10 µL TFA): δ (ppm) 8.31, 9.48 (d, J = 3.4), 19.87, 27.43, 29.73, 40.35, 65.85, 110.98 (d, J = 24.1), 112.61 (d, J = 9.5), 112.63, 114.30 (d, J = 27.1), 115.41 (q, J = 289.0, TFA), 115.69, 119.10, 128.19, 132.28 (d, J = 10.3), 133.15, 140.20, 154.97 (d, J = 252.0), 158.75 (q, J = 37.8, TFA), 161.70, 176.27.MS (LC-MS, ESI): *m/z* 412.22 [M+H$^+$]. HRMS (ESI-MS): *m/z* [M+H$^+$] calcd. for $C_{22}H_{27}FN_5O_2^+$: 412.2143, found: 412.2147.

3.5.2.8 Preparation of the carboxylic amides **3.31**-**3.37**

General procedure for the preparation of 3.31-3.32[9] ***by amide coupling***

The respective carboxylic acid (1 eq) was dissolved in anhydrous THF. EDC × HCl (1 eq), HOBt × H_2O (1 eq) and DIPEA (1.5 eq) were added, and the reaction mixture was stirred at rt under argon atmosphere for 2 h. Subsequently, the building block **3.22** or **3.23** (1 eq) and DIPEA (2.5 eq), dissolved in anhydrous THF were added in one portion. The solution was stirred at rt for 20 h. The

solvent was evaporated under reduced pressure and the residue was dissolved in CH_2Cl_2 (25 mL). The solution was washed with saturated $NaHCO_{3(aq.)}$ and brine, dried over anhydrous Na_2SO_4 and concentrated *in vacuo*. The crude product was purified by flash-chromatography (eluent CH_2Cl_2 (A), MeOH (B); gradient: 0 to 40 min: A/B 100/0 – 90/10 (*v/v*), SF 15-8 g) and afforded a white solid.

N-(3-(4-(1H-Benzo[d]imidazol-2-yl)phenoxy)propyl)propionamide (3.31)

The title compound was prepared from propionic acid (14 mg, 0.182 mmol), EDC × HCl (35 mg, 0.182 mmol), HOBt × H_2O (28 mg, 0.182 mmol) and DIPEA (35 mg, 0.270 mmol) in THF (2 mL), followed by the addition of **3.23** (90 mg, 0.182 mmol) and DIPEA (59 mg, 0.600 mmol) in THF (0.5 mL) (38 mg, 48%). R_f = 0.35 (CH_2Cl_2/MeOH 90/10). UV/VIS (20 mM HCl): λ_{max} 311, 217, 197 nm. RP-HPLC (220 nm): 99.4% (gradient: 0−30 min: MeCN/0.1% aq. TFA 30/70−60/40, 31-40 min: 90/10, t_R = 9.0 min, *k* = 2.2). ^{1}H-NMR (300 MHz, MeOH-d_4): δ (ppm) 1.13 (t, *J* = 7.6, 3H), 2.01 (p, *J* = 6.5, 2H), 2.21 (q, *J* = 7.6, 2H), 3.39 (t, *J* = 6.9, 2H), 4.11 (t, *J* = 6.2, 2H), 7.05-7.13 (m, 2H), 7.20-7.26 (m, 2H), 7.54-7.61 (m, 2H), 7.98-8.06 (m, 2H). ^{13}C-NMR (151 MHz, DMSO-d_6 + 10 µL TFA): δ (ppm) 9.96, 28.53, 28.78, 35.37, 66.05, 112.52 (2C), 114.86, 115.40 (q, *J* = 289.8, TFA), 115.73 (2C), 125.81 (2C), 130.01 (2C), 131.64 (2C), 149.10, 158.47 (q, *J* = 37.4, TFA), 162.73, 172.98. MS (LC-MS, ESI): *m/z* 323.9 [M+H$^+$]. HRMS (EI-MS): *m/z* M$^{+\bullet}$ calcd. for $C_{19}H_{21}N_3O_2$: 323.1634, found: 323.1635.

N-{3-[4-(5-Fluoro-4-methyl-1H-benzo[d]imidazol-2-yl)-3-methylphenoxy]propyl}propionamide (hydrotrifluoroacetate) (3.32)

The title compound was prepared from propionic acid (11 mg, 0.148 mmol), EDC × HCl (28 mg, 0.148 mmol), HOBt × H_2O (23 mg, 0.148 mmol) and DIPEA (29 mg, 0.222 mmol) in THF (2 mL), followed by the addition of **3.22** (80 mg, 0.148 mmol) and DIPEA (48 mg, 0.369 mmol) in THF (0.5 mL) (Yield: 29 mg, 41%.) R_f = 0.41 (CH_2Cl_2/MeOH 90/10). UV/VIS (20 mM HCl): λ_{max} 292, 218, 197 nm. RP-HPLC (220 nm): 100% (gradient: 0−30 min: MeCN/0.1% aq. TFA 30/70−60/40, 31-40 min: 90/10, t_R = 12.7 min, *k* = 3.5). ^{1}H-NMR (300 MHz, $CDCl_3$): δ (ppm) 1.11 (t, *J* = 7.6, 3H), 1.92 (p, *J* = 6.3, 2H), 2.18 (q, *J* = 7.6, 2H), 2.45 (s, 3H), 2.52 (d, *J* = 1.1, 3H), 3.38 (q, *J* = 6.5, 2H), 3.94 (t, *J* = 5.9, 2H), 6.13 (bs, 1H), 6.58 (dd, *J*=2.4, 8.5, 1H), 6.69 (d, *J*=2.3, 1H), 6.90-7.02 (m, 1H), 7.27-7.38 (m, 2H). ^{13}C-NMR (151 MHz, DMSO-d_6 + 10 µL TFA): δ (ppm) 9.34 (d, *J* = 3.2), 9.97, 19.73, 28.69, 35.42, 65.80, 79.19, 110.81 (d, *J* = 23.7), 112.44 (d, *J* = 10.1), 112.52, 114.07 (d, *J* = 27.0), 115.25 (q, *J* = 289.2, TFA), 115.38, 117.18, 128.08, 132.20 (d, *J* = 9.8), 132.94, 140.02, 150.88, 158.03 (d, *J* = 236.8), 158.43 (q, *J* = 38.0, TFA), 161.76, 179.98. MS (LC-MS, ESI): *m/z* 370.0 [M+H$^+$]. HRMS (EI-MS): *m/z* M$^{+\bullet}$ calcd. for $C_{21}H_{24}FN_3O_2$: 369.1853, found: 369.1848.

General procedure for the preparation of 3.33-3.36 by amide coupling

The acid (1.1 eq) was dissolved in DMF (3 mL). DIPEA (3 eq) and TBTU (1.1 eq) were added and the reaction mixture was stirred at rt under argon atmosphere for 10 min. The building block **3.22** (1 eq) and DIPEA (3 eq), dissolved in DMF (1 mL) were added slowly and stirring was continued for 20 h. The crude product was purified by preparative RP-HPLC (column: Gemini-NX C18, 250 × 21 mm). MeCN was removed under reduced pressure. After lyophilisation **3.33**-**3.36** was obtained as white fluffy solid (TFA-salts).

N-{3-[4-(5-Fluoro-4-methyl-1H-benzo[d]imidazol-2-yl)-3-methylphenoxy]propyl}-3-[(5-methyl-1H-imidazol-4-yl)methylsulfanyl] propionamide (bis(hydrotrifluoroacetate)) (3.33)

The title compound was prepared from 2-[(5-methyl-1*H*-imidazol-4-yl)methylsulfanyl]acetic acid (UR-PG139)[55] (30 mg, 0.163 mmol),TBTU (52 mg, 0.163 mmol) and DIPEA (57 mg, 0.443 mmol) in DMF (3 mL), followed by the addition of **3.22** (80 mg, 0.148 mmol) and DIPEA (57 mg, 0.443 mmol) in THF (1 mL) according to general procedure (gradient for HPLC purification: 0−30 min: MeCN/0.1% aq. TFA 15/85−40/60, t_R = 13.2 min; Yield: 43 mg, 41%). R_f = 0.13 (CH_2Cl_2/MeOH 90/10, as free base). UV/VIS (20 mM HCl): λ_{max} 292, 248, 227, 217 nm. RP-HPLC (220 nm): 100% (gradient: 0−30 min: MeCN/0.1% aq. TFA 20/80−80/20, 31-40 min: 90/10, t_R = 13.3 min, k = 4.7). ^{1}H-NMR (400 MHz, DMSO-d_6 + 10 µL TFA): δ (ppm) 1.90 (p, *J* = 6.4, 2H), 2.26 (s, 3H), 2.49 (s, 3H), 2.53 (d, *J* = 0.9, 3H), 3.09 (s, 2H), 3.25 (d, *J* = 6.7, 2H), 3.90 (s, 2H), 4.12 (t, *J* = 6.2, 2H), 7.04-7.12 (m, 2H), 7.39-7.46 (m, 1H), 7.67-7.74 (m, 2H), 8.17 (t, *J* = 5.5, 1H), 8.92 (s, 1H), 9.15 (bs, TFA), 14.25 (bs, 2H) .^{13}C-NMR (101 MHz, DMSO-d_6 + 10 µL TFA): δ (ppm) 8.41, 9.16 (d, *J* = 3.1), 19.57, 23.61, 28.49, 33.58, 35.69, 65.54, 110.66 (d, *J* = 23.8), 112.31 (d, *J* = 10.5), 112.36, 113.92 (d, *J* = 27.0), 115.15 (q, *J* = 289.3, TFA), 115.31, 117.00, 125.11, 126.26, 127.96, 132.06 (d, *J* = 10.3), 132.80, 132.94, 139.89, 150.70, 157.90 (d, *J* = 239.5), 158.33 (q, *J* = 37.8, TFA), 161.56, 168.68. MS (LC-MS, ESI): *m/z* 482.20 [M+H$^+$]. HRMS (ESI-MS): *m/z* [M+H$^+$] calcd. for $C_{25}H_{29}FN_5O_2S^+$: 482.2021, found: 482.2022.

5-Chloro-N-{3-[4-(5-fluoro-4-methyl-1H-benzo[d]imidazol-2-yl)-3-methylphenoxy]propyl}-1H-indole-2-carboxamide (hydrotrifluoroacetate) (3.34)

The title compound was prepared from 5-chloro-1*H*-indole-2-carboxylic acid (32 mg, 0.163 mmol), TBTU (52 mg, 0.163 mmol) and DIPEA (57 mg, 0.443 mmol) in 3 mL of DMF, followed by the addition of **3.22** (80 mg, 0.148 mmol) and DIPEA (57 mg, 0.443 mmol) in THF (1 mL) according to general procedure (gradient for HPLC purification: 0−30 min: MeCN/0.1% aq. TFA 30/70−60/40, t_R = 16.8 min; Yield: 12 mg, 13%). R_f = 0.16 (CH_2Cl_2/MeOH 90/10, as free base). UV/VIS (20 mM HCl): λ_{max} 290, 223,

198 nm. RP-HPLC (220 nm): 100% (gradient: 0−30 min: MeCN/0.1% aq. TFA 40/60−90/10, 31-40 min: 90/10, t_R = 16.6 min, k = 6.1). ^{1}H-NMR (400 MHz, DMSO-d_6 + 10 µL TFA): δ (ppm) 1.98-2.10 (m, 2H), 3.49 (dd, J = 12.2, 6.3 Hz, 2H), 4.18 (t, J = 6.0 Hz, 2H), 7.01-7.27 (m, 5H), 7.37-7.47 (m, 2H), 7.61-7.77 (m, 3H), 8.69 (t, J = 5.4, 1H), 11.79 (s, 1H), 11.97 (bs, TFA). ^{13}C-NMR (151 MHz, DMSO-d_6 + 10 µL TFA): δ (ppm) 9.42 (d, J = 3.0), 19.78, 28.93, 35.98, 65.95, 106.91, 110.93 (d, J = 23.9), 112.52 (d, J = 9.6), 112.67, 114.09 (d, J = 28.3), 115.35, 115.20 (q, J = 288.3, TFA), 117.30, 120.63, 123.47, 124.51, 128.00, 128.04, 128.29, 130.10, 132.16 (d, J = 10.0), 133.09, 134.93, 140.16, 150.93, 158.11 (d, J = 239.1), 158.55 (q, J = 38.4, TFA), 161.02, 161.97. MS (LC-MS, ESI): *m/z* 491.16 [M+H$^+$]. HRMS (ESI-MS): *m/z* [M+H$^+$] calcd. for $C_{27}H_{25}ClFN_4O_2^+$: 491.1645, found: 491.1654.

N-{3-[4-(5-Fluoro-4-methyl-1H-benzo[d]imidazol-2-yl)-3-methylphenoxy]propyl}-3-(4-fluorophenyl)-3-phenylacrylamide (hydrotrifluoroacetate) (3.35)

The title compound was prepared from 3-(4-fluorophenyl)-3-phenylacrylic acid (PG17) (39 mg, 0.163 mmol), TBTU (52 mg, 0.163 mmol) and DIPEA (57 mg, 0.443 mmol) in DMF (3 mL), followed by the addition of **3.22** (80 mg, 0.148 mmol) and DIPEA (57 mg, 0.443 mmol) in THF (1 mL) according to general procedure (gradient for HPLC purification: 0−30 min: MeCN/0.1% aq. TFA 40/70−70/30, t_R = 10.4 min; Yield: 53 mg, 55%). R_f = 0.15 (CH_2Cl_2/MeOH 90/10, as free base). UV/VIS (20 mM HCl): λ_{max} 294, 253, 228, 218 nm. RP-HPLC (220 nm): 99.9% (gradient: 0−30 min: MeCN/0.1% aq. TFA 40/60−90/10, 31-40 min: 90/10, t_R = 17.5 min, k = 6.5). ^{1}H-NMR (400 MHz, DMSO-d_6 + 10 µL TFA): δ (ppm) 1.70-1.90 (m, 2H), 2.49 (s, 3H), 2.53 (s, 3H), 3.11-3.28 (m, 2H), 3.98 (dt, J = 20.1, 6.2 Hz, 2H), 6.44 (d, J = 9.8 Hz, 1H), 6.99-7.09 (m, 2H), 7.10-7.38 (m, 8H), 7.38-7.47 (m, 1H), 7.66-7.75 (m, 2H), 8.07 (dt, J = 5.6, 32.3, 1H), 11.35 (bs, TFA). ^{13}C-NMR (101 MHz, DMSO-d_6 + 10 µL TFA): δ (ppm) 9.38 (d, J = 3.2), 19.78, 28.74, 35.36 (d, J = 6.1), 65.76, 110.89 (d, J = 23.7) 112.51 (d, J = 10.6), 112.61, 114.19 (d, J = 26.4), 114.65 (d, J = 21.4), 115.26 (d, J = 288.8), 115.36, 115.42 (d, J = 21.6), 117.20, 122.89 (d, J = 7.0), 127.70, 127.89, 127.92 (d, J = 33.1), 128.58, 129.33, 129.77 (d, J = 8.4), 131.47 (d, J = 8.3), 132.19 (d, J = 10.2), 133.01, 135.40, 138.99, 140.09 (d, J = 2.8), 141.26, 147.46 (d, J = 46.7), 150.92, 158.13 (d, J = 236.5), 158.53 (q, J = 38.2, TFA), 161.78 (d, J = 244.3), 161.85, 165.45 (d, J = 12.3). MS (LC-MS, ESI): *m/z* 538.23 [M+H$^+$]. HRMS (ESI-MS): *m/z* [M+H$^+$] calcd. for $C_{33}H_{30}F_2N_3O_2^+$: 538.2301, found: 538.2305.

N-{3-[4-(5-Fluoro-4-methyl-1H-benzo[d]imidazol-2-yl)-3-methylphenoxy]propyl}-4-(4-fluorophenyl)-3-methylbutanamide (hydrotrifluoroacetate) (3.36)

The title compound was prepared from 4-(4-fluorophenyl)-3-methylbutanoic acid (AK318) (32 mg, 0.163 mmol), TBTU (52 mg, 0.163 mmol) and DIPEA (57 mg, 0.443 mmol) in DMF (3 mL), followed by

the addition of **3.22** (80 mg, 0.148 mmol) and DIPEA (57 mg, 0.443 mmol) in THF (1 mL) according to the general procedure (gradient for HPLC purification: 0−30 min: MeCN/0.1% aq. TFA 37/63−67/33, t_R = 10.2 min; Yield: 38 mg, 43%). R_f = 0.13 (CH_2Cl_2/MeOH 90/10, as free base). UV/VIS (20 mM HCl): λ_{max} 299, 250, 229, 218 nm. RP-HPLC (220 nm): 99.6% (gradient: 0−30 min: MeCN/0.1% aq. TFA 40/60−90/10, 31-40 min: 90/10, t_R = 15.7 min, k = 5.7). ^{1}H-NMR (400 MHz, DMSO-d_6 + 10 µL TFA): δ (ppm) 0.80 (d, J = 6.5, 3H), 1.81-1.98 (m, 3H), 2.04-2.22 (m, 2H), 2.42 (dd, J = 7.8, 13.2, 1H), 2.47 (s, 3H), 2.53 (d, J = 1.0, 3H), 2.61 (dd, J = 6.1, 13.2, 1H), 3.23 (q, J = 6.5, 2H), 4.11 (t, J = 6.2, 2H), 6.94-7.02 (m, 3H), 7.04-7.10 (m, 2H), 7.26-7.35 (m, 1H), 7.38-7.46 (m, 1H), 7.66-7.73 (m, 2H), 7.95 (t, J = 5.4, 1H), 11.96 (bs, TFA). ^{13}C-NMR (101 MHz, DMSO-d_6 + 10 µL TFA): δ (ppm) 9.38 (d, J = 3.3), 19.06, 19.76, 28.95, 32.04, 35.44, 42.02, 42.41, 65.85, 110.90 (d, J = 23.7), 112.52 (d, J = 12.5), 112.59, 112.79, 114.20 (d, J = 26.9), 115.25 (q, J = 288.6), 115.36, 115.76 (d, J = 20.6), 117.23, 125.26 (d, J = 2.4), 128.07, 130.01 (d, J = 8.5), 132.18 (d, J = 10.2), 133.03, 140.11, 143.60 (d, J = 7.2), 150.92, 158.16 (d, J = 239.2), 158.54 (q, J = 38.2), 161.89 (s), 162.27 (d, J = 243.0), 171.51. MS (LC-MS, ESI): *m/z* 492.25 [M+H$^+$]. HRMS (ESI-MS): *m/z* [M+H$^+$] calcd. for $C_{29}H_{32}F_2N_3O_2^+$: 492.2457, found: 492.2468.

N-{3-[4-(5-Fluoro-4-methyl-1H-benzo[d]imidazol-2-yl)-3-methylphenoxy]propyl}-3-phenylpropanamide (hydrotrifluoroacetate) (3.37)

A solution of **3.23** (bis(hydrotrifluoroacetate)) (8.57 g, 34.0 mmol) and DIPEA (3.59 g, 35.0 mmol, 1.05 eq) in CH_2Cl_2 (1.8 mL) was cooled to 0 °C, and 3-phenylpropanoyl chloride (10.0 g, 35.0mmol) was added. The mixture was allowed to warm to rt within 1 h and stirred for further 8 h. Subsequently, CH_2Cl_2 (23 mL) was added, the solution was transferred to a separation funnel and washed with saturated $NaHSO_{3(aq.)}$ and brine. The organic phase was dried over anhydrous Na_2SO_4 and concentrated *in vacuo*. The crude product was purified by preparative RP-HPLC (column: Nucleodur 250 × 21 mm; gradient: 0−30 min: MeCN/0.1% aq. TFA 30/70−60/40, t_R = 16.5 min). MeCN was removed under reduced pressure. After lyophilisation **3.37** (hydrotrifluoroacetate) was obtained as white fluffy solid (24.4 mg, 59%.). R_f = 0.13 (CH_2Cl_2/MeOH 90/10, as free base). UV/VIS (20 mM HCl): λ_{max} 277, 205, 190 nm. RP-HPLC (220 nm): 98.3% (gradient: 0−30 min: MeCN/0.1% aq. TFA 5/95-80/20, 31-40 min: 90/10, t_R = 20.2 min, k = 11.0). ^{1}H-NMR (400 MHz, DMSO-d_6 + 10 µL TFA): δ (ppm) 1.85 (p, J = 6.5, 3H), 2.38 (t, J = 7.7, 3H), 2.49 (s, 3H), 2.53 (d, J = 1.0, 3H), 2.82 (t, J = 7.7, 2H), 3.21 (q, J = 6.5, 2H), 4.03 (t, J = 6.3, 2H), 7.01-7.09 (m, 2H), 7.12-7.27 (m, 5H), 7.39-7.47 (m, 1H), 7.66-7.74 (m, 2H), 7.93 (t, J = 5.4, 1H), 11.96 (bs, TFA). ^{13}C-NMR (101 MHz, DMSO-d_6 + 10 µL TFA): δ (ppm) 9.40 (d, J = 3.0), 19.78, 28.82, 31.19, 35.41, 37.09, 65.72, 110.87 (d, J = 23.7), 112.48 (d, J = 10.4), 112.58, 114.15 (d, J = 25.1), 115.23 (d, J = 288.9, TFA), 115.35, 117.21, 125.93, 128.07, 128.28 (2C), 128.30 (2C), 132.19 (d, J = 10.0), 132.99, 140.06, 141.36, 150.90, 157.96 (d, J = 288.7), 158.47 (q, J = 38.1,

TFA), 161.81, 171.47. MS (LC-MS, ESI): *m/z* 446.23 [M+H$^+$]. HRMS (ESI-MS): *m/z* [M+H$^+$] calcd. for $C_{27}H_{29}FN_3O_2^+$: 446.2238, found: 446.2246.

3.5.2.9 Preparation of the histamine homolog **3.41**

2-[2-(5-Methyl-1H-imidazol-4-yl)ethyl]isoindoline-1,3-dione (3.39)[62]

Compound **3.38**[62,63] (600 mg, 1.94 mmol) was dissolved in formamide (20 mL) and the mixture was stirred at 170 °C for 4 h. The solution was taken up in 250 mL of saturated $NaHCO_{3(aq.)}$ and extracted with $CHCl_3$ (2 x 250 mL). The organic layer was dried over $MgSO_4$ and evaporated *in vacuo*. Flash-chromatography (eluent CH_2Cl_2 (A), MeOH (B); gradient: 0 to 25 min: A/B 100/0 – 90/10 (*v/v*), SF 15-12 g) yielded a yellow solid (238 mg, 48%). mp 228 °C. R_f = 0.15 (CH_2Cl_2/MeOH 96/4). ^{1}H-NMR (300 MHz, $CDCl_3$): δ (ppm) 2.10 (s, 3H), 2.92 (t, *J* = 7.1, 2H), 3.89 (t, *J* = 7.1, 2H), 7.52 (s, 1H), 7.60-7.86 (m, 4H), 10.36 (s, 1H). ^{13}C-NMR (75 MHz, $CDCl_3$): δ (ppm) 10.21, 24.77, 37.75, 123.17 (2C), 128.26, 132.00 (2C), 133.29, 133.93 (2C), 168.20 (2C). MS (LC-MS, ESI): *m/z* 255.9 [M+H$^+$]. $C_{14}H_{13}N_3O_2$ (255.27).

2-[2-(5-Methyl-1-trityl-1H-imidazol-4-yl)ethyl]isoindoline-1,3-dione (3.40)

To a solution of **3.39** (130 mg, 0.509 mmol, 1 eq) and NEt_3 (92 mg, 0.917 mmol, 1.8 eq) in 2.5 mL of MeCN was added dropwise a solution of trityl chloride (170 mg, 0.611 mmol, 1.2 eq) in MeCN (0.5 mL). After stirring the mixture for 27 h, of $CHCl_3$ (150 mL) was added and washed with water (100 mL). The organic phase was dried over anhydrous Na_2SO_4 and concentrated *in vacuo*. The crude product was purified by flash-chromatography (eluent CH_2Cl_2 (A), MeOH (B); gradient: 0 to 40 min: A/B 100/0 – 90/10 (*v/v*), SF 15-12 g) and afforded a yellow foam-like solid (241 mg, 95%), mp 190 °C. R_f = 0.35 (CH_2Cl_2/MeOH 96/4). ^{1}H-NMR (300 MHz, $CDCl_3$): δ (ppm) 1.28 (s, 3H), 2.89 (t, *J* = 6.9, 2H), 3.97 (t, *J* = 6.9, 2H), 7.03-7.11 (m, 6H), 7.19 (m, 1H), 7.21-7.28 (m, 9H), 7.65-7.85 (m, 4H). ^{13}C-NMR (75 MHz, $CDCl_3$): δ (ppm) 11.54, 26.37, 38.07, 74.78, 123.21 (2C), 126.14, 127.79 (3C), 127.98 (6C), 130.10 (6C), 132.26 (2C), 133.81 (2C), 136.72, 137.64, 141.99 (3C), 168.25 (2C). MS (LC-MS, ESI): *m/z* 498.0 [M+H$^+$]. $C_{33}H_{27}N_3O_2$ (497.59).

2-(5-Methyl-1-trityl-1H-imidazol-4-yl)ethanamine (3.41)[24]

A mixture of **3.40** (235 mg, 0.472 mmol, 1 eq) and hydrazine monohydrate (66 mg, 2.36 mmol, 5 eq) in EtOH (2.4 mL) was stirred at rt for 24 h. After removal of insoluble material, the filtrate was evaporated giving a pale brownish solid (167 g, 96%). mp 82 °C. R_f = 0.07 (CH_2Cl_2/MeOH 90/10).

^{1}H-NMR (300 MHz, $CDCl_3$): δ (ppm) 1.38 (s, 3H), 2.61 (t, *J* = 6.6, 2H), 2.97 (t, *J* = 6.6, 2H), 7.10-7.15 (m, 6H), 7.21 (s, 1H), 7.26-7.34 (m, 9H). ^{13}C-NMR (75 MHz, $CDCl_3$): δ (ppm) ^{13}C NMR (75 MHz, $CDCl_3$) δ 11.68, 25.62, 41.95, 74.78, 125.82, 127.84 (3C), 127.99 (3C), 130.05 (3C), 137.50, 138.00, 141.95 (3C). MS (LC-MS, ESI): *m/z* 368.21 [M+H$^+$]. $C_{25}H_{25}N_3$ (367.49).

3.5.2.10 Preparation of the secondary amine **3.45**

4,5,6,7-Tetrahydro-3H-imidazo[4,5-c]pyridine dihydrochloride (3.42)[22,23]

Histamine dihydrochloride (2.04 g, 11.1 mmol, 1 eq) was dissolved in hydrochloric acid (0.01 M, 87 mL). After the addition of dimethoxymethane (0.837 g, 11.1 mmol, 1 eq), the mixture was heated at reflux for 19 h. Subsequently, the mixture was evaporated to dryness. The solid obtained was stirred in EtOH (30 mL) for 2 h, filtered off and dried *in vacuo* to give **3.42** (dihydrochloride) as white crystals (1.57 g, 72%). mp 270 °C (lit.[22] 270 °C). R_f = 0.07 (CH_2Cl_2/MeOH 90/10). UV/VIS (20 mM HCl): λ_{max} 209, 192. IR (KBr): 3104, 2927, 2281, 1653, 1578, 1500, 1466, 1410 cm^{-1}. RP-HPLC (200 nm): 99.3% (gradient: 0−30 min: MeCN/0.1% aq. TFA 5/95-50/50, 31-40 min: 90/10, t_R = 2.5 min, *k* = 0.5). ^{1}H-NMR (300 MHz, MeOH-d_4): δ (ppm) 3.13 (t, *J* = 6.1, 2H), 3.66 (t, *J* = 6.1, 2H), 4.47 (s, 2H), 8.95 (s, 1H). ^{13}C-NMR (75 MHz, MeOH-d_4): δ (ppm) 19.31, 40.28, 42.45, 122.13, 126.47, 135.95. MS (LC-MS, ESI): *m/z* 124.09 [M+H$^+$]. HRMS (ESI-MS): *m/z* [M+H$^+$] calcd. for $C_6H_9N_3$: 124.0869, found: 124.0871.

Benzyl-6,7-dihydro-3H-imidazo[4,5-c]pyridine-5(4H)-carboxylate (3.43)[64]

To a solution of **3.42** (495 mg, 2.53 mmol, 1 eq) and NEt_3 (728 mg, 7.20 mmol, 3 eq) in CH_2Cl_2 (40 mL) at 0 °C, benzyl succinimidyl carbonate (597 mg, 2.40 mmol, 0.95 eq) in DMF (10 mL) was added dropwise within 10 min. After stirring for 10 min at the same temperature, the mixture was allowed to come to rt and stirring was continued for 1 h. Subsequently, the reaction mixture was transferred to a separation funnel, 400 mL of saturated $K_2CO_{3(aq)}$ and 400 mL of EtOAc were added and the pH of the aqueous phase was adjusted to pH 10 by addition of 1 M $NaOH_{(aq)}$. The organic phase was washed with 150 mL of brine, dried over $MgSO_4$ and concentrated *in vacuo*. The crude product was purified by flash-chromatography (eluent CH_2Cl_2 (A), MeOH (B); gradient: 0 to 40 min: A/B 100/0 – 90/10 (*v/v*), SF 25-40 g) and afforded a yellow oil (377 mg, 58%). R_f = 0.35 (CH_2Cl_2/MeOH 90/10). ^{1}H-NMR (300 MHz, $CDCl_3$): δ (ppm) 2.66 (t, *J* = 4.8, 2H), 3.76 (t, *J* = 4.8, 2H), 4.54 (s, 2H), 5.15 (s, 2H), 7.26-7.41 (m, 5H), 7.47 (s, 1H), 8.31 (bs, 1H). ^{13}C-NMR (75 MHz, $CDCl_3$): δ (ppm) 22.10, 41.78, 42.78, 67.39, 125.29, 127.83 (3C), 128.12, 128.53 (2C), 134.18, 136.46, 155.85. MS (LC-MS, ESI): *m/z* 258.12 [M+H$^+$]. $C_{14}H_{15}N_3O_2$ (257.29).

Benzyl 3-trityl-6,7-dihydro-3H-imidazo[4,5-c]pyridine-5(4H)-carboxylate (3.44)

To a solution of **3.43** (282 mg, 1.10 mmol, 1 eq) and NEt_3 (333 mg, 3.29 mmol, 3 eq) in MeCN (40 mL) was added dropwise a solution of trityl chloride (458 mg, 1.64 mmol, 1.5 eq) in MeCN (10 mL). After stirring the mixture for 24 h, the solvent was removed under reduced pressure and the residue was purified by flash-chromatography (eluent CH_2Cl_2 (A), MeOH (B); gradient: 0 to 40 min: A/B 100/0 – 90/10 (*v/v*), SF 25-40 g) and afforded a yellow foam-like solid (360 mg, 66%), mp 86 °C. R_f = 0.45 (CH_2Cl_2/MeOH 96/4). ^{1}H-NMR (400 MHz, $CDCl_3$): δ (ppm) 1.67 (bs, 2H), 3.47 (bs, 2H), 4.60 (s, 2H), 5.12 (s, 2H), 7.08-7.18 (m, 7H), 7.23-7.38 (m, 13H), 7.35 (s, 1H). ^{13}C NMR (101 MHz, $CDCl_3$): δ (ppm) 24.32, 41.34, 43.75, 53.55, 67.19, 74.84, 127.83 (2C), 128.00, 128.10 (3H), 128.16 (6C), 128.22, 128.49 (2C), 129.96 (6C), 138.17, 141.30, 141.62 (3C), 155.69. MS (LC-MS, ESI): *m/z* 500.23 [$M+H^+$]. $C_{33}H_{29}N_3O_2$ (499.60).

3-Trityl-4,5,6,7-tetrahydro-3H-imidazo[4,5-c]pyridine (3.45)

To a solution of **3.44** (300 mg, 0.601 mmol, 1 eq) in MeOH (10 mL), 10% palladium-on-charcoal catalyst (30 mg) was added and a slow stream of hydrogen was led through a glass tube into the vigorously stirred suspension. After depletion of the starting material (4 h; control by TLC) the catalyst was removed by filtration through Celite. The filtrate was concentrated *in vacuo* to give the product as a clear sticky oil which was used in the next step without further purification (198 mg, 90%). R_f = 0.15 (CH_2Cl_2/MeOH 96/4). ^{1}H-NMR (300 MHz, $CDCl_3$): δ (ppm) 1.87 (bs, 2H), 3.02 (bs, 2H), 4.15 (s, 2H), 7.00-7.10 (m, 6H), 7.20-7.31 (m, 10H). MS (LC-MS, ESI): *m/z* 366.20 [$M+H^+$]. $C_{25}H_{23}N_3$ (365.47).

3.5.2.11 Preparation of the primary amines **3.48**-**3.50**

Benzyl 4-{3-[2-(tert-butoxycarbonylamino)ethylamino]-3-oxoprop-1-enyl}-1H-imidazole-1-carboxylate (3.47)

To a solution of **3.46** (UR-MK251, 558 mg, 1.99 mmol, 1 eq) and NEt_3 (806 mg, 7.96 mmol, 4 eq) in DMF (40 mL), benzyl chloroformate (679 mg, 3.98 mmol, 2 eq) in DMF (10 mL) were added dropwise within 10 min and the mixture was stirred at rt for 24 h. Subsequently, the reaction mixture was transferred to a separation funnel, 400 mL of 1 M $NaOH_{(aq)}$, 200 mL of EtOAc and 450 mL of water was added. The organic phase was washed with 200 mL of brine, dried over $MgSO_4$ concentrated *in vacuo*. The crude product was purified by flash-chromatography (eluent CH_2Cl_2 (A), MeOH (B); gradient: 0 to 50 min: A/B 100/0 – 90/10 (*v/v*), SF 25-40 g) and afforded a yellow foam-like solid

(668 mg, 81%), mp 153 °C. R_f = 0.35 (CH_2Cl_2/MeOH 90/10). ^{1}H-NMR (400 MHz, $CDCl_3$): δ (ppm) 1.38 (s, 9H), 3.16-3.44 (m, 4H), 4.64 (s, 2H), 6.64 (d, *J* = 15.2, 1H), 7.03 (s, 1H), 7.18-7.45 (m, 6H), 8.00 (s, 1H). MS (LC-MS, ESI): *m/z* 415.20 [M+H$^+$]. $C_{21}H_{26}N_4O_5$ (414.45).

Benzyl 4-[3-(2-aminoethylamino)-3-oxoprop-1-enyl]-1H-imidazole-1-carboxylate bis(hydrotrifluoroacetate) (3.48)

To a solution of **3.47** (334 mg, 0.807 mmol) in CH_2Cl_2 (2 mL), TFA (1 mL) was added dropwise. After stirring for 4 h, the solvent was removed under reduced pressure, resuspended twice in CH_2Cl_2 (10 mL) to remove remains of TFA. Subsequently, the residue was dissolved in water (10 mL) and dried by lyophilisation to afford **3.49** (bis(hydrotrifluoroacetate)) as a white powder (360 mg, 96%). R_f = 0.05 (CH_2Cl_2/MeOH 90/10). ^{1}H-NMR (300 MHz, DMSO-d_6 + 10 µL TFA): δ (ppm) 2.79-3.02 (m, 2H), 3.41 (q, *J* = 6.2, 2H), 5.15 (s, 2H), 6.64 (d, *J* = 16.0, 1H), 7.24-7.49 (m, 6H), 7.99 (s, 3H), 8.51 (t, *J* = 5.7, 2H), 9.09 (bs, TFA), 9.16 (s, 1H). MS (LC-MS, ESI): *m/z* 315.15 [M+H$^+$]. $C_{16}H_{18}N_4O_3$ (314.34).

N-(2-Aminoethyl)-3-(1H-imidazol-4-yl)acrylamide bis(hydrotrifluoroacetate) (3.49)

To a solution of **3.46** (0.50 g, 1.78 mmol) in CH_2Cl_2 (2 mL), TFA (1 mL) was added dropwise. After stirring for 4 h, the solvent was removed under reduced pressure, resuspended twice in CH_2Cl_2 (10 mL) to remove remains of TFA. Subsequently, the residue was dissolved in water (10 mL) and dried by lyophilisation to afford **3.49** as a white powder (714 mg, 98%). A sample of 50 mg was purified by preparative HPLC (column: Nucleodur 250 × 21 mm; gradient: 0−30 min: MeCN/0.1% aq. TFA 3/97, 31−40 min: 90/10 min, t_R = 5.5 min). MeCN was removed under reduced pressure. After lyophilisation **3.49** (bis(hydrotrifluoroacetate)) was obtained as white fluffy solid (38 mg, 76%). R_f = 0.16 (CH_2Cl_2/MeOH/NH_3 80/19/1). UV/VIS (20 mM HCl): λ_{max} 266, 192 nm. RP-HPLC (220 nm): 99.6% (gradient: 0−30 min: MeCN/0.1% aq. TFA 3/97, 31-40 min: 90/10, t_R = 8.7 min, *k* = 2.1). ^{1}H-NMR (300 MHz, MeOH-d_4): δ (ppm) 3.13 (t, *J* = 5.9, 2H), 3.60 (t, *J* = 5.9, 2H), 6.75 (d, *J* = 15.9, 1H), 7.49 (d, *J* = 15.9, 1H), 7.84 (s, 1H), 8.96 (s, 1H). ^{13}C NMR (75 MHz, MeOH-d_4): δ (ppm) 38.51, 40.75, 121.18, 125.00, 126.31, 131.34, 137.13, 168.09.MS (LC-MS, ESI): *m/z* 181.04 [M+H$^+$]. HRMS (ESI-MS): *m/z* [M+H$^+$] calcd. for $C_8H_{13}N_4O^+$: 181.1084, found: 181.1088.

N-(2-Aminoethyl)-3-(1H-imidazol-4-yl)propanamide bis(hydrotrifluoroacetate) (3.50)

To a solution of **3.46** (194 mg, 0.475 mmol, 1 eq) in MeCN (10 mL), 10% palladium-on-charcoal catalyst (19 mg) was added and a slow stream of hydrogen was led through a glass tube into the vigorously stirred suspension for 4 h. Subsequently, stirring was continued at 1 atm H_2 for 16 h. After depletion of the starting material (control by TLC) the catalyst was removed by filtration through Celite. The filtrate was concentrated *in vacuo* to give the product as a white solid (170 mg, 88%). A sample of 50 mg was purified by preparative HPLC (column: Nucleodur 250 × 21 mm; gradient: 0−30 min: MeCN/0.1% aq. TFA 3/97, 31−40 min: 90/10 min, t_R = 5.8 min). MeCN was removed under reduced pressure. After lyophilisation **3.50** (bis(hydrotrifluoroacetate)) was obtained as white fluffy solid (28 mg, 56%). R_f = 0.15 (CH_2Cl_2/MeOH/NH_3 80/19/1). UV/VIS (20 mM HCl): λ_{max} 222, 212 nm. RP-HPLC (220 nm): 98.3% (gradient: 0−30 min: MeCN/0.1% aq. TFA 3/97, 31-40 min: 90/10, t_R = 5.0 min, k = 0.8). ^{1}H-NMR (300 MHz, MeOH-d_4): δ (ppm) 2.65 (t, J = 7.3, 1H). 2.99-3.09 (m, 2H), 3.46 (t, J = 5.9, 1H), 7.31 (d, J = 0.8, 1H), 8.77 (d, J = 1.3, 1H). ^{13}C NMR (75 MHz, MeOH-d_4): δ (ppm) 21.07, 34.90, 38.23, 40.75, 117.01, 134.59, 134.67, 174.94. MS (LC-MS, ESI): *m/z* 183.12 [M+H$^+$]. HRMS (ESI-MS): *m/z* [M+H$^+$] calcd. for $C_8H_{15}N_4O^+$: 183.1240, found: 183.1240.

3.5.2.12 Preparation of the primary amines **3.58**-**3.60**

General procedure for the preparation of the imidazoles 3.53 and 3.54

The respective amine (1 eq), phthalic anhydride (7 eq) and NEt_3 (3 eq) were put together in toluene connected with a water separator and refluxed for 24 h. The mixture was cooled to rt and the solvent was removed under reduced pressure. Subsequently, the residue was transferred to a separation funnel, 100 mL of EtOAc and 100 mL of brine were added and the pH of the aqueous phase was adjusted to pH 11 by addition of 1 M $NaOH_{(aq)}$. The aqueous phase was washed with 100 mL of EtOAc for three times and the combined organic phases were dried over $MgSO_4$ and concentrated *in vacuo* to afford **3.53** or **3.54** as pale yellow solid which was used in the next step without further purification.

2-[4-(1H-Imidazol-4-yl)butyl]isoindoline-1,3-dione (3.53)[52]

The title compound was prepared from **3.51** (imbutamine dihydrobromide, 5.75 g, 19.1 mmol), phthalic anhydride (19.8 g, 133 mmol) and NEt_3 (5.80 mg, 57.1 mmol) in toluene (150 mL) according to general procedure. (Yield: 2.47 g, 48%.). R_f = 0.45 (CH_2Cl_2/MeOH 90/10). mp 151 °C (lit.[52] 158-160 °C). ^{1}H-NMR (300 MHz, MeOH-d_4): δ (ppm). 1.57-1.73 (m, 4H), 2.63 (t, J = 6.9, 2H), 3.67 (t, J = 6.6, 2H), 6.81 (s, 1H), 7.66 (s, 1H), 7.73-7.84 (m, 4H). ^{13}C NMR (75 MHz, MeOH-d_4): δ (ppm) 26.72,

27.77, 29.05, 38.53, 118.03, 124.09 (2C), 133.38 (2C), 135.35 (2C), 135.65, 137.46, 169.85 (2C). MS (LC-MS, ESI): *m/z* 270.13 [M+H$^+$]. $C_{15}H_{15}N_3O_2$ (269.30).

2-[5-(1H-Imidazol-4-yl)pentyl]isoindoline-1,3-dione (3.54)

The title compound was prepared from **3.52** (impentamine, 0.670 g, 4.78 mmol), phthalic anhydride (4.54 g, 30.6 mmol) and NEt_3 (1.33 mg, 13.1 mmol) in toluene (25 mL) according to general procedure. (Yield: 0.657 g, 53%). R_f = 0.45 (CH_2Cl_2/MeOH 90/10). ^{1}H-NMR (300 MHz, MeOH-d_4): δ (ppm) 1.22-1.40 (m, 2H), 1.57-1.72 (m, 4H), 2.55 (t, *J* = 7.5, 2H), 3.61 (t, *J* = 7.2, 2H), 6.74 (s, 1H), 7.57 (s, 1H), 7.70-7.82 (m, 4H), 7.88 (s, 1H). ^{13}C NMR (75 MHz, MeOH-d_4): δ (ppm) 27.08, 27.34, 29.20, 29.90, 38.66, 118.18, 123.99 (2C), 133.22 (2C), 135.23 (2C), 135.50, 137.53, 169.69 (2C). MS (LC-MS, ESI): *m/z* 284.14 [M+H$^+$]. $C_{16}H_{17}N_3O_2$ (283.33).

General procedure for the preparation of the trityl-prot*ECt*ed imidazoles 3.56 and 3.57

To a solution of **3.56 or 3.57** (1 eq) and NEt_3 (1.5-3.0 eq) in MeCN was added dropwise a solution of trityl chloride (1.3 eq) in MeCN. After stirring the mixture for 24 h, the solvent was removed under reduced pressure. The crude product was purified by flash-chromatography.

2-[4-(1-Trityl-1H-imidazol-4-yl)butyl]isoindoline-1,3-dione (3.56)[65]

The title compound was prepared from **3.53** (500 mg, 1.86 mmol), trityl chloride (673 mg, 2.41 mmol) and NEt_3 (282 mg, 2.79 mmol) in MeCN (75 mL) according to general procedure. The crude product was purified by flash-chromatography (eluent CH_2Cl_2 (A), MeOH (B); gradient: 0 to 50 min: A/B 100/0 – 90/10 (*v/v*), SF 25-40 g) and afforded a yellow foam-like solid (860 mg, 91%), mp 56 °C. R_f = 0.61 (CH_2Cl_2/MeOH 90/10). ^{1}H-NMR (400 MHz, $CDCl_3$): δ (ppm) 1.64 (bs, 4H), 2.54 (bs, 2H), 3.61 (bs, 2H), 6.50 (s, 1H), 7.04-7.12 (m, 6H), 7.20-7.27 (m, 9H), 7.32 (s, 1H), 7.54-7.78 (m, 4H). ^{13}C NMR (101 MHz, $CDCl_3$): δ (ppm) 26.44, 27.66, 27.95, 37.62, 74.93, 117.86, 122.89 (2C), 127.77 (3C), 127.83 (6C), 129.58 (6C), 132.00 (2C), 133.62 (2C), 138.08, 140.92, 142.34 (3C), 168.08 (2C). MS (LC-MS, ESI): *m/z* 512.23 [M+H$^+$]. $C_{34}H_{29}N_3O_2$ (511.61).

2-[5-(1-Trityl-1H-imidazol-4-yl)pentyl]isoindoline-1,3-dione (3.57)[66]

The title compound was prepared from **3.54** (272 mg, 0.960 mmol), trityl chloride (348 mg, 1.25 mmol) and NEt_3 (291 mg, 2.79 mmol) in MeCN (50 mL) according to general procedure. The crude product was purified by flash-chromatography (eluent CH_2Cl_2 (A), MeOH (B); gradient: 0 to

50 min: A/B 100/0 – 90/10 (*v/v*), SF 25-40 g) and afforded a yellow foam-like solid (200 mg, 40%), mp 73 °C. R_f = 0.45 (CH_2Cl_2/MeOH 90/10). ^{1}H-NMR (400 MHz, DMSO-d_6 + 10 µL TFA): δ (ppm) 1.28-1.39 (m, 2H), 1.58-1.71 (m, 4H), 2.50 (t, *J* = 7.5, 2H), 3.62 (t, *J* = 7.3, 2H), 6.48 (s, 1H), 7.08-7.14 (m, 6H), 7.25-7.30 (m, 9H), 7.31 (s, 1H), 7.60-7.81 (m, 4H). ^{13}C NMR (101 MHz, $CDCl_3$): δ (ppm) 26.50, 28.20, 28.40, 28.87, 38.02, 75.06, 117.79, 123.11 (2C), 127.94 (3C), 127.98 (6C), 129.77 (6C), 132.17 (2C), 133.81 (2C), 138.21, 141.58, 142.57 (3C), 168.37 (2C). MS (LC-MS, ESI): *m/z* 526.25 [M+H$^+$]. $C_{35}H_{31}N_3O_2$ (525.64).

General procedure for the preparation of the imidazoles 3.58 - 3.60

A mixture of **3.55**-**3.57** (1 eq) and hydrazine monohydrate (5-6.3 eq) in EtOH or *n*-butanol was stirred at rt for 24 h. After removal of insoluble material, the filtrate was evaporated giving a pale brownish solid which was used in the next step without further purification.

3-(1-Trityl-1H-imidazol-4-yl)propan-1-amine (3.58)[67]

The title compound was prepared from **3.55** (1.58 g, 3.18 mmol) and hydrazine monohydrate (1.00 g, 20.0 mmol, 6.3 eq) in *n*-butanol (25 mL) according to general procedure, affording a yellow foam-like solid which was used in the next step without further purification (1.17 g, 100%), mp 107 °C (lit.[52] 106-108 °C). R_f = 0.10 (CH_2Cl_2/MeOH 90/10). ^{1}H-NMR (300 MHz, $CDCl_3$): δ (ppm) 1.59-1.75 (m, 2H), 2.47 (t, *J* = 7.5, 2H), 2.60 (t, *J* = 7.0, 2H), 6.43 (s, 1H), 6.97-7.08 (m, 6H), 7.15-7.21 (m, 9H), 7.25 (s, 1H). ^{13}C-NMR (75 MHz, $CDCl_3$): δ (ppm) 25.67, 32.91, 41.49, 75.02, 117.80, 127.95 (3C), 127.97 (6C), 129.72 (3C), 138.27, 141.23, 142.50 (3C). MS (LC-MS, ESI): *m/z* 368.0 [M+H$^+$]. $C_{25}H_{25}N_3$ (367.49).

4-(1-Trityl-1H-imidazol-4-yl)butan-1-amine (3.59)[65]

The title compound was prepared from **3.56** (430 mg, 0.841 mmol) and hydrazine monohydrate (210 mg, 4.20 mmol, 5 eq) in EtOH (6 mL) according to general procedure, affording a yellow sticky solid which was used in the next step without further purification (308 mg, 96%). mp 63 °C. R_f = 0.10 (CH_2Cl_2/MeOH 90/10). ^{1}H-NMR (300 MHz, $CDCl_3$): δ (ppm) 1.36-1.68 (m, 4H), 2.45 (t, *J* = 7.5, 2H), 2.65 (t, *J* = 6.9, 2H), 6.46 (s, 1H), 7.01-7.11 (m, 6H), 7.20-7.28– (m, 9H), 7.29 (s, 1H). ^{13}C-NMR (75 MHz, $CDCl_3$): δ (ppm) 26.43, 27.92, 32.06, 41.21, 74.98, 117.70, 127.92 (9C), 129.66 (6C), 138.10, 141.40, 142.39 (3C). MS (LC-MS, ESI): *m/z* 382.23 [M+H$^+$]. $C_{26}H_{27}N_3$ (381.51).

5-(1-Trityl-1H-imidazol-4-yl)pentan-1-amine (3.60)[65]

The title compound was prepared from **3.57** (200 mg, 0.381 mmol) and hydrazine monohydrate (95 mg, 1.90 mmol, 5 eq) in EtOH (3 mL) according to general procedure, affording a yellow foam-like solid which was used in the next step without further purification (148 mg, 98%), mp 73 °C. R_f = 0.10 (CH_2Cl_2/MeOH 90/10). ^{1}H-NMR (300 MHz, $CDCl_3$): δ (ppm) 1.23-1.68 (m, 6H), 2.39-2.79 (m, 4H), 6.46 (s, 1H), 7.04-7.15 (m, 6H), 7.25-7.34 (m, 10H). ^{13}C-NMR (75 MHz, $CDCl_3$): δ (ppm) 26.37, 28.18, 29.00, 31.96, 41.41, 75.04, 117.75, 127.99 (9C), 129.77 (6C), 138.14, 141.69, 142.51 (3C). MS (LC-MS, ESI): *m/z* 396.24 [M+H$^+$]. $C_{27}H_{29}N_3$ (395.54).

3.5.2.13 Preparation of the amines **3.62**-**3.73**

5-Fluoro-2-[4-(3-iodopropoxy)-2-methylphenyl]-4-methyl-1H-benzo[d]imidazole (3.61)

A mixture of **3.11** (1.36 g, 4.09 mmol, 1 eq) and NaI (1.39 g, 27.8 mmol, 6.8 eq) in acetone (7 mL) was refluxed for 72 h. Subsequently, the solvent was removed und reduced pressure, the residue was dissolved in CH_2Cl_2 (20 mL), sonificated, filtered and dried *in vacuo* to afford a yellow foam-like solid (1.56 g, 90%). mp 76-78 °C. R_f = 0.41 (hexanes/EtOAc 2/1) nm. RP-HPLC (220 nm): 97% (gradient: 0−30 min: MeCN/0.1% aq. TFA 5/95−80/20, 31-40 min: 90/10, t_R = 26.0 min, *k* = 10.1). ^{1}H-NMR (400 MHz, $CDCl_3$): δ (ppm) 2.27 (p, *J* = 6.3, 1H), 2.44 (s, 3H), 2.49 (d, *J* = 1.4, 3H), 3.37 (t, *J* = 6.7, 2H), 4.03 (t, *J* = 5.8, 2H), 6.64 (dd, *J* = 2.5, 8.5, 1H), 6.75 (d, *J* = 2.5, 1H), 6.95 (dd, *J* = 8.8, 10.1, 1H), 7.24 (dd, *J* = 4.4, 8.7, 1H), 7.37 (d, *J* = 8.5, 1H). ^{13}C-NMR (101 MHz, DMSO-d_6 + 10 µL TFA) 3.76, 9.42 (d, *J* = 3.2), 19.81, 32.36, 67.85, 110.97 (d, *J* = 23.7), 112.58 (d, *J* = 10.1), 112.72, 114.29 (d, *J* = 26.8), 115.35 (d, *J* = 288.8, TFA), 115.68, 117.34, 128.13, 132.24 (d, *J* = 10.3), 133.15, 140.29, 150.94, 158.24 (d, *J* = 239.6), 158.65 (q, *J* = 38.1, TFA), 161.75. MS (LC-MS, ESI): *m/z* 425.05 [M+H$^+$]. HRMS (ESI-MS): *m/z* [M+H$^+$] calcd. for $C_{18}H_{19}FIN_2O^+$: 425.0521, found: 425.0522.

General procedure for the preparation of the s*EC*ondary amines 3.62 and 3.73

The iodinated compound **3.61** (1 eq), the pertinent amine (2-3.5 eq) and K_2CO_3 (4-7 eq) in MeCN were heated under microwave irradiation at 130 °C for 20 min. Subsequently, the solvent was removed *in vacuo*. For **3.65** and **3.66**, the crude product was purified by preparative RP-HPLC. For all other compounds, the residue was dissolved in CH_2Cl_2, TFA was added and the reaction mixture was stirred until the protection group was removed (5-8 h, TLC control). After evaporation of the solvent *in vacuo*, the crude product was purified by preparative RP-HPLC.

3-[4-(5-Fluoro-4-methyl-1H-benzo[d]imidazol-2-yl)-3-methylphenoxy]-N-[2-(5-methyl-1H-imidazol-4-yl)ethyl]propan-1-amine tris(hydrotrifluoroacetate) (3.62)

The title compound was prepared from **3.61** (50 mg, 0.118 mmol, 1 eq), **3.41** (152 mg, 0.413 mmol, 3.5 eq) and K_2CO_3 (114 mg, 0.825 mmol, 7 eq) in MeCN (2.5 mL) according to general procedure. Deprotection in CH_2Cl_2 (5 mL) and TFA (2 mL) followed by preparative RP-HPLC (column: Nucleodur 250 × 21 mm; gradient: 0–30 min: MeCN/0.1% aq. TFA 10/90–45/55, t_R = 12.8 min) afforded **3.62** (tris(hydrotrifluoroacetate)) as white fluffy solid (38 mg, 42%). R_f = 0.11 (CH_2Cl_2/MeOH/NH_3 80/19/1). UV/VIS (20 mM HCl): λ_{max} 295, 252, 209, 192 nm. RP-HPLC (220 nm): 98.8% (gradient: 0–30 min: MeCN/0.1% aq. TFA 5/95-80/20, 31-40 min: 90/10, t_R = 13.3 min, k = 6.9). ^{1}H-NMR (400 MHz, DMSO-d_6 + 10 µL TFA): δ (ppm) 2.07-2.17 (m, 2H), 2.25 (s, 3H), 2.50 (s, 3H, superimposed by solvent), 2.53 (d, J = 1.0, 3H), 3.01 (t, J = 7.4, 2H), 3.11-3.28 (m, 4H), 4.19 (t, J = 6.0, 2H), 7.05-7.10 (m, 2H), 7.38-7.47 (m, 1H), 7.70 (dd, J = 4.4, 9.1, 1H), 7.74 (d, J = 8.7, 1H), 8.87 (bs, 1H), 8.95 (s, 1H), 13.17 (bs, TFA), 14.22 (bs, 2H). ^{13}C-NMR (101 MHz, DMSO-d_6 + 10 µL TFA): δ (ppm) 8.61, 9.38 (d, J = 3.1), 19.79, 20.23, 25.51, 44.32, 45.56, 65.21, 110.89 (d, J = 23.4), 112.55 (d, J = 9.9), 112.57, 114.17 (d, J = 26.3), 115.31 (q, J = 288.9, TFA), 115.80, 117.16, 123.85, 126.28, 128.19, 132.28 (d, J = 10.4), 132.97, 133.07, 140.17, 150.80, 158.14 (d, J = 239.3), 158.56 (q, J = 38.0, TFA), 161.47. MS (LC-MS, ESI): *m/z* 422.24 [M+H$^+$]. HRMS (ESI-MS): *m/z* [M+H$^+$] calcd. for $C_{24}H_{29}FN_5O^+$: 422.2351, found: 422,2354.

N-[3-(1H-Imidazol-4-yl)propyl]-3-[4-(5-fluoro-4-methyl-1H-benzo[d]imidazol-2-yl)-3-methylphenoxy]propan-1-amine tris(hydrotrifluoroacetate) (3.63)

The title compound was prepared from **3.61** (116 mg, 0.272 mmol, 1 eq), **3.58** (305 mg, 0.817 mmol, 3 eq) and K_2CO_3 (263 mg, 1.91 mmol, 7 eq) in MeCN (5.5 mL) according to the general procedure. Deprotection in CH_2Cl_2 (5 mL) and TFA (2 mL) followed by preparative RP-HPLC (column: Nucleodur 250 × 21 mm; gradient: 0–30 min: MeCN/0.1% aq. TFA 20/80–50/50, t_R = 9.0 min) afforded **3.63** (tris(hydrotrifluoroacetate)) as white fluffy solid (58.2 mg, 28%). R_f = 0.13 (CH_2Cl_2/MeOH/NH_3 80/19/1). UV/VIS (20 mM HCl): λ_{max} 294, 252, 205 nm. RP-HPLC (220 nm): 99.3% (gradient: 0–30 min: MeCN/0.1% aq. TFA 5/95-80/20, 31-40 min: 90/10, t_R = 13.1 min, k = 6.8). ^{1}H-NMR (400 MHz, DMSO-d_6 + 10 µL TFA): δ (ppm) 1.91-2.02 (m, 2H), 2.06-2.16 (m, 2H), 2.49 (s, 3H), 2.53 (d, J = 1.2, 3H), 2.76 (t, J = 7.4, 2H), 2.94-3.05 (m, 2H), 3.06-3.18 (m, 2H), 4.18 (t, J = 6.0, 2H), 7.03-7.10 (m, 2H), 7.39-7.45 (m, 1H), 7.46 (s, 1H), 7.65-7.77 (m, 2H), 8.70 (bs, 2H), 9.01 (s, 1H), 13.17 (bs, TFA), 14.24 (bs, 2H). ^{13}C-NMR (101 MHz, DMSO-d_6 + 10 µL TFA): δ (ppm) 9.14 (d, J = 3.3), 19.56, 20.92, 24.25, 25.35, 44.07, 45.83, 64.98, 110.67 (d, J = 23.7), 112.32 (d, J = 10.1), 112.33, 113.96 (d, J = 28.2), 115.09 (q, J = 288.8, TFA), 115.55, 115.67, 116.94, 127.95, 131.89, 132.04 (d, J = 10.5), 132.84, 133.93, 139.94,

150.57, 157.92 (d, *J* = 239.5), 158.33 (q, *J* = 38.0), 161.27. MS (LC-MS, ESI): *m/z* 422.24 [M+H$^+$]. HRMS (ESI-MS): *m/z* [M+H$^+$] calcd. for $C_{24}H_{29}FN_5O^+$: 422.2351, found: 422.2346.

***N*-{3-[4-(5-Fluoro-4-methyl-1*H*-benzo[d]imidazol-2-yl)-3-methylphenoxy]propyl}-4-(1*H*-imidazol-4-yl)butan-1-amine tris(hydrotrifluoroacetate) (3.64)**

The title compound was prepared from **3.61** (60 mg, 0.141 mmol, 1 eq), **3.59** (184 mg, 0.481 mmol, 3.4 eq) and K_2CO_3 (133 mg, 0.962 mmol, 6.8 eq) in MeCN (2.5 mL) according to the general procedure. Deprotection in CH_2Cl_2 (5 mL) and TFA (2 mL) followed by preparative RP-HPLC (column: Nucleodur 250 × 21 mm; gradient: 0–30 min: MeCN/0.1% aq. TFA 10/90–45/55, t_R = 9.5 min) afforded **3.64** (tris(hydrotrifluoroacetate)) as white fluffy solid (42.9 mg, 39%). R_f = 0.12 (CH_2Cl_2/MeOH/NH_3 80/19/1). UV/VIS (20 mM HCl): λ_{max} 291, 249, 208, 192 nm. RP-HPLC (220 nm): 99.4% (gradient: 0–30 min: MeCN/0.1% aq. TFA 10/90–80/20, 31-40 min: 90/10, t_R = 14.9 min, *k* = 5.4). ^{1}H-NMR (400 MHz, DMSO-d_6 + 10 µL TFA): δ (ppm) 1.54-1.75 (m, 4H), 2.04-2.18 (m, 2H), 2.50 (s, 3H, superimposed by solvent), 2.53 (d, *J* = 1.0, 3H), 2.69 (t, *J* = 6.9, 2H), 2.91-3.04 (m, 2H), 3.05-3.17 (m, 2H), 4.19 (t, *J* = 6.0, 2H), 7.04-7.10 (m, 2H), 7.38-7.48 (m, 2H), 7.71 (dd, *J* = 4.8, 9.6, 1H), 7.74 (d, *J* = 8.5, 1H), 8.63 (bs, 2H), 8.99 (s, 1H), 13.54 (bs, TFA), 14.48 (bs, 2H). ^{13}C-NMR (101 MHz, DMSO-d_6 + 10 µL TFA): δ (ppm) 9.35 (d, *J* = 3.4), 19.79, 23.31, 24.84, 24.93, 25.58, 44.27, 46.58, 65.21, 110.89 (d, *J* = 23.6), 112.56 (d, *J* = 10.1), 112.57, 114.13 (d, *J* = 29.5), 115.42 (q, *J* = 289.5, TFA), 115.72, 115.82, 117.17, 128.24, 132.32 (d, *J* = 10.0), 132.97, 133.06, 133.93, 140.16, 150.84, 158.14 (d, *J* = 239.3), 158.60 (q, *J* = 37.7, TFA), 161.49. MS (LC-MS, ESI): *m/z* 436.25 [M+H$^+$]. HRMS (ESI-MS): *m/z* [M+H$^+$] calcd. for $C_{25}H_{31}FN_5O^+$: 436.2507, found: 436.2506.

***N*-{3-[4-(5-Fluoro-4-methyl-1*H*-benzo[d]imidazol-2-yl)-3-methylphenoxy]propyl}-4-(5-methyl-1*H*-imidazol-4-yl)butan-1-amine tris(hydrotrifluoroacetate) (3.65)**

The title compound was prepared from **3.61** (50 mg, 0.118 mmol, 1 eq), 4-(5-methyl-1*H*-imidazol-4-yl)butan-1-amine (5-methylimbutamine, 63 mg, 0.413 mmol, 3.5 eq) and K_2CO_3 (114 mg, 0.825 mmol, 7 eq) in MeCN (2.5 mL) according to the general procedure. Preparative RP-HPLC (column: Interchim, Puriflash C18HQ, 15 µm, 120 g; gradient: 0–30 min: MeCN/0.1% aq. TFA 10/90–48/52, t_R = 11.2 min) afforded **3.65** (tris(hydrotrifluoroacetate)) as white fluffy solid (57.8 mg, 62%). R_f = 0.13 (CH_2Cl_2/MeOH/NH_3 80/19/1). UV/VIS (20 mM HCl): λ_{max} 298, 256, 211, 192 nm. RP-HPLC (220 nm): 100% (gradient: 0–30 min: MeCN/0.1% aq. TFA 10/90–80/20, 31-40 min: 90/10, t_R = 11.3 min, *k* = 3.8). ^{1}H-NMR (400 MHz, DMSO-d_6 + 10 µL TFA): δ (ppm) 1.52-1.68 (m, 4H), 2.02-2.17 (m, 2H), 2.22 (s, 3H), 2.49 (s, 3H), 2.53 (d, *J* = 1.1, 3H), 2.64 (t, *J* = 6.5, 2H), 2.96 (bs, 2H), 3.10 (bs, 2H), 4.18 (t, *J* = 6.0, 2H), 7.02-7.10 (m, 2H), 7.38-7.47 (m, 1H), 7.67-7.77 (m, 2H), 8.59 (bs, 2H), 8.89 (s, 1H),

13.09 (bs, TFA), 14.14 (bs, 2H). ^{13}C-NMR (101 MHz, DMSO-d_6 + 10 µL TFA): δ (ppm) 8.57, 9.38 (d, *J* = 3.3), 19.79, 22.33, 24.90, 25.57, 44.29, 46.65, 65.21, 110.91 (d, *J* = 23.6), 112.55 (d, *J* = 9.8), 112.58, 114.20 (d, *J* = 27.1), 115.30 (q, *J* = 288.9, TFA), 115.77, 117.18, 124.62, 127.96, 132.19 (d, *J* = 10.1), 132.32, 133.08, 134.30, 140.18, 150.81, 158.16 (d, *J* = 239.7), 158.56 (q, *J* = 38.1, TFA), 161.52. MS (LC-MS, ESI): *m/z* 450.27 [M+H$^+$]. HRMS (ESI-MS): *m/z* [M+H$^+$] calcd. for $C_{26}H_{33}FN_5O^+$: 450.2664, found: 450.2657.

3-[4-(5-Fluoro-4-methyl-1H-benzo[d]imidazol-2-yl)-3-methylphenoxy]-N-{2-[(5-methyl-1H-imidazol-4-yl)methylsulfanyl]ethyl}propan-1-amine tris(hydrotrifluoroacetate) (3.66)

The title compound was prepared from **3.61** (50 mg, 0.118 mmol, 1 eq), 2-[(5-methyl-1*H*-imidazol-4-yl)methylsulfanyl)ethanamine dihydrochloride (101 mg, 0.413 mmol, 3.5 eq) and K_2CO_3 (114 mg, 0.825 mmol, 7 eq) in MeCN (2.5 mL) according to general procedure. Preparative RP-HPLC (column: Interchim, Puriflash C18HQ, 15 µm, 120 g; gradient: 0−30 min: MeCN/0.1% aq. TFA 10/90−48/52, t_R = 11.0 min) afforded **3.66** (tris(hydrotrifluoroacetate)) as white fluffy solid (54.4 mg, 57%). R_f = 0.07 (CH_2Cl_2/MeOH/NH_3 80/19/1). UV/VIS (20 mM HCl): λ_{max} 293, 251, 209, 192 nm. RP-HPLC (220 nm): 100% (gradient: 0−30 min: MeCN/0.1% aq. TFA 10/90−80/20, 31-40 min: 90/10, t_R = 15.2 min, *k* = 5.5). ^{1}H-NMR (400 MHz, DMSO-d_6 + 10 µL TFA): δ (ppm) 2.08-2.18 (m, 2H), 2.29 (s, 3H), 2.50 (s, 3H, superimposed by solvent), 2.53 (d, *J* = 1.0, 3H), 2.74 (t, *J* = 7.7, 2H), 3.09-3.27 (m, 4H), 3.92 (s, 2H), 4.19 (t, *J* = 5.9, 2H), 7.04-7.10 (m, 2H), 7.39-7.46 (m, 1H), 7.70 (dd, *J* = 4.2, 9.0, 1H), 7.74 (d, *J* = 8.4, 1H), 8.80 (bs, 2H), 8.95 (s, 1H), 12.24 (bs, TFA), 14.32 (bs, 2H). ^{13}C-NMR (101 MHz, DMSO-d_6 + 10 µL TFA): δ (ppm) 8.65, 9.37 (d, *J* = 3.0), 19.79, 22.92, 25.52, 26.52, 44.35, 46.02, 65.25, 110.89 (d, *J* = 23.7), 112.55 (d, *J* = 10.1), 112.57, 114.16 (d, *J*= 26.6), 115.36 (q, J = 289.2, TFA), 115.82, 117.17, 125.27,126.48, 128.22, 132.31 (d, *J* = 10.0), 133.06, 133.32, 140.16, 150.83, 158.14 (d, *J* = 239.3 Hz), 158.58 (q, *J* = 37.8 Hz, TFA), 161.48. MS (LC-MS, ESI): *m/z* 468.22 [M+H$^+$]. HRMS (EI-MS): *m/z* M$^{+\bullet}$ calcd. for $C_{25}H_{31}FN_5OS^+$: 468.2228, found: 468.2232.

N-{3-[4-(5-Fluoro-4-methyl-1H-benzo[d]imidazol-2-yl)-3-methylphenoxy]propyl}-5-(1H-imidazol-4-yl)pentan-1-amine tris(hydrotrifluoroacetate) (3.67)

The title compound was prepared from **3.61** (60 mg, 0.141 mmol, 1 eq), **3.60** (178 mg, 0.450 mmol, 3.2 eq) and K_2CO_3 (133 mg, 0.962 mmol, 6.8 eq) in MeCN (2.5 mL) according to the general procedure. Deprotection in CH_2Cl_2 (5 mL) and TFA (2 mL) followed by preparative RP-HPLC (column: Nucleodur 250 × 21 mm; gradient: 0−30 min: MeCN/0.1% aq. TFA 10/90−45/55, t_R = 13.5 min) afforded **3.67** (tris(hydrotrifluoroacetate)) as white fluffy solid (35.8 mg, 32%). R_f = 0.12 (CH_2Cl_2/MeOH/NH_3 80/19/1). UV/VIS (20 mM HCl): λ_{max} 294, 252, 206, 193 nm. RP-HPLC (220 nm):

98.6% (gradient: 0−30 min: MeCN/0.1% aq. TFA 10/90−80/20, 31-40 min: 90/10, t_R = 14.4 min, k = 5.2). ^{1}H-NMR (400 MHz, DMSO-d_6 + 10 µL TFA): δ (ppm) 1.30-1.40 (m, 2H), 1.56-1.70 (m, 4H), 2.04-2.17 (m, 2H), 2.50 (s, 3H), 2.53 (d, J = 0.7, 3H), 2.65 (t, J = 7.6, 2H), 2.90-3.02 (m, 2H), 3.05-3.16 (m, 2H), 4.18 (t, J = 5.9, 2H), 7.04-7.10 (m, 2H), 7.39-7.46 (m, 2H), 7.70 (dd, J = 4.3, 9.0, 1H), 7.74 (d, J = 8.3, 1H), 8.61 (bs, 2H), 8.98 (s, 1H), 9.98 (bs, TFA), 14.43 (bs, 2H). ^{13}C-NMR (101 MHz, DMSO-d_6 + 10 µL TFA): δ (ppm) 9.36 (d, J = 3.2), 19.78, 23.63, 25.22, 25.30, 25.51, 27.37, 44.19, 46.79, 65.16, 110.84 (d, J = 22.9), 112.50, 112.51 (d, J = 9.4), 114.05 (d, J = 28.2), 115.35 (q, J = 289.4), 115.51, 115.88, 117.12, 128.28, 132.38 (d, J = 10.3), 132.98, 133.25, 133.78, 140.09, 150.82, 158.05 (d, J = 240.2), 158.49 (q, J = 37.7, TFA), 161.38. MS (LC-MS, ESI): *m/z* 450.27 [M+H$^+$]. HRMS (ESI-MS): *m/z* [M+H$^+$] calcd. for $C_{26}H_{31}FN_5O^+$: 450.2664, found: 450.2667.

N-{3-[4-(5-Fluoro-4-methyl-1H-benzo[d]imidazol-2-yl)-3-methylphenoxy]propyl}ethane-1,2-diamine tris(hydrotrifluoroacetate) (3.68)

The title compound was prepared from **3.61** (50 mg, 0.118 mmol, 1 eq), *tert*-butyl 2-aminoethylcarbamate (60 mg, 0.375 mmol, 3 eq) and K_2CO_3 (98 mg, 0.710 mmol, 6 eq) in MeCN (2.5 mL) according to the general procedure. Deprotection in CH_2Cl_2 (5 mL) and TFA (2 mL) followed by preparative RP-HPLC (column: Nucleodur 250 × 21 mm; gradient: 0−30 min: MeCN/0.1% aq. TFA 10/90−45/55, t_R = 9.1 min) afforded **3.68** (tris(hydrotrifluoroacetate)) as white fluffy solid (39.8 mg, 48%). R_f = 0.07 (CH_2Cl_2/MeOH/NH_3 80/19/1). UV/VIS (20 mM HCl): λ_{max} 291, 254, 208, 192 nm. RP-HPLC (220 nm): 96.4% (gradient: 0−30 min: MeCN/0.1% aq. TFA 5/95-80/20, 31-40 min: 90/10, t_R = 13.0 min, k = 6.7). ^{1}H-NMR (400 MHz, DMSO-d_6 + 10 µL TFA): δ (ppm) 2.05-2.18 (m, 2H), 2.50 (s, 3H, superimposed by solvent), 2.53 (d, J = 1.0, 3H), 3.07-3.29 (m, 6H), 4.19 (t, J = 6.0, 2H), 7.05-7.11 (m, 1H), 7.39-7.46 (m, 1H), 7.70 (dd, J = 4.4, 9.1, 1H), 7.74 (d, J = 8.6, 1H), 8.05 (bs, 3H), 8.92 (bs, 2H), 13.27 (bs, TFA). ^{13}C-NMR (101 MHz, DMSO-d_6 + 10 µL TFA): δ (ppm) 9.38 (d, J = 3.1), 19.79, 25.65, 35.40, 44.23, 44.61, 65.16, 110.89 (d, J = 22.6), 112.55 (d, J = 9.7), 112.58, 114.19 (d, J = 27.0), 115.31 (q, J = 288.9, TFA), 115.81, 117.19, 128.18, 132.27 (d, J = 10.2), 133.07, 140.17, 150.81, 158.15 (d, J = 239.6), 158.57 (q, J = 38.0, TFA), 161.47. MS (LC-MS, ESI): *m/z* 357.21 [M+H$^+$]. HRMS (ESI-MS): *m/z* [M+H$^+$] calcd. for $C_{20}H_{26}FN_4O^+$: 357.2085, found: 357.2086.

5-Fluoro-4-methyl-2-{2-methyl-4-[3-(piperazin-1-yl)propoxy]phenyl}-1H-benzo[d]imidazole tris(hydrotrifluoroacetate) (3.69)

The title compound was prepared from **3.61** (120 mg, 0.283 mmol, 1 eq), **6.1** (179 mg, 0.962 mmol, 3.4 eq) and K_2CO_3 (98 mg, 1.92 mmol, 6.8 eq) in MeCN (2.5 mL) according to the general procedure. Deprotection in CH_2Cl_2 (5 mL) and TFA (2 mL) followed by preparative RP-HPLC (column: Interchim,

Puriflash C18HQ, 15 µm, 120 g; gradient: 0−30 min: MeCN/0.1% aq. TFA 10/90−60/40, t_R = 9.5 min) afforded **3.69** (tris(hydrotrifluoroacetate)) as white fluffy solid (134 mg, 65%). R_f = 0.10 (CH_2Cl_2/MeOH/NH_3 80/19/1). UV/VIS (20 mM HCl): λ_{max} 293, 251, 206, 190 nm. RP-HPLC (220 nm): 99.3% (gradient: 0−30 min: MeCN/0.1% aq. TFA 10/90−70/30, 31-40 min: 90/10, t_R = 14.4 min, k = 5.2). ^{1}H-NMR (400 MHz, DMSO-d_6 + 10 µL TFA): δ (ppm) 2.14-2.25 (m, 2H), 2.50 (s, 3H, superimposed by solvent), 2.53(d, J = 1.0, 3H), 3.32-3.72 (m, 10H), 4.19 (t, J = 6.0, 2H), 7.05-7.11 (m, 2H), 7.38-7.46 (m, 1H), 7.71 (dd, J = 4.2, 9.0, 1H), 7.74 (d, J = 8.4, 1H), 9.42 (bs, 2H), 13.27 (bs, TFA). ^{13}C-NMR (101 MHz, DMSO-d_6 + 10 µL TFA): δ (ppm) 9.37 (d, J = 3.3), 19.81, 23.42, 40.38 (2C), 48.30 (2C), 53.30, 65.22, 110.89 (d, J = 23.6), 112.57 (d, J = 10.1), 112.58, 114.09 (d, J = 27.8), 115.67 (q, J = 290.6), 116.01, 117.20, 128.35, 132.44 (d, J = 10.2), 133.03, 140.16, 150.85, 158.11 (d, J = 239.5), 158.75 (q, J = 36.8, TFA), 161.37. MS (LC-MS, ESI): *m/z* 383.22 [M+H$^+$]. HRMS (ESI-MS): *m/z* [M+H$^+$] calcd. for $C_{22}H_{28}FN_4O^+$: 383.2242, found: 383.2243.

N-(2-{3-[4-(5-Fluoro-4-methyl-1H-benzo[d]imidazol-2-yl)-3-methylphenoxy]propylamino}ethyl)-3-(1H-imidazol-4-yl)acrylamide tris(hydrotrifluoroacetate) (3.70)

The title compound was prepared from **3.61** (60 mg, 0.141 mmol, 1 eq), **3.48** (151 mg, 0.450 mmol, 3.4 eq) and K_2CO_3 (133 mg, 0.962 mmol, 6.8 eq) in MeCN (2.5 mL) according to the general procedure. Deprotection in CH_2Cl_2 (5 mL) and TFA (2 mL) followed by preparative RP-HPLC (column: Nucleodur 250 × 21 mm; gradient: 0−30 min: MeCN/0.1% aq. TFA 10/90−45/55, t_R = 9.6 min) afforded **3.70** (tris(hydrotrifluoroacetate)) as white fluffy solid (35.9 mg, 43%). R_f = 0.09 (CH_2Cl_2/MeOH/NH_3 80/19/1). UV/VIS (20 mM HCl): λ_{max} 276, 257, 210, 190 nm. RP-HPLC (220 nm): 99.3% (gradient: 0−30 min: MeCN/0.1% aq. TFA 10/90−70/30, 31-40 min: 90/10, t_R = 14.0 min, k = 5.0). ^{1}H-NMR (400 MHz, DMSO-d_6 + 10 µL TFA): δ (ppm) 2.05-2.18 (m, 2H). 2.50 (s, 3H, superimposed by solvent), 2.53 (d, J = 0.9, 3H), 3.06-3.23 (m, 4H), 3.47-3.56 (m, 2H), 4.19 (t, J = 5.9, 2H), 6.67 (d, J = 16.0, 1H), 7.05-7.11 (m, 2H), 7.41 (d, J = 15.8, 1H), 7.40-7.46 (m, 1H), 7.70 (dd, J = 4.3, 9.0, 1H), 7.74 (d, J = 8.3, 1H), 8.58 (t, J = 5.7, 1H), 8.70 (bs, 2H), 9.17 (s, 1H), 10.05 (bs, TFA). ^{13}C-NMR (101 MHz, DMSO-d_6 + 10 µL TFA): δ (ppm) 9.36 (d, J = 3.5), 19.79, 25.49, 35.71, 44.51, 46.58, 65.23, 110.83 (d, J = 22.9), 112.51 (d, J = 9.0), 112.52, 115.39 (q, J = 289.7, TFA), 115.90, 117.00 (d, J = 33.5), 119.71, 120.29, 123.86, 124.74, 128.30, 129.09, 132.40 (d, J = 10.2), 132.96, 136.29, 140.07, 150.83, 158.50 (q, J = 37.5, TFA), 158.60 (d, J = 243.7), 161.37, 164.98. MS (LC-MS, ESI): *m/z* 477.25 [M+H$^+$]. HRMS (ESI-MS): *m/z* [M+H$^+$] calcd. for $C_{26}H_{30}FN_6O_2^+$: 477.2409, found: 477.2404.

5-{3-[4-(5-Fluoro-4-methyl-1H-benzo[d]imidazol-2-yl)-3-methylphenoxy]propyl}-4,5,6,7-tetrahydro-3H-imidazo[4,5-c]pyridine tris(hydrotrifluoroacetate) (3.71)

The title compound was prepared from **3.61** (60 mg, 0.141 mmol, 1 eq), **3.45** (176 mg, 0.450mmol, 3.4 eq) and K_2CO_3 (133 mg, 0.962 mmol, 6.8 eq) in MeCN (2.5 mL) according to the general procedure. Deprotection in CH_2Cl_2 (5 mL) and TFA (2 mL) followed by preparative RP-HPLC (column: Interchim, Puriflash C18HQ, 15 µm, 120 g; gradient: 0−10 min: MeCN/0.1% aq. TFA 10/90, 10−40 min: 10/90−30/40, t_R = 7.2 min) afforded **3.71** (tris(hydrotrifluoroacetate))) as white fluffy solid (39.9 mg, 37%). R_f = 0.10 (CH_2Cl_2/MeOH/NH_3 80/19/1). UV/VIS (20 mM HCl): λ_{max} 291, 249, 207, 192 nm. RP-HPLC (220 nm): 99.9% (gradient: 0−30 min: MeCN/0.1% aq. TFA 10/90−80/20, 31-40 min: 90/10, t_R = 14.4 min, k = 5.2). ^{1}H-NMR (400 MHz, DMSO-d_6 + 10 µL TFA): δ (ppm) 2.23-2.34 (m, 2H), 2.50 (s, 3H, superimposed by solvent), 2.53 (d, J = 0.9, 3H), 3.07 (t, J = 5.1, 2H), 3.46-3.55 (m, 2H), 3.70 (bs, 2H), 4.22 (t, J = 5.9 Hz, 2H), 4.59 (bs, 2H), 7.04-7.12 (m, 2H), 7.37-7.45 (m, 1H), 7.71 (dd, J = 4.3, 9.0, 1H), 7.74 (d, J = 8.3, 1H), 9.04 (s, 1H), 13.16 (bs, TFA). ^{13}C-NMR (101 MHz, DMSO-d_6 + 10 µL TFA): δ (ppm) 9.13 (d, J = 3.3), 17.88, 19.57, 23.68, 46.28, 48.59, 52.14, 65.05, 110.66 (d, J = 23.6), 112.33, 112.34 (d, J = 9.9), 113.89 (d, J = 27.0), 115.27 (q, J = 289.9, TFA), 115.71, 116.97, 120.43, 124.30, 128.04, 132.13 (d, J = 10.1), 132.83, 134.96, 139.94, 150.59, 157.90 (d, J = 239.4), 158.44 (q, J = 37.3, TFA), 161.19. MS (LC-MS, ESI): *m/z* 420.22 [M+H$^+$]. HRMS (ESI-MS): *m/z* [M+H$^+$] calcd. for $C_{24}H_{27}FN_5O^+$: 420.2194, found: 420.2195.

(5-Chloro-1H-indol-2-yl)(4-{3-[4-(5-fluoro-4-methyl-1H-benzo[d]imidazol-2-yl)-3-methylphenoxy]propyl}piperazin-1-yl)methanone bis(hydrotrifluoroacetate) (3.72)

The title compound was prepared from **3.61** (34 mg, 0.080 mmol, 1 eq), **6.3** (60 mg, 0.159 mmol, 2 eq) and K_2CO_3 (44 mg, 0.318 mmol, 6.8 eq) in MeCN (2.5 mL) according to the general procedure. Preparative RP-HPLC (column: Nucleodur 250 × 21 mm; gradient: 0−30 min: MeCN/0.1% aq. TFA 20/80−50/50, t_R = 18.5 min) afforded **3.72** (bis(hydrotrifluoroacetate)) as white fluffy solid (35.4 mg, 56%). R_f = 0.24 (CH_2Cl_2/MeOH/NH_3 80/19/1). UV/VIS (20 mM HCl): λ_{max} 297, 227, 217, 193 nm. RP-HPLC (220 nm): 99.0% (gradient: 0−30 min: MeCN/0.1% aq. TFA 10/90−80/20, 31-40 min: 90/10, t_R = 17.1 min, k = 6.3). ^{1}H-NMR (400 MHz, DMSO-d_6 + 10 µL TFA): δ (ppm) 2.15-2.29 (m, 2H), 2.50 (s, 3H, superimposed by solvent), 2.54 (d, J = 0.9, 3H), 3.13-3.79 (m, 8H), 4.21 (t, J = 5.8, 2H), 4.53-4.74 (m, 2H), 6.91 (d, J = 1.5, 1H), 7.06-7.14 (m, 2H), 7.22 (dd, J = 2.1, 8.7, 1H), 7.39-7.50 (m, 2H), 7.68 (d, J = 2.0, 1H), 7.71 (dd, J = 4.3, 9.0, 1H), 7.75 (d, J = 8.5, 1H), 10.26 (bs, 1H), 11.88 (s, 1H), 13.02 (bs, TFA). ^{13}C-NMR (101 MHz, DMSO-d_6 + 10 µL TFA): δ (ppm) 9.38 (d, J = 3.2), 19.80, 23.48, 51.07 (2C), 51.11, 53.30 (2C), 65.34, 104.50, 110.91 (d, J = 23.5), 112.56 (d, J = 9.6), 112.61, 113.93, 114.20 (d, J = 28.2), 115.32 (q, J = 288.9), 115.86, 117.23, 120.56, 123.84, 124.55, 127.90, 128.19, 130.52, 132.29 (d, J=

8.6), 133.10, 134.73, 140.20, 150.82, 158.16 (d, *J* = 239.4), 158.57 (q, *J* = 38.0, TFA), 161.46, 161.84. MS (LC-MS, ESI): *m/z* 560.22 [M+H$^+$]. HRMS (ESI-MS): *m/z* [M+H$^+$] calcd. for $C_{31}H_{32}ClFN_5O_2^+$: 560.2223, found: 560.2229.

3.5.2.14 Preparation of the amide **3.75**

Benzyl 2-aminoethyl{3-[4-(5-fluoro-4-methyl-1H-benzo[d]imidazol-2-yl)-3-methylphenoxy]propyl}-carbamate bis(hydrotrifluoroacetate) (3.74)

3.61 (194 mg, 0.457 mmol, 1 eq), *tert*-butyl 2-aminoethylcarbamate (249 mg, 1.56 mmol, 3.4 eq) and K_2CO_3 (430 mg, 3.11 mmol, 6.8 eq) in MeCN (2.5 mL) were heated under microwave irradiation at 130 °C for 20 min. The solvent was removed under reduced pressure and the residue was dried *in vacuo*. Subsequently, NEt_3 (162 mg, 1.60 mmol, 3.5 eq) in CH_2Cl_2 (2 mL) and benzyl chloroformate (273 mg, 1.60 mmol, 3.5 eq) in CH_2Cl_2 (1 mL) were added dropwise at 0 °C within 10 min and the mixture was stirred at rt for 24 h. The reaction mixture was concentrated *in vacuo*. The crude product was purified by flash-chromatography (eluent CH_2Cl_2 (A), MeOH (B); gradient: 0 to 40 min: A/B 100/0 – 90/10 (*v/v*), SF 25-40 g) affording a white solid. mp 115 °C. R_f = 0.35 (CH_2Cl_2/MeOH 90/10). Subsequently, 4 mL of CH_2Cl_2 and 1 mL of TFA was added dropwise. After stirring for 4 h, the solvent was removed under reduced pressure, resuspended twice in 10 mL of CH_2Cl_2 to remove remains of TFA. The residue was dissolved in 10 mL of water and dried by lyophilisation to afford **3.74** (bis(hydrotrifluoroacetate)) as a white powder (182 mg, 55%). R_f = 0.05 (CH_2Cl_2/MeOH 90/10). ^{1}H-NMR (400 MHz, MeOH-d_4): δ (ppm) 2.09 (bs, 2H), 2.50 (s, 3H), 2.58 (d, *J* = 1.4, 3H), 3.18 (bs, 2H), 3.59 (bs, 2H), 3.64 (t, *J* = 6.1, 2H), 4.10 (bs, 2H), 5.10 (s, 2H), 6.91-7.09 (m, 2H), 7.28-7.43 (m, 6H), 7.61-7.70 (m, 2H). ^{13}C-NMR (101 MHz, MeOH-d_4): δ (ppm) 9.39 (d, *J* = 3.8), 20.16, 29.07, 39.79, 46.13, 49.34, 49.55, 67.12, 68.86, 112.45 (d, *J* = 23.8), 113.33 (d, *J* = 10.1), 113.97, 115.95 (d, *J* = 27.6), 116.50, 118.56, 129.14, 129.28 (2C), 129.34, 129.67 (2C), 133.55 (d, *J* = 9.9), 133.68, 137.78, 141.53, 152.70, 160.34 (d, *J* = 241.6), 163.90. MS (LC-MS, ESI): *m/z* 491.25 [M+H$^+$]. HRMS (ESI-MS): *m/z* [M+H$^+$] calcd. for $C_{28}H_{32}FN_4O_3^+$: 491.2453, found: 491.2449.

N-(2-{3-[4-(5-Fluoro-4-methyl-1H-benzo[d]imidazol-2-yl)-3-methylphenoxy]propylamino}ethyl)-propionamide bis(hydrotrifluoroacetate) (3.75)

To a solution of **3.75** (135 mg, 0.188 mmol, 1 eq) and NEt_3 (95 mg, 0.939 mmol, 5 eq) in MeCN/DMF (1/1, 2 mL), succinimidyl propionate (39 mg, 0.225 mmol, 1.2 eq) was added. After stirring at rt for 24 h, the solvent was removed under reduced pressure. For deprotection, TFA (1.5 mg, 0.013 mmol, 0.07 eq) in MeCN (3 mL) and 10% palladium-on-charcoal catalyst (11 mg) were added and a slow

stream of hydrogen was led through a glass tube into the vigorously stirred suspension for 4 h. Subsequently, stirring was continued at 1 atm H_2 for further 16 h. After depletion of the starting material (control by TLC) the catalyst by filtration through Celite. The filtrate was concentrated *in vacuo*, followed by preparative RP-HPLC (column: Interchim, Puriflash C18HQ, 15 µm, 120 g; gradient: 0−30 min: MeCN/0.1% aq. TFA 10/90−45/55, t_R = 12.2 min) affording **3.75** (bis(hydrotrifluoroacetate)) as a white fluffy solid (120 mg, 65%). R_f = 0.20 (CH_2Cl_2/MeOH/NH_3 80/19/1). UV/VIS (20 mM HCl): λ_{max} 292, 252, 198, 192 nm. RP-HPLC (220 nm): 99.9% (gradient: 0−30 min: MeCN/0.1% aq. TFA 10/90−80/20, 31-40 min: 90/10, t_R = 15.4 min, k = 5.6). ^{1}H-NMR (400 MHz, DMSO-d_6 + 10 µL TFA): δ (ppm) 1.01 (t, J = 7.6, 3H), 2.06-2.18 (m, 4H), 2.50 (s, 3H, superimposed by solvent), 2.53 (d, J = 1.2, 3H), 2.97-3.21 (m, 4H), 3.36 (q, J = 6.1, 2H), 4.18 (t, J = 5.9, 2H), 7.03-7.13 (m, 2H), 7.37-7.46 (m, 1H), 7.70 (dd, J = 4.2, 8.9, 1H), 7.74 (d, J = 8.4, 1H), 8.06 (t, J = 5.5, 1H), 8.67 (bs, 2H), 10.39 (bs, TFA). ^{13}C-NMR (101 MHz, DMSO-d_6 + 10 µL TFA): δ (ppm) 9.34 (d, J = 3.1), 9.58, 19.80, 25.47, 28.42, 35.30, 44.43, 46.79, 65.26, 111.10 (d, J = 31.7), 112.52, 112.52 (d, J = 9.9), 113.97 (d, J = 27.5), 115.59 (q, J = 290.4, TFA), 115.97, 117.18, 128.39, 132.48 (d, J = 9.9), 132.93, 140.05, 150.87, 158.02 (d, J = 239.1), 158.56 (q, J = 36.7, TFA), 161.35, 174.00. MS (LC-MS, ESI): *m/z* 413.24 [M+H$^+$]. HRMS (ESI-MS): *m/z* [M+H$^+$] calcd. for $C_{23}H_{30}FN_4O_2^+$: 413.2347, found: 413.2349.

3.5.2.15 Preparation of the amide **3.76**

1-(4-{3-[4-(5-Fluoro-4-methyl-1H-benzo[d]imidazol-2-yl)-3-methylphenoxy]propyl}piperazin-1-yl)propan-1-one bis(hydrotrifluoroacetate) (3.76)

To a solution of **3.69** (50 mg, 0.082 mmol, 1 eq) and NEt_3 (27 mg, 0.270 mmol, 3.3 eq) in MeCN (2.5 mL), succinimidyl propionate (17 mg, 0.098 mmol, 1.2 eq) was added. After stirring at rt for 24 h, the solvent was removed under reduced pressure. Preparative RP-HPLC (column: Interchim, Puriflash C18HQ, 15 µm, 120 g; gradient: 0−30 min: MeCN/0.1% aq. TFA 10/90−50/50, t_R = 10.7 min) afforded **3.78** (bis(hydrotrifluoroacetate)) as a white solid (35.0 mg, 76%). R_f = 0.22 (CH_2Cl_2/MeOH/NH_3 80/19/1). UV/VIS (20 mM HCl): λ_{max} 293, 249, 192 nm. RP-HPLC (220 nm): 99.9% (gradient: 0−30 min: MeCN/0.1% aq. TFA 10/90−80/20, 31-40 min: 90/10, t_R = 16.1 min, k = 5.9). ^{1}H-NMR (400 MHz, DMSO-d_6 + 10 µL TFA): δ (ppm) 1.00 (t, J = 7.4, 3H), 2.13-2.27 (m, 2H), 2.30-2.45 (m, 2H), 2.50 (s, 3H, superimposed by solvent), 2.53 (d, J = 1.2, 3H), 2.86-3.68 (m, 8H), 4.19 (t, J = 5.9, 2H), 4.00-4.58 (m, 2H), 7.05-7.11 (m, 2H), 7.37-7.48 (m, 1H), 7.71 (dd, J = 9.0, 4.3, 1H), 7.74 (d, J = 8.4, 1H), 10.11 (bs, 1H), 12.32 (bs, TFA). ^{13}C-NMR (101 MHz, DMSO-d_6 + 10 µL TFA): δ (ppm) 9.12, 9.37 (d, J = 3.2), 19.79, 23.43, 25.30, 38.19, 41.85, 50.98, 51.22, 53.23, 65.32, 110.89 (d, J = 23.7), 112.54 (d, J = 8.0), 112.59, 114.16 (d, J = 26.9), 115.38 (q, J = 289.3, TFA), 115.88, 117.21, 128.22, 132.31 (d, J = 10.4), 133.07,

140.18, 150.82, 158.14 (d, *J* = 239.5), 158.58 (q, *J* = 37.8, TFA), 161.42, 171.75. MS (LC-MS, ESI): *m/z* 439.25 [M+H$^+$]. HRMS (ESI-MS): *m/z* [M+H$^+$] calcd. for $C_{25}H_{32}FN_4O_2^+$: 439.2504, found: 439.2408.

3.5.3 Pharmacological Methods

Histamine dihydrochloride was purchased from Alfa Aesar GmbH & Co. KG (Karlsruhe, Germany). Guanosine diphosphate (GDP) was from Sigma-Aldrich Chemie GmbH (Munich, Germany), unlabeled GTPγS was from Roche (Mannheim, Germany) and thioperamide was from R&D Systems (Wiesbaden, Germany) [^{3}H]pyrilamine and [^{3}H]N$^\alpha$-methylhistamine and [^{3}H]histamine was purchased from Hartmann Analytic (Braunschweig, Germany). [^{35}S]GTPγS was from PerkinElmer Life Sciences (Boston, MA) or Hartmann Analytic GmbH (Braunschweig, Germany). [^{3}H]UR-DE257 (*N*-[6-(3,4-dioxo-2-{3-[3-(piperidin-1-ylmethyl)phenoxy]propylamino}-cyclobut-1-enylamino)hexyl]-[2,3-$^3H_2$]-propionamide) was synthesized as described in Chapter 5.

3.5.3.1 Competition binding experiments on membrane preparations of Sf9 insect cells

Competition binding experiments were performed on membrane preparations of Sf9 insect cells expressing the hH_1R + RGS4, hH_2R-$G_{s\alpha S}$, hH_3R + $G_{\alpha i2}$ + $\beta_1\gamma_2$ or the hH_4R + $G_{\alpha i2}$ + $\beta_1\gamma_2$. General procedures for the generation of recombinant baculoviruses, culture of Sf9 cells and membrane preparation have been described elsewhere.[48,68] The respective membranes were thawed and sedimented by centrifugation at 4 °C and 13000 g for 10 min. Membranes were resuspended in binding buffer (12.5 mM $MgCl_2$, 1 mM EDTA, and 75 mM Tris/HCl, pH 7.4). Each tube (total volume 100 µL) contained 30 µg (hH_1R), 40 µg (hH_2R), 60 µg (hH_3R) or 100 µg (hH_4R) of membrane protein and increasing concentrations of unlabeled ligands. Radioligands: H_1R: [^{3}H]pyrilamine, specific activity 20.0 Ci/mmol, K_d = 4.5 nM, c = 5 nM, nonspecific binding determined in the presence of 10 µM of diphenhydramine; H_2R: [^{3}H]UR-DE257 (radioligand was diluted with unlabeled ligand due to economic reasons), specific activity 63.0 Ci/mmol, K_d = 31 nM, c = 30 nM, nonspecific binding determined in the presence of 10 µM of famotidine; H_3R: [^{3}H]N$^\alpha$-methylhistamine, specific activity 85.3 Ci/mmol, K_d = 8.6 nM, c = 3 nM, nonspecific binding determined in the presence of 10 µM of thioperamide; H_4R: [^{3}H]histamine, specific activity 25 Ci/mmol, K_d = 16 nM, c = 10 nM, nonspecific binding determined in the presence of 10 µM of histamine. Filtration through 0.3% polyethyleneimine-pretreated glass microfiber filters (Whatman GF/B, Maidstone, UK) using a Brandel 96 sample harvester (Brandel, Gaithersburg, MD) separated unbound from membrane associated radioligand. After three washing steps with binding buffer, filter pieces for each well were punched and transferred into untapped 96-well sample plates 1450-401 (Perkin Elmer, Rodgau,

Germany). Each well was supplemented with 200 µL of scintillation cocktail (Rotiscint Eco plus, Roth, Karlsruhe, Germany) and incubated in the dark. Radioactivity was measured with a Micro Beta^2 1450 scintillation counter (Perkin Elmer, Rodgau, Germany). Protein concentration was determined by the method of Lowry using bovine serum albumin as standard.[69] Data analysis of the resulting competition curves was accomplished by non-linear regression analysis using the algorithms in PRISM GraphPad Software (GraphPad Prism 5.0 software, San Diego, CA). K_i values were derived from the corresponding EC_{50} data utilizing the equation of Cheng and Prusoff.[39] Values represent the mean ± SEM of 2-3 independent experiments each performed in triplicate.

3.5.3.2 Steady-State [γ-^{33}P]GTPase activity assay

GTPase activity assays were performed as previously described.[32-34,55]

H_1R assays: Sf9 insect cell membranes coexpressing the hH_1R and RGS4 were employed.

3.5.3.3 [^{35}S]GTPγS binding assay[70,71]

[^{35}S]GTPγS binding assays were performed as previously described for the H_2R,[35,36] H_3R[37,38] and H_4R.[33,49] Histamine dihydrochloride was purchased from Alfa Aesar (Karlsruhe, Germany). thioperamide was from R&D Systems (Wiesbaden, Germany), guanosine diphosphate (GDP) was from Sigma-Aldrich (Munich, Germany), unlabeled GTPγS was from Roche (Mannheim, Germany). [^{35}S]GTPγS was from PerkinElmer Life Sciences (Boston, MA) or Hartmann Analytic GmbH (Braunschweig, Germany). GF/C filters were from Whatman (Maidstone, UK). H_2R assays: Sf9 insect cell membranes expressing the hH_2R-$Gs_{\alpha S}$ fusion protein were employed, H_3R assays: Sf9 insect cell membranes coexpressing the hH_3R, mammalian $G\alpha_{i2}$ and $G\beta_1\gamma_2$ were employed, H_4R assays: Sf9 insect cell membranes coexpressing the hH_4R or the mH_4R, mammalian $G\alpha_{i2}$ and $G\beta_1\gamma_2$ were employed. The respective membranes were thawed and sedimented by 10 min centrifugation at 4 °C and 13000 *g.* Membranes were resuspended in binding buffer (12.5 mM $MgCl_2$, 1 mM EDTA, and 75 mM Tris/HCl, pH 7.4). Each assay tube contained Sf9 membranes expressing the respective H_xR subtype (10-20 µG-Protein/tube), 1 µM GDP, 0.05% (*w/v*) bovine serum albumin, 0.2 nM [^{35}S]GTPγS and the investigated ligands (dissolved in millipore water or in a mixture (*v/v*) of 80% millipore water and 20% DMSO) at various concentrations in binding buffer (total volume 100 µL). All H_4R assays additionally contained 100 mM NaCl. For the determination of K_b values (antagonist mode of the [^{35}S]GTPγS binding assay) histamine was added to the reaction mixtures (final concentrations: $hH_{3/4}R$: 100 nM, hH_2R: 1 µM, mH_4R: 10 µM). Incubation was conducted for 90 min at 25 °C and shaking at 250 rpm. Bound [^{35}S]GTPγS was separated from free [^{35}S]GTPγS by filtration through GF/C filters,

followed by three washing steps with 2 mL of binding buffer (4 °C) using a Brandel Harvester. Filter-bound radioactivity was determined after an equilibration phase of at least 12 h by liquid scintillation counting. The experimental conditions chosen ensured that not more than 10% of the total amount of [^{35}S]GTPγS added was bound to the filters. Nonspecific binding was determined in the presence of 10 µM unlabeled GTPγS. IC_{50} values were converted to K_b values using the Cheng-Prussoff equation.[39] EC_{50} and K_b values from the functional GTPγS assays were analyzed by nonlinear regression and best fit to sigmoidal concentration-response curves (GraphPad Prism 5.0 software, San Diego, CA).

3.5.3.4 Radioligand binding assay using HEK-293 cells expressing the mH_4R[51,72]

With some modifications, the radioligand binding assay was performed as described previously.[51,72] HEK293-SF-mH_4R-His_6 cells were seeded into 175-cm^2 culture flasks until they reached 80-100% confluency. After trypsinization, the cells were detached with Leibovitz's L-15 medium without phenol red (Invitrogen, Karlsruhe, Germany) including 1% FCS and centrifuged for 10 min at 300 *g*. The supernatant was discarded and the cells were re-suspended in the aforementioned medium. After counting the cells in a hemocytometer, the cell density was adjusted to 2-3·10^6 cells/mL. As radioactive tracer [^{3}H]UR-PI294 was used, which was synthesized in our laboratory (K_d = 75 nM).[5] For competition binding experiments, cells (160 µL of the cell suspension) were incubated with increasing concentrations of the unlabelled ligands in presence of 50 nM [^{3}H]UR-PI294 in a 96-well plate (Greiner, Germany) (total volume 200 µL). Samples were shaken at 100 rpm for 90 min under light protection prior to harvesting. Cell-bound radioactivity was transferred to a glass fibre filter GF/C (Skatron) pre-treated with polyethyleneimine (0.3% (*v/v*) by a Combi Cell Harvester 11025. The filter was washed with PBS (4 °C) for approx. 10 s. Filter-bound radioactivity was determined after an equilibration phase of at least 12 h by liquid scintillation counting.

3.5.3.5 Radioligand binding studies on hM_1R or hM_2R expressing CHO-K9 cells

CHO-K9 cells stably transfected with the human muscarinic receptors M_x (x = 1 or 2) were purchased from Missouri S&T cDNA Resource Centre and were cultured in HAM's F12 medium supplemented with FCS (10%) and geneticin (750 µg/mL). The muscarinic receptor (MR) competitive antagonist [^{3}H]-*N*-methylscopolamine ([^{3}H]-NMS) (a_s = 80 Ci/mmol, purchased from Hartman Analytic GmbH, Germany) was used as radioligand. Prior to competition binding experiments the K_d values of [^{3}H]-NMS were determined in saturation binding experiments at the distinct receptor subtypes. CHO cells were seeded in tissue-culture treated white 96-well plates with clear bottom (Corning Incorporated Life Sciences, Tewksbury, MA; Corning cat. no. 3610) one or two days prior to the experiment. Depending on the level of receptor expression the confluence of the cells was 10-20%

(high receptor density), 40-60% (medium receptor density) or 100% (low receptor content) on the day of the experiment (totally bound radioligand should not exceed 1,500 dpm per well). The culture medium was removed by suction, the cells were washed with phosphate buffered saline (PBS) (200 µL) and covered with Leibovitz's L15 culture medium (Gibco, Life Technologies GmbH, Darmstadt, Germany) supplemented with 1% BSA (in the following referred to as L15 medium) (150 µL). For total binding L15 medium (18.8 µL) and L15 medium (18.8 µL) containing the radioligand (10-fold concentrated) was added. For non-specific binding and displacement of [^{3}H]-NMS L15 medium (18.8 µL) containing the competitor (10-fold concentrated) and L15 medium (18.8 µL) containing the radioligand (10-fold concentrated) was added. The plates were shaken during incubation at ambient temperature (21-23 °C). After 3 h of incubation the medium was removed, the cells were washed twice with ice-cold PBS (200 µL; washing period ≤ 2 min) and lysis solution (urea (8 M), acetic acid (3 M) and Triton-X-100 (1%) in water) (25 µL) was added. The plates were shaken for 20 min, scintillation liquid (Optiphase Supermix, PerkinElmer, Überlingen, Germany) (200 µL) was added and the plates were sealed with a transparent sealing tape (permanent seal for microplates, PerkinElmer, prod. no. 1450-461). The plates were held up side down several times in order to achieve a complete mixing of scintillator and lysis solution. The samples were kept in darkness for at least 1 h prior to the measurement of radioactivity with a MicroBeta2 plate counter for 24 and 96 well plates (PerkinElmer) using a tritium dpm program linked with quench correction data determined in the same type of 96 well plate. The radioligand concentration was 0.2 nM throughout. Non-specific binding was determined in the presence of atropine (500-fold excess) and amounted to < 10% of total binding. Data analysis of the resulting competition curves was accomplished by non-linear regression analysis using the algorithms in PRISM GraphPad Software (GraphPad Prism 5.0 software, San Diego, CA). K_i values were derived from the corresponding EC_{50} data utilizing the equation of Cheng and Prusoff.[39]

3.5.3.6 Data analysis and pharmacological parameters

All data are presented as mean of n independent experiments ± SEM. Dpm (decays per minute) values of total and nonspecific binding were processed with GraphPad Prism® 5 (GraphPad Software, San Diego (CA), USA). Specific binding was calculated by subtraction of nonspecific binding from the respective values for total binding. Agonist potencies were given as EC_{50} values (molar concentration of the agonist causing 50% of the maximal response). Maximal responses (intrinsic activities) were expressed as *a* values. The *a* value of histamine was set to 1.00, *a* values of other compounds were referred to this value. IC_{50} values were converted to K_i and K_b values using the Cheng-Prusoff equation.[39] pK_i values were analyzed by nonlinear regression and best fit to one-site (monophasic)

competition isotherms. pEC_{50} and pK_b values from the functional [^{35}S]GTPγS and [^{33}P]GTPase assays were analyzed by nonlinear regression and best fit to sigmoidal concentration-response curves.

3.6 References

1. Igel, P.; Dove, S.; Buschauer, A. Histamine H_4 receptor agonists. *Bioorg. Med. Chem. Lett.* **2010**, 20, 7191-7199.
2. Schreeb, A.; Łażewska, D.; Dove, S.; Buschauer, A.; Kieć-Kononowicz, K.; Stark, H. Histamine H4 Receptor Ligands. In *Histamine H_4 Receptor: A Novel Drug Target in Immunoregulation and Inflammation*, Stark, H., Ed. Versita: London, **2013**; pp 21-62.
3. Savall, B. M.; Edwards, J. P.; Venable, J. D.; Buzard, D. J.; Thurmond, R.; Hack, M.; McGovern, P. Agonist/antagonist modulation in a series of 2-aryl benzimidazole H_4 receptor ligands. *Bioorg. Med. Chem. Lett.* **2010**, 20, 3367-3371.
4. Geyer, R.; Kaske, M.; Baumeister, P.; Buschauer, A. Synthesis and Functional Characterization of Imbutamine Analogs as Histamine H_3 and H_4 Receptor Ligands. *Arch. Pharm. (Weinheim).* **2014**, 347, 77-88.
5. Igel, P.; Schnell, D.; Bernhardt, G.; Seifert, R.; Buschauer, A. Tritium-Labeled N^1-[3-(1H-imidazol-4-yl)propyl]-N^2-propionylguanidine ([^{3}H]UR-PI294), a High-Affinity Histamine H_3 and H_4 Receptor Radioligand. *ChemMedChem* **2009**, 4, 225-231.
6. Keller, M.; Bernhardt, G.; Buschauer, A. [^{3}H]UR-MK136: A Highly Potent and Selective Radioligand for Neuropeptide Y Y_1 Receptors. *ChemMedChem* **2011**, 6, 1566-1571.
7. Keller, M.; Pop, N.; Hutzler, C.; Beck-Sickinger, A. G.; Bernhardt, G.; Buschauer, A. Guanidine-acylguanidine bioisosteric approach in the design of radioligands: synthesis of a tritium-labeled N^G-propionylargininamide ([^{3}H]-UR-MK114) as a highly potent and selective neuropeptide Y Y_1 receptor antagonist. *J. Med. Chem.* **2008**, 51, 8168-8172.
8. Pluym, N.; Baumeister, P.; Keller, M.; Bernhardt, G.; Buschauer, A. [^{3}H]UR-PLN196: a selective nonpeptide radioligand and insurmountable antagonist for the neuropeptide Y Y_2 receptor. *ChemMedChem* **2013**, 8, 587-593.
9. Savall, B. M.; Fontimayor, J. R.; Edwards, J. P. Selective phenol alkylation for an improved synthesis of 2-arylbenzimidazole H_4 receptor ligands. *Tetrahedron Lett.* **2009**, 50, 2490-2492.
10. Ghorai, P.; Kraus, A.; Keller, M.; Götte, C.; Igel, P.; Schneider, E.; Schnell, D.; Bernhardt, G.; Dove, S.; Zabel, M.; Elz, S.; Seifert, R.; Buschauer, A. Acylguanidines as Bioisosteres of Guanidines: N^G-Acylated Imidazolylpropylguanidines, a New Class of Histamine H_2 Receptor Agonists. *J. Med. Chem.* **2008**, 51, 7193-7204.
11. Feichtinger, K.; Zapf, C.; Sings, H. L.; Goodman, M. Diprotected Triflylguanidines: A New Class of Guanidinylation Reagents. *J. Org. Chem.* **1998**, 63, 3804-3805.
12. Kraus, A.; Ghorai, P.; Birnkammer, T.; Schnell, D.; Elz, S.; Seifert, R.; Dove, S.; Bernhardt, G.; Buschauer, A. N^G-Acylated Aminothiazolylpropylguanidines as Potent and Selective Histamine H_2 Receptor Agonists. *ChemMedChem* **2009**, 4, 232-240.
13. Iwanowicz, E. J.; Poss, M. A.; Lin, J. Preparation of *N*,*N*'-bis-*tert*-Butoxycarbonylthiourea *Synth. Commun.* **1993**, 23, 1443-1445.
14. Poss, M. A.; Iwanowicz, E.; Reid, J. A.; Lin, J.; Gu, Z. A mild and efficient method for the preparation of guanidines. *Tetrahedron Lett.* **1992**, 33, 5933-5936.
15. Gausepohl, H.; Pieles, U.; Frank, R. W. In Schiff base analog formation during in situ activation by HBTU and TBTU, **1992**; ESCOM: **1992**; pp 523-524.
16. DeMong, D. E.; Williams, R. M. The asymmetric synthesis of (2*S*,3*R*)-capreomycidine. *Tetrahedron Lett.* **2001**, 42, 3529-3532.
17. Kim, K. S.; Qian, L. Improved method for the preparation of guanidines. *Tetrahedron Lett.* **1993**, 34, 7677-7680.
18. Ghorai, P. Arpromidine-related acylguanidines: synthesis and structure activity relationships of a new class of guanidine-type histamine H_2 receptor agonists with reduced basicity. University of Regensburg, Regensburg, Doctoral thesis, **2006**.

19. Kraus, A. Highly Potent, Selective Acylguanidine-Type Histamine H_2 Receptor Agonists: Synthesis and Structure-Activity Relationships. University of Regensburg, Regensburg, Doctoral thesis, **2007**.
20. Elz, S.; Schunack, W. An alternative synthesis of homohistamine and structurally related (imidazol-4-yl)alkylamines. *Z. Naturforsch., B: Chem. Sci.* **1987**, 42, 238-242.
21. Bredereck, H.; Theilig, G. Untersuchungen in der Oxazolreihe und Umwandlungen von Oxazolen in Imidazole mittels Formamids (Formamid-Reaktionen, I. Mitteil.). *Chem. Ber.* **1953**, 86, 96-109.
22. Mach, U. R.; Hackling, A. E.; Perachon, S.; Ferry, S.; Wermuth, C. G.; Schwartz, J. C.; Sokoloff, P.; Stark, H. Development of novel 1,2,3,4-tetrahydroisoquinoline derivatives and closely related compounds as potent and selective dopamine D_3 receptor ligands. *ChemBioChem* **2004**, 5, 508-518.
23. Habermehl, G. G.; Ecsy, W. The condensation of histamine with carbonyl compounds. *Heterocycles* **1976**, 5, 127-134.
24. Igel, P. Synthesis and structure-activity relationships of N^G-acylated arylalkylguanidines and related compounds as histamine receptor ligands: Searching for selective H_4R agonists. University of Regensburg, Regensburg, Doctoral thesis, **2008**.
25. Finkelstein, H. Darstellung organischer Jodide aus den entsprechenden Bromiden und Chloriden. *Ber. Dtsch. Chem. Ges.* **1910**, 43, 1528-1532.
26. Durant, G. J.; Emmett, J. C.; Ganellin, C. R.; Miles, P. D.; Parsons, M. E.; Prain, H. D.; White, G. R. Cyanoguanidine-thiourea eqalence in the development of the histamine H_2-receptor antagonist, cimetidine. *J. Med. Chem.* **1977**, 20, 901-906.
27. Keller, M.; Erdmann, D.; Pop, N.; Pluym, N.; Teng, S.; Bernhardt, G.; Buschauer, A. Red-fluorescent argininamide-type NPY Y_1 receptor antagonists as pharmacological tools. *Bioorg. Med. Chem.* **2011**, 19, 2859-2878.
28. Xu, C.-P.; Xiao, Z.-H.; Zhuo, B.-Q.; Wang, Y.-H.; Huang, P.-Q. Efficient and chemoselective alkylation of amines/amino acids using alcohols as alkylating reagents under mild conditions. *Chem. Commun.* **2010**, 46, 7834-7836.
29. Bodensteiner, J.; Baumeister, P.; Geyer, R.; Buschauer, A.; Reiser, O. Synthesis and pharmacological characterization of new tetrahydrofuran based compounds as conformationally constrained histamine receptor ligands. *Org. Biomol. Chem.* **2013**, 11, 4040-4055.
30. Yellin, T. O.; Buck, S. H.; Gilman, D. J.; Jones, D. F.; Wardleworth, J. M. ICI 125,211: A new gastric antisecretory agent acting on histamine H_2-receptors. *Life Sci.* **1979**, 25, 2001-2009.
31. Ghorai, P.; Kraus, A.; Birnkammer, T.; Geyer, R.; Bernhardt, G.; Dove, S.; Seifert, R.; Elz, S.; Buschauer, A. Chiral N^G-acylated hetarylpropylguanidine-type histamine H_2 receptor agonists do not show significant stereoselectivity. *Bioorg. Med. Chem. Lett.* **2010**, 20, 3173-3176.
32. Kelley, M. T.; Bürckstümmer, T.; Wenzel-Seifert, K.; Dove, S.; Buschauer, A.; Seifert, R. Distinct Interaction of Human and Guinea Pig Histamine H_2-Receptor with Guanidine-Type Agonists. *Mol. Pharmacol.* **2001**, 60, 1210-1225.
33. Schneider, E. H.; Schnell, D.; Papa, D.; Seifert, R. High Constitutive Activity and a G-Protein-Independent High-Affinity State of the Human Histamine H_4-Receptor. *Biochemistry* **2009**, 48, 1424-1438.
34. Seifert, R.; Wenzel-Seifert, K.; Bürckstümmer, T.; Pertz, H. H.; Schunack, W.; Dove, S.; Buschauer, A.; Elz, S. Multiple Differences in Agonist and Antagonist Pharmacology between Human and Guinea Pig Histamine H_1-Receptor. *J. Pharmacol. Exp. Ther.* **2003**, 305, 1104-1115.
35. Houston, C.; Wenzel-Seifert, K.; Bürckstümmer, T.; Seifert, R. The human histamine H_2-receptor couples more eficiently to Sf9 insect cell G_s-proteins than to insect cell G_q-proteins: limitations of Sf9 cells for the analysis of receptor/G_q-protein coupling. *J. Neurochem.* **2002**, 80, 678-696.
36. Wenzel-Seifert, K.; Kelley, M. T.; Buschauer, A.; Seifert, R. Similar Apparent Constitutive Activity of Human Histamine H_2-Receptor Fused to Long and Short Splice Variants of Gs_a. *J. Pharmacol. Exp. Ther.* **2001**, 299, 1013-1020.
37. Rouleau, A.; Ligneau, X.; Tardivel-Lacombe, J.; Morisset, S.; Gbahou, F.; Schwartz, J. C.; Arrang, J. M. Histamine H_3-receptor-mediated [^{35}S]GTPγS binding: evidence for constitutive activity of the recombinant and native rat and human H_3 receptors. *Br. J. Pharmacol.* **2002**, 135, 383-392.

38. Schnell, D.; Burleigh, K.; Trick, J.; Seifert, R. No Evidence for Functional Selectivity of Proxyfan at the Human Histamine H_3 Receptor Coupled to Defined G_i/G_o Protein Heterotrimers. *J. Pharmacol. Exp. Ther.* **2010**, 332, 996-1005.
39. Cheng, Y.; Prusoff, W. H. Relationship between the inhibition constant (K_1) and the concentration of inhibitor which causes 50 per cent inhibition (I_{50}) of an enzymatic reaction. *Biochem. Pharmacol.* **1973**, 22, 3099-3108.
40. Xie, S.-X.; Ghorai, P.; Ye, Q.-Z.; Buschauer, A.; Seifert, R. Probing Ligand-Specific Histamine H_1- and H_2-Receptor Conformations with N^G-Acylated Imidazolylpropylguanidines. *J. Pharmacol. Exp. Ther.* **2006**, 317, 139-146.
41. Lim, H. D.; van Rijn, R. M.; Ling, P.; Bakker, R. A.; Thurmond, R. L.; Leurs, R. Evaluation of histamine H_1-, H_2-, and H_3-receptor ligands at the human histamine H_4 receptor: identification of 4-methylhistamine as the first potent and selective H_4 receptor agonist. *J. Pharmacol. Exp. Ther.* **2005**, 314, 1310-1321.
42. Hagelüken, A.; Grünbaum, L.; Klinker, J. F.; Nürnberg, B.; Harhammer, R.; Schultz, G.; Leschke, C.; Schunack, W.; Seifert, R. Histamine receptor-dependent and/or -independent activation of guanine nucleotide-bindinG-Proteins by histamine and 2-substituted histamine derivatives in human leukemia (HL-60) and human erythroleukemia (HEL) cells. *Biochem. Pharmacol.* **1995**, 49, 901-914.
43. Klinker, J. F.; Seifert, R. Rezeptor-unabhängige Aktivierung von G-Proteinen. *Pharm. Unserer Zeit* **1995**, 24, 250-263.
44. Seifert, R.; Hageluken, A.; Hoer, A.; Hoer, D.; Grunbaum, L.; Offermanns, S.; Schwaner, I.; Zingel, V.; Schunack, W.; Schultz, G. The H_1 receptor agonist 2-(3-chlorophenyl)histamine activates G_i proteins in HL-60 cells through a mechanism that is independent of known histamine receptor subtypes. *Mol. Pharmacol.* **1994**, 45, 578-586.
45. Mousli, M.; Bueb, J.-L.; Bronner, C.; Rouot, B.; Landry, Y. G-Protein activation: a receptor-independent mode of action for cationic amphiphilic neuropeptides and venom peptides. *Trends Pharmacol. Sci.* **1990**, 11, 358-362.
46. Wifling, D.; Löffel, K.; Nordemann, U.; Strasser, A.; Bernhardt, G.; Dove, S.; Seifert, R.; Buschauer, A. Molecular determinants for the high constitutive activity of the human histamine H_4 receptor: Functional studies on orthologs and mutants. *Br. J. Pharmacol.* **2014**, in press, doi: 10.1111/bph.12801.
47. Lim, H. D.; de Graaf, C.; Jiang, W.; Sadek, P.; McGovern, P. M.; Istyastono, E. P.; Bakker, R. A.; de Esch, I. J.; Thurmond, R. L.; Leurs, R. Molecular determinants of ligand binding to H_4R species variants. *Mol. Pharmacol.* **2010**, 77, 734-743.
48. Schnell, D.; Brunskole, I.; Ladova, K.; Schneider, E.; Igel, P.; Dove, S.; Buschauer, A.; Seifert, R. Expression and functional properties of canine, rat, and murine histamine H_4 receptors in Sf9 insect cells. *Naunyn-Schmiedeberg's Arch. Pharmacol.* **2011**, 383, 457-470.
49. Nordemann, U.; Wifling, D.; Schnell, D.; Bernhardt, G.; Stark, H.; Seifert, R.; Buschauer, A. Luciferase Reporter Gene Assay on Human, Murine and Rat Histamine H_4 Receptor Orthologs: Correlations and Discrepancies between Distal and Proximal Readouts. *PLoS ONE* **2013**, 8, e73961.
50. Liu, C.; Ma, X.-J.; Jiang, X.; Wilson, S. J.; Hofstra, C. L.; Blevitt, J.; Pyati, J.; Li, X.; Chai, W.; Carruthers, N.; Lovenberg, T. W. Cloning and Pharmacological Characterization of a Fourth Histamine Receptor (H_4) Expressed in Bone Marrow. *Mol. Pharmacol.* **2001**, 59, 420-426.
51. Nordemann, U. Radioligand binding and reporter gene assays for histamine H_3 and H_4 receptor species orthologs. University of Regensburg, Regensburg, Doctoral thesis, **2013**.
52. Igel, P.; Geyer, R.; Strasser, A.; Dove, S.; Seifert, R.; Buschauer, A. Synthesis and Structure−Activity Relationships of Cyanoguanidine-Type and Structurally Related Histamine H_4 Receptor Agonists. *J. Med. Chem.* **2009**, 52, 6297-6313.
53. Spasov, A. A.; Yozhitsa, I. N.; Bugaeva, L. I.; Anisimova, V. A. Benzimidazole derivatives: Spectrum of pharmacological activity and toxicological properties (a review). *Pharm Chem J* **1999**, 33, 232-243.
54. Bansal, Y.; Silakari, O. The therapeutic journey of benzimidazoles: a review. *Bioorg. Med. Chem.* **2012**, 20, 6208-6236.
55. Ghorai, P.; Kraus, A.; Keller, M.; Goette, C.; Igel, P.; Schneider, E.; Schnell, D.; Bernhardt, G.; Dove, S.; Zabel, M.; Elz, S.; Seifert, R.; Buschauer, A. Acylguanidines as Bioisosteres of Guanidines: N^G-Acylated

Imidazolylpropylguanidines, a New Class of Histamine H_2 Receptor Agonists. *J. Med. Chem.* **2008**, 51, 7193-7204.

56. Eleftheriou, S.; Gatos, D.; Panagopoulos, A.; Stathopoulos, S.; Barlos, K. Attachment of histidine, histamine and urocanic acid to resins of the trityl-type. *Tetrahedron Lett.* **1999**, 40, 2825-2828.
57. Charlton, P. T.; Maliphant, G. M.; Oxley, P.; Peak, D. A. Antituberculous compounds. VII. Some further *N*-substituted amidines and analogs. *J. Chem. Soc.* **1951**, 485-492.
58. Lee, B. H.; Miller, M. J. Natural ferric ionophores: total synthesis of schizokinen, schizokinen A, and arthrobactin. *J. Org. Chem.* **1983**, 48, 24-31.
59. Roy, S.; Eastman, A.; Gribble, G. W. Synthesis of bisindolylmaleimides related to GF109203x and their efficient conversion to the bioactive indolocarbazoles. *Org. Biomol. Chem.* **2006**, 4, 3228-3234.
60. Dodd, D. S.; Kozikowski, A. P. Conversion of Alcohols to Protected Guanidines Using the Mitsunobu Protocol. *Tetrahedron Lett.* **1994**, 35, 977-980.
61. Pluym, N.; Brennauer, A.; Keller, M.; Ziemek, R.; Pop, N.; Bernhardt, G.; Buschauer, A. Application of the Guanidine–Acylguanidine Bioisosteric Approach to Argininamide-Type NPY Y_2 Receptor Antagonists. *ChemMedChem* **2011**, 6, 1727-1738.
62. Eriks, J. C.; Van der Goot, H.; Timmerman, H.; Koper, J. G. Preparation of (un)substituted 4(5)-(*ω*-aminoalkyl)imidazoles for the treatment of heart failures or allergic conditions. WO8910360A1, **1989**.
63. Elz, S.; Schunack, W. An alternative synthesis of homohistamine and structurally related (imidazol-4-yl)alkylamines. *Z. Naturforsch. B* **1987**, 42, 238-242.
64. Badorc, A.; Boldron, C.; Delesque, N.; Fossey, V.; Lassalle, G.; Yvon, X. Derivatives of *N*-[(1*H*-pyrazol-1-yl)aryl]-1*H*-indole-3-carboxamide and *N*-[(1*H*-pyrazol-1-yl)aryl]-1*H*-indazole-3-carboxamide, their preparation and their use as P2Y12 antagonists. WO2012146318A1, **2012**.
65. Wolin, R.; Connolly, M.; Afonso, A.; Hey, J. A.; She, H.; Rivelli, M. A.; Willams, S. M.; West Jr, R. E. Novel H_3 receptor antagonists. Sulfonamide homologs of histamine. *Bioorg. Med. Chem. Lett.* **1998**, 8, 2157-2162.
66. Bouix-Peter, C.; Carlavan, I.; Soulet, C.; Parnet, V.; Voegel, J. Preparation of amino acid azetidine amide derivatives, as selective melanocortin receptor MC4R antagonists for pharmaceutical use. WO2010052256A1, **2010**.
67. Ankersen, M.; Crider, M.; Liu, S.; Ho, B.; Andersen, H. S.; Stidsen, C. Discovery of a Novel Non-Peptide Somatostatin Agonist with SST4 Selectivity. *J. Am. Chem. Soc.* **1998**, 120, 1368-1373.
68. Pop, N.; Igel, P.; Brennauer, A.; Cabrele, C.; Bernhardt, G. N.; Seifert, R.; Buschauer, A. Functional reconstitution of human neuropeptide Y (NPY) Y_2 and Y_4 receptors in Sf9 insect cells. *J. Recept. Signal Transduct.* **2011**, 31, 271-285.
69. Lowry, O. H.; Rosebrough, N. J.; Farr, A. L.; Randall, R. J. Protein measurement with the Folin phenol reagent. *J. Biol. Chem.* **1951**, 193, 265-275.
70. Asano, T.; Pedersen, S. E.; Scott, C. W.; Ross, E. Reconstitution of catecholamine-stimulated binding of guanosine 5'-O-(3-thiotriphosphate) to the stimulatory GTP-bindinG-Protein of adenylate cyclase. *Biochemistry* **1984**, 23, 5460-5467.
71. Hilf, G.; Gierschik, P.; Jakobs, K. H. Muscarinic acetylcholine receptor-stimulated binding of guanosine 5'-O-(3-thiotriphosphate) to guanine-nucleotide-bindinG-Proteins in cardiac membranes. *Eur. J. Biochem.* **1989**, 186, 725-731.
72. Mosandl, J. Radiochemical and luminescence-based binding and functional assays for human histamine receptors using genetically engineered cells. University of Regensburg, Regensburg, Doctoral thesis, **2009**.

Chapter 4

Synthesis and Pharmacological Characterization of VUF 8430 Derivatives as Histamine H_4 Receptor Ligands

4.1 Introduction

The early pharmacological and physiological characterization of the H_4R was based on the investigation of compounds previously known as ligands of the other histamine receptor subtypes. For example, the H_3R/H_4R agonists imetit[1] and VUF 8328,[2] the H_3R antagonist/H_4R agonist clobenpropit[3] and the H_3R antagonist/H_4R inverse agonist thioperamide[4] show comparable affinities to both receptors.[5] N^G-alkylated and acylated imidazolyl-propylguanidines were originally developed as H_2R agonists.[6-12] However, the parent compound, imidazolyl-propylguanidine (SK&F-91486),[13] N^G-alkylated analogs such as impromidine[6] and N^G-acylated analogs such as UR-AK24, UR-AK51[12] and UR-PG80[14] were found to possess H_3R and H_4R affinity, too. Modification of the N^G-acyl groups in UR-AK24 resulted in potent nearly full H_4R agonists such as UR-PI287, UR-PI288, UR-PI294 and UR-PI295 with pEC_{50} values of 7.8 to 8.6 and 25- to 300-fold selectivity over the hH_2R.[15] The major drawback of imidazole-containing hH_4R agonists is the lack of selectivity over the other histamine receptor subtypes, in particular the hH_3R. In addition, imidazole derivatives are potential inhibitors of cytochrome P450 enzymes.[16,17] Replacement of the imidazole ring by various heterocycles as potential bioisosteres revealed only weak activity of most of the synthesized hetarylalkylamines at the H_3R and the H_4R.[18] Interestingly, VUF 8430, combining a guanidine *via* an ethylene spacer with an isothiourea group, was also initially designed as an H_2R agonist related to dimaprit,[19] but proved to

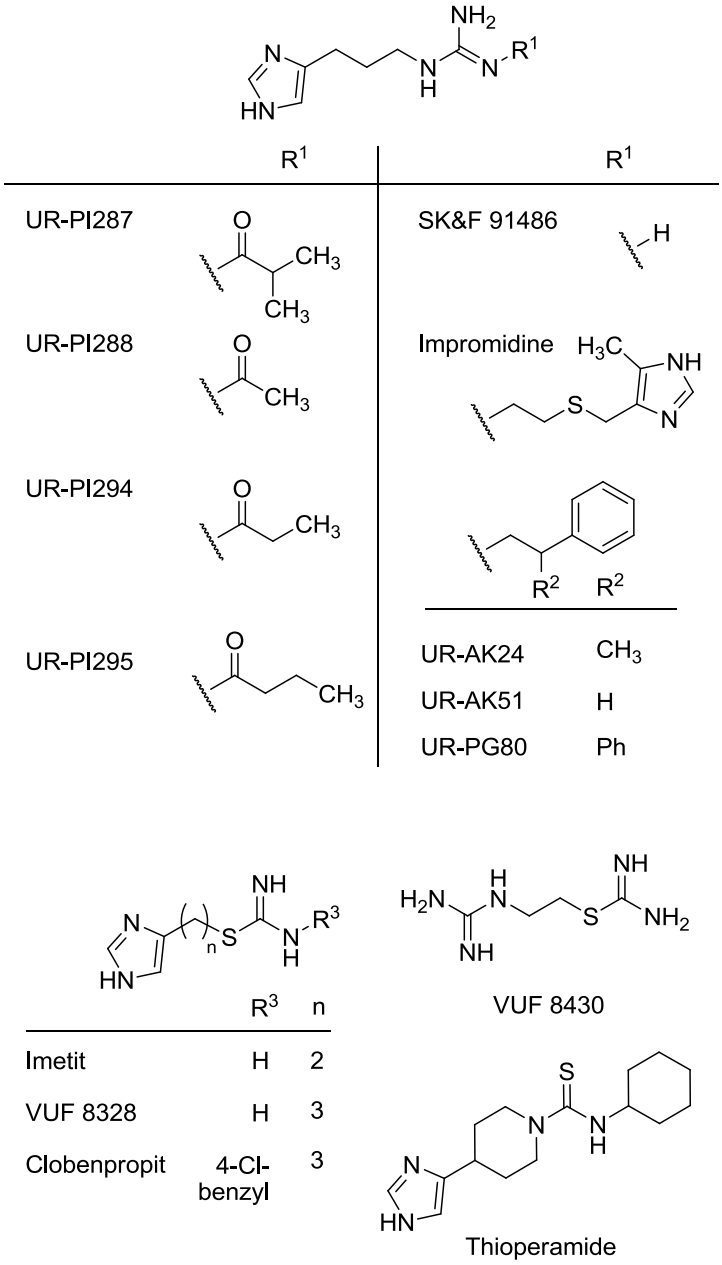

Figure 4.1 Histamine receptor ligands with agonistic activities at the hH_4R.

be a potent hH_4R agonist with ~30-fold selectivity over the hH_3R (full agonism) and negligible affinity for hH_1R and hH_2R (partial agonism).[20,21]

Aiming at H_4R agonists with increased selectivity over the other H_xR subtypes, the present study was focused on the combination of crucial structural features of VUF 8430 and N^G-acylated imidazolylpropylguanidines, i. e. guanidine and acylguanidine groups, as shown in Figure 4.2. In a first approach either a guanidine and an N^G-acylated guanidine moiety or two acylguanidines were connected by an ethylene or a trimethylene spacer. The residues 'R' were selected with respect to comparison of the structure-activity relationship with those of the previously published imidazolylpropylguanidines,[12,14,15] containing small residues such as ethoxycarbonyl or butyryl residues as well as more bulky moieties such as aromatic rings. Moreover, structural analogs bearing an isothiourea instead of a guanidine group were synthesized.

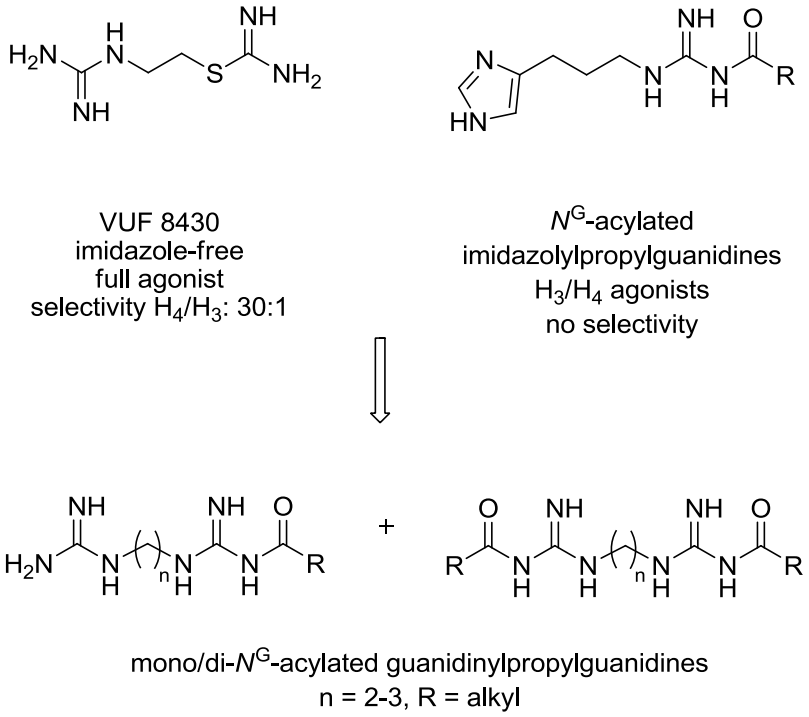

Figure 4.2 Replacement of the imidazole-ring by guanidine and N^G-acylated guanidine groups.

4.2 Chemistry

The preparation of **4.12**-**4.39** was performed according to Scheme 4.1, starting with the synthesis of the required guanidinylating reagents **4.3**-**4.11**. The *N*-Boc protected *S*-methyisothiourea **4.2** and the di-protected analog **4.3** were synthesized as described previously.[22-25] Acylation of **4.2** with the pertinent acids under standard conditions for amide coupling using TBTU yielded **4.4**-**4.11** in very good yields.[26]

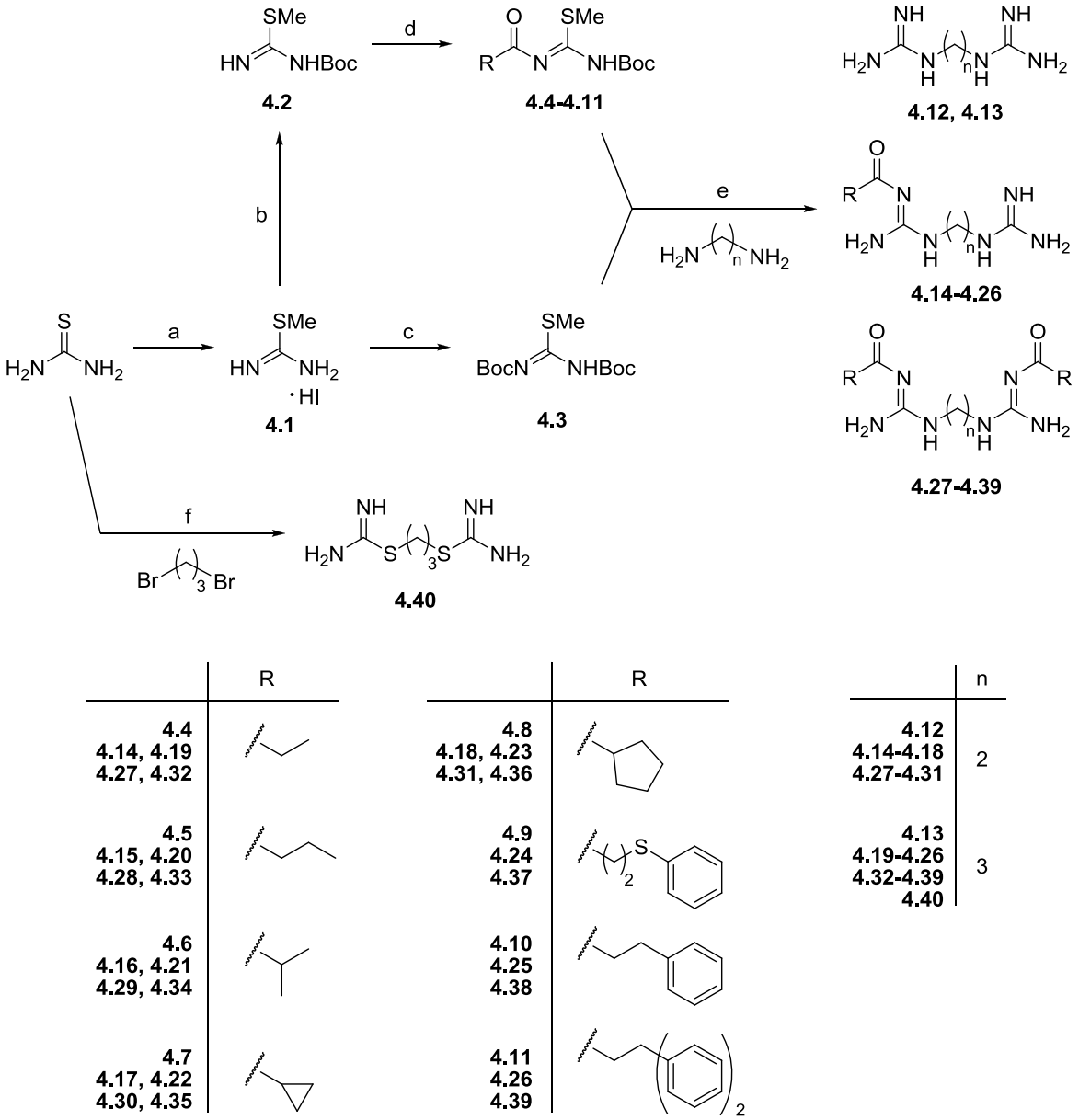

Scheme 4.1 Synthesis of the acylguanidines **4.12**-**4.39** and the dimeric isothiourea **4.40**. Reagents and conditions: (a) Thiourea, MeI, MeOH, rt, 1 h, 98%; (b) Boc_2O, NEt_3, rt, 20 h, 74%; (c) Boc_2O, NEt_3, rt, 22 h, 56%; (d) respective acid, TBTU, DIPEA, rt, O/N, 55-89%; (e) 1) ethanediamine or propanediamine, **4.4**-**4.11**, **4.3**, $HgCl_2$, NEt_3, CH_2Cl_2, rt, 24-48 h, 2) 5% TFA in CH_2Cl_2, rt, 4-8 h, 4-26%; (f) 1,3-dibromopropane, thiourea, EtOH, microwave 125 °C, 15 min, 65%.

Ethandiamine or propanediamine were treated with the isothiourea derivatives **4.2** and **4.4**-**4.11**, in the presence of $HgCl_2$. Hereby, the metal ion acts as a desulfurizing agent *via* complex formation.[27,28] After acidic cleavage of the protecting groups, purification by preparative HPLC afforded **4.12**-**4.39** in low to moderate yields. According to this combinatorial approach, the synthesis of 30 compounds *via* 14 reactions became feasible. The preparation of the **4.40** was performed from 1,3-dibrom-propane and thiourea under microwave irradiation (cf. Scheme 4.1). Synthesis of **4.43** started from guanidinylating reagents **3.25** and 3-amino-propanol to obtain intermediate **4.41** in excellent yield.[29]

Conversion of the terminal hydroxyl-group to the bromide by refluxing with concentrated HBr yielded **4.42**, which was subsequently allowed to react with thiourea under microwave irradiation to give **4.43** (cf. Scheme 4.2).[20]

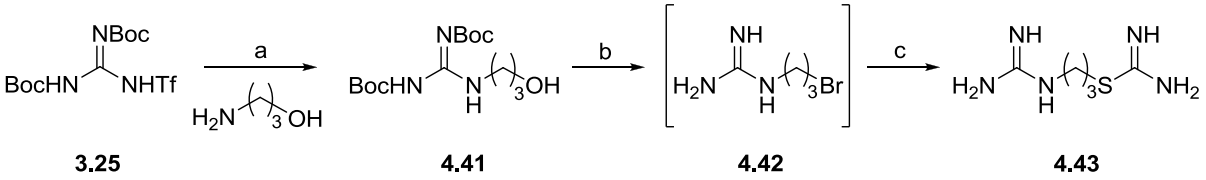

3.25 **4.41** **4.42** **4.43**

Scheme 4.2 Synthesis of the VUF 8430 analog **4.43**. Reagents and conditions: (a) 3-Aminopropan-1-ol, NEt_3, CH_2Cl_2 ml, rt, 40 min, 95%; (b) 47% $HBr_{(aq.)}$, 100 °C, 30 h; (c) thiourea, EtOH, microwave 125 °C, 15 min, 10% over two steps.

4.3 Pharmacological Results and Discussion

The synthesized compounds **4.12**-**4.40** and **4.43** were investigated at the hH_3R and hH_4R in radioligand binding assays using membrane preparations of Sf9 insect cells coexpressing the hH_3R + $G\alpha_{i2}$ + $G\beta_1\gamma_2$ or hH_4R + $G\alpha_{i2}$ + $G\beta_1\gamma_2$, respectively. Additionally, selected compounds were tested for hH_2R affinity at the hH_2R−$Gs_{\alpha s}$ fusion protein. For comparison, VUF 8430 was included as a reference compound. The data are summarized in Table 4.1.

VUF 8430 revealed a K_i value of 17.7 nM and a 33-fold selectivity over the hH_3R, which were in good agreement with the pharmacological data reported for cell homogenates of SK-N-MC expressing the hH_4R (K_i = 31.6 nM, 30-fold selectivity over the hH_3R).[20] The extension of the ethylene linker by one methylene group (**4.43**) resulted in a decrease in affinity (K_i = 104 nM), whereas the selectivity ratio was retained. The results for **4.43** were inconsistent with reported data (K_i ~8000 nM)[20] for unknown reasons. The introduction of two guanidines (**4.12**), led to a 200-fold decrease in affinity at the hH_4R compared to VUF 8430. Interestingly, the decrease in affinity was less pronounced in case of the homolog **4.13** (K_i = 442, $K_{i(ref)}$[20] = ~400 nM). The dimeric isothiourea **4.40** revealed a switch in receptor subtype preference with a lower K_i value at the hH_3R (K_i = 1010 nM) compared to the hH_4R (K_i = 4200 nM).

The bioisosteric exchange of an isothiourea by an acylguanidine group resulted in the derivatives **4.14**-**4.18**. In comparison to VUF8430, all of these compounds had lower affinities at the hH_4R (K_i = 550-1860 nM) and reduced selectivities towards the hH_3R (2- to 5-fold). Analogs separating the guanidine and N^G-acylated guanidines by a three-membered carbon spacer have higher affinity for the hH_4R (compare **4.19**-**4.23**) than their lower homologs, but were still inferior to VUF 8430.

Table 4.1 Binding data of compounds **4.12**-**4.40** and **4.43** at the histamine receptor subtypes H_2, H_3 and H_4[a]

Compound	**hH_2R**		**hH_3R**		**hH_4R**		Selectivity $H_4 : H_3$
	K_i / nM	n	K_i / nM	n	K_i / nM	n	
Histamine	n.d.		20.1 ± 3.1	4	13.1 ± 1.1	4	1.5 : 1
VUF 8430	>20000	2	587 ± 75	2	17.7 ± 1.4	4	33 : 1
4.12	>20000	2	10100 ± 3760	3	3650 ± 290	2	2.8 : 1
4.13	>20000	2	2310 ± 340	3	442 ± 79	3	5.2 : 1
4.14	>10000	2	7000 ± 170	2	1400 ± 340	3	5 : 1
4.15	n.a.[b]	2	2520 ± 630	2	1040 ± 9	2	1.8 : 1
4.16	n.d.		6010 ± 1360	2	1820 ± 250	2	3.3 : 1
4.17	n.a.[b]	2	3260 ± 480	2	1860 ± 170	2	1.8 : 1
4.18	n.d.		1110 ± 160	3	550 ± 33	2	2 : 1
4.19	n.d.		6240 ± 840	2	104 ± 41	2	60 : 1
4.20	n.d.		12200 ± 1040	2	500 ± 40	2	24 : 1
4.21	n.d.		4410 ± 580	2	98.3 ± 5.8	3	45 : 1
4.22	n.d.		11300 ± 2300	2	350 ± 46	3	32 : 1
4.23	n.d.		2360 ± 430	3	227 ± 35	3	10 : 1
4.24	n.d.		2470 ± 1390	2	4670 ± 570	2	1 : 1.9
4.25	n.d.		4620 ± 510	2	2870 ± 36	2	1.6 : 1
4.26	n.d.		9410 ± 1100	2	7030 ± 250	2	1.3 : 1
4.27	>10000	2	9300 ± 1650	2	9260 ± 2450	2	1 : 1
4.28	n.d.		> 20000	2	> 30000	2	-
4.29	n.d.		19300 ± 25	2	8360 ± 370	2	2.3 : 1
4.30	n.d.		> 20000	2	> 20000	2	-
4.31	n.d.		8170 ± 1790	2	6150 ± 2580	2	1.3 : 1
4.32	n.d.		11100 ± 1800	2	2770 ± 30	2	4 : 1
4.33	n.d.		8510 ± 2390	2	2890 ± 1280	3	3 : 1
4.34	n.d.		45100 ± 4350	2	1580 ± 400	2	29 : 1
4.35	n.d.		34300 ± 2420	2	6190 ± 1100	2	5.5 : 1
4.36	n.d.		4030 ± 330	3	1380 ± 250	3	2.9 : 1
4.37	n.d.		8090 ± 140	2	9270 ± 1790	2	1 : 1.2
4.38	n.d.		7050 ± 660	2	3850 ± 1000	2	1.8 : 1
4.39	n.d.		n.a.[b]		n.a[b]		-
4.40	> 20000	2	1010 ± 420	3	4200 ± 590	3	1 : 4.2
4.43	n.d.		2670 ± 570	2	104 ± 0.2	2	26 : 1

[a] Determined on membrane preparations of Sf9 insect cells expressing hH_2R-$Gs_{\alpha s}$ fusion protein, hH_3R + $G\alpha_{i2}$ + $G\beta_1\gamma_2$ or the hH_4R + $G\alpha_{i2}$ + $G\beta_1\gamma_2$; radioligands: for hH_2R: [^{3}H]UR-DE257, c = 20 nM), for hH_3R: [^{3}H]N^{α}-methylhistamine (c = 3 nM), for hH_4R: [^{3}H]Histamine (c = 10 nM); [b] no binding up to a concentration of 100 μM; n gives the number of independent experiments performed in triplicate; n.d. = not determined.

Highest affinities were obtained for the propionylguanidine **4.19** (K_i = 104 nM) and its isobutyryl analog **4.21** (K_i = 98 nM). Compared to VUF 8430, both compounds showed slightly higher selectivities for the hH_4R over the hH_3R (60-fold for **4.19** and 45-fold for **4.21**, respectively). Among the acylguanidines **4.14**-**4.26** the H_4R affinity and selectivity was strongly dependent on the structure of the N^G-acyl substituent (cf. R in Scheme 4.1). Only small aliphatic residues were tolerated to retain submicromolar K_i values at the hH_4R, which is in accordance to previously published data.[15,30] Compounds bearing a phenyl group in the acyl moiety (**4.24**-**4.26**) showed only affinities in the micromolar range and were devoid of receptor subtype selectivity. For the dimeric acylguanidines **4.27**-**4.39**, the K_i values at the hH_4R were also in the micromolar range and the selectivity towards the hH_3R was reduced, regardless whether an ethylene or a trimethylene linker was incorporated. Noteworthy is compound **4.34** with a trimethylene spacer which had moderate affinity (K_i = 1580 nM) but retained selectivity towards the hH_3R. At the hH_2R all investigated compounds of this series revealed K_i values higher than 10000 nM, which was in the same range as for VUF 8430.

4.4 Summary and Outlook

The bioisosteric replacment of the isothiourea group or both the guanidine and the isothiourea group in VUF 8430 by various N^G-acylguanidine moieties (**4.14**-**4.39**) resulted in compounds with reduced hH_4R affinities compared to the reference substance. Among these VUF 8430 analogs, highest affinity resided in compounds **4.19** and **4.21** with K_i values of around 100 nM at the hH_4R and slightly higher selectivity over the H_3R (60-fold for **4.19** and 45-fold for **4.21**, respectively). Compounds comprising two chemically different basic moieties revealed higher hH_4R binding than homodimeric analogs, i. e. compounds with two guanidine (**4.12** and **4.13**, respectively), two isothiourea (**4.43**) or two acylguanidine (**4.27**-**4.39**) groups. In the series acylguanidines **4.14**-**4.39** only small aliphatic residues 'R' were tolerated to achieve submicromolar K_i values at the hH_4R, and compounds with a linker length of three methylene groups were superior to the lower homologs.

Suggestions for future structural modifications are shown in Figure 4.3. It is rather likely that the isothiourea group is accepted by the H_4R as a bioisosteric mimic of the imidazole ring in histamine. Therefore, the combination of the acylguanidine with an isothiourea moiety should be taken into consideration. The influence of further extended linkers on H_4R affinity should also be explored. Moreover, rigidization has been proven successful to improve the selectivity of H_4R ligands.[31-34] This approach might be applied to non-imidazoles, e. g. by introduction of a ring or a multiple bond in the linker or by the incorporation of one of the basic centers in a heterocycle.

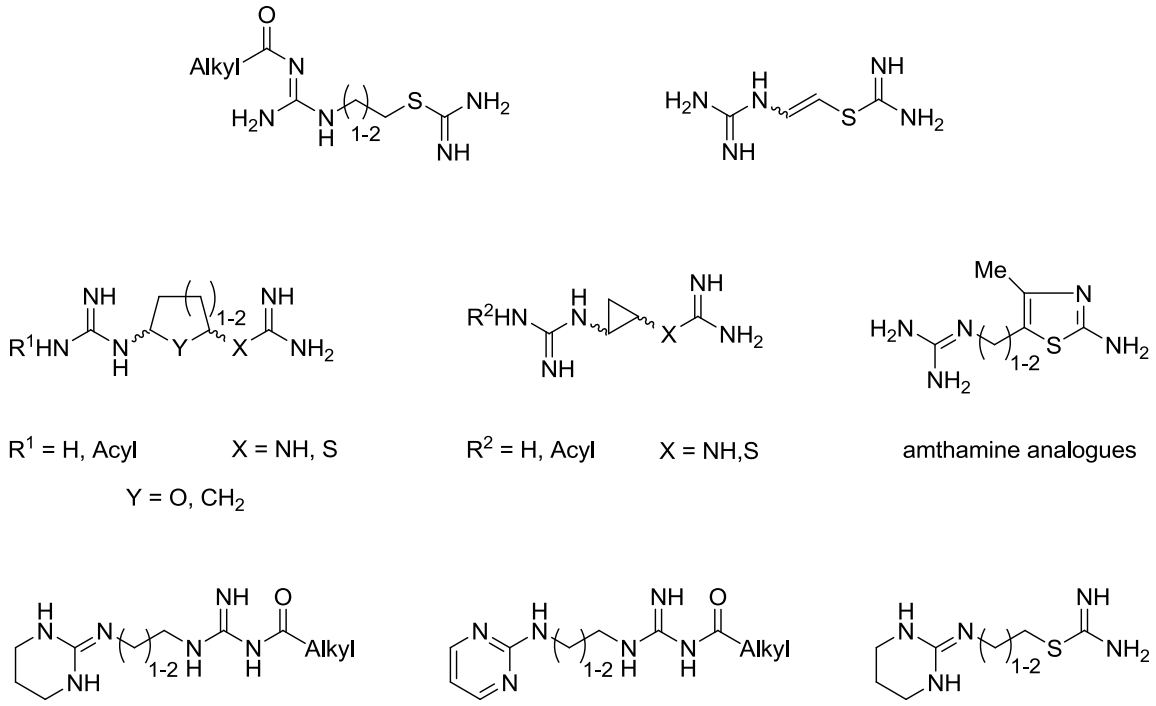

Figure 4.3 Suggestions of future structural variations H_4R ligands derived from VUF 8430.

4.5 Experimental Section

4.5.1 Chemistry

4.5.1.1 General conditions

See section 3.4.1.1

Except for **4.23**, **4.24**, **4.26**-**4.29** and **4.38**-**4.44** the HPLC column was a Eurospher-100 (250 x 4 mm, 5 µm) (Knauer, Berlin, Germany, t_0 = 3.32 min) at a flow rate of 0.8 ml/min. For **4.23**, **4.24**, **4.26**-**4.29** and **4.38**-**4.44** the column was a Luna C18(2) (150 × 4.6 mm, 3 µm) (Phenomenex, Aschaffenburg, Germany, t_0 = 2.88 min). UV detection was done at 200 nm. VUF 8430 was synthesized by Dr. Roland Geyer in our research group by analogy with a previously published synthesis.[20]

4.5.1.2 Preparation of the isothiourea derivatives **4.2** and **4.3**

General procedure for the synthesis of the guanidinylating reagents 4.2 and 4.3

S-Methylthiouronium iodide (4.1)[22]

Thiourea (12.9 g, 169 mmol, 1 eq) and MeI (10.6 g, 169 mmol, 1 eq) in MeOH (130 ml) were refluxed for 1 h. After evaporation of the solvent under reduced pressure the crude product was triturated with Et_2O, filtered and washed twice with Et_2O to yield the desired product as white solid (36.2 g, 98%). The crude product was used in the next step without further purification. mp 111 °C (lit.[35] 113.5-115 °C). ^{1}H-NMR (300 MHz, DMSO-d_6): δ (ppm) 2.56 (s, 3H), 8.86 (bs, s, 4H). ^{13}C-NMR (75 MHz, DMSO-d_6): δ (ppm) 13.58, 171.10. MS (LC-MS, ESI): *m/z* 91.1 [M+H$^+$]. $C_2H_6N_2S$ (90.15).

N-tert-Butoxycarbonyl-S-methylisothiourea (4.2)[22]

To a solution of **4.1** (15.0 g, 68.8 mmol, 1 eq) and NEt_3 (6.95 g, 68.8 mmol, 1 eq) in CH_2Cl_2 (107 ml) was added Boc_2O (15.0 g, 68.8 mmol, 1 eq) in CH_2Cl_2 (27 ml) and the reaction was stirred for 20 h at room temperature. Subsequently, the mixture was washed with water, the organic layer dried over anhydrous Na_2SO_4 and concentrated *in vacuo*. The crude product was purified by flash-chromatography (eluent hexanes (A), EtOAc (B); gradient: 0 to 60 min: A/B 100/0 – 0/100 v/v, SF 65-400 g) affording a white solid (9.63 g, 74%). mp 82 °C (lit.[36] 77 °C). R_f = 0.29 (hexane/EtOAc 5:1). ^{1}H-NMR (300 MHz, $CDCl_3$): δ (ppm) 1.49 (s, 9H), 2.43 (s, 3H), 7.52 (bs, 2H). MS (LC-MS, ESI): *m/z* 191.0 [M+H$^+$]. $C_7H_{14}N_2O_2S$ (190.26).

N,N'-Bis(tert-butoxycarbonyl)-S-methylisothiourea (4.3)[35,37]

To a solution of **4.1** (10.0 g, 45.9 mmol, 1 eq) and NEt_3 (11.6 g, 115 mmol, 2.5 eq) in CH_2Cl_2 (80 ml) was added Boc_2O (25 g, 115 mmol, 2.5 eq) in CH_2Cl_2 (80 ml). The mixture was stirred for 22 h at room temperature and subsequently washed with water and brine. The organic layer was dried over anhydrous $MgSO_4$ and concentrated *in vacuo*. The crude product was purified by flash-chromatography (eluent hexanes (A), EtOAc (B); gradient: 0 to 60 min: A/B 100/0 – 3/1 v/v, SF 65-400 g) affording a white solid (7.41 g, 56%). mp 122 °C (lit.[37] 122 – 123 °C). R_f = 0.52 (hexane/EtOAc 5:1). ^{1}H-NMR (300 MHz, $CDCl_3$): δ (ppm) 1.50 (s, 9H), 1.52 (s, 9H), 2.39 (s, 3H), 11.60 (s, 1H). MS (LC-MS, ESI): *m/z* 291.0 [M+H$^+$]. $C_{12}H_{22}N_2O_4S$ (290.38).

4.5.1.3 Preparation of N^G-acylated isothiourea derivatives **4.4**-**4.11**

General procedure for the synthesis of the isothiourea derivatives 4.4-4.11

The pertinent acid (1 eq) was dissolved in CH_2Cl_2 (15-30 ml), DIPEA (3 eq) and TBTU (1.2 eq) were added and the reaction mixture was stirred at room temperature under argon atmosphere for 20 min. The acylated isothiourea derivative (1 eq), dissolved in CH_2Cl_2 (5-15 ml) was added slowly, and stirring was continued overnight. The mixture was poured into ice cold water (20 ml), acidified with 0.1 M HCl (pH 4) and extracted two times with CH_2Cl_2 (20-40 ml). The combined organic phase was dried over anhydrous Na_2SO_4 and concentrated *in vacuo*. The crude product was purified by flash-chromatography.

N-tert-Butoxycarbonyl-N'-ethoxycarbonyl-S-methylisothiourea (4.4)[38]

The title compound was prepared from propionic acid (390 mg, 5.26 mmol, 1 eq), DIPEA (2.08 g, 15.78 mmol, 3 eq), TBTU (2.03 g, 6.31 mmol, 1.2 eq) and **4.2** (1.00 g, 5.26 mmol, 1 eq). The crude product was purified by flash-chromatography (eluent CH_2Cl_2, isocratic, SF 15-24 g) affording a pale yellow solid (1.15 g, 89%). mp 114 °C. R_f = 0.46 (hexane/EtOAc 5:1). ^{1}H-NMR (300 MHz, DMSO-d_6): δ (ppm) 1.00 (t, *J* = 7.4, 3H), 1.42 (s, 9H), 2.28 (s, 3H), 2.36 (q, *J* = 7.4, 2H), 11.21 (bs, 1H). ^{13}C-NMR (75 MHz, $CDCl_3$): δ (ppm) 8.81, 14.46, 27.97 (3C), 31.15, 81.67 (br), 161.36, 171.02 (br), 172.00 (br). MS (LC-MS, ESI): *m/z* 247.0 [M+H$^+$]. $C_{10}H_{18}N_2O_3S$ (246.33).

N-tert-Butoxycarbonyl-N'-(butyryl)-S-methylisothiourea (4.5)

The title compound was prepared from butyric acid (278 mg, 3.15 mmol, 1 eq), DIPEA (2.08 g, 15.78 mmol, 3 eq), TBTU (1.22 g, 3.78 mmol, 1.2 eq) and **4.2** (600 mg, 3.15 mmol, 1 eq). The crude

product was purified by flash-chromatography (eluent CH_2Cl_2, isocratic, SF 15-24 g) affording a white solid (689 mg, 84%). mp 82 °C. R_f = 0.45 (hexane/EtOAc 5:1). ^{1}H-NMR (300 MHz, $CDCl_3$): δ (ppm) 0.97 (t, *J* = 7.4, 3H), 1.51 (s, 9H), 1.63-1.77 (m, 2H), 2.39 (s, 3H), 2.42 (d, *J* = 7.3, 2H), 12.44 (bs, 1H). ^{13}C-NMR (75 MHz, $CDCl_3$): δ (ppm) 13.62, 14.45, 18.25, 27.97 (3C), 39.77, 81.54, 160.77, 170.98, 172.07. MS (LC-MS, ESI): *m/z* 261.13 [M+H$^+$]. $C_{11}H_{20}N_2O_3S$ (260.35).

N-tert-Butoxycarbonyl-N'-(isobutyryl)-S-methylisothiourea (4.6)

The title compound was prepared from isobutyric acid (277.8 mg, 3.15 mmol, 1 eq), DIPEA (2.08 g, 15.78 mmol, 3 eq), TBTU (1.22 g, 3.78 mmol, 1.2 eq) and **4.2** (600 mg, 3.15 mmol, 1 eq). The crude product was purified by flash-chromatography (eluent CH_2Cl_2, isocratic, SF 15-24 g) affording a white solid (706 mg, 86%). mp 86 °C. R_f = 0.52 (hexanes/EtOAc 5:1). ^{1}H-NMR (300 MHz, $CDCl_3$): δ (ppm) 1.15 (d, J = 7.0, 1H), 1.45 (s, 9H), 2.33 (s, 3H), 2.47-2.63 (m, 1H), 12.47 (bs, 1H). ^{13}C-NMR (75 MHz, $CDCl_3$): δ (ppm) 14.48, 18.96 (2C), 27.94 (3C), 36.71, 81.62, 160.75 (br), 171.29, 175.28 (br). MS (LC-MS, ESI): *m/z* 261.13 [M+H$^+$]. $C_{11}H_{20}N_2O_3S$ (260.35).

N-tert-Butoxycarbonyl-N'-(cyclopropylcarbonyl)-S-methylisothiourea (4.7)

The title compound was prepared from cyclopropanecarboxylic acid (272 mg, 3.15 mmol, 1 eq), DIPEA (2.08 g, 15.78 mmol, 3 eq), TBTU (1.22 g, 3.78 mmol, 1.2 eq) and **4.2** (600 mg, 3.15 mmol, 1 eq). The crude product was purified by flash-chromatography (eluent CH_2Cl_2, isocratic, SF 15-24 g) affording a white solid (644 mg, 79%). mp 59 °C. R_f = 0.60 (hexane/EtOAc 5:1). ^{1}H-NMR (300 MHz, $CDCl_3$): δ (ppm) 0.87-0.98 (m, 2H), 1.05-1.14 (m, 2H), 1.50 (s, 9H), 1.71 (s, 1H), 2.37 (s, 3H), 12.48 (bs, 1H). ^{13}C-NMR (75 MHz, $CDCl_3$): δ (ppm) 10.00, 10.30, 14.49, 20.27, 28.06 (3C), 81.42, 161.00, 171.12, 172.45. MS (LC-MS, ESI): *m/z* 259.11 [M+H$^+$]. $C_{11}H_{18}N_2O_3S$ (258.34).

N-tert-Butoxycarbonyl-N'-(cyclopentylcarbonyl)-S-methylisothiourea (4.8)

The title compound was prepared from cyclopentanecarboxylic acid (721 mg, 6.31 mmol, 1 eq), DIPEA (2.45 g, 18.94 mmol, 3 eq), TBTU (2.43 g, 7.58 mmol, 1.2 eq) and **4.2** (1.20 g, 6.31 mmol, 1 eq). The crude product was purified by flash-chromatography (eluent CH_2Cl_2, isocratic, SF 15-24 g) affording a white solid (1.61 g, 89%). mp 81 °C. R_f = 0.46 (hexane/EtOAc 5:1). ^{1}H-NMR (300 MHz, $CDCl_3$): δ (ppm) 1.53 (s, 9H), 1.56-2.00 (m, 8H), 2.39 (s, 3H), 2.76 (p, *J* = 8.0, 1H), 12.49 (s, 1H). ^{13}C-NMR (75 MHz, $CDCl_3$): δ (ppm) 14.48, 25.88 (2C), 27.97 (3C), 29.96 (2C), 46.73, 81.28, 160.78, 171.15, 175.36. MS (LC-MS, ESI): *m/z* 287.2 [M+H$^+$]. $C_{13}H_{22}N_2O_3S$ (286.39).

N-tert-Butoxycarbonyl-N'-[2-(phenylsulfanyl)acetyl]-S-methylisothiourea (4.9)

The title compound was prepared from 3-(phenylsulfanyl)propanoic acid (562 mg, 3.08 mmol, 1 eq), DIPEA (1.20 g, 9.25 mmol, 3 eq), TBTU (1.19 g, 3.70 mmol, 1.2 eq) and **4.2** (586 mg, 3.08 mmol, 1 eq). The crude product was purified by flash-chromatography (eluent hexanes (A), EtOAc (B); gradient: 0 to 30 min: A/B 100/0 – 10/1 v/v, SF 15-24 g) affording a white solid (600 mg, 55 %). mp 66 °C. R_f = 0.50 (hexane/EtOAc 10:1). ^{1}H-NMR (300 MHz, $CDCl_3$): δ (ppm) 1.50 (s, 9H), 2.38 (s, 3H), 2.64-2.87 (m, 2H), 3.23 (t, *J* = 7.2, 2H), 7.17-7.24 (m, 1H), 7.29 (t, *J* = 7.4, 2H), 7.37 (d, *J* = 7.5, 2H), 12.14 (s, 1H). ^{13}C-NMR (75 MHz, $CDCl_3$): δ (ppm) 14.48, 25.88 (2C), 27.97 (3C), 29.96 (2C), 46.73, 81.28, 160.78, 171.15, 175.36. MS (LC-MS, ESI): *m/z* 354.9 [M+H$^+$]. $C_{16}H_{22}N_2O_3S_2$ (354.49).

N-tert-Butoxycarbonyl-N'-(3-phenylpropanoyl)-S-methylisothiourea (4.10)[38]

The title compound was prepared from 3-phenylpropanoic acid (948 mg, 6.31 mmol, 1 eq), DIPEA (2.45 g, 18.94 mmol, 3 eq), TBTU (2.43 g, 7.58 mmol, 1.2 eq) and **4.2** (1.20 g, 6.31 mmol, 1 eq). The crude product was purified by flash-chromatography (eluent CH_2Cl_2, isocratic, SF 15-24 g) affording a white solid (1.58 mg, 78%). mp 103 °C. R_f = 0.52 (100% CH_2Cl_2). ^{1}H-NMR (300 MHz, $CDCl_3$): δ (ppm) 1.51 (s, 9H), 2.39 (s, 3H), 2.70-2.87 (m, 2H), 2.96-3.04 (m, 2H), 7.17-7.24 (m, 3H), 7.26-7.32 (m, 2H), 12.48 (s, 1H). ^{13}C-NMR (75 MHz, $CDCl_3$): δ (ppm) 14.52, 28.11 (3C), 30.39, 39.01, 81.28, 126.48, 128.32 (2C), 128.59 (2C), 139.90, 160.95, 170.51, 171.15. MS (LC-MS, ESI): *m/z* 323.0 [M+H$^+$]. $C_{16}H_{22}N_2O_3S$ (322.42).

N-tert-Butoxycarbonyl-N'-(3,3-diphenylpropanoyl)-S-methylisothiourea (4.11)

The title compound was prepared from 3,3-diphenylpropanoic acid (1.43 mg, 6.31 mmol, 1 eq), DIPEA (2.45 g, 18.94 mmol, 3 eq), TBTU (2.43 g, 7.58 mmol, 1.2 eq) and **4.2** (1.20 g, 6.31 mmol, 1 eq). The crude product was purified by flash-chromatography (eluent CH_2Cl_2, isocratic, SF 15-24 g) affording a white solid (1.85 mg, 74%). mp 123 °C. R_f = 0.67 (100% CH_2Cl_2). ^{1}H-NMR (300 MHz, $CDCl_3$): δ (ppm) 1.47 (s, 9H), 2.36 (s, 3H), 3.08-3.33 (m, 2H), 4.56-4.73 (m, 1H), 7.14-7.32 (m, 10H), 11.94 (s, 1H). ^{13}C-NMR (75 MHz, $CDCl_3$): δ (ppm) 14.69, 28.03 (3C), 43.93, 46.70, 126.44, 126.83, 127.74 (2C), 127.84 (2C), 128.61 (2C), 128.79 (2C), 142.98, 144.18, 160.94, 170.86, 184.34. MS (LC-MS, ESI): *m/z* 399.1 [M+H$^+$]. $C_{22}H_{26}N_2O_3S$ (398.52).

4.5.1.4 Preparation of the guanidine derivatives **4.12**-**4.39**

General procedure for the synthesis of the guanidine derivatives 4.12-4.39

The diamine (1 eq), one of the guanidinylating reagents **4.4**-**4.11** (1 eq), the guanidinylating reagent **4.3** (1 eq) and $HgCl_2$ (4 eq) were dissolved in anhydrous CH_2Cl_2 (4-10 ml). NEt_3 (4 eq) was added and the mixture was stirred at ambient temperature for 24 to 48 h. Subsequently, the precipitate was filtered over Celite and dried *in vacuo*. The residue was dissolved in CH_2Cl_2. TFA (50% final concentration) was added and the reaction mixture was stirred until the protection groups were removed (3–8 h, TLC control). After evaporation of the solvent *in vacuo*, the crude product was purified by preparative RP-HPLC. MeCN was removed under reduced pressure. After lyophilisation **4.12**-**4.39** (bis(hydrotrifluoroacetate)) were obtained as white fluffy hydroscopic solids.

1,1'-(Ethane-1,2-diyl)diguanidine bis(hydrotrifluoroacetate) (4.12), N-[N-(2-guanidinoethyl)-carbamimidoyl]propionamide bis(hydrotrifluoroacetate) (4.14) and N,N'-[ethane-1,2-diylbis-(azanediyl)]bis(iminomethylene)dipropionamide bis(hydrotrifluoroacetate) (4.27)

The three title compounds were prepared in a one-pot reaction from ethane-1,2-diamine (41 mg, 0.681 mmol, 1 eq), **4.3** (198 mg, 0.681 mmol, 1 eq), **4.4** (168 mg, 0.681 mmol, 1 eq), $HgCl_2$ (740 mg, 2.72 mmol, 4 eq) and NEt_3 (276 mg, 2.72 mmol, 4 eq). Deprotection in CH_2Cl_2 (5 ml) and TFA (5 ml) followed by preparative RP-HPLC (column: Nucleodur 250 × 21 mm; gradient: 0−30 min: MeCN/0.1% aq. TFA 5/95−25/75) afforded **4.12** bis(hydrotrifluoroacetate) as white fluffy solid (27.9 mg, 22%, t_R = 6.0 min), **4.14** bis(hydrotrifluoroacetate) as white fluffy solid (26.8 mg, 18%, t_R = 11.3 min) and **4.27** bis(hydrotrifluoroacetate) as white fluffy solid (42.9 mg, 26%, t_R = 21.4 min).

4.12:

R_f = 0.10 (CH_2Cl_2/MeOH/NH_3 80/19/1). UV/VIS (20 mM HCl): λ_{max} 231, 191 nm. RP-HPLC (200 nm): 97.3% (gradient: 0−30 min: MeCN/0.1% aq. TFA 5/95−30/70, 31-40 min: 90/10, t_R = 3.7 min, k = 0.6). ^{1}H-NMR (300 MHz, DMSO-d_6): δ (ppm) 3.17-3.28 (m, 4H), 7.30 (bs, 6H), 7.66 (bs, 2H). ^{13}C-NMR (75 MHz, DMSO-d_6 + TFA): δ (ppm) 40.03 (2C), 115.28 (q, J = 287.9, TFA), 157.02 (2C), 158.57 (q, J = 38.2, TFA). MS (LC-MS, ESI): *m/z* 145.12 [M+H$^+$]. HRMS (ESI-MS): *m/z* [M+H$^+$] calcd. for $C_4H_{13}N_6^+$: 145.1196, found: 145.1194.

4.14:

R_f = 0.14 (CH_2Cl_2/MeOH/NH_3 80/19/1). UV/VIS (20 mM HCl): λ_{max} 230, 204, 191 nm. RP-HPLC (200 nm): 99.8% (gradient: 0−30 min: MeCN/0.1% aq. TFA 5/95−30/70, 31-40 min: 90/10, t_R = 9.3 min, k = 3.0). ^{1}H-NMR (300 MHz, DMSO-d_6 + TFA): δ (ppm) 1.04 (t, J = 7.4, 2H), 2.44 (q, J = 7.4, 1H), 3.24-3.48 (m, 4H), 7.32 (bs, 2H), 7.72 (t, J = 5.7, 1H), 8.85 (bs, 2H), 9.35 (bs, 1H), 11.03 (bs, TFA), 11.96 (s, 1H).

^{13}C-NMR (75 MHz, DMSO-d_6 + TFA): δ (ppm) 8.25, 29.69, 39.04 (superimposed by solvent), 40.20, 115.44 (q, *J* = 288.3, TFA), 153.60, 157.10, 158.72 (q, *J* = 37.6, TFA), 176.25. MS (LC-MS, ESI): *m/z* 201.15 [M+H$^+$]. HRMS (ESI-MS): *m/z* [M+H$^+$] calcd. for $C_7H_{17}N_6O^+$: 201.1458, found: 201.1460.

4.27:

R_f = 0.22 (CH_2Cl_2/MeOH/NH_3 80/19/1). UV/VIS (20 mM HCl): λ_{max} 230, 204, 190 nm. RP-HPLC (200 nm): 98.9% (gradient: 0−30 min: MeCN/0.1% aq. TFA 5/95−30/70, 31-40 min: 90/10, t_R = 15.0 min, *k* = 5.5). ^{1}H-NMR (400 MHz, DMSO-d_6 + TFA): δ (ppm) 1.04 (t, *J* = 7.4, 6H), 2.44 (q, *J* = 7.4, 4H), 3.39-3.55 (m, 4H), 8.81 (bs, 4H), 9.32 (bs, 2H), 11.03 (bs, TFA), 11.85 (bs, 2H). ^{13}C-NMR (75 MHz, DMSO-d_6 + TFA): δ (ppm) 8.26 (2C), 29.74 (2C), 40.30 (2C), 115.34 (q, *J* = 288.6, TFA), 157.99 (2C), 158.75 (q, *J* = 38.2, TFA), 176.14 (2C). MS (LC-MS, ESI): *m/z* 257.17 [M+H$^+$]. HRMS (ESI-MS): *m/z* [M+H$^+$] calcd. for $C_{10}H_{21}N_6O_2^+$: 257.1721, found: 257.1721.

N-[N-(2-Guanidinoethyl)carbamimidoyl]butyramide bis(hydrotrifluoroacetate) (4.15) and N,N'-[ethane-1,2-diylbis(azanediyl)]bis(iminomethylene)dibutyramide bis(hydrotrifluoroacetate) (4.28)

The title compounds were prepared in a one-pot reaction from ethane-1,2-diamine (50 mg, 0.827 mmol, 1 eq), **4.3** (240 mg, 0.827 mmol, 1 eq), **4.5** (215 mg, 0.827 mmol, 1 eq), $HgCl_2$ (898 mg, 3.31 mmol, 4 eq) and NEt_3 (335 mg, 3.31 mmol, 4 eq). Deprotection in CH_2Cl_2 (5 ml) and TFA (5 ml) followed by preparative RP-HPLC (column: Nucleodur 250 × 21 mm; gradient: 0−5 min: MeCN/0.1% aq. TFA 5/95, 5−37 min: MeCN/0.1% aq. TFA 5/95−40/60) affording **4.15** bis(hydrotrifluoroacetate) as white fluffy solid (43.3 mg, 24%, t_R = 16.1 min) and **4.28** bis(hydrotrifluoroacetate) as white fluffy solid (67.5 mg, 32%, t_R = 23.4 min). Note: Compound **4.12** (see above) was not isolated from this reaction mixture.

4.15:

R_f = 0.11 (CH_2Cl_2/MeOH/NH_3 80/19/1). UV/VIS (20 mM HCl): λ_{max} 200, 191 nm. RP-HPLC (200 nm): 98.2% (gradient: 0−30 min: MeCN/0.1% aq. TFA 5/95−43/57, 31-40 min: 90/10, t_R = 11.8 min, *k* = 4.1). ^{1}H-NMR (400 MHz, DMSO-d_6 + TFA): δ (ppm) 0.89 (t, *J* = 7.4, 3H), 1.58 (h, *J* = 7.3, 2H), 2.40 (t, *J* = 7.2, 2H), 3.27-3.48 (m, 4H), 7.31 (bs, 2H), 7.72 (t, *J* = 5.7, 1H), 8.88 (bs, 2H), 9.37 (bs, 1H), 11.97 (s, 1H), 13.78 (bs, TFA). ^{13}C-NMR (101 MHz, DMSO-d_6 + TFA): δ (ppm) 13.27, 17.49, 38.07, 39.25 (superimposed by solvent), 40.21, 115.52 (d, *J* = 293.6, TFA), 153.60, 157.14, 158.76 (q, *J* = 37.6, TFA), 175.44. MS (LC-MS, ESI): *m/z* 215.16 [M+H$^+$]. HRMS (ESI-MS): *m/z* [M+H$^+$] calcd. for $C_8H_{19}N_6O^+$: 215.1615, found: 215.1614.

4.28:

R_f = 0.24 (CH_2Cl_2/MeOH/NH_3 80/19/1). UV/VIS (20 mM HCl): λ_{max} 206, 200, 191 nm. RP-HPLC (200 nm): 99.7% (gradient: 0−30 min: MeCN/0.1% aq. TFA 5/95−43/57, 31-40 min: 90/10, t_R = 20.4 min, k = 7.8). ^{1}H-NMR (600 MHz, DMSO-d_6 + TFA): δ (ppm) 0.90 (t, J = 7.4, 6H), 1.58 (h, J = 7.3, 4H), 2.40 (t, J = 7.2, 4H), 3.45-3.52 (m, 4H), 8.84 (bs, 4H), 9.36 (s, 2H), 11.89 (s, 2H), 12.40 (bs, TFA). ^{13}C-NMR (101 MHz, DMSO-d_6 + TFA): δ (ppm) 13.25 (2C), 17.46 (2C), 38.04 (2C), 54.93 (2C), 115.31 (q, J = 289.0, TFA). 153.55 (2C), 158.68 (q, J = 38.0, TFA), 175.26 (2C). MS (LC-MS, ESI): *m/z* 285.20 [M+H$^+$]. HRMS (ESI-MS): *m/z* [M+H$^+$] calcd. for $C_{10}H_{21}N_6O_2^+$: 285.2034, found: 285.2038.

N-[N-(2-Guanidinoethyl)carbamimidoyl]-2-methylpropanamide bis(hydrotrifluoroacetate) (4.16) and N,N'-[ethane-1,2-diylbis(azanediyl)]bis(iminomethylene)bis(2-methylpropanamide) bis(hydrotrifluoroacetate) (4.29)

The title compounds were prepared in a one-pot reaction from ethane-1,2-diamine (41 mg, 0.681 mmol, 1 eq), **4.3** (198 mg, 0.681 mmol, 1 eq), **4.6** (168 mg, 0.681 mmol, 1 eq), $HgCl_2$ (740 mg, 2.72 mmol, 4 eq) and NEt_3 (276 mg, 2.72 mmol, 4 eq). Deprotection in CH_2Cl_2 (5 ml) and TFA (5 ml) followed by preparative RP-HPLC (column: Nucleodur 250 × 21 mm; gradient: 0−5 min: MeCN/0.1% aq. TFA 5/95, 5−35 min: MeCN/0.1% aq. TFA 5/95−40/60) afforded **4.16** bis(hydrotrifluoroacetate) as white fluffy solid (18.0 mg, 12%, t_R = 15.8 min) and **4.29** bis(hydrotrifluoroacetate) as white fluffy solid (90.4 mg, 52%, t_R = 24.6 min). Note: Compound **4.12** (see above) was not isolated from this reaction mixture.

4.16:

R_f = 0.15 (CH_2Cl_2/MeOH/NH_3 80/19/1). UV/VIS (20 mM HCl): λ_{max} 193 nm. RP-HPLC (200 nm): 97.3% (gradient: 0−30 min: MeCN/0.1% aq. TFA 5/95−43/57, 31-40 min: 90/10, t_R = 11.4 min, k = 3.9). ^{1}H-NMR (400 MHz, DMSO-d_6 + TFA): δ (ppm) 1.10 (d, J = 6.8, 2H), 2.60-2.70 (m, 1H), 3.25-3.49 (m, 4H), 7.32 (bs, 2H), 7.74 (t, J = 5.7, 1H), 8.91 (bs, 2H), 9.39 (s, 1H), 9.80 (bs, TFA), 11.92 (s, 1H). ^{13}C-NMR (101 MHz, DMSO-d_6 + TFA): δ (ppm) 18.47, 35.28, 39.15 (superimposed by solvent), 40.19, 115.64 (d, J = 288.5, TFA), 153.76, 157.06, 158.68 (q, J = 37.3, TFA), 179.21. MS (LC-MS, ESI): *m/z* 215.16 [M+H$^+$]. HRMS (ESI-MS): *m/z* [M+H$^+$] calcd. for $C_8H_{19}N_6O^+$: 215.1615, found: 215.1617.

4.29:

R_f = 0.20 (CH_2Cl_2/MeOH/NH_3 80/19/1). UV/VIS (20 mM HCl): λ_{max} 192 nm. RP-HPLC (200 nm): 99.3% (gradient: 0−30 min: MeCN/0.1% aq. TFA 5/95−43/57, 31-40 min: 90/10, t_R = 17.7 min, k = 6.6). ^{1}H-NMR (400 MHz, DMSO-d_6 + TFA): δ (ppm) 1.10 (d, J = 6.8, 12H), 2.59-2.70 (m, 2H), 3.42-3.56 (m, 4H), 8.89 (bs, 4H), 9.40 (s, 2H), 9.81 (bs, TFA), 11.86 (s, 2H). ^{13}C-NMR (101 MHz, DMSO-d_6 + TFA):

δ (ppm) 18.46 (4C), 35.28 (2C), 40.20 (2C), 115.38 (q, *J* = 289.6, TFA). 153.76 (2C), 158.69 (q, *J* = 37.6, TFA), 179.07 (2C). MS (LC-MS, ESI): *m/z* 285.20 [M+H$^+$]. HRMS (ESI-MS): *m/z* [M+H$^+$] calcd. for $C_{10}H_{21}N_6O_2^+$: 285.2034, found: 285.2038.

N-[N-(2-Guanidinoethyl)carbamimidoyl]cyclopropanecarboxamide bis(hydrotrifluoroacetate) (4.17) and N,N'-[ethane-1,2-diylbis(azanediyl)]]bis(iminomethylene)dicyclopropanecarboxamide bis-(hydrotrifluoroacetate) (4.30)

The title compounds were prepared in a one-pot synthesis from ethane-1,2-diamine (53 mg, 0.884 mmol, 1 eq), **4.3** (257 mg, 0.884 mmol, 1 eq), **4.7** (228 mg, 0.884 mmol, 1 eq), $HgCl_2$ (960 mg, 3.54 mmol, 4 eq) and NEt_3 (358 mg, 3.54 mmol, 4 eq). Deprotection in CH_2Cl_2 (5 ml) and TFA (5 ml) followed by preparative RP-HPLC (column: Nucleodur 250 × 21 mm; gradient: 0−5 min: MeCN/0.1% aq. TFA 5/95, 5−37 min: MeCN/0.1% aq. TFA 5/95−40/60) affording **4.17** bis(hydrotrifluoroacetate) as white fluffy solid (46.7 mg, 24%, t_R = 16.1 min) and **4.30** bis(hydrotrifluoroacetate) as white fluffy solid (62.5 mg, 28%, t_R = 16.1 min). Note: Compound **4.12** (see above) was not isolated from this reaction mixture.

4.17:

R_f = 0.12 (CH_2Cl_2/MeOH/NH_3 80/19/1). UV/VIS (20 mM HCl): λ_{max} 229, 204, 190 nm. RP-HPLC (200 nm): 98.3% (gradient: 0−30 min: MeCN/0.1% aq. TFA 5/95−43/57, 31-40 min: 90/10, t_R = 10.1 min, *k* = 3.3). ^{1}H-NMR (400 MHz, DMSO-d_6 + TFA): δ (ppm) 0.86-1.11 (m, 4H), 1.77-1.91 (m, 1H), 3.24-3.48 (m, 4H), 7.29 (bs, 2H), 7.69 (t, *J* = 5.6, 1H), 9.42 (s, 1H), 9.54 (bs, TFA), 12.42 (s, 1H). ^{13}C-NMR (101 MHz, DMSO-d_6): δ (ppm) 9.41 (2C), 14.53, 39.10 (superimposed by solvent), 40.07, 153.02, 156.75, 175.72. MS (LC-MS, ESI): *m/z* 213.15 [M+H$^+$]. HRMS (ESI-MS): *m/z* [M+H$^+$] calcd. for $C_8H_{17}N_6O^+$: 213.1458, found: 213.1459.

4.30:

R_f = 0.25 (CH_2Cl_2/MeOH/NH_3 80/19/1). UV/VIS (20 mM HCl): λ_{max} 229, 202, 191 nm. RP-HPLC (200 nm): 99.7% (gradient: 0−30 min: MeCN/0.1% aq. TFA 5/95−43/57, 31-40 min: 90/10, t_R = 17.1 min, *k* = 6.3). ^{1}H-NMR (600 MHz, DMSO-d_6 + TFA): δ (ppm) 0.89-0.96 (m, 4H), 0.99-1.05 (m, 4H), 1.78-1.90 (m, 2H), 3.40-3.54 (m, 4H), 8.84 (bs, 4H), 9.37 (s, 2H), 12.25 (s, 2H), 12.37 (bs, TFA). ^{13}C-NMR (151 MHz, DMSO-d_6 + TFA): δ (ppm) 9.67 (4c), 14.87 (2C), 40.06 (2C), 115.27 (q, *J* = 288.7, TFA), 153.28 (2C), 158.63 (q, *J* = 38.1, TFA), 175.86 (2C). MS (LC-MS, ESI): *m/z* 281.17 [M+H$^+$]. HRMS (ESI-MS): *m/z* [M+H$^+$] calcd. for $C_{12}H_{21}N_6O_2^+$: 281.1721, found: 281.1721.

N-[N-(2-Guanidinoethyl)carbamimidoyl]cyclopentanecarboxamide bis(hydrotrifluoroacetate) (4.18) and N,N'-[ethane-1,2-diylbis(azanediyl)]bis(iminomethylene)dicyclopentanecarboxamide bis-(hydrotrifluoroacetate) (4.31)

The title compounds were prepared in a one-pot synthesis from ethane-1,2-diamine (41 mg, 0.681 mmol, 1 eq), **4.3** (198 mg, 0.681 mmol, 1 eq), **4.8** (195 mg, 0.681 mmol, 1 eq), $HgCl_2$ (740 mg, 2.72 mmol, 4 eq) and NEt_3 (276 mg, 2.72 mmol, 4 eq). Deprotection in CH_2Cl_2 (5 ml) and TFA (5 ml) followed by preparative RP-HPLC (column: Nucleodur 250 × 21 mm; gradient: 0−5 min: MeCN/0.1% aq. TFA 5/95, 5−35 min: MeCN/0.1% aq. TFA 5/95−45/55) afforded **4.18** bis(hydrotrifluoroacetate) as white fluffy solid (31.7 mg, 20%, t_R = 21.2 min) and **4.31** bis(hydrotrifluoroacetate) as white fluffy solid (19.6 mg, 10%, t_R = 30.1 min). Note: Compound **4.12** (see above) was not isolated from this reaction mixture.

4.18:

R_f = 0.16 (CH_2Cl_2/MeOH/NH_3 80/19/1). UV/VIS (20 mM HCl): λ_{max} 219, 204, 191 nm. RP-HPLC (200 nm): 97.1% (gradient: 0−30 min: MeCN/0.1% aq. TFA 10/90−70/30, 31-40 min: 90/10, t_R = 16.5 min, k = 6.1). ^{1}H-NMR (600 MHz, DMSO-d_6 + TFA): δ (ppm) 1.52-1.64 (m, 4H), 1.66-1.75 (m, 2H), 1.81-1.90 (m, 2H), 2.85 (p, J = 7.8, 1H), 3.32 (q, J = 6.1, 2H), 3.42 (q, J = 6.1, 2H), 7.28 (bs, 4H), 7.67 (t, J = 5.9, 1H), 8.81 (bs, 2H), 9.31 (s, 1H), 11.78 (s, 1H), 12.89 (bs, TFA). ^{13}C-NMR (151 MHz, DMSO-d_6 + TFA): δ (ppm) 25.62 (2C), 29.47 (2C), 40.06, 40.23, 45.31, 115.29 (q, J = 288.9, TFA), 153.65, 157.05, 158.61 (q, J = 38.0, TFA), 178.38. MS (LC-MS, ESI): *m/z* 241.18 [M+H$^+$]. HRMS (ESI-MS): *m/z* [M+H$^+$] calcd. for $C_{10}H_{21}N_6O^+$: 241.1771, found: 241.1774.

4.31:

R_f = 0.30 (CH_2Cl_2/MeOH/NH_3 80/19/1). UV/VIS (20 mM HCl): λ_{max} 220, 200, 191 nm. RP-HPLC (200 nm): 98.9% (gradient: 0−30 min: MeCN/0.1% aq. TFA 10/90−70/30, 31-40 min: 90/10, t_R = 27.4 min, k = 10.8). ^{1}H-NMR (600 MHz, DMSO-d_6 + TFA): δ (ppm) 1.52-1.66 (m, 8H), 1.67-1.76 (m, 4H), 1.82-1.91 (m, 4H), 2.85 (p, J = 7.8, 2H), 3.45-3.53 (m, 4H), 8.81 (bs, 4H), 9.31 (s, 2H), 11.74 (s, 2H), 12.02 (bs, TFA). ^{13}C-NMR (151 MHz, DMSO-d_6 + TFA): δ (ppm) 25.61 (4C), 29.47 (4C), 40.06 (2C), 45.28 (2C), 115.22 (q, J = 288.6, TFA), 153.65 (2C), 158.56 (q, J = 38.2, TFA), 178.26 (2C). MS (LC-MS, ESI): *m/z* 337.23 [M+H$^+$]. HRMS (ESI-MS): *m/z* [M+H$^+$] calcd. for $C_{16}H_{29}N_6O_2^+$: 337.2347, found: 337.2343.

1,1'-(Propane-1,3-diyl)diguanidine bis(hydrotrifluoroacetate) (4.13), N-[N-(3-guanidinopropyl)carbamimidoyl]propionamide bis(hydrotrifluoroacetate) (4.19) and N,N'-[propane-1,3-diylbis(azanediyl)]bis(iminomethylene)dipropionamide bis(hydrotrifluoroacetate) (4.32)

The title compounds were prepared in a one-pot synthesis from propane-1,3-diamine (60 mg, 0.813 mmol, 1 eq), **4.3** (237 mg, 0.813 mmol, 1 eq), **4.4** (200 mg, 0.813 mmol, 1 eq), $HgCl_2$ (885 mg, 3.26 mmol, 4 eq) and NEt_3 (330 mg, 3.26 mmol, 4 eq). Deprotection in CH_2Cl_2 (5 ml) and TFA (5 ml) followed by preparative RP-HPLC (column: Nucleodur 250 × 21 mm; gradient: 0−30 min: MeCN/0.1% aq. TFA 10/90−25/75) afforded **4.13** bis(hydrotrifluoroacetate) as white fluffy solid (22.0 mg, 14%, t_R = 5.4 min), **4.19** bis(hydrotrifluoroacetate) as white fluffy solid (18.3 mg, 10%, t_R = 12.8 min) and **4.32** bis(hydrotrifluoroacetate) as white fluffy solid (36.5 mg, 18%, t_R = 26.1 min).

4.13:

R_f = 0.05 (CH_2Cl_2/MeOH/NH_3 80/19/1). UV/VIS (20 mM HCl): λ_{max} 200, 191 nm. RP-HPLC (200 nm): 96.8% (gradient: 0−30 min: MeCN/0.1% aq. TFA 5/95−30/70, 31-40 min: 90/10, t_R = 3.9 min, k = 0.7). ^{1}H-NMR (300 MHz, DMSO-d_6): δ (ppm) 1.69 (p, J = 7.1, 2H), 3.12 (dd, J = 6.7, 4H), 7.23 (bs, 4H), 7.82 (t, J = 5.3, 2H). ^{13}C-NMR (75 MHz, DMSO-d_6): δ (ppm) 27.74, 38.08 (2C), 156.84 (2C). MS (LC-MS, ESI): *m/z* 159.1 [M+H$^+$]. HRMS (ESI-MS): *m/z* [M+H$^+$] calcd. for $C_5H_{15}N_6^+$: 159.1353, found: 159.1347.

4.19:

R_f = 0.18 (CH_2Cl_2/MeOH/NH_3 80/19/1). UV/VIS (20 mM HCl): λ_{max} 207, 192 nm. RP-HPLC (200 nm): 99.0% (gradient: 0−30 min: MeCN/0.1% aq. TFA 5/95−30/70, 31-40 min: 90/10, t_R = 7.5 min, k = 2.2). ^{1}H-NMR (300 MHz, MeOH-d_4): δ (ppm) 1.14 (t, J = 7.4, 3H), 1.88-1.99 (m, 2H), 2.50 (q, J = 7.4, 2H), 3.21-3.44 (m, 4H). ^{13}C-NMR (101 MHz, DMSO-d_6): δ (ppm) 1.04 (t, J = 7.4, 3H), 1.74 (p, J = 6.9, 2H), 2.43 (q, J = 7.4, 2H), 3.14 (q, J = 6.5, 2H), 3.29 (q, J = 6.5, 2H), 7.35 (bs, 4H), 7.97 (t, J = 5.3, 1H), 8.94 (bs, 2H), 9.56 (s, 1H), 12.20 (s, 1H). MS (LC-MS, EI): *m/z* 214.15 [M$^{+\bullet}$]. HRMS (ESI-MS): *m/z* [M+H$^+$] calcd. for $C_{10}H_{21}N_6O^+$: 215.1615, found: 215.1617.

4.32:

R_f = 0.22 (CH_2Cl_2/MeOH/NH_3 80/19/1). UV/VIS (20 mM HCl): λ_{max} 209, 194 nm. RP-HPLC (200 nm): 99.3% (gradient: 0−30 min: MeCN/0.1% aq. TFA 5/95−30/70, 31-40 min: 90/10, t_R = 16.7 min, k = 6.2). ^{1}H-NMR (400 MHz, DMSO-d_6): δ (ppm) 1.05 (t, J = 7.4, 6H), 1.72-1.88 (m, 2H), 2.44 (q, J = 7.4, 4H), 3.23-3.41 (m, 4H), 8.85 (bs, 4H), 9.46 (s, 2H), 12.00 (s, 2H). ^{13}C-NMR (101 MHz, DMSO-d_6): δ (ppm) 8.18 (2C), 26.36, 29.50 (2C), 38.45 (2C), 153.12 (2C), 175.96 (2C). MS (LC-MS, ESI): *m/z* 271.1 [M+H$^+$]. HRMS (EI-MS): *m/z* [M+H$^+$] calcd. for $C_{16}H_{29}N_6O_2^+$: 271.1877, found: 271.1877.

N-[N-(3-Guanidinopropyl)carbamimidoyl]butyramide bis(hydrotrifluoroacetate) (4.20) and N,N'-[propane-1,3-diylbis(azanediyl)]bis(iminomethylene)dibutyramide bis(hydrotrifluoroacetate) (4.33)

The title compounds were prepared in a one-pot synthesis from propane-1,3-diamine (71 mg, 0.960 mmol, 1 eq), **4.3** (279 mg, 0.960 mmol, 1 eq), **4.5** (250 mg, 0.960 mmol, 1 eq), $HgCl_2$ (1.04 g, 3.84 mmol, 4 eq) and NEt_3 (388 mg, 3.84 mmol, 4 eq). Deprotection in CH_2Cl_2 (5 ml) and TFA (5 ml) followed by preparative RP-HPLC (column: Nucleodur 250 × 21 mm; gradient: 0−5 min: MeCN/0.1% aq. TFA 5/95, 5−35 min: MeCN/0.1% aq. TFA 5/95−40/60) afforded **4.20** bis(hydrotrifluoroacetate) as white fluffy solid (74.8 mg, 34%, t_R = 17.4 min) and **4.33** bis(hydrotrifluoroacetate) as white fluffy solid (55.3 mg, 22%, t_R = 24.5 min). Note: Compound **4.13** (see above) was not isolated from this reaction mixture.

4.20:

R_f = 0.20 (CH_2Cl_2/MeOH/NH_3 80/19/1). UV/VIS (20 mM HCl): λ_{max} 190 nm. RP-HPLC (200 nm): 98.8% (gradient: 0−30 min: MeCN/0.1% aq. TFA 5/95−50/50, 31-40 min: 90/10, t_R = 10.5 min, k = 5.2). ^{1}H-NMR (600 MHz, DMSO-d_6 + TFA): δ (ppm) 0.90 (t, J = 7.4, 3H), 1.55-1.61 (m, 2H), 1.74 (p, J = 7.1, 2H), 2.39 (t, J = 7.2, 2H), 3.14 (q, J = 6.6, 2H), 3.28 (q, J = 6.6, 2H), 7.19 (bs, 4H), 7.67 (t, J = 5.5, 1H), 8.76 (bs, 2H), 9.29 (s, 1H), 11.29 (bs, TFA), 11.75 (s, 1H). ^{13}C-NMR (151 MHz, DMSO-d_6 + TFA): δ (ppm) 13.29, 17.47, 27.26, 38.07, 38.27, 38.59, 115.24 (q, J = 288.6, TFA), 153.16, 156.88, 158.58 (q, J = 38.2, TFA), 175.22. MS (LC-MS, ESI): *m/z* 229.18 [M+H$^+$]. HRMS (ESI-MS): *m/z* [M+H$^+$] calcd. for $C_9H_{21}N_6O^+$: 229.1771, found: 229.1771.

4.33:

R_f = 0.30 (CH_2Cl_2/MeOH/NH_3 80/19/1). UV/VIS (20 mM HCl): λ_{max} 193 nm. RP-HPLC (200 nm): 100% (gradient: 0−30 min: MeCN/0.1% aq. TFA 5/95−50/50, 31-40 min: 90/10, t_R = 17.8 min, k = 9.5). ^{1}H-NMR (600 MHz, DMSO-d_6 + TFA): δ (ppm) 0.90 (t, J = 7.4, 6H), 1.58 (h, J = 7.3, 4H), 1.79 (p, J = 6.8, 2H), 2.39 (t, J = 7.2, 4H), 3.31 (q, J = 6.6, 4H), 8.70 (s, 4H), 9.25 (s, 2H), 11.65 (s, 2H), 12.17 (bs, TFA). ^{13}C-NMR (101 MHz, DMSO-d_6 + TFA): δ (ppm) 13.30 (2C), 17.47 (2C), 26.52, 38.09 (2C), 38.60 (2C), 115.17 (q, J = 288.3, TFA), 153.10 (2C), 175.14 (2C), 158.54 (q, J = 38.5, TFA). MS (LC-MS, ESI): *m/z* 299.22 [M+H$^+$]. HRMS (ESI-MS): *m/z* [M+H$^+$] calcd. for $C_{13}H_{27}N_6O_2^+$: 299.2190, found: 299.2184.

N-[N-(3-Guanidinopropyl)carbamimidoyl]-2-methylpropanamide bis(hydrotrifluoroacetate) (4.21) and N,N'-[propane-1,3-diylbis(azanediyl)]bis(iminomethylene)bis(2-methylpropanamide) bis(hydrotrifluoroacetate) (4.34)

The title compounds were prepared from propane-1,3-diamine (71 mg, 0.960 mmol, 1 eq), **4.3** (279 mg, 0.960 mmol, 1 eq), **4.6** (250 mg, 0.960 mmol, 1 eq), $HgCl_2$ (1.04 g, 3.84 mmol, 4 eq) and NEt_3

(388 mg, 3.84 mmol, 4 eq). Deprotection in CH_2Cl_2 (5 ml) and TFA (5 ml) followed by preparative RP-HPLC (column: Nucleodur 250 × 21 mm; gradient: 0−5 min: MeCN/0.1% aq. TFA 5/95, 5−35 min: MeCN/0.1% aq. TFA 5/95−40/60) afforded **4.21** bis(hydrotrifluoroacetate) as white fluffy solid (26.8 mg, 22%, t_R = 17.6 min) and **4.34** bis(hydrotrifluoroacetate) as white fluffy solid (110.2 mg, 44%, t_R = 25.7 min). Note: Compound **4.13** (see above) was not isolated from this reaction mixture.

4.21:

R_f = 0.15 (CH_2Cl_2/MeOH/NH_3 80/19/1). UV/VIS (20 mM HCl): λ_{max} 192 nm. RP-HPLC (200 nm): 95.2% (gradient: 0−30 min: MeCN/0.1% aq. TFA 5/95−50/50, 31-40 min: 90/10, t_R = 10.2 min, k = 5.0). ^{1}H-NMR (600 MHz, DMSO-d_6 + TFA): δ (ppm) 1.10 (d, J = 6.8, 6H), 1.74 (p, J = 7.1, 2H), 2.63 (p, J = 6.8, 1H), 3.14 (q, J = 6.6, 2H), 3.29 (q, J = 6.6, 2H), 7.11 (bs, 4H), 7.69 (t, J = 5.5, 1H), 8.79 (bs, 2H), 9.32 (s, 1H), 11.70 (s, 1H), 11.84 (bs, TFA). ^{13}C-NMR (151 MHz, DMSO-d_6 + TFA): δ (ppm) 18.50, 27.21, 35.33, 38.27, 38.63, 115.27 (q, J = 288.8, TFA), 153.39, 156.88, 158.59 (q, J = 38.1, TFA), 179.03. MS (LC-MS, ESI): *m/z* 229.18 [M+H$^+$]. HRMS (ESI-MS): *m/z* [M+H$^+$] calcd. for $C_9H_{21}N_6O^+$: 229.1771, found: 229.1774.

4.34:

R_f = 0.30 (CH_2Cl_2/MeOH/NH_3 80/19/1). UV/VIS (20 mM HCl): λ_{max} 193 nm. RP-HPLC (200 nm): 100% (gradient: 0−30 min: MeCN/0.1% aq. TFA 5/95−50/50, 31-40 min: 90/10, t_R = 14.3 min, k = 7.5). ^{1}H-NMR (600 MHz, DMSO-d_6 + TFA): δ (ppm) 1.10 (d, J = 6.9, 6H), 1.80 (p, J = 6.8, 2H), 2.63 (p, J = 6.7, 2H), 3.32 (q, J = 6.6, 4H), 8.75 (bs, 4H), 9.31 (s, 2H), 11.63 (s, 2H), 12.74 (bs, TFA). ^{13}C-NMR (151 MHz, DMSO-d_6 + TFA): δ (ppm) 18.50 (4C), 26.43, 35.34 (2C), 38.65 (2C), 115.21 (q, J = 288.6, TFA). 153.34 (2C), 158.57 (q, J = 38.3, TFA), 178.95 (2C). MS (LC-MS, ESI): *m/z* 299.22 [M+H$^+$]. HRMS (ESI-MS): *m/z* [M+H$^+$] calcd. for $C_{13}H_{27}N_6O_2^+$: 299.2190, found: 299.2194.

N-[N-(3-Guanidinopropyl)carbamimidoyl]cyclopropanecarboxamide bis(hydrotrifluoroacetate) (4.22) and N,N'-[propane-1,3-diylbis(azanediyl)]bis(iminomethylene)dicyclopropanecarboxamide bis(hydrotrifluoroacetate) (4.35)

The title compounds were prepared in a one-pot synthesis from propane-1,3-diamine (64 mg, 0.867 mmol, 1 eq), **4.3** (252 mg, 0.867 mmol, 1 eq), **4.7** (224 mg, 0.867 mmol, 1 eq), $HgCl_2$ (941 mg, 3.47 mmol, 4 eq) and NEt_3 (351 mg, 3.47 mmol, 4 eq). Deprotection in CH_2Cl_2 (5 ml) and TFA (5 ml) followed by preparative RP-HPLC (column: Nucleodur 250 × 21 mm; gradient: 0−5 min: MeCN/0.1% aq. TFA 5/95, 5−35 min: MeCN/0.1% aq. TFA 5/95−40/60) afforded **4.22** bis(hydrotrifluoroacetate) as white fluffy solid (15.4 mg, 8%, t_R = 12.6 min) and **4.35** bis(hydrotrifluoroacetate) as white fluffy solid (40.6 mg, 18%, t_R = 20.0 min). Note: Compound **4.13** (see above) was not isolated from this reaction mixture.

4.22:

R_f = 0.11 (CH_2Cl_2/MeOH/NH_3 80/19/1). UV/VIS (20 mM HCl): λ_{max} 205, 192 nm. RP-HPLC (200 nm): 97.0% (gradient: 0–30 min: MeCN/0.1% aq. TFA 5/95–40/60, 31-40 min: 90/10, t_R = 13.6 min, k = 4.9). ^{1}H-NMR (400 MHz, DMSO-d_6 + TFA): δ (ppm) 0.89-1.07 (m, 4H), 1.74 (p, J = 7.0, 2H), 1.79-1.90 (m, 1H), 3.14 (q, J = 6.6, 2H), 3.29 (q, J = 6.6, 2H), 7.15 (bs, 4H), 7.72 (t, J = 5.5, 2H), 8.83 (bs, 2H), 9.42 (s, 1H), 9.75 (bs, TFA), 12.33 (s, 1H). ^{13}C-NMR (101 MHz, DMSO-d_6 + TFA): δ (ppm) 8.30, 9.61, 14.79, 27.18, 38.20, 38.53, 115.21 (q, J = 287.9, TFA), 152.94, 156.85, 158.60 (q, J = 37.3, TFA), 175.83. MS (LC-MS, ESI): *m/z* 227.16 [M+H$^+$]. HRMS (ESI-MS): *m/z* [M+H$^+$] calcd. for $C_9H_{17}N_6O^+$: 227.1615, found: 227.1616.

4.35:

R_f = 0.25 (CH_2Cl_2/MeOH/NH_3 80/19/1). UV/VIS (20 mM HCl): λ_{max} 203, 193 nm. RP-HPLC (200 nm): 95.8% (gradient: 0–30 min: MeCN/0.1% aq. TFA 5/95–50/50, 31-40 min: 90/10, t_R = 13.0 min, k = 6.7). ^{1}H-NMR (600 MHz, DMSO-d_6 + TFA): δ (ppm) 0.90-1.04 (m, 8H), 1.73-1.92 (m, 3H), 3.31 (q, J = 6.5, 1H), 8.73 (s, 4H), 9.31 (s, 2H), 12.10 (s, 2H), 12.16 (bs, TFA). ^{13}C-NMR (151 MHz, DMSO-d_6 + TFA): δ (ppm) 9.63 (4C), 14.88 (2C), 26.44, 38.60 (2C), 115.19 (q, J = 288.5), 152.86 (2C), 158.55 (q, J = 38.4), 175.77 (2C). MS (LC-MS, ESI): *m/z* 295.19 [M+H$^+$]. HRMS (ESI-MS): *m/z* [M+H$^+$] calcd. for $C_{13}H_{21}N_6O_2^+$: 295.1877, found: 295.1880.

N-[N-(3-Guanidinopropyl)carbamimidoyl]cyclopentanecarboxamide bis(hydrotrifluoroacetate) (4.23) and N,N'-[propane-1,3-diylbis(azanediyl)]bis(iminomethylene)dicyclopentanecarboxamide bis(hydro-trifluoroacetate) (4.36)

The title compounds were prepared from propane-1,3-diamine (60 mg, 0.812 mmol, 1 eq), **4.3** (237-mg, 0.812 mmol, 1 eq), **4.8** (333 mg, 0.812 mmol, 1 eq), $HgCl_2$ (882 mg, 3.25 mmol, 4 eq) and NEt_3 (329 mg, 3.25 mmol, 4 eq). Deprotection in CH_2Cl_2 (5 ml) and TFA (5 ml) followed by preparative RP-HPLC (column: Nucleodur 250 × 21 mm; gradient: 0–30 min: MeCN/0.1% aq. TFA 20/80–50/50) afforded **4.23** bis(hydrotrifluoroacetate) as white fluffy solid (31.7 mg, 16%, t_R = 13.6 min) and **4.36** bis(hydrotrifluoroacetate) as white fluffy solid (60.9 mg, 26%, t_R = 28.8 min). Note: Compound **4.13** (see above) was not isolated from this reaction mixture.

4.23:

R_f = 0.25 (CH_2Cl_2/MeOH/NH_3 80/19/1). UV/VIS (20 mM HCl): λ_{max} 211, 204, 191 nm. RP-HPLC (200-nm): 97.1% (gradient: 0–30 min: MeCN/0.1% aq. TFA 5/95–50/50, 31-40 min: 90/10, t_R = 12.6 min, k = 6.5). ^{1}H-NMR (300 MHz, MeOH-d_4): δ (ppm) 1.41-1.86 (m, 10H), 2.78-3.01 (m, 2H), 3.17 (q, J = 6.5, 2H), 3.43 (q, J = 6.7, 2H). ^{13}C-NMR (75 MHz, DMSO-d_6 + TFA): δ (ppm) 24.56 (2C), 26.18,

28.91 (2C), 38.21, 38.51, 45.86, 115.24 (q, *J* = 288.7, TFA), 153.94, 156.87, 158.60 (q, *J* = 37.3, TFA), 178.21. MS (LC-MS, ESI): *m/z* 255.1 [M+H$^+$]. HRMS (ESI-MS): *m/z* [M+H$^+$] calcd. for $C_{11}H_{23}N_6O^+$: 255.1928, found: 255.1928.

4.36:

R_f = 0.35 (CH_2Cl_2/MeOH/NH_3 80/19/1). UV/VIS (20 mM HCl): λ_{max} 212, 205, 191 nm. RP-HPLC (200-nm): 98.8% (gradient: 0−30 min: MeCN/0.1% aq. TFA 20/80−50/50, 31-40 min: 90/10, t_R = 17.3-min, *k* = 5.1). ^{1}H-NMR (400 MHz, DMSO-d_6): δ (ppm) 1.46-1.96 (m, 18H), 2.75-2.97 (m, 2H), 3.32 (q, *J* = 6.0, 4H), 8.85 (bs, 4H), 9.46 (s, 2H), 11.92 (s, 2H). ^{13}C-NMR (101 MHz, DMSO-d_6): δ (ppm) 25.59 (4C), 26.31, 29.40 (4C), 38.53 (2C), 45.11 (2C), 153.24 (2C), 178.18 (2C). MS (LC-MS, ESI): *m/z* 351.2 [M+H$^+$]. HRMS (ESI-MS): *m/z* [M+H$^+$] calcd. for $C_{17}H_{31}N_6O_2^+$: 351.2503, found: 351.2501.

N-[N-(3-Guanidinopropyl)carbamimidoyl]-3-(phenylsulfanyl)propanamide bis(hydrotrifluoro-acetate) (4.24) and N,N'-[propane-1,3-diylbis(azanediyl)]bis(iminomethylene)bis[3-(phenylsulfanyl)propanamide] bis(hydrotrifluoroacetate) (4.37)

The title compounds were prepared from propane-1,3-diamine (46 mg, 0.620 mmol, 1 eq), **4.3** (180 mg, 0.620 mmol, 1 eq), **4.9** (220 mg, 0.620 mmol, 1 eq), $HgCl_2$ (673 mg, 2.48 mmol, 4 eq) and NEt_3 (251 mg, 2.48 mmol, 4 eq). Deprotection in CH_2Cl_2 (5 ml) and TFA (5 ml) followed by preparative RP-HPLC (column: Nucleodur 250 × 21 mm; gradient: 0−30 min: MeCN/0.1% aq. TFA 20/80−50/50) afforded **4.24** bis(hydrotrifluoroacetate) as white fluffy solid (39.3 mg, 24%, t_R = 14.0 min) and **4.37** bis(hydrotrifluoroacetate) as white fluffy solid (26.6 mg, 12%, t_R = 18.3 min). Note: Compound **4.13** (see above) was not isolated from this reaction mixture.

4.24:

R_f = 0.20 (CH_2Cl_2/MeOH/NH_3 80/19/1). UV/VIS (20 mM HCl): λ_{max} 276, 213, 191 nm. RP-HPLC (200 nm): 97.5% (gradient: 0−30 min: MeCN/0.1% aq. TFA 5/95−50/50, 31-40 min: 90/10, t_R = 16.3 min, *k* = 8.7). ^{1}H-NMR (300 MHz, DMSO-d_6): δ (ppm) 1.73 (p, *J* = 6.8, 2H), 2.77 (t, *J* = 6.8, 2H), 3.13 (q, *J* = 6.6, 2H), 3.21 (t, *J* = 6.9, 2H), 3.28 (q, *J* = 6.2, 2H), 6.94-7.43 (m, 9H), 7.73 (t, *J* = 5.4, 1H), 8.80 (bs, 2H), 9.32 (bs, 1H), 11.98 (bs, 1H). ^{13}C-NMR (101 MHz, DMSO-d_6 + TFA): δ (ppm) 25.48, 26.85, 28.88, 36.18, 38.15, 126.20, 128.66 (2C), 129.19 (2C), 131.41, 156.79, 162.31, 176.75. MS (LC-MS, ESI): *m/z* 323.17 [M+H$^+$]. HRMS (ESI-MS): *m/z* [M+H$^+$] calcd. for $C_{14}H_{23}N_6OS^+$: 323.1649, found: 323.1651.

4.37:

R_f = 0.35 (CH_2Cl_2/MeOH/NH_3 80/19/1). UV/VIS (20 mM HCl): λ_{max} 282, 215, 191 nm. RP-HPLC (200 nm): 98.7% (gradient: 0−30 min: MeCN/0.1% aq. TFA 5/95−50/50, 31-40 min: 90/10, t_R =

23.1 min, *k* = 12.7). ^{1}H-NMR (300 MHz, DMSO-d_6): δ (ppm) 1.77 (p, *J* = 6.3, 2H), 2.77 (t, *J* = 6.9, 4H), 3.21 (t, *J* = 6.9, 4H), 3.30 (q, *J* = 6.1, 4H), 7.14-7.42 (m, 10H), 8.83 (bs, 4H), 9.41 (s, 2H), 12.10 (s, 2H). ^{13}C-NMR (75 MHz, DMSO-d_6): δ (ppm) 26.35, 26.88 (2C), 36.14 (2C), 38.47 (2C), 126.15 (2C), 128.59 (4C), 129.18 (4C), 135.20 (2C), 152.86 (2C), 173.30 (2C). MS (LC-MS, ESI): *m/z* 487.19 [M+H$^+$]. HRMS (ESI-MS): *m/z* [M+H$^+$] calcd. for $C_{23}H_{32}N_6O_2S_2^+$: 487.1944, found: 487.1948.

N-[N-(3-Guanidinopropyl)carbamimidoyl]-3-phenylpropanamide bis(hydrotrifluoroacetate) (4.25) and N,N'-[propane-1,3-diylbis(azanediyl)]bis(iminomethylene)bis(3-phenylpropanamide) bis(hydrotrifluoroacetate) (4.38)

The title compounds were prepared from propane-1,3-diamine (60 mg, 0.812 mmol, 1 eq), **4.3** (237 mg, 0.812 mmol, 1 eq), **4.10** (323 mg, 0.812 mmol, 1 eq), $HgCl_2$ (882 mg, 3.25 mmol, 4 eq) and NEt_3 (329 mg, 3.25 mmol, 4 eq). Deprotection in CH_2Cl_2 (5 ml) and TFA (5 ml) followed by preparative RP-HPLC (column: Nucleodur 250 × 21 mm; gradient: 0−30 min: MeCN/0.1% aq. TFA 30/70−60/40) afforded **4.25** bis(hydrotrifluoroacetate) as white fluffy solid (33.4 mg, 16%, t_R = 14.7 min) and **4.38** bis(hydrotrifluoroacetate) as white fluffy solid (37.0 mg, 14%, t_R = 18.7 min). Note: Compound **4.13** (see above) was not isolated from this reaction mixture.

4.25:

R_f = 0.45 (CH_2Cl_2/MeOH/NH_3 80/19/1). UV/VIS (20 mM HCl): λ_{max} 278, 205, 191 nm. RP-HPLC (200 nm): 99.9% (gradient: 0−30 min: MeCN/0.1% aq. TFA 5/95−50/50, 31-40 min: 90/10, t_R = 15.0 min, *k* = 7.9). ^{1}H-NMR (400 MHz, DMSO-d_6): δ (ppm) 1.73 (p, *J* = 7.0, 2H), 2.75 (t, *J* = 7.5, 2H), 2.88 (t, *J* = 7.4, 2H), 3.13 (q, *J* = 6.6, 2H), 3.28 (q, *J* = 6.6, 2H), 6.93-7.60 (m, 9H), 7.83 (t, *J* = 5.5, 1H), 8.90 (bs, 2H), 9.48 (s, 1H), 12.19 (s, 1H). ^{13}C-NMR (101 MHz, DMSO-d_6): δ (ppm) 27.12, 29.54, 37.65, 38.15, 38.48, 126.21, 128.26 (2C), 128.41 (2C), 140.18, 153.09, 156.84, 174.49. MS (LC-MS, ESI): *m/z* 291.2 [M+H$^+$]. $C_{14}H_{22}N_6O$ (290.36).

4.38:

R_f = 0.60 (CH_2Cl_2/MeOH/NH_3 80/19/1). UV/VIS (20 mM HCl): λ_{max} 285, 218, 193 nm. RP-HPLC (200 nm): 95.6% (gradient: 0−30 min: MeCN/0.1% aq. TFA 5/95−50/50, 31-40 min: 90/10, t_R = 23.3 min, *k* = 12.8). ^{1}H-NMR (400 MHz, DMSO-d_6): δ (ppm) 1.78 (p, *J* = 6.5, 2H), 2.75 (t, *J* = 7.5, 2H), 2.88 (t, *J* = 7.4, 2H), 3.30 (q, *J* = 6.3, 2H), 7.11-7.38 (m, 10H), 8.85 (bs, 4H), 9.45 (s, 2H), 12.10 (s, 2H). ^{13}C-NMR (101 MHz, DMSO-d_6): δ (ppm) 26.34, 29.52 (2C), 37.64 (2C), 38.45 (2C), 126.20 (2C), 128.25 (4C), 128.40 (4C), 140.15 (2C), 153.01 (2C), 174.40 (2C). MS (LC-MS, ESI): *m/z* 423.1 [M+H$^+$]. HRMS (ESI-MS): *m/z* [M+H$^+$] calcd. for $C_{23}H_{31}N_6O_2^+$: 423.2503, found: 423.2506.

N-[N-(3-Guanidinopropyl)carbamimidoyl]-3,3-diphenylpropanamide bis(hydrotrifluoroacetate) (4.26) and N,N'-[propane-1,3-diylbis(azanediyl)]bis(iminomethylene)bis(3,3-diphenylpropanamide) bis(hydro-trifluoroacetate) (4.39)

The title compounds were prepared in a one-pot synthesis from propane-1,3-diamine (60 mg, 0.812 mmol, 1 eq), **4.3** (237 mg, 0.812 mmol, 1 eq), **4.11** (323 mg, 0.812 mmol, 1 eq), $HgCl_2$ (882 mg, 3.25 mmol, 4 eq) and NEt_3 (329 mg, 3.25 mmol, 4 eq). Deprotection in CH_2Cl_2 (5 ml) and TFA (5 ml) followed by preparative RP-HPLC (column: Nucleodur 250 × 21 mm; gradient: 0−30 min: MeCN/0.1% aq. TFA 25/75−60/40) afforded **4.26** bis(hydrotrifluoroacetate) as white fluffy solid (62.6 mg, 26%, t_R = 13.6 min) and **4.39** bis(hydrotrifluoroacetate) as white fluffy solid (26.0 mg, 8%, t_R = 28.8 min). Note: Compound **4.13** (see above) was not isolated from this reaction mixture.

4.26:

R_f = 0.35 (CH_2Cl_2/MeOH/NH_3 80/19/1). UV/VIS (20 mM HCl): λ_{max} 284, 221, 196 nm. RP-HPLC (200 nm): 98.3% (gradient: 0−30 min: MeCN/0.1% aq. TFA 5/95−60/40, 31-40 min: 90/10, t_R = 18.7 min, k = 10.1). ^{1}H-NMR (300 MHz, DMSO-d_6 + TFA): δ (ppm) 1.69-1.84 (m, 2H), 2.67-2.86 (m, 2H), 3.20-3.36 (m, 4H), 4.52 (t, J = 7.9, 1H), 7.10-7.37 (m, 10H), 7.75 (bs, 4H), 8.79 (bs, 2H), 9.33 (b, 1H), 12.11 (s, 1H), 12.37 (bs, TFA). ^{13}C-NMR (75 MHz, DMSO-d_6 + TFA): δ (ppm) 25.89, 36.28, 38.08, 41.70, 45.93, 115.41 (d, J = 289.2, TFA), 126.55 (2C), 127.49 (4C), 128.62 (4C), 143.46 (2C), 158.33, 158.53 (d, J = 37.5, TFA), 159.31, 173.24. MS (LC-MS, ESI): *m/z* 367.2 [M+H$^+$]. $C_{20}H_{26}N_6O$ (366.46).

4.39:

R_f = 0.55 (CH_2Cl_2/MeOH/NH_3 80/19/1). UV/VIS (20 mM HCl): λ_{max} 285, 226, 191 nm. RP-HPLC (200 nm): 99.8% (gradient: 0−30 min: MeCN/0.1% aq. TFA 5/95−60/50, 31-40 min: 90/10, t_R = 23.9 min, k = 13.1). ^{1}H-NMR (300 MHz, DMSO-d_6): δ (ppm) 1.63-1.90 (m, 2H), 3.15-3.39 (m, 8H), 4.36-4.50 (m, 2H), 7.10-7.37 (m, 20H), 8.00 (bs, 4H), 9.45 (bs, 2H), 12.46 (s, 2H). ^{13}C-NMR (75 MHz, DMSO-d_6): δ (ppm) 28.11, 31.19 (2C), 37.96 (2C), 38.22 (2C), 46.61 (2C), 126.18 (4C), 127.37 (8C), 128.27 (8C), 143.71 (4C), 159.69 (2C), 171.03 (2C). MS (LC-MS, ESI): *m/z* 575.4 [M+H$^+$]. HRMS (EI-MS): *m/z* [M+H$^+$] calcd. for $C_{35}H_{39}N_6O_2$: 575.3129, found: 575.3134.

4.5.1.5 Preparation of the dicarbamimidothioate **4.40**

Propane-1,3-diyl dicarbamimidothioate (dihydrobromide) (4.40)[39]

Thiourea (45 mg, 0.594 mmol, 2 eq) and 1,3-dibromopropane (60 mg, 0.297 mmol, 1 eq) in EtOH (2 ml) were heated under microwave irradiation at 125 °C for 15 min. While the reaction mixture was allowed to cool to room temperature **4.40** was precipitating as white crystals (37 mg, 65%). mp 186 °C (lit.[39] 204-205 °C). R_f = 0.55 (CH_2Cl_2/MeOH/NH_3 80/19/1). UV/VIS (20 mM HCl): λ_{max} 222,

192 nm. RP-HPLC (200 nm): 98.2% (gradient: 0−30 min: MeCN/0.1% aq. TFA 5/95−43/57, 31-40 min: 90/10, t_R = 4.8 min, k = 0.7). ^{1}H-NMR (300 MHz, DMSO-d_6): δ (ppm) 1.95 (p, J = 6.8, 2H), 3.24 (t, J = 7.3, 4H), 9.07 (s, 8H). ^{13}C-NMR (75 MHz, DMSO-d_6): δ (ppm) 28.43 (3C), 169.33 (2C). MS (LC-MS, ESI): *m/z* 193.0 [M+H$^+$]. HRMS (ESI-MS): *m/z* [M+H$^+$] calcd. for $C_5H_{13}N_4S_2^+$: 193.0576, found: 193.0580.

4.5.1.6 Preparation of VUF 8430 analog **4.43**

1-(3-Hydroxypropyl)-N-,N'-Bis(tert-butoxycarbonyl)guanidine (4.41)[29]

Neat 3-Aminopropan-1-ol (1.92 g, 25.6 mmol, 1.1 eq) was added to a solution of *N*,*N'*-Di-boc-*N''*-trifluoromethanesulfonylguanidine (**3.25**, 9.00 g, 23.0 mmol, 1 eq) and triethylamine (2.59 g, 25.6 mmol, 1.1 eq) in CH_2Cl_2 (100 ml) and the mixture was stirred at room temperature for 40 min. The mixture was diluted with CH_2Cl_2 (100 ml), washed with saturated $KHSO_4$(aq.), saturated $NaHCO_3$(aq.)) and water, dried over anhydrous Na_2SO_4 and concentrated *in vacuo*. A white solid was obtained (6.91 g, 95%). mp 105 °C (lit.[40] 112-113 °C).. R_f = 0.20 (CH_2Cl_2/MeOH 50:1). ^{1}H-NMR (300 MHz, DMSO-d_6): δ (ppm) 1.39 (s, 9H), 1.47 (s, 9H), 1.62 (p, J = 6.4, 2H), 3.35 (t, J = 6.6, 2H), 3.44 (q, J = 5.9, 2H), 4.64 (t, J = 5.2, 1H), 8.41 (t, J = 5.4, 1H), 11.48 (s, 1H). ^{13}C-NMR (75 MHz, DMSO-d_6): δ (ppm) 27.50 (3C), 27.87 (3C), 31.31, 37.91, 58.38, 77.98, 82.70, 151.88, 155.11. MS (LC-MS, ESI): *m/z* 318.0 [M+H$^+$]. $C_{14}H_{27}N_3O_5$ (317.38).

3-Guanidinopropyl carbamimidothioate bis(hydrotrifluoroacetate) (4.43)[41]

4.41 (203 mg, 0.630 mmol, 1 eq) in 47% $HBr_{(aq.)}$ (6 ml) was heated at 100 °C for 30 h. After evaporation of the solvent *in vacuo*, thiourea (48 mg, 0.630 mmol, 1 eq) in EtOH (2 ml) was added and the mixture was heated under microwave irradiation at 125 °C for 15 min. After evaporation of the solvent *in vacuo*, the crude product was purified by preparative RP-HPLC (column: Nucleodur 250 × 21 mm; gradient: 0−30 min: MeCN/0.1% aq. TFA 3/97) afforded **4.43** bis(hydrotrifluoroacetate) as white fluffy solid (25.2 mg, 10%, t_R = 6.0 min). R_f = 0.15 (CH_2Cl_2/MeOH/NH_3 80/19/1). UV/VIS (20 mM HCl): λ_{max} 218, 196 nm. RP-HPLC (200 nm): 98.2% (gradient: 0−30 min: MeCN/0.1% aq. TFA 5/95−43/57, 31-40 min: 90/10, t_R = 4.8 min, k = 0.7). ^{1}H-NMR (300 MHz, DMSO-d_6): δ (ppm) 1.80 (p, J = 7.1, 1H), 3.06-3.23 (m, 4H), 7.26 (bs, 4H), 7.87 (t, J = 5.4, 1H), 9.35 (bs, 2H), 9.08 (bs, 2H). ^{13}C-NMR (75 MHz, DMSO-d_6): δ (ppm) 27.04, 27.95, 39.25, 156.70, 169.51. MS (LC-MS, ESI): *m/z* 176.0 [M+H$^+$]. HRMS (ESI-MS): *m/z* [M+H$^+$] calcd. for $C_5H_{14}N_5S^+$: 176.0964, found: 176.0962.

4.5.2 Pharmacological Methods

4.5.2.1 General

See section 3.4.3.1

4.5.2.2 Competition binding experiments on membrane preparations of Sf9 insect cells

See section 3.4.3.2

4.6 References

1. Garbarg, M.; Arrang, J. M.; Rouleau, A.; Ligneau, X.; Tuong, M. D.; Schwartz, J. C.; Ganellin, C. R. S-[2-(4-imidazolyl)ethyl]isothiourea, a highly specific and potent histamine H_3 receptor agonist. *J. Pharmacol. Exp. Ther.* **1992**, 263, 304-310.
2. Alves-Rodrigues, A.; Lemstra, S.; Vollinga, R. C.; Menge, W. M.; Timmerman, H.; Leurs, R. Pharmacological analysis of immepip and imetit homologues. Further evidence for histamine H_3 receptor heterogeneity? *Behav. Brain Res.* **2001**, 124, 121-127.
3. Kathmann, M.; Schlicker, E.; Detzner, M.; Timmerman, H. Nordimaprit, homodimaprit, clobenpropit and imetit: affinities for H_3 binding sites and potencies in a functional H_3 receptor model. *Naunyn-Schmiedeberg's Arch. Pharmacol.* **1993**, 348, 498-503.
4. Arrang, J. M.; Garbarg, M.; Lancelot, J. C.; Lecomte, J. M.; Pollard, H.; Robba, M.; Schunack, W.; Schwartz, J. C. Highly potent and selective ligands for histamine H_3-receptors. *Nature* **1987**, 327, 117-123.
5. Lim, H. D.; van Rijn, R. M.; Ling, P.; Bakker, R. A.; Thurmond, R. L.; Leurs, R. Evaluation of histamine H_1-, H_2-, and H_3-receptor ligands at the human histamine H_4 receptor: identification of 4-methylhistamine as the first potent and selective H_4 receptor agonist. *J. Pharmacol. Exp. Ther.* **2005**, 314, 1310-1321.
6. Durant, G. J.; Ganellin, C. R.; Hills, D. W.; Miles, P. D.; Parsons, M. E.; Pepper, E. S.; White, G. R. The Histamine H_2 Receptor Agonist Impromidine: Synthesis and Structure-Activity Considerations. *J. Med. Chem.* **1985**, 28, 1414-1422.
7. Buschauer, A. Synthesis and in vitro pharmacology of arpromidine and related phenyl(pyridylalkyl)guanidines, a potential new class of positive inotropic drugs. *J. Med. Chem.* **1989**, 32, 1963-1970.
8. Buschauer, A.; Friese-Kimmel, A.; Baumann, G.; Schunack, W. Synthesis and histamine H_2 agonistic activity of arpromidine analogs: replacement of the pheniramine-like moiety by non-heterocyclic groups. *Eur. J. Med. Chem.* **1992**, 27, 321-330.
9. Dove, S.; Elz, S.; Seifert, R.; Buschauer, A. Structure-activity relationships of histamine H_2 receptor ligands. *Mini. Rev. Med. Chem.* **2004**, 4, 941-954.
10. Xie, S.-X.; Ghorai, P.; Ye, Q.-Z.; Buschauer, A.; Seifert, R. Probing Ligand-Specific Histamine H_1- and H_2-Receptor Conformations with N^G-Acylated Imidazolylpropylguanidines. *J. Pharmacol. Exp. Ther.* **2006**, 317, 139-146.
11. Xie, S.-X.; Petrache, G.; Schneider, E.; Ye, Q.-Z.; Bernhardt, G.; Seifert, R.; Buschauer, A. Synthesis and pharmacological characterization of novel fluorescent histamine H_2-receptor ligands derived from aminopotentidine. *Bioorg. Med. Chem. Lett.* **2006**, 16, 3886-3890.
12. Ghorai, P.; Kraus, A.; Keller, M.; Goette, C.; Igel, P.; Schneider, E.; Schnell, D.; Bernhardt, G.; Dove, S.; Zabel, M.; Elz, S.; Seifert, R.; Buschauer, A. Acylguanidines as Bioisosteres of Guanidines: N^G-Acylated Imidazolylpropylguanidines, a New Class of Histamine H_2 Receptor Agonists. *J. Med. Chem.* **2008**, 51, 7193-7204.
13. Parsons, M. E.; Blakemore, R. C.; Durant, G. J.; Ganellin, C. R.; Rasmussen, A. C. Proceedings: 3-(4(5)-imidazolyl) propylguanidine (SK&F 91486) - a partial agonist at histamine H_2-receptors. *Agents Actions* **1975**, 5, 464.
14. Ghorai, P.; Kraus, A.; Birnkammer, T.; Geyer, R.; Bernhardt, G.; Dove, S.; Seifert, R.; Elz, S.; Buschauer, A. Chiral N^G-acylated hetarylpropylguanidine-type histamine H_2 receptor agonists do not show significant stereoselectivity. *Bioorg. Med. Chem. Lett.* **2010**, 20, 3173-3176.
15. Igel, P.; Schneider, E.; Schnell, D.; Elz, S.; Seifert, R.; Buschauer, A. N^G-Acylated Imidazolylpropylguanidines as Potent Histamine H_4 Receptor Agonists: Selectivity by Variation of the N^G-Substituent. *J. Med. Chem.* **2009**, 52, 2623-2627.
16. Parsons, M. E.; Ganellin, C. R. Histamine and its receptors. *Br. J. Pharmacol.* **2006**, 147, S127-S135.

17. Schreeb, A.; Łażewska, D.; Dove, S.; Buschauer, A.; Kieć-Kononowicz, K.; Stark, H. Histamine H_4 Receptor Ligands. In *Histamine H_4 Receptor: A Novel Drug Target in Immunoregulation and Inflammation*, Stark, H., Ed. Versita: London, **2013**; pp 21-62.
18. Geyer, R.; Kaske, M.; Baumeister, P.; Buschauer, A. Synthesis and Functional Characterization of Imbutamine Analogs as Histamine H_3 and H_4 Receptor Ligands. *Arch. Pharm. (Weinheim).* **2014**, 347, 77-88.
19. Sterk, G. J.; van der Goot, H.; Timmerman, H. The influence of guanidino and isothiourea groups in histaminergic compounds on H_2-activity. *Agents Actions* **1986**, 18, 137-140.
20. Lim, H. D.; Smits, R. A.; Bakker, R. A.; vanDam, C. M. E.; deEsch, I. J. P.; Leurs, R. Discovery of *S*-(2-Guanidylethyl)-isothiourea (VUF 8430) as a Potent Nonimidazole Histamine H_4 Receptor Agonist. *J. Med. Chem.* **2006**, 49, 6650-6651.
21. Lim, H. D.; Adami, M.; Guaita, E.; Werfel, T.; Smits, R. A.; de Esch, I. J.; Bakker, R. A.; Gutzmer, R.; Coruzzi, G.; Leurs, R. Pharmacological characterization of the new histamine H_4 receptor agonist VUF 8430. *Br. J. Pharmacol.* **2009**, 157, 34-43.
22. Kraus, A.; Ghorai, P.; Birnkammer, T.; Schnell, D.; Elz, S.; Seifert, R.; Dove, S.; Bernhardt, G.; Buschauer, A. N^G-Acylated Aminothiazolylpropylguanidines as Potent and Selective Histamine H_2 Receptor Agonists. *ChemMedChem* **2009**, 4, 232-240.
23. Iwanowicz, E. J.; Poss, M. A.; Lin, J. Preparation of *N*,*N*'-bis-*tert*-Butoxycarbonylthiourea *Synth. Commun.* **1993**, 23, 1443-1445.
24. Poss, M. A.; Iwanowicz, E.; Reid, J. A.; Lin, J.; Gu, Z. A mild and efficient method for the preparation of guanidines. *Tetrahedron Lett.* **1992**, 33, 5933-5936.
25. Rasmussen, C. R.; Villani Jr, F. J.; Reynolds, B. E.; Plampin, J. N.; Hood, A. R.; Hecker, L. R.; Nortey, S. O.; Hanslin, A.; Costanzo, M. J.; Howse Jr, R. M.; Molinari, A. J. A Versatile Synthesis of Novel *N*,*N*,*N*-Trisubstituted Guanidines. *Synthesis* **1988**, 1988, 460-466.
26. Gausepohl, H.; Pieles, U.; Frank, R. W. In Schiff base analog formation during in situ activation by HBTU and TBTU, **1992**; ESCOM: **1992**; pp 523-524.
27. DeMong, D. E.; Williams, R. M. The asymmetric synthesis of (2*S*,3*R*)-capreomycidine. *Tetrahedron Lett.* **2001**, 42, 3529-3532.
28. Kim, K. S.; Qian, L. Improved method for the preparation of guanidines. *Tetrahedron Lett.* **1993**, 34, 7677-7680.
29. Feichtinger, K.; Zapf, C.; Sings, H. L.; Goodman, M. Diprotected Triflylguanidines: A New Class of Guanidinylation Reagents. *J. Org. Chem.* **1998**, 63, 3804-3805.
30. Igel, P.; Dove, S.; Buschauer, A. Histamine H_4 receptor agonists. *Bioorg. Med. Chem. Lett.* **2010**, 20, 7191-7199.
31. Geyer, R. Hetarylalkyl(aryl)cyanoguanidines as histamine H_4 receptor ligands: Synthesis, chiral separation, pharmacological characterization, structureactivity and -selectivity relationships. University of Regensburg, Regensburg, Doctoral thesis, **2011**.
32. Hashimoto, T.; Harusawa, S.; Araki, L.; Zuiderveld, O. P.; Smit, M. J.; Imazu, T.; Takashima, S.; Yamamoto, Y.; Sakamoto, Y.; Kurihara, T.; Leurs, R.; Bakker, R. A.; Yamatodani, A. A Selective Human H_4-Receptor Agonist: (-)-2-Cyano-1-methyl-3-(2*R*,5*R*)-5-[1*H*-imidazol-4(5)-yl]tetrahydrofuran-2-ylmethylguanidine. *J. Med. Chem.* **2003**, 46, 3162-3165.
33. Kobayashi, T.; Watanabe, M.; Yoshida, A.; Yamada, S.; Ito, M.; Abe, H.; Ito, Y.; Arisawa, M.; Shuto, S. Synthesis and structural and pharmacological properties of cyclopropane-based conformationally restricted analogs of 4-methylhistamine as histamine H_3/H_4 receptor ligands. *Bioorg. Med. Chem.* **2010**, 18, 1076-1082.
34. Bodensteiner, J.; Baumeister, P.; Geyer, R.; Buschauer, A.; Reiser, O. Synthesis and pharmacological characterization of new tetrahydrofuran based compounds as conformationally constrained histamine receptor ligands. *Org. Biomol. Chem.* **2013**, 11, 4040-4055.
35. Chen, X.; Wang, J.; Sun, S.; Fan, J.; Wu, S.; Liu, J.; Ma, S.; Zhang, L.; Peng, X. Efficient enhancement of DNA cleavage activity by introducing guanidinium groups into diiron(III) complex. *Bioorg. Med. Chem. Lett.* **2008**, 18, 109-113.

36. Weiss, S.; Keller, M.; Bernhardt, G.; Buschauer, A.; Konig, B. Modular synthesis of non-peptidic bivalent NPY Y_1 receptor antagonists. *Bioorg. Med. Chem.* **2008**, 16, 9858-9866.
37. Bergeron, R. J.; McManis, J. S. Total synthesis of (+-)-15-deoxyspergualin. *J. Org. Chem.* **1987**, 52, 1700-1703.
38. Pluym, N.; Brennauer, A.; Keller, M.; Ziemek, R.; Pop, N.; Bernhardt, G.; Buschauer, A. Application of the Guanidine–Acylguanidine Bioisosteric Approach to Argininamide-Type NPY Y_2 Receptor Antagonists. *ChemMedChem* **2011**, 6, 1727-1738.
39. Grogan, C. H.; Rice, L. M.; Sullivan, M. X. Diisothiuronium dihydrohalide salts. *J. Org. Chem.* **1953**, 18, 728-735.
40. Rerat, V.; Dive, G.; Cordi, A. A.; Tucker, G. C.; Bareille, R.; Amédée, J.; Bordenave, L.; Marchand-Brynaert, J. $\alpha_v\beta_3$ Integrin-Targeting Arg-Gly-Asp (RGD) Peptidomimetics Containing Oligoethylene Glycol (OEG) Spacers. *J. Med. Chem.* **2009**, 52, 7029-7043.
41. Sterk, G. J.; van Der Goot, H.; Timmerman, H. Studies on Histaminergic Compounds, IV Non-isosterism between the Imidazole, Guanidino and Isothiourea Moieties at the H_2-Receptor. *Arch. Pharm. (Weinheim).* **1986**, 319, 1057-1064.

Chapter 5

[^{3}H]UR-DE257: A Selective and Highly Potent Tritium-Labeled Squaramide-type Histamine H_2 Receptor Antagonist

5.1 Introduction

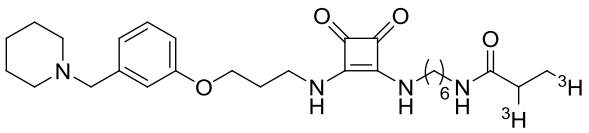

[^{3}H]UR-DE257

Figure 5.1 Structure of [^{3}H]UR-DE257.

The H_2 receptor (H_2R) is known as the target of drugs such as cimetidine, ranitidine, famotidine or roxatidine (Figure 1.6), which have been used, e.g., for the treatment of gastric or duodenal ulcers.[1,2] Apart from marketed drugs, numerous structurally related compounds,[3,4] e.g. iodoaminopotentidine,[5] BMY 25368,[6] and tiotidine,[7] are known as H_2R antagonists. Histamine as well as several of the antagonists were radiolabeled as pharmacological tools (for review see[8]).[9-11] Nevertheless, [^{3}H]histamine, [^{3}H]ranitidine,[12] [^{3}H]cimetidine[13] and [^{3}H]tiotidine[14] are far from being ideal. The H_2R affinities of the endogenous (non-selective) agonist and the antagonists cimetidine and ranitidine are low. [^{3}H]Tiotidine,[14,15] although used as a standard radioligand for a long period of time, is known for high unspecific binding. [^{125}I]Iodoamino-potentidine[10] has the highest affinity of all reported H_2R ligands and was used, for instance, for autoradiography of the H_2R in heart and brain of the guinea pig. Compared to tritium-labeled compounds, iodinated radioligands have the advantage of higher specific activity.[16] However, [^{125}I]iodoaminopotentidine is not commercially available and can only be used within 4-6 weeks after preparation. Selective H_2R radioligands are indispensable for histamine receptor research including studies on receptor subtypes other than the H_2R. In previous work, aiming at the development of high-affinity labeled H_2R antagonists, the piperidinomethylphenoxyalkyl portion of aminopotentidine and related substances was retained, the polar group ('urea eqalent'), was optimized by exploring cyanoguanidine, nitroethenediamine, amide or squaric amide moieties, and a terminal amino group, connected via a linker of different length, was introduced.[17] In this series highest affinity and selectivity was found for UR-DE257, determined in radioligand binding assays, using membrane preparations of Sf9 insect cells, expressing the respective hH_xR subtype (hH_1R: K_i: >10000 nM, hH_2R: K_i: 28 nM (K_b: 38 nM, neutral antagonism in the GTPase assay), hH_3R: K_i: 3800 nM, hH_4R: K_i: >10000 nM). The propionyl group allowed coupling with succinimidyl [2,3-^{3}H]propionate, which is commercially available, under standard laboratory conditions.[18-21] Herein, the radiosynthesis of [^{3}H]UR-DE257 and its pharmacological characterization is shown. In addition, the applicability to autoradiographic binding studies cryosections of a rat or guinea-pig brain and guinea-pig heart were incubated with [^{3}H]UR-DE257.

5.2 Results and Discussion

5.2.1 Radiosynthesis

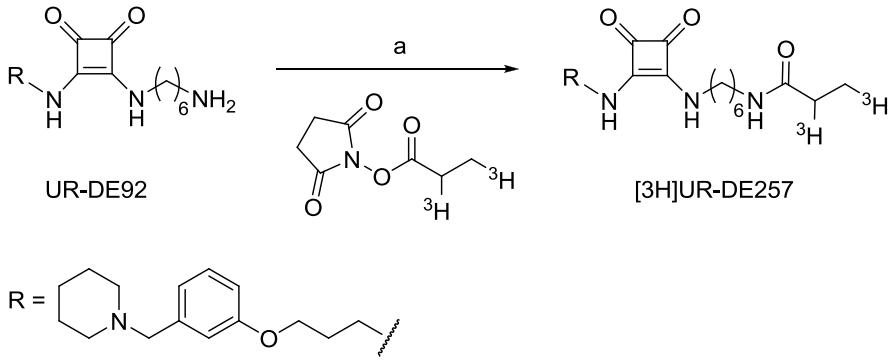

Scheme 5.1 Synthesis of [^{3}H]UR-DE257. Reagents and conditions: UR-DE92, succinimidyl [2,3-^{3}H]-propionate, CH_3CN/DMSO (1:1), NEt_3, rt, 18 h, 44.6%.

The [2,3-^{3}H]propionyl-substituted amide ([^{3}H]UR-DE257, *N*-{6-[3,4-dioxo-2-({3-[3-(piperidin-1-ylmethyl)phenoxy]propylamino})-cyclo-but-1-enylamino]hexyl}-(2,3-$^3H_2$)-propionamide), the 'hot' form of UR-DE257, was prepared by acylation of an excess of amine precursor UR-DE92 in the presence of triethylamine with commercially available tritiated succinimidyl propionate (Scheme 5.1, cf.[18-21]). After purification by HPLC, [^{3}H]UR-DE257 was obtained in a radiochemical purity of >99% (Figure 5.2) with a specific activity (a_s) of 63.0 Ci/mmol. The identity of the radioligand was confirmed by HPLC analysis of labeled and unlabeled UR-DE257. Moreover, chemical stability in EtOH at -20 °C was proven over a period of at least 24 months (cf. Figure 5.3).

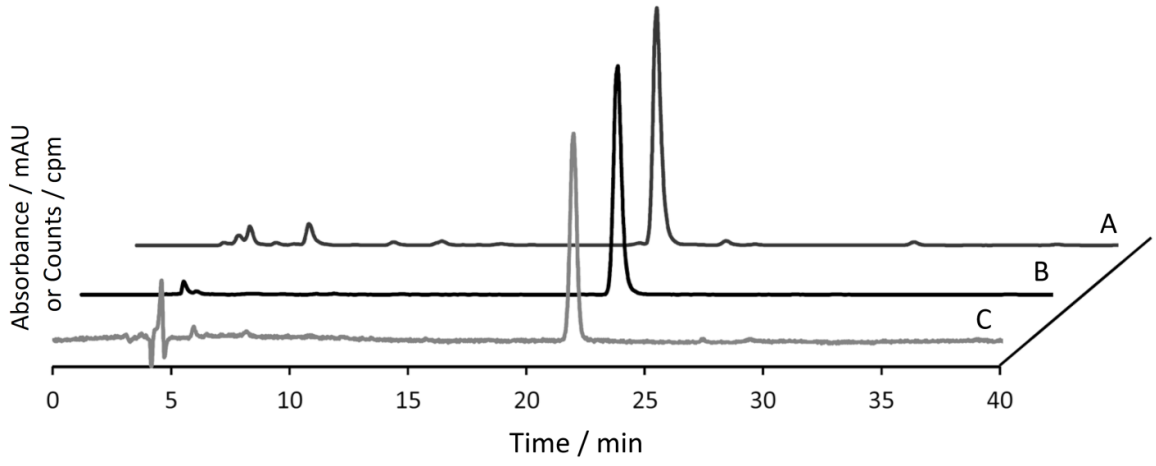

Figure 5.2 Identity and purity control of [^{3}H]UR-DE257. A: Reaction control after 20 h. B: Purity control after purification (radiochromatograms). C: UV (λ = 280 nm) chromatogram of UR-DE257, c: 100 µM.

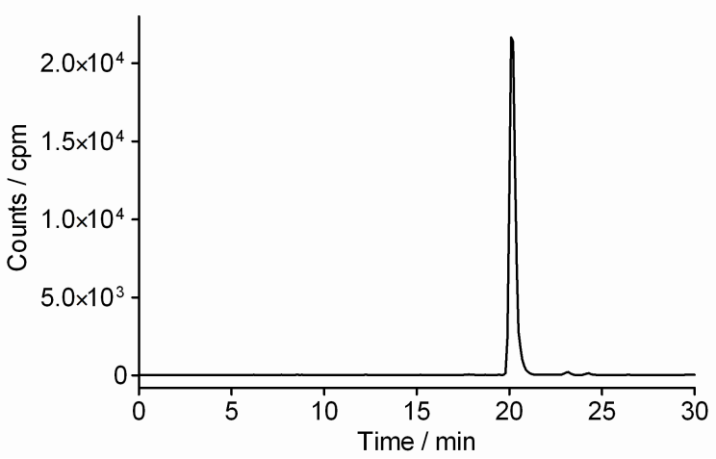

Figure 5.3 Example of a radiochromatogram of [^{3}H]UR-DE257 after storage in ethanol at -20 °C for a period of 24 months.

5.2.2 Determination of binding constants of [^{3}H]UR-DE257

[^{3}H]UR-DE257 was characterized by saturation and kinetic binding experiments on membrane preparations of Sf9 insect cells expressing the fusion proteins hH_2R-$G_{s\alpha S}$, gpH_2R-$G_{s\alpha S}$ or rH_2R-$G_{s\alpha S}$ or on HEK293T CRE-Luc hH_2R cells stably expressing the hH_2R. [^{3}H]UR-DE257 was bound in a saturable manner (cf. Figure 5.4 for the hH_2R; Figure 5.5 for the gpH_2R, Figure 5.6 for the rH_2R at Sf9 insect cell membranes and Figure 5.7 for the hH_2R experiments on HEK cells). Up to a radioligand concentration of 200 nM, nonspecific binding, determined in the presence of famotidine (10 µM), was low, amounting to 5–20% of total binding. Specific binding versus [^{3}H]UR-DE257 concentration was best fitted by nonlinear regression to a one-site binding model, nonspecific binding to a standard linear curve. The determined K_d values (27-55 nM, Table 5.1) were comparable with the K_b values from functional GTPase assays (K_b = 38 nM).[17] Moreover, the K_i values of [^{3}H]UR-DE257 determined in radioligand binding assays on different H_2R species orthologs using membrane preparations and whole cells, respectively, were in the same range (K_i = 16-44 nM). The maximum number of binding sites (B_{max}) ranged between 0.8 and 4.1 pmol/mg membrane protein in the Sf9 cell membranes and 2.4 x 10^6 sites on HEK cells. In all cases, within the investigated concentration range, the Scatchard plots were linear, in agreement with the binding of [^{3}H]UR-DE257 to a single binding site, following the law of mass action (Figure 5.4-5.7 C).

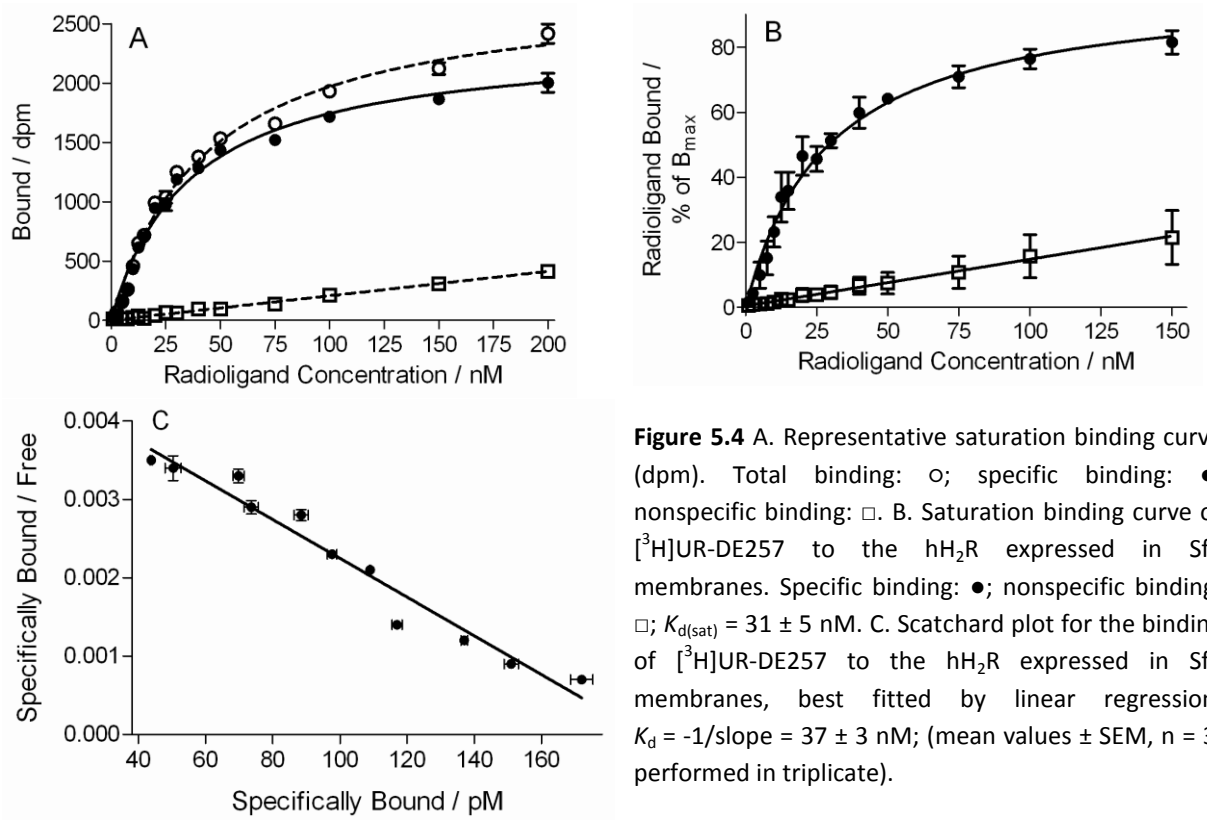

Figure 5.4 A. Representative saturation binding curve (dpm). Total binding: ○; specific binding: ●; nonspecific binding: □. B. Saturation binding curve of [^{3}H]UR-DE257 to the hH_2R expressed in Sf9 membranes. Specific binding: ●; nonspecific binding: □; $K_{d(sat)}$ = 31 ± 5 nM. C. Scatchard plot for the binding of [^{3}H]UR-DE257 to the hH_2R expressed in Sf9 membranes, best fitted by linear regression, K_d = -1/slope = 37 ± 3 nM; (mean values ± SEM, n = 3, performed in triplicate).

Table 5.1 Saturation binding parameters of [^{3}H]UR-DE257 on membranes of Sf9 cells expressing human, guinea pig and rat H_2R and at hH_2R in HEK293T CRE-Luc hH_2R cells.[a]

	K_d / nM	$K_{d\ (scatchard)}$ / nM	B_{max} / pmol/mG-Protein	Specific binding sites / well
hH_2R[b]	31 ± 5	37 ± 3	0.78 ± 0.08	4.8 x 10^{10}
hH_2R[c]	55 ± 8	52 ± 9	-	2.4 x 10^{6}[d]
gpH_2R[b]	37 ± 13	39 ± 24	0.77 ± 0.03	3.0 x 10^{10}
rH_2R[b]	29 ± 2	40 ± 12	4.07 ± 0.11	13.6 x 10^{10}

[a] Data are the mean of two independent experiments, each performed in triplicate. [b] Binding data determined on membranes of Sf9 insect cells expressing the respective xH_2R-$G_{s\alpha S}$ fusion protein (x = h, gp or r); radioligand: [^{3}H]UR-DE257 (30 nM). [c] hH_2R binding: HEK293T CRE-Luc hH_2R cells; radioligand: [^{3}H]UR-DE257 (30 nM). [d] Estimated B_{max} (sites / cell).

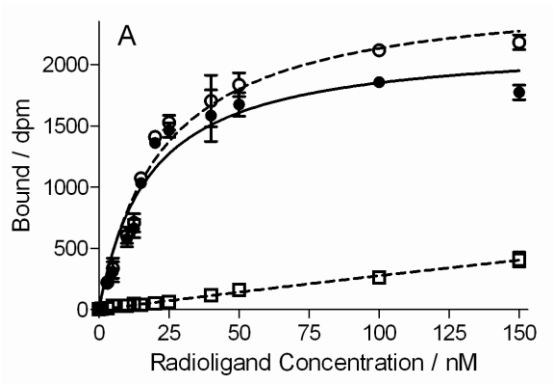

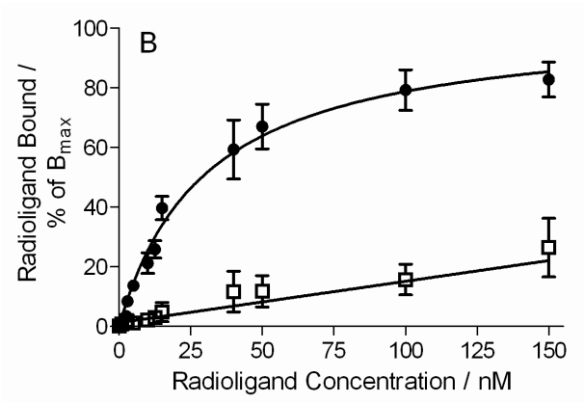

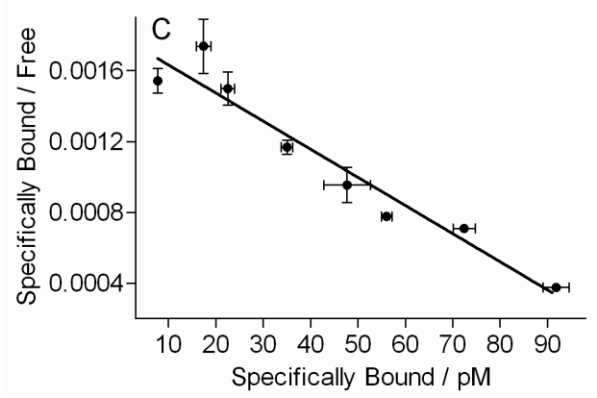

Figure 5.5 A. Representative saturation binding curve (dpm). Total binding: ○; specific binding: ●; nonspecific binding: □. B. Saturation binding curve of [^{3}H]UR-DE257 on membranes of Sf9 cells expressing the gpH_2R. Specific binding: ●; nonspecific binding: □; $K_{d(sat)}$ = 37 ± 13 nM. C. Scatchard plot for the binding of [^{3}H]UR-DE257 to the gpH_2R expressed in Sf9 membranes, best fitted by linear regression, K_d = -1/slope = 39 ± 24 nM. (mean values ± SEM, n = 2, performed in triplicate).

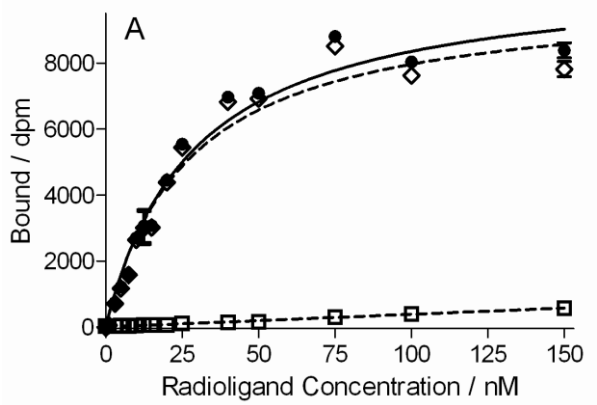

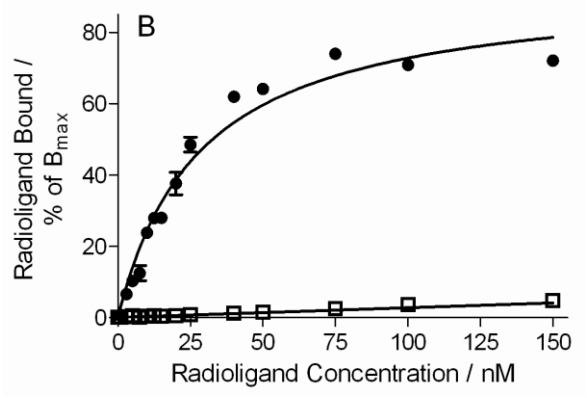

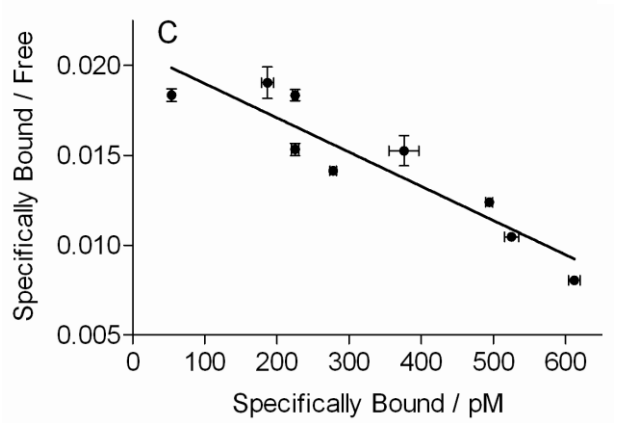

Figure 5.6 A. Representative saturation binding curve (dpm). Total binding: ○; specific binding: ●; nonspecific binding: □. B. Saturation binding curve of [^{3}H]UR-DE257 on membranes of Sf9 cells expressing the rH_2R. Specific binding: ●; nonspecific binding: □; $K_{d(sat)}$ = 29 ± 2 nM. C. Scatchard plot for the binding of [^{3}H]UR-DE257 to the rH_2R expressed in Sf9 membranes, best fitted by linear regression, K_d = –1/slope = 40 ± 12 nM; (mean values ± SEM, n = 2, performed in triplicate).

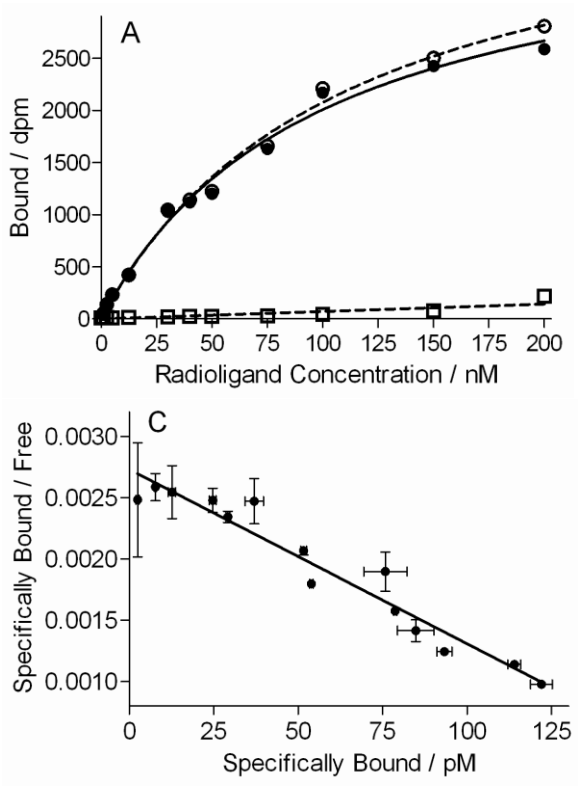

Figure 5.7 A. Representative saturation binding curve (dpm). Total binding: ○; specific binding: ●; nonspecific binding: □. B. Saturation binding curve of [^{3}H]UR-DE257 to the hH_2R expressed HEK293T CRE-Luc hH_2R cells. Specific binding: ●; nonspecific binding: □; $K_{d(sat)}$ = 55 ± 8 nM. C. Scatchard plot for the binding of [^{3}H]UR-DE257 to the hH_2R stably expressed in HEK293T CRE-Luc hH_2R cells, best fitted by linear regression, K_d = –1/slope = 52 ± 9 nM. (mean values ± SEM, n = 3, performed in triplicate).

The results of kinetic studies of [^{3}H]UR-DE257 (c = 30 nM) at the hH_2R on Sf9 cell membranes at 22 °C are presented in Figure 5.8. Similar data were obtained for gpH_2R and rH_2R (Sf9 cell membranes) and hH_2R expressed in HEK293 cells (cf. Figures 5.10-5.12). Linearization of the association curves revealed straight lines with k_{ob} values ranging from 0.050 to 0.073 min^{-1}. Dissociation in the presence of famotidine (Figure 5.8 C) was slow and gave comparable results for all investigated H_2R orthologs in Sf9 membranes and HEK293 cells. After 90 minutes the residual specific binding of the tritiated compound amounted to approximately 60-70%, suggesting (pseudo)irreversible binding (cf.[21]). Linearization of the dissociation kinetics revealed two straight lines with different slopes (Figure 5.8 B and Figures 5.10-5.12 B, inset). The equilibrium dissociation constant of [^{3}H]UR-DE257, calculated from kinetics (K_d = k_{off}/k_{on} = 13-20 nM; Figure 5.8 and Figures 5.10-5.12, Table 5.2), was consistent with the K_d values derived from saturation binding experiments (K_d = 27-55 nM), proving that radioligand [^{3}H]UR-DE257 follows the law of mass action,[22] provided that the k_{off} value of the fast dissociation was considered.

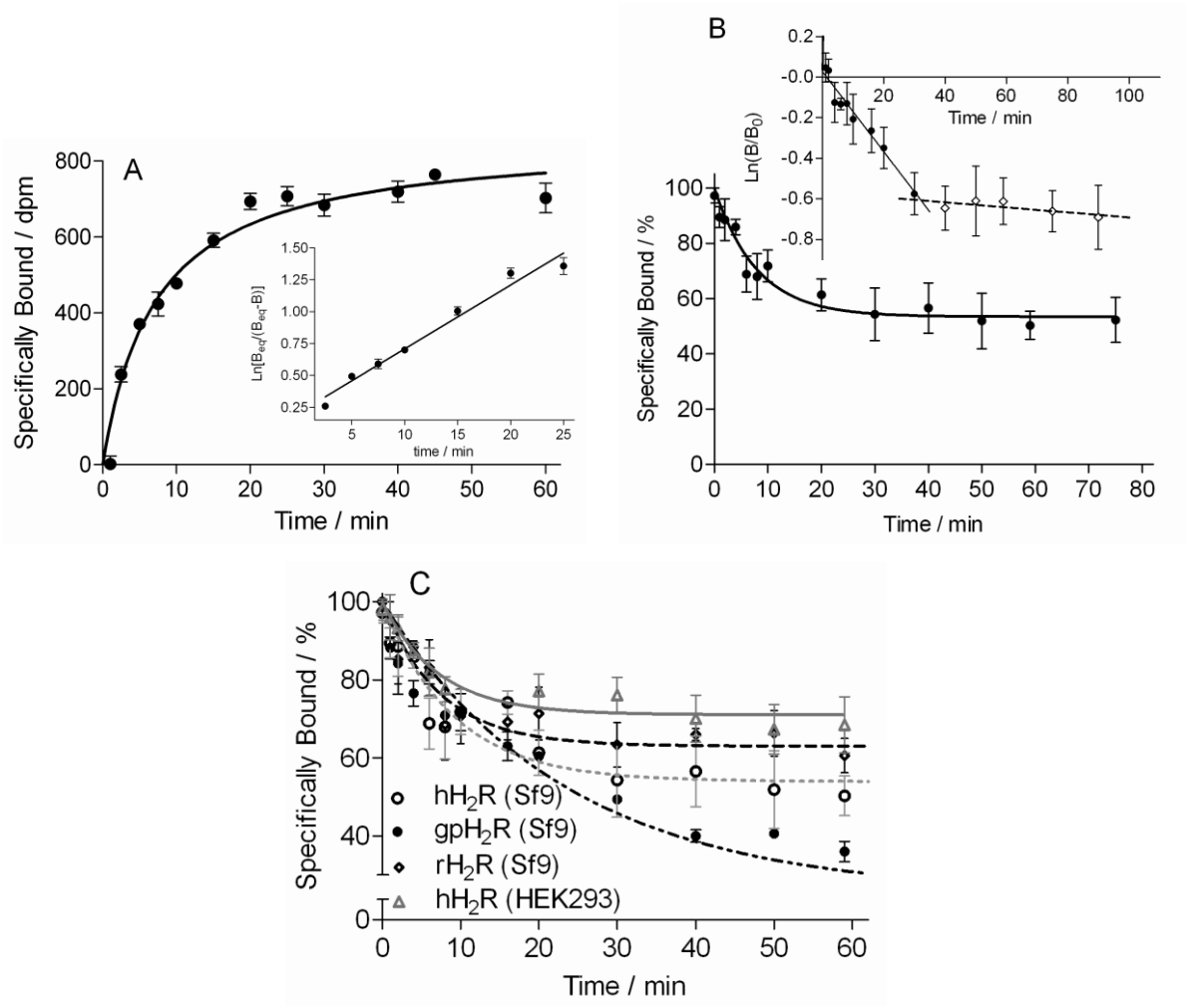

Figure 5.8 Association and dissociation kinetics of the radiolabeled H_2R antagonist [^{3}H]UR-DE257 on hH_2R-$G_{s\alpha S}$ (Sf9 cell membranes). A. Radioligand (c = 30 nM) association as a function of time. Inset: Linearization $\ln[B_{eq}/(B_{eq}-B)]$ versus time of the association kinetic for the determination of k_{ob} and k_{on}, slope = k_{ob} = 0.050 min^{-1}, k_{on} = (k_{ob} - k_{off})/[L] = 8.6 x 10^{-4} min^{-1} x nM^{-1}. B. Radioligand (c = 30 nM, pre-incubation for 60 min) dissociation as a function of time, monophasic exponential fit, $t_{1/2}$ = 5.5 min, dissociation determined in the presence of a 100-fold excess of famotidine. Inset: Linearization $\ln(B/B_0)$ versus time of the dissociation kinetics for the determination of k_{off} = slope^{-1} = 0.020 min^{-1}. (mean values ± SEM, n = 4) Inset: Representative dissociation curve (dpm) for linearization. C. Comparison of the radioligand (c = 30 nM, pre-incubation for 60 min) dissociation as a function of time, monophasic exponential fit, determined in Sf9 insect cell membranes expressing the respective xH_2R-$G_{s\alpha S}$ subtype or in HEK293T CRE-Luc hH_2R cells.

The pseudo-irreversibility of binding is reminiscent of the pharmacological behavior reported for several classes of H_2R antagonists, for instance, piperidinylmethylphenoxyalkyl substituted squaramides, thiadiazolamines or aminotriazoles.[6,23-25] Piperidinylmethylphenoxyalkyl-substituted squaramides such as BMY 25368 (Figure 1.6) were described as insurmountable H_2R antagonists, causing a concentration- dependent depression of the maximal response to the agonist and tight binding to the H_2R in the guinea pig right atrium (K_b = 13 nM) compared to standard ligands such as famotidine.[26]

Such peculiar behavior at the guinea pig right atrium was also confirmed for UR-DE91 (pA_2 = 7.36 ± 0.14) and UR-DE111 (pA_2 = 7.22 ± 0.08).[17]

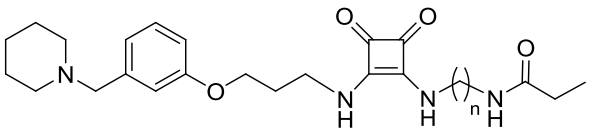

	n
UR-DE91	2
UR-DE111	3

Figure 5.9 Structures of UR-DE91 and UR-DE111.

Both compounds caused a concentration-dependent decrease in the maximum response to histamine (at antagonist concentration of 1 µM: E_{max} (histamine): 54% (UR-DE91) and 77% (UR-DE111), respectively).[17] Recently, a Y_2R selective radioligand with similar properties in kinetic and functional experiments was reported as an insurmountable pseudo-irreversible non-peptide neuropeptide Y antagonist.[21] Possible explanations are a slow rate of dissociation from the receptor[27], a slow rate of interconversion between inactive and active receptor conformations[28,29] or stabilization of a ligand (antagonist) specific inactive receptor conformation.[30]

Table 5.2 H_2R binding and functional characteristics of [^{3}H]UR-DE257.

Receptor	k_{off} / min^{-1}[a]	k_{on} / min^{-1} nM^{-1}[b]	k_{off}/k_{on} / nM[c]	K_d / nM[d]	$t_{1/2}$ / min[e]
hH_2R (Sf9)	0.024	0.00086	20	31	5.5
gpH_2R (Sf9)	0.015	0.00033	44	37	16
rH_2R (Sf9)	0.019	0.0015	13	29	5.1
hH_2R (HEK293)	0.025	0.0016	16	55	5.9

[a] Dissociation rate constant determined by linear regression. [b] Association rate constant determined by linear regression. [c] Kinetically determined dissociation constant. [d] Equilibrium dissociation constant determined by saturation binding experiments. [e] Dissociation half-life.

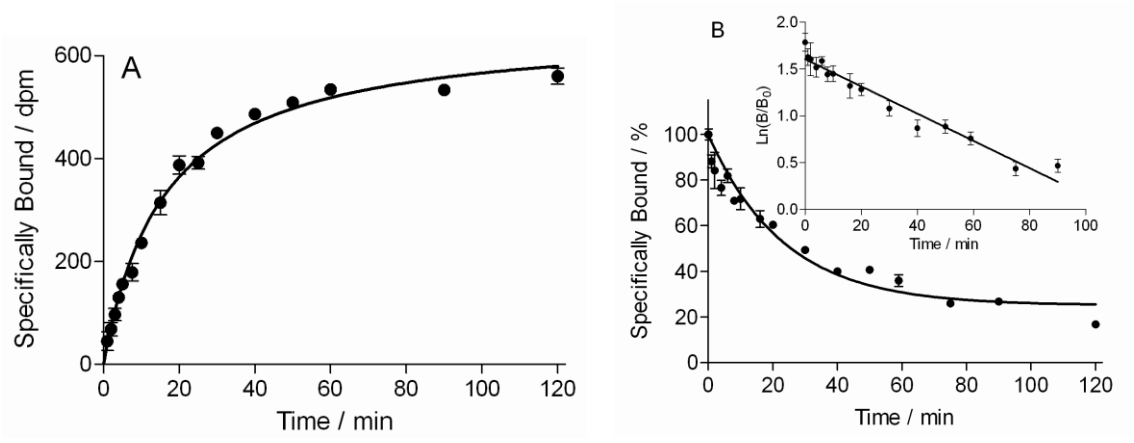

Figure 5.10 Association and dissociation kinetics of the specific gpH_2R binding of [^{3}H]UR-DE257 in Sf9 membranes. a) Radioligand (c = 30 nM) association as a function of time. Inset: Linearization $\ln[B_{eq}/(B_{eq}-B)]$ versus time of the association kinetic for the determination of k_{ob} and k_{on}, slope = k_{ob} = 0.025 min^{-1}, k_{on} = (k_{ob} - k_{off})/[L] = 3.3 x 10^{-4} min^{-1} x nM^{-1}. b) Radioligand (c = 30 nM, pre-incubation for 60 min) dissociation as a function of time, monophasic exponential fit, $t_{1/2}$ = 16 min, dissociation performed with 100-fold excess of Famotidine. c) Linearization $\ln(B/B_0)$ versus time of the dissociation kinetic for the determination of k_{off} = slope^{-1} = 0.015 min^{-1}. (mean values ± SEM, n = 4) Inset: Representative dissociation curve (dpm) for linearization.

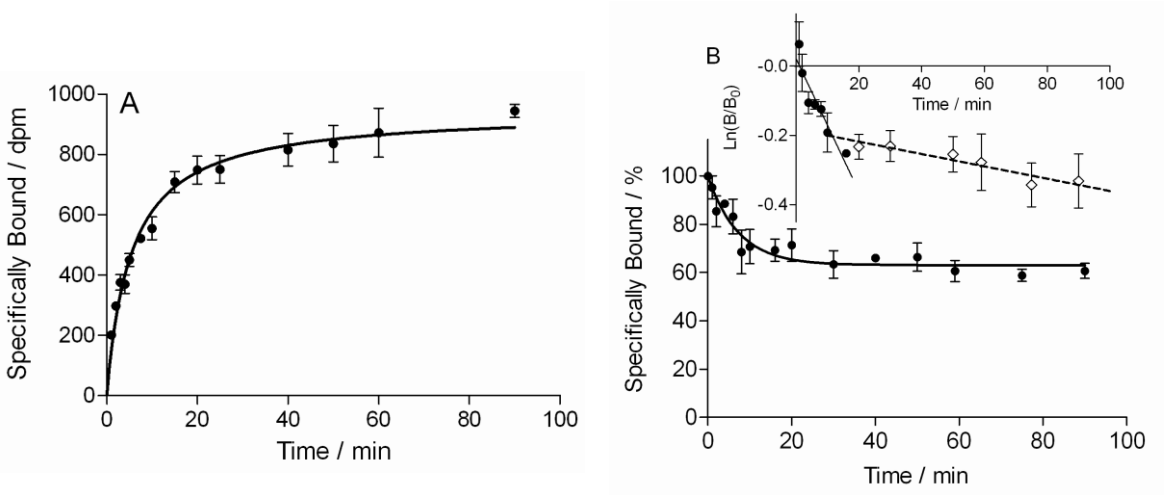

Figure 5.11 Association and dissociation kinetics of the specific rH_2R binding of [^{3}H]UR-DE257 in Sf9 membranes. a) Radioligand (c = 30 nM) association as a function of time. Inset: Linearization ln[B_{eq}/(B_{eq}-B)] versus time of the association kinetic for the determination of k_{ob} and k_{on}, slope = k_{ob} = 0.065 min^{-1}, k_{on} = (k_{ob} - k_{off})/[L] = 1,5 x 10^{-3} min^{-1} x nM^{-1}. b) Radioligand (c = 30 nM, pre-incubation for 60 min) dissociation as a function of time, monophasic exponential fit, $t_{1/2}$ = 5.1 min, dissociation performed with 100-fold excess of famotidine. c) Linearization ln(B/B_0) versus time of the dissociation kinetic for the determination of k_{off} = slope^{-1} = 0.019 min^{-1}. (mean values ± SEM, n = 2) Inset: Representative dissociation curve (dpm) for linearization.

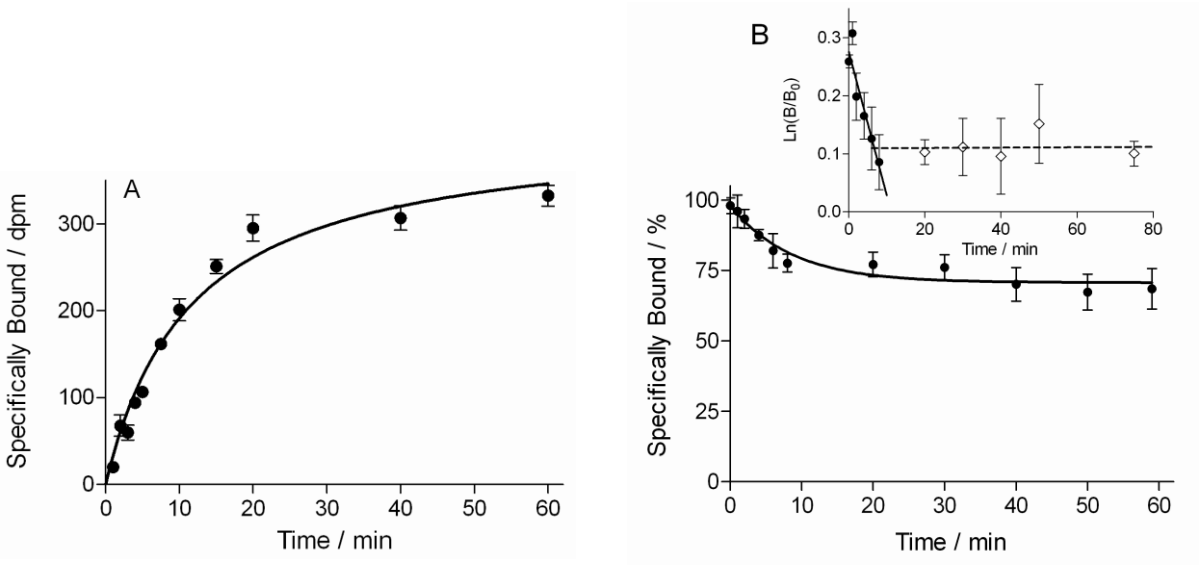

Figure 5.12 Association and dissociation kinetics of the specific H_2R binding of [^{3}H]UR-DE257 in HEK293T CRE-Luc hH_2R cells. a) Radioligand (c = 30 nM) association as a function of time. Inset: Linearization ln[B_{eq}/(B_{eq}-B)] versus time of the association kinetic for the determination of k_{ob} and k_{on}, slope = k_{ob} = 0.073 min^{-1}, k_{on} = (k_{ob} - k_{off})/[L] = 0.0016 min^{-1} x nM^{-1}. b) Radioligand (c = 30 nM, pre-incubation for 60 min) dissociation as a function of time, monophasic exponential fit, $t_{1/2}$ = 5.9 min, dissociation performed with 100-fold excess of Famotidine. c) Linearization ln(B/B_0) versus time of the dissociation kinetic for the determination of k_{off} = slope^{-1} = 0.025 min^{-1}. (mean values ± SEM, n = 4)

Regardless of the apparent incomplete dissociation (Figure 5.8 B and Figures 5.10-5.12 B) in competition binding studies, the radioligand [^{3}H]UR-DE257 was completely displaceable and proved to be a very useful tool to determine the binding data of H_2R agonists and antagonists as shown for

some reference compounds in Figures 5.13-5.16. The K_d value determined from binding kinetics was applied for the calculation of K_i values by means of the Cheng-Prusoff equation.[31] The hH_2R binding affinity of the agonists histamine (K_i = 534 nM), amthamine (K_i = 244 nM), UR-Bit24[32] (K_i = 7.1 nM) and UR-AK480[33] (K_i = 1.9 nM) and the antagonists famotidine (K_i = 136 nM), ranitidine (K_i = 1730 nM), BMY 25368 (K_i = 19 nM) and iodoaminopotentidine (K_i = 0.31 nm) performed on Sf9 insect cell membranes expressing the hH_2R-$G_{s\alpha S}$ fusion protein were consistent with reported data from functional and binding experiments, respectively.[26,34] The K_i value of UR-DE257 (28 nM), determined by competition binding experiments with the labeled analog [^{3}H]UR-DE257, corresponds very well to the K_d value of [^{3}H]UR-DE257 (31 nM).

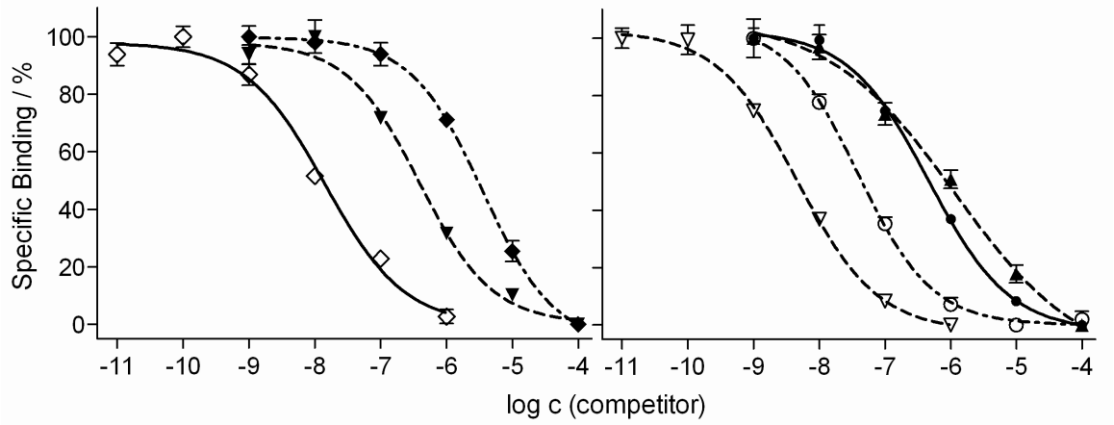

Figure 5.13 Displacement of [^{3}H]UR-DE257 (c = 30 nM, K_d = 31 nM) by the histamine H_2R ligands UR-AK480 (∇, K_i = 1.9 ± 0.5 nM), UR-DE257 (○, K_i = 28 ± 2 nM), famotidine (●, K_i = 136 ± 17 nM), histamine (▲, K_i = 534 ± 52 nM), UR-Bit24 (◊, K_i = 7.1 ± 1.2 nM), amthamine (▼, K_i = 244 ± 46 nM) and ranitidine (♦, K_i = 1730 ± 220 nM). The assay was performed on Sf9 insect cell membranes expressing the hH_2R-$G_{s\alpha S}$ fusion protein. The incubation period was 60 min. Data are mean values ± SEM (n = 2-3).

Table 5.3 H_2R binding to the human/guinea-pig and rat receptor subtype of H_2R agonists and antagonists.

Compound	K_i / nM			
	hH_2R[b]	**rH_2R[b]**	**gpH_2R[b]**	**hH_2R[c]**
Histamine	534 ± 52	486 ± 106	150 ± 29	99700 ± 21500
Amthamine	244 ± 46	-	-	19900 ± 4940
UR-AK480	1.9 ± 0.5	1.7 ± 0.5	0.15 ± 0.02	8.2 ± 3
UR-Bit24	7.1 ± 1.2	54 ± 3	9.5 ± 2	107 ± 32
Famotidine	136 ± 17	423 ± 33	107 ± 5	147 ± 43
Ranitidine	1730 ± 220	-	-	-
Iodoaminopotentine	0.31 ± 0.04	-	-	-
BMY 25368	19 ± 1	-	-	-
UR-DE257	28 ± 2	16 ± 1	43 ± 30	-

[a] Length of the linker expressed as number of atoms connecting the 'urea eqalent' and the ω-amino function (structures cf. Scheme 3); [b] h/gp/rH_2R binding: Sf9 insect cell membranes expressing the respective xH_2R-$G_{s\alpha S}$ subtype; [c] hH_2R binding: HEK293T CRE-Luc hH_2R cells. radioligand: [^{3}H]UR-DE257. (30 nM); value represents the mean ± SEM of 2-3 independent experiments each performed in triplicate.

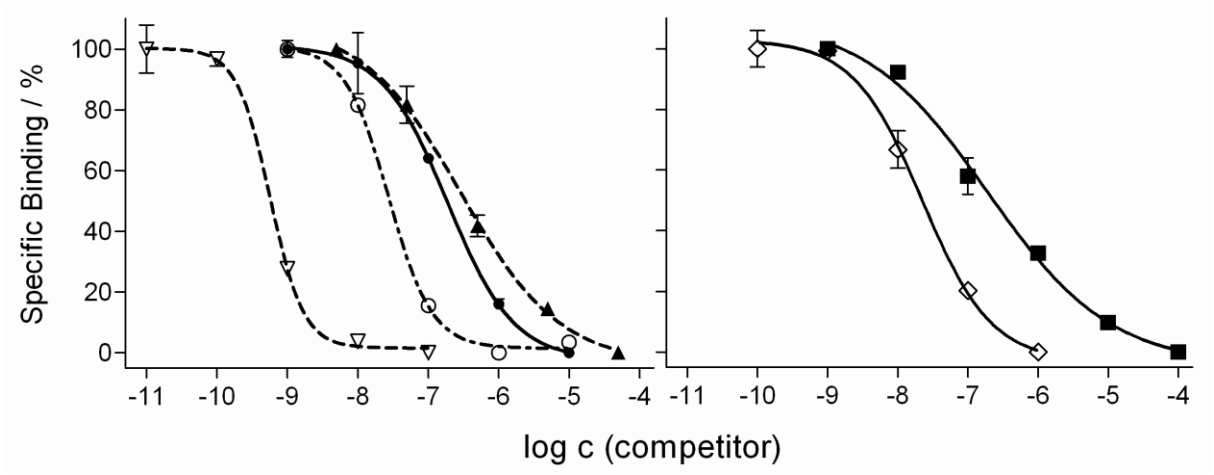

Figure 5.14 Displacement of the radioligand [^{3}H]UR-DE257 (c = 30 nM, K_d = 37 nM) by histamine H_2R ligands UR-Ak480[33] (∇, K_i = 0.15 ± 0.02 nM), UR-DE257 (○, K_i = 43 ± 30 nM), famotidine (●, K_i = 107 ± 5 nM), histamine (▲, K_i = 150 ± 29 nM), UR-Bit24[32] (◊, K_i = 9.5 ± 2 nM) and dimaprit (■, K_i = 104 ± 20 nM). The assay was performed on membranes of Sf9 insect cells expressing the gpH_2R-$G_{s\alpha S}$; incubation period: 60 min, data represent mean values ± SEM (n = 2).

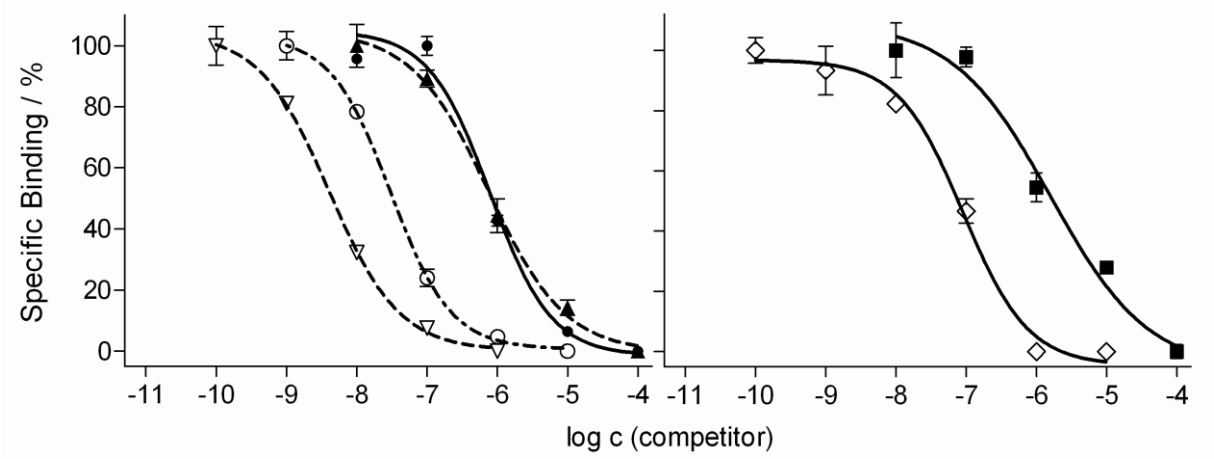

Figure 5.15 Displacement of the radioligand [^{3}H]UR-DE257 (c = 30 nM, K_d = 29 nM) by histamine H_2R ligands UR-AK480 (∇, K_i = 1.7 ± 0.5 nM), UR-DE257 (○, K_i = 16 ± 1 nM), famotidine (●, K_i = 423 ± 33 nM), histamine (▲, K_i = 486 ± 106 nM), UR-Bit24 (◊, K_i = 54 ± 3 nM) and dimaprit (■, K_i = 600 nM). The assay was performed on membranes of Sf9 insect cells expressing the rH_2R-$G_{s\alpha S}$ with an incubation period of 60 min (mean values ± SEM, n = 1-2).

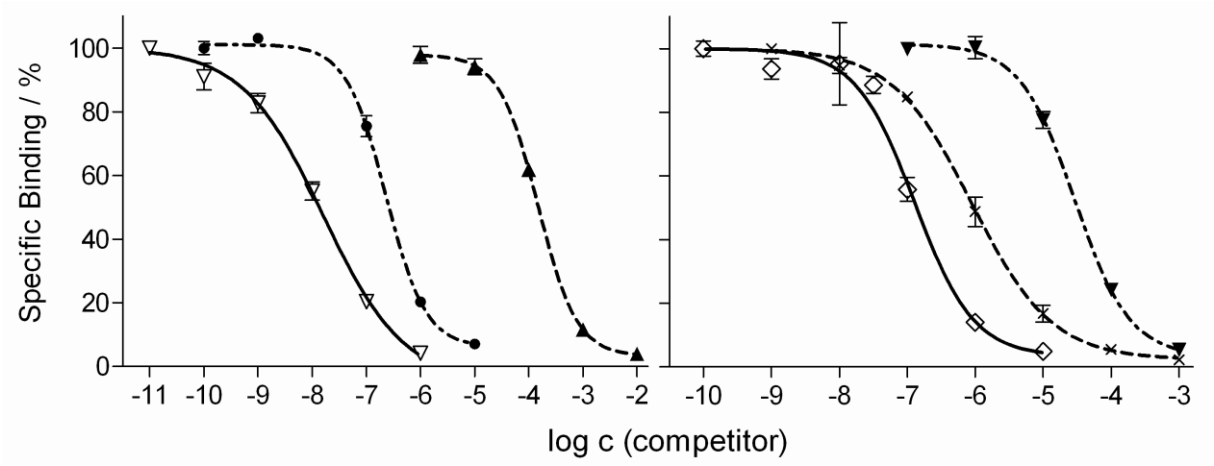

Figure 5.16 Displacement of the radioligand [^{3}H]UR-DE257 (c = 30 nM, K_d = 55 nM) by histamine H_2R ligands UR-AK480 (∇, K_i = 8.2 ± 3 nM), famotidine (●, K_i = 147 ± 43 nM), histamine (▲, K_i = 100 ± 18 µM), UR-Bit24 (◊, K_i = 107 ± 32 nM), cimetidine (x, K_i = 428 ± 7 nM) and amthamine (▼, K_i = 20 ± 1 µM). The assay was performed on HEK293T CRE-Luc hH_2R cells with an incubation period of 60 min (mean values ± SEM, n = 2-3).

5.2.3 Autoradiography

In the guinea-pig brain, with [^{125}I]iodoaminopotentidine as radioligand, H_2R binding sites were described in the cerebral cortex in layers I-III (I: molecular layer; II: external granular layer; III: layer of medium-sized pyramidal cells), in the thalamus, and in the hippocampus .[10,34,35] To explore, if [^{3}H]UR-DE257 is also a useful radioligand for autoradiography, cryosections of guinea-pig and rat brain were incubated with [^{3}H]UR-DE257. However, there were no significant differences between the autoradiographs representing specific and nonspecific binding (cf. Figure 5.17-5.20).

To identify H_2R binding sites in guinea-pig heart, adjacent transverse ventricular or atrium cryosections were incubated with [^{3}H]UR-DE257. Unfortunately, as depicted in Figure 5.21 and 5.22 there was no indication of specific binding.

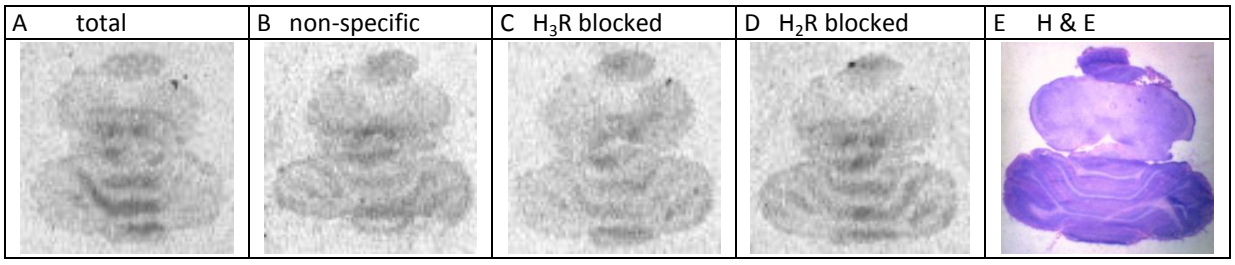

Figure 5.17 Binding of the tritiated H_2R antagonist [^{3}H]UR-DE257 (c = 30 nM) to adjacent coronal cerebrallar sections of rat brain (male Wistar rat, 3-4 month old). A. Total binding. B. Non-specific binding, determined with famotidine (c = 6 µM) and histamine (c = 6 µM) for blocking all histamine receptor subtypes. C. Binding of [^{3}H]UR-DE257 (c = 30 nM) with thioperamide (c = 6 µM) for blocking the H_3R. D. Binding of [^{3}H]UR-DE257 (c = 30 nM) with famotidine (c = 6 µM) for blocking the H_2R. E. H & E stained adjacent section.

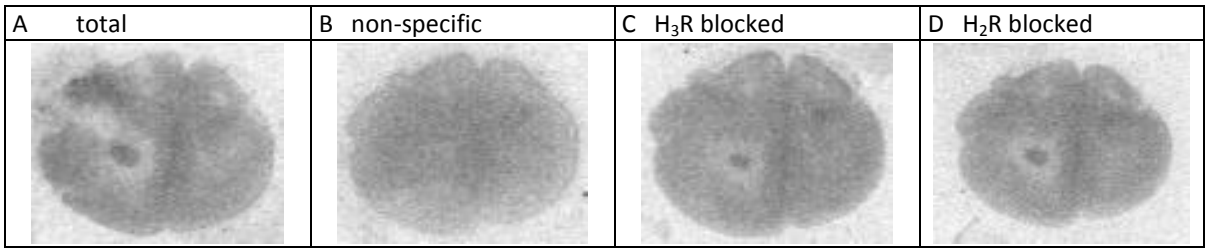

Figure 5.18 Binding of the tritiated H_2R antagonist [^{3}H]UR-DE257 (c = 30 nM) to adjacent coronal frontal lobe sections of rat brain (male Wistar rat, 3-4 month old). A. Total binding. B. Non-specific binding, determined with famotidine (c = 6 µM) and histamine (c = 6 µM) for blocking all histamine receptor subtypes. C. Binding of [^{3}H]UR-DE257 (c = 30 nM) with thioperamide (c = 6 µM) for blocking the H_3R. D. Binding of [^{3}H]UR-DE257 (c = 30 nM) with famotidine (c = 6 µM) for blocking the H_2R. E. H & E stained adjacent section.

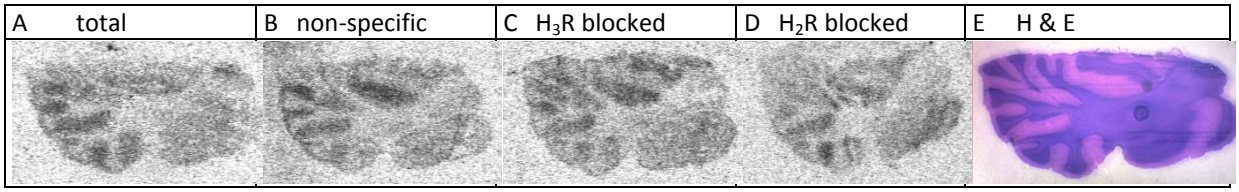

Figure 5.19 Binding of the tritiated H_2R antagonist [^{3}H]UR-DE257 (c = 30 nM) to adjacent coronal cerebral sections of guinea-pig brain (female guinea-pig, 2 month old). A. Total binding. B. Non-specific binding, determined with famotidine (c = 6 µM) and histamine (c = 6 µM) for blocking all histamine receptor subtypes. C. Binding of [^{3}H]UR-DE257 (c = 30 nM) with thioperamide (c = 6 µM) for blocking the H_3R. D. Binding of [^{3}H]UR-DE257 (c = 30 nM) with famotidine (c = 6 µM) for blocking the H_2R. E. H & E stained adjacent section.

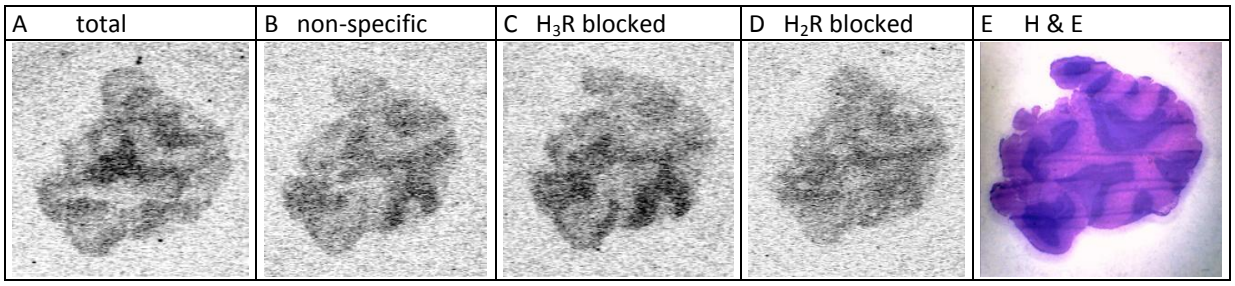

Figure 5.20 Binding of the tritiated H_2R antagonist [^{3}H]UR-DE257 (c = 30 nM) to adjacent coronal olfactory bulb sections of guine-pig brain (female guinea-pig, 2 month old). A. Total binding. B. Non-specific binding, determined with famotidine (c = 6 µM) and histamine (c = 6 µM) for blocking all histamine receptor subtypes. C. Binding of [^{3}H]UR-DE257 (c = 30 nM) with thioperamide (c = 6 µM) for blocking the H_3R. D. Binding of [^{3}H]UR-DE257 (c = 30 nM) with famotidine (c = 6 µM) for blocking the H_2R. E. H & E stained adjacent section.

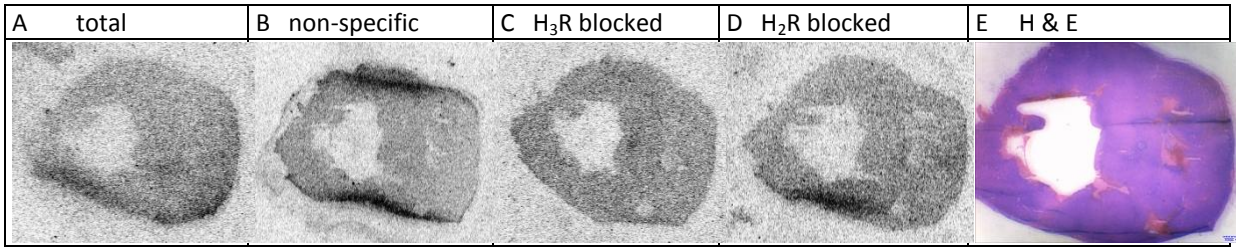

Figure 5.21 Binding of the tritiated H_2R antagonist [^{3}H]UR-DE257 (c = 30 nM) to adjacent transverse ventricular sections of guinea-pig heart (female guinea-pig, 2 month old). A. Total binding. B. Non-specific binding, determined with famotidine (c = 6 µM) and histamine (c = 6 µM) for blocking all histamine receptor subtypes. C. Binding of [^{3}H]UR-DE257 (c = 30 nM) with thioperamide (c = 6 µM) for blocking the H_3R. D. Binding of [^{3}H]UR-DE257 (c = 30 nM) with famotidine (c = 6 µM) for blocking the H_2R. E. H & E stained adjacent section.

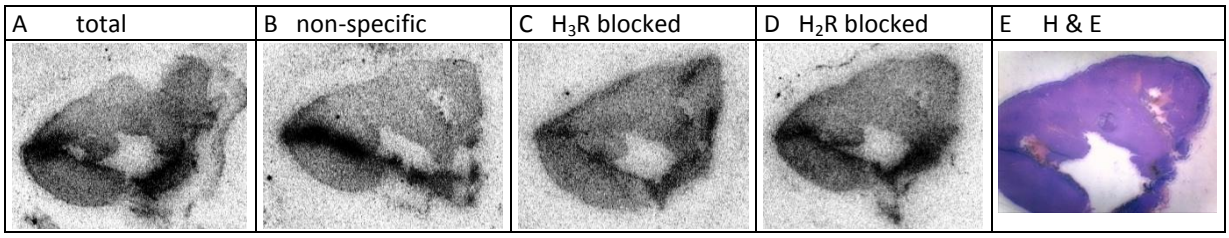

Figure 5.22 Binding of the tritiated H_2R antagonist [^{3}H]UR-DE257 (c = 30 nM) to adjacent transverse atrium sections of guine-pig heart (female guinea-pig, 2 month old). A. Total binding. B. Non-specific binding, determined with famotidine (c = 6 µM) and histamine (c = 6 µM) for blocking all histamine receptor subtypes. C. Binding of [^{3}H]UR-DE257 (c = 30 nM) with thioperamide (c = 6 µM) for blocking the H_3R. D. Binding of [^{3}H]UR-DE257 (c = 30 nM) with famotidine (c = 6 µM) for blocking the H_2R. E. H & E stained adjacent section.

5.3 Summary

There has been a shortage of high affinity radioligands for the investigation of the histamine H_2 receptor. Therefore, *N*-[6-(3,4-dioxo-2-{3-[3-(piperidin-1-ylmethyl)phenoxy]-propylamino}cyclobut-1-enylamino)-hexyl]-(2,3-$^3H_2$)propionamide ([^{3}H]UR-DE257) as a tritium-labeled H_2R antagonist (K_b: 38 nM, GTPase assay) was synthesized and characterized. Acylation of the amine precursor with succinimidyl [2,3-$^3H_2$]propionate gave the tritium-labeled radioligand with a high specific activity (63 Ci/mmol). This compound binds with high affinity (K_d, from saturation binding: 31 nM, kinetic studies: 20 nM) and selectivity for the hH_2R over the other HR subtypes. Affinities and selectivities of the unlabeled form, UR-DE257, were determined in radioligand binding assays, using membrane preparations of Sf9 insect cells, expressing the respective hH_xR subtype (K_i values: hH_1R: >10000 nM, hH_2R: 28 nM, hH_3R: 3800 nM, hH_4R: >10000 nM). The determined K_d value (20 nM) from kinetic experiments was in good agreement with the dissociation equilibrium constant (31 nM) from saturation analysis. [^{3}H]UR-DE257 proved to be a useful tool to determine the H_2R binding affinities of unlabeled compounds in competition binding experiments, as confirmed for a set of reference ligands. [^{3}H]UR-DE257 is an attractive alternative to [^{3}H]tiotidine,[14,15] which showed a high degree of unspecific binding. Compared to [^{125}I]iodoaminopotentidine,[10] [^{3}H]UR-DE257 has a longer half-life, which is of advantage with respect to performing both synthesis and pharmacological studies, and the compound is more convenient to handle with respect to safety precautions.

5.4 Experimental Section

5.4.1 General conditions for radiosynthesis

Chemicals and solvents were purchased from Merck KGaA (Darmstadt, Germany) and Sigma Aldrich GmbH (Munich, Germany) and were used without further purification unless otherwise stated. All solvents were of analytical grade, and DMSO was distilled prior to use and stored over 4 Å molecular sieves. Succinimidyl [2,3-^{3}H]-propionate was purchased from Hartmann Analytic GmbH (Braunschweig, Germany) and provided in ethyl acetate (specific activity a_s = 2.96 TBq/mmol, 80/mmol; a_v =185 MBq/mL, 5 mCi/mL). Scintillation cocktail Rotiscint Eco Plus was from Carl Roth (Karlsruhe, Germany). Analytical HPLC was performed on a system from Waters (Eschborn, Germany), equipped with a pump control module, a 510 HPLC pump, a 486 UV/VIS detector, and a Flo-One beta series A-500 radiodetector (Packard, Meriden, USA). The stationary phase was a Synergi Hydro-RP (250 x 4.6 mm, 4 µM) column equipped with a Luna C18 (4 x 3.0 mm) column guard (Phenomenex, Aschaffenburg, Germany). Linear gradients of CH_3CN/TFA 0.05% (*v/v*) and H_2O/TFA 0.05% (*v/v*) were used as mobile phases at a flow rate of 0.8 mL/min. Absorbance was detected at 280 nM, and radioactivity was measured with the radiodetector by liquid scintillation counting (liquid scintillator: Rotiscint Eco Plus, flow rate: 3.8 mL/min).

5.4.2 Synthesis of *N*-[6-(3,4-Dioxo-2-{3-[3-(piperidin-1-ylmethyl)phenoxy]propyl-amino}-cyclobut-1-enylamino)hexyl]-[2,3-$^{3}H_2$]propionamide ([^{3}H]UR-DE257):

Succinimidyl [2,3-$^{3}H_2$]propionate (5.35 µg, 0.0313 µmol, 1 eq, 2.5 mCi) in 500 µL ethyl acetate were transferred in a 1.5 mL Eppendorf reaction vessel (screw top) and the solvent was removed in a vacuum concentrator (40 °C) over a period of 30 min. Compound 12 (553 µg, 1.25 µmol, 40 eq) in DMSO (69 µL) and NEt_3 (253 µg, 2.50 µmol, 80 eq) in CH_3CN (69 µL) were added. After addition of 62 µL of CH_3CN, the reaction mixture was vigorously blended (vortexer), briefly centrifuged and stirred with a magnetic microstirrer for 18 h at room temperature. The reaction was monitored by HPLC. Reaction mixture (0.5 µL) was added to 105 µL of unlabeled compound UR-DE92 solution (50 µM), the 'cold' version of [^{3}H]UR-DE257, to allow for UV detection in addition to radiodetection; injection volume: 100 µL). For purification, the reaction mixture was diluted with 1060 µL of a mixture of CH_3CN/H_2O 20:80 (*v/v*) containing 0.05% TFA and the product was isolated (seven injections, 180 µL each) with analytical HPLC. In this instance, radiometric detection was not performed. Fractions containing the radioligand were collected at ~20 min (gradient: 0.05% TFA in CH_3CN/0.05% TFA in H_20: 0 min: 20:80 (*v/v*), 37 min: 30:70 (*v/v*), 38 min 90:10 (*v/v*), 48 min 90:10 (*v/v*)). The solvent of the combined fractions was evaporated under reduced pressure, the product dissolved in 1000 µL ethanol and transferred to an Amersham glass vial.

Quantification: A four-point calibration was performed with the unlabeled ligand UR-DE257 (1.0, 2.5, 5.0 and 7.5 µM, inj. vol.: 100 µL, gradient: 0.05% TFA in CH_3CN/0.05% TFA in H_2O: 0 min: 20:80 (*v/v*), 15 min: 52.5:47.5 (*v/v*), 16 min: 90:10 (*v/v*), 21 min: 90:10 (*v/v*), t_R ~ 14 min, see Figure 5.2). The solutions for injection were prepared in CH_3CN/0.05% aq. TFA (20/80) less than 5 min prior to injection. All standard solutions were prepared from a 100 µM solution of UR-DE257 (in CH_3CN/0.05% aq. TFA 20:80), which was freshly made from a 10 mM stock solution of UR-DE257 in CH_3CN. Two aliquots (2.0 µL) of the ethanolic solution of the product were diluted with 100 µL of CH_3CN/0.05% aq. TFA (20:80), and 100 µL were analyzed by HPLC. Whereas one sample was only used for quantification of the product by UV detection, the second sample was additionally monitored radiometrically to determine radiochemical purity. The molarity of the ethanolic solution of [^{3}H]UR-DE257 was calculated from the mean of the peak areas, and the linear calibration curve was obtained from the peak areas of the standards. Yield: 7.01 µg (14.0 nmol, 44.6%).

Determination of the specific activity: An aliquot (1.5 µL) of the ethanolic solution was diluted with 448.5 mL of a mixture of CH_3CN and H_2O (20:80) in duplicate, and 50 µL of the 1:300 dilutions were counted three times in Rotiszint eco plus (3 mL) in a LS 6500 liquid scintillation counter (Beckmann Coulter, München, Germany). The total activity in 1000 µL stock solution amounted to 32.5 MBq (0.877 mCi), resulting in a calculated specific activity of 2.33 TBq/mmol (63.0 Ci/mmol). The activity of the stock solution was adjusted to 9.25 MBq/mL, (0.25 mCi/mL, c = 3.97 µM) by adding EtOH. HPLC analysis showed a radiochemical purity of >99%. The identity of the radioligand was confirmed by HPLC analysis of labeled and unlabeled UR-DE257 under the same conditions, resulting in identical retention times. [^{3}H]UR-DE257 was stored at –20 °C.

Control of chemical stability of [^{3}H]UR-DE257 by HPLC: 2 µL of the adjusted stock solution of [^{3}H]UR-DE257 (activity concentration: 9.25 MBq/mL) in ethanol was diluted with 100 µL of CH_3CN/0.1% aq. TFA (20:80) to a total volume of 102 µL. 100 µL of this solution were injected into the HPLC system and analyzed by means of radiometric- and UV-detection. (gradient: 0.05% TFA in CH_3CN/0.05% TFA in H_20: 0 min: 20:80 (*v/v*), 37 min: 30:70 (*v/v*), 38 min 90:10 (*v/v*), 48 min 90:10 (*v/v*)).

5.4.3 Pharmacological methods

5.4.3.1 Histamine radioligand binding assays on membrane preparations of Sf9 insect cells

5.4.3.1.1 Competition binding experiments

Competition binding experiments were performed on membrane preparations of Sf9 insect cells expressing the hH_1R + RGS4, hH_2R-$G_{s\alpha S}$, gpH_2R-$G_{s\alpha S}$, rH_2R-$G_{s\alpha S}$, hH_3R + $G_{\alpha i2}$ + $\beta_1\gamma_2$ or the hH_4R + $G_{\alpha i2}$ + $\beta_1\gamma_2$ as described in Section 3.5.1.3.

5.4.3.1.2 Saturation binding experiments

Saturation binding experiments were conducted with radioligand concentrations (final concentration) between 1 nM and 200 nM. There, unspecific binding was determined with 10 µM famotidine. The membrane-ligand mixtures were incubated for 60 min at RT und shaking at 300 rpm. Separation of bound and unbound radioligand was performed by filtration as described before.

5.4.3.1.3 Kinetic experiments

In kinetic experiments the membranes were prepared as described before. Association and dissociation kinetic experiments were started by addition of [^{3}H]UR-DE257 (final concentration = 30 nM). During incubation the plate was shaken (300 rpm) at 22 °C. The wells for total binding in association experiments additionally contained 10 µL H_2O (millipore), the wells for unspecific binding 10 µL of a 100 µM solution of famotidine (final concentration = 10 µM) in H_2O (millipore). The respective radioligand or radioligand plus famotidine was added at different time points (0-180 min) to the membrane containing wells. After the last addition of radioligand bound radioligand was separated from free radioligand. Thus the last time point (last addition of radioligand) represented the shortest incubation time (0 min), whereas the first time point represents the longest incubation time (180 min). In dissociation experiments all wells were preincubated with [^{3}H]UR-DE257 (without 10 µM famotidine for total binding, with 10 µM famotidine for unspecific binding, final concentration: 30 nM in each well) for 60 min, before starting dissociation by addition of famotidine (final concentration: 10 µm/well). Preincubation was started for each data set at different time points. Dissociation kinetics was measured over 120 min. After the last addition of radioligand bound radioligand was separated from free radioligand by filtration. Thus the last time point (last addition of famotidine) represented the shortest dissociation time, whereas the first time point represents the longest dissociation time.

5.4.3.2 Radioligand binding assay at HEK293T CRE-Luc hH_2R cells

Leibovitz without phenol red (L15) from Life Technologies GmbH (Darmstadt, Germany), PP-96-well plates flat bottom from Greiner (Frickenhausen, Germany), GF/C filters from Skatron Instruments AS (Lier, Norway), fetal bovine serum (FBS) and G418 from Biochrom AG (Berlin, Germany), hygromycin B from MoBiTec GmbH (Göttingen, Germany) and Rotiszint eco plus from Carl Roth GmbH (Karslruhe, Germany). Separation of bound radioactivity from free radioactive tracer was done with a Brandel Harvester (CH-620), Robotic Cell Harvester, Gaithersburg, MD, US) and radioactivity could be measured by scintillation counting on a microplate counter (Microbeta 2450) from Perkin Elmer (Waltham, MA, US). HEK293T CRE-Luc hH_2R cells were essentially cultured and used as described[40] with minor modifications: Cells were cultured in DMEM with 10% FBS and selection antibiotics

(600 µg/mL of G418 and 250 µg/mL of hygromycin B) in a water saturated atmosphere containing 5% CO_2 at 37 °C. Cells were seeded into 175 cm^2 culture flasks (Sarstedt, Nümbrecht, Germany) and grown to approximately 90% confluence. The radioligand assay was performed as described previously,[40] with some modifications: On the day of the investigation the cells were detached with trypsin, suspended in L15 and centrifuged for 10 min at 300 *g*. The medium was discarded and the cells were resuspended in L15. After counting the cells, the cell density was adjusted to approximately 1-1.5 x 10^6 cells/mL. PP-96-well plates were either provided with 10 µL Leibovitz medium for the determination of total binding or 10 µL of famotidine (10 µM, final concentration) to determine the unspecific binding. 80 µL of the cell suspension were added per well. The samples were completed by adding 10 µL of radioligand. Samples were incubated for 60 minutes at 300 rpm. Competition binding experiments were performed in analogy to described methods with minor modifications. In brief: 160 µL of the suspended cells (2-4 x106 cells/mL in L15) were used per well (96 well plate). The cells were incubated in the presence of 30 nM [^{3}H]UR-DE257 (final concentration in L-15, K_d: 55 nM) with the ligand of interest at various concentrations (0.1 nM - 1 mM, final concentration) to measure total binding. Unspecific binding was the value determined at the highest concentration of the ligand of interest (1 µM-1 mM, final concentration) in the presence of 30 nM [^{3}H]UR-DE257 (final concentration). This concentration was sufficient to prevent specific binding of the radioactive tracer. The well plate was shaken (RT, light protection) for 60 min at 300 rpm. Separation of bound and unbound radioligand was performed by filtration as described before. Saturation binding and kinetic experiments were performed in the same manner as mentioned for membrane preparations of Sf9 insect cells.

5.4.4 Autoradiography

The rat brain (female Wistar rat, 3-4 month, 250 g), the guinea-pig brain and the guinea-pig heart were taken from the animals (24-48 h prior to experiment), immediately frozen in Tissue-Tek with the help of a mixture of dry ice and 2-propanol, and stored at -18 °C. Cryosections (10 µm) were obtained at -18 °C (for brain tissues) or -16 °C (for the guinea-pig heart) with a 2800 Frigocut E freezing microtome (Reichert-Jung/Leica, Germany). Two adjacent sections were mounted on a microscopic slide (Superfrost Plus, 75 × 25 × 1 mm), put 1 min into a chamber of 100% humidity and then carefully covered with binding buffer (800 µL) or fixed for 20 s in an alcoholic formaldehyde fixative (40 mL of 37% formaldehyde, 360 mL of 95% ethanol and 0.2 g calcium acetate.[41] The binding buffer was removed (after a period of less than 60 min under cooling) by putting the slides uprightly on a paper towel (~1 min). For total binding the sections were covered with binding buffer (about 600 to 800 µL for one slide) containing [^{3}H]UR-DE257 (30 nM). For non-specific binding the sections were covered with binding buffer containing [^{3}H]UR-DE257 (30 nM) and either famotidine (6 µM) for

blocking the H_2R, thioperamide (6 µM) for blocking the H_3R or famotidine (6 µM) and histamine (6 µM) for blocking all histamine receptor subtypes. The sections were incubated at room temperature (22-25 °C) for a period of 30 min. After incubation the binding buffer was removed, the slides were immerged three times into binding buffer split to 3 vessels (4 °C, 10 s) and finally rinsed with distilled water (4 °C, 10 s). The slides were put uprightly on a paper towel for 1 min and then dried in horizontal position in a desiccator over P_4O_{10} under reduced pressure. The slides were set in close contact with a tritium sensitive screen (PerkinElmer, 192 × 125 mm, Überlingen, Germany) using an X-ray film cassette and stored in a dark room for 14-17 d. The autoradiographic image was generated from the tritium screen using a phosphor imager (Cyclone Storage Phosphor System, Packard, Meriden, USA). The fixed sections were stained with haematoxylin and eosin: H & E: rinsing (H_2O_{demin}), Mayer's S11 haemalum solution (Merck) 1:3 diluted in water (11 min), rinsing (tap water), 1% aq. acetic acid (3 × immersion), running tap water (10 min), rinsing (H_2O_{demin}), eosin standard solution (2 min), running H_2O_{demin} (5 min); 96% aq. EtOH (2 × 3 min), 100% EtOH (2 × 3 min), 100% xylene (3 min). Entellan (Merck) was used for covering.

5.5 References

1. Parsons, M. E.; Ganellin, C. R. Histamine and its receptors. *Br. J. Pharmacol.* **2006**, 147 Suppl 1, S127-135.
2. Hill, S. J.; Ganellin, C. R.; Timmerman, H.; Schwartz, J. C.; Shankley, N. P.; Young, J. M.; Schunack, W.; Levi, R.; Haas, H. L. International Union of Pharmacology. XIII. Classification of histamine receptors. *Pharmacol. Rev.* **1997**, 49, 253-278.
3. Dove, S.; Elz, S.; Seifert, R.; Buschauer, A. Structure-activity relationships of histamine H_2 receptor ligands. *Mini. Rev. Med. Chem.* **2004**, 4, 941-954.
4. Seifert, R.; Strasser, A.; Schneider, E. H.; Neumann, D.; Dove, S.; Buschauer, A. Molecular and cellular analysis of human histamine receptor subtypes. *Trends Pharmacol. Sci.* **2013**, 34, 33-58.
5. Hirschfeld, J.; Buschauer, A.; Elz, S.; Schunack, W.; Ruat, M.; Traiffort, E.; Schwartz, J. C. Iodoaminopotentidine and related compounds: a new class of ligands with high affinity and selectivity for the histamine H_2 receptor. *J. Med. Chem.* **1992**, 35, 2231-2238.
6. Cavanagh, R. L.; Buyniski, J. P. Effect of BMY-25368, a potent and long-acting histamine H_2-receptor antagonist, on gastric secretion and aspirin-induced gastric lesions in the dog. *Aliment. Pharmacol. Ther.* **1989**, 3, 299-313.
7. Yellin, T. O.; Buck, S. H.; Gilman, D. J.; Jones, D. F.; Wardleworth, J. M. ICI 125,211: A new gastric antisecretory agent acting on histamine H_2-receptors. *Life Sci.* **1979**, 25, 2001-2009.
8. van der Goot, H.; Timmerman, H. Selective ligands as tools to study histamine receptors. *Eur. J. Med. Chem.* **2000**, 35, 5-20.
9. Leurs, R.; Smit, M. J.; Menge, W. M.; Timmerman, H. Pharmacological characterization of the human histamine H_2 receptor stably expressed in Chinese hamster ovary cells. *Br. J. Pharmacol.* **1994**, 112, 847-854.
10. Ruat, M.; Traiffort, E.; Bouthenet, M. L.; Schwartz, J. C.; Hirschfeld, J.; Buschauer, A.; Schunack, W. Reversible and irreversible labeling and autoradiographic localization of the cerebral histamine H_2 receptor using [^{125}I]iodinated probes. *Proc. Natl. Acad. Sci. U.S.A.* **1990**, 87, 1658-1662.

11. Kelley, M. T.; Burckstummer, T.; Wenzel-Seifert, K.; Dove, S.; Buschauer, A.; Seifert, R. Distinct interaction of human and guinea pig histamine H_2-receptor with guanidine-type agonists. *Mol. Pharmacol.* **2001**, 60, 1210-1225.
12. Bristow, D. R.; Hare, J. R.; Hearn, J. R.; Martin, L. E. PROCEEDINGS OF THE British Pharmacological Society 10th-12th September, 1980. *Br. J. Pharmacol.* **1981**, 72, 487P-590P.
13. Warrander, S. E.; Norris, D. B.; Rising, R. J.; Wood, T. P. [^{3}H]-cimetidine and the H_2-receptor. *Life Sci.* **1983**, 33, 1119-1126.
14. Gajtkowski, G. A.; Norris, D. B.; Rising, T. J.; Wood, T. P. Specific binding of ^{3}H-tiotidine to histamine H_2 receptors in guinea pig cerebral cortex. *Nature* **1983**, 304, 65-67.
15. Monczor, F.; Fernandez, N.; Legnazzi, B. L.; Riveiro, M. E.; Baldi, A.; Shayo, C.; Davio, C. Tiotidine, a histamine H_2 receptor inverse agonist that binds with high affinity to an inactive G-protein-coupled form of the receptor. Experimental support for the cubic ternary complex model. *Mol. Pharmacol.* **2003**, 64, 512-520.
16. Bylund, D. B.; Toews, M. L. Radioligand binding methods for membrane preparations and intact cells. In *R*EC*eptor Signal Transduction Protocols*, 2011/05/25 ed.; Willars, G. B.; Challiss, R. A. J., Eds., Springer: Leicester, 2011; Vol. 746, pp 135-164.
17. Erdmann, D. Histamine H_2- and H_3- Receptor Antagonists: Synthesis and Characterization of Radiolabelled and Flourescent Pharmacological Tools. *Doctoral Thesis, University of Regensburg,* **2010**.
18. Keller, M.; Pop, N.; Hutzler, C.; Beck-Sickinger, A. G.; Bernhardt, G.; Buschauer, A. Guanidine-acylguanidine bioisosteric approach in the design of radioligands: synthesis of a tritium-labeled N^G-propionylargininamide ([^{3}H]-UR-MK114) as a highly potent and selective neuropeptide Y Y_1 receptor antagonist. *J. Med. Chem.* **2008**, 51, 8168-8172.
19. Igel, P.; Schnell, D.; Bernhardt, G.; Seifert, R.; Buschauer, A. Tritium-Labeled N^1-[3-(1H-imidazol-4-yl)propyl]-N^2-propionylguanidine ([^{3}H]UR-PI294), a High-Affinity Histamine H_3 and H_4 Receptor Radioligand. *ChemMedChem* **2009**, 4, 225-231.
20. Keller, M.; Bernhardt, G.; Buschauer, A. [^{3}H]UR-MK136: A Highly Potent and Selective Radioligand for Neuropeptide Y Y_1 Receptors. *ChemMedChem* **2011**, 6, 1566-1571.
21. Pluym, N.; Baumeister, P.; Keller, M.; Bernhardt, G.; Buschauer, A. [^{3}H]UR-PLN196: A Selective Nonpeptide Radioligand and Insurmountable Antagonist for the Neuropeptide Y Y_2 Receptor. *ChemMedChem* **2013**, 8, 587-593.
22. Vauquelin, G.; Van Liefde, I.; Birzbier, B. B.; Vanderheyden, P. M. New insights in insurmountable antagonism. *Fundam. Clin. Pharmacol.* **2002**, 16, 263-272.
23. Torchiana, M. L.; Pendleton, R. G.; Cook, P. G.; Hanson, C. A.; Clineschmidt, B. V. Apparent irreversible H_2-receptor blocking and prolonged gastric antisecretory activities of 3-*N*-(3-[3-(1-piperidinomethyl)phenoxy]propyl) amino-4-amino-1,2,5-thiadiazole-1-oxide (L-643, 441). *J. Pharmacol. Exp. Ther.* **1983**, 224, 514-519.
24. Brittain, R. T.; Jack, D.; Reeves, J. J.; Stables, R. Pharmacological basis for the induction of gastric carcinoid tumours in the rat by loxtidine, an insurmountable histamine H_2-receptor blocking drug. *Br. J. Pharmacol.* **1985**, 85, 843-847.
25. Stables, R.; Daly, M. J.; Humphray, J. M. Comparison of antisecretory potency and duration of action of the H_2-receptor antagonists AH 22216, cimetidine, ranitidine and SK & F 93479 in the dog. *Agents Actions* **1983**, 13, 166-169.
26. Buyniski, J. P.; Cavanagh, R. L.; Pircio, A. W.; Algieri, A. A.; Crenshaw, R. R. Structure-activity Relationships among newer Histamine H_2 Receptor Antagonists. *Highlights in Receptor Chemistry* **1984**, 195-215.
27. Mullins, D.; Adham, N.; Hesk, D.; Wu, Y.; Kelly, J.; Huang, Y.; Guzzi, M.; Zhang, X.; McCombie, S.; Stamford, A.; Parker, E. Identification and characterization of pseudoirreversible nonpeptide antagonists of the neuropeptide Y Y_5 receptor and development of a novel Y_5-selective radioligand. *Eur. J. Pharmacol.* **2008**, 601, 1-7.

28. Meini, S.; Patacchini, R.; Lecci, A.; Quartara, L.; Maggi, C. A. Peptide and non-peptide bradykinin B_2 receptor agonists and antagonists: a reappraisal of their pharmacology in the guinea-pig ileum. *Eur. J. Pharmacol.* **2000**, 409, 185-194.
29. Fierens, F. L. P.; Vanderheyden, P. M. L.; De Backer, J.-P.; Vauquelin, G. Insurmountable angiotensin AT_1 receptor antagonists: the role of tight antagonist binding. *Eur. J. Pharmacol.* **1999**, 372, 199-206.
30. Vauquelin, G.; Morsing, P.; Fierens, F. L.; De Backer, J. P.; Vanderheyden, P. M. A two-state receptor model for the interaction between angiotensin II type 1 receptors and non-peptide antagonists. *Biochem. Pharmacol.* **2001**, 61, 277-284.
31. Cheng, Y.; Prusoff, W. H. Relationship between the inhibition constant (K_1) and the concentration of inhibitor which causes 50 per cent inhibition (I_{50}) of an enzymatic reaction. *Biochem. Pharmacol.* **1973**, 22, 3099-3108.
32. Birnkammer, T.; Spickenreither, A.; Brunskole, I.; Lopuch, M.; Kagermeier, N.; Bernhardt, G.; Dove, S.; Seifert, R.; Elz, S.; Buschauer, A. The Bivalent Ligand Approach Leads to Highly Potent and Selective Acylguanidine-Type Histamine H_2 Receptor Agonists. *J. Med. Chem.* **2012**, 55, 1147-1160.
33. Kraus, A.; Ghorai, P.; Birnkammer, T.; Schnell, D.; Elz, S.; Seifert, R.; Dove, S.; Bernhardt, G.; Buschauer, A. N^G-Acylated Aminothiazolylpropylguanidines as Potent and Selective Histamine H_2 Receptor Agonists. *ChemMedChem* **2009**, 4, 232-240.
34. Ruat, M.; Traiffort, E.; Bouthenet, M. L.; Souil, E.; Pollard, H.; Moreau, J.; Schwartz, J. C.; Martinez-Mir, I.; Palacios, J. M.; Hirschfeld, J.; et al. Reversible and irreversible labelling of H_1- and H_2 -receptors using novel [^{125}I] probes. *Agents Actions Suppl.* **1991**, 33, 123-144.
35. Vizuete, M. L.; Traiffort, E.; Bouthenet, M. L.; Ruat, M.; Souil, E.; Tardivel-Lacombe, J.; Schwartz, J. C. Detailed mapping of the histamine H_2 receptor and its gene transcripts in guinea-pig brain. *Neuroscience* **1997**, 80, 321-343.
36. Saher, G.; Brugger, B.; Lappe-Siefke, C.; Mobius, W.; Tozawa, R.-i.; Wehr, M. C.; Wieland, F.; Ishibashi, S.; Nave, K.-A. High cholesterol level is essential for myelin membrane growth. *Nat. Neurosci.* **2005**, 8, 468-475.
37. Pop, N.; Igel, P.; Brennauer, A.; Cabrele, C.; Bernhardt, G. N.; Seifert, R.; Buschauer, A. Functional reconstitution of human neuropeptide Y (NPY) Y_2 and Y_4 receptors in Sf9 insect cells. *J. Recept. Signal Transduct. Res.* **2011**, 31, 271-285.
38. Schnell, D.; Brunskole, I.; Ladova, K.; Schneider, E. H.; Igel, P.; Dove, S.; Buschauer, A.; Seifert, R. Expression and functional properties of canine, rat, and murine histamine H_4 receptors in Sf9 insect cells. *Naunyn-Schmiedeberg's Arch. Pharmacol.* **2011**, 383, 457-470.
39. Lowry, O. H.; Rosebrough, N. J.; Farr, A. L.; Randall, R. J. Protein measurement with the Folin phenol reagent. *J. Biol. Chem.* **1951**, 193, 265-275.
40. Nordemann, U.; Wifling, D.; Schnell, D.; Bernhardt, G.; Stark, H.; Seifert, R.; Buschauer, A. Luciferase Reporter Gene Assay on Human, Murine and Rat Histamine H_4 Receptor Orthologs: Correlations and Discrepancies between Distal and Proximal Readouts. *PLoS ONE* **2013**, 8, e73961.
41. Bancroft, J. D.; Gamble, M. *Theory and Practice of Histological Techniques*. 5 th ed.; Churchill Livingstone: London, **2002**.

Chapter 6

[^{3}H]JNJ7777120: A Tritium-Labeled Histamine H_4 Receptor Antagonist

6.1 Introduction

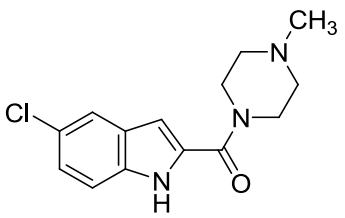

Figure 6.1 JNJ7777120.

JNJ7777120 (1-[(5-Chloro-1*H*-indol-2-yl)carbonyl]-4-methyl-piperazine) has been described as the first potent and selective antagonist at the H_4 receptor in 2003.[1,2] It resulted from in-house high-throughput screening (HTS) followed by optimization at Johnson & Johnson (J&J). JNJ7777120 binds to the human H_4 receptor with high affinity (K_i = 4.1 nM), it is also considered to be equipotent at the mouse and rat receptors and has a high selectivity over the other three histamine receptor subtypes. The antagonist properties of this compound have been described against histamine in a forskolin-stimulated cAMP-mediated reporter gene assay with a resulting pA_2 of 8.1 for the human H_4R and comparable values for other H_4R orthologs.[3,4] Regardless of unfavourable pharmacokinetic properties (short half-life), JNJ7777120 has been widely used to investigate the physiological role of the H_4R in various animal modelsR.[5-18] Meanwhile, apart from off-target effects at higher concentrations, the 'standard' H_4R antagonist JNJ7777120 was reported to produce H_4R-mediated paradoxical effects, for example regarding arrestin recruitment and agonist-like properties, depending on the assay and the H_4R species ortholog considered.[19-22] A detailed overview over the behavior of JNJ7777120 in different in vitro test systems is given by Seifert *et al*.[19] In principle, differential activation or inhibition of signaling pathways including G-protein- and β-arrestin-mediated responses is compatible with the concept of functional selectivity or biased signaling,[19] assuming unique ligand-specific receptor conformations with distinct signal transduction capabilities. In addition, discrepancies between pharmacological data may result from the substantially different constitutive activities of H_4R species orthologs.[20]

In general, the investigation of the (patho)physiological role of the H_4R and its validation as a drug target in translational animal models are compromised by distinct species-dependent discrepancies regarding potencies and receptor subtype selectivities of the pharmacological tools. Moreover, the pharmacological evaluation of murine cell systems is hampered by the lack of selective and suitable pharmacological tools like fluorescent- or radioligands. Radioligand binding studies at the H_4R, using [^{3}H]histamine,[20-24] [^{3}H]JNJ7777120,[3,25] the iodinated H_3R ligand [^{125}I]iodophenpropit[25,26] and the recently developed high affinity $hH_{3/4}R$ radioligand [^{3}H]UR-PI294[27] have were published. [^{3}H]Thioperamide[28] was reported as a radioligand for the H_3R, but radioligand binding studies for the H_4R are not available. Yet, none of these radiotracers is universally applicable. [^{3}H]Histamine binding data were reported for the hH_4R,[20-24] the cH_4R,[4] the mH_4R[21,22] and the rH_4R.[21] However, the analysis of radioligand binding studies with [^{3}H]histamine at the mH_4R and the rH_4R turned out to be difficult if not impossible, at least in the Sf9 cell system, due to too low specific binding of [^{3}H]histamine at

these H_4R species orthologs.[20,29] Further drawbacks of [^{3}H]histamine are low specific activity (10-25 Ci/mmol) of the commercially available radioligand and lack of HR subtype selectivity. [^{125}I]iodophenpropit, a radioligand with high affinity to the H_3R (pK_i = 8.2) showed also rather high affinity to the hH_4R (pK_i = 7.8) and was considered as a potential hH_4R radioligand, but its use was limited due to a high level of nonspecific binding and a B_{max} value varying from the expected one, determined with [^{3}H]histamine.[25] [^{3}H]UR-PI294 was applied in binding studies on the hH_4R and the mH_4R, using Sf9 cell membranes and HEK293T cells.[27] However, the pharmacological evaluation of mH_4R binding is hampered by lower affinity of UR-PI294 to the mH_4R.[30] Furthermore, as [^{3}H]UR-PI294 and [^{3}H]histamine are agonist at the hH_4R, binding can influenced by G-protein coupling,[31,32] preference for a receptor subpopulation[33] (the high affinity state) or internalization. As an antagonist, [^{3}H]JNJ7777120 should be superior to labeled agonists. Unfortunately, [^{3}H]JNJ7777120 is not commercially available and a consumer commissioned synthesis is overpriced. Hence, we decided to synthesize [^{3}H]JNJ7777120 in house and to evaluate the suitability of this radioligand at the hH_4R and the mH_4R using Sf9 cell membranes and HEK293T cells expressing the receptor of interest.

6.2 Chemistry

6.2.1 Optimization of the synthesis

The key step in radiosynthesis is the introduction of a radiolabeled group. Due to the practicability and easier handling with respect to safety precautions this should be done in the last step of the synthesis. In search for a suitable commercially available precursor we found [^{3}H]MeI as an appropriate methylation reagent.[34] In order to be able to use [^{3}H]MeI in the last step, we adapted the procedure of the published synthesis[1] of JNJ7777120 accordingly (Scheme 6.1). Preparation of JNJ7777120 (**6.4a**) started from piperazine, which was converted to the mono-Boc-protected derivative (**6.1**) in the first step. Reaction of **6.2** with 5-chloroindol-2-carboxylic acid under amide coupling conditions using EDC/HOBT followed by acidic Boc-deprotection yielded the des-methylated JNJ7777120 derivative **6.3** as di-TFA salt. In the next step methylation reaction was explored under HPLC control (cf. Table 6.1).

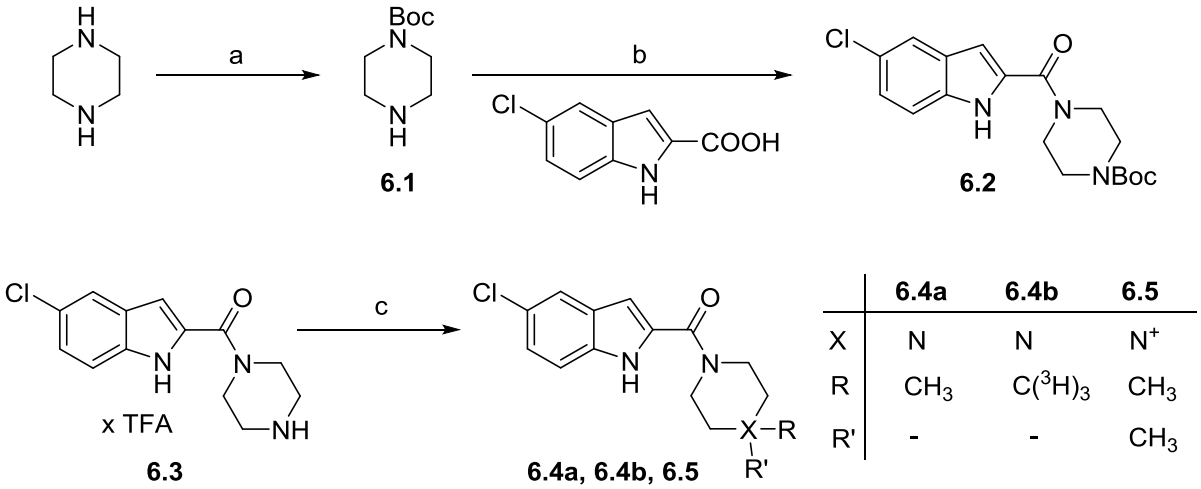

Scheme 6.1 Synthesis of JNJ7777120 (**6.4a**), [^{3}H]JNJ7777120 (**6.4b**) and **6.5**. Reagents and conditions: (a) Boc_2O, CH_2Cl_2, 0 °C, 2 h, 71%; (b) 5-chloroindole-2-carboxylic acid, EDC x HCl, HOBt x H_2O, DIPEA, THF, 26 h, rt, 52%; (c) for **6.4a**: MeI, K_2CO_3, acetone/toluene (20:1), 24 h, rt, 56%; for **6.4b**: [^{3}H]MeI, K_2CO_3, acetone/toluene (20:1), 24 h, rt, 9.6%; for **6.5**: MeI, K_2CO_3, acetone, 24 h, rt, 98%.

The ratio of building block **6.3**, K_2CO_3 and MeI was optimized to prevent the formation of the quaternary ammonium compound **6.5**. A ratio of 1 eq MeI, 10 eq of **6.3** and 30 eq of K_2CO_3 in a mixture of MeCN and toluene gave exclusively **6.4a**. Toluene was added because [^{3}H]MeI was provided as a solution in toluene. To identify the tertiary amine and the quaternary ammonium compound in HPLC analysis, for comparison, the di-methylated product **6.5** was synthesized from **6.3** with a large excess of MeI in acetone.

Table 6.1 Test reactions[a] for the methylation of compound **6.3**.

eq MeI	eq **6.3**	eq K_2CO_3	Product ratio (**6.3** : **6.4a** : **6.5**)	N
1	1	3	18 : 69 : 13	1
1	5	15	80 : 18 : 2	1
1	10	30	90 : 10 : 0	3

[a] Reagents and conditions: 190 µL acetone, 10 µL toluene, rt, 24 h.

6.2.2 Radiosynthesis of [^{3}H]JNJ7777120

The [^{3}H]methylated indol **6.4b** ([^{3}H]JNJ7777120, [^{3}H](5-chloro-1*H*-indol-2-yl)(4-methylpiperazin-1-yl)-methanone), the 'hot' form of **6.4a**, was prepared by methylation of an excess of amine precursor **6.3** in the presence of K_2CO_3 with commercially available [^{3}H]MeI in a mixture of MeCN and toluene (Scheme 6.1). Purification by HPLC afforded the radioligand **6.4b** in a radiochemical purity of >97% (Figure 6.2 A) with a specific activity (a_s) of 78.3 Ci/mmol.

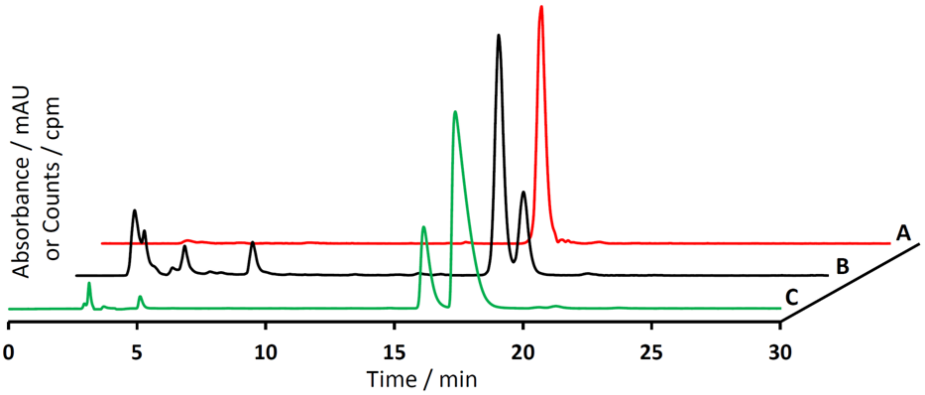

Figure 6.2 Identity and purity control of [^{3}H]JNJ7777120 (**6.4b**). A: Purity control (radiochromatogram) after isolation by HPLC. B: Reaction control after 22 h. C: UV (λ = 220 nm) chromatogram of the reaction mixture spiked with **6.4a**, c: 100 µM, column: Agilent Scalar C18 (4.6 x 250 mm, 5 µm), gradient: 0.05% TFA in CH_3CN/0.05% TFA in H_2O: 0 min 25:75 (*v/v*), 30 min 25:75 (*v/v*), 31 min 95:5 (*v/v*), 40 min 95:5 (*v/v*). The minor difference in retention times (t_R) of both chromatograms results from the setup of the UV and the radioactivity detector in series.

The identity of the radioligand was confirmed by comparing the HPLC retention times (t_R) of labeled (**6.4b**) and unlabeled JNJ7777120 (**6.4a**, cf. Figure 6.2). To exclude that di-methylation of **6.3** had occurred during the radiosynthesis, HPLC analysis was performed. Labeled JNJ7777120 (**6.4b**), unlabeled JNJ7777120 (**6.4a**) and the di-methylated analog (**6.5**) were compared on a YMC Triart C18 column, which is stable under basic conditions. Under these conditions the quaternary amine **6.5** is permanently charged and its retention time is very different from that of JNJ7777120 (cf. Figure 6.3). Lastly, chemical stability in EtOH/H_2O 1:1 (*v/v*) at -20 °C was proven over a period of at least 12 months (cf. Figure 6.4).

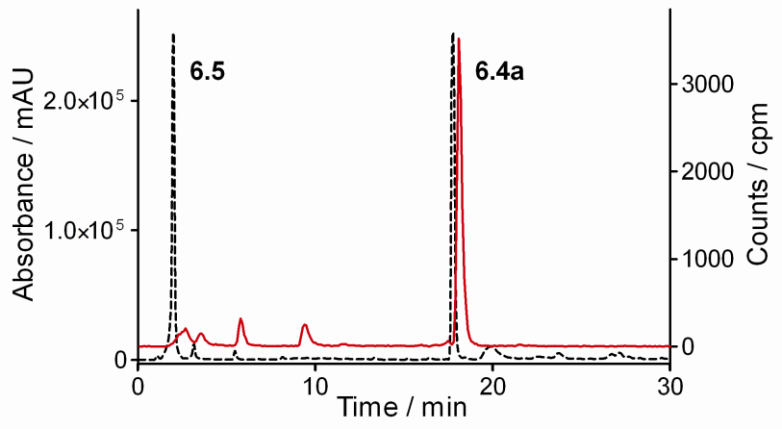

Figure 6.3 Identity control of [^{3}H]JNJ7777120 (**6.4b**). Red line: Radiochromatogram of **6.4b**; black dashed line: UV (λ = 220 nm) chromatogram of the **6.4a** (c = 100 µM) and **6.5** (c = 100 µM), column: YMC Triart C18 (150 x 2 mm, 5 µm). The minor difference in retention times (t_R) of both chromatograms results from the setup of the UV and the radioactivity detector in series. gradient: 0.5% NH_3 in CH_3CN/0.5% NH_3 in H_2O: 0 min 50:50 (*v/v*), 30 min 80:20 (*v/v*), 31 min 95:5 (*v/v*), 40 min 95:5 (*v/v*).

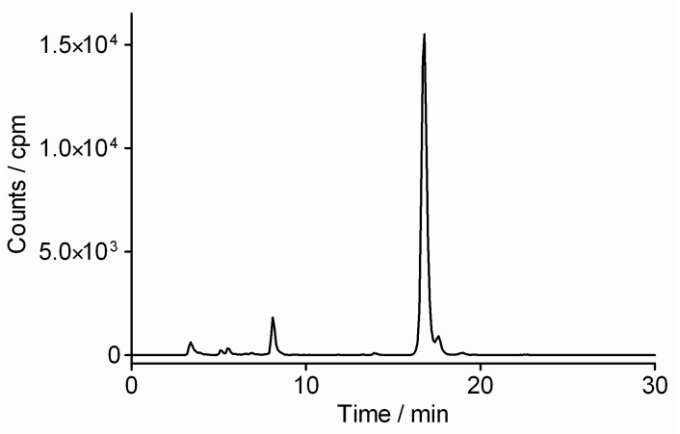

Figure 6.4 Long-term stability of [^{3}H]JNJ7777120. Example of a radiochromatogram of **6.4b** after storage in EtOH/H_2O (9:1 (*v/v*) at -20 °C for a period of 12 months, column: Agilent Scalar C18 (4.6 x 250 mm, 5 µm), gradient: 0.05% TFA in CH_3CN/0.05% TFA in H_2O: 0 min 25:75 (*v/v*), 30 min 25:75 (*v/v*), 31 min 95:5 (*v/v*), 40 min 95:5 (*v/v*).

6.3 Results and Discussion

6.3.1 Histamine receptor subtype affinities

The synthesized compounds **6.3** and **6.4a** (JNJ7777120) were investigated at the hH_3R and hH_4R in radioligand binding assays using membrane preparations of Sf9 insect cells expressing the hH_3R + $G\alpha_{i2}$ + $G\beta_1\gamma_2$ or hH_4R + $G\alpha_{i2}$ + $G\beta_1\gamma_2$, respectively as reported before.[35] Surprisingly, the demethylated compound **6.3** showed higher affinity to the hH_4R (K_i = 39.6 nM) and higher selectivity for the hH_4R versus the hH_3R (hH_3R: K_i = 35700 nM, selectivity H_4:H_3: 900:1) than JNJ7777120 (**6.4a**). Even though it is not crucial for the further investigation of JNJ7777120 as a radioligand, it is noteworthy that methylation of the free piperazine nitrogen is not mandatory for potential H_4R ligands. The affinities of JNJ7777120 (**6.4a**) to both receptors (hH_3R: K_i = 13100 nM, hH_4R: K_i = 39.6 nM) were in good agreement with reported data in a Sf9 membrane system.[20]

Table 6.2 Binding data of **6.3** and **6.4a** at the hH_3R and hH_4R.[a]

Compound	**hH_3R**		**hH_4R**		Selectivity
	K_i / nM	n	K_i / nM	n	H_4:H_3
Histamine	20.1 ± 3.1	4	13.1 ± 1.1	4	0.65 : 1
6.3	35700 ± 5900	2	39.6 ± 1.4	2	900 : 1
6.4a (JNJ7777120)	13100 ± 3500	2	65.3 ± 12.8	2	200 :1

[a] Determined on membrane preparations of Sf9 insect cells expressing the hH_3R + $G\alpha_{i2}$ + $G\beta_1\gamma_2$ or hH_4R + $G\alpha_{i2}$ + $G\beta_1\gamma_2$; radioligands: for hH_3R: [^{3}H]N^{α}-methylhistamine (c =3 nM), for hH_4R: [^{3}H]Histamine (c =10 nM). n gives the number of independent experiments, each performed in triplicate.

6.3.2 Pharmacological characterization of [^{3}H]JNJ7777120 (**6.4b**) on Sf9 cell membranes

6.3.2.1 Saturation binding of [^{3}H]JNJ7777120 at the hH_4R

Binding of [^{3}H]JNJ7777120 (**6.4b**) was determined on membranes of Sf9 insect cell expressing the hH_4R. Nonspecific binding was determined in the presence of an excess of histamine (100 µM), thioperamide (10 µM) or JNJ7777120 (**6.4a**, 10µM). Thereby, histamine or thioperamide revealed comparable results as competitor.

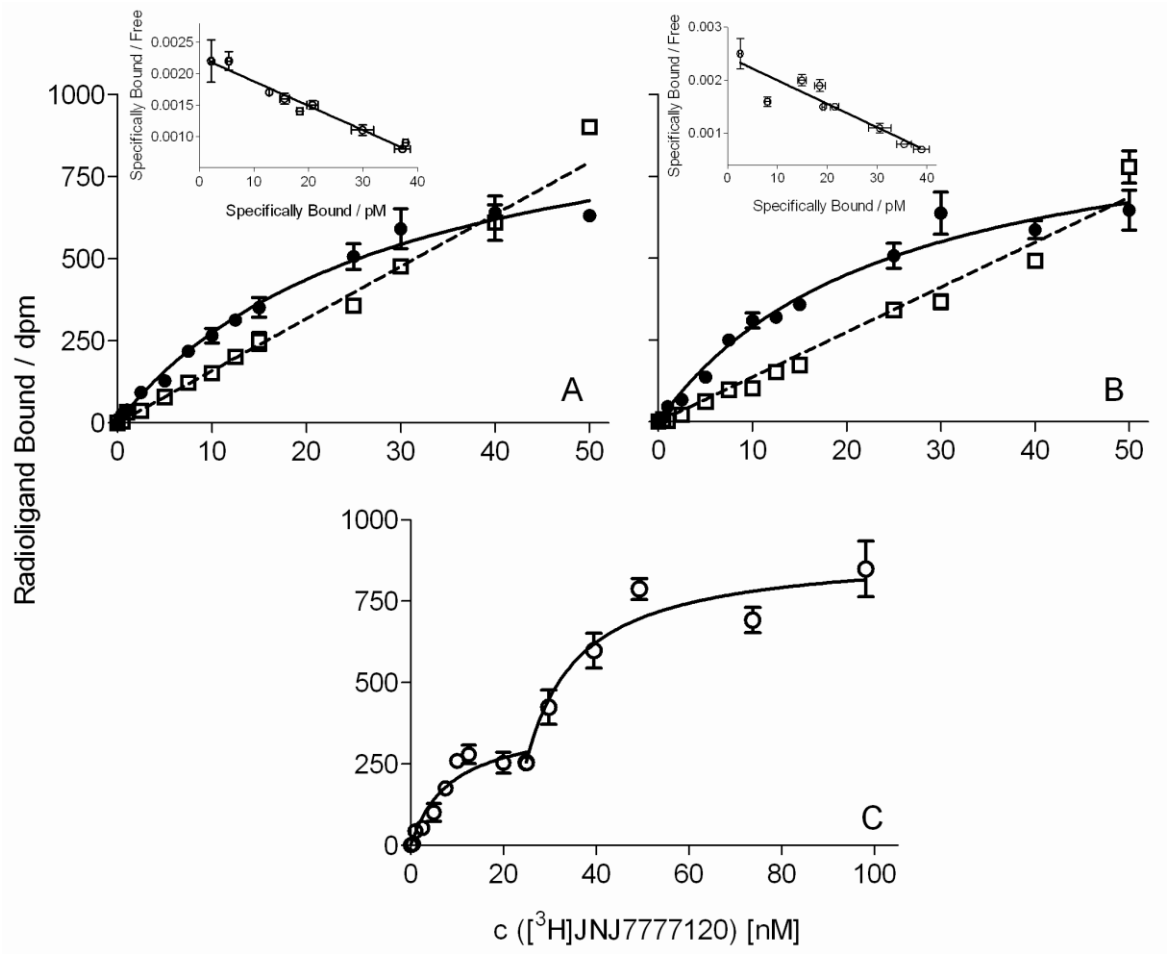

Figure 6.5 Saturation binding of **6.4b** to the hH_4R expressed in Sf9 membranes. A. Competitor: Histamine (c = 100 µM); specific binding: ●; nonspecific binding: □; $K_{d(sat)}$ = 29.5 ± 4.0 nM; inset: Scatchard plot for the binding of **6.4b**, K_d = –1/slope = 25.8 nM). B. Competitor: thioperamide (c = 100 µM); specific binding: ●; nonspecific binding: □; $K_{d(sat)}$ = 25.1 ± 4.6 nM; inset: Scatchard plot for the binding of 6.4b, K_d = –1/slope = 22.6 nM). C. Competitor: JNJ7777120 (**6.4a**, c = 10 µM); specific binding: ○; nonspecific binding: Not shown, amounted to ~50% (cf. appendix); $K_{d(sat)low}$ = 8.7 ± 3.8 nM; $K_{d(sat)high}$ = 36.8 ± 5.8 nM. Best fitted by nonlinear regression for specific binding and linear regression for nonspecific binding; mean values ± SEM, two independent experiments, each performed in triplicate.

In both cases, [^{3}H]JNJ7777120 (**6.4b**) specifically bound to the hH_4R (Figure 6.7 A+B) in a saturable manner with a K_d value of 29.5 nM for histamine and 25.1 nM for thioperamide, respectively, which were in good agreement with the potency determined in the steady-state GTPase assay (EC_{50} = 31.6 nM)[20] and the affinity determined with [^{3}H]histamine (K_i = 65 nM). Within the investigated concentration range, nonspecific binding amounted to approximately 30-40% of total binding and the calculated B_{max} values were 0.94 pmol per mg membrane for histamine and 0.90 pmol per mg membrane for thioperamide. The Scatchard plots of both experiments were linear, according to the binding of [^{3}H]JNJ7777120 to a single binding site, following the law of mass action (Figure 6.7 A+B: Insets).

Table 6.3 Saturation binding of [^{3}H]JNJ7777120 (**6.4b**) at the hH_4R in Sf9 cells membranes compared to [^{3}H]histamine as a radioligand.

Radioligand	Nonspecific binding determined by co-incubation with:	K_d / nM	$K_{d\ (scatchard)}$ / nM	B_{max} / pmol x mg membrane^{-1}	$N_{receptor}$ / well
6.4b[a]	Histamine[b]	29.5 ± 4.0	25.8	0.94	15.3 x 10^9
6.4b[a]	Thioperamide[b]	25.1 ± 4.6	22.6	0.90	14.6 x 10^9
6.4b[a]	JNJ7777120[c]	8.7 ± 3.8	n.d.	0.32[d]	5.2 x 10^{9}[d]
		36.8 ± 5.8	n.d.	0.60[d]	9.7 x 10^{9}[d]
[^{3}H]Histamine[a]	Histamine[c]	9.5 ± 1.2	n.d.	1.06	13.0 x 10^9

[a] Concentration range: 0.5-100 nM; [b] final concentration : 100 µM; [c] final concentration competitor: 10 µM. [d] ∑ B_{max} = 0.92 pmol/mg membrane; ∑ $N_{receptor}$/well = 14.9 x 10^{10}.

By contrast, when JNJ7777120 (**6.4a**) was used as a competitor, **6.4b** seemed to bind in a biphasic manner (Figure 6.7 C), resulting in a low K_d value of 8.7 nM with a B_{max} of 0.32 pmol per mg membrane and a high K_d value of 36.8 nM with a B_{max} of 1.52 pmol per mg membrane. This might be interpreted as a hint to conformational states with different accessibility for the antagonist JNJ7777120 compared to the endogenous agonist histamine or the inverse agonist thioperamide. The sum (0.92 pmol per mg membrane) of the B_{max} values for the two putative binding sites determined in the presence of unlabeled JNJ7777120 (**6.4a**) was in good agreement with the B_{max} values in the presence of histamine or thioperamide. However, displacement of the radioligand by its unlabeled version from a JNJ7777120-specific site different from the H_4R cannot be ruled out.

6.3.2.2 Kinetics at the hH_4R

The results of kinetic studies with [^{3}H]JNJ7777120 (c = 20 nM) at the hH_4R in Sf9 cell membranes at 20 °C are presented in Figure 6.6. Association was almost complete after 20 minutes. Linearization of

the association curves revealed a straight line with a k_{ob} value of 0.062 min^{-1}. Dissociation, initiated by JNJ7777120 (**6.4a**) was almost complete after 10 min indicating that [^{3}H]JNJ7777120 binds reversibly to the receptor ($t_{1/2}$ = 4.8 min). The resulting dissociation rate constant (k_{off}) was 0.171 min^{-1}. The determination of a K_d value from the ratio of the k_{off} and k_{on} values failed because the k_{on} value was not calculable from $k_{on} = (k_{ob} - k_{off})/[L]$, indicating [^{3}H]JNJ7777120 did not follow the law of mass action as also assumed by the varying results from saturation binding.

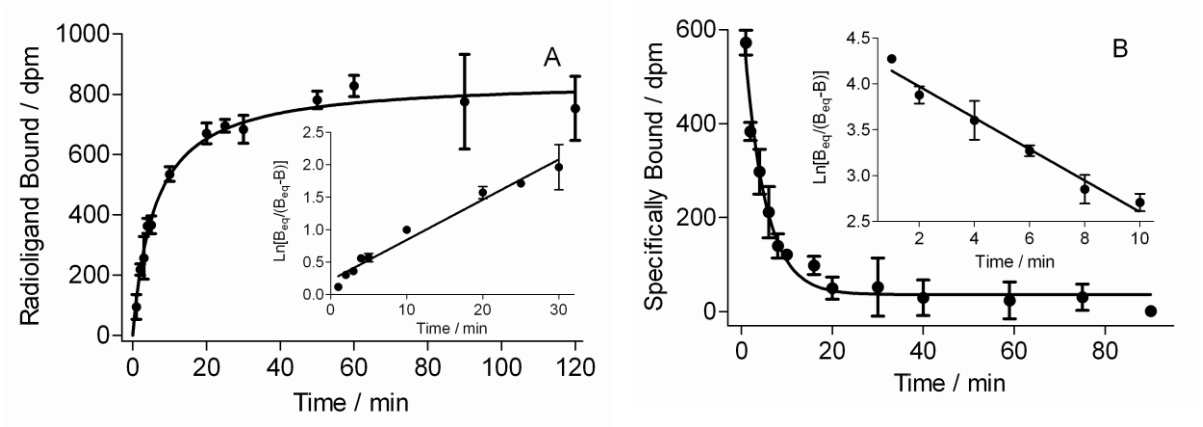

Figure 6.6 Association and dissociation kinetics of the specific H_4R binding of **6.4b** in Sf9 membranes. A: Radioligand (c = 20 nM) association as a function of time; inset: Linearization $\ln[B_{eq}/(B_{eq}-B)]$ versus time of the association kinetics for the determination of k_{ob}, slope = k_{ob} = 0.062 min^{-1}. B: Radioligand (c = 20 nM, pre-incubation for 60 min) dissociation as a function of time, monophasic exponential fit, $t_{1/2}$ = 4.8 min, dissociation performed with 100 µM of JNJ7777120 (**6.4a**); inset: Linearization $\ln(B/B_0)$ versus time of the dissociation kinetic for the determination of k_{off} = slope^{-1} = 0.171 min^{-1}.

6.3.2.3 Competition binding at the hH_4R

Regardless of the inconsistent saturation binding and kinetic experiments, competition binding studies showed that [^{3}H]JNJ7777120 (c = 20 nM) was completely displaceable and proved to be useful as a radioligand in competition binding studies with H_4R agonists and antagonists as shown in Figure 6.7. K_i values were calculated by means of the Cheng-Prusoff equation.[36] Therein, the K_d value was set to 20 nM. Due to the varying K_d values in saturation binding experiments (cf. Table 6.3) a more precise value was not available. The hH_4R binding affinity of histamine (K_i = 2.4 ± 0.4 nM), 5-methylhistamine (K_i = 49.1 ± 8.1 nM), VUF 8430 (K_i = 39.8 ± 15.7 nM), **3.16** (K_i = 4.2 ± 1.2 nM) and UR-PI376 (K_i = 58.4 ± 22.2 nM) are consistent with K_i values from binding experiments with [^{3}H]histamine and reported data (cf. Table 6.4).

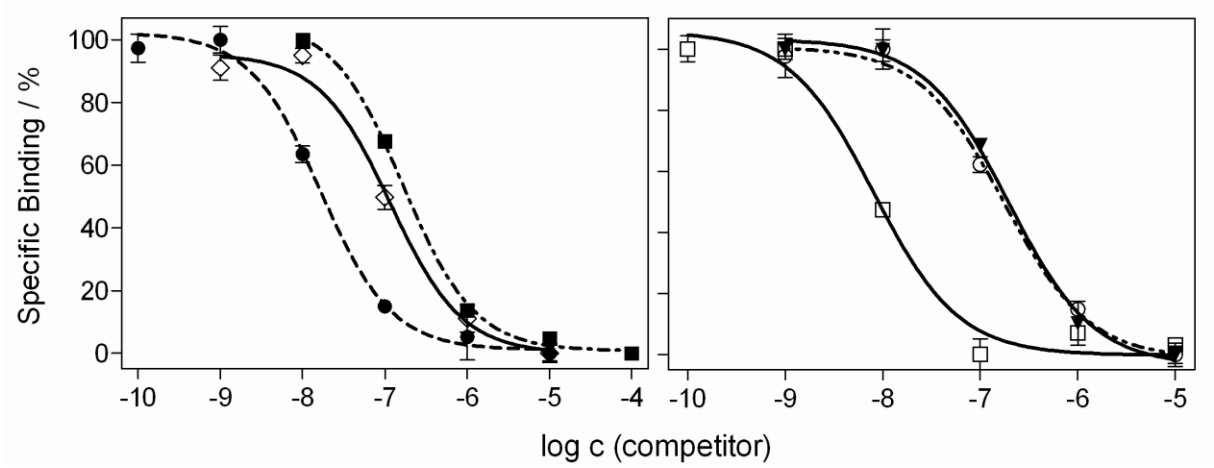

Figure 6.7 Displacement of the radioligand **6.4b** (c = 20 nM) by histamine H_4R ligands histamine (□, K_i = 2.4 ± 0.4 nM), 5-methylhistamine (**20a**, ▼, K_i = 49.1 ± 8.1 nM), VUF 8430 (○, K_i = 39.8 ± 15.7 nM), 3.16 (●, K_i = 4.2 ± 1.2 nM), UR-PI376 (◊, K_i = 58.4 ± 22.2 nM) and JNJ7777120 (**6.4a**, ■, K_i = 39.1 ± 8.2 nM). Assaya were performed on Sf9 insect cell membranes expressing the hH_4R + $G_{\alpha i2}$ + $\beta_1\gamma_2$ with an incubation period of 60 min (mean values ± SEM, n = 3).

The K_i value of JNJ7777120 (**6.4a**, K_i = 39.1 ± 8.2 nM), determined by competition binding experiments with the labeled analog **6.4b**, were in the same range as the K_d value of compound **6.4b** (~20 nM, cf. Table 6.4).

Table 6.4 Displacement of the radioligands [^{3}H]JNJ7777120 (**6.4b**) and [^{3}H]histamine by H_4R standard ligands.

Compound	[^{3}H]Histamine[a]		[^{3}H]JNJ7777120[b]		Reference data	
	K_i / nM	n	K_i / nM	n	K_i / nM	n
Histamine	13.1 ± 1.1	4	2.4 ± 0.4	3	12.7 ± 1.5[c]	3
5-Me-histamine	28.5 ± 4.4	3	49.1 ± 8.1	3	50.1 ± 10.3[d]	-
VUF8430	17.7 ± 1.4	4	39.8 ± 15.7	3	31.6[e]	-
UR-PI376	n.d.		58.4 ± 22.2	3	57.5 ± 11.8[f]	3
JNJ7777120	65.3 ± 12.8	3	39.1 ± 8.2	3	16[d]	-
3.16	11.2 ± 1.8	3	4.2 ± 1.2	3	0.21[g]	-

[a] Radioligand: [^{3}H]Histamine (c = 10 nM, K_d = 15.9 nM); [b] radioligand: **6.4b** (c = 20 nM, K_d = 8.7 nM); [c] Geyer *et al*. 2014;[35] [d] Lim *et al*. 2005;[25] [e] Igel *et al*. 2010;[37] [f] Igel *et al*. 2009;[38] [f] Savall *et al*. 2010.[39] Assays were performed on Sf9 insect cell membranes expressing the hH_4R with an incubation period of 60 min (mean values ± SEM). n gives the number of independent experiments, each performed in triplicate.

6.3.2.4 Membranes of Sf9 cells expressing the mH_4R

As high affinity of JNJ7777120 to the mH_4R was reported,[3] we performed binding experiments on membranes of Sf9 insect cells expressing the mH_4R. Nonspecific binding was detected with 'cold'

JNJ7777120 at a concentration of 100 µM. As presented in Figure 6.8, no specific binding was detectable up to a concentration of 150 nM of [^{3}H]JNJ7777120. Possible reasons are low affinity of JNJ7777120 to the mH_4R in the Sf9 membrane system, high nonspecific binding to membranes, or the presence of a receptor conformation, which is not accessible for JNJ7777120. A similar phenomenon was observed for binding experiments with [^{3}H]histamine at the mH_4R using Sf9 membranes, suggesting that it is exceedingly difficult to perform meaningful radioligand binding studies in this system.[20] Competition binding experiments were performed in order to elucidate if [^{3}H]JNJ7777120 is displaceable from the mH_4R, although specific binding could not be determined. The concentration of [^{3}H]JNJ7777120 was set to 20 nM, but neither agonists, nor antagonists displaced [^{3}H]JNJ7777120 from mH_4R expressing membranes (data not shown).

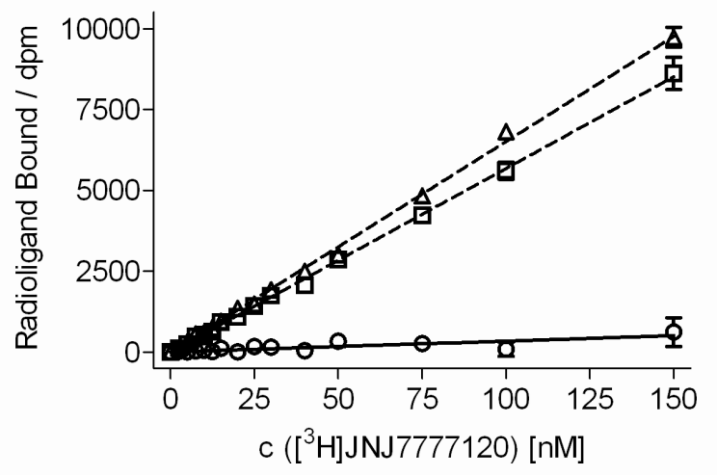

Figure 6.8 Saturation binding of **6.4b** to the mH_4R expressed in Sf9 membranes. Competitor: JNJ7777120 (c = 100 µM); total binding: Δ; specific binding: ○; nonspecific binding: □.

6.3.3 Saturation binding at HEK293-SF-H_4R-His_6 cells

Saturation binding experiments were performed on HEK cells stably expressing the hH_4R (HEK293-SF-hH_4R-His_6 cells) to explore the applicability of [^{3}H]JNJ7777120 in mammalian systems. In these studies binding was not saturable up to a concentration of 150 nM and the amount of nonspecific binding depended on the ligand used as a competitor (cf. Figure 6.9 A+B). In the presence of the 'cold' analog **6.4a** (c = 10 µM), nonspecific binding was approximately 50%, in the presence histamine (c = 100µM) nonspecific and total binding were in the same range. This suggests that [^{3}H]JNJ7777120 bound in a way or at a site, making the displacement by histamine impossible at the chosen concentration. For further exploration, control experiments were performed on parental HEK293-CRE-Luc cells, not expressing the hH_4R. As displayed in Figure 6.9 (C+D), the results were the same. Pseudospecific binding was found, when unlabeled JNJ7777120 was used as a competitor. This demonstrates that there is no specific binding of [^{3}H]JNJ7777120 to the hH_4R on HEK cells stably

expressing the hH_4R. In conclusion, [^{3}H]JNJ7777120 was inappropriate for the pharmacological characterization of HEK293-SF-H_4R-His_6 cells.

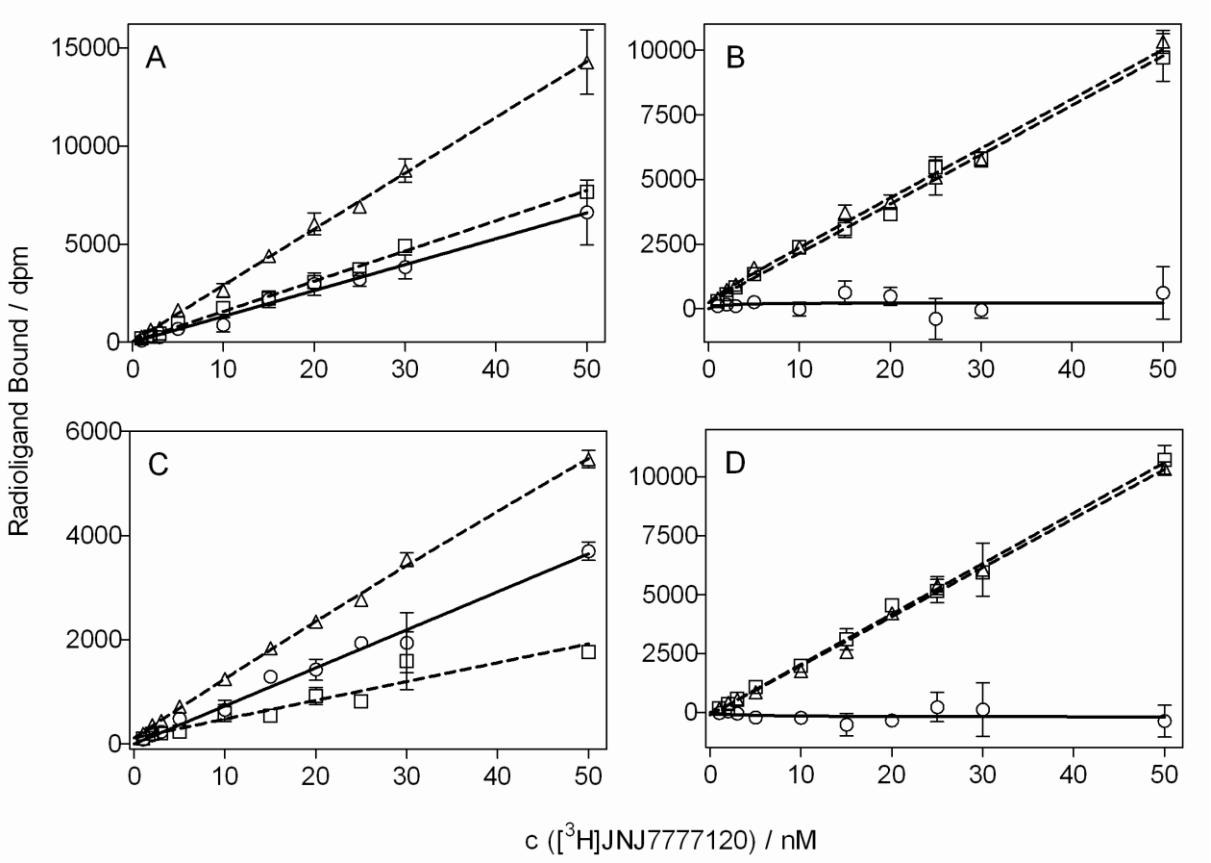

Figure 6.9 Saturation binding of **6.4b** to the hH_4R expressed in HEK cells. A: Cells: HEK293-SF-hH_4R-His_6; competitor: **6.4a** (c = 10 µM); total binding: Δ; specific binding: ○; nonspecific binding: □. B: Cells: HEK293-SF-hH_4R-His_6; competitor: Histamine (c = 100 µM); total binding: Δ; specific binding: ○; nonspecific binding: □. C: Cells: HEK293-CRE-Luc; competitor: **6.4a** (c = 10 µM); total binding: Δ; specific binding: ○; nonspecific binding: □. D: Cells: HEK293-CRE-Luc; histamine (c = 100 µM); total binding: Δ; specific binding: ○; nonspecific binding: □.

6.4 Summary and Conclusion

The tritium-labeled version of the widely use potent H_4R ligand JNJ7777120 was synthesized and pharmacologically characterized. The radioligand proved to be suitable for the investigation of the hH_4R in Sf9 insect cell membranes. However, saturation binding revealed discrepancies, when different competitors were used. With histamine and the inverse agonist thioperamide as competitors, [^{3}H]JNJ7777120 bound monophasic. In case that 'cold' JNJ7777120 was used, a biphasic curve with a low and a high K_d value could be fitted, suggesting the binding to different H_4R subpopulations (conformations). The association of [^{3}H]JNJ7777120 at the hH_4R in Sf9 cell membranes was almost complete after 20 min, whereas dissociation after almost 10 min. Linearization of both curve indicated, that [^{3}H]JNJ7777120 did not follow the law of mass action.

Above all, competition binding experiments were in good accordance to reported data. Even high affinity to the mH_4R is reported,[3] saturation and competition binding did not work with Sf9 cell membranes expressing the mH_4R. Similarly, the mH_4R/Sf9 cell system also failed when [^{3}H]histamine was used as a radioligand, suggesting that Sf9 cells membranes were not appropriate for mH_4R binding studies. Binding of [^{3}H]JNJ7777120 at HEK-hH_4R cells (HEK293-SF-hH_4R-His_6 cells) was not saturable and revealed 'pseudospecific' in binding experiments, just when the 'cold' analog JNJ7777120 was used as a competitor. Control experiments with HEK cells (HEK293-CRE-Luc) not expressing the hH_4R proved hH_4R-independent binding.

In summary, although JNJ7777120 has been used for the study of the H_4R in animal models, the investigation of the tritiated version, [^{3}H]JNJ7777120, revealed that this compound is far from being an ideal standard ligand or an optimal pharmacological tool. Due to very high non-specific binding an expected advantage of [^{3}H]JNJ7777120 as a H_4R selective antagonist compared to [^{3}H]histamine, a non-selective H_xR radiolabeled agonist could not be confirmed. On the whole, a 'perfect' radioligand for the H_4R is not available so far. This holds, in particular, for the analysis of the murine H_4R, due to substantially reduced or lack of mH_4R affinity of several reference compounds compared to the hH_4R, depending on the test system, for example, membrane preparations or mammalian cells. Thus, there is still a need for molecular tools such as high affinity fluorescent and radiolabeled H_4R ligands for the study of various H_4R species orthologs.

6.5 Experimental Section

6.5.1 Chemistry

6.5.1.1 General

See section 3.5.1.1

6.5.1.2 Preparation of the indol derivatives **6.4a** and **6.5**

tert-Butyl piperazine-1-carboxylate (6.1)[40]

A solution of 10.91 g (0.05 mol, 1eq) of di-*tert*-butyl dicarbonate in anhydrous CH_2Cl_2 (20 mL) was added dropwise within 30 min to a stirred solution of 8.61 g (0.10 mol, 2eq) of piperazine in anhydrous CH_2Cl_2 (100 mL) and stirred for 2 h. The precipitate was filtered off and washed with CH_2Cl_2 (3 × 50 mL). The solvent was removed under reduced pressure, the colorless oily residue was dissolved in 100 mL of water and stirred for 1 h. The insoluble bis(*tert*-butoxycarbonyl) derivative was removed by filtration and washed with water. The filtrate was saturated with K_2CO_3, extracted with diethyl ether (3 × 100 mL) and dried over anhydrous Na_2SO_4. Concentration *in vacuo* afforded the product as a white crystalline solid (6.40 g, 71%), mp 47 °C (lit.[41] 45-46 °C). R_f = 0.7 (CH_2Cl_2/MeOH 25:1). ^{1}H-NMR (300 MHz, DMSO-d_6): δ (ppm) 1.39 (s, 9H), 3.15-3.25 (m, 4H), 2.56-2.63 (m, 4H). ^{13}C-NMR (75 MHz, DMSO-d_6): δ = 28.07 (3C), 45.44, 78.49, 153.95. MS (GC-MS, CI): *m/z* 187.2 [M+H$^+$]. $C_9H_{18}N_2O_2$ (186.25).

tert-Butyl 4-(5-chloro-1H-indole-2-carbonyl)piperazine-1-carboxylate (6.2)[42]

EDC × HCl (0.49 g, 2.56 mmol, 1 eq), HOBt × H_2O (0.39 g, 2.56 mmol, 1 eq), 5-chloro-1*H*-indole-2-carboxylic acid (0.50 g, 2.56 mmol, 1 eq) and DIPEA (0.48 g, 3.74 mmol, 1.46 eq) were dissolved in anhydrous THF (20 mL), cooled to 0 °C and stirred for 2 h. Subsequently, **6.1** (0.52 g, 2.77 mmol, 1.08 eq) in anhydrous THF (5 mL) was added within 5 min. The reaction mixture was stirred for 26 h at room temperature. The solvent was evaporated and the residue was dissolved in CH_2Cl_2 (50 mL). The solution was washed with saturated $NaHCO_{3(aq.)}$ and brine, dried over anhydrous Na_2SO_4 and concentrated *in vacuo*. The crude product was purified by flash-chromatography (eluent CH_2Cl_2 (A), MeOH (B); gradient: 0 to 30 min: A/B 100/0 - 90/10 v/v, SF15-12 g) and afforded a white powder (0.48 g, 52%). R_f = 0.15 (CH_2Cl_2/MeOH 10:1). ^{1}H-NMR (300 MHz, DMSO-d_6): δ (ppm) 1.42 (s, 9H), 3.39-3.50 (m, 4H), 3.73 (br, 4H), 6.79 (d, J = 1.6, 1H), 7.17 (dd, J = 8.7, 2.0, 1H), 7.43 (d, J = 8.7, 1H), 7.63 (d, J = 1.8, 1H), 11.80 (s, 1H). ^{13}C-NMR (75 MHz, DMSO-d_6): δ (ppm) 28.03 (3C), 78.50, 78.94, 79.19 (2C), 79.38, 103.75, 113.65, 120.33, 123.36, 124.24, 127.82, 131.18, 134.37, 153.78, 161.75. MS (LC-MS, ESI): *m/z* 364.0 [M+H$^+$]. $C_{18}H_{22}ClN_3O_3$ (363.84).

(5-Chloro-1H-indol-2-yl)(piperazin-1-yl)methanone hydrotrifluoroacetate (6.3)[42]

6.2 (0.38 g, 1.04 mmol) was dissolved in anhydrous CH_2Cl_2 (4.5 mL) and TFA (0.5 mL) was added dropwise. The mixture was stirred at room temperature for 4 h and the solvents were removed under reduced pressure. CH_2Cl_2 (3 x 10 mL) was added and evaporated to remove remaining TFA. The crude product was obtained as a beige-colored solid (0.43 g, 83%) and used without further purification. 50 mg of the crude product were purified with preparative HPLC (column: Nucleodur 250 × 21 mm; gradient: 0–5 min: MeCN/0.1% aq. TFA 5/95, 5–35 min: MeCN/0.1% aq. TFA 5/95–40/60) and removal of the solvent from the eluate by evaporation and lyophilisation afforded **6.2** (hydrotrifluoroacetate) as a white fluffy solid (33 mg, 66%). R_f = 0.05 (CH_2Cl_2/MeOH 5:1). UV/VIS (20 mM HCl): λ_{max} 293, 233, 213 nm. RP-HPLC (220 nm): 99.0% (gradient: 0–30 min: MeCN/0.1% aq. TFA 5/95–80/20, 31-40 min: 90/10, t_R = 15.3 min, k = 8.1). ^{1}H NMR (300 MHz, DMSO-d_6): δ (ppm) 3.23 (br, 4H), 3.94 (br, 4H), 6.89 (d, J = 1.6, 1H), 7.21 (dd, J = 1.7, 8.7, 1H), 7.45 (dd, J = 1.5, 8.7, 1H), 7.67 (d, J = 1.9, 1H), 8.99 (s, 2H), 11.85 (s, 1H). ^{13}C NMR (75 MHz, DMSO-d_6): δ (ppm) 42.75, 104.26, 113.82, 120.45, 123.65, 124.35, 127.81, 130.61, 134.57, 161.89. MS (LC-MS, ESI): *m/z* 264.0 [M+H$^+$]. HRMS (EI-MS): *m/z* $M^{+\bullet}$ calcd. for $C_{13}H_{14}ClN_3O$: 263.0825, found: 263.0831.

(5-Chloro-1H-indol-2-yl)(4-methylpiperazin-1-yl)methanone hydrotrifluoroacetate (JNJ7777120, 6.4a)[1,42]

To a mixture of **6.3** (50 mg, 0.132 mmol, 1eq) and powdered K_2CO_3 (54.9 mg, 0.397 mmol, 3 eq) in acetone (1 mL), MeI (18.8 mg, 0.132 mmol, 1 eq) in acetone (100 µL) was added. The resulting white suspension was stirred for 6 h, quenched with water (20 mL), extracted with EtOAc (3 x 25ml), dried over anhydrous Na_2SO_4 and dried *in vacuo*. The product was purified with preparative HPLC (column: Nucleodur 250 × 21 mm; gradient: 0–30 min: MeCN/0.1% aq. TFA 30/70–60/40, t_R = 23.3 min) and removal of the solvent from the eluent by evaporation and lyophilisation afforded **6.4a** (hydrotrifluoroacetate) as a white fluffy solid (29 mg, 56%). R_f = 0.05 (CH_2Cl_2/MeOH 5:1). UV/VIS (20 mM HCl): λ_{max} 294, 235, 219 nm. RP-HPLC (220 nm): 99.5% (gradient: 0–30 min: MeCN/0.1% aq. TFA 5/95–80/20, 31-40 min: 90/10, t_R = 15.9 min, k = 8.4). ^{1}H NMR (300 MHz, DMSO-d_6, **6.4a** x HCl): δ (ppm) 2.78 (d, J = 3.3, 3H), 3.01-3.22 (m, 2H), 3.37-3.69 (br, 4H, superimposed by water), 4.53 (br, 2H), 6.89 (d, J = 1.6, 1H), 7.21 (dd, J = 2.1, 8.7, 1H), 7.46 (d, J = 8.7, 1H) 7.67 (d, J = 2.0, 1H), 11.49 (br, 1H), 11.92 (s, 1H). ^{13}C NMR (75 MHz, DMSO-d_6): δ (ppm) 41.98 (2C), 52.02 (2C), 104.33, 113.81, 120.44, 123.65, 124.32, 127.77, 130.46, 134.56, 161.75. MS (LC-MS, ESI): *m/z* 278.0 [M+H$^+$]. HRMS (EI-MS): *m/z* $M^{+\bullet}$ calcd. for $C_{14}H_{16}ClN_3O$: 277.0982, found: 277.0980.

4-[(5-Chloro-1H-indol-2-yl)carbonyl]-1,1-dimethylpiperazinium trifluoroacetate (6.5)

To a mixture of **6.3** (5.0 mg, 0.0132 mmol, 1eq) and powdered K_2CO_3 (24 mg, 0.174 mmol, 13 eq) in acetone (0.4 mL), MeI (681 mg, 4.798 mmol, 364 eq) was added. The resulting white suspension was stirred at rt for 16 h and the solvent was evaporated under reduced pressure affording a white powder (5.2 mg, 98%). R_f = 0.03 (CH_2Cl_2/MeOH 5:1). RP-HPLC (220 nm): 99.5% (gradient: 0−30 min: MeCN/0.1% aq. TFA 5/95−80/20, 31-40 min: 90/10, t_R = 16.4 min, *k* = 8.7). ^{1}H NMR (300 MHz, DMSO-d_6): δ (ppm) 3,15 (s, 6H), 3.25 (br, 2H), 3.38-3.79 (br, 4H), 4.35 (br, 2H), 6.91 (d, J = 1.8, 1H) , 7.02 (dd, J = 1.6, 8.5, 1H), 7.38 (dd, J = 1.9, 8.2, 1H) 7.60 (d, J = 1.7, 1H), 11.57 (s, 1H). MS (LC-MS, ESI): *m/z* 293.0 [M+H$^+$].

Optimization of the methylation of compound 6.3

To a mixture of **6.3** (hydrotrifluoroacetate) and powdered K_2CO_3 in a mixture of acetone (90 µL) and toluene (10 µL), MeI (0.177 mg, 1.25 µmol, 1 eq, 78 nl) in acetone (90 µL) was added. The resulting white suspension was stirred for 24 h, quenched with 0.1% $TFA_{(aq.)}$ and the reaction was controlled by analytical HPLC. The ratio of **6.3** and the reagents was varied as summarized in Table 6.5.

Table 6.5 Testreactions for the methylation of compound **6.3** (x TFA).

6.3 (x TFA)			**K_2CO_3**			**Product ratio (6.3 : 6.4a : 6.5)**	**N**
eq	n[a] / µmol	m[b] / mg	eq	n / µmol	m /mg		
1	1.25	0.47	3	3.75	5.2	18 : 69 : 13	1
2	2.5	0.94	6	7.5	10.4	80 : 18 : 2	1
10	12.5	4.7	30	37.5	51.8	90 : 10 : 0	3

[a] n = amount of substance; [b] m = weight; N gives the number of independent experiments.

6.5.2 Preparation of [^{3}H]JNJ7777120 (**6.4b**)

General conditions for radiosynthesis

Commercial reagents and solvents were purchased from Acros Organics (Geel, Belgium), Alfa Aesar (Karlsruhe, Germany), Sigma Aldrich GmbH (Munich, Germany), TCI Deutschland (Eschborn, Germany) or Merck KGaA (Darmstadt, Germany) and were used without further purification unless otherwise stated. All solvents were of analytical grade. [^{3}H]Methyl iodide dissolved in toluene (a_s = 2.96 TBq/mmol, 80 Ci/mmol; a_v = 18.5 GBq/ml, 0.5 Ci/ml) was from Hartmann Analytic (Braunschweig, Germany). Scintillation cocktail Rotiscint Eco Plus was from Carl Roth (Karlsruhe, Germany). Analytical HPLC was performed on a system from Waters (Eschborn, Germany), equipped

with a pump control module, a 510 HPLC pump, a 486 UV/VIS detector, and a Flo-One beta series A-500 radiodetector (Packard, Meriden, USA). The stationary phase was a Agilent Scalar C18 column (250 × 4.6 mm, 5 µm) equipped with a Luna C18 (4 x 3.0 mm) column guard (Phenomenex, Aschaffenburg, Germany) or a YMC Triart C18 (150 x 2 mm, 5 µm) equipped with a Luna C18 (4 x 3.0 mm) column guard (Phenomenex, Aschaffenburg, Germany). Linear gradients or isocratic mixtures of CH_3CN/TFA 0.05% (*v/v*) and H_2O/TFA 0.05% (*v/v*) were used as mobile phases at a flow rate of 0.8 mL/min. Absorbance was detected at 220 nm, and radioactivity was measured with the radiodetector by liquid scintillation counting (liquid scintillator: Rotiscint Eco Plus, flow rate: 3.8 mL/min).

(5-Chloro-1H-indol-2-yl)[4-(methyl-t_3)piperazin-1-yl]methanone hydrotrifluoroacetate (6.4b, [^{3}H]JNJ7777120)

Compound **6.3** hydrotrifluoroacetate (0.307 mg, 0.625 µmol, 10 eq) and powdered K_2CO_3 (0.259 mg, 1.875 µmol, 30 eq) dissolved in acetone (190 µL) were added to a solution of [^{3}H]MeI (8.875 µg, 0.0625 mmol, 1 eq, 5 mCi) in toluene (10 µL), and stirred for 22 h at room temperature. The reaction was monitored by HPLC. The reaction mixture (1 µL) was added to a solution of unlabeled compound **6.4a** (99 µL, c = 100 µM), the 'cold' version of **6.4b**, to allow UV detection in addition to radiodetection; injection volume: 95 µL. The solvent was removed under reduced pressure, and the residue was redissolved in 600 µL of a mixture of CH_3CN/H_2O 25:75 (*v/v*) containing 0.05% TFA. For isolation of **6.4b**, aliquots (12 x 60µl) were injected into an HPLC instrument. Fractions containing the radioligand were collected at ~17 min (gradient: 0.05% TFA in CH_3CN/0.05% TFA in H_2O: 0 min 25:75 (*v/v*), 30 min 25:75 (*v/v*), 31 min 95:5 (*v/v*), 40 min 95:5 (*v/v*), 41 min 25:75 (*v/v*), 50 min 25:75 (*v/v*). The solvent of the combined fractions was evaporated, and the residue was dissolved in 150 µL of a mixture of CH_3CN/H_2O 25:75 (*v/v*) containing 0.05% TFA. The supernatant were purified by HPLC to achieve high purity. The solvent of the combined fractions was evaporated and the residue was redissolved in 650 µL of EtOH/H_2O 9:1 (*v/v*), and transferred into a 5 mL Amersham glass vial.

Quantification: A five-point calibration was performed with the unlabeled ligand **6.4b** (0.5, 1.0, 2.0, 3.0 and 5.0 µM, inj. vol.: 100 µL, (gradient: 0.05% TFA in CH_3CN/0.05% TFA in H_2O: 0 min 25:75 (*v/v*), 30 min 25:75 (*v/v*), 31 min 95:5 (*v/v*), 40 min 95:5 (*v/v*), 41 min 25:75 (*v/v*), 50 min 25:75 (*v/v*), t_R ~17 min. The solutions for injection were prepared in 0.05% TFA in CH_3CN/0.05% TFA 25:75 (*v/v*) less than 5 min prior to injection. All standard solutions were prepared from a 100 µM solution of **6.4a** (in CH_3CN/0.05% TFA 25:75 (*v/v)*), which was freshly made from a 10 mM stock solution of **6.4a** in EtOH. Two aliquots (10.5 µL) of the ethanolic solution of the product were diluted with 94.5 µL of CH_3CN/0.05% TFA 25:75 (*v/v*), and 100 µL were analyzed by HPLC. Whereas one sample was only

used for quantification of the product by UV detection, the second sample was additionally monitored radiometrically to determine radiochemical purity (cf. Figure 6.2). The minor difference in retention times (t_R) of both chromatograms results from the setup of the UV and the radiodetector in series. The molarity of the ethanolic solution of **6.4b** was calculated from the mean of the peak areas, and the linear calibration curve was obtained from the peak areas of the standards. Yield: 1.70 µg (5.98 nmol, 9.6%).

Determination of the specific activity: An aliquot (5 µL, in duplicate) of the ethanolic solution was diluted with 445 mL of a mixture of CH_3CN and H_2O 25:75 (*v/v*) in duplicate, and 50 µL of 1:300 dilutions were counted three times in Rotiszint eco plus (3 mL) in a LS 6500 liquid scintillation counter (Beckmann Coulter, München, Germany). The total activity in the stock solution amounted to 17.3 MBq (0.468 mCi), corresponding to a calculated specific activity of 2.90 TBq/mmol (78.3 Ci/mmol). The activity of the stock solution was adjusted to 9.25 MBq/ml, (0.25 mCi/ml, c = 2.99 µM) by adding EtOH/H_2O 1:1 (*v/v*). HPLC analysis showed a radiochemical purity of >97%. The identity of the radioligand was confirmed by HPLC analysis of labeled **6.4b** and unlabeled **6.4a** under the same conditions, resulting in identical retention times. The radioligand **6.4b** was stored at –20 °C.

Control of chemical stability of [^{3}H]JNJ7777120 by HPLC: 1 µL of the adjusted stock solution of [^{3}H]JNJ7777120 (a_v: 9.25 MBq/ml) in EtOH/H_2O 1:1 (*v/v*) was diluted with 109 µL of CH_3CN/0.05% TFA 25:75 (*v/v*) to a total volume of 110 µL. 100 µL of this solution were injected into the HPLC system and analyzed by radiometric detection. Gradient: 0.05% TFA in CH_3CN/0.05% TFA in H_2O: 0 min 25:75 (*v/v*), 30 min 25:75 (*v/v*), 31 min 95:5 (*v/v*), 40 min 95:5 (*v/v*).

6.5.3 Radioligand binding assay for the hH_xR

See Chapter 5.4.3

6.5.4 Saturation binding assay for the mH_4R

Saturation binding experiments using HEK293-SF-mH4R-His6 cells were performed by Dr. Uwe Nordemann in our research group as described previously.[30]

6.6 References

1. Jablonowski, J. A.; Grice, C. A.; Chai, W.; Dvorak, C. A.; Venable, J. D.; Kwok, A. K.; Ly, K. S.; Wei, J.; Baker, S. M.; Desai, P. J.; Jiang, W.; Wilson, S. J.; Thurmond, R. L.; Karlsson, L.; Edwards, J. P.; Lovenberg, T. W.; Carruthers, N. I. The First Potent and Selective Non-Imidazole Human Histamine H_4 Receptor Antagonists. *J. Med. Chem.* **2003**, 46, 3957-3960.
2. Venable, J. D.; Cai, H.; Chai, W.; Dvorak, C. A.; Grice, C. A.; Jablonowski, J. A.; Shah, C. R.; Kwok, A. K.; Ly, K. S.; Pio, B.; Wei, J.; Desai, P. J.; Jiang, W.; Nguyen, S.; Ling, P.; Wilson, S. J.; Dunford, P. J.; Thurmond, R. L.; Lovenberg, T. W.; Karlsson, L.; Carruthers, N. I.; Edwards, J. P. Preparation and biological evaluation of indole, benzimidazole, and thienopyrrole piperazine carboxamides: potent human histamine H_4 antagonists. *J. Med. Chem.* **2005**, 48, 8289-8298.
3. Thurmond, R. L.; Desai, P. J.; Dunford, P. J.; Fung-Leung, W. P.; Hofstra, C. L.; Jiang, W.; Nguyen, S.; Riley, J. P.; Sun, S.; Williams, K. N.; Edwards, J. P.; Karlsson, L. A potent and selective histamine H_4 receptor antagonist with anti-inflammatory properties. *J. Pharmacol. Exp. Ther.* **2004**, 309, 404-413.
4. Jiang, W.; Lim, H. D.; Zhang, M.; Desai, P.; Dai, H.; Colling, P. M.; Leurs, R.; Thurmond, R. L. Cloning and pharmacological characterization of the dog histamine H_4 receptor. *Eur. J. Pharmacol.* **2008**, 592, 26-32.
5. Coruzzi, G.; Adami, M.; Guaita, E.; de Esch, I. J.; Leurs, R. Antiinflammatory and antinociceptive effects of the selective histamine H_4-receptor antagonists JNJ7777120 and VUF6002 in a rat model of carrageenan-induced acute inflammation. *Eur. J. Pharmacol.* **2007**, 563, 240-244.
6. Cowden, J. M.; Zhang, M.; Dunford, P. J.; Thurmond, R. L. The histamine H_4 receptor mediates inflammation and pruritus in Th2-dependent dermal inflammation. *J. Invest. Dermatol.* **2010**, 130, 1023-1033.
7. Deml, K. F.; Beermann, S.; Neumann, D.; Strasser, A.; Seifert, R. Interactions of histamine H_1-receptor agonists and antagonists with the human histamine H4-receptor. *Mol. Pharmacol.* **2009**, 76, 1019-1030.
8. Dunford, P. J.; O'Donnell, N.; Riley, J. P.; Williams, K. N.; Karlsson, L.; Thurmond, R. L. The histamine H_4 receptor mediates allergic airway inflammation by regulating the activation of CD4+ T cells. *J. Immunol.* **2006**, 176, 7062-7070.
9. Morgan, R. K.; McAllister, B.; Cross, L.; Green, D. S.; Kornfeld, H.; Center, D. M.; Cruikshank, W. W. Histamine 4 receptor activation induces recruitment of FoxP3+ T cells and inhibits allergic asthma in a murine model. *J. Immunol.* **2007**, 178, 8081-8089.
10. Roßbach, K.; Stark, H.; Sander, K.; Leurs, R.; Kietzmann, M.; Bäumer, W. The histamine H_4 receptor as a new target for treatment of canine inflammatory skin diseases. *Vet. Dermatol.* **2009**, 20, 555-561.
11. Roßbach, K.; Wendorff, S.; Sander, K.; Stark, H.; Gutzmer, R.; Werfel, T.; Kietzmann, M.; Baumer, W. Histamine H_4 receptor antagonism reduces hapten-induced scratching behaviour but not inflammation. *Exp. Dermatol.* **2009**, 18, 57-63.
12. Zampeli, E.; Thurmond, R. L.; Tiligada, E. The histamine H_4 receptor antagonist JNJ7777120 induces increases in the histamine content of the rat conjunctiva. *Inflamm. Res.* **2009**, 58, 285-291.
13. Beermann, S.; Glage, S.; Jonigk, D.; Seifert, R.; Neumann, D. Opposite Effects of Mepyramine on JNJ7777120-Induced Amelioration of Experimentally Induced Asthma in Mice in Sensitization and Provocation. *PLoS ONE* **2012**, 7, e30285.
14. Deiteren, A.; De Man, J. G.; Ruyssers, N. E.; Moreels, T. G.; Pelckmans, P. A.; De Winter, B. Y. Histamine H_4 and H_1 receptors contribute to postinflammatory visceral hypersensitivity. *Gut* **2014**.
15. Pini, A.; Somma, T.; Formicola, G.; Lucarini, L.; Bani, D.; Thurmond, R.; Masini, E. Effects Of A Selective Histamine H_4R Antagonist On Inflammation In A Model Of Carrageenan-Induced Pleurisy In The Rat. *Curr. Pharm. Des.* **2013**.
16. Martinel Lamas, D. J.; Carabajal, E.; Prestifilippo, J. P.; Rossi, L.; Elverdin, J. C.; Merani, S.; Bergoc, R. M.; Rivera, E. S.; Medina, V. A. Protection of radiation-induced damage to the hematopoietic system, small intestine and salivary glands in rats by JNJ7777120 compound, a histamine H_4 ligand. *PLoS ONE* **2013**, 8, e69106.

17. Cowden, J. M.; Yu, F.; Challapalli, M.; Huang, J. F.; Kim, S.; Fung-Leung, W. P.; Ma, J. Y.; Riley, J. P.; Zhang, M.; Dunford, P. J.; Thurmond, R. L. Antagonism of the histamine H_4 receptor reduces LPS-induced TNF production in vivo. *Inflamm. Res.* **2013**, 62, 599-607.
18. Matsushita, A.; Seike, M.; Okawa, H.; Kadawaki, Y.; Ohtsu, H. Advantages of histamine H_4 receptor antagonist usage with H_1 receptor antagonist for the treatment of murine allergic contact dermatitis. *Exp. Dermatol.* **2012**, 21, 714-715.
19. Seifert, R.; Schneider, E. H.; Dove, S.; Brunskole, I.; Neumann, D.; Strasser, A.; Buschauer, A. Paradoxical stimulatory effects of the "standard" histamine H_4-receptor antagonist JNJ7777120: the H_4 receptor joins the club of 7 transmembrane domain receptors exhibiting functional selectivity. *Mol. Pharmacol.* **2011**, 79, 631-638.
20. Schnell, D.; Brunskole, I.; Ladova, K.; Schneider, E.; Igel, P.; Dove, S.; Buschauer, A.; Seifert, R. Expression and functional properties of canine, rat, and murine histamine H_4 receptors in Sf9 insect cells. *Naunyn-Schmiedeberg's Arch. Pharmacol.* **2011**, 383, 457-470.
21. Liu, C.; Wilson, S. J.; Kuei, C.; Lovenberg, T. W. Comparison of human, mouse, rat, and guinea pig histamine H_4 receptors reveals substantial pharmacological species variation. *J. Pharmacol. Exp. Ther.* **2001**, 299, 121-130.
22. Lim, H. D.; de Graaf, C.; Jiang, W.; Sadek, P.; McGovern, P. M.; Istyastono, E. P.; Bakker, R. A.; de Esch, I. J.; Thurmond, R. L.; Leurs, R. Molecular determinants of ligand binding to H_4R species variants. *Mol. Pharmacol.* **2010**, 77, 734-743.
23. Zhu, Y.; Michalovich, D.; Wu, H.; Tan, K. B.; Dytko, G. M.; Mannan, I. J.; Boyce, R.; Alston, J.; Tierney, L. A.; Li, X.; Herrity, N. C.; Vawter, L.; Sarau, H. M.; Ames, R. S.; Davenport, C. M.; Hieble, J. P.; Wilson, S.; Bergsma, D. J.; Fitzgerald, L. R. Cloning, expression, and pharmacological characterization of a novel human histamine receptor. *Mol. Pharmacol.* **2001**, 59, 434-441.
24. Morse, K. L.; Behan, J.; Laz, T. M.; West, R. E., Jr.; Greenfeder, S. A.; Anthes, J. C.; Umland, S.; Wan, Y.; Hipkin, R. W.; Gonsiorek, W.; Shin, N.; Gustafson, E. L.; Qiao, X.; Wang, S.; Hedrick, J. A.; Greene, J.; Bayne, M.; Monsma, F. J., Jr. Cloning and characterization of a novel human histamine receptor. *J. Pharmacol. Exp. Ther.* **2001**, 296, 1058-1066.
25. Lim, H. D.; van Rijn, R. M.; Ling, P.; Bakker, R. A.; Thurmond, R. L.; Leurs, R. Evaluation of histamine H_1-, H_2-, and H_3-receptor ligands at the human histamine H_4 receptor: identification of 4-methylhistamine as the first potent and selective H_4 receptor agonist. *J. Pharmacol. Exp. Ther.* **2005**, 314, 1310-1321.
26. Jansen, F. P.; Rademaker, B.; Bast, A.; Timmerman, H. The first radiolabeled histamine H_3 receptor antagonist, [^{125}I]iodophenpropit: saturable and reversible binding to rat cortex membranes. *Eur. J. Pharmacol.* **1992**, 217, 203-205.
27. Igel, P.; Schnell, D.; Bernhardt, G.; Seifert, R.; Buschauer, A. Tritium-Labeled *N*^{1}-[3-(1*H*-imidazol-4-yl)propyl]-*N*^{2}-propionylguanidine ([^{3}H]UR-PI294), a High-Affinity Histamine H_3 and H_4 Receptor Radioligand. *ChemMedChem* **2009**, 4, 225-231.
28. Alves-Rodrigues, A.; Leurs, R.; Wu, T. S.; Prell, G. D.; Foged, C.; Timmerman, H. [^{3}H]-thioperamide as a radioligand for the histamine H_3 receptor in rat cerebral cortex. *Br. J. Pharmacol.* **1996**, 118, 2045-2052.
29. Wifling, D.; Löffel, K.; Nordemann, U.; Strasser, A.; Bernhardt, G.; Dove, S.; Seifert, R.; Buschauer, A. Molecular determinants for the high constitutive activity of the human histamine H_4 receptor: Functional studies on orthologs and mutants. *Br. J. Pharmacol.* **2014**, in press, doi: 10.1111/bph.12801.
30. Nordemann, U. Radioligand binding and reporter gene assays for histamine H_3 and H_4 receptor species orthologs. University of Regensburg, Regensburg, Doctoral thesis, **2013**.
31. Kenakin, T. P. A pharmacology primer : theory, applications, and methods. In Boston: Academic Press/Elsevier: Amsterdam, **2009**; Vol. xix, p 389 pp.
32. Lazareno, S. Quantification of receptor interactions using binding methods. *J. Recept. Signal. Transduct. Res.* **2001**, 21, 139-165.
33. Bylund, D. B.; Toews, M. L. Radioligand binding methods: practical guide and tips. *Am. J. Physiol.* **1993**, 265, L421-429.

34. Bernat, V.; Heinrich, M. R.; Baumeister, P.; Buschauer, A.; Tschammer, N. Synthesis and application of the first radioligand targeting the allosteric binding pocket of chemokine receptor CXCR3. *ChemMedChem* **2012**, 7, 1481-1489.
35. Geyer, R.; Kaske, M.; Baumeister, P.; Buschauer, A. Synthesis and functional characterization of imbutamine analogs as histamine H_3 and H_4 receptor ligands. *Arch. Pharm.* **2014**, 347, 77-88.
36. Cheng, Y.; Prusoff, W. H. Relationship between the inhibition constant (K_1) and the concentration of inhibitor which causes 50 per cent inhibition (I_{50}) of an enzymatic reaction. *Biochem. Pharmacol.* **1973**, 22, 3099-3108.
37. Igel, P.; Dove, S.; Buschauer, A. Histamine H_4 receptor agonists. *Bioorg. Med. Chem. Lett.* **2010**, 20, 7191-7199.
38. Igel, P.; Geyer, R.; Strasser, A.; Dove, S.; Seifert, R.; Buschauer, A. Synthesis and structure-activity relationships of cyanoguanidine-type and structurally related histamine H_4 receptor agonists. *J. Med. Chem.* **2009**, 52, 6297-6313.
39. Savall, B. M.; Edwards, J. P.; Venable, J. D.; Buzard, D. J.; Thurmond, R.; Hack, M.; McGovern, P. Agonist/antagonist modulation in a series of 2-aryl benzimidazole H4 receptor ligands. *Bioorg. Med. Chem. Lett.* **2010**, 20, 3367-3371.
40. Lu, C. F.; Xie, C.; Chen, Z. X.; Yang, G. C. Synthesis of new soluble dendrimers on poly(ethylene glycol) sublayer. *Russian Journal of Organic Chemistry* **2009**, 45, 788-791.
41. Bradbury, B. J.; Baumgold, J.; Paek, R.; Kammula, U.; Zimmet, J.; Jacobson, K. A. Muscarinic receptor binding and activation of second messengers by substituted *N*-methyl-*N*-[4-(1-azacycloalkyl)-2-butynyl]acetamides. *J. Med. Chem.* **1991**, 34, 1073-1079.
42. Carruthers, N. I.; Chai, W.; Dvorak, C. A.; Edwards, J. P.; Grice, C. A.; Jablonowski, J. A.; Karlsson, L.; Khatuya, H.; Kreisberg, J. D.; Kwok, A. K.; Lovenberg, T. W.; Ly, K. S.; Pio, B.; Shah, C. R.; Sun, S.; Thurmond, R. L.; Wei, J.; Xiao, W. Preparation of piperazinylcarbonylindoles as histamine H_4 antagonists. WO2002072548A2, **2002**.

Chapter 7

Subtype-selective Nonpeptide Radioligands for the NPY Y_2 Receptor

7.1 Introduction

The (*S*)-configured arginine-amide BIIE 0246, the first potent and selective Y_2R receptor (Y_2R) antagonist, has been widely used as a pharmacological tool for the investigation of the physiological role of the Y_2R.[1] Aiming at potent and subtype selective tracers for the Y_2R, a series of derivatives of BIIE 0246 was synthesized.[3] Application of the guanidine-acylguanidine bioisosteric approach resulted in the first tritiated Y_2R selective non-peptide radioligand, [^{3}H]UR-PLN196.[2] More detailed binding and functional studies of UR-PLN196 revealed insurmountable antagonism versus pNPY and pseudo-irreversible binding at the Y_2R. Here the synthesis and characterization of [^{3}H]UR-PLN208, a structurally related radiotracer is reported and binding as well as functional data are compared with those of [^{3}H]UR-PLN196 and the unlabeled analogs.

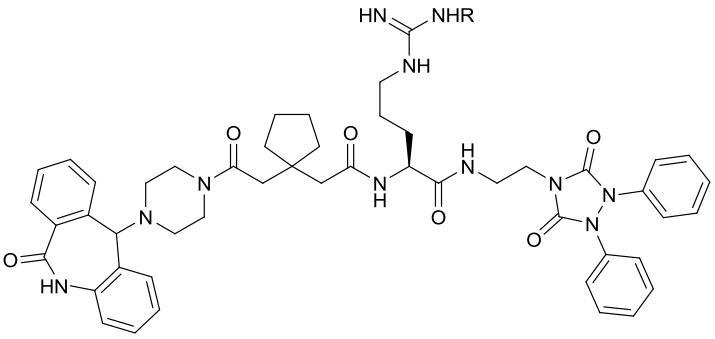

R =		K_d	K_b	K_i
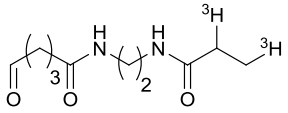	[^{3}H]UR-PLN196	67 nM	9.9 nM	16 nM
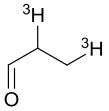	[^{3}H]UR-PLN208	20 nM	8.2 nM	5.2 nM
H	BIIE 0246	-	5.6 nM	2.6 nM

Figure 7.1 Structure and pharmacological profile of BIIE 0246[1] and the argininamide-type radioligands [^{3}H]UR-PLN196[2] and [^{3}H]UR-PLN208.

7.2 Results and Discussion

7.2.1 Synthesis of [^{3}H]UR-PLN208

[^{3}H]UR-PLN208 was synthesized, as the 'cold' analog showed improved binding affinity compared to the previously prepared radioligand [^{3}H]UR-PLN196 (K_i = 5.2 nM vs. 16 nM) in a flow cytometric binding assay, using CHO cells stably expressing the human Y_2 receptor (hY_2R)[4] and fluorescence-labeled pNPY (Cy5-pNPY or Dy-635- pNPY).[5] Antagonistic activity (K_b = 8.2 nM) was proven in a spectrofluorimetric Ca^{2+} assay (Fura-2 assay)[6] with CHO cells stably expressing the hY_2R compared to UR-PLN196.[2] Moreover, high selectivity for the hY_2R over the other hY_xR-subtypes was observed for UR-PLN208 (K_i values: hY_1R: >3500 nM; hY_4R: >6500 nM; hY_5R: >5000 nM).[7]

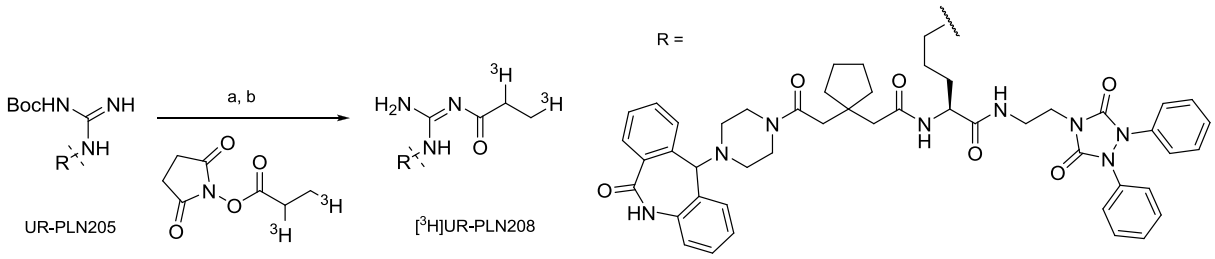

Scheme 7.1 Synthesis of [^{3}H]UR-PLN208. Reagents and conditions: a) UR-PLN205, succinimidyl [2,3-^{3}H]-propionate, NEt_3, MeCN, rt, 16 h; b) TFA, rt, 2 h, 7.9%.

[^{3}H]UR-PLN208 was obtained by direct acylation of UR-PLN205, the mono-Boc protected analog of BIIE 0246, with commercially available succinimidyl [2,3-$^3H_2$]propionate in the presence of triethylamine followed by *in situ* deprotection with TFA (Scheme 7.1). After purification by HPLC, the radioligand was obtained with a high specific activity (a_s) of 75 Ci/mmol in radiochemical purity of >99% (cf. Figure 7.2), similar to [^{3}H]UR-PLN196 (81 Ci/mmol; radiochemical purity >99%). The identity of the radioligand was confirmed by HPLC analysis of labeled and unlabeled UR-PLN208. Furthermore, chemical stability in ethanol at -20 °C was proven over a period of at least 12 months (cf. Figure 7.3).

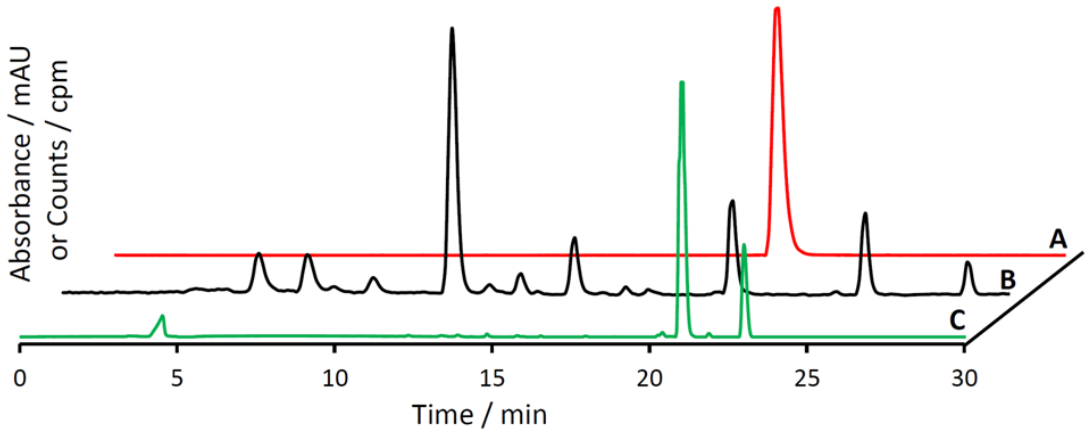

Figure 7.2 Identity and purity control of [^{3}H]UR-PLN208. A: Purity control after isolation by HPLC (radiochromatogram). B: Reaction control after 18 h. C: UV (λ = 220 nm) chromatogram of the reaction control spiked with 'cold' UR-PLN208, c = 100 µM; gradient: CH_3CN/0.1% TFA in H_20: 0 min: 25:75 (*v/v*), 30 min: 90:10 (*v/v*), 40 min 90:10 (*v/v*).

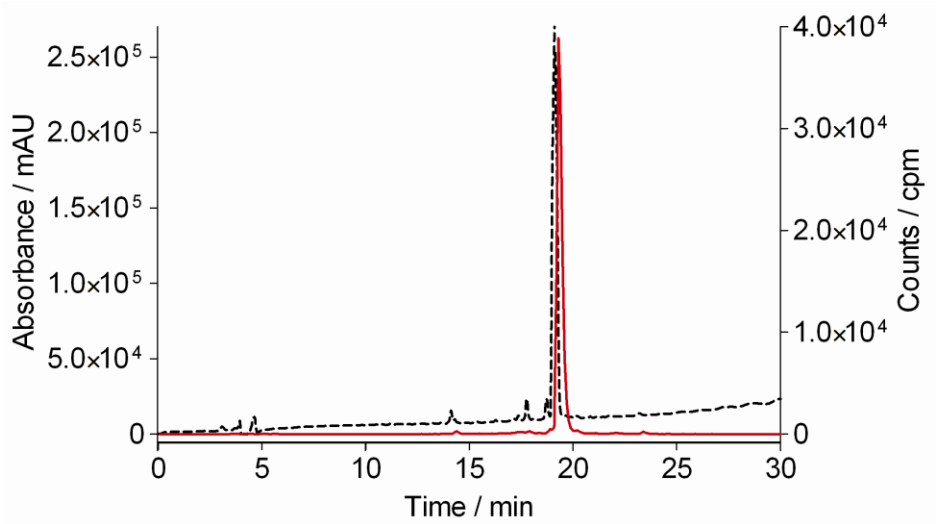

Figure 7.3 Long-term stability of [^{3}H]UR-PLN208. Example of a radiochromatogram (red solid line) after storage in ethanol (+ 50 µM TFA) at -20 °C for a period of 12 months. The identity of [^{3}H]UR-PLN208 was confirmed by spiking with larger amounts of the 'cold' form of UR-PLN208 (c = 100 µM), which allowed UV detection (black dashed line). The minor difference in retention times (t_R) of both chromatograms results from the setup of the UV and the radiodetector in series. gradient: CH_3CN/0.1% TFA in H_20: 0 min: 25:75 (*v/v*), 30 min: 90:10 (*v/v*), 40 min 90:10 (*v/v*).

7.2.2 Pharmacological characterization of [^{3}H]UR-PLN208 and 'cold' analogs at CHO-hY_2R cells

7.2.2.1 Determination of binding constants of [^{3}H]UR-PLN208

The radioligand [^{3}H]UR-PLN208 was characterized by saturation binding experiments within a concentration range of 0.5 to 150 nM using CHO-hY_2R cells as shown in Figure 7.4. For these experiments special surface-modified plates (BD Primaria 96-well plates; Becton Dickinson GmbH, Germany) were used to reduce the adsorption of the radioligand to the plastic as reported previously.[7] Nonspecific binding was determined in the presence of BIIE 0246 (30-fold concentrated), a structurally related antagonist, or pNPY (100-fold concentrated), a peptidic agonist. Nonspecific binding in the presence of pNPY was more than twice as high (~60%) as in the presence of BIIE 0246 (~25%). This may be interpreted a hint to different binding modes of peptidic (endogenous) Y_2R ligands and non-peptidic BIIE 0246-type antagonists, binding of the radioligand, at least in part, to a site distinct from the peptide agonist binding site. Most probably, the Y_2R binding sites of BIIE 0246-like antagonists and NPY overlap only partially,[8] as also reported for other GPCRs.[9] It is also conceivable that cellular uptake of the radioligand is involved, e. g. via transporters, which could be occupied by BIIE 0246, resulting in reduced [^{3}H]UR-PLN208 uptake and unspecific binding, respectively.[10] Hence, the maximum number of binding sites (B_{max}) amounted to approximately 387,000 and 108,000 per cell in the presence of BIIE 0246 pNPY, respectively. Regardless of that, [^{3}H]UR-PLN208 bound in a saturable manner in both experiments with similar K_d values up to a

concentration of 40 nM, ($K_{d(pNPY)}$ = 23.5 ± 2.3 nM, $K_{d(BIIE\ 0246)}$ = 19.2 ± 2.3 nM; $K_{d(\Sigma)}$ 21.3 ± 1.8 nM; Figure 7.4 C, D). A more complex binding behavior became obvious when concentrations higher than 40 nM of [^{3}H]UR-PLN208 were taken into account. Between 50 and 150 nM, specific binding of [^{3}H]UR-PLN208 increased again and was saturable, fitted by nonlinear regression with a K_d value of approximately 100 nM (Figure 7.4 A, B). For elucidation of a real second binding site, higher concentrations of [^{3}H]UR-PLN208 would be required to achieve saturation. Unfortunately, the radioligand was not available in sufficiently large amount.

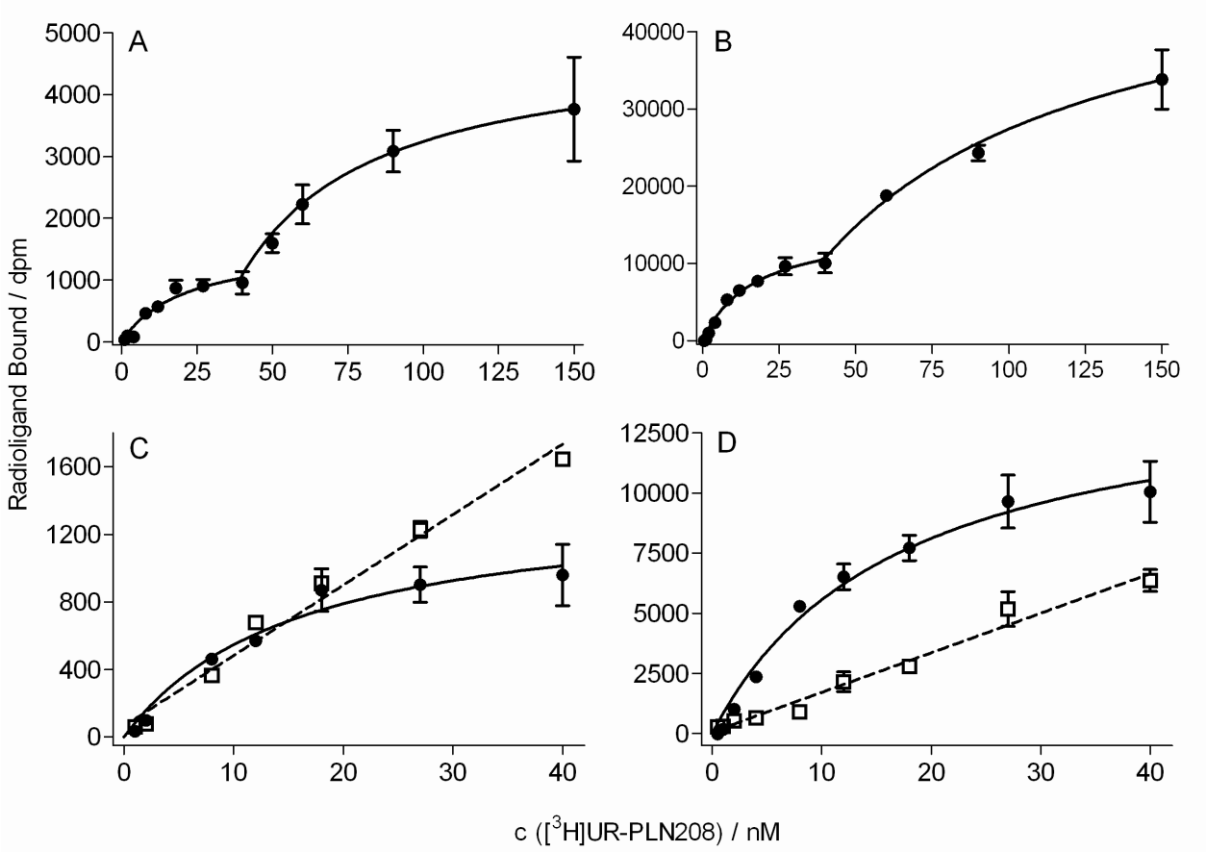

Figure 7.4 Saturation binding of [^{3}H]UR-PLN208 at CHO-hY2R cells. A: Biphasic curve (c([^{3}H]UR-PLN208) = 0-150 nM); Nonspecific binding determined by co-incubation with: pNPY (100-fold concentration of [^{3}H]UR-PLN208); specific binding: ●; nonspecific binding: not shown cf. appendix; $K_{d(sat)low}$ = 23.5 ± 2.3 nM; $K_{d(sat)high}$ = 66.2 ± 6.9 nM. B: Biphasic curve (c([^{3}H]UR-PLN208) = 0-150 nM); Nonspecific binding determined by co-incubation with: BIIE 0246 (30-fold concentration of [^{3}H]UR-PLN208); specific binding: ●; nonspecific binding: not shown cf. appendix; $K_{d(sat)low}$ = 19.2 ± 2.3 nM; $K_{d(sat)high}$ = 107.7 ± 29.3 nM. C: Monophasic curve (c([^{3}H]UR-PLN208) = 0-40 nM); Nonspecific binding determined by co-incubation with: pNPY (100-fold concentration of [^{3}H]UR-PLN208); specific binding: ●; nonspecific binding: □; $K_{d(sat)}$ = 23.5 ± 2.3 nM. D: Monophasic curve (c([^{3}H]UR-PLN208) = 0-40 nM); Nonspecific binding determined by co-incubation with: BIIE 0246 (30-fold concentration of [^{3}H]UR-PLN208); specific binding: ●; nonspecific binding: □; $K_{d(sat)}$ = 19.2 ± 2.3 nM. n = 2; best fitted by nonlinear regression for specific binding and linear regression for nonspecific binding; mean values ± SEM, performed in triplicate.

In short, binding was saturable up to a concentration of 40 nM, but there were differences in the portion of specific binding compared to nonspecific binding depending on the chosen competitor. The results suggest the existence of a second binding site, which is sensitive to BIIE 0246-related

compounds, but this could not be proven due to limited amounts of available radioligand. In contrast, [^{3}H]UR-PLN196 did not show such discrepancies in saturation experiments up to a concentration of 150 nM. Yet, as the K_d value of [^{3}H]UR-PLN196 (67 nM)[2] for the so-called high-affinity binding site was higher than that of [^{3}H]UR-PLN208, presumably, a second binding site might not have been detected within the investigated concentration range (up to 200 nM).

Table 7.1 Saturation binding parameters of [^{3}H]UR-PLN208 at CHO-hY_2R cells.

Competitor	K_d / nM	Estimated B_{max} (sites / cell).
BIIE 0246[a]	19.2 ± 2.3 (high)[b]	387,400
	107.7 ± 29.3 (low)[b]	1,107,500
pNPY[c]	23.5 ± 2.3 (high)[b]	107,500
	66.2 ± 6.9 (low)[b]	271,000
Mean value[d]	21.3 ± 1.8[e]	-

[a] 30-fold concentration of [^{3}H]UR-PLN208; [b] n = 2; [c] 30-fold concentration of [^{3}H]UR-PLN208; [d] mean value of 4 independent experiments (high affintiy binding site), twice performed with BIIE 0246 as competitor, twice with pNPY; [e] n = 4.

7.2.2.2 Association and dissociation kinetics of [^{3}H]UR-PLN208

In spite of differences regarding saturation binding, the analysis of the association kinetics for the specific Y_2R binding of [^{3}H]UR-PLN196 and [^{3}H]UR-PLN208 at CHO-hY_2R cells revealed comparable results. In both cases, association was almost complete after 30 minutes (cf. Figure 7.5 A). In dissociation experiments the residual specific binding of the tritiated compounds amounted to approximately 25% for [^{3}H]UR-PLN196 and 60% for [^{3}H]UR-PLN208 after preincubation of the CHO-hY_2R cells with the respective radioligand for 60 min (cf. Figure 7.5 B). Dissociation was induced by removing the free radioligand by suction and addition of a 100-fold excess of BIIE 0246 to prevent reassociation. For both radioligands the results suggest in part irreversible binding to a specific binding site. Further possible explanations for such a behavior are a slow rate of dissociation from the receptor,[11] a slow rate of interconversion between inactive and active receptor conformations,[12,13] or stabilization of an inactive ligand (antagonist)-specific receptor conformation.[14]

To elucidate if the residual binding of [^{3}H]UR-PLN208 is time-dependent, the dissociation experiment was repeated with different periods of preincubation 30 and 90 min. However, the amount of residual binding remained unchanged (data not shown). A preincubation period shorter than 30 min

is inappropriate due to incomplete association as shown before. Therefore, a time-dependency of the incomplete dissociation could not be detected in the evaluable time range.

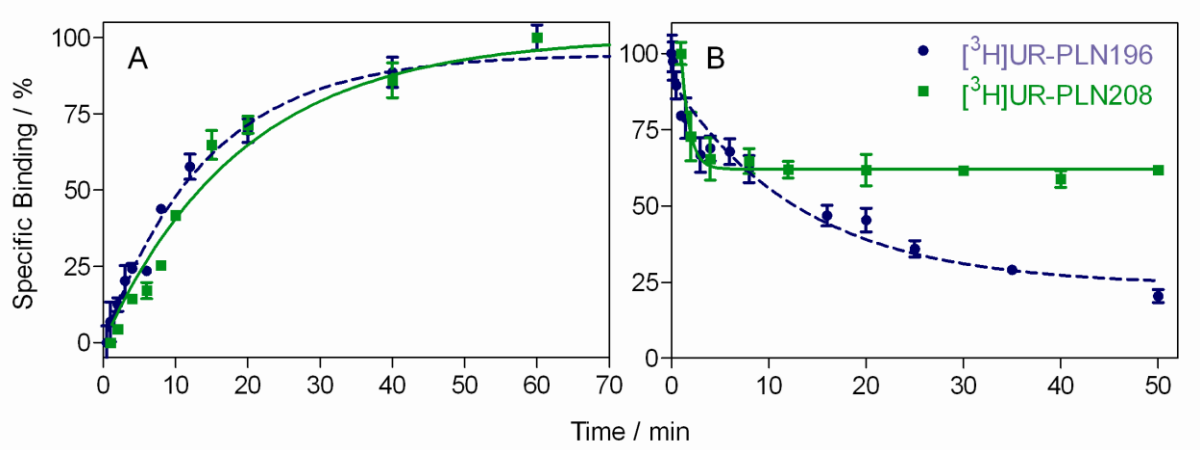

Figure 7.5 Association and dissociation kinetics of [^{3}H]UR-PLN196 and [^{3}H]UR-PLN208 at CHO-hY_2R cells. A: Radioligand association kinetics ([^{3}H]UR-PLN196 (c = 75 nM, ●, blue curve); [^{3}H]UR-PLN208 (c = 30 nM, ■, green curve)). B: Radioligand dissociation kinetics ([^{3}H]UR-PLN196 (c = 75 nM, ●, blue curve); [^{3}H]UR-PLN208 (c = 30 nM, ■, green curve), preincubation for 60 min)), monophasic exponential fit, dissociation performed in the presence of a 100-fold excess of BIIE 0246.

7.2.2.3 Competition binding experiments

Contrary to the incomplete dissociation in kinetic studies, the radioligands [^{3}H]UR-PLN196 and [^{3}H]UR-PLN208 were completely displaceable in competition binding studies. Interestingly, tremendous discrepancies became obvious when competitors of different chemical nature were used. In case of nonpeptide Y_2R antagonists (BIIE 0246,[1] SF-11[15] and CMY9484[16]) (for structures see Chapter 1) the displacement was monophasic (cf. Table 7.2 A). The peptidic agonist pNPY displaced [^{3}H]UR-PLN196 in a biphasic manner, indicative of a high (K_i = 2.0 nM) and a low affinity binding site (K_i = 1300 nM, cf. Table 7.2 B).[2] By contrast, displacement of [^{3}H]UR-PLN208 with pNPY revealed only a low affinity binding site (K_i = 2100 nM), suggesting either pseudo-irreversible binding or stabilization of a ligand specific Y_2R conformation. When the competition binding experiment was performed in an inverse manner, that is to say by displacing Dy-635-pNPY with 'cold' UR-PLN196 in a flow cytometric assay, the K_i value of UR-PLN196 was comparable with the K_d value of [^{3}H]UR-PLN196.[2]

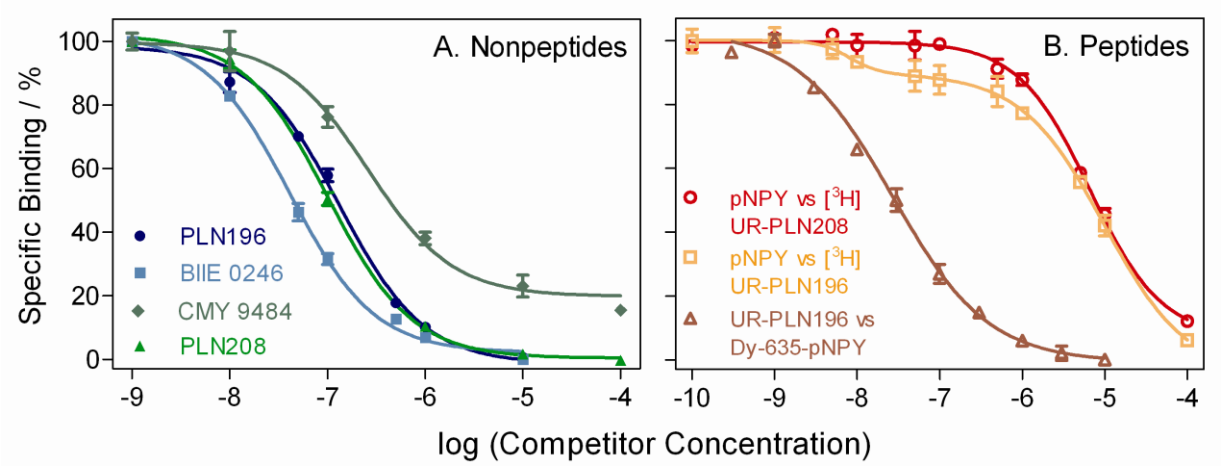

Figure 7.6 A. Displacement of [^{3}H]UR-PLN208 by hY_2R antagonists at CHO-hY_2R cells. B. Competition binding experiments of different radio- and fluorescent ligands. Data represent the mean ± SEM (n=2–5, see also Table 7.2).

Such differences became also obvious when [^{3}H]UR-PLN208 was displaced with the peptidic ligands pPYY, hPP, $pNPY_{13-36}$ and $pNPY_{22-36}$. The hY_2R affinity was at least 70-fold lower than data obtained from the displacement of [^{3}H]pNPY or Dy-635-pNPY. This indicates that the apparent discrepancies at the hY_2R are characteristic for peptidic agonists, when BIIE 0246-type radioligands are used. In competition binding experiments with peptidic agonists such as pNPY, an incubation time of at least 90 min is recommended, due to slow association of pNPY to the receptor.[17] To clarify if the displacement curve as shown in Figure 7.6 B (○, pNPY vs [^{3}H]UR-PLN208) is time-dependent, the incubation time was set to 60 or 120 min, respectively. The received K_i values and the shape of the curves revealed no differences in the displacement of pNPY by [^{3}H]UR-PLN208 between 60 and 120 min (cf. Figure 7.7).

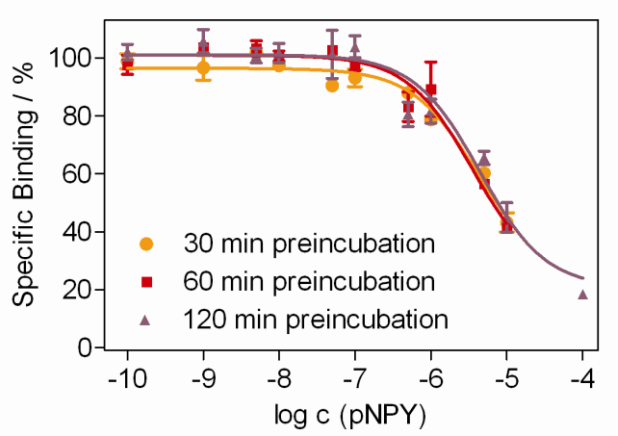

Incubation time / min	**hY_2R**
	K_i (pNPY) /nM
30	1630
60	1410
120	1750

Figure 7.7 Displacement of [^{3}H]UR-PLN208 by pNPY at CHO-hY_2R cells after different periods of incubation. hY_2R radioligand binding assay on CHO cells, stably expressing the hY_2R; radioligand: [^{3}H]UR-PLN208 (20 nM); incubation time: 30 min (●, orange curve, K_i = 1630 nM); 60 min (■, red curve, K_i = 1410 nM); 120 min (▲, brown curve, K_i = 1750 nM).

Table 7.2 K_i values of hY_2R ligands, determined with [^{3}H]UR-PLN196, [^{3}H]UR-PLN208, Dy-635-pNPY or [^{3}H]pNPY, and functional data at CHO-hY_2R cells; **A**: Nonpeptidic antagonists, **B**: Peptidic agonists.

	Compound	**hY_2R binding: K_i / nM, determined with**				**hY_2R antagonism:**
		[^{3}H]UR-PLN196[a]	[^{3}H]UR-PLN208[b]	Cy5-pNPY[c]	[^{3}H]pNPY[d]	K_b[e] or (IC_{50})[f] / nM
A	PLN196	47 ± 7	80 ± 13	9.9 ± 1[g]	n.d.	16 ± 8[g]
	PLN208	33 ± 7	39 ± 1	5.2 ± 2[g]	n.d.	8.2 ± 0[g]
	BIIE 0246	17 ± 3	21 ± 5	2.6 ± 1.2[h]	24.2[l]	6.0 ± 0[h]
	SF11[f]	2800 ± 710	840 ± 110	1300 ± 350[i]	n.d.	(190 ± 10)[j]
	CMY 9484	8.3 ± 0.5	200 ± 64	n.d.	n.d.	(19)[i]
B	pNPY: K_i high	**2.0 ± 1.1**	-	**0.8 ± 0.2**[k]	**0.4 ± 0.1**[k]	n.d.
	low	**1300 ± 700**	**2100 ± 170**	-	-	
	$pNPY_{13-36}$	n.d.	3600 ± 87	1.7 ± 0.4[k]	1.7 ± 0.4[k]	n.d.
	$pNPY_{22-36}$	n.d.	9800 ± 2200	110 ± 37[j]	n.d.	n.d.
	hPP	n.d.	5000 ± 1700	n.d.	68 ± 1[l]	n.d.
	pPYY	n.d.	n.a.[m]	0.4 ± 1[k]	0.06 ± 0.01[k]	n.d.

[a] hY_2R radioligand binding assay with CHO cells, stably expressing the hY_2R; radioligand: [^{3}H]UR-PLN196 (75 nM); [b] hY_2R radioligand binding assay on CHO cells, stably expressing the hY_2R; radioligand: [^{3}H]UR-PLN208 (20 nM); [c] hY_2R flow cytometric competition binding assay on CHO cells, stably expressing the hY_2R; fluorescent ligand: Cy5-pNPY (5 nM); [d] hY_2R radioligand binding assay with CHO cells, stably expressing the hY_2R; radioligand: [^{3}H]pNPY (1 nM); [e] inhibition of pNPY (70 nM)-induced $[Ca^{2+}]_i$ mobilization in hY_2R-expressing CHO cells; [f] data from a Y_2R cAMP biosensor assay; [g] Pluym *et al*. 2013;[2] [h] Pluym *et al*. 2011;[3] [i] Pluym, N. 2011;[7] [j]Kaske, M. 2012;[18] [k]Ziemek *et al*. 2006;[4] [l] Ziemek, R. 2006;[19] [m] up to a concentration of 10 µM. incubation time: 30-90 min, mean values ± SEM, n = 2-5, n.d. means not determined.

7.2.2.4 Calcium assay on hY_2R-expressing CHO cells

Y_2R antagonism of UR-PLN196 and UR-PLN208 was investigated in a Fura-2 based Ca^{2+} assay on hY_2R-expressing CHO cells, revealing K_b values of 16 nM for UR-PLN196 and 8.2 nM for UR-PLN208, respectively. Moreover, concentration-response curves (CRCs) of NPY were constructed in the absence and presence of different concentrations of the antagonist UR-PLN196.[2] Simultaneous addition of pNPY and UR-PLN196 suggested competitive antagonism. By contrast, pretreatment with UR-PLN196 for 20 min caused a decrease in the maximal agonist response in a concentration-dependent manner, indicating insurmountable antagonism against pNPY by analogy with previous reports on BIIE 0246.[20,4] In addition to concentration-dependency of insurmountable antagonism, time-dependency was investigated. The concentrations of pNPY and the antagonists UR-PLN196 or UR-PLN208 were kept constant and the time interval between addition of the antagonist and pNPY was varied as shown in Figure 7.8. The depression of the maximal response to pNPY (c = 300 nM) by

UR-PLN196 proved to be both concentration- and time dependent: At a concentration of 30 nM of UR-PLN196 the maximum response of pNPY was reduced to 60% after 20 minutes, at a concentration of 75 nM the effect of pNPY amounted to 40% after the same time. Pretreatment with 30 nM of UR-PLN208 for 10 minutes completely inhibited the Ca^{2+} response of pNPY (c = 300 nM). These results were in good accordance to the incomplete dissociation rates for both radioligands from the receptor in dissociation experiments. Apart from classical irreversible binding, the aforementioned stabilization of an inactive ligand (antagonist)-specific receptor conformation[14], which is not accessible for pNPY any longer, could explain this phenomenon.

Irreversibly binding antagonists could be useful tools for the determination of spare receptors. Lipophilic antagonists capable of stabilizing the receptor in an inactive state, have been taken for co-crystallization of different GPCRs.[21-23] Therefore, the (pseudo)irreversibly binding BIIE-type ligands might be useful for the crystallization of the NPY Y_2R.

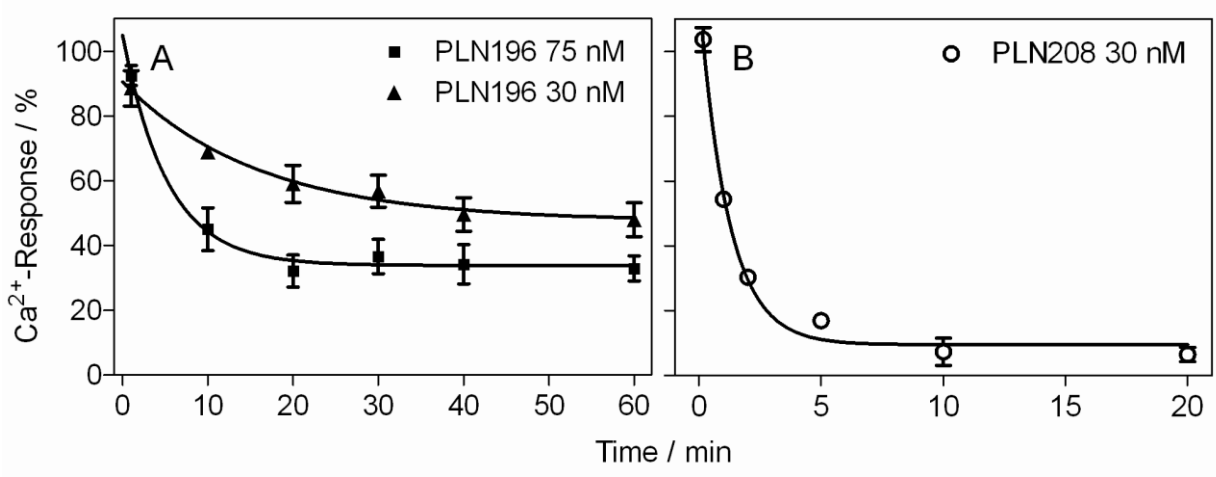

Figure 7.8 Time course of the pNPY (c = 300 nM)-induced Ca^{2+} signal in the presence of BIIE 0246-type antagonists. Fura-2 assay on CHO-hY_2R cells performed after pretreatment of the cells with UR-PLN196 (**A**: ▲: c = 30 nM; ■: c = 75 nM) or UR-PLN208 (**B**: ○: c = 30 nM) for different periods of time; mean values ± SEM, n = 2-3.

7.2.3 Pharmacological characterization of [^{3}H]UR-PLN208 and non-labeled analogs on the hY_2R at Sf9 insect cell membranes

7.2.3.1 hY_2R antagonist activity of BIIE 0246 and related compounds in thesteady-state [γ-^{33}P]GTPase assay

The steady-state [γ-^{33}P]GTPase activity assay using the baculovirus/Sf9 cell system has been established as a reliable functional readout for the analysis of hY_2R ligands.[24] It is characterized by a high signal-to-noise ratio and the proximal readout avoids bias from downstream signaling.[25] Therefore, the GTPase assay is well suited to complement the data from the Fura-2 assay, to

compare K_b values from different readouts and to examine, whether insurmountable antagonism of BIIE 0246-related compounds is detectable in the GTPase assay too. As displayed in Table 7.3, the K_b values for BIIE 0246 ($K_{b(GTPase)}$ = 11.9 ± 1.7), UR-PLN74 ($K_{b(GTPase)}$ = 4.2 ± 0.1, structure is shown in Figure 7.11), UR-PLN196 ($K_{b(GTPase)}$ = 4.3 ± 1.6) and UR-PLN208 ($K_{b(GTPase)}$ = 8.3 ± 0.5) determined in the GTPase assay, were in good accordance to the K_b values determined in the Fura-2 assay.[2,3] Also for SF11, a Y_2R antagonist with a different scaffold, the determined K_b value of 59.0 ± 34.5 was in the same range as published data.[15]

Table 7.3 hY_2R antagonism of selected ligands the GTPase assay compared to reported data from functional and binding assays.

Compound	**hY_2R**			
	$K_{b(GTPase)}$ / nM[a]	n	$K_{b(Ca\text{-}assay)}$ or (IC_{50}) / nM[b]	K_i / nM[c]
BIIE 0246	11.9 ± 1.7	2	5.6 ± 0.4[d]	2.6 ± 1.2[d]
UR-PLN74	4.2 ± 0.1	2	1.8 ± 0.2[e]	3.2 ± 0.3[e]
UR-PLN196	4.3 ± 1.6	4	16 ± 8[e]	9.9 ± 1.0[e]
UR-PLN208	8.3 ± 0.5	4	8.2 ± 0.4[e]	5.2 ± 1.8[e]
SF11[f]	59.0 ± 34.5	2	(190 ± 10)[f]	1.6 ± 0.9[f]

[a] Steady-state GTPase assay on membranes of Sf9 cells expressing the hY_2R + $G\alpha_{i2}$ + $G\beta_1\gamma_2$, mean values ± SEM, performed in duplicate, K_b values were calculated according to the Cheng-Prusoff equation;[26] [b] inhibition of pNPY (70 nM)-induced $[Ca^{2+}]_i$ mobilization in hY_2R-expressing CHO cells; mean values ± SEM; [c] K_i values were determined in a flow cytometric binding assay from the displacement of Cy5-pNPY (K_d=5.2 nM, c=5 nM) at CHO-hY_2R cells; [d] Pluym *et al.* 2011;[3] [e] Pluym *et al.* 2013;[2] [f] Brothers *et al.* 2010;[15] IC_{50} obtained from an antagonist concentration-response curve in a Y_2R cAMP biosensor assay, K_i obtained from displacement of ^{125}I-PYY from Y_2R-expressing cells.

To investigate if the maximum response of pNPY is reduced by BIIE 0246-type antagonists in the GTPase assay, the typical experimental procedure was modified. Instead of inducing the maximum response of the system by the addition of pNPY at first, followed by addition of the antagonists, the receptor ligands were added in inverse order. Different concentrations of UR-PLN196 or UR-PLN208 were incubated with the Y_2R containing cell membranes in the absence of pNPY for different periods of time (0, 15, 30 min) followed by addition of pNPY (c = 100 nM). The minimum and maximum values were compared among the concentration response curves as well as the K_b values determined at different time points. Neither UR-PLN196 nor UR-PLN208 showed significant changes in maximal responses or K_b values (cf. Figure 7.9 and Table 7.4), which would be expected in case of insurmountable antagonism. It is difficult to provide a satisfactory explanation for the discrepancy between the results from GTPase and Ca^{2+} assay. These two artificial test systems are different, using insect cell membranes and mammalian cells, respectively, distinct functional readouts (GTPase

activity vs. Ca^{2+}-signal) and a different experimental setup. It is worth mentioning that the addition of BIIE 0246-related compounds without the addition of pNPY did not reduce the constitutive activity of the hY_2R in the GTPase assay, indicating that these compounds do not act as inverse agonists but as neutral antagonists.

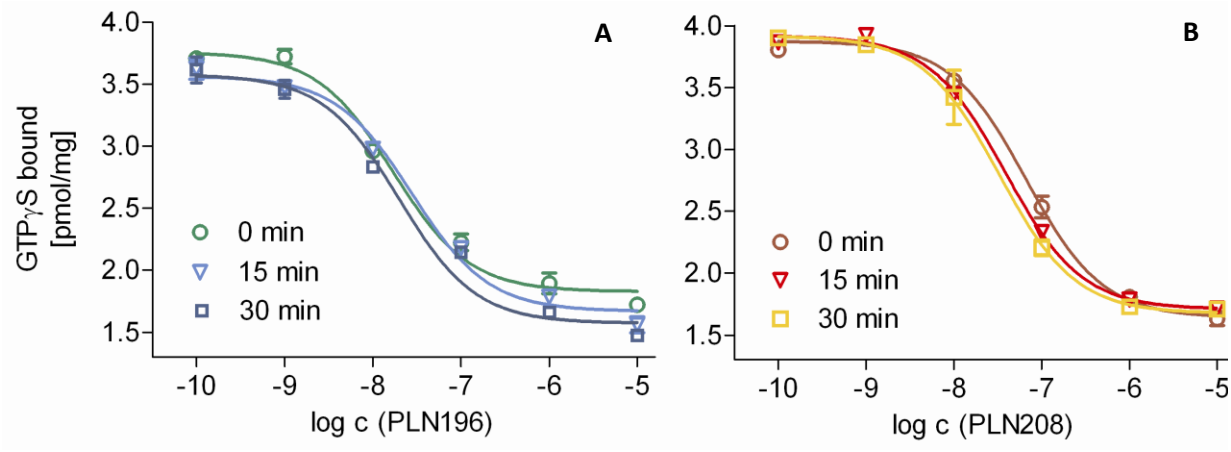

Figure 7.9 Concentration-response curves of the hY_2R ligands UR-PLN196 and UR-PLN208. Determined vs. 100 nM pNPY in a steady-state GTPase assay with membranes expressing the hY_2R + $G\alpha_{i2}$ + $G\beta_1\gamma_2$ after pretreatment of the membranes with UR-PLN196 (A. ○: 0 min, Δ: 15 min; □: 30 min) or UR-PLN208 (B. ○: 0 min, Δ: 15 min; □: 30 min) for different periods of time ; mean values ± SEM, n = 2-4.

Table 7.4 hY_2R antagonism of UR-PLN196 and UR-PLN208 in the GTPase assay determined after different periods of preincubation manner.[a]

Compound	Preincubation with antagonist:		
	0 min	**15 min**	**30 min**
	K_b / nM]	K_b / nM]	K_b / nM]
UR-PLN196	4.4 ± 2.5	3.8 ± 0.2	4.8 ± 0.6
UR-PLN208	2.4 ± 0.5	3.8 ± 0.8	3.6 ± 1.1

[a] Data are mean values ± SEM from 2 independent experiments performed in duplicate.

7.2.3.2 Saturation binding of [^{3}H]UR-PLN208 using hY_2R-insect cell membrane preparations

The functional data for the BIIE 0246-type antagonists gained from the steady-state GTPase assay on membranes of Sf9 insect cells expressing the hY_2R were in good agreement with the K_b values determined in the calcium assay on hY_2R expressing CHO cells. In order to explore if membranes of Sf9 insect cells are suitable for binding studies on the hY_2R using radioligands such as UR-PLN208, a saturation binding experiment was performed. For these experiments BD Primaria 96-well plates

(Becton Dickinson GmbH, Germany) were used to reduce the adsorption of the radioligand to the plastic as reported previously.[7]

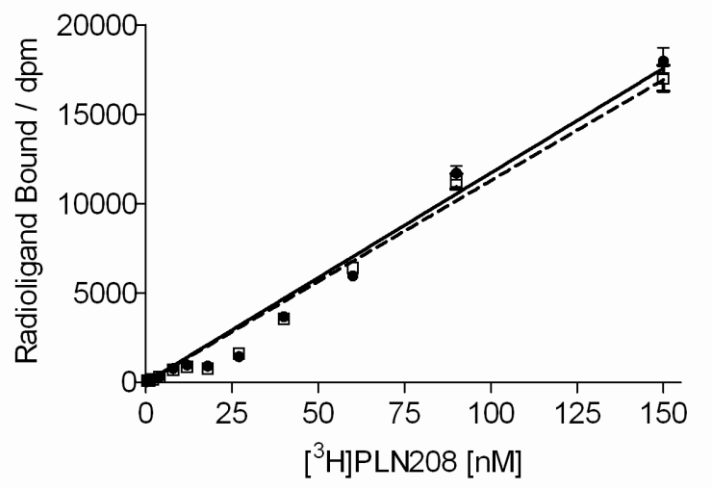

Figure 7.10 Saturation binding of [^{3}H]UR-PLN208 at Sf9-hY_2R cells membrane preparations. Total binding: ●; nonspecific binding: □; n = 2.

As shown in Figure 7.10, no specific binding was detected within the investigated concentration range of 0.5-150 nM. It is rather likely that membrane preparations are not suitable for lipophilic ligands like UR-PLN208, due to nonspecific binding to membrane lipids or the formation of micelles which include the lipophilic compounds. Similar findings in membrane systems have been reported for [^{3}H]iodophenpropit[27], [^{3}H]tiotidine[28] and [^{3}H]JNJ7777120 (cf. Chapter 6). Moreover, the work-up *via* filtration over GF/C cellulose filters could lead to such high nonspecific binding, although the filters were pretreated with PEI (polyethylenimine) to prevent the binding of the positively charged radioligand to the filters. Optimization of the work-up procedure or the addition of a detergent like Triton X might be beneficial, but such attempts were not taken into account due to the limited available amounts of the radioligand [^{3}H]UR-PLN208.

7.2.4 Stability of argininamide-type NPY Y_2R antagonists

As recently reported, N^{ω}-acylated argininamides have to be considered critically with respect to chemical stability, depending on the structure of the acyl substituent.[29-32] Therefore, a selection of compounds with different substituents at the guanidine group (UR-PLN26, UR-PLN74 and UR-PLN208, for structures cf. Figure 7.11) were investigated with regard to decomposition giving BIIE 0246 under assay-like conditions (aqueous buffer, pH 7.4, 20 °C, time scale 90 min to 48 h, cf. Figure 7.11). As such compounds are of potential value as ligands for Y_2R crystallization experiments, stability was also investigated over a longer time period (24 and 48 h, respectively) than required for pharmacological in vitro studies (incubation time: 90 min).[7] In the latter the release of BIIE 0246

under assay conditions has to be taken into account, because the high potency of cleavage product BIIE 0246 (K_i = 2.6 nM) might feign or mask the activity of the decomposing Y_2R antagonist. Cleavage of aminoalkanoylguanidines was already observed for N^G-acylated argininamide-type Y_1R antagonists.[29,32]

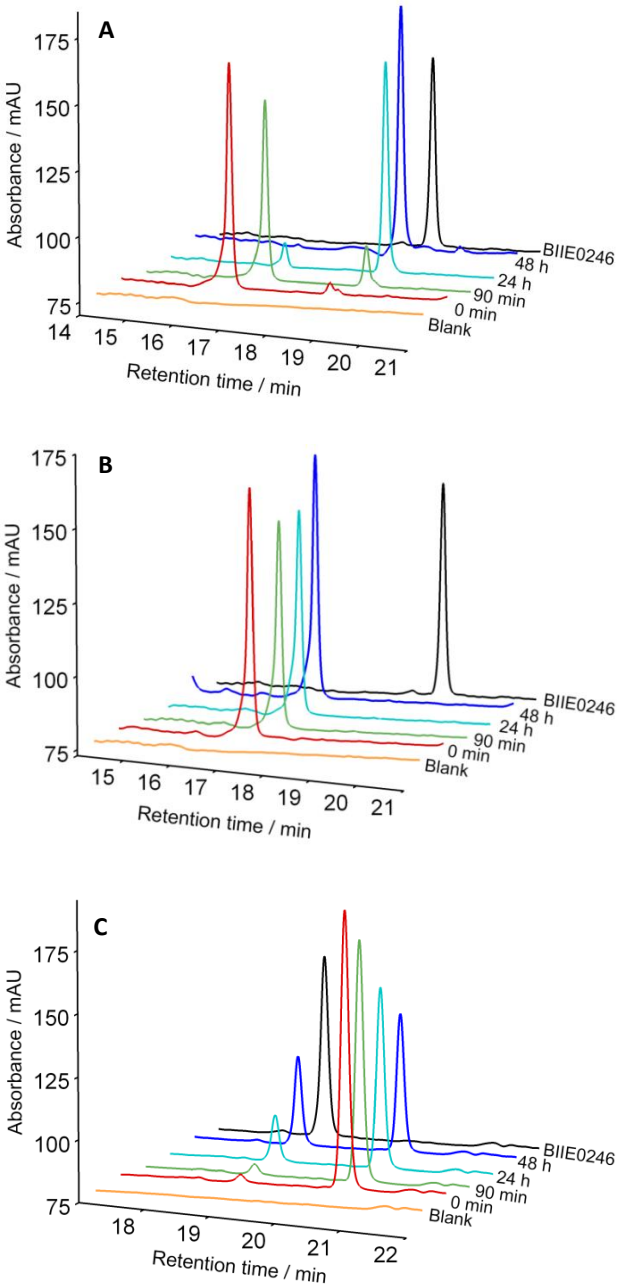

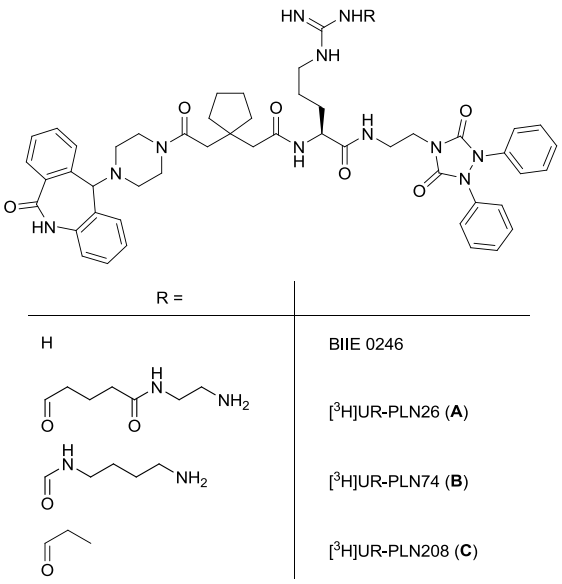

D

Time	Peak ratio (UV detection) / %		
	UR-PLN26 : BIIE 0246	UR-PLN74 : BIIE 0246	UR-PLN208 : BIIE 0246
0 min	97 : 3	100 : 0	97 : 3
90 min	83 : 17	100 : 0	96 : 4
24 h	11 : 89	100 : 0	79 : 21
48 h	0 : 100	100 : 0	61 : 39

Figure 7.11 HPLC analysis of the chemical stability of N^G-substituted Y_2R antagonists. BIIE 0246 is formed by decomposition of the ligands. Incubation: 0 min, 90 min, 24 h and 48 h in buffer, c = 50 µM, pH 7.4, 20 °C (A. UR-PLN26; B. UR-PLN74; C. UR-PLN208; cf. Appendix for the complete chromatograms; D. Ratios calculated from the peak ratio (UV detection) of the respective antagonist and BIIE 0246 after different periods of time.

In case of the Y_2R antagonists the deacylation proved to be rapid in case of UR-PLN26 (90 min: almost 20% decomposition, 24 h: 90%), probably favored by an intramolecular nucleophilic attack at the carbonyl group. In case of the propionylated radioligand UR-PLN208, only traces of the parent compound BIIE 0246 were detected after 90 min (4%), but the amount of BIIE 0246 was increasing from 24 h (~20%) to 48 h (~40%). The exchange of the acylguanidine moiety by carbamoylated analogs led to high stability, as shown for UR-PLN74 in Figure 7.11 B. Recently, considerably improved stability of carbamoylguanidines compared to acylguanidines has been demonstrated for radiolabeled and fluorescent Y_1R antagonists.[30,31] Thus, the carbamoylguanidine structural motif should be preferred for future design of BIIE 0246-type ligands.

7.3 Summary and Outlook

The guanidine-acylguanidine bioisosteric approach was applied to the preparation of the tritiated Y_2R-selective radioligands [^{3}H]UR-PLN196[2] and [^{3}H]UR-PLN208. The difference between peptidic agonists and nonpeptide antagonists regarding displacement of both radioligands suggests a slow interconversion between inactive and active receptor conformations,[12,13] a slow rate of dissociation from the receptor,[11] stabilization of an inactive ligand-specific receptor conformation,[14] or binding to a site distinct from the peptide agonist binding site. The presented data also indicate that the Y_2R binding sites of BIIE 0246-derived antagonists and NPY are different or overlap only partially. Recently, a Y_5R-selective radioligand with similar behavior in kinetic and functional studies was reported as an insurmountable pseudo-irreversible nonpeptide antagonist.[33] Regardless of insurmountable antagonism and pseudo-irreversible binding, both radioligands are valuable pharmacological tools for the detection of Y_2R binding sites, investigations on ligand binding modes and the characterization of nonpeptide Y_2 receptor antagonists. The steady-state GTPase assay revealed K_b values consistent with reported data from the Ca^{2+} (Fura-2) assay, but did not show insurmountable antagonism of the BIIE 0246-related compounds. The pharmacological characterization of [^{3}H]UR-PLN208 at the hY_2R using membrane preparations of Sf9 insect cells failed due to high degree of nonspecific binding, presumably resulting from the physicochemical properties of this ligand. High stability under physiological conditions over severals days is crucial for crystallization experiments and was shown for carbamoylguanidines such as UR-PLN74. Therefore, future design of argininamide-type Y_2R antagonists should be focused on carbamoylguanidines instead of less stable acylguanidines. With [^{3}H]UR-PLN187 and [^{3}H]propionyl-NPY, two additional radioligands were synthesized in our working group. In comparison, these ligands can hopefully give new insights in the mechanism of both, agonist and antagonist binding at the hY_2R. Future direction in search for new radioligands should focus on antagonists structurally distinct from BIIE 0246-type ligands to compare the binding behavior of antagonists with different scaffolds.

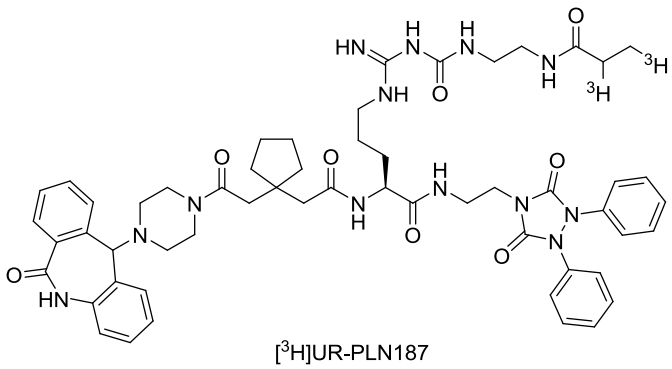

Figure 7.12 Structure of [^{3}H]PLN187.

7.4 Experimental Section

7.4.1 General

Chemicals and solvents were purchased from Merck KGaA (Darmstadt, Germany) and Sigma Aldrich GmbH (Munich, Germany) and were used without further purification unless otherwise stated. BIIE 0246, UR-PLN26, UR-PLN74, UR-PLN205 and 'cold' UR-PLN208 were synthesized by Dr. Nikola Pluym in our research group as part of his doctoral project.[7] Porcine NPY (pNPY) was kindly provided by Prof. Dr. C. Cabrele (Paris-Lodron-University, Salzburg, Austria). SF-11 was purchased from Tocris Bioscience (Bristol, United Kingdom). CMY 9484 was synthesized by Kilian Kuhn in our research group by analogy with a previously published synthesis.[16] Succinimidyl [2,3-$^3H_2$]-propionate was purchased from Hartmann Analytic GmbH (Braunschweig, Germany) and provided as solution in ethyl acetate (specific activity a_s = 2.96 TBq/mmol, 80 Ci/mmol; a_v =185 MBq/mL, 5 mCi/mL). Scintillation cocktail Rotiscint Eco Plus was from Carl Roth (Karlsruhe, Germany). Radioanalytical HPLC was performed on a system from Waters (Eschborn, Germany), equipped with a pump control module, a 510 HPLC pump, a 486 UV/VIS detector, and a Flo-One beta series A-500 radiodetector (Packard, Meriden, USA). The stationary phase was a Synergi Hydro-RP (250 x 4.6 mm, 4 µm) column equipped with a Luna C18 (4 x 3.0 mm) column guard (Phenomenex, Aschaffenburg, Germany). Linear gradients of CH_3CN/TFA 0.05% and H_2O/TFA 0.05% were used as mobile phases at a flow rate of 0.8 mL/min. Absorbance was detected at 220 nm, and radioactivity was measured with the radiodetector by liquid scintillation counting (liquid scintillator: Rotiscint Eco Plus, flow rate: 3.8 mL/min). Chemical stability investigations of UR-PLN26, UR-PLN74 and UR-PLN208 were performed on a HPLC system from Merck, composed of an L-5000 controller, a 655A-12 pump, a 655A-40 auto sampler and an L-4250 UV-VIS detector. The column was a Eurospher-100 (250 x 4 mm, 5 µm) (Knauer, Berlin, Germany) at a flow rate of 0.8 mL/min. UV-detection was done at 220 nm. Mixtures of 0.05% TFA in acetonitrile and 0.05% aq. TFA were used as mobile phase. Helium degassing prior to HPLC analysis

was necessary. Compound purities were calculated as percentage peak area of the analyzed compound by UV detection at 220 nm.

7.4.2 Synthesis of (2*S*)-*N*-[2-(3,5-Dioxo-1,2-diphenyl-1,2,4-triazolidin-4-yl)ethyl]-N^{α}-{2-[1-({2-oxo-2-[4-(6-oxo-6,11-dihydro-5*H*-dibenzo[*b*,*e*]azepin-11-yl)piperazin-1-yl]ethyl})cyclopentyl]acetyl}-N^{ω}-([2,3-$^{3}H_2$]propanoyl)argininamide ([^{3}H]UR-PLN208)

Succinimidyl [2,3-$^{3}H_2$]propionate (5.35 µg, 31.25 nmol, 1 eq, 2.5 mCi) in 800 µL ethyl acetate was transferred into a 1.5 mL Eppendorf reaction vessel (screw top) and the solvent was removed in a vacuum concentrator (40 °C) over a period of 30 min. UR-PLN205 (1.245 mg, 1.250 µmol, 40 eq) in MeCN (125 µL) and NEt_3 (253.0 µg, 2.50 µmol, 80 eq) in CH_3CN (5 µL) were added, the components were mixed (vortex), briefly centrifuged and stirred with a magnetic microstirrer for 16 h at room temperature. Subsequently, 25 µL TFA were added and stirred for further 2 h. The reaction was monitored by HPLC. Reaction mixture (0.5 µL) was added to 105 µL of unlabeled UR-PLN208 solution (100 µM, CH_3CN/H_2O 20:80 (*v/v*)), the 'cold' version of [^{3}H]UR-PLN208, to allow UV detection in addition to radiodetection; injection volume: 100 µL). For purification, the reaction mixture was diluted with 400 µL H_2O containing 0.05% TFA and the product was isolated (3 injections, 175 µL each) by analytical HPLC. In this instance, radiometric detection was not performed. Fractions containing the radioligand were collected at ~21 min (gradient: 0.05% TFA in CH_3CN/0.05% TFA in $H_2$0: 0 min: 20:80 (*v/v*), 30 min: 95:5 (*v/v*), 40 min 95:5 (*v/v*), 41 min 20:80 (*v/v*), 50 min 20:80 (*v/v*)). The solvent of the combined fractions was evaporated, and the residue was dissolved in 190 µL of CH_3CN/H_2O 20:80 (*v/v*) containing 0.05% TFA. The supernatant was purified by HPLC to achieve high purity. The solvent of the combined fractions was evaporated under reduced pressure, the product dissolved in 200 µL EtOH containing 100 µM TFA and transferred to an Amersham glass vial.

Quantification: A five-point calibration was performed with the unlabeled ligand UR-PLN208 (2.5, 5.0, 7.5, 10 µM and 15 µM, inj. vol.: 100 µL, gradient: 0.05% TFA in CH_3CN/0.05% TFA in H_2O: 0 min: 50:50 (*v/v*), 20 min: 80:20 (*v/v*), 21 min: 95:5 (*v/v*), 25 min: 95:5 (*v/v*), 26 min: 50:50 (*v/v*), 30 min: 50:50 (*v/v*). t_R ~ 21 min). The solutions for injection were prepared in CH_3CN/0.05% aq. TFA (20/80) less than 5 min prior to injection. All standard solutions were prepared from a 100 µM solution of UR-PLN208 (in CH_3CN/0.05% aq. TFA 20:80) which was freshly made from a 10 mM stock solution of UR-PLN208 in DMSO. Two aliquots (2.0 µL) of the ethanolic solution of the product were diluted with 100 µL of CH_3CN/0.05% aq. TFA (20:80), and 100 µL were analyzed by HPLC. Whereas one sample was only used for quantification of the product by UV detection, the second sample was additionally monitored radiometrically to determine radiochemical purity. The molarity of the ethanolic solution

of [^{3}H]UR-PLN208 was calculated from the mean of the peak areas, and the linear calibration curve was obtained from the peak areas of the standards. Yield: 2.35 µg (2.46 nmol, 7.9%).

Determination of the specific activity: An aliquot (1.5 µL) of the ethanolic solution was diluted with 448.5 µL of a mixture of CH_3CN/H_2O 20:80 (*v/v*) in duplicate, and 50 µL of the 1:90 dilutions were counted three times in Rotiszint eco plus (3 mL) in a LS 6500 liquid scintillation counter (Beckmann Coulter, München, Germany). The total activity in 200 µL stock solution amounted to 6.823 MBq (0.1844 mCi), resulting in a calculated specific activity of 2.772 TBq/mmol (74.92 Ci/mmol). The activity of the stock solution was adjusted to 9.25 MBq/mL, (0.25 mCi/mL, c = 3.337 µM) by adding EtOH. HPLC analysis showed a radiochemical purity of >98%. The identity of the radioligand was confirmed by HPLC analysis of labeled and unlabeled UR-PLN208 under the same conditions, resulting in identical retention times. The radioligand was stored at –20 °C.

Control of chemical stability of [^{3}H]UR-PLN208 by HPLC: 2 µL of the adjusted stock solution of [^{3}H]UR-PLN208 (a_v: 9.25 MBq/mL) in ethanol containing TFA (100 µM) was diluted with 108 µL of CH_3CN/0.1% aq. TFA (20:80) containing 102 µM of 'cold' UR-PLN208 to a total volume of 110 µL. 100 µL of this solution were injected into the HPLC system and analyzed by radiometric and UV detection. Gradient: CH_3CN/0.1% TFA in H_20: 0 min: 25:75 (*v/v*), 30 min: 90:10 (*v/v*), 40 min 90:10 (*v/v*).

7.4.3 Investigation of the chemical stability

The stability of the Y_2R antagonists UR-PLN26, UR-PLN74 and UR-PLN208 regarding the formation of BIIE 0246 was investigated at neutral pH in binding buffer. Incubation was started by addition of 50 µL of a 1 mM solution of the compounds in DMSO/H_2O 1:1, which was freshly prepared from a 10 mM stock solution in DMSO, to 950 µL of buffer to give a final concentration of 50 µM. After 1.5 h, 24 h and 48 h a 150 µL aliquot was taken and diluted with 150 µL of a mixture of acetonitrile, H_2O and 1 % aq. TFA (60:90:1). 150 µL of the resulting solution were analyzed by HPLC on a RP-column (Eurospher-100 C18, 250 × 4 mm, 5 µm, Knauer, Berlin, Germany). Gradient: CH_3CN/0.1% TFA in H_2O: 0 min: 20:80 (*v/v*), 30 min: 95:5 (*v/v*), 40 min: 95:5. The flow rate was set to 0.8 mL/min, the column temperature to 30 °C and the detection wavelength to 220 nm. The quantity of decomposition product BIIE 0246 was estimated from the peak integrals of the incubation sample and a reference chromatogram of the analyzed compound. The blank HPLC run was performed under identical conditions without any Y_2R antagonist. For the reference HPLC runs (0 min equal to purity control of the stock solutions) of UR-PLN26, UR-PLN74**,** UR-PLN208 and BIIE 0246, 25 µM solutions in 300 µL of CH_3CN/0.1% TFA in H_2O 20:80 (*v/v*) was prepared from the respective 1 mM solution in DMSO/H_2O 1:1 (*v/v*).

7.4.4 Pharmacological methods

7.4.4.1 Cell culture

CHO-hY_2-K9-qi5-K9-mtAEQ-A7 (abbreviated: CHO-hY_2R) cells were cultured as described elsewhere.[4]

7.4.4.2 Spectrofluorimetric Ca^{2+} assay (Fura-2 assay)

Y_2R antagonistic activities (K_b values) were determined by spectrofluorimetric measurement of the inhibition of pNPY-induced (70 nM) mobilization of intracellular $[Ca^{2+}]_i$ in CHO-hY_2R cells by analogy with the general procedure described previously,[6] using a LS50 B spectrofluorimeter from Perkin Elmer (Überlingen, Germany).

7.4.4.3 Radioligand binding assay

General. The buffer for the Y_2R binding studies of [^{3}H]UR-PLN208 was prepared by the addition of 1% BSA to Leibovitz medium without phenol red (L15) from Life Technologies GmbH (Darmstadt, Germany). Bacitracin (100 µg/mL) was added for binding studies with pNPY. PBS (phosphate buffered saline) buffer without additives was used to wash the cells previous to and after radioligand binding. The lysis solution for the radioligand binding assays consisted of urea (8 M), acetic acid (3 M), and Triton-X-100 (1%) in H_2O. Stock solutions of all compounds were prepared in DMSO (10 mM) and stored at –20 °C.

Protocol. The radioligand binding assay was essentially performed as described.[4] The radioligand was diluted 1:10 with unlabeled ligand due to economic reasons. Cells were seeded in BD Primaria 96-well plates (Becton Dickinson GmbH, Germany) 3-4 days prior to the experiment. On the day of the experiment, confluency of the cells was at least 90%. The culture medium was removed by suction, the cells were washed once with PBS buffer (200 µL), and covered with Leibovitz medium. Leibovitz medium (10 µL) and Leibovitz medium (10 µL) containing [^{3}H]UR-PLN208 (10-fold concentrated) was added for total binding. For non-specific binding and displacement of UR-PLN208 Leibovitz medium (10 µL) containing the respective competitor 10-fold concentrated and Leibovitz medium (10 µL) with [^{3}H]UR-PLN208 (10-fold concentrated) were added. During incubation at room temperature the plates were shaken at 300 rpm. After incubation (saturation experiments and competition with nonpeptidic Y_2R antagonists: 30 min; competition with peptidic agonists: 2 h) the binding buffer was removed, the cells were washed twice with PBS buffer (200 µL, 4 °C), covered with lysis solution (25 µL) and the plates were gently shaken for at least 30 min. The lysates were transferred into 96-well sample plates 1450-401 (Perkin Elmer, Rodgau, Germany) and washed once with lysis solution (25 µL). Each well was supplemented with 200 µL of scintillation cocktail (Rotiscint Eco plus, Roth, Karlsruhe, Germany) and incubated in the dark. Radioactivity was measured with a Micro Beta^2 1450

scintillation counter (Perkin Elmer, Rodgau, Germany). In case of determining the dissociation kinetics, the cells were incubated with Leibovitz medium (100 µL) containing the respective competitor (BIIE 0246: 30-fold-, pNPY: 100-fold higher concentrated than the radioligand). After incubation with [^{3}H]UR-PLN208 (20 nM) and subsequent washing (200 µL, 4 °C, twice). After different periods of time, the cells were washed twice with PBS buffer (200 µL, 4 °C) followed by the addition of lysis solution. For association kinetics, cells were incubated with [^{3}H]UR-PLN208 (20 nM) in Leibovitz medium (100 µL). The supernatant was sucked off after different periods of time and the adherent cells were washed twice with cold PBS buffer (200 µL, 4 °C) before lysis solution was added. Non-specific binding was determined with BIIE 0246 (30-fold higher concentrated than the radioligand) in kinetic studies. Assays were performed in triplicate.

7.4.4.4 Steady-state GTPase activity assay

GTPase activity assays were performed as previously described.[24] hY_2R assays: Sf9 insect cell membranes coexpressing the hY_2R, mammalian Gα_{i2} and G$\beta_1\gamma_2$ were employed. The membranes were thawed, sedimented by centrifugation at 4 °C and 13,000 *g* for 10 min. Membranes were resuspended in 10 mM Tris/HCl, pH 7.4. Each assay tube contained the hY_2R expressing Sf9 membranes, (10 µG-Protein/tube), 2 mM $MgCl_2$, 200 µM EDTA, 200 µM ATP, 200 nM GTP, 200 µM adenylyl imidophosphate, 2.4 mM creatine phosphate, 2 µg creatine kinase and 0.4% (*w/v*) bovine serum albumin in 100 mM Tris/HCl, pH 7.4 and the investigated ligands at various concentrations. For the determination of pK_b values (antagonist mode of the GTPase activity assay), pNPY was added to the reaction mixtures (final concentrations: 100 nM). The reaction mixtures (80 µL) were incubated for 2 min at 25 °C. After the addition of 20 µL of [^{33}P]GTP (0.1 µCi/tube), the reaction mixtures were incubated for 20 min at 25 °C. Reactions were terminated by the addition of 900 µL slurry consisting of 5% (w/v) activated charcoal and 50 mM NaH_2PO_4, pH 2.0. The charcoal-quenched reaction mixtures were centrifuged for 7 min at room temperature at 13,000 *g*. 600 µL of the supernatant were removed and $^{33}P_i$ was determined by liquid scintillation counting. Spontaneous [^{33}P]GTP degradation was determined in tubes containing all components described above, plus a high concentration of unlabeled GTP (1 mM), which, due to competition with [^{33}P]GTP, prevents [^{33}P]GTP hydrolysis by enzymatic activities present in Sf9 membranes. Spontaneous [^{33}P]GTP degradation was <1% of the total amount of radioactivity added. The experimental conditions chosen ensured that not more than 10% of the total amount of [^{33}P]GTP added was converted to $^{33}P_i$.

7.4.4.5 Saturation binding of [^{3}H]UR-PLN208 at the hY_2R on membrane preparations of Sf9 insect cells

For membrane preparation see 7.4.4.4

The radioligand was diluted 1:10 with unlabeled ligand due to economic reasons. Saturation binding experiments were conducted with radioligand concentrations (final conc.) between 1 nM and 150 nM. There, unspecific binding was determined with 30-fold excess of BIIE 0246. The membrane-ligand mixtures were incubated for 60 min at RT and shaking at 300 rpm. Separation of bound and unbound radioligand was performed by filtration as described before (cf. Chapter 5).

7.5 References

1. Doods, H.; Gaida, W.; Wieland, H. A.; Dollinger, H.; Schnorrenberg, G.; Esser, F.; Engel, W.; Eberlein, W.; Rudolf, K. BIIE0246: a selective and high affinity neuropeptide Y Y_2 receptor antagonist. *Eur. J. Pharmacol.* **1999**, 384, R3-5.
2. Pluym, N.; Baumeister, P.; Keller, M.; Bernhardt, G.; Buschauer, A. [^{3}H]UR-PLN196: a selective nonpeptide radioligand and insurmountable antagonist for the neuropeptide Y Y_2 receptor. *ChemMedChem* **2013**, 8, 587-593.
3. Pluym, N.; Brennauer, A.; Keller, M.; Ziemek, R.; Pop, N.; Bernhardt, G.; Buschauer, A. Application of the Guanidine-Acylguanidine Bioisosteric Approach to Argininamide-Type NPY Y_2 Receptor Antagonists. *ChemMedChem* **2011**.
4. Ziemek, R.; Brennauer, A.; Schneider, E.; Cabrele, C.; Beck-Sickinger, A. G.; Bernhardt, G.; Buschauer, A. Fluorescence- and luminescence-based methods for the determination of affinity and activity of neuropeptide Y_2 receptor ligands. *Eur. J. Pharmacol.* **2006**, 551, 10-18.
5. Schneider, E.; Mayer, M.; Ziemek, R.; Li, L.; Hutzler, C.; Bernhardt, G.; Buschauer, A. A simple and powerful flow cytometric method for the simultaneous determination of multiple parameters at G-Protein-coupled receptor subtypes. *ChemBioChem* **2006**, 7, 1400-1409.
6. Müller, M.; Knieps, S.; Gessele, K.; Dove, S.; Bernhardt, G.; Buschauer, A. Synthesis and neuropeptide Y Y_1 receptor antagonistic activity of *N*,*N*-disubstituted ω-guanidino- and ω-aminoalkanoic acid amides. *Arch. Pharm. (Weinheim).* **1997**, 330, 333-342.
7. Pluym, N. Application of the Guanidine–Acylguanidine Bioisosteric Approach to NPY Y_2 Receptor Antagonists: Bivalent, Radiolabeled and Fluorescent Pharmacological Tools. University of Regensburg, Regensburg, Doctoral thesis, **2011**.
8. Xu, B.; Fällmar, H.; Boukharta, L.; Pruner, J.; Lundell, I.; Mohell, N.; Gutiérrez-de-Terán, H.; Åqvist, J.; Larhammar, D. Mutagenesis and Computational Modeling of Human G-Protein-Coupled Receptor Y_2 for Neuropeptide Y and Peptide YY. *Biochemistry* **2013**, 52, 7987-7998.
9. Lazareno, S.; Birdsall, N. J. Detection, quantitation, and verification of allosteric interactions of agents with labeled and unlabeled ligands at G-Protein-coupled receptors: interactions of strychnine and acetylcholine at muscarinic receptors. *Mol. Pharmacol.* **1995**, 48, 362-378.
10. Bylund, D. B.; Toews, M. L. Radioligand binding methods for membrane preparations and intact cells. In *Recept. Signal Transduct. Prot.*, 2011/05/25 ed.; Willars, G. B.; Challiss, R. A. J., Eds., Springer: Leicester, **2011**; Vol. 746, pp 135-164.
11. Meini, S.; Patacchini, R.; Lecci, A.; Quartara, L.; Maggi, C. A. Peptide and non-peptide bradykinin B_2 receptor agonists and antagonists: a reappraisal of their pharmacology in the guinea-pig ileum. *Eur. J. Pharmacol.* **2000**, 409, 185-194.
12. Fierens, F. L.; Vanderheyden, P. M.; De Backer, J. P.; Vauquelin, G. Insurmountable angiotensin AT_1 receptor antagonists: the role of tight antagonist binding. *Eur. J. Pharmacol.* **1999**, 372, 199-206.
13. Vauquelin, G.; Morsing, P.; Fierens, F. L.; De Backer, J. P.; Vanderheyden, P. M. A two-state receptor model for the interaction between angiotensin II type 1 receptors and non-peptide antagonists. *Biochem. Pharmacol.* **2001**, 61, 277-284.
14. Seifert, R.; Schneider, E. H.; Dove, S.; Brunskole, I.; Neumann, D.; Strasser, A.; Buschauer, A. Paradoxical stimulatory effects of the "standard" histamine H_4-receptor antagonist JNJ7777120: the H_4 receptor joins the club of 7 transmembrane domain receptors exhibiting functional selectivity. *Mol. Pharmacol.* **2011**, 79, 631-638.
15. Brothers, S. P.; Saldanha, S. A.; Spicer, T. P.; Cameron, M.; Mercer, B. A.; Chase, P.; McDonald, P.; Wahlestedt, C.; Hodder, P. S. Selective and brain penetrant neuropeptide Y Y_2 receptor antagonists discovered by whole-cell high-throughput screening. *Mol. Pharmacol.* **2010**, 77, 46-57.
16. Mittapalli, G. K.; Vellucci, D.; Yang, J.; Toussaint, M.; Brothers, S. P.; Wahlestedt, C.; Roberts, E. Synthesis and SAR of selective small molecule neuropeptide Y Y_2 receptor antagonists. *Bioorg. Med. Chem. Lett.* **2012**, 22, 3916-3920.

17. Vanderheyden, P. M. L.; Van Liefde, I.; De Backer, J. P.; Vauquelin, G. [^{3}H]-BIBP3226 and [^{3}H]-NPY Binding to Intact SK-N-MC Cells and CHO Cells Expressing the Human Y_1 Receptor. *J. RECept. Signal Transduct. Res.* **1998**, 18, 363-385.
18. Kaske, M. In search for potent and selective NPY Y_4 receptor ligands: acylguanidines, argininamides and peptide analogs. University of Regensburg, Regensburg, Doctoral thesis, **2012**.
19. Ziemek, R. Development of binding and functional assays for the neuropeptide Y Y_2 and Y_4 receptors. University of Regensburg, Regensburg, Doctoral thesis, **2006**.
20. Dautzenberg, F. M.; Neysari, S. Irreversible binding kinetics of neuropeptide Y ligands to Y_2 but not to Y_1 and Y_5 receptors. *Pharmacology* **2005**, 75, 21-29.
21. Jaakola, V. P.; Griffith, M. T.; Hanson, M. A.; Cherezov, V.; Chien, E. Y.; Lane, J. R.; Ijzerman, A. P.; Stevens, R. C. The 2.6 angstrom crystal structure of a human A_{2A} adenosine receptor bound to an antagonist. *Science* **2008**, 322, 1211-1217.
22. Shimamura, T.; Shiroishi, M.; Weyand, S.; Tsujimoto, H.; Winter, G.; Katritch, V.; Abagyan, R.; Cherezov, V.; Liu, W.; Han, G. W.; Kobayashi, T.; Stevens, R. C.; Iwata, S. Structure of the human histamine H_1 receptor complex with doxepin. *Nature* **2011**, 475, 65-70.
23. Manglik, A.; Kruse, A. C.; Kobilka, T. S.; Thian, F. S.; Mathiesen, J. M.; Sunahara, R. K.; Pardo, L.; Weis, W. I.; Kobilka, B. K.; Granier, S. Crystal structure of the μ-opioid receptor bound to a morphinan antagonist. *Nature* **2012**, 485, 321-326.
24. Pop, N.; Igel, P.; Brennauer, A.; Cabrele, C.; Bernhardt, G. N.; Seifert, R.; Buschauer, A. Functional reconstitution of human neuropeptide Y (NPY) Y_2 and Y_4 receptors in Sf9 insect cells. *J. Recept. Sig. Transd.* **2011**, 31, 271-285.
25. Schneider, E. H.; Seifert, R. Sf9 cells: a versatile model system to investigate the pharmacological properties of G-Protein-coupled receptors. *Pharmacol. Ther.* **2010**, 128, 387-418.
26. Cheng, Y.; Prusoff, W. H. Relationship between the inhibition constant (K_1) and the concentration of inhibitor which causes 50 per cent inhibition (I_{50}) of an enzymatic reaction. *Biochem. Pharmacol.* **1973**, 22, 3099-3108.
27. Lim, H. D.; van Rijn, R. M.; Ling, P.; Bakker, R. A.; Thurmond, R. L.; Leurs, R. Evaluation of histamine H_1-, H_2-, and H_3-receptor ligands at the human histamine H_4 receptor: identification of 4-methylhistamine as the first potent and selective H_4 receptor agonist. *J. Pharmacol. Exp. Ther.* **2005**, 314, 1310-1321.
28. Kelley, M. T.; Burckstummer, T.; Wenzel-Seifert, K.; Dove, S.; Buschauer, A.; Seifert, R. Distinct interaction of human and guinea pig histamine H_2-receptor with guanidine-type agonists. *Mol. Pharmacol.* **2001**, 60, 1210-1225.
29. Weiss, S.; Keller, M.; Bernhardt, G.; Buschauer, A.; König, B. N^G-Acyl-argininamides as NPY Y_1 receptor antagonists: Influence of structurally diverse acyl substituents on stability and affinity. *Bioorg. Med. Chem.* **2010**, 18, 6292-6304.
30. Keller, M.; Bernhardt, G.; Buschauer, A. [^{3}H]UR-MK136: A Highly Potent and Selective Radioligand for Neuropeptide Y Y_1 Receptors. *ChemMedChem* **2011**, 6, 1566-1571.
31. Keller, M.; Erdmann, D.; Pop, N.; Pluym, N.; Teng, S.; Bernhardt, G.; Buschauer, A. Red-fluorescent argininamide-type NPY Y_1 receptor antagonists as pharmacological tools. *Bioorg. Med. Chem.* **2011**, 19, 2859-2878.
32. Brennauer, A.; Keller, M.; Freund, M.; Bernhardt, G.; Buschauer, A. Decomposition of 1-(ω-aminoalkanoyl)guanidines under alkaline conditions. *Tetrahedron Lett.* **2007**, 48, 6996-6999.
33. Mullins, D.; Adham, N.; Hesk, D.; Wu, Y.; Kelly, J.; Huang, Y.; Guzzi, M.; Zhang, X.; McCombie, S.; Stamford, A.; Parker, E. Identification and characterization of pseudoirreversible nonpeptide antagonists of the neuropeptide Y Y_5 receptor and development of a novel Y_5-selective radioligand. *Eur. J. Pharmacol.* **2008**, 601, 1-7.

Chapter 8

Summary

G-protein coupled receptors (GPCRs) are the most important class of biological targets for the currently available pharmacotherapeutics and hold great potential for the development of future drugs as well. Histamine and neuropeptide Y (NPY) receptors may be considered representative examples of aminergic and peptidergic GPCRs, respectively.

The histamine H_4 receptor (H_4R), the latest addition to the histamine receptor family, has been suggested as a potential therapeutic target for the modulation of various inflammatory and immunological disorders. However, the (patho)physiological role of the H_4R is far from being fully understood, and its elucidation is hampered by substantial species-dependent differences of available ligands regarding potency, receptor selectivity and even the quality of action. Therefore, additional potent and receptor subtype selective H_4R ligands, antagonists as well as agonists, are required as molecular tools.

In search for agonists for the human (h) and murine (m) H_4R, a series of 2-arylbenzimidazoles was synthesized, inspired by the structure of a recently published H_4R agonist (*N*-[2-(1*H*-imidazol-4-yl)ethyl]-3-[4-(5-fluoro-4-methyl-1*H*-benzo[*d*]imidazol-2-yl)-3-methylphenoxy]propan-1-amine), bearing a histamine moiety. The compounds were pharmacologically characterized *in vitro* in radioligand and [^{35}S]GTPγS binding assays using membrane preparations of Sf9 insect cells expressing the human and murine H_xR subtypes and in radioligand binding studies on HEK293 cells stably expressing the mH_4R. The substitution pattern at the benzimidazole moiety proved to be important with regard to selectivity for the H_4R over the other hH_xR subtypes. Extension of the carbon chain between the imidazole and the amino group by two methylene groups (imbutamine derivative) was tolerated, revealing higher affinities and potencies, in part in the subnanomolar range (K_i = 0.58 nM, EC_{50} = 1.2 nM). By incorporation of the higher homolog impentamine, agonism switched to antagonism at the hH_4R and antagonism to agonism at the hH_3R. In addition to the introduction of a 5-methyl substituent at the imidazole ring, rigidization to a spinaceamine derivative was most effective regarding H_4R selectivity. Structural changes aiming at replacing the imidazole moiety, e. g. by guanidines, amides and aromatic residues, resulted in a decrease in affinity at the hH_4R. Affinities and activities at the mH_4R were lower compared to the data for the hH_4R. Nevertheless, the 5-methylimbutamine derivative, surprisingly, revealed an EC_{50} value of 7.0 nM at the mH_4R with almost full agonist activity. Moreover, high affinity at the hH_2R, the hH_3R, the hH_4R and the mH_4R depending on the substitution pattern make the 2-arylbenzimidazole building block an extremely versatile scaffold to tune subtype, functional and ortholog selectivity in the histamine receptor field.

It is not astonishing that ligands incorporating an imidazole moiety as the endogenous ligand histamine, showed low selectivity for a unique histamine receptor subtype. Aiming at H_4R agonists with increased selectivity for the H_4R over the other H_xR subtypes, the combination of the imidazole-

free molecule VUF 8430 (*S*-(2-guanidinylethyl)isothiourea, K_i (hH_4R) = 17.7 nM)) with the putatively bioisosteric acylguanidine moiety of the N^G-acylated imidazolylalkylguanidines was applied. This approach resulted in compounds with reduced hH_4R affinities compared to the reference substance. Highest hH_4R affinity (K_i value ca. 100 nM) and slightly higher selectivity over the H_3R than VUF 8430 were found for small alkanoyl residues (propanoyl/isobutyryl) at the guanidine group in combination with a 3-membered linker.

Due to a shortage of high affinity radioligands for the investigation of the histamine H_2 receptor, the squaramide [^{3}H]UR-DE257 (*N*-{6-[3,4-dioxo-2-({3-[3-(piperidin-1-ylmethyl)phenoxy]propylamino})-cyclo-but-1-enylamino]hexyl}-(2,3-$^3H_2$)-propionamide) was synthesized and pharmacologically characterized. The K_d-value (20 nM) determined from kinetic experiments was in good agreement with the dissociation equilibrium constant (31 nM) from saturation analysis. [^{3}H]UR-DE257 proved to be a useful tool to determine the H_2R binding affinities of unlabeled ligands in competition binding experiments. Future detailed analyses on the binding kinetics and quality of action (insurmountable H_2R antagonism) must show, if [^{3}H]UR-DE257 is an appropriate molecular tool to study functional selectivity at H_2R and receptor dynamics.

The tritium-labeled version of the widely used potent H_4R antagonist JNJ7777120 ((5-chloro-1*H*-indol-2-yl)(4-methylpiperazine-1-yl)methanone) was synthesized and pharmacologically characterized. The radioligand proved to be suitable for the investigation of the hH_4R in Sf9 insect cell membranes. Although JNJ7777120 has been used for the study of the H_4R in animal models, the investigation of the tritiated version, [^{3}H]JNJ7777120, revealed that this compound is far from being an ideal standard ligand or, not to mention, an optimal pharmacological tool. Due to very high non-specific binding, an advantage of [^{3}H]JNJ7777120 as a radiolabeled selective H_4R antagonist compared to the non-selective H_xR agonist [^{3}H]histamine was not confirmed. Nevertheless, the results of competition binding experiments were in good accordance to reported data. The exceptionally high affinity of JNJ7777120 for the murine H_4R, reported in literature, could not be confirmed in saturation and competition binding studies on Sf9 cell membranes. Binding of [^{3}H]JNJ7777120 at HEK-hH_4R cell membranes was insaturable and was predominantly hH_4R-independent.

To better understand the biological role of the NPY Y_2 receptor (Y_2R) subtype, pharmacological tools such as radioligands are required. The guanidine-acylguanidine bioisosteric approach was applied to the preparation of the tritiated argininamide-type Y_2R-selective radioligand [^{3}H]UR-PLN208, structurally related to the previously published [^{3}H]UR-PLN196 from our laboratory. Pharmacological investigation revealed differences between peptidic agonists and nonpeptide antagonists regarding

displacement of the radioligand, compatible with the concept of insurmountable antagonism and pseudo-irreversible binding, and discrepancies depending on the assays used. Whereas time-dependent depression of the NPY-induced Ca^{2+}-response was demonstrated in the fura-2 assay on hY_2R expressing CHO cells, insurmountable antagonism was not detectable in the steady-state GTPase assay on Sf9 cell membranes, but the K_b values from both assays were consistent. The data suggest different or partially overlapping binding sites of BIIE 0246-like antagonists and NPY, supporting the idea of ligand-specific receptor conformations. Yet, [^{3}H]UR-PLN208 is a valuable pharmacological tool for the detection of Y_2R binding sites, investigations on ligand binding modes and the characterization of nonpeptide Y_2R antagonists.

Taken together, several of the synthesized 2-arylbenzimidazoles harbor the potential of molecular tools and will hopefully contribute to a better understanding of the structure-activity- and structure-selectivity relationships of H_4R ligands on human and murine receptor orthologs. The synthesized and pharmacologically characterized tritium-labeled radioligands [^{3}H]UR-DE257, [^{3}H]JNJ7777120 and [^{3}H]UR-PLN208 for GPCRs are proven pharmacological tools for the detection of the respective receptor *in vitro* and for investigations on the antagonistic binding mode, respectively, as well as for the identification and characterization of new ligands at the respective target.

Chapter 9

Appendix

9.1 Synthesis and Application of the First Radioligand Targeting the Allosteric Binding Pocket of Chemokine Receptor CXCR3

As part of a cooperation with the working group of Dr. Nuska Tschammer at the FAU Erlangen-Nürnberg a radioligand called RAMX3 was synthesized and purified for further pharmacological investigation. These results are published in:

Bernat, V.; Heinrich, M. R.; Baumeister, P.; Buschauer, A.; Tschammer, N. Synthesis and application of the first radioligand targeting the allosteric binding pocket of chemokine receptor CXCR3. *ChemMedChem* **2012**, 7, 1481-1489. doi: 10.1002/cmdc.201200184.

Contribution of Paul Baumeister: Synthesis, analytical and radiochemical characterization of the radiolabeled form of RAMX3 as outlined in the following.

9.1.1 Abstract

Strategies for the identification of allosteric modulators of chemokine receptors largely rely on various cell-based functional assays. Radioligand binding assays are typically not available for allosteric binding sites. We synthesized, purified, and applied the first tritium-labeled allosteric modulator of the human chemokine receptor CXCR3 (RAMX3, [^{3}H]*N*-{1-[3-(4-ethoxyphenyl)-4-oxo-3,4-dihydropyrido[2,3-*d*]pyrimidin-2-yl]ethyl}-2-[4-fluoro-3-(trifluoromethyl)phenyl]-*N*-[(1-methylpiperidin-4-yl)methyl]acet-amide). RAMX3 is chemically derived from 8-azaquinazolinone-type allosteric modulators and binds to the CXCR3 receptor with a K_d value of 1.08 nM (specific activity: 80.4 Ci/mmol). Radioligand displacement assays showed potent negative cooperativity between RAMX3 and chemokine CXCL11, providing a basis for the use of RAMX3 to investigate other potential allosteric modulators. Additionally, the synthesis and characterization of a number of other full and truncated 8-azaquinazoline analogs were used to validate the binding properties of RAMX3. We demonstrate that RAMX3 can be efficiently used to facilitate the discovery and characterization of small molecules as allosteric modulators of the CXCR3 receptor.

9.1.2 General conditions for radiosynthesis:

Commercial reagents and solvents were purchased from Acros Organics (Geel, Belgium), Alfa Aesar (Karlsruhe, Germany), or Merck KGaA (Darmstadt, Germany) and were used without further purification unless otherwise stated. All solvents were of analytical grade, and DMSO was distilled prior to use and stored over 4 Å molecular sieves. [^{3}H]Methyl iodide dissolved in toluene (a_s = 3.15 TBq/mmol, 85 Ci/mmol; a_v = 37 GBq/mL, 1 Ci/mL) was from Hartmann Analytic (Braunschweig,

Germany). Compound 9.1 and 'cold' RAMX3 was synthesized in the laboratory of Dr. Nuska Tschammer by Viachaslau Bernat (FAU Erlangen-Nürnberng, Germany). Scintillation cocktail Rotiscint Eco Plus was from Carl Roth (Karlsruhe, Germany). Analytical HPLC was performed on a system from Waters (Eschborn, Germany), equipped with a pump control module, a 510 HPLC pump, a 486 UV/VIS detector, and a Flo-One beta series A-500 radiodetector (Packard, Meriden, USA). The stationary phase was a Synergi Hydro-RP (250 x 4.6 mm, 4 µm) column equipped with a Luna C18 (4 x 3.0 mm) column guard (Phenomenex, Aschaffenburg, Germany). Linear gradients of CH_3CN/TFA 0.05% (*v/v*) and H_2O/TFA 0.05% (*v/v*) were used as mobile phases at a flow rate of 0.8 mL/min. Absorbance was detected at 220 nm, and radioactivity was measured with the radiodetector by liquid scintillation counting (liquid scintillator: Rotiscint Eco Plus, flow rate: 3.8 mL/min).

9.1.3 Radiosynthesis of [^{3}H]*N*-{1-[3-(4-Ethoxyphenyl)-4-oxo-3,4-dihydropyrido[2,3-*d*]pyrimidin-2-yl]ethyl}-2-[4-fluoro-3-(trifluoromethyl)phenyl]-*N*-[(1-methylpiperidin-4-yl)methyl]acetamide (RAMX3)

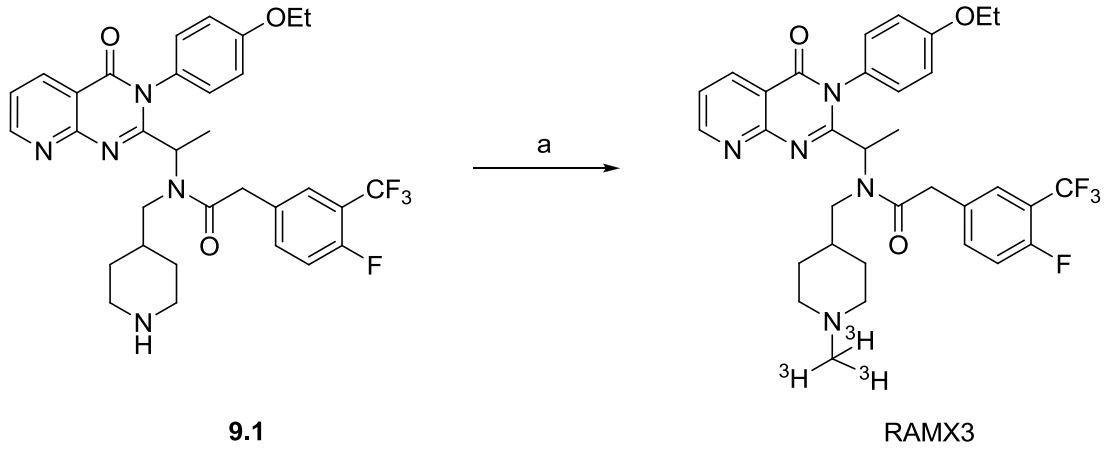

9.1 RAMX3

Scheme 9.1 Synthesis of radioligand RAMX3. Reagents and conditions: a) [^{3}H]MeI, DIPEA, CH_2Cl_2, 20 h, RT, 20.7%.

Compound **9.1** (402.7 mg, 0.6588 mmol, 11.2 eq), dissolved in CH_2Cl_2 (50 µL), and DIPEA (123.9 mg, 0.9588 mmol, 16.3 eq) in CH_2Cl_2 (50 µL) were added to a solution of [^{3}H]methyl iodide (8.875 mg, 0.0588 mmol, 1 eq, 5 mCi) in toluene (5 µL), and the reaction mixture was diluted with CH_2Cl_2 (100 µL) and stirred for 20 h at room temperature. The reaction was monitored by HPLC. Reaction mixture (1 µL) was added to 104 µL of 'cold' RAMX3 solution (100 µM) to allow for UV detection in addition to radiodetection; injection volume: 100 µL, see Figure 9.1). The solvent was removed under reduced pressure, and the residue was redissolved in 1000 µL of a mixture of CH_3CN/H_2O 95:5 (*v/v*) containing 0.05% TFA.

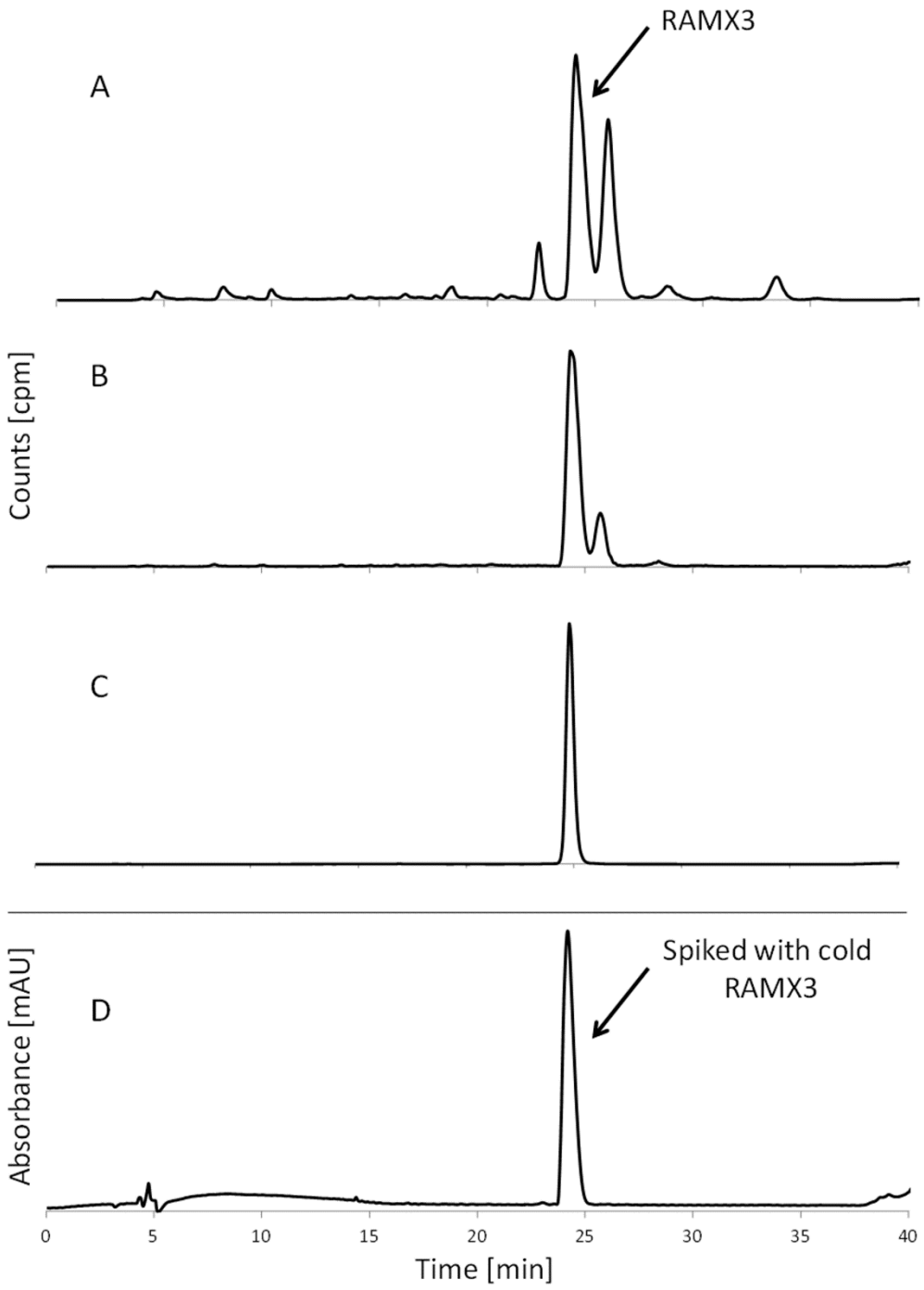

Figure 9.1 Identity and purity control of RAMX3 by HPLC. A. Reaction control after 20 h; B. Purity control after first purification; C. Final purity control; D. UV (λ = 220 nm) chromatogram of unlabeled RAMX at 100 µM. Conditions: injection volume: 100 µL, gradient: 0.05% TFA in CH_3CN (*v/v*)/0.05% TFA in H_2O (*v/v*): 0 min 5:95, 10 min 45:55, 34 min 35:65, 36 min 95:5, 41 min 95:5, 43 min 5:95, 50 min 5:95, flow: 0.8 mL/min, t_R~25 min. Minor differences in retention times (t_R) result from the setup of the UV and the radiodetector in series. The identity of RAMX3 was confirmed by spiking with 'cold' RAMX3.

For isolation of RAMX3, aliquots (1 x 100 µL, 5 x 180 µL) were injected into an HPLC instrument. Fractions containing the radioligand were collected at ~24 min (gradient: 0.05% TFA in CH_3CN/0.05% TFA in H_2O: 0 min 5:95 (*v/v*), 10 min 45:55 (*v/v*), 34 min 35:65 (*v/v*), 36 min 95:5 (*v/v*), 41 min 95:5 (v/v), 43 min 5:95 (*v/v*), 50 min 5:95 (*v/v*)). The solvent of the combined fractions was evaporated,

and the residue was dissolved in 540 mL of a mixture of CH_3CN/H_2O 5:95 (*v/v*) containing 0.05% TFA. Aliquots (3 x 180 µL) of the supernatant were purified by HPLC to achieve high purity. The solvent of the combined fractions was evaporated and the residue was re-dissolved in freshly distilled DMSO (720 µL) and transferred into a 5 mL Amersham glass vial.

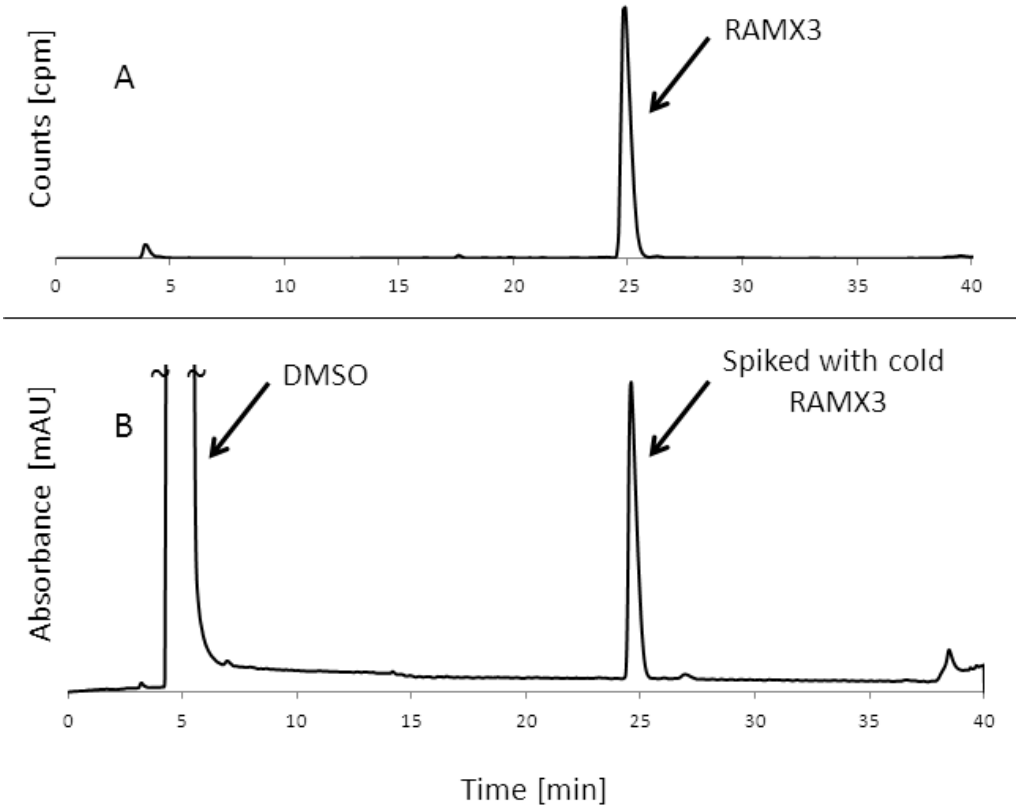

Figure 9.2 Purity control of RAMX3 by HPLC after storage at room temperature for five months. A. Radiochromatogram of RAMX3. B. UV detection (λ = 220 nm) of RAMX3 spiked with unlabeled RAMX3, c: 100 µM. Conditions: injection volume: 100 µL, gradient: 0.05% TFA in MeCN (*v/v*) / 0.05% TFA in H_2O (*v/v*): 0 min: 5/95, 10 min: 45/55, 34 min: 35/65, 36 min: 95/5, 41 min: 95/5, 43 min: 5/95, 50 min: 5/95, flow: 0.8 mL/min, t_R ~25 min. The minor difference in retention times (t_R) results from the setup of the UV and the radiodetector in series. The identity of RAMX3 was confirmed by spiking with 'cold' RAMX3.

The concentration of the radioligand in the stock solution was determined from a five point calibration curve for unlabeled ligand RAMX3 (1.0, 2.5, 5.0, 7.5, and 10 µM; inj. vol.: 100 µL; HPLC: λ=220 nm, gradient: 0.05% TFA in CH_3CN/0.05% TFA in H_2O: 0 min 5:95 (*v/v*), 10 min 75:25 (*v/v*), 20 min 85:15 (*v/v*), 21 min 95:5 (*v/v*), 25 min 95:5 (*v/v*), 26 min 5:95 (*v/v*), 30 min 5:95 (*v/v*), t_R~14 min) from the peak area of 100 µL of a mixture of stock solution (10.5 µL) diluted with 94.5 µL CH_3CN/H_2O 5:95 (*v/v*) containing 0.05% TFA (16.86 µM, 12.14 nmol, yield: 20.7 %). All standard solutions were prepared separately from a 100 µM solution of unlabeled RAMX3 in a mixture of CH_3CN/H_2O 5:95 (*v/v*) containing 0.05% TFA, which was freshly prepared from a 10 mM solution of unlabeled RAMX3 in CH_3CN. To determine the total radioactivity of RAMX3, stock solution (5 µL) was diluted with 445 µL of a mixture of CH_3CN/H_2O 5:95 (*v/v*) containing 0.05% TFA, and 50 µL of this

solution was measured three times in scintillation cocktail Rotiscint Eco Plus (3 mL) in a LS 6500 liquid scintillation counter (Beckmann Coulter, München, Germany). The total activity in 720 µL stock solution amounted to 36.1 MBq (0.976 mCi), resulting in a calculated specific activity of 2.98 TBq/mmol (80.4 Ci/mmol). The activity of the stock solution was adjusted to 37 MBq/mL; (1 mCi/mL, c=12.40 µM) by adding a mixture of DMSO/EtOH 98:2 (*v/v*) containing 100 µM TFA. HPLC analysis showed a radiochemical purity of >99.9 %. The identity of the radioligand was confirmed by HPLC analysis of labeled and unlabeled RAMX3 under the same conditions, resulting in identical retention times. Moreover, chemical stability in DMSO/EtOH 98:2 (*v/v*) containing 100 µM TFA at room temperature was proven over a period of at least 5 months (see Figure 9.2).

9.2 Nonspecific binding of [^{3}H]JNJ7777120 at the hH_4R in Sf9 cell membranes (cf. Chapter 6)

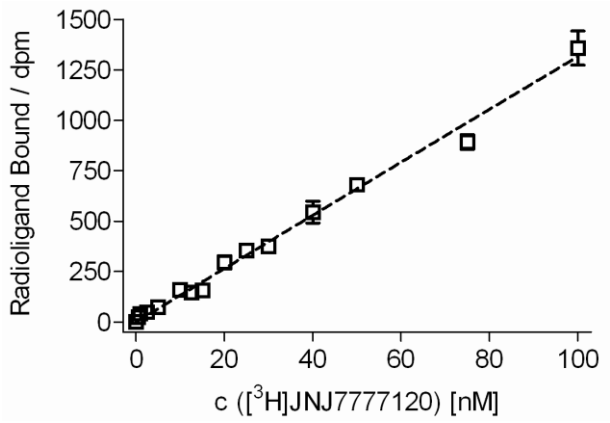

Figure 9.3 Nonspecific binding of [^{3}H]JNJ7777120 at the hH_4R in Sf9 insect cell membranes. A. Nonspecific binding: □; competitor: JNJ7777120 (**6.4a**) (c = 10µM); specific binding is shown in Figure 6.5.

9.3 Nonspecific binding of [^{3}H]UR-PLN208 at CHO-hY_2R cells (cf. Chapter 7)

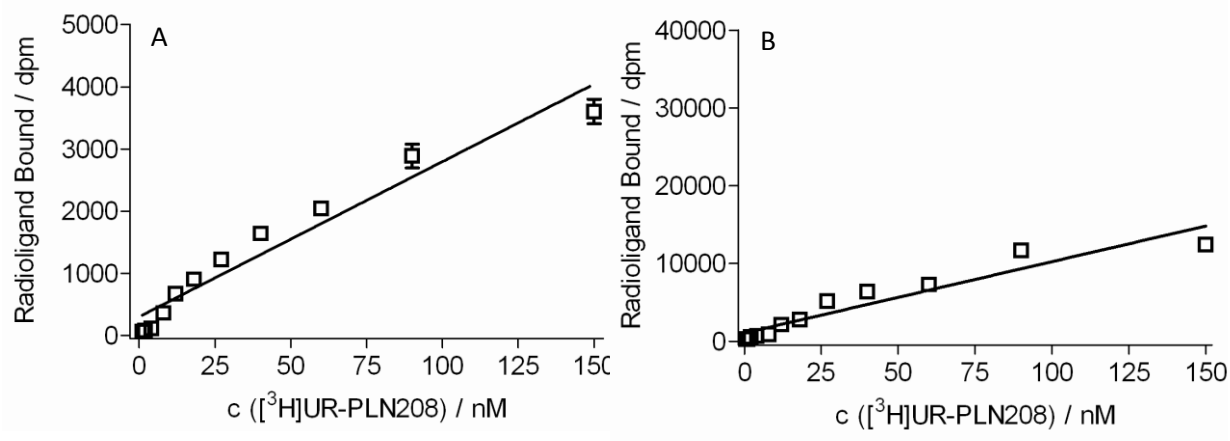

Figure 9.4 Nonspecific binding of [^{3}H]UR-PLN208 at CHO-hY_2R cells. A. Nonspecific binding: □; competitor: pNPY (100 fold concentration of [^{3}H]UR-PLN208); specific binding is shown in Figure 7.4. B. Nonspecific binding: □; competitor: BIIE 0246 (30 fold concentration of [^{3}H]UR-PLN208); specific binding is shown in Figure 7.4.

9.4 NMR-Spectra of selected compounds

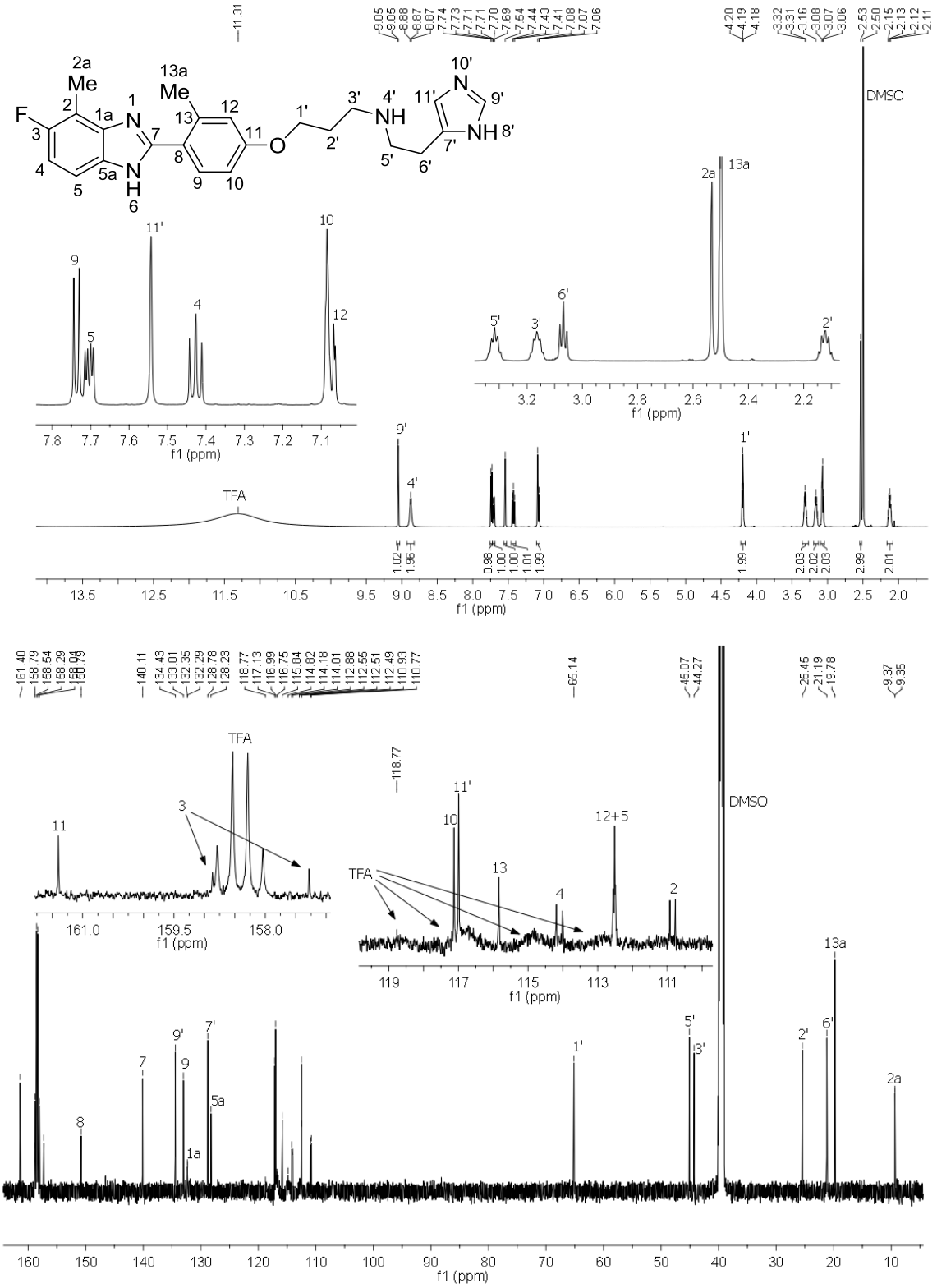

Figure 9.5 ^{1}H- & ^{13}C-Spectra of **3.16**.

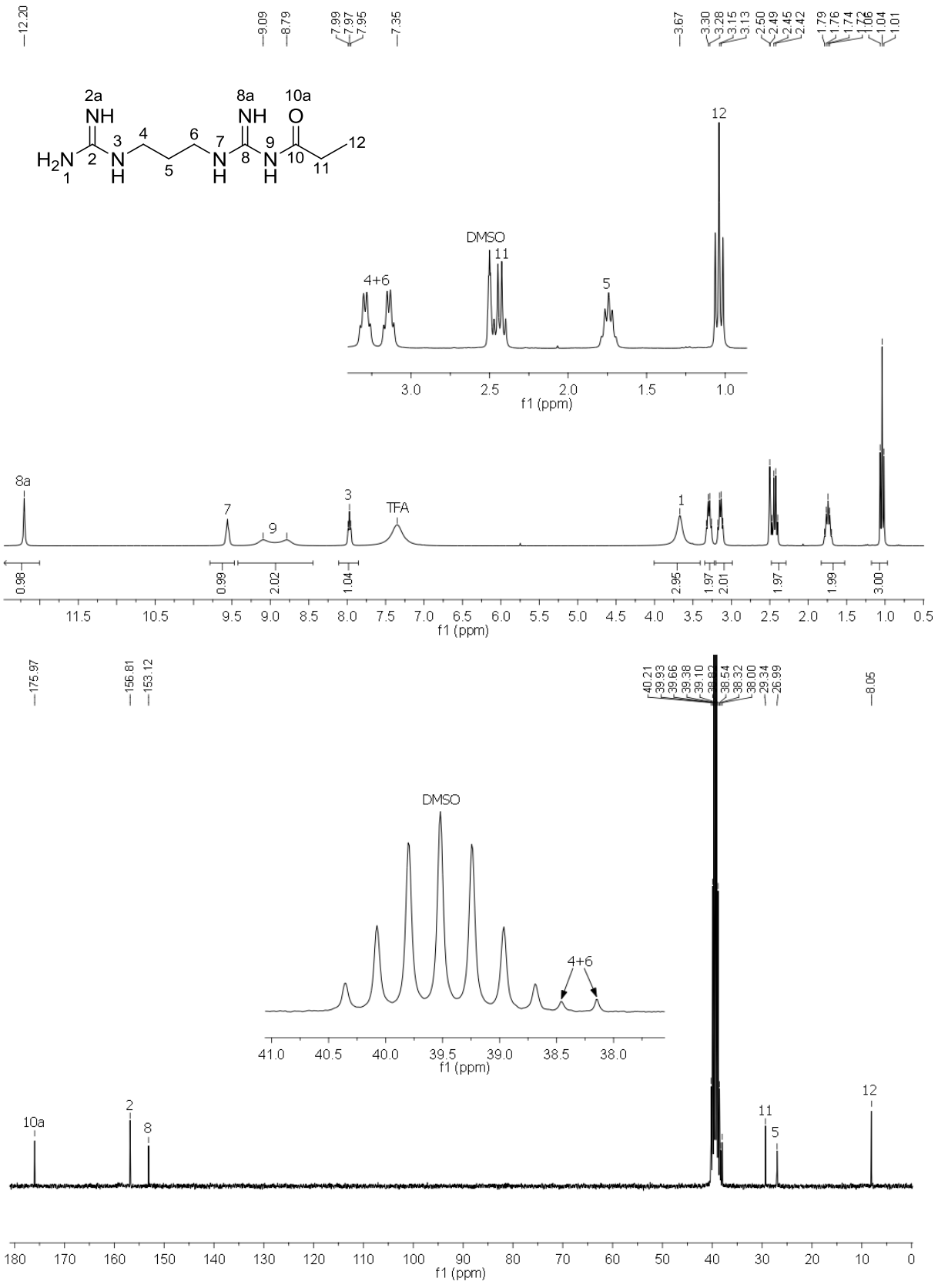

Figure 9.6 ^{1}H- & ^{13}C-Spectra of **4.19**.

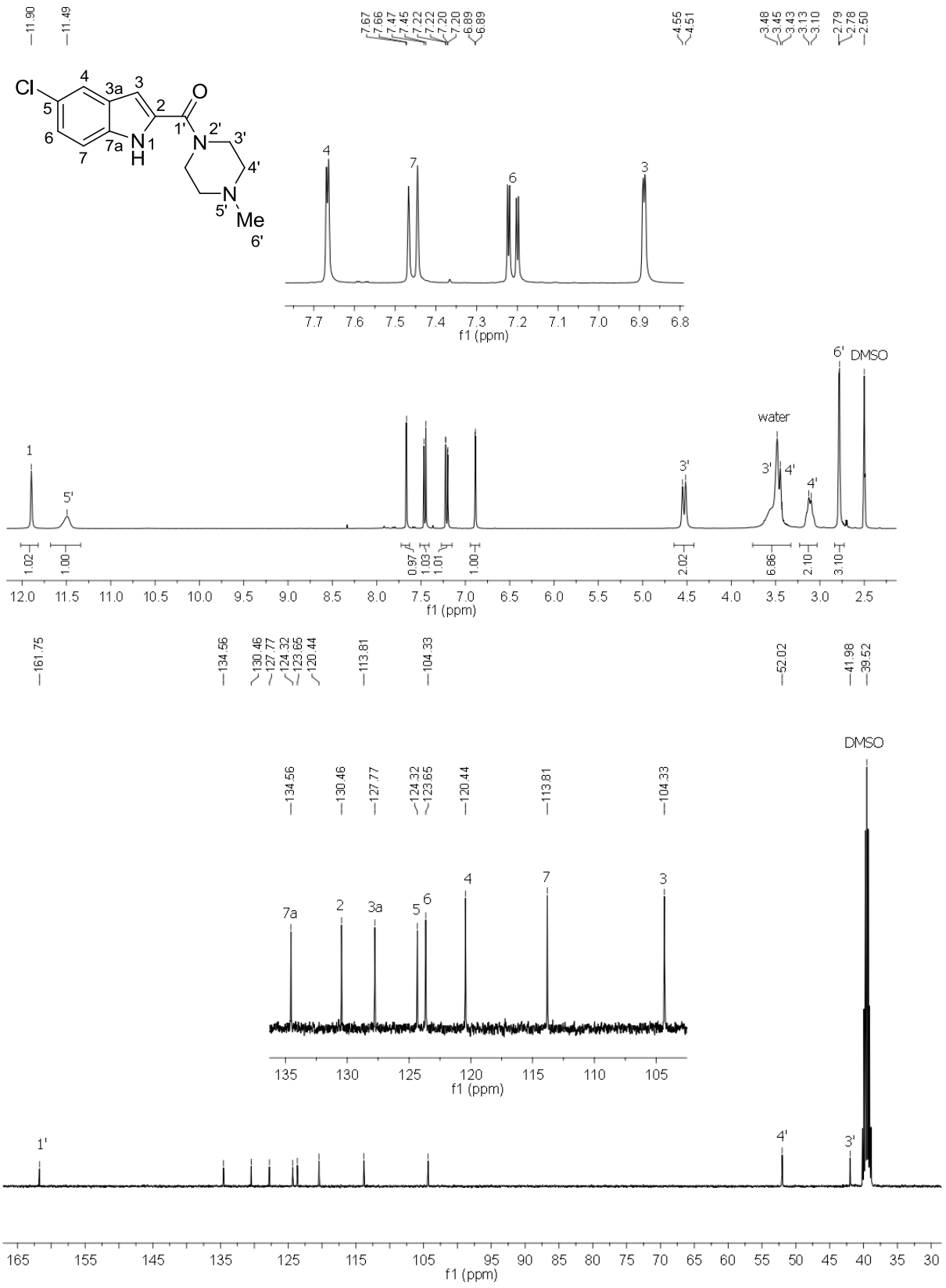

Figure 9.7 ^{1}H- & ^{13}C-Spectra of JNJ7777120 (**6.4a**).

9.5 HPLC Purity Data

No	Gradient	λ / nm	t_R	k	Purity / %
3.11	30/70-60/40	220	22.5	10.1	99.4
3.16	20/80-50/50	220	11.2	3.0	99.9
3.17	20/80−50/50	220	6.9	1.5	99.6
3.18	20/80−50/50	220	10.9	2.9	99.6
3.19	20/80−50/50	220	6.5	1.3	99.8
3.20	10/90−80/20	220	6.5	1.3	99.8
3.22	20/80−50/50	220	12.3	3.4	99.2
3.23	30/70−60/40	220	7.6	1.6	100
3.26	20/80−50/50	220	16.9	6.3	98.7
3.30	5/95-80/20	220	15.7	8.3	97.8
3.31	30/70−60/40	220	9.0	2.2	99.4
3.32	30/70−60/40	220	12.7	3.5	100
3.33	20/80−80/20	220	13.3	4.7	100
3.34	40/60−90/10	220	16.6	6.1	100
3.35	40/60−90/10	220	17.5	6.5	99.9
3.36	40/60−90/10	220	15.7	5.7	99.6
3.37	5/95-80/20	220	20.2	11.0	98.3
3.42	5/95-50/50	220	2.5	0.5	99.3
3.49	3/97 (isocratic)	220	8.7	2.1	99.6
3.50	3/97 (isocratic)	220	5.0	0.8	98.3
3.61	5/95−80/20	220	26.0	10.1	97.0
3.62	5/95-80/20	220	13.3	6.9	98.8
3.63	5/95-80/20	220	13.1	6.8	99.3
3.64	10/90−80/20	220	14.9	5.4	99.4
3.65	10/90−80/20	220	11.3	3.8	100
3.66	10/90−80/20	220	15.2	5.5	100
3.67	10/90−80/20	220	14.4	5.2	98.6
3.68	5/95-80/20	220	13.0	6.7	96.4
3.69	10/90−70/30	220	14.4	5.2	99.3
3.70	10/90−70/30	220	14.0	5.0	99.3
3.71	10/90−80/20	220	14.4	5.2	99.9
3.72	10/90−80/20	220	17.1	6.3	99.0
3.77	10/90−80/20	220	15.4	5.6	99.9
3.78	10/90−80/20	220	16.1	5.9	99.9

No	Gradient	λ / nm	t_R	*k*	Purity / %
4.12	5/95−30/70	200	3.7	0.6	97.3
4.13	5/95−30/70	200	3.9	0.7	96.8
4.14	5/95−30/70	200	9.3	3.0	99.8
4.15	5/95−43/57	200	11.8	4.1	98.2
4.16	5/95−43/57	200	11.4	3.9	97.3
4.17	5/95−43/57	200	10.1	3.3	98.3
4.18	10/90−70/30	200	16.5	6.1	97.1
4.19	5/95−30/70	200	7.5	2.2	99.0
4.20	5/95−50/50	200	10.5	5.2	98.8
4.21	5/95−50/50	200	10.2	5.0	95.2
4.22	5/95−40/60	200	13.6	4.9	97.0
4.23	5/95−50/50	200	12.6	6.5	97.1
4.24	5/95−50/50	200	16.3	8.7	97.5
4.25	5/95−50/50	200	15.0	7.9	99.9
4.26	5/95−60/40	200	18.7	10.1	98.3
4.27	5/95−30/70	200	15.0	5.5	98.9
4.28	5/95−43/57	200	20.4	7.8	99.7
4.29	5/95−43/57	200	17.7	6.6	99.3
4.30	5/95−43/57	200	17.1	6.3	99.7
4.31	10/90−70/30	200	27.4	10.8	98.9
4.32	5/95−30/70	200	16.7	6.2	99.3
4.33	5/95−50/50	200	17.8	9.5	100
4.34	5/95−50/50	200	14.3	7.5	100
4.35	5/95−50/50	200	13.0	6.7	95.8
4.36	20/80−50/50	200	17.3	5.1	98.8
4.37	5/95−50/50	200	23.1	12.7	98.7
4.38	5/95−50/50	200	23.3	12.8	95.6
4.39	5/95−60/50	200	23.9	13.1	99.8
4.40	5/95−43/57	200	4.8	0.7	98.2
4.43	5/95−43/57	200	4.8	0.7	98.2
6.3	5/95-80/20	220	15.3	8.1	99.0
6.4a	5/95-80/20	220	15.9	8.4	99.5

Regular column: Eurospher-100 (250 x 4 mm, 5 µm) (Knauer, Berlin, Germany, t_0 = 3.32 min); flow rate: 0.8 mL/min; column for **3.30**, **3.37**, **3.42**, **3.62**, **3.63**, **3.68**, **4.23**, **4.24**, **4.26**-**4.29**, **4.38**-**4.44**, **6.3** and **6.4a**: Luna C18(2) (150 × 4.6 mm, 3 µm) (Phenomenex, Aschaffenburg, Germany, t_0 = 2.88 min); solvent mixture: 0.05% TFA in MeCN and 0.05% aq. TFA; gradient: 0-30 min: see table, 31-40 min: 95/5; compound purities were calculated as percentage peak area of the analyzed compound by UV detection at 200/220 nm. The capacity (retention) factors were calculated according to $k = (t_R-t_0)/t_0$.

9.6 Abbreviations

α	intrinsic activity or selectivity factor
A	agonist
abs	absolute
AC	adenylyl cyclase
aq	aqueous
a_s	specific activity
atm	atmosphere
ATP	adenosine triphosphate
a_v	activity concentration
Boc	*tert*-butoxycarbonyl
Boc_2O	di-*tert*-butyl dicarbonate
Bq	becquerel
bs	broad singulet
c	concentration
calcd.	calculated
cAMP	cyclic 3', 5'-adenosine monophosphate
cat.	catalytical amounts
CH_2Cl_2	dichloromethane
$CHCl_3$	chloroform
CH_3CN	acetonitrile
Ci	curie
CI	chemical ionization
CNS	central nervous system
COSY	correlated spectroscopy
cpm	counts per minute
C_{quat}	quaternary carbon atom
Cs_2CO_3	caesium carbonate
d	day or doublet
DAG	diacylglycerol
dd	doublet of doublets
DIPEA	diisopropylethylamine
DMF	dimethylformamide
DMSO	dimethylsulfoxide
EC_{50}	molar concentration of the agonist causing 50 % of the maximal response

EDC x HCl	*N*-(3-dimethylaminopropyl)-*N*'-ethylcarbodiimide hydrochloride
eq	equivalents
EI	electron ionization
E_{max}	maximal response relative to the endogenous ligand (1.00)
ESI	electrospray ionization
Et_2O	diethylether
EtOAc	ethyl acetate
EtOH	ethanol
FBS	fetal bovine serum
G	giga or G-Protein
GC	gas chromatography
GDP	guanosine diphosphate
GF/C	glass microfibre, grade c (fine)
GPCR	G-Protein coupled receptor
GTP	guanosine triphosphate
GTPγS	guanosine 5'-thiotriphosphate
h	hour(s) or human
HCl	hydrochloric acid
HEK	human embryonic kidney
HOBt x H_2O	1-Hydroxybenzotriazole hydrate
HPLC	high-performance liquid chromatography
HR	histamine receptor
hH_1R	human histamine H_1 receptor
hH_2R	human histamine H_2 receptor
hH_2R-$Gs\alpha_S$	fusion protein between the hH_2R and short splice variant of Gsα
hH_3R	human histamine H_3 receptor
hH_4R	human histamine H_4 receptor
HMBC	heteronulcear multiple bond correlation
HMQC	heteronuclear multiple quantum correlation
H_1R, H_2R, H_3R, H_4R	histamine receptor subtypes
HRMS	high resolution mass spectroscopy
HSQC	heteronuclear single quantum correlation
hY_2R	human Y_2 receptor
Hz	hertz
IC_{50}	functional assay: antagonist (inverse agonist) concentration suppressing 50 % of an agonist induced effect

	radioligand binding assay: ligand concentration inhibiting the binding of a radioligand by 50 %
IP_3	inositol-1,4,5-trisphosphate
IR	infrared
J	coupling constant
k	capacity factor
K_b	dissociation constant (functional assay)
KBr	potassium bromide
K_2CO_3	potassium carbonate
K_d	dissociation constant (saturation binding)
$KHSO_4$	potassium bisulfate
K_i	dissociation constant (competition binding)
k_{ob}	observed rate constant
k_{off}	dissociation rate constant
k_{on}	association rate constant
L	liter
LC	liquid chromatography
m	multiplet or milli or mouse
M	mega or mol/L
MAPK	mitogen-activated protein kinase
mAU	milli absorbance units
MeCN	acetonitrile
mH_4R	mouse histamine H_4 receptor
MeI	methyl iodide
MeOD	deuterated methanol
MeOH	methanol
$MgSO_4$	magnesium sulfate
min	minute(s)
µ	micro
mp	melting point
MS	mass spectrometry
n	nano or amount of substance
$NaHCO_3$	sodium bicarbonate
NaI	sodium iodide
NaOH	sodium hydroxide
Na_2SO_4	sodium sulfate
$Na_2S_2O_5$	sodium metabisulfite

NEt_3	triethylamine
N^G	guanidino-nitrogen
NHS	*N*-hydroxysuccinimide
nm	nanometer
NMR	nuclear magnetic resonance
NOESY	nuclear overhauser enhancement spectroscopy
NP	normal phase
NPY	neuropeptide Y
p	quintet
PBS	phoshpate buffered saline
PE	petroleum ether
pEC_{50}	negative decadic logarithm of the molar concentration of the agonist causing 50 % of the maximal response
PEI	polyethyleneimine
Ph	phenyl
P_i	inorganic phosphate
PIP_2	phosphatidylinositol-4,5-bisphosphate
PKA	protein kinase A
PKC	protein kinase C
PLA_2	phospholipase A_2
PLC_β	phospholipase C_β
Phthal	phthalimide
ppm	parts per million
q	quartet
R	inactive state of a GPCR
R*	active state of a GPCR
ref	reference
R_f	retardation factor
RGS	regulator of G-protein signaling
RP	reversed phase
rpm	revolutions per minute
rt	room temperature
s	singlet
sat.	saturated
SEM	standard error of the mean
SF	SuperFlash
Sf9	*Spodoptera frugiperda* insect cell line

SK-N-MC cells	human neuroblastoma cell line established from the supraorbital metastasis of a neuroblastoma of a 14-year old girl in 1971
t	triplet
T	tera
t_0	dead time
TBTU	2-(1*H*-Benzotriazole-1-yl)-1,1,3,3-tetramethylaminium tetrafluoroborate
TFA	trifluoroacetic acid
THF	tetrahydrofuran
TLC	thin layer chromatography
TM	transmembrane
TMS	trimethylsilyl
t_R	retention time
Tris	tris(hydroxymethyl)aminomethane
Trt	trityl, triphenylmethyl
UV	ultraviolett
Vis	visible

Ich erkläre hiermit an Eides statt, dass ich die vorliegende Arbeit ohne unzulässige Hilfe Dritter und ohne Benutzung anderer als der angegebenen Hilfsmittel angefertigt habe; die aus anderen Quellen direkt oder indirekt übernommenen Daten und Konzepte sind unter Angabe des Literaturzitats gekennzeichnet.

Regensburg, _____

Paul Baumeister